N 121868

AD 654783

LRC66-509

LOCKHEED-GEORGIA COMPANY

A DIVISION OF LOCKHEED AIRCRAFT CORPORATION

DISCLAIMER NOTICE

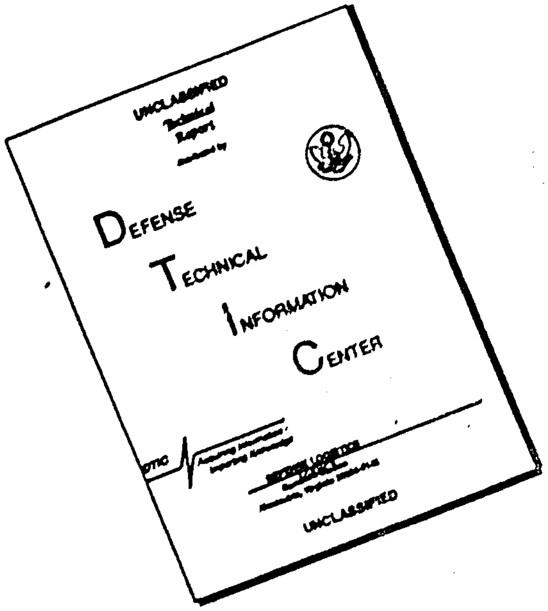

THIS DOCUMENT IS BEST QUALITY AVAILABLE. THE COPY FURNISHED TO DTIC CONTAINED A SIGNIFICANT NUMBER OF PAGES WHICH DO NOT REPRODUCE LEGIBLY.

REPORT NO. ER-7634

DATED 12 January 1965

LOCKHEED-GEORGIA COMPANY

A DIVISION OF LOCKHEED AIRCRAFT CORPORATION

MARIETTA GEORGIA

TITLE

FULL SCALE TESTS OF THE XV-4A HUMMINGBIRD IN THE AMES 40 X 80 FOOT WIND TUNNEL

SUBMITTED UNDER

Contract No. DA 44-177-TC-773

MODEL XV-4A

REFERENCE Contract No. DA 44-177-TC-773

PREPARED BY O. G. Barnes, Jr.

GROUP Department 72-10

CHECKED BY

APPROVED BY

APPROVED BY J. G. McReynolds, Jr.

APPROVED BY A. W. Mooney

DATE	REV. BY	PAGES AFFECTED	REMARKS

FORM 402-2

CONTENTS

Section	Title	Page
	FIGURE INDEX	ii
I	INTRODUCTION	1
II	SUMMARY	2
III	DESCRIPTION OF AIRCRAFT AND TEST SETUP	4
IV	DATA REDUCTION	7
V	SCOPE OF THE TESTS	10
VI	PLOTTED COEFFICIENT DATA	13
VII	ANALYSIS OF THE CONVENTIONAL FLIGHT DATA	14
VIII	ANALYSIS OF THE HOVER AND TRANSITION DATA	17
IX	REFERENCES	28

FIGURE INDEX

Figure	Title	Page
1	Hummingbird Installed in the 40 x 80 Foot Wind Tunnel	29
2	Hummingbird General Arrangement	30
3	Theoretical Aerodynamic Data	31
4	Remote Readout Panel	33
5	Table of Symbols	34
6	Run Schedule Summary	36
7	Power Effects on Lift in Hover	40
8	Power Effects on Drag in Hover	41
9	Power Effects on Pitching Moment in Hover	42
10	Power Effect on Lift Coefficient in Conventional Flight at 40 Knots	43
11	Power Effect on Drag Coefficient in Conventional Flight at 40 Knots	44
12	Power Effect on Pitching Moment Coefficient in Conventional Flight at 40 Knots	45
13	Power Effect on Lift Coefficient in Conventional Flight at 80 Knots	46
14	Power Effect on Drag Coefficient in Conventional Flight at 80 Knots	47
15	Power Effect on Pitching Moment Coefficient in Conventional Flight at 80 Knots	48
16	Elevator Effect on Lift in Hover	49
17	Elevator Effect on Drag in Hover	50
18	Elevator Effect on Pitching Moment in Hover	51
19	Aileron Effect on Side Force in Hover	52
20	Aileron Effect on Yawing Moment in Hover	53
21	Aileron Effect on Rolling Moment in Hover	54
22	Rudder Effect on Side Force in Hover	55

FIGURE INDEX (Continued)

Figure	Title	Page
23	Rudder Effect on Yawing Moment in Hover	56
24	Rudder Effect on Rolling Moment in Hover	57
25	Lift Coefficient in Phase I Flight at 20 Knots	58
26	Drag Coefficient in Phase I Flight at 20 Knots	59
27	Pitching Moment Coefficient in Phase I Flight at 20 Knots	60
28	Side Force Coefficient in Phase I Flight at 20 Knots	61
29	Yawing Moment Coefficient in Phase I Flight at 20 Knots	62
30	Rolling Moment Coefficient in Phase I Flight at 20 Knots	63
31	Elevator Effect on Lift Coefficient in Phase I Flight at 20 Knots	64
32	Elevator Effect on Drag Coefficient in Phase I Flight at 20 Knots	65
33	Elevator Effect on Pitching Moment Coefficient in Phase I Flight at 20 Knots	66
34	Aileron Effect on Side Force Coefficient in Phase I Flight at 20 Knots	67
35	Aileron Effect on Yawing Moment Coefficient in Phase I Flight at 20 Knots	68
36	Aileron Effect on Rolling Moment Coefficient in Phase I Flight at 20 Knots	69
37	Rudder Effect on Side Force Coefficient in Phase I Flight at 20 Knots ($\psi = 0$)	70
38	Rudder Effect on Yawing Moment Coefficient in Phase I Flight at 20 Knots ($\psi = 0$)	71
39	Rudder Effect on Rolling Moment Coefficient in Phase I Flight at 20 Knots ($\psi = 0$)	72
40	Rudder Effect on Side Force Coefficient in Phase I Flight at 20 Knots ($\psi = 10$)	73
41	Rudder Effect on Yawing Moment Coefficient in Phase I Flight at 20 Knots ($\psi = 10$)	74

FIGURE INDEX (Continued)

Figure	Title	Page
42	Rudder Effect on Rolling Moment Coefficient in Phase I Flight at 20 Knots (ψ = 10)	75
43	Lift Coefficient in Phase I Flight at 30 Knots	76
44	Drag Coefficient in Phase I Flight at 30 Knots	77
45	Pitching Moment Coefficient in Phase I Flight at 30 Knots	78
46	Side Force Coefficient in Phase I Flight at 30 Knots	79
47	Yawing Moment Coefficient in Phase I Flight at 30 Knots	80
48	Rolling Moment Coefficient in Phase I Flight at 30 Knots	81
49	Elevator Effect on Lift Coefficient in Phase I Flight at 30 Knots	82
50	Elevator Effect on Drag Coefficient in Phase I Flight at 30 Knots	83
51	Elevator Effect on Pitching Moment Coefficient in Phase I Flight at 30 Knots	84
52	Aileron Effect on Side Force Coefficient in Phase I at 30 Knots	85
53	Aileron Effect on Yawing Moment Coefficient in Phase I at 30 Knots	86
54	Aileron Effect on Rolling Moment Coefficient in Phase I at 30 Knots	87
55	Rudder Effect on Side Force Coefficient in Phase I Flight at 30 Knots	88
56	Rudder Effect on Yawing Moment Coefficient in Phase I Flight at 30 Knots	89
57	Rudder Effect on Rolling Moment Coefficient in Phase I Flight at 30 Knots	90
58	Lift Coefficient in Phase I Flight at 40 Knots	91
59	Drag Coefficient in Phase I Flight at 40 Knots	92
60	Pitching Moment Coefficient in Phase I Flight at 40 Knots	93
61	Side Force Coefficient in Phase I Flight at 40 Knots	94

FIGURE INDEX (Continued)

Figure	Title	Page
62	Yawing Moment Coefficient in Phase I Flight at 40 Knots	95
63	Rolling Moment Coefficient in Phase I Flight at 40 Knots	96
64	Elevator Effect on Lift Coefficient in Phase I Flight at 40 Knots	97
65	Elevator Effect on Drag Coefficient in Phase I Flight at 40 Knots	98
66	Elevator Effect on Pitching Moment Coefficient in Phase I Flight at 40 Knots	99
67	Aileron Effect on Side Force Coefficient in Phase I Flight at 40 Knots	100
68	Aileron Effect on Yawing Moment Coefficient in Phase I Flight at 40 Knots	101
69	Aileron Effect on Rolling Moment Coefficient in Phase I Flight at 40 Knots	102
70	Rudder Effect on Side Force Coefficient in Phase I Flight at 40 Knots	103
71	Rudder Effect on Yawing Moment Coefficient in Phase I Flight at 40 Knots	104
72	Rudder Effect on Rolling Moment Coefficient in Phase I Flight at 40 Knots	105
73	Lift Coefficient in Phase I Flight at 50 Knots	106
74	Drag Coefficient in Phase I Flight at 50 Knots	107
75	Pitching Moment Coefficient in Phase I Flight at 50 Knots	108
76	Side Force Coefficient in Phase I at 50 Knots	109
77	Yawing Moment Coefficient in Phase I at 50 Knots	110
78	Rolling Moment Coefficient in Phase I at 50 Knots	111
79	Elevator Effect on Lift Coefficient in Phase I Flight at 50 Knots (BLC on)	112
80	Elevator Effect on Drag Coefficient in Phase I Flight at 50 Knots (BLC on)	113

FIGURE INDEX (Continued)

Figure	Title	Page
81	Elevator Effect on Pitching Moment Coefficient in Phase I Flight at 50 Knots (BLC on)	114
82	Elevator Effect on Lift Coefficient in Phase I Flight at 50 Knots (BLC off)	115
83	Elevator Effect on Drag Coefficient in Phase I Flight at 50 Knots (BLC off)	116
84	Elevator Effect on Pitching Moment Coefficient in Phase I Flight at 50 Knots (BLC off)	117
85	Aileron Effect on Side Force Coefficient in Phase I Flight at 50 Knots	118
86	Aileron Effect on Yawing Moment Coefficient in Phase I Flight at 50 Knots	119
87	Aileron Effect on Rolling Moment Coefficient in Phase I Flight at 50 Knots	120
88	Rudder Effect on Side Force Coefficient in Phase I Flight at 50 Knots	121
89	Rudder Effect on Yawing Moment Coefficient in Phase I Flight at 50 Knots	122
90	Rudder Effect on Rolling Moment Coefficient in Phase I Flight at 50 Knots	123
91	Lift Coefficient in Phase I Flight at 70 Knots	124
92	Drag Coefficient in Phase I Flight at 70 Knots	125
93	Pitching Moment Coefficient in Phase I Flight at 70 Knots	126
94	Elevator Effect on Lift Coefficient in Phase I Flight at 70 Knots	127
95	Elevator Effect on Drag Coefficient in Phase I Flight at 70 Knots	128
96	Elevator Effect on Pitching Moment Coefficient in Phase I Flight at 70 Knots	129
97	Lift Coefficient in Phase II Flight at 50 Knots	130
98	Drag Coefficient in Phase II Flight at 50 Knots	131

FIGURE INDEX (Continued)

Figure	Title	Page
99	Pitching Moment Coefficient in Phase II Flight at 50 Knots	132
100	Elevator Effect on Lift Coefficient in Phase II at 50 Knots	133
101	Elevator Effect on Drag Coefficient in Phase II at 50 Knots	134
102	Elevator Effect on Pitching Moment Coefficient in Phase II at 50 Knots	135
103	Lift Coefficient in Phase II Flight at 67 Knots	136
104	Drag Coefficient in Phase II Flight at 67 Knots	137
105	Pitching Moment Coefficient in Phase II Flight at 67 Knots	138
106	Elevator Effect on Lift Coefficient in Phase II Flight at 67 Knots	139
107	Elevator Effect on Drag Coefficient in Phase II Flight at 67 Knots	140
108	Elevator Effect on Pitching Moment Coefficient in Phase II Flight at 67 Knots	141
109	Lift Coefficient in Phase II Flight at 85 Knots	142
110	Drag Coefficient in Phase II Flight at 85 Knots	143
111	Pitching Moment Coefficient in Phase II Flight at 85 Knots	143
112	Elevator Effect on Lift Coefficient in Phase II Flight at 85 Knots	145
113	Elevator Effect on Drag Coefficient in Phase II Flight at 85 Knots	146
114	Elevator Effect on Pitching Moment Coefficient in Phase II Flight at 85 Knots	147
115	Lift Coefficient in Phase II Flight at 100 Knots	148
116	Drag Coefficient in Phase II Flight at 100 Knots	149
117	Pitching Moment Coefficient in Phase II Flight at 100 Knots	150
118	Elevator Effect on Lift Coefficient in Phase II Flight at 100 Knots	151
119	Elevator Effect on Drag Coefficient in Phase II Flight at 100 Knots	152

FIGURE INDEX (Continued)

Figure	Title	Page
120	Elevator Effect on Pitching Moment Coefficient in Phase II Flight at 100 Knots	153
121	Aileron Effect on Side Force Coefficient in Phase II Flight at 100 Knots	154
122	Aileron Effect on Yawing Moment Coefficient in Phase II Flight at 100 Knots	155
123	Aileron Effect on Rolling Moment Coefficient in Phase II Flight at 100 Knots	156
124	Rudder Effect on Side Force Coefficient in Phase II Flight at 100 Knots	157
125	Rudder Effect on Yawing Moment Coefficient in Phase II Flight at 100 Knots	158
126	Rudder Effect on Rolling Moment Coefficient in Phase II Flight at 100 Knots	159
127	Lift Coefficient in Phase III Flight at 80 Knots	160
128	Drag Polar for Phase III Flight at 80 Knots	161
129	Pitching Moment Characteristics in Phase III Flight at 80 Knots	162
130	Side Force Coefficient in Phase III Flight at 80 Knots	163
131	Yawing Moment Coefficient in Phase III Flight at 80 Knots	164
132	Rolling Moment Coefficient in Phase III Flight at 80 Knots	165
133	Lift Coefficient in Conventional Flight at 40 Knots	166
134	Drag Polar in Conventional Flight at 40 Knots	167
135	Pitching Moment Characteristics in Conventional Flight at 40 Knots	168
136	Lift Coefficient in Conventional Flight at 80 Knots (Power Off)	169
137	Drag Polar in Conventional Flight at 80 Knots (Power Off)	170
138	Pitching Moment Characteristics in Conventional Flight at 80 Knots (Power Off)	171

FIGURE INDEX (Continued)

Figure	Title	Page
139	Side Force Coefficient in Conventional Flight at 80 Knots (Power Off)	172
140	Yawing Moment Coefficient in Conventional Flight at 80 Knots (Power Off)	173
141	Rolling Moment Coefficient in Conventional Flight at 80 Knots (Power Off)	174
142	Elevator Effect on Lift Coefficient in Conventional Flight at 80 Knots (Power Off)	175
143	Elevator Effect on Drag Coefficient in Conventional Flight at 80 Knots (Power Off)	176
144	Elevator Effect on Pitching Moment Coefficient in Conventional Flight at 80 Knots (Power Off)	177
145	Aileron Effect on Side Force Coefficient in Conventional Flight at 80 Knots (Power Off)	177A
146	Aileron Effect on Yawing Moment Coefficient in Conventional Flight at 80 Knots (Power Off)	178
147	Aileron Effect on Rolling Moment Coefficient in Conventional Flight at 80 Knots (Power Off)	179
148	Rudder Effect on Side Force Coefficient in Conventional Flight at 80 Knots (Power Off)	180
149	Rudder Effect on Yawing Moment Coefficient in Conventional Flight at 80 Knots (Power Off)	181
150	Rudder Effect on Rolling Moment Coefficient in Conventional Flight at 80 Knots (Power Off)	182
151	Lift Coefficient in Conventional Flight at 80 Knots (Power On)	183
152	Drag Polar in Conventional Flight at 80 Knots (Power On)	184
153	Pitching Moment Characteristics in Conventional Flight at 80 Knots (Power On)	185
154	Elevator Effect on Lift Coefficient in Conventional Flight at 80 Knots (Power On)	186
155	Elevator Effect on Drag Coefficient in Conventional Flight at 80 Knots (Power On)	187
156	Elevator Effect on Pitching Moment Coefficient in Conventional Flight at 80 Knots (Power On)	188

FIGURE INDEX (Continued)

Figure	Title	Page
157	Tunnel Dynamic Pressure Effect on Data Presentation	189
158	Stability and Control Comparison in Conventional Flight	190
159	Lift in Phase I Flight at 20 Knots and EPR = 1.53	191
160	Drag in Phase I Flight at 20 Knots and EPR = 1.53	192
161	Pitching Moment in Phase I Flight at 20 Knots and EPR = 1.53	193
162	Side Force in Phase I Flight at 20 Knots and EPR = 1.53	194
163	Yawing Moment in Phase I Flight at 20 Knots and EPR = 1.53	195
164	Rolling Moment in Phase I Flight at 20 Knots and EPR = 1.53	196
165	Elevator Effectiveness in Phase I Flight at 20 Knots and EPR = 1.53	197
166	Aileron Effect on Side Force in Phase I Flight at 20 Knots and EPR = 1.53	198
167	Aileron Effect on Yaw in Phase I Flight at 20 Knots and EPR = 1.53	199
168	Aileron Effect on Roll in Phase I Flight at 20 Knots and EPR = 1.53	200
169	Rudder Effect on Side Force in Phase I Flight at 20 Knots and EPR = 1.53	201
170	Rudder Effect on Yaw in Phase I Flight at 20 Knots and EPR = 1.53	202
171	Rudder Effect on Roll in Phase I Flight at 20 Knots and EPR = 1.53	203
172	Lift in Phase I Flight at 30 Knots and EPR = 1.53	204
173	Drag in Phase I Flight at 30 Knots and EPR = 1.53	205
174	Pitching Moment in Phase I Flight at 30 Knots and EPR = 1.53	206
175	Side Force in Phase I Flight at 30 Knots and EPR = 1.53	207
176	Yawing Moment in Phase I Flight at 30 Knots and EPR = 1.53	208
177	Rolling Moment in Phase I Flight at 30 Knots and EPR = 1.53	209

FIGURE INDEX (Continued)

Figure	Title	Page
178	Elevator Effectiveness in Phase I Flight at 30 Knots and EPR = 1.53	210
179	Aileron Effect on Side Force in Phase I Flight at 30 Knots and EPR = 1.53	211
180	Aileron Effect on Yaw in Phase I Flight at 30 Knots and EPR = 1.53	212
181	Aileron Effect on Roll in Phase I Flight at 30 Knots and EPR = 1.53	213
182	Rudder Effect on Side Force in Phase I Flight at 30 Knots and EPR = 1.53	214
183	Rudder Effect on Yaw in Phase I Flight at 30 Knots and EPR = 1.53	215
184	Rudder Effect on Roll in Phase I Flight at 30 Knots and EPR = 1.53	216
185	Lift in Phase I Flight at 40 Knots and EPR = 1.53	217
186	Drag in Phase I Flight at 40 Knots and EPR = 1.53	218
187	Pitching Moment in Phase I Flight at 40 Knots and EPR = 1.53	219
188	Side Force in Phase I Flight at 40 Knots and EPR = 1.53	220
189	Yawing Moment in Phase I Flight at 40 Knots and EPR = 1.53	221
190	Rolling Moment in Phase I Flight at 40 Knots and EPR = 1.53	222
191	Elevator Effectiveness in Phase I Flight at 40 Knots and EPR = 1.53	223
192	Aileron Effect on Side Force in Phase I Flight at 40 Knots and EPR = 1.53	224
193	Aileron Effect on Yaw in Phase I Flight at 40 Knots and EPR = 1.53	225
194	Aileron Effect on Roll in Phase I Flight at 40 Knots and EPR = 1.53	226
195	Rudder Effect on Side Force in Phase I Flight at 40 Knots and EPR = 1.53	227
196	Rudder Effect on Yaw in Phase I Flight at 40 Knots and EPR = 1.53	228

FIGURE INDEX (Continued)

Figure	Title	Page
197	Rudder Effect on Roll in Phase I Flight at 40 Knots and EPR = 1.53	229
198	Lift in Phase I Flight at 50 Knots and EPR = 1.53	230
199	Drag in Phase I Flight at 50 Knots and EPR = 1.53	231
200	Pitching Moment in Phase I Flight at 50 Knots and EPR = 1.53	232
201	Side Force in Phase I Flight at 50 Knots and EPR = 1.53	233
202	Yawing Moment in Phase I Flight at 50 Knots and EPR = 1.53	234
203	Rolling Moment in Phase I Flight at 50 Knots and EPR = 1.53	235
204	Elevator Effectiveness in Phase I Flight at 50 Knots and EPR = 1.53	236
205	Aileron Effect on Side Force in Phase I Flight at 50 Knots and EPR = 1.53	237
206	Aileron Effect on Yaw in Phase I Flight at 50 Knots and EPR = 1.53	238
207	Aileron Effect on Roll in Phase I Flight at 50 Knots and EPR = 1.53	239
208	Elevator Effectiveness in Hover at EPR = 1.99	240
209	Aileron Effect on Side Force in Hover at EPR = 1.99	241
210	Aileron Effect on Yaw in Hover at EPR = 1.99	242
211	Aileron Effect on Roll in Hover at EPR = 1.99	243
212	Rudder Effect on Side Force in Hover at EPR = 1.99	244
213	Rudder Effect on Yaw in Hover at EPR = 1.99	245
214	Rudder Effect on Roll in Hover at EPR = 1.99	246
215	Lift in Phase I Flight at 30 Knots and EPR = 1.99	247
216	Drag in Phase I Flight at 30 Knots and EPR = 1.99	248
217	Pitching Moment in Phase I Flight at 30 Knots and EPR = 1.99	249
218	Elevator Effectiveness in Phase I Flight at 30 Knots and EPR = 1.99	250

FIGURE INDEX (Continued)

Figure	Title	Page
219	Aileron Effect on Side Force in Phase I Flight at 30 Knots and EPR = 1.99	251
220	Aileron Effect on Yaw in Phase I Flight at 30 Knots and EPR = 1.99	252
221	Aileron Effect on Roll in Phase I Flight at 30 Knots and EPR = 1.99	253
222	Rudder Effect on Side Force in Phase I Flight at 30 Knots and EPR = 1.99	254
223	Rudder Effect on Yaw in Phase I Flight at 30 Knots and EPR = 1.99	255
224	Rudder Effect on Roll in Phase I Flight at 30 Knots and EPR = 1.99	256
225	Aileron Effect on Side Force in Phase I Flight at 40 Knots and EPR = 1.99	257
226	Aileron Effect on Yaw in Phase I Flight at 40 Knots and EPR = 1.99	258
227	Aileron Effect on Roll in Phase I Flight at 40 Knots and EPR = 1.99	259
228	Rudder Effect on Side Force in Phase I Flight at 40 Knots and EPR = 1.99	260
229	Rudder Effect on Yaw in Phase I Flight at 40 Knots and EPR = 1.99	261
230	Rudder Effect on Roll in Phase I Flight at 40 Knots and EPR = 1.99	262
231	Lift in Phase I Flight at 50 Knots and EPR = 1.99	263
232	Drag in Phase I Flight at 50 Knots and EPR = 1.99	264
233	Pitching Moment in Phase I Flight at 50 Knots and EPR = 1.99	265
234	Elevator Effectiveness in Phase I Flight at 50 Knots and EPR = 1.99	266
235	Aileron Effect on Side Force in Phase I Flight at 50 Knots and EPR = 1.99	267
236	Aileron Effect on Yaw in Phase I Flight at 50 Knots and EPR = 1.99	268

FIGURE INDEX (Continued)

Figure	Title	Page
237	Aileron Effects on Roll in Phase I Flight at 50 Knots and EPR = 1.99	269
238	Rudder Effect on Side Force in Phase I Flight at 50 Knots and EPR = 1.99	270
239	Rudder Effect on Yaw in Phase Flight at 50 Knots and EPR = 1.99	271
240	Rudder Effect on Roll in Phase I Flight at 50 Knots and EPR = 1.99	272
241	Lift in Phase I Flight at 70 Knots and EPR = 1.99	273
242	Drag in Phase I Flight at 70 Knots and EPR = 1.99	274
243	Pitching Moment in Phase I Flight at 70 Knots and EPR = 1.99	275
244	Elevator Effectiveness in Phase I Flight at 70 Knots and EPR = 1.99	276
245	Lift in Phase II Flight at 50 Knots and EPR = 1.53	277
246	Drag in Phase II Flight at 50 Knots and EPR = 1.53	278
247	Pitching Moment in Phase II Flight at 50 Knots and EPR = 1.53	279
248	Elevator Effectiveness in Phase II Flight at 50 Knots and EPR = 1.53	280
249	Lift in Phase II Flight at 67 Knots and EPR = 1.53	281
250	Drag in Phase II Flight at 67 Knots and EPR = 1.53	282
251	Pitching Moment in Phase II Flight at 67 Knots and EPR = 1.53	283
252	Elevator Effectiveness in Phase II Flight at 67 Knots and EPR = 1.53	284
253	Lift in Phase II Flight at 85 Knots and EPR = 1.53	285
254	Drag in Phase II Flight at 85 Knots and EPR = 1.53	286
255	Pitching Moment in Phase II Flight at 85 Knots and EPR = 1.53	287
256	Elevator Effectiveness in Phase II Flight at 85 Knots and EPR = 1.53	288
257	Lift in Phase II Flight at 100 Knots and EPR = 1.99	289
258	Drag in Phase II Flight at 100 Knots and EPR = 1.99	290

FIGURE INDEX (Continued)

Figure	Title	Page
259	Pitching Moment in Phase II Flight at 100 Knots and EPR = 1.99	291
260	Elevator Effectiveness in Phase II Flight at 100 Knots and EPR = 1.99	292
261	Aileron Effect on Side Force in Phase II Flight at 100 Knots and EPR = 1.99	293
262	Aileron Effect on Yaw in Phase II Flight at 100 Knots and EPR = 1.99	294
263	Aileron Effect on Roll in Phase II Flight at 100 Knots and EPR = 1.99	295
264	Rudder Effect on Side Force in Phase II Flight at 100 Knots and EPR = 1.99	296
265	Rudder Effect on Yaw in Phase II Flight at 100 Knots and EPR = 1.99	297
266	Rudder Effect on Roll in Phase II Flight at 100 Knots and EPR = 1.99	298
267	Static Aircraft Thrust	299
268	Reaction Control Pitching Moment	300
269	Reaction Control Yawing Moment (EPR = 1.53)	301
270	Reaction Control Yawing Moment (EPR = 1.99)	302
271	Reaction Control Rolling Moment	303

I. INTRODUCTION

The U. S. Army XV-4A Hummingbird Aircraft Serial Number 24504 was tested in the 40 x 80 Foot Wind Tunnel of the Ames Research Center from August 28, 1964, through September 11, 1964. As a part of the original Hummingbird contract (DA 44-177-TC-773), these tests were to have been accomplished prior to the first transition attempts. A number of postponements resulted in the wind tunnel tests being conducted nearly a year after successful transitions were performed.

The tests consisted of 41 runs and a total of 944 test points. Tests were conducted over a range of speeds in all phases of flight from hover through transition to conventional flight. Pitch and yaw runs, as well as control effectiveness runs in all three modes were made. Many of the pitch runs were made well into the so-called deep stall angle of attack range.

II. SUMMARY

The results of the XV-4A Hummingbird tests in the Ames 40 x 80 Foot Wind Tunnel are presented and analyzed. The 41 runs made included pitch, yaw, and control effectiveness tests in hover, transition, and conventional flight.

As tested in the wind tunnel, the Hummingbird configuration was the same as that flight tested. To accomplish the test, the main landing gear was removed for attachment of the wind tunnel main supports, some wiring was run externally, and the rear wind tunnel support was attached to the aft fuselage. Electric actuators were provided for the remote control of all aircraft control systems. Control surface position potentiometers provided signals for the indication of control deflections on a remote readout panel adjacent to the remote control panel located in the wind tunnel control room.

The minimum printout unit values of 12 pounds in lift for pitching moment, 6 pounds in lift difference for rolling moment, and 2.4 pounds for the other components are larger than those desirable for the magnitude of forces and moments generated by the Hummingbird. Only a small percentage of the balance system capability was used for these tests. The IBM data reduction system used reduced data promptly.

The final wind tunnel data are plotted in two forms. A standard aerodynamic coefficient form is used for presentation of all of the data. In addition, the hover and transition data are also presented in the form of forces and moments. Only the conventional flight configuration test data are analyzed in the coefficient form, and the hover and transition data are analyzed in the dimensional form.

The tests of the conventional flight configuration with the engines thrusting indicate good agreement with other data in all parameters except the pitching

moment coefficient at zero lift with neutral elevator and the directional stability level. The pitching moment and yawing moment coefficients generated by the drag of the unshielded rear support can account for the majority of the discrepancy.

Good agreement is obtained between forces from the data based on the equations derived from the small scale wind tunnel tests of Reference 1, the limited flight test data, and the full scale wind tunnel test data in hover and transition except a partially unexplained 750 pound reduction in the ejector net force value from the full scale wind tunnel tests. The agreement between the moment data is not quite as good with the full scale wind tunnel data indicating increased stability in all modes, limited control effectiveness in some cases and a nose down shift in the pitching moment data. Although a crude shield for the rear support was installed and indicated little change in the data, the shift in the pitching moment data and the directional stability level change can be generated by the drag of the unshielded rear support which was used throughout the major portion of the tests.

If these tests had been conducted previous to successful transition flights of the Hummingbird, none of the results would have prevented these flights, but some of the data indicate the need for additional analyses to explain some of the differences observed between the full scale wind tunnel tests and the equations derived from the small scale wind tunnel tests with additional full scale tests probably being indicated in some areas.

III. DESCRIPTION OF AIRCRAFT AND TEST SETUP

The external configuration of the aircraft was unchanged from that which was flight tested, except that some wiring and plumbing had to be attached to the skin externally. The external wiring and plumbing were held to a minimum and were located mostly in the nacelle and under fuselage areas. Two external longitudinal tunnels were used under the fuselage between the ejectors, but these tunnels were also present during flight tests. The leads from the tail angle of attack indicator were attached to the lower surface of the horizontal stabilizer between the boom and the point where they entered the vertical stabilizer.

Figure 1 shows the Hummingbird mounted in the Ames 40 x 80 Foot Wind Tunnel, and Figure 2 gives the general arrangement with the basic dimensions of the aircraft noted on this figure. The theoretical aerodynamic data for the Hummingbird are given in Figure 3.

The aircraft was equipped for complete remote operation from the control panel located in the wind tunnel control room. This remote control panel supplied all functions necessary for operation of the aircraft in all flight regimes and included the controls for the fire extinguishing system. The engine fuel controls were positioned from the remote control panel by means of electrical actuators located in each nacelle. Fuel was supplied from an external tank to each wheel well with all internal tankage having been removed from the aircraft.

Electrical actuators, operated from the remote control panel, were located in the cockpit and supplied the forces and motions to the aircraft control system similar to normal pilot inputs. From this point, the normal aircraft control systems were used to position the aerodynamic control surfaces and the respective reaction controls. The ejection seat and much of the pilot's instrumentation were removed from the cockpit to provide space for mounting the electrical control actuators. The existing aircraft systems were used through remote controls to position the flaps, the ejector inlet and exit doors, the nose gear, the boundary layer control air valve for the horizontal tail, the engine diverter valves, and the bleed air valves for the lateral reaction controls.

The positions of the various controls were shown by indicators mounted in the remote readout panel. These indicators were positioned by potentiometers installed at the respective control surfaces. Figure 4 is a typical picture of the remote readout panel as photographed for data recording. In addition to the control positions, operating pressures for the reaction control systems, the horizontal tail boundary layer control pressures, angle of attack, angle of sideslip, tail angle of attack, boom airspeed pressures, and engine tail pipe pressures (P_{t_5}'s) were presented on the remote readout panel.

The Hummingbird was mounted on the conventional wind tunnel three-strut support system, which is connected to the external balance. Special mounting pads were manufactured and installed in place of the main landing gear to which the ball and socket attachments of the two main wind tunnel struts were fastened. These mounting pads were designed to provide a distance between the main strut attachment points, or tread, of 88 inches, which permitted a yaw angle of 20 degrees before interference was encountered on the mounting system in the tunnel. A special fitting designed to distribute the load equally to three of the aft fuselage frames provided a mounting pad for the ball and socket of the rear wind tunnel strut. Since these frames are not normally subjected to high concentrated loads, local beefup of the three frames was required to transmit the loads into the aft fuselage basic structure. The tail length, or distance from the main strut center line to the center line of the tail strut socket, was 133.6 inches.

The remote control leads, instrumentation leads, fuel lines, CO_2 lines, and electrical start power lines were run from the wheel wells down the main struts. These leads were taped solid to the exposed potion of the struts and were run down through the windshields which protected the remainder of the forward struts from airloads which otherwise would be measured by the balance system. The regular fairing or windshield for the rear strut was damaged in the test preceding the Hummingbird test and was not used. However, a crude stationary windshield was fabricated and installed previous to Run 37. Runs 37 through 41 include the effect of this crude rear strut windshield.

Basically, the rear strut of the support system is designed to carry axial loads only, having a ball and socket mount at the aircraft and a gimbel attachment to the balance system underneath the tunnel floor. As the aircraft is yawed, the rear strut attachment under the tunnel floor follows a path perpendicular to the center line of the tunnel by means of a separate drive system controlled by limit switches. The main support struts remain vertical at all times, and move fore and aft, as well as crosswise, in the tunnel as the aircraft is yawed.

The external balance system of the tunnel is composed of four lift posts, two side force links, and one drag link. The details of the support and balance system are described more fully in Reference 2.

IV. DATA REDUCTION

All wind tunnel data were read on the external balance system and reduced to coefficient form based on the wing chord plane dimensions. The moment data were transferred to the stability axes with an origin at the 10 percent mean aerodynamic chord point which is located in the aircraft at fuselage station 285.5 and water line 100.0. Wing dimensions used for data reduction to coefficient form are:

Wing Area (S) = 104.17 square feet

Mean Aerodynamic Chord ($\bar{c}$) = 4.43 feet

Wing Span (b) = 25.0 feet

The wing span dimension used by Ames for their data reduction was 25.9 feet. However, for the data presented in this report, a correction was made to reflect a wing span of 25.0 feet as noted above. This correction was made to facilitate correlation with other data which were based on this theoretical value.

The control surface sign conventions used in all plotted data are included in the definition of symbols presented in Figure 5. These are used throughout the entire report.

In addition to the normal wind tunnel weight and data tares, a special correction was included in the data reduction for the drag of the rear strut which was not protected by a fairing or windshield. This drag value was based upon tunnel free-stream q; however, in most instances at least a portion of the rear strut was exposed to flow from the ejector which in general was at a much higher q than the free stream tunnel value, thus having a higher drag value than indicated by the correction. The drag on the rear strut also introduces a pitching moment into the data. No attempt was made to correct the data for this induced pitching moment, which is in a nose down or negative direction. The magnitude of this correction is discussed in Section VII. For Runs 37 through 41, a crude stationary fairing was installed in the wind tunnel to protect the rear strut from most of the drag load induced by the air flow.

Normal wind tunnel wall effects corrections were applied to the data for the conventional flight configuration of the aircraft. Wall corrections were not applied to the transitional flight configurations data since the major portion of the lift forces are generated by engine thrust rather than by aerodynamic means and thus the wind tunnel wall effects are not well defined. In addition, Ames personnel expressed the opinion that the wall effects for the 40 x 80 Foot Wind Tunnel are negligible for transition tests. These tests were to serve as a check of wall effects by comparison with flight test data and the small scale wind tunnel tests. The amount of flight test data is too limited for a reasonable evaluation.

Two methods were used for recording the forces as indicated on the readout scales. One was a card punch system which recorded 10 samples for each data point. The IBM data reduction system averaged these 10 samples to give a single value for each of the components reduced for each test point. Prompt data reduction was supplied by this system throughout the test.

The smallest unit recorded on the data punch cards had the following values: 12 pounds in lift summation for pitching moment; 6 pounds in lift difference for rolling moment; and 2.4 pounds for drag or side force. When these values are reflected into moments, the printout accuracies are as follows: approximately 400 foot-pounds in pitching moment; approximately 200 foot-pounds in rolling moment, and approximately 60 foot-pounds in yawing moment. The overall accuracy of the balance system is not quoted; however, it was used to a small percentage of its capacity.

The second, or backup method of recording data consisted of a tape printout system at each of the individual scales. Five data samples were printed for each test point. These tapes had to be read manually and were used only in case of a failure of the primary card punch system or in case there was any question of the final reduced values as obtained from the card punch system. The tapes were read to the nearest 5 pounds on all four lift values and to the nearest one pound on the other components. For the Hummingbird test, the card punched data was used entirely except for 3 or 4 runs in which cases significant discrepancies were found in the values used to determine the pitching moment. For these cases, the tape values were read and later used in the IBM reduction programs.

V. SCOPE OF THE TESTS

The full scale tests of the Hummingbird included some runs within all regimes of flight for VTOL aircraft consisting of hover, transition and conventional flight. The amount of hover testing was quite limited, primarily due to the restrictions imposed by the wind tunnel. Although the overhead doors of the test section were open for all hover testing, the tunnel walls still introduced certain restrictions on the test conditions, and continued hover testing induced tunnel q. The major portions of the tests were performed in the transition regime, which is the more difficult operational region for all VTOL aircraft. A few runs were made in the conventional flight regime at two velocities, in an attempt to determine some Reynolds number effects. In addition, an engine calibration run was made at zero tunnel q.

Figure 6 is a summary of the runs that were made during the test. The definitions of the various phases of transition which have been used throughout the entire Hummingbird program were adopted for the full scale test and are used in this figure. These phases are defined as follows:

Phase I - Both engines are diverted through the ejector lift system.

Phase II - Engine #1 is exhausting through the conventional tailpipe and engine #2 is diverted through the ejector lift system.

Phase III - Both engines are exhausting through the conventional tailpipes but with the ejector doors still opened.

The test speed is noted for each run with all runs being made between 0 and 100 knots. The engine thrust level for each of the runs is indicated by a P_{t_5} value which is the engine tailpipe pressure expressed in inches of mercury with a value of 30 noted for the engine inoperative condition.

Ejector exit rake surveys were made during the first two runs in an attempt to determine the gross thrust level of the ejector. These rakes were installed in the left ejector bays. Since the amount of pressure instrumentation provided by the limited number of rakes was considered to be inadequate, no data are presented; however, an examination of data by Ames showed fairly close agreement between the gross thrust values derived from these data and the net thrust values obtained from the balance system. After Runs 1 and 2 were completed these rakes were removed and no pressure instrumentation of any sort was used within the ejectors for the remainder of the test.

The maximum range of angles of attack for the polars was from -12 degrees to +28 degrees; however, many of the polars did not span this complete range of angles but were shortened somewhat on either end. The yaw angles tested ranged from -4 degrees to +10 degrees with many of the yaw runs only going to +8 degrees. For the powered runs, the P_{t_5}'s tested ranged between 35 and 66 inches of mercury. Nominal values of P_{t_5} of 46 inches of mercury and 60 inches of mercury were used for the constant thrust runs.

The control effectiveness runs were made over the complete range of deflections for each control surface. In the VTOL configurations, the elevator deflections tested were between 0 and 52 degrees. In the conventional flight configuration, these limits were plus and minus 30 degrees. The range of rudder deflections tested was between -20 and +17 degrees. For aileron effectiveness, the deflections varied from -17 to +17 degrees per aileron. In general, these control surface deflection limits were somewhat less than the design values for the airplane. One reason for this was the fact that the remote control actuators did not permit full deflection of most surfaces. However, in some cases, the actual design values were not realized partially because of control system deflections and stretch under load.

Since the Hummingbird was rigged for complete remote operation, the same number of test points could have been accumulated in a shorter period of time if it had not been for certain limitations on the tunnel operation, or conversely, more test points could have been accumulated during the span of the test. These limitations were temperature and contamination caused by the operation of the engines. Since the wind tunnel does not have facilities for exchanging the air while running, much time was consumed in airing out the tunnel between runs by opening the overhead test section doors while maintaining low tunnel q. An arbitrary limit on the maximum allowable temperature of the tunnel was originally set at 115 degrees F; however, on many runs this value was exceeded with the temperature during one run actually reaching 135 degrees F.

VI. PLOTTED COEFFICIENT DATA

All of the data accumulated during the tests are plotted in Figures 7 through 156 in the form of aerodynamic coefficients with the exception of the data for the effects of power and control in hover presented in actual forces and moments. These data are plotted in the standard form for wind tunnel test results, except that drag coefficients and pitching moment coefficients are plotted as a function of angle of attack rather than lift coefficient. Angle of attack is used for convenience since the lift coefficients have such high values for the transitional tests where test speeds are low and the forces due to ejector thrust are large.

The tunnel q values varied substantially during a constant q run. In the normal IBM data reduction procedures each test point is reduced at the individual q of the test point rather than at a nominal value for the complete run. For the tests in Phase I and Phase II of transition, the amount of scatter introduced by using individual q's is greater than that experienced in the conventional configuration since the forces and moments are primarily the result of the ejector thrust rather than normal aerodynamic forces and moments. The coefficient data as shown in this report have been reduced to a constant q value for each run thereby minimizing the amount of scatter due to the variation of q within a single run. The single value of q used is that based upon the specified test value of velocity for each run. Figure 157 gives a typical comparison of the coefficient data as presented by Ames using the individual q values for each test point and the coefficient data based upon a constant q throughout the entire run. To be consistent, all of the coefficient data are based upon the constant q value for each run.

VII. ANALYSIS OF THE CONVENTIONAL FLIGHT DATA

Since the Hummingbird has flight and handling characteristics similar to any other aircraft in the normal or conventional flight regime, the coefficient form of the wind tunnel data is used for this analysis. Figure 158 is a tabulation of the stability and control levels indicated by the full scale data in the conventional flight configuration and corresponding estimates based upon the results of the small scale wind tunnel tests of Reference 1. All of the normal aerodynamic parameters of interest are tabulated. A comparison of the two sets of data, point by point, indicates good agreement for the lift and side force coefficients. The agreement between the other components is somewhat poorer.

Although the agreement between the pitching moment coefficients is not very good for the power-off test, the agreement with power on is quite good except for the C_{M_o} value. The disagreement shown in the C_{M_o} values is probably due to the pitching moment caused by the drag of the unshielded rear strut. Using a C_{D_o} value of 1.18 for the drag coefficient of the circular rear strut as shown by Reference 3, an average diameter of 6 inches, a length of 20 feet, and the center of the strut drag 10 feet (d_1) below the Hummingbird center of gravity, an estimate of the generated pitching moment coefficient is as follows:

$$M = -D \times d_1 = -10D = -10\ C_D\ q\ S_{strut}$$

$$M = -10\ C_D\ q\ (20 \times 0.5) = -100\ C_D\ q$$

$$C_M = \frac{M}{q\ S_w\ \bar{c}_w} = \frac{M}{q\ (104.2)\ (4.43)} = \frac{-100\ C_D\ q}{q\ (104.2)\ (4.43)}$$

$$C_M = -0.217\ C_D = -0.217\ (1.18) = -0.256$$

$$C_M = -0.256$$

The data of Figure 158 show a difference in C_{M_o} of -0.358 between the full scale wind tunnel data and the estimates from the small scale wind tunnel data. A large percentage of the discrepancy in C_{M_o} can be accounted for by considering the moment due to the rear strut drag in conventional flight. A forty percent increase in the rear strut drag over the above calculated value would give complete agreement.

A similar analysis of the effect of the rear strut drag on the directional stability (C_{N_β}) follows:

$$D = C_D \, q \, S_{strut} = 1.18 \, (10) \, q$$

$$N = D \, l_t \sin\beta \quad = 11.8 \, q \, (\frac{133.6}{12}) \sin\beta$$

For small angles,

$$\sin\beta \quad = \quad \beta/57.3$$

where β is in degrees, and

$$N = 11.8 \, q \, (\frac{133.6}{12}) \quad \beta/57.3 = 2.293 \, q \, \beta$$

$$C_N = 2.293 \, q \, \beta \; /qS_w b_w = \frac{2.293 \, \beta}{(104.17)(25.0)} = 0.00088 \, \beta$$

$$C_{N_\beta} = 0.00088/\text{Deg.}$$

This analysis indicates that the level (0.0045) shown for the full scale wind tunnel test data is too great by the 0.0009 value. A reduction by this amount gives a C_{N_β} level of 0.0036 as compared to 0.0030 for the small scale value. If the forty percent increase in the rear strut drag to give complete agreement for the C_{M_o} value is used, the C_{N_β} value becomes 0.0033 for the full scale wind tunnel tests which is good agreement.

The poor agreement, power off, may be partially explained by the change in the flow pattern about the aircraft due to the windmilling engines. The small scale model actually had open, free flow type nacelles, and the internal drag of the nacelle system was removed from the wind tunnel data. Unfortunately, most of the full scale data were run with the engines windmilling rather than power on. All of the lateral directional tests were made with engines windmilling.

Little flight test data are available for comparison with the wind tunnel data of the conventional flight configuration. However, based upon pilot comments and observations, the flight characteristics of the Hummingbird tend to more nearly substantiate the estimates based upon the equation data derived from the small scale wind tunnel test data rather than the values obtained from the full scale wind tunnel data. The trim elevator settings required for the Hummingbird correspond more nearly with the small scale data, but good correlation with the full scale data can also be obtained if the above correction to C_{M_0} is made for the effect of the drag of the unprotected rear strut.

VIII. ANALYSIS OF THE HOVER AND TRANSITION DATA

All of the hover and transition data from the full scale tests of the Hummingbird are given in Figures 159 through 266 in terms of forces and moments rather than in coefficient form. This form of presentation is used for these data since the forces and moments are primarily a result of ejector thrust rather than the result of normal aerodynamic effects, and is considered more meaningful than the coefficient form. In addition, the equations of Reference 1, used to predict the Hummingbird characteristics in hover and transition, are written in terms of forces and moments rather than in the coefficient form. Values determined from these equations for the full scale wind tunnel test conditions are also plotted on Figures 159 through 266 for comparison with the actual full scale wind tunnel data. These calculated forces and moments are based on a net ejector hover thrust of 6650 pounds for sea level day take-off thrust on the two JT-12 engines installed in the aircraft.

The pitch reaction controls under these design conditions produce a thrust of 450 pounds which, when added to the net ejector thrust value, gives a net airplane thrust equal to 7100 pounds as shown in the data of Figure 267. This is the value obtained when the test data are extrapolated to the take-off thrust engine pressure ratio of 2.28. The lift and drag values of the four runs have been combined to give the resultant force curve shown in this figure. With everything considered, the data show a surprisingly small mount of scatter. However, the net ejector static thrust value of 6650 pounds at the design engine pressure ratio of 2.28 is 750 pounds less than the value of 7400 pounds which has been shown for the same ejector configuration on tests in the Lift Improvement Program conducted at the Lockheed-Georgia Company. The possibility of a small difference in the primary nozzle area of the manifolds of the two tests and some small secondary configuration differences exist which may account for some of the difference in these thrust values.

The 750 pound discrepancy in net ejector static thrust also may be partially explained by the vertical component of the ejector exit flow along the unshielded rear wind tunnel support. The moment generated by this negative lift force is positive or nose up which is opposite to the net moment generated as compared with the Lift Improvement Program data. However, the drag force on the rear strut generated by the horizontal component of the ejector exit flow acts at a larger arm near the wind tunnel floor giving a negative moment. With a drag force of the same order of magnitude as the negative lift on the rear strut, the pitching moment from drag is approximately twice that generated by negative lift. Although exact values cannot be placed on these effects, both the lift deficiency and the change in pitching moment can be generated by forces acting on the unshielded rear wind tunnel support even in the hover mode.

The value of net ejector thrust used in the small scale equations was the 6650 pound level indicated by the static test in the full scale wind tunnel. This value seems to match the lift data observed on the transition tests more nearly than would the 7400 pound thrust level. The use of this lower value also gives a more conservative comparison with the full scale wind tunnel results. A limited quantity of flight test data have been reduced. These values are shown on the corresponding plots of full scale wind tunnel data of Figures 217, 233, and 243.

The aerodynamic characteristics of the Hummingbird as predicted by the equations based on the small scale wind tunnel data of Reference 1 do not include the effects of the reaction controls. The reaction control effects are evaluated separately and added to the equation values. Figure 268 presents the reaction control pitching moments available as a function of elevator deflection for the two constant engine pressure ratios used throughout the test. The engine pressure ratio of 1.53 corresponds to a tailpipe pressure, P_{t_5}, of 46 inches of mercury and the pressure ratio value of 1.99 corresponds to a P_{t_5} value of 60 inches of mercury. These engine pressure ratios are based on the average ambient pressure of 30.1 inches of mercury as observed during the test.

The yawing moments produced by reaction controls as a function of rudder deflection are shown in Figures 269 and 270 for fixed elevator deflections and for the two normally tested engine pressure ratios. The yawing moments are presented for the various elevator deflections which cover the test range to give the effect of the pitch reaction control on the yawing moment.

Figure 271 presents the rolling moment available from reaction control as a function of aileron deflection. The same two values of engine pressure ratio are used for these data.

All of the reaction control moments presented in these figures are based on the calibration curves for the aircraft as tested and on the respective gas flows for the particular reaction control corresponding to the test engine pressure ratio. The reaction control gas flows are based upon previously determined values for an engine design pressure ratio of 2.28. The estimated values of gas flow were used since the values which could be determined from the data presented on the readout panel during the test are open to question. The test values are questionable because time was not allowed for some test pressure gages to reach steady state values. The time required for some of the gages was quite large and was not expended in an attempt to obtain as many runs as possible during the limited span of the test.

The data of Figures 208 through 213 compare the actual reaction control effectiveness obtained in Run 39 for the Hummingbird as tested, with the values evaluated for addition to the small scale equations as described above. The pitching moment available from reaction control shows excellent agreement with the test data of Figure 208; however, at the high elevator deflections, some discrepancy does exist.

The agreement shown in Figure 211 for the reaction control in roll is acceptable, but the test data have been displaced through zero aileron deflection by approximately 2700 foot-pounds, and the test reaction control is not as effective for the negative aileron deflections. Figure 213 shows a slightly higher effectiveness from the yaw reaction control as determined for addition to the small scale equation data than the value obtained from the actual test points. However, the computed values are certainly within acceptable tolerances.

The pitch reaction control duct pressure data of points 12 through 17 of Run 26 indicate total pressure duct losses approximately equal to those originally estimated. These same points are used to evaluate the boom angle of attack and airspeed indicators. Of the six points, four show perfect correlation with wind tunnel angle of attack and the other two indicate 1/2 of a degree low. Half of the points indicate perfect agreement with the wind tunnel airspeed; the other half indicate 1/2 of a knot low.

An examination of the total duct pressures of the roll reaction control system of Run 18 indicates reasonable agreement with the expected values. No attempt to completely analyze the roll reaction control system is made because the duct q data are open to question. As mentioned above, these are the gages which were slow to indicate steady state values.

Each plot in this section of the report is not analyzed individually since comparative data are plotted on each figure. In general, the agreement obtained from the lift data is good between the full scale test and the data based on the small scale equations. For some test conditions, the equation data give slightly higher values of lift than do the full scale wind tunnel data; and for other test conditions, the reverse is true with the full scale wind tunnel data indicating higher values of lift. As mentioned previously, the equation data are based on a net ejector thrust value of 6650 pounds rather than the 7400 pound level indicated in the Lift Improvement Program data. The possible reason for this 750 pound deficiency is discussed above.

The agreement obtained between the two sets of drag data is not as good as that obtained for the lift data. Except for a very few cases, the drag values obtained from the full scale wind tunnel data are greater than those obtained from the equation data. This higher drag value for the aircraft is easily explained when the condition of the airplane as tested is compared with the condition of the model on which the small scale equations are based. A general cleanup of the aircraft would certainly give an appreciable reduction in its drag level and produce a better agreement between the two sets of data. The influence of the ejector flow on the drag of the rear support strut is also reflected in this comparison.

A comparison of the side force data obtained from the test completes the picture so far as force data are concerned. Similar to the lift analysis, good agreement is obtained between the full scale wind tunnel data and the side force data based upon the equations derived from the small scale wind tunnel test data. Although the side force data are, in general, quite good, there are a few cases where the side forces do not pass through zero, but at zero sideslip, are offset by an appreciable amount parallel to the predicted levels. In other cases, a discontinuity in side force is shown for sideslip angles close to zero.

With generally good agreement of all of the force data, the same would be expected of the moment data, but this is not the case. A comparison between the two sets of pitching moment data indicates a somewhat higher stability level for the full scale wind tunnel test results and the total nose up pitching moment is shown to be less. Because of these two factors, although a reduction in the control effectiveness in pitch is indicated, the elevator angle required to trim under all test conditions is less than that shown by the equations based on the small scale wind tunnel tests. A comparison of the elevator effectiveness (M_{δ_e}) through the mid deflection range indicates fairly good agreement between the two sets of data. However, the total effectiveness (total pitching moment produced in going from zero to maximum elevator deflection) shown by the full scale data is considerably less than that indicated by the equations. Some of this reduction in total elevator effectiveness is certainly due to the rigging of the control system so that the reaction controls tend to level off at a moderate deflection of the elevator.

Detailed analysis of the data by removing the reaction control effects indicates that the elevator alone is tending to reach its maximum effectiveness point at a relatively low deflection. For angles beyond 35 to 40 degrees, the additional pitching moment available with increasing elevator deflection appears to be quite small. This effect is hard to explain since observations of tufts on the horizontal tail indicated that the complete tail, including the elevator, was effective at large elevator deflections and large angles of attack of the aircraft. In spite of this reduced effectiveness, the pitch control system is shown capable of trimming the aircraft throughout the complete angle of attack range investigated. This included high angles of attack in the so-called deep stall regime.

In attempting to explain differences in the pitching moment data, discussions with Ames personnel indicated that the moment reference point used for data reduction was 2.6 inches ahead of the actual location of this point as tested. The original data from the test indicated an even higher longitudinal stability level than that shown by the data of this report since these data have been corrected for the 2.6 inch change in reference point. The effect of changing the data by this amount is the same as shifting the reference point 2.6 inches aft without changing the notation for the new location. The pitching moment data and all other moment data are still presented about the 10 percent mean aerodynamic chord point.

The difference of 2.6 inches consists of three small changes in the apparent dimensions. The attachment holes for the ball and socket attachments to the main mounting pads supplied with the Hummingbird were not located at the points originally intended. The use of the 10 degree wedge between the socket attachments and the mounting pads also changed the locations of the balls and sockets relative to the airplane. An error of an additional one inch was found in a basic dimension used in the data reduction equations. Lengthy examination revealed no other dimensional changes of the location of the airplane in the full scale wind tunnel. However, lost motion in the actuation system and connections of the support system could possibly account for some small differences in this area.

The conventional flight data, as presented in this report which includes the 2.6 inch change in the location of the Hummingbird within the tunnel, indicate excellent agreement in the longitudinal stability levels for the tests with power on. The only serious discrepancy in the comparison for this condition is the pitching moment coefficient for zero lift at zero elevator deflection. Most of this difference is explained by the drag of the unshielded rear strut. Everything else on this run tends to verify the revised location of the reference point of the airplane within the full scale tunnel.

Some of the remote readout panel data have been read for the tail angle of attack values indicated by the vane located on the boom ahead of the horizontal tail. Points from some of the transition tests were read and supplied by Ames personnel. In addition, some of the conventional flight values have been read in an attempt to explain some of the discrepancies in the pitching moment data. The reading accuracy of only ± 1.5 degrees when coupled with the general erratic nature of the downwash values obtained from the tail angle of attack indication makes the data most questionable, and none of these data are presented in this report. A random single point downwash value, no matter how accurate, is not indicative of the average effective downwash field experienced by the horizontal tail.

In Phase I of transition the lateral and directional stability levels were tested only at the lower thrust level corresponding to a P_{t_5} of 46 inches of mercury. No lateral-directional tests were made in the Phase II configuration. The Phase I test results indicate increased stability levels in both the lateral and directional modes as compared to the levels predicted from the small scale tests. The indicated increase in directional stability can be accounted for by drag of the rear mounting strut as shown in Section VII. The indicated increase in lateral stability or dihedral effect is more difficult to explain. Although no direct effect of the unshielded rear strut on rolling moment has been isolated, an induced effect similar to those in pitching and yawing moments is not out of reason since the ejector exit flow induces angularity to the flow at the rear strut as the airplane is pitched and yawed.

In some of the tests, the data indicate that there is a discontinuity in both rolling moment and yawing moment through zero sideslip angle. In performing the yaw test, the aircraft was generally yawed from zero in one direction, returned to zero and yawed in the opposite direction, and finally returned to the zero yaw condition. By running the yaw test in this manner, the zero condition was approached from opposite directions during each run. Any lost motion in either the drive mechanism or the angle of yaw indication mechanism would result in a discontinuity of the data through zero, since the Hummingbird actually would be at a slightly different angle in the tunnel when a zero yawed condition is indicated.

Both lateral and directional control effectiveness data were run for all test conditions in Phase I of transition except at the extreme speed and thrust condition of 70 knots for an EPR of 1.99. The only lateral directional control effectiveness tests performed in Phase II were at 100 knots and at an EPR of 1.99. In general, the lateral directional control effectiveness data obtained in the full scale wind tunnel tests are in agreement with those predicted by the equations based on the small scale wind tunnel tests. Some minor differences do exist in a few cases. However, the only significant difference indicated by the full scale wind tunnel data is the reduction in aileron effectiveness including the reaction control with negative deflection of the aileron. In most tests, this reduction in aileron effectiveness for negative deflections was quite pronounced, and in many cases the effectiveness actually went to zero. The only logical explanation of this effect was that some portion of the roll control system must have malfunctioned during the test.

Checks of the roll reaction control valves following the test indicated that the upward pointed valves under certain conditions could go into an overcenter control lever position. Under this condition, the affected roll control valve would remain at essentially a full open condition although the aileron was returned to its neutral position. Deflection of the aileron to a negative position would cause the valve to move toward its closed position. Evidence of such an overcenter condition was found for the upward pointing valve on the right wing tip. This evidence consisted of a bent place in the bullet fairing which houses the roll control valves. The size of the dent indicates that full down travel of the right aileron probably occurred with the roll control valve in the overcenter position.

The magnitude of the discrepancies observed in some cases cannot be explained entirely by this overcenter condition. Although the right upward pointed reaction control valve would be the one involved with a negative deflection of the ailerons, other minor malfunctions in the roll control system or in the wind tunnel force readout system could have been associated with this condition also.

Although the control effectiveness level appeared good, in some cases the lateral directional data indicate a constant shift in the side force, rolling moment, or yawing moment levels occurred throughout the complete run. In other words, the full scale data show a control level parallel to that predicted from the small scale data but displaced by a constant increment. When this occurred in one component, one of the others usually indicated the same trend. The conclusion drawn is that one of the wind tunnel force readouts must have malfunctioned or shifted slightly during each of these tests. Normally, the magnitude of this shift is well within a reasonable change in force level.

The data of Run 41 plotted in Figures 261 through 266 indicate that such a shift or displacement occurred throughout the lateral directional control effectiveness portion of this run which was made with a constant foul indicated on the balance system. For the aileron effectiveness portion, a shift is observed in all three components: side force, yawing moment and rolling moment. Similar shifts occurred during the directional control effectiveness portion of this run. A comparison of these data indicate that the same shift, magnitude-wise, occurred in both sets of data for each component. The same thing occurred on a few other runs, but in general, only two out of the three components would be affected by this constant shift. The data so affected still appears to be valid so long as this shift is recognized. In many cases, the value of the shift which occurred is well within the accuracy expected of such a test.

With the exceptions noted, the agreement between the full scale wind tunnel test data and the data predicted by the equations based on the small scale test data are good. A slight change in the horizontal tail incidence of the aircraft or a minor change in the downwash field at the horizontal tail, coupled with the pitching moment due to the drag of the unshielded rear support, accounts for the differences indicated in the pitching moments for zero lift at zero elevator deflection. The changes in stability level throughout Phases I and II of transition are not too alarming, nor are the orders of magnitude too great. The reduction in total effectiveness of the pitch control system going from zero elevator deflection to full elevator deflection is completely unexplained, but the level indicated by the full scale data still provides adequate control capability for the aircraft.

In general, nothing was indicated by the full scale wind tunnel test which would have prevented the aircraft having been flight tested throughout the transition regime, had the data been collected previous to the actual attempts. However, a more extensive or exhaustive examination of the data would certainly have been in order, since the differences between the full scale wind tunnel tests and the data derived from the small scale equations are partially unexplained in some areas. The largest discrepancy, of course, is in the net ejector lift value which was determined for the static test and used in the small scale equations data comparison for the other tests throughout transition. The shift in the zero lift value of pitching moment and the reduction in the overall value of reaction control in pitch are disturbing. The fact that the data indicate that successful transitions are completely feasible was verified by the number of transitions made in actual flight test.

IX. REFERENCES

1. Barnes, C. C., Jr., "The VZ-10 Hummingbird 0.19 Scale Model Wind Tunnel Test Results." Lockheed-Georgia Company ER-5623, April, 1962.

2. NACA, "Guide for Planning Investigations in the Ames 40- by 80- Foot Wind Tunnel," Ames Aeronautical Laboratory, January, 1957.

3. Hoerner, Sighard F., Fluid-Dynamic Drag. Published by the Author, 1958.

FIGURE 3

THEORETICAL AERODYNAMIC DATA

Wing	
Area	104.17 ft.
Aspect Ratio	6.0
Span	25.0 ft.
Flap Area	13.02 sq. ft.
Aileron Area	4.28 sq. ft.
Sweep at 50% Chord	0
Root Chord	72.0 in.
Root Airfoil	64_A012
Root Incidence	1.5°
Tip Chord	28.0 in.
Tip Airfoil	64_A212
Tip Incidence	1.5°
M.A.C. Length	53.23 in.
Vertical Tail	
Area	21.93 sq. ft.
Aspect Ratio	1.194
Span	61.414 in.
Rudder Area	4.59 sq. ft.
Root Chord	66.0 in.
Tip Chord	36.85 in.
Sweep at 25% Chord	32° 8'
Airfoil	64_A012
M.A.C. Length	52.491 in.
Volume Coefficient	0.1098

FIGURE 3 (Continued)

Horizontal Tail

Area	26.44 sq. ft.
Aspect Ratio	4.303
Span	128.0 in.
Elevator Area	5.29 sq. ft.
Root Chord	42.5 in.
Tip Chord	17.0 in.
Incidence	0
Airfoil	0010-2.00 - 40/1.575
M.A.C. Length	31.5[illegible]1
Volume Coefficient	0.895

FIGURE 5

TABLE OF SYMBOLS

b	theoretical wingspan (25.0 ft.)
$\bar{c}$	mean aerodynamic chord (4.43 ft.)
C_D	drag coefficient (D/qS)
C_L	lift coefficient (L/qS)
C_l	rolling moment coefficient l/qSb)
C_m	pitching moment coefficient ($M/q\bar{c}S$)
C_n	yawing moment coefficient (N/qSb)
C_y	side force coefficient (Y/qS)
D	drag (lb, aft positive)
L	lift (lb, up positive)
l	rolling moment (ft-lb, right wing down positive)
M	pitching moment (ft-lb, nose up positive)
N	yawing moment (ft-lb, nose right positive)
Y	side force (lb, right positive)
EPR	engine pressure ratio (P_{t_5}/P_a)
P_a	ambient pressure (in. Hg)
P_{t_5}	engine tailpipe pressure (in. Hg)
q	dynamic pressure ($1/2\ \rho V^2$, lb/ft^2)
S	wing planform area (104.17 ft^2)
V	airspeed
α	angle of attack (deg, nose up positive)
β	angle of sideslip (deg, nose left positive)
δ_a	aileron deflection angle (deg, trailing edge down positive, total aileron is equal to right aileron deflection minus left aileron deflection)

FIGURE 5 (Continued)

δ_e	elevator deflection angle (deg, trailing edge down positive)
δ_r	rudder deflection angle (deg, trailing edge left positive)
ρ	atmospheric density (lb sec^2/ft^4)
ψ	angle of yaw (deg, nose right positive)

FIGURE 6

RUN SCHEDULE SUMMARY

Run	P_{t_5} (in. Hg)	V (knots)	Phase	Type of Run
1	Varied	Varied	I	Ejector Exit Rake Survey
			II	Ejector Exit Rake Survey
2	Varied	Varied	I	Ejector Exit Rake Survey
			II	Ejector Exit Rake Survey
3	Varied	0	I	Static Run $\alpha = 12$
	46	30	I	Polar
				Elevator Effectiveness $\alpha = 0$
4	46	50	I	Polar
5	46	40	I	Polar
6	46	67	II	Polar
				Elevator Effectiveness $\alpha = 0$
7	46	40	I	Polar
				Elevator Effectiveness $\alpha = -6$
8	46	85	II	Polar
				Elevator Effectiveness $\alpha = 0$
9	46	30	I	Polar
10	46	50	I	Elevator Effectiveness $\alpha = -10$
			II	Elevator Effectiveness $\alpha = 0$
11	46	40	I	Polar
12	46	50	II	Polar
13	46	20	I	Polar
14	46	20	I	Polar

FIGURE 6 (Continued)

Run	P_{t_5} (in. Hg)	V (knots)	Phase	Type of Run	
15	46	50	I	Polar	
				Elevator Effectiveness	$\alpha = 20$
	46	50		Yaw Run	
				Aileron Effectiveness	$\psi = 0$
16	46	20	I	Elevator Effectiveness	$\alpha = 0$
17	46	40	I	Yaw Run	
				Aileron Effectiveness	$\psi = 0$ & 8
				Rudder Effectiveness	$\psi = 0$ & 8
18	60	40	I	Aileron Effectiveness	$\psi = 0$
				Rudder Effectiveness	$\psi = 0$
19	46	30	I	Yaw Run	
20	46	40	I	Polar	
21	46	50	I	Polar	
22	60	30	I	Aileron Effectiveness	$\psi = 0$
				Rudder Effectiveness	$\psi = 0$
	46	30	I	Aileron Effectiveness	$\psi = 0$ & 10
				Rudder Effectiveness	$\psi = 0$ & 10
23	46	20	I	Aileron Effectiveness	$\psi = 0$ & 10
				Rudder Effectiveness	$\psi = 0$ & 10
				Yaw Run	
24	60	50	I	Polar	
				Elevator Effectiveness	$\alpha = 0$ & 20
25	60	[illegible]	I	Aileron Effectiveness	$\psi = 0$
				Rudder Effectiveness	$\psi = 0$

FIGURE 6 (Continued)

Run	P_{t_5} (in. Hg)	V (knots)	Phase	Type of Run
26	60	70	I	Polar
				Elevator Effectiveness $\alpha = 0$
27	60	30	I	Polar
				Elevator Effectiveness $\alpha = 0$
28	30	80	Conventional	Polar
				Elevator Effectiveness $\alpha = 0$
				Aileron Effectiveness $\psi = 0$
				Rudder Effectiveness $\psi = 0$
29	30	40	Conventional	Polar
30	30	80	Conventional	Yaw Run
				Aileron Effectiveness $\psi = 0$ & 8
				Rudder Effectiveness $\psi = 8$
31	30	80	Conventional	Polar
				Yaw Run
				Elevator Effectiveness $\alpha = 0$
				Aileron Effectiveness $\psi = 8$
				Rudder Effectiveness $\psi = 8$
32	Varied	0	Conventional	Power Effects $\alpha = 0$
33	Varied	80	Conventional	Power Effects $\alpha = 0$
	46	80	Conventional	Polar
				Elevator Effectiveness $\alpha = 0$
34	Varied	40	Conventional	Power Effects $\alpha = 0$
35	30	80	III	Polar
				Yaw Run $\alpha = 0$ & 8

FIGURE 6 (Continued)

Run	P_{t_5} (in. Hg)	V (knots)	Phase	Type of Run
36	60	100	II	Polar
37	Varied	0	I	Power Effects $\alpha = -12$
	46	30	I	Polar
				Elevator Effectiveness $\alpha = 0$
38	Varied	0	I	Power Effects $\alpha = 0$
	46	40	I	Polar
	46	40	I	Elevator Effectiveness $\alpha = 0$
				Aileron Effectiveness $\psi = 0$
				Rudder Effectiveness $\psi = 0$
39	Varied	0	I	Power Effects $\alpha = 12$
	60	0	I	Elevator Effectiveness $\alpha = 12$
				Aileron Effectiveness $\psi = 0$
				Rudder Effectiveness $\psi = 0$
40	60	50	I	Polar
				Elevator Effectiveness $\alpha = 0$
41	46	50	I	Polar
				Elevator Effectiveness $\alpha = 0$
	60	100	II	Elevator Effectiveness $\alpha = 0$ & 8
				Aileron Effectiveness $\psi = 0$
				Rudder Effectiveness $\psi = 0$

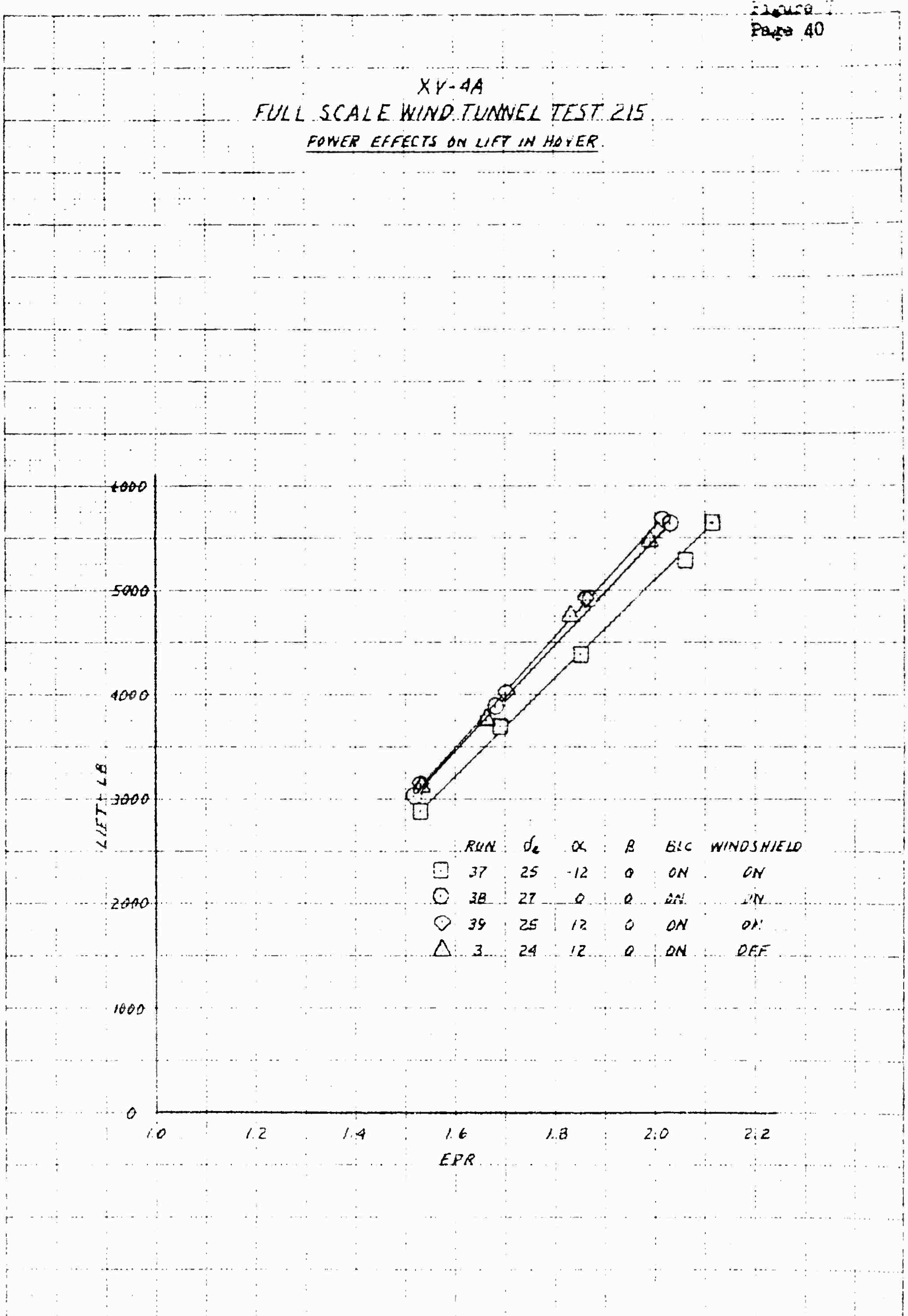
XV-4A
FULL SCALE WIND TUNNEL TEST 215
POWER EFFECTS ON LIFT IN HOVER
LIFT - LB
6000
5000
4000
3000
2000
1000
0
1.0
1.2
1.4
1.6
1.8
2.0
2.2
EPR
RUN δe α β BLC WINDSHIELD
37 25 -12 0 ON ON
38 27 0 0 ON ON
39 25 12 0 ON ON
3 24 12 0 ON OFF

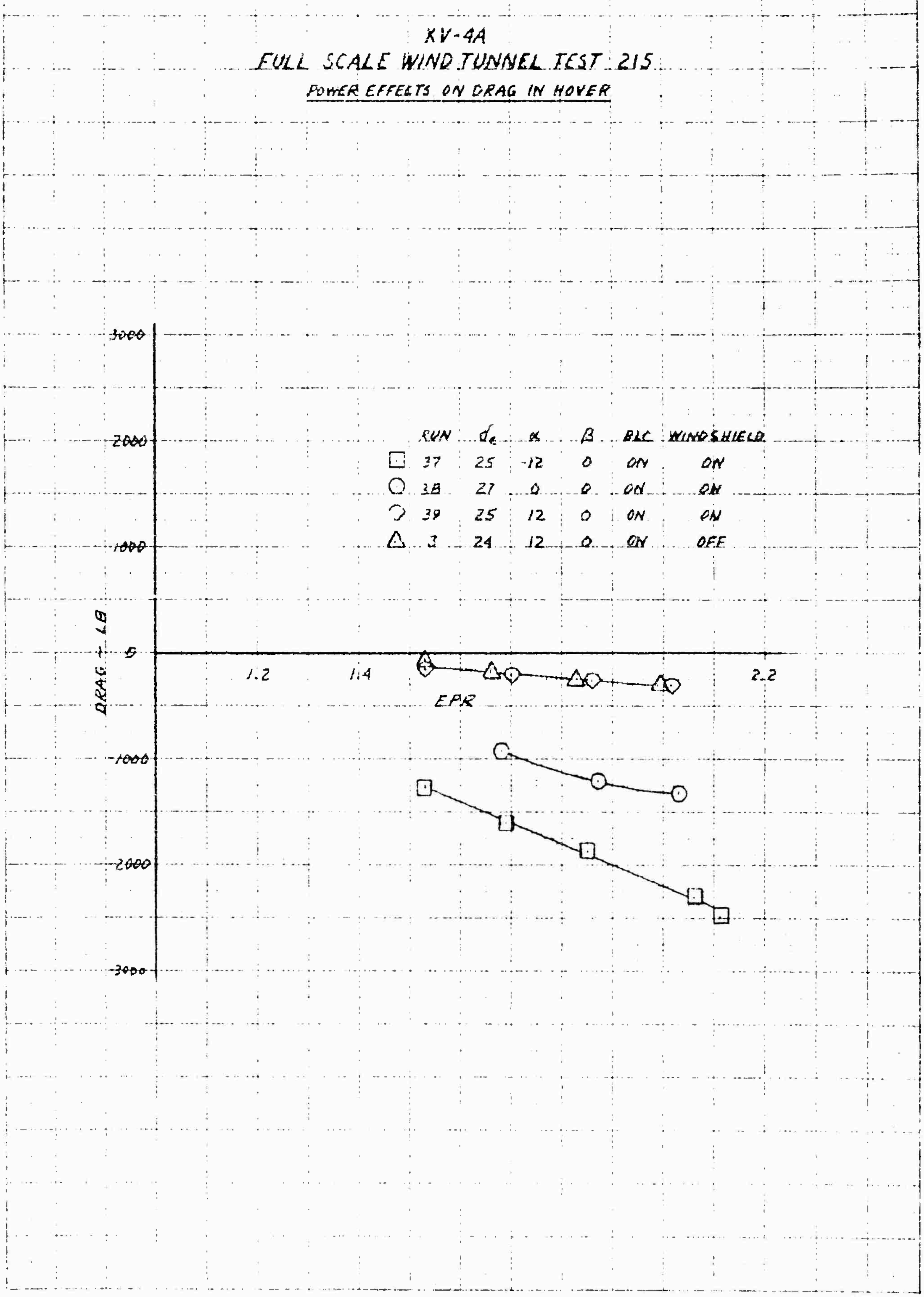
XV-4A
FULL SCALE WIND TUNNEL TEST 215
POWER EFFECTS ON DRAG IN HOVER
RUN δ_e α β BLC WINDSHIELD
37 25 -12 0 ON ON
38 27 0 0 ON ON
39 25 12 0 ON ON
3 24 12 0 ON OFF
3000
2000
1000
0
-1000
-2000
-3000
DRAG ~ LB
1.2
1.4
2.2
EPR

XV-4A
FULL SCALE WIND TUNNEL TEST 215
POWER EFFECTS ON PITCHING MOMENT IN HOVER

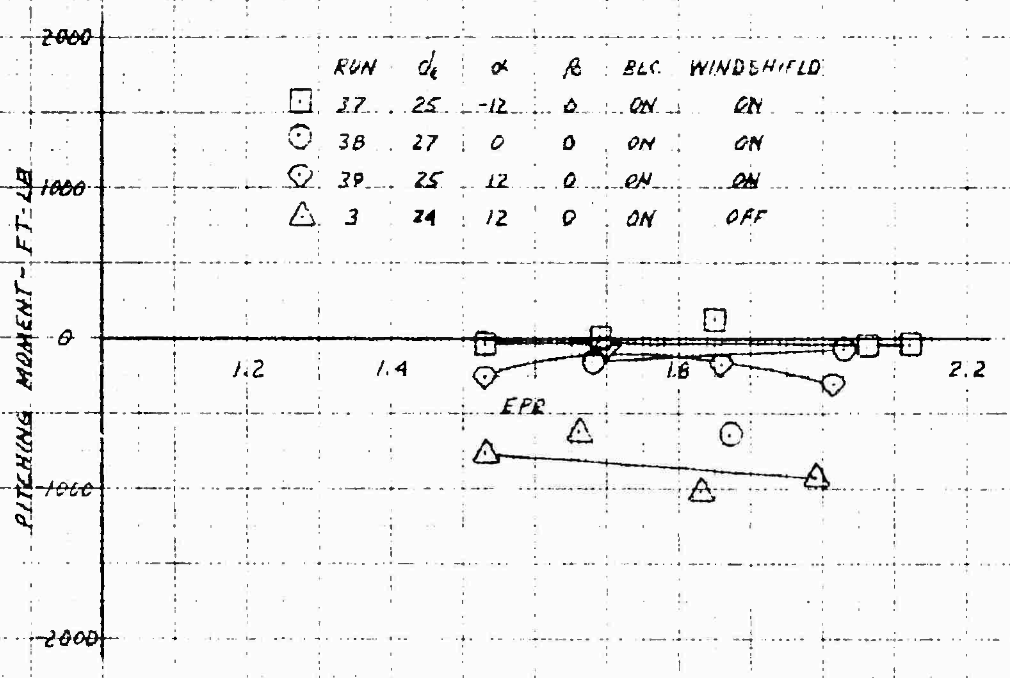

XV-4A

FULL SCALE WIND TUNNEL TEST 215

POWER EFFECT ON LIFT COEFFICIENT IN CONVENTIONAL FLIGHT AT 40 KNOTS

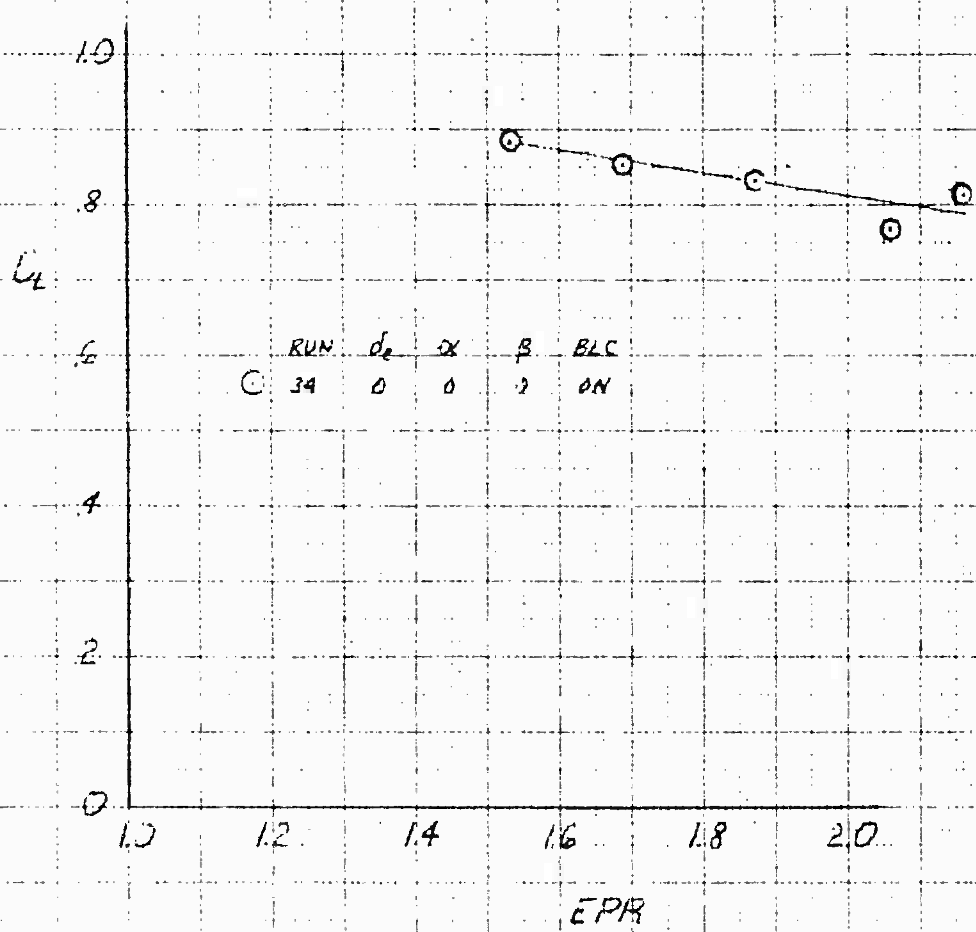

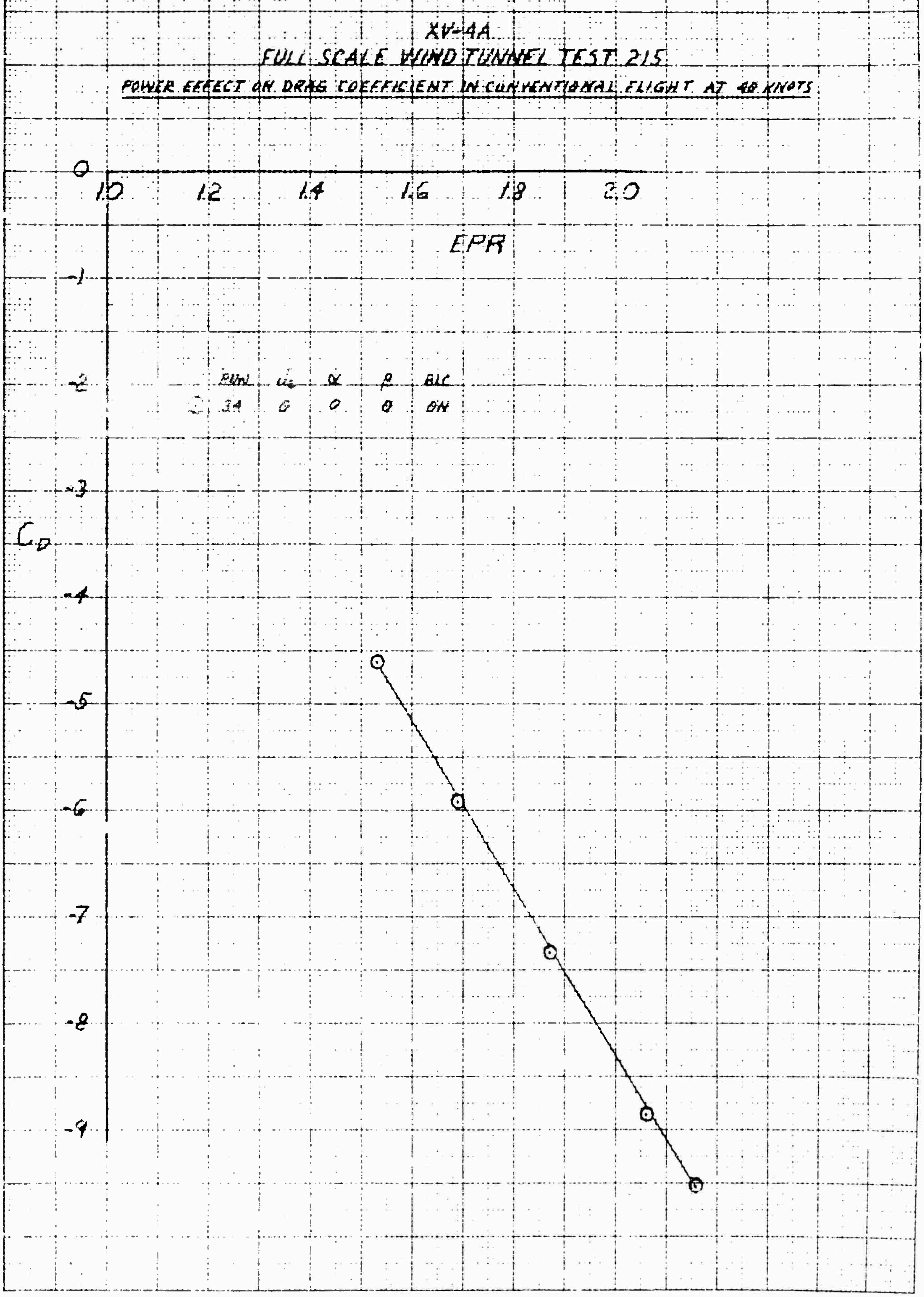

XV-4A
FULL SCALE WIND TUNNEL TEST 215
POWER EFFECT ON DRAG COEFFICIENT IN CONVENTIONAL FLIGHT AT 40 KNOTS
0
1.0
1.2
1.4
1.6
1.8
2.0
EPR
-1
-2
-3
-4
-5
-6
-7
-8
-9
C_D
RUN
α
β
BLC
34
0
0
0
ON

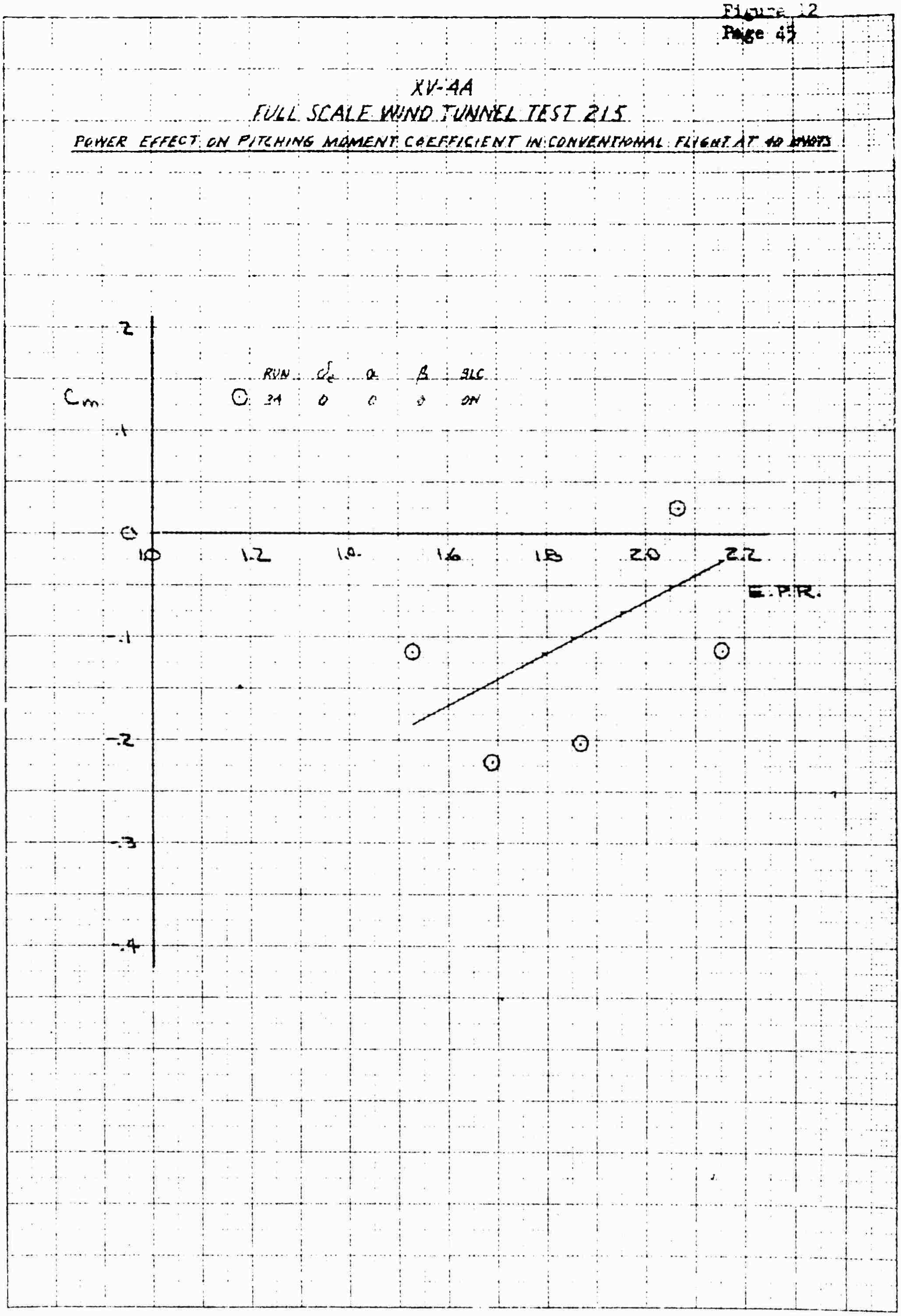
XV-4A
FULL SCALE WIND TUNNEL TEST 215
POWER EFFECT ON PITCHING MOMENT COEFFICIENT IN CONVENTIONAL FLIGHT AT 40 KNOTS
RUN
α
β
BLC
31
0
0
0
ON
C_m
.2
.1
0
-.1
-.2
-.3
-.4
1.0
1.2
1.4
1.6
1.8
2.0
2.2
E.P.R.

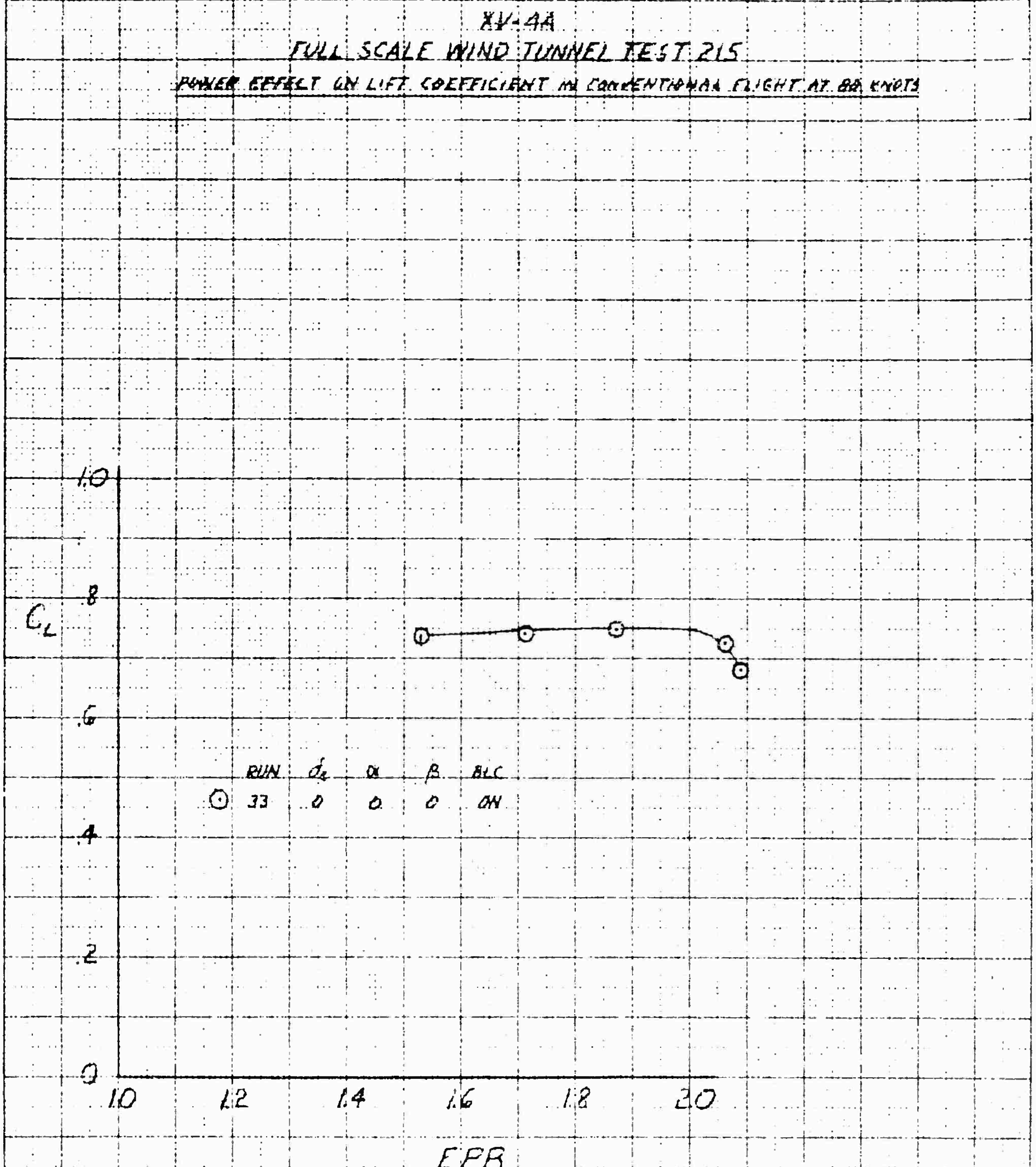
XV-4A
FULL SCALE WIND TUNNEL TEST 215
POWER EFFECT ON LIFT COEFFICIENT IN CONVENTIONAL FLIGHT AT 80 KNOTS
C_L
1.0
.8
.6
.4
.2
0
1.0
1.2
1.4
1.6
1.8
2.0
EPR
RUN δ α β BLC
33 0 0 0 ON

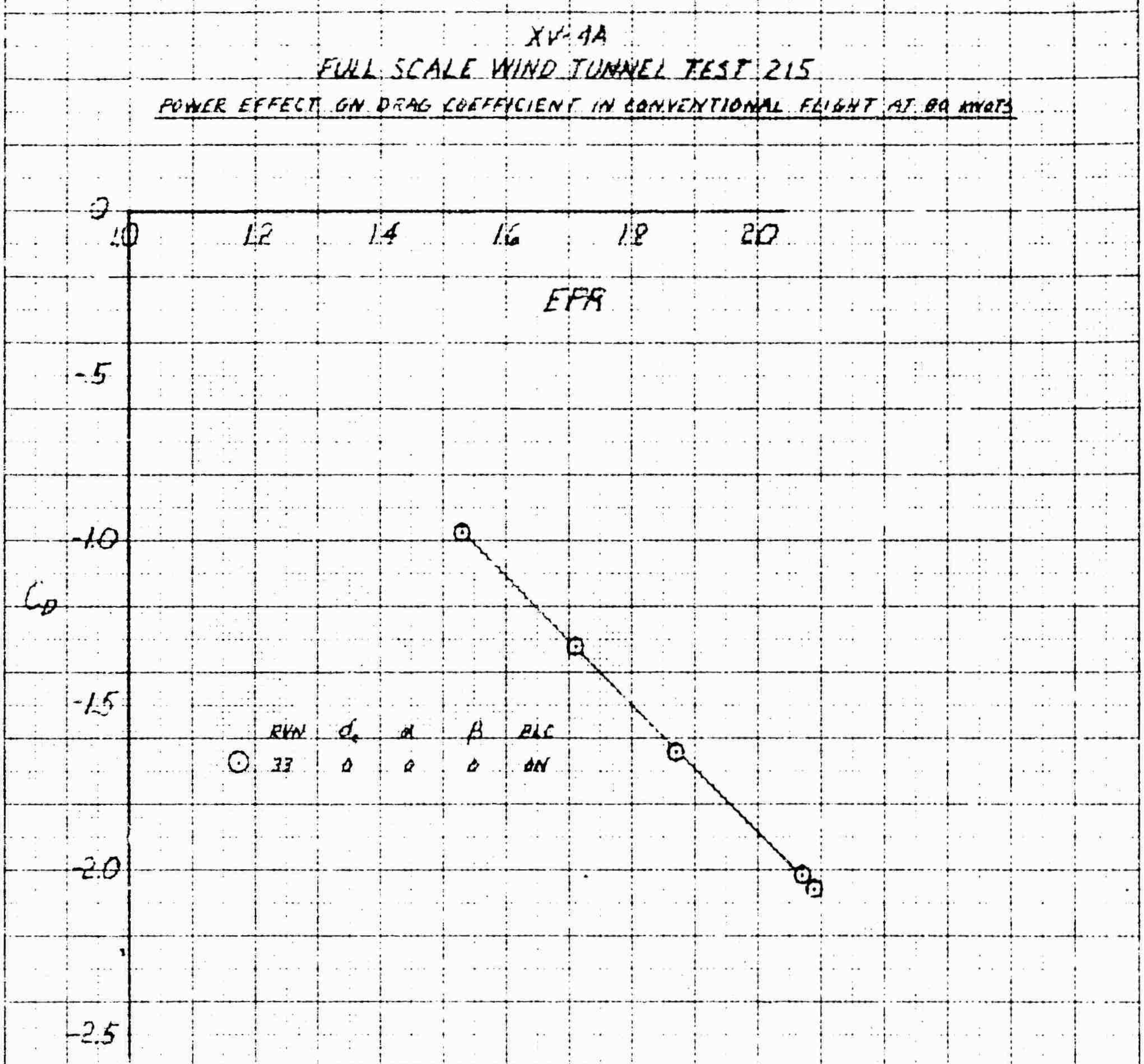
XV-4A
FULL SCALE WIND TUNNEL TEST 215
POWER EFFECT ON DRAG COEFFICIENT IN CONVENTIONAL FLIGHT AT 80 KNOTS
0
1.0
1.2
1.4
1.6
1.8
2.0
EPR
-.5
-1.0
C_D
-1.5
-2.0
-2.5
RUN
δ_e
α
β
BLC
33
0
0
0
ON

XV-4A

FULL SCALE WIND TUNNEL TEST 215

POWER EFFECT ON PITCHING MOMENT COEFFICIENT IN CONVENTIONAL FLIGHT AT 80 KNOTS

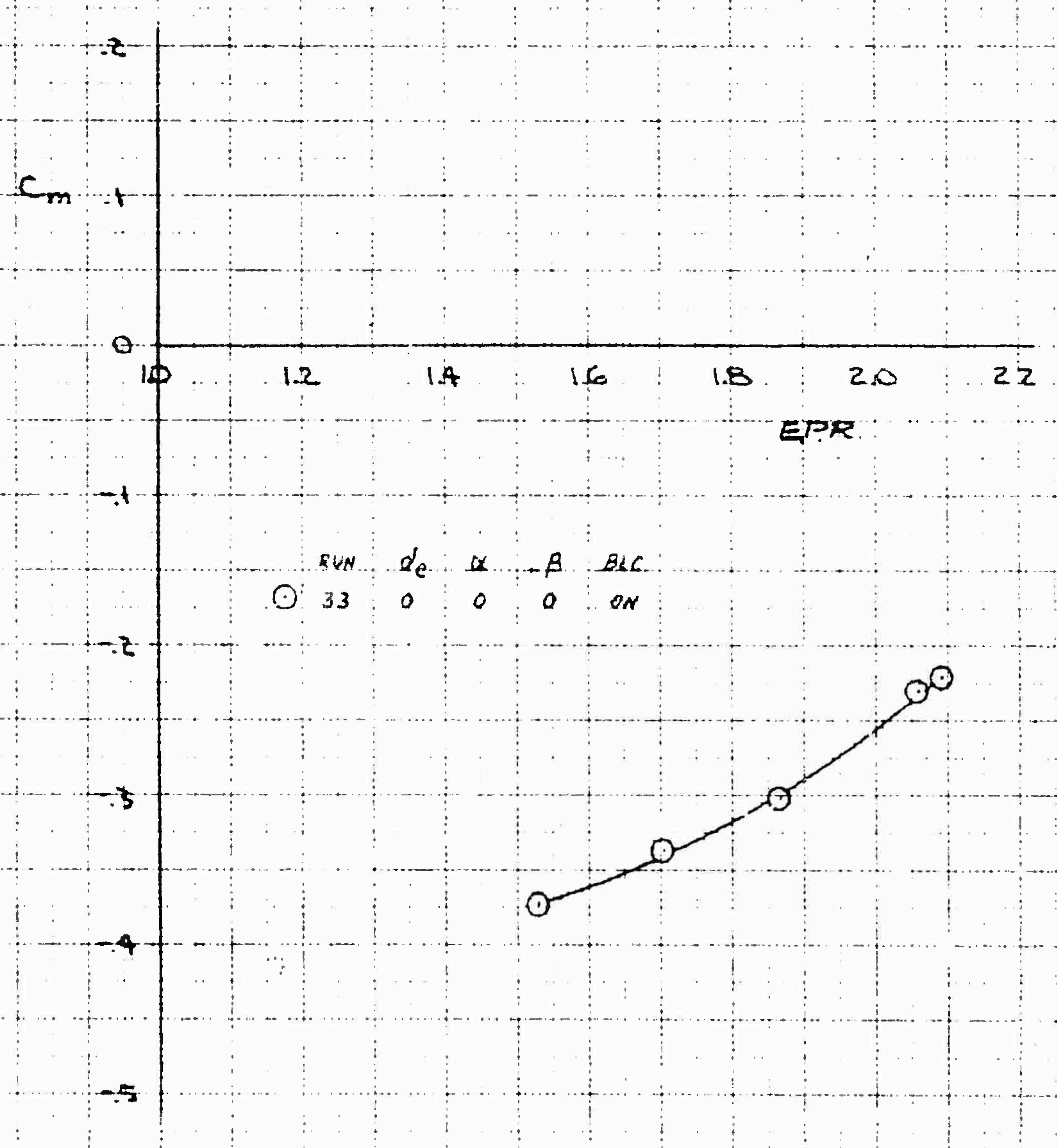

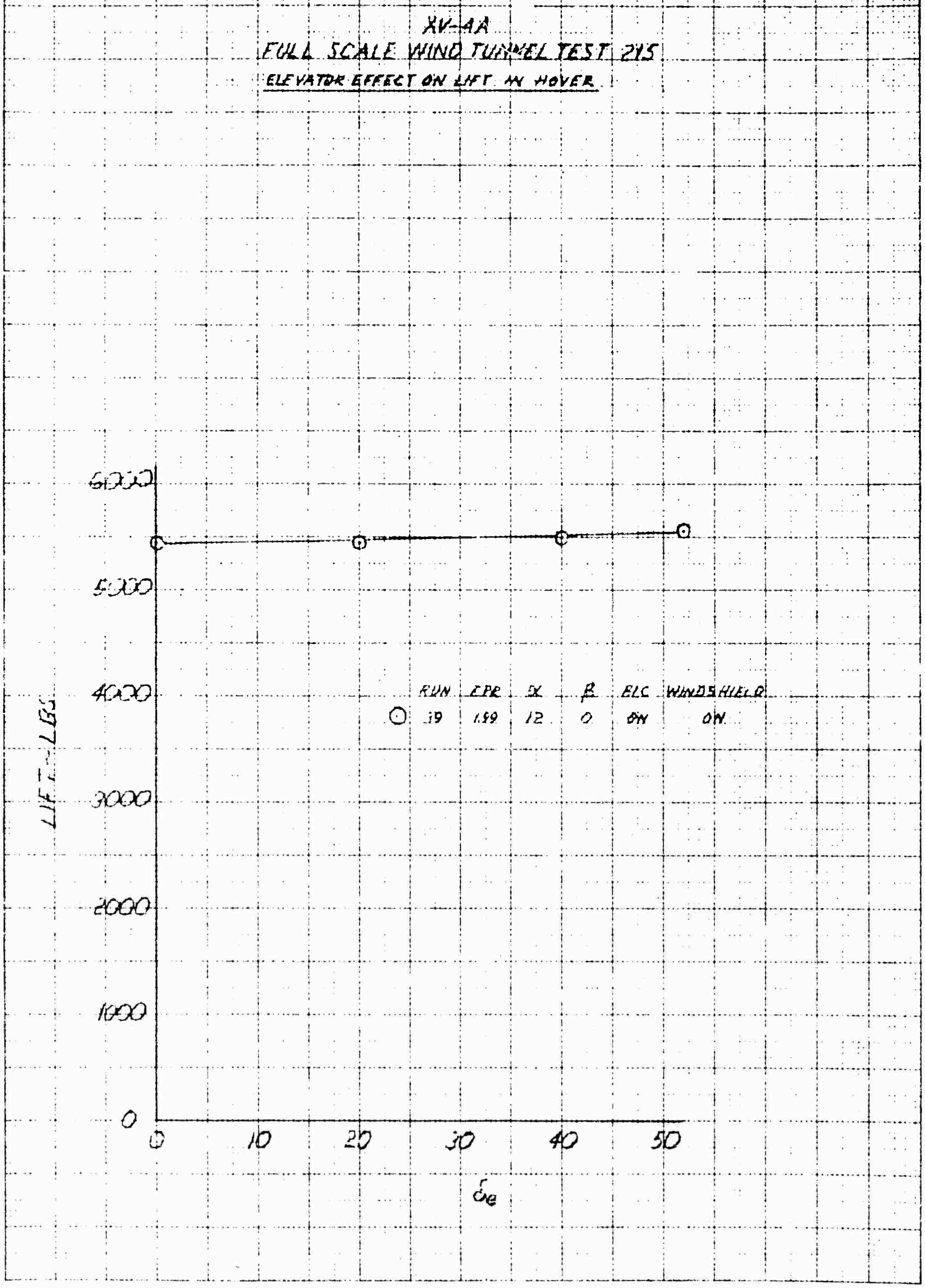
XV-4A
FULL SCALE WIND TUNNEL TEST 215
ELEVATOR EFFECT ON LIFT IN HOVER
LIFT ~ LBS
6000
5000
4000
3000
2000
1000
0
0
10
20
30
40
50
δe
RUN EPR EX β ELC WINDSHIELD
39 1.99 12 0 ON ON

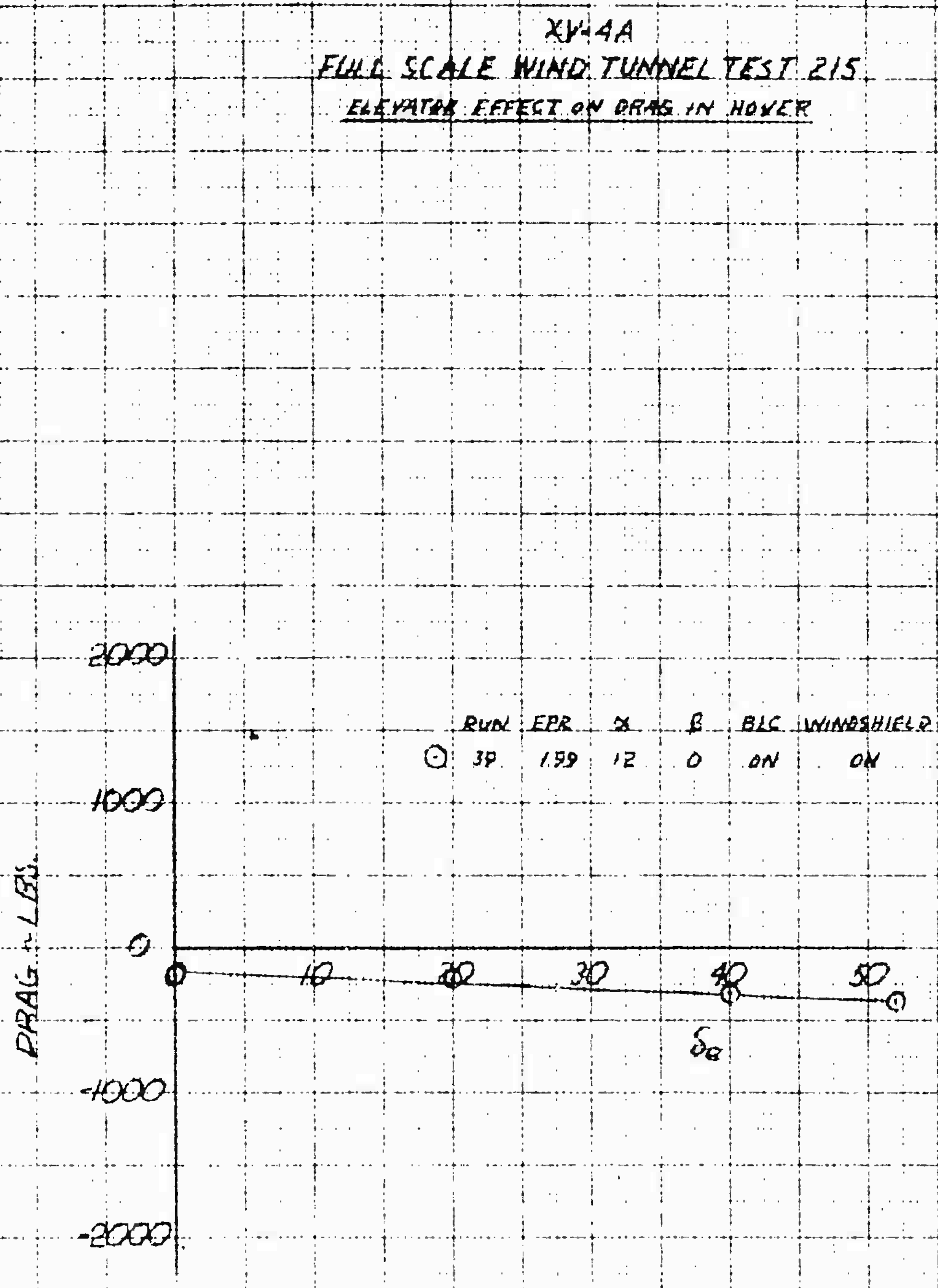
XV-4A
FULL SCALE WIND TUNNEL TEST 215
ELEVATOR EFFECT ON DRAG IN HOVER
RUN EPR α β BLC WINDSHIELD
39 1.99 12 0 ON ON
2000
1000
0
-1000
-2000
DRAG ~ LBS.
0
10
20
30
40
50
δe

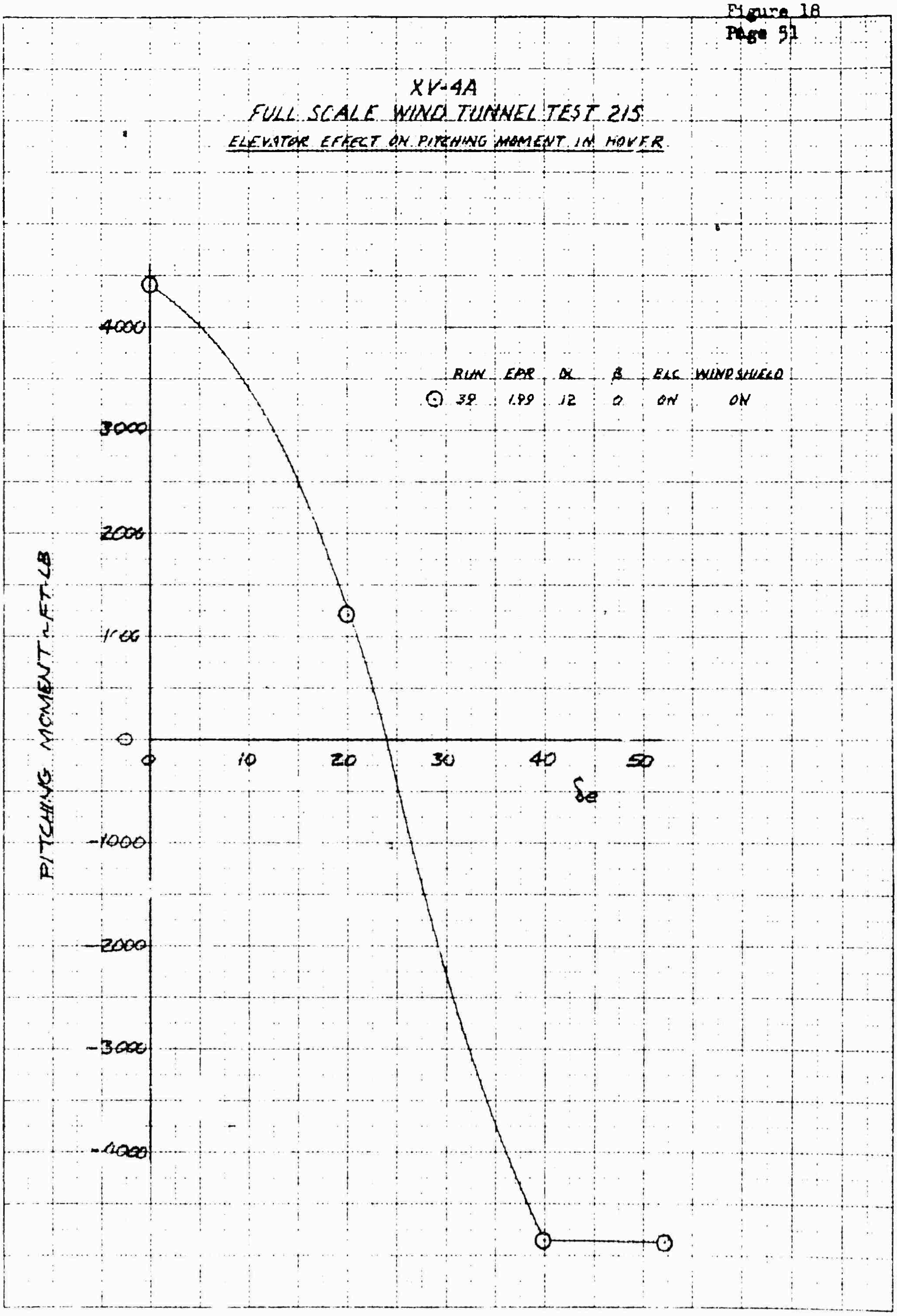
XV-4A
FULL SCALE WIND TUNNEL TEST 215
ELEVATOR EFFECT ON PITCHING MOMENT IN HOVER
RUN EPR α β ELC WINDSHIELD
39 1.99 12 0 ON ON
PITCHING MOMENT ~ FT-LB
4000
3000
2000
1000
0
-1000
-2000
-3000
-4000
0
10
20
30
40
50
δe

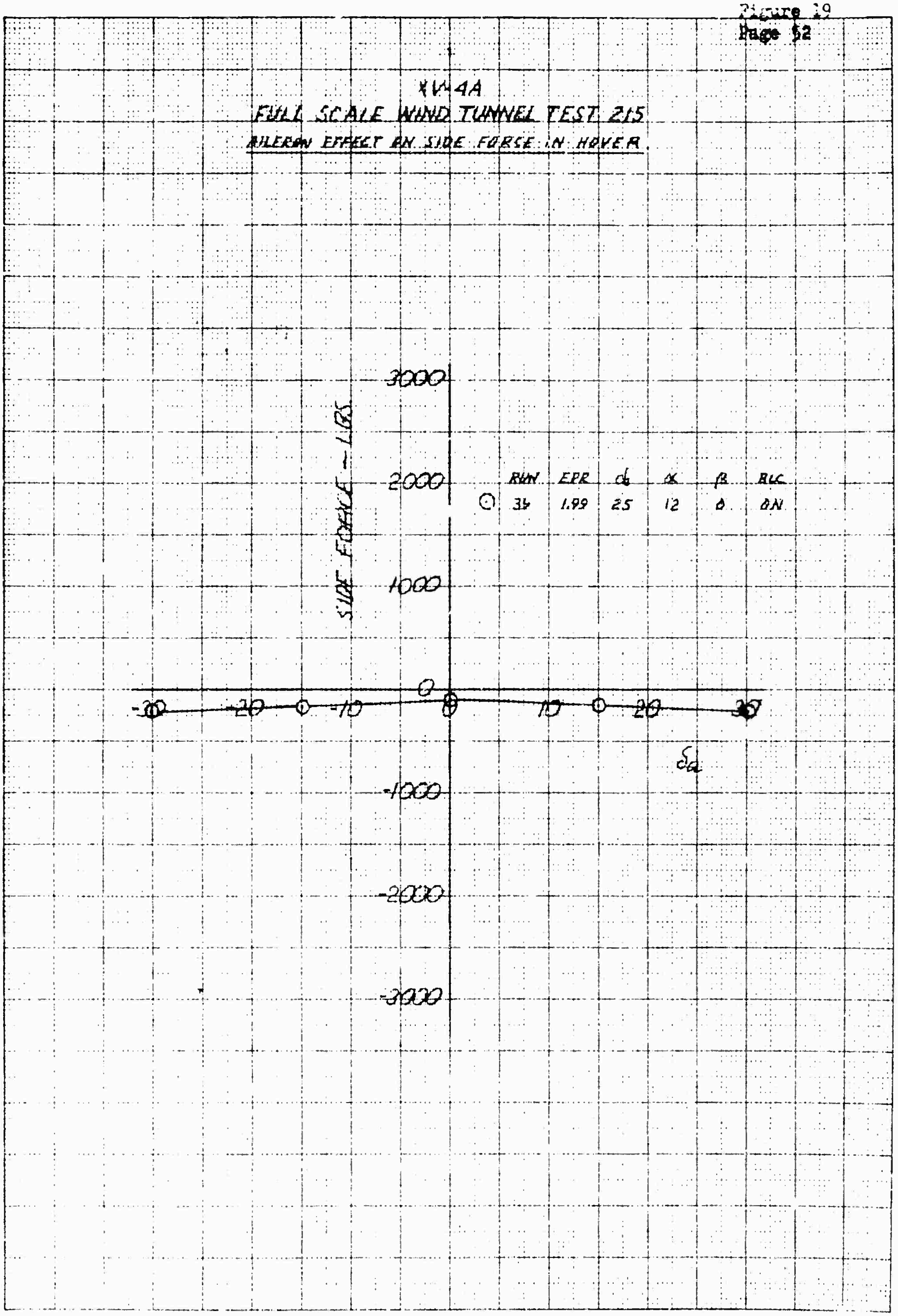
XV-4A
FULL SCALE WIND TUNNEL TEST 215
AILERON EFFECT ON SIDE FORCE IN HOVER
SIDE FORCE — LBS
3000
2000
1000
0
-1000
-2000
-3000
-30
-20
-10
10
20
30
δa
RUN EPR d α β BLC
36 1.99 25 12 0 ON

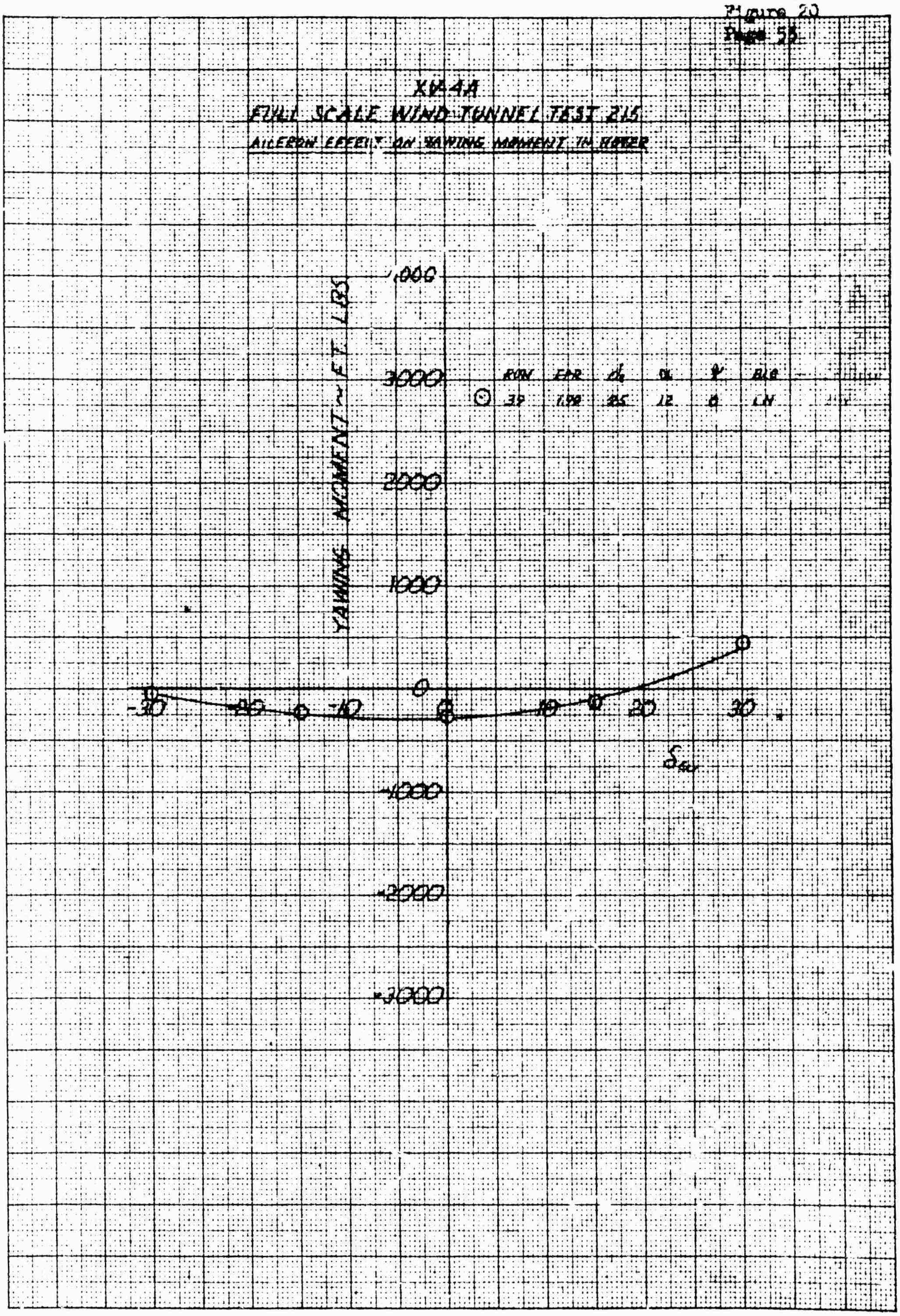
XV-4A
FULL SCALE WIND TUNNEL TEST 215
AILERON EFFECT ON YAWING MOMENT IN HOVER
YAWING MOMENT ~ FT LBS
3000
2000
1000
0
-1000
-2000
-3000
39 1.98 85 12 0 LH
-30
-20
-10
10
20
30

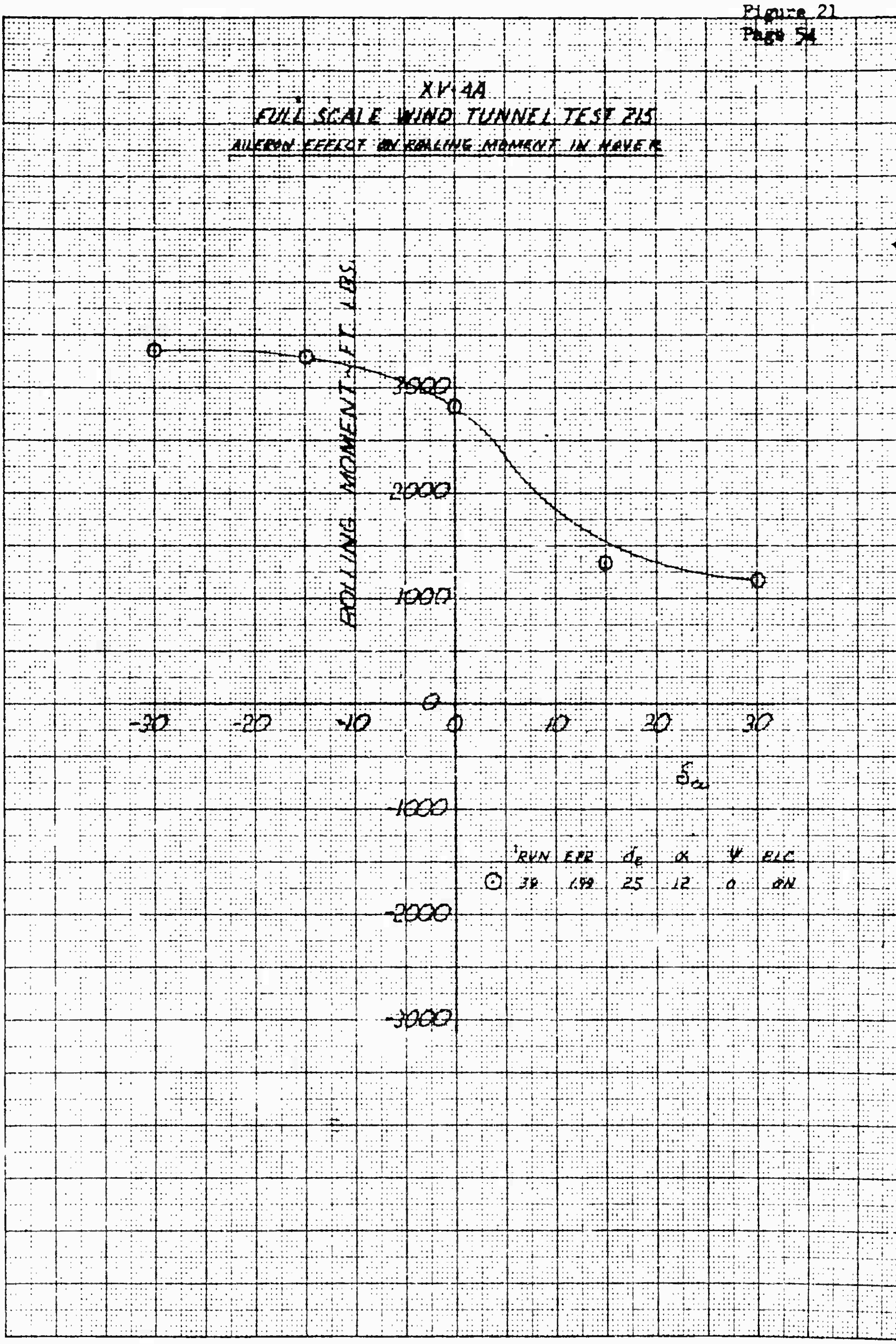
XV-4A
FULL SCALE WIND TUNNEL TEST 215
AILERON EFFECT ON ROLLING MOMENT IN HOVER
ROLLING MOMENT - FT. LBS.
3000
2000
1000
0
-1000
-2000
-3000
-30
-20
-10
0
10
20
30
δa
RUN
EPR
δe
α
ψ
ELC
39
1.99
25
12
0
8N

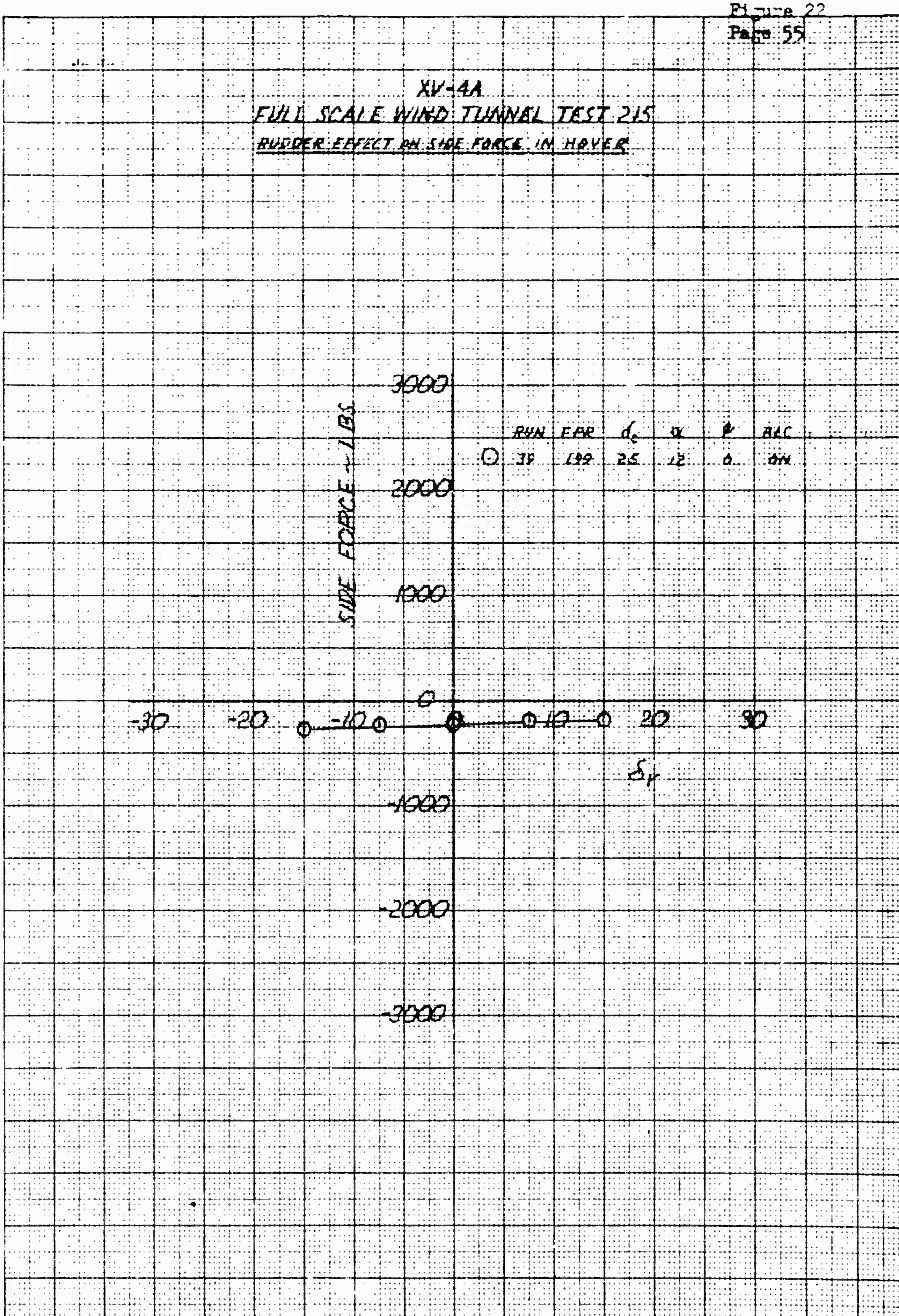
XV-4A
FULL SCALE WIND TUNNEL TEST 215
RUDDER EFFECT ON SIDE FORCE IN HOVER
RUN EPR d_c α ψ BLC
39 199 25 12 0 ON
SIDE FORCE ~ LBS
3000
2000
1000
0
-1000
-2000
-3000
-30 -20 -10 10 20 30
δ_r

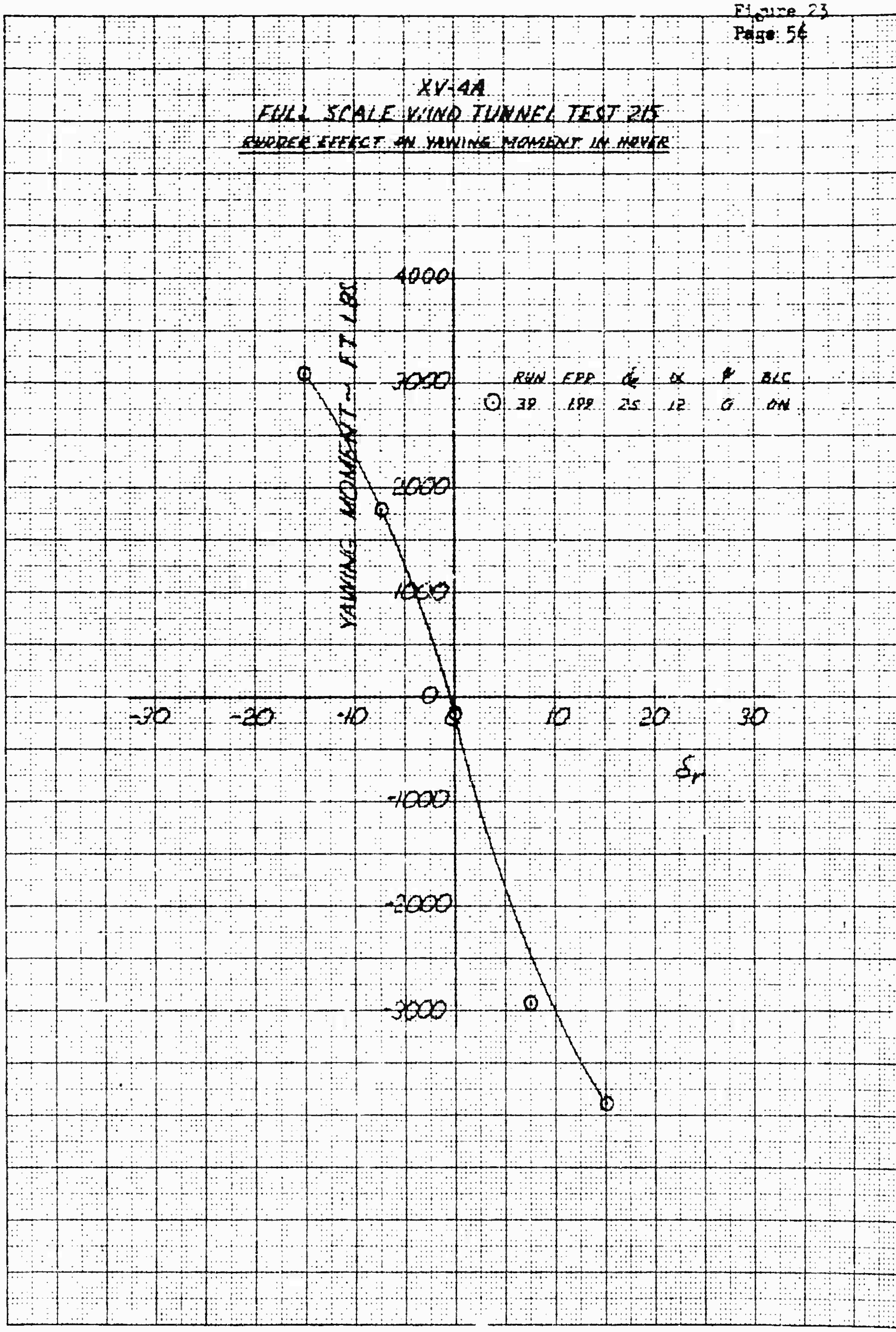
XV-4A
FULL SCALE WIND TUNNEL TEST 215
RUDDER EFFECT ON YAWING MOMENT IN HOVER
RUN EPR δ α ψ BLC
⊙ 39 .199 25 12 0 ON
YAWING MOMENT ~ FT LBS
4000
3000
2000
1000
0
-1000
-2000
-3000
-30 -20 -10 0 10 20 30
δr

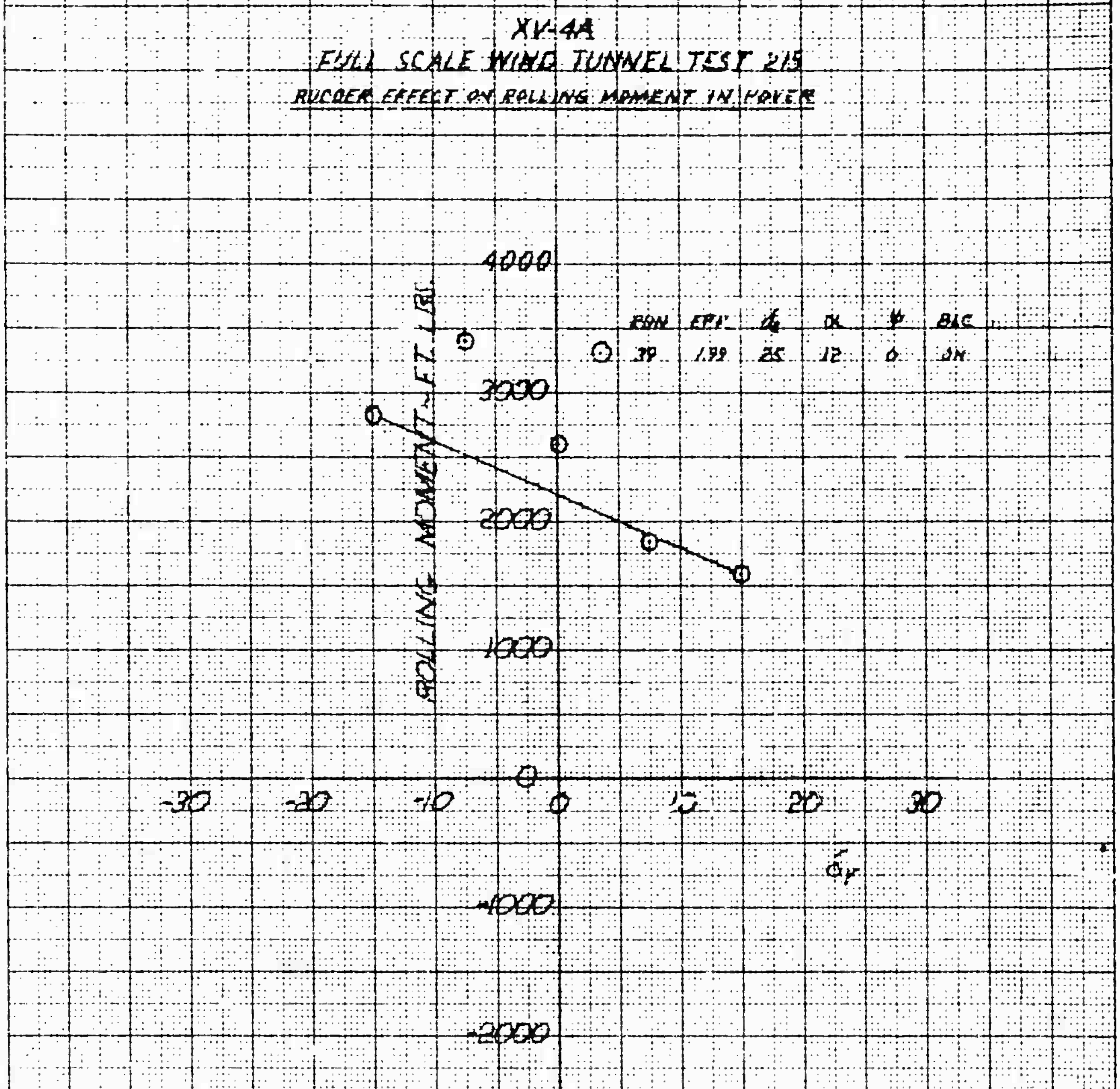
XV-4A
FULL SCALE WIND TUNNEL TEST 215
RUDDER EFFECT ON ROLLING MOMENT IN HOVER
RUN
EPI
α
ψ
BLC
39
1.99
25
12
0
ON
4000
3000
2000
1000
-1000
-2000
-3000
ROLLING MOMENT ~ FT. LB.
-30
-20
-10
0
10
20
30
δ_r

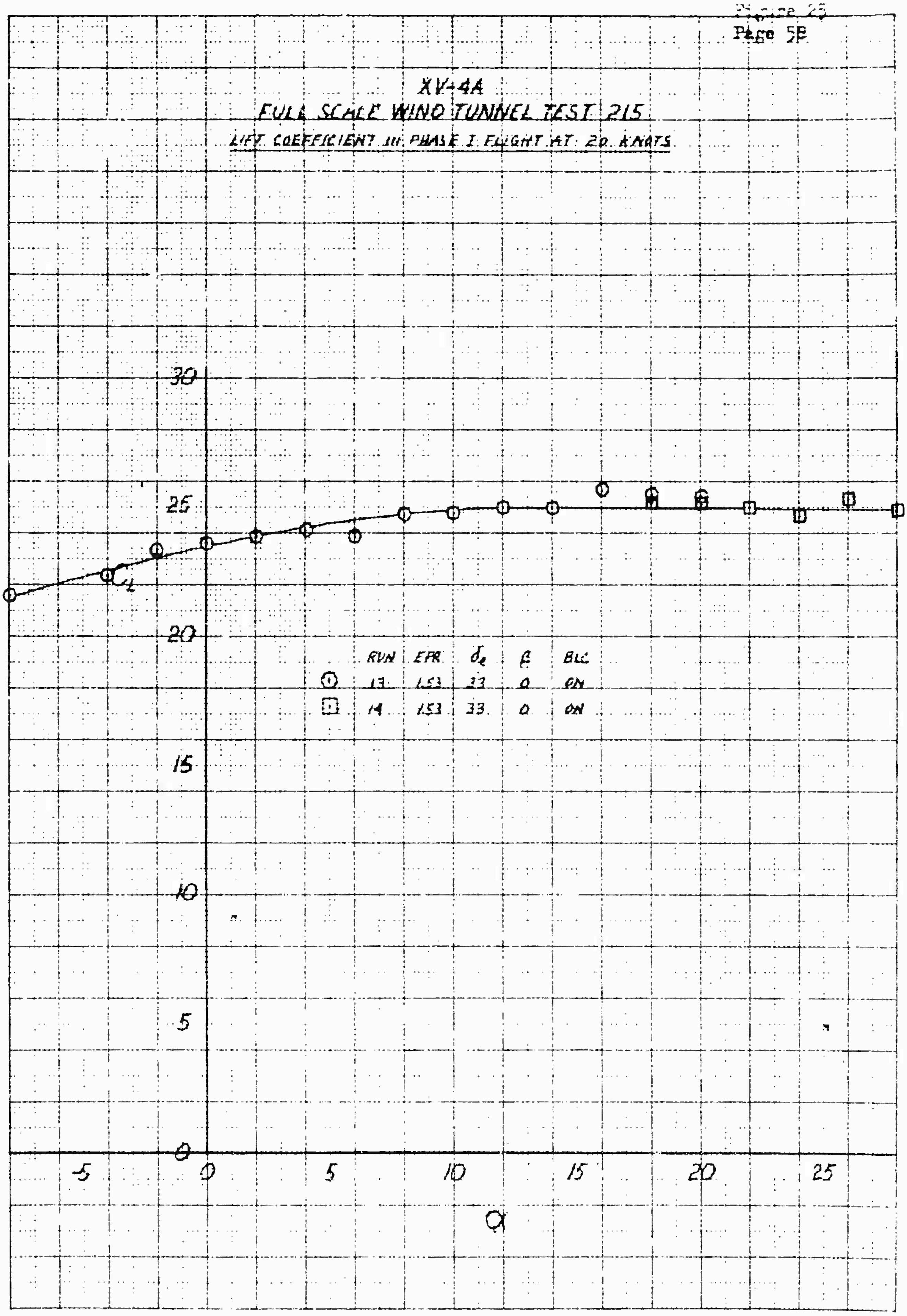
XV-4A
FULL SCALE WIND TUNNEL TEST 215
LIFT COEFFICIENT IN PHASE I FLIGHT AT 20 KNOTS
30
25
20
15
10
5
0
C_L
RUN EPR δ_e β BLC
13 1.53 33 0 ON
14 1.53 33 0 ON
-5
0
5
10
15
20
25
α

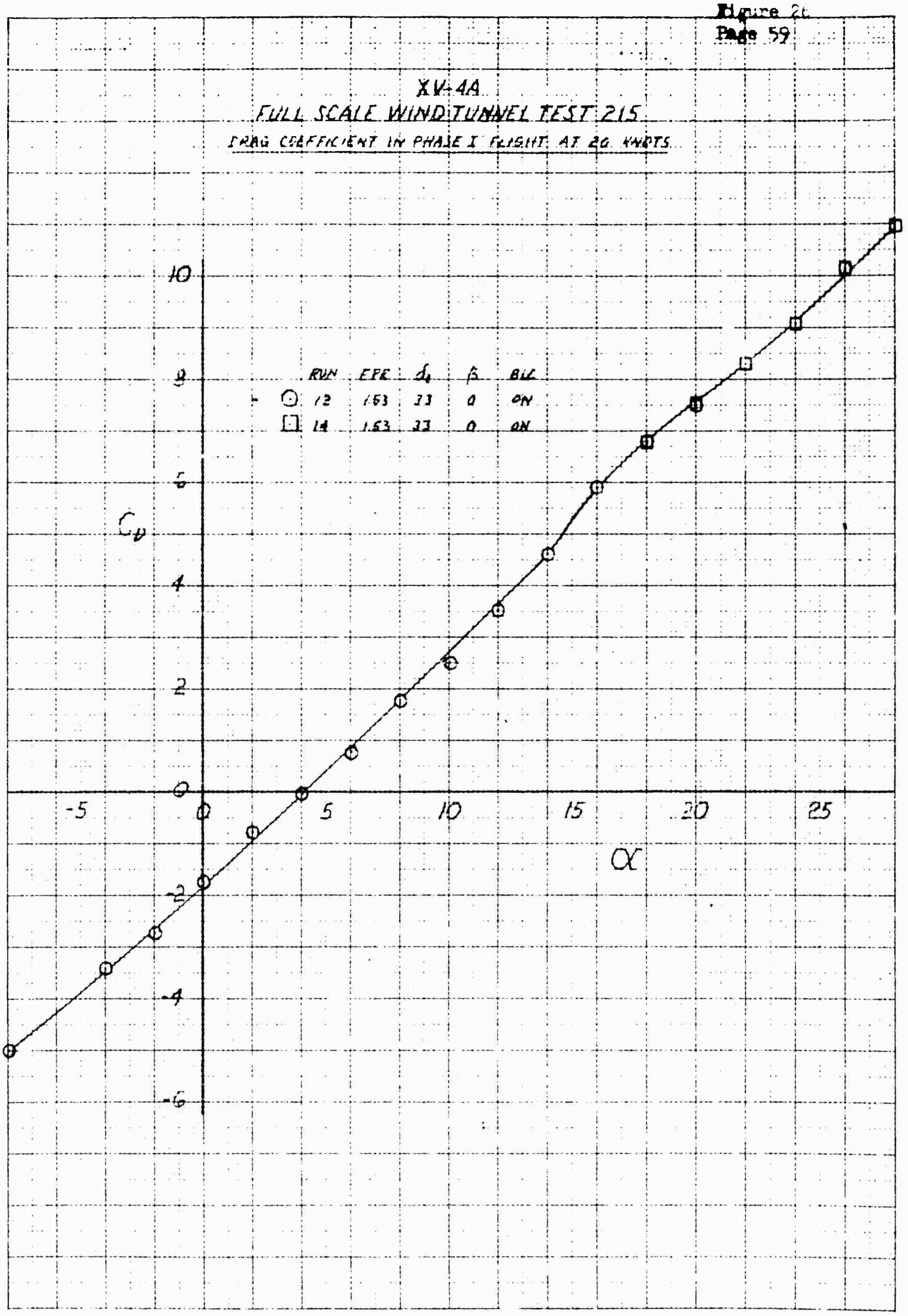
XV-4A
FULL SCALE WIND TUNNEL TEST 215
DRAG COEFFICIENT IN PHASE I FLIGHT AT 20 KNOTS
RUN EPE δ_f β BLC
12 1.53 33 0 ON
14 1.53 33 0 ON
C_D
α
10
8
6
4
2
0
-2
-4
-6
-5
0
5
10
15
20
25

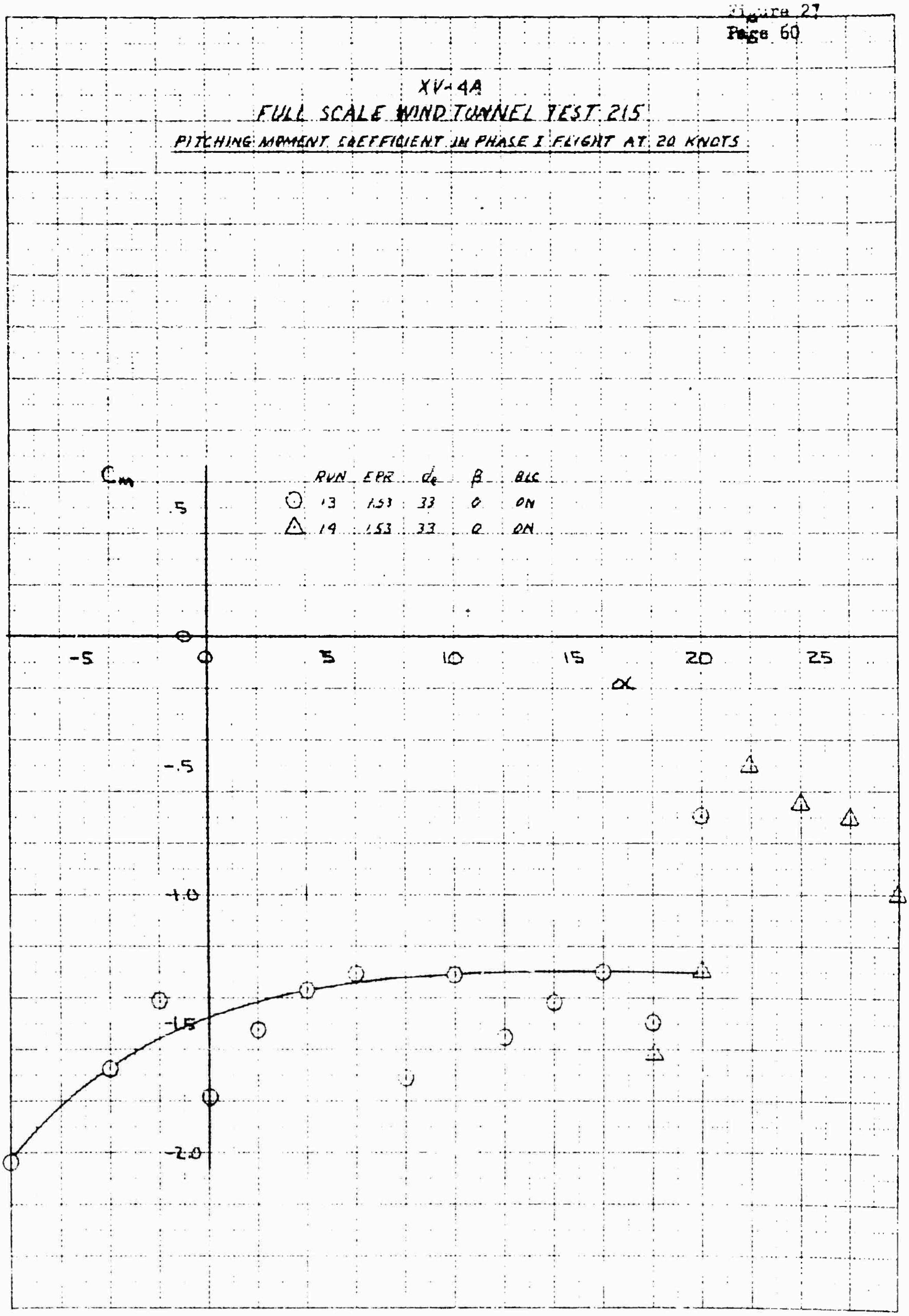
XV-4A
FULL SCALE WIND TUNNEL TEST 215
PITCHING MOMENT COEFFICIENT IN PHASE I FLIGHT AT 20 KNOTS
Cm
RUN EPR δ_e β BLC
13 1.53 33 0 ON
19 1.53 33 0 ON
.5
-5
0
5
10
15
20
25
α
-.5
-1.0
-1.5
-2.0

XV-4A
FULL SCALE WIND TUNNEL TEST 215
SIDE FORCE COEFFICIENT IN PHASE I FLIGHT AT 20 KNOTS

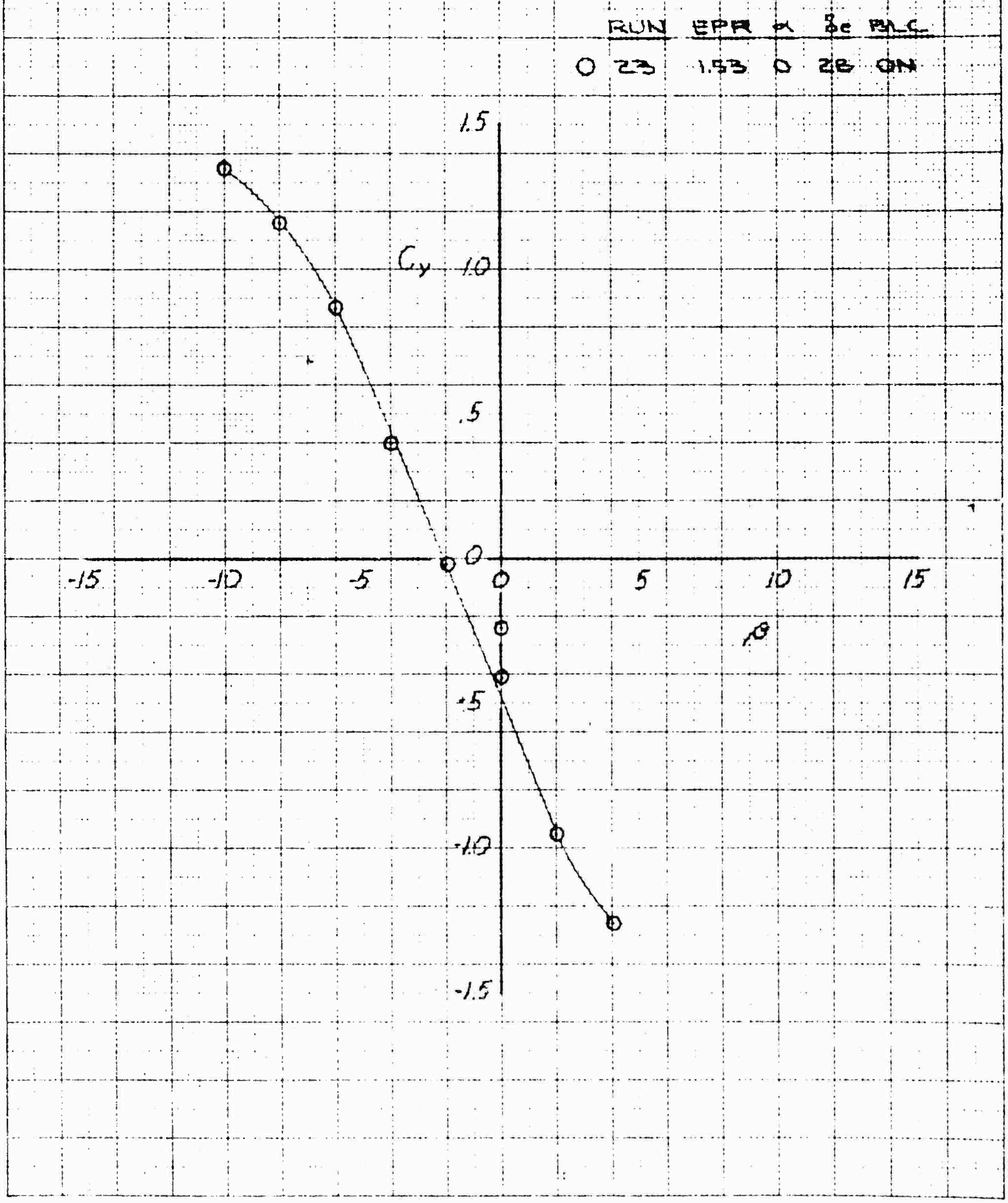

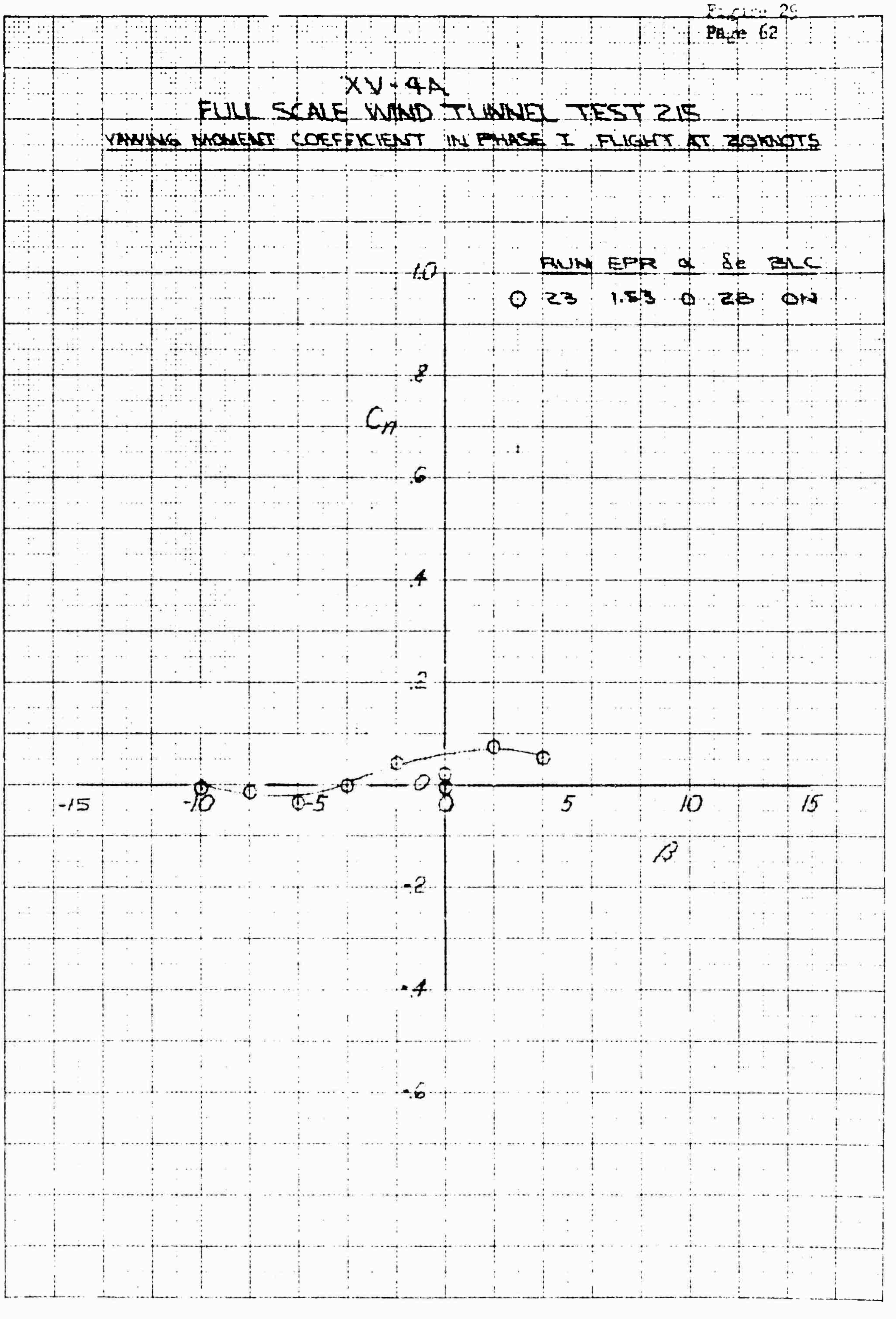
XV-4A
FULL SCALE WIND TUNNEL TEST 215
YAWING MOMENT COEFFICIENT IN PHASE I FLIGHT AT 20 KNOTS
RUN EPR α δe BLC
23 1.53 0 28 ON
C_n
1.0
.8
.6
.4
.2
0
-.2
-.4
-.6
-15
-10
-5
0
5
10
15
β

XV-4A
FULL SCALE WIND TUNNEL TEST 215
ROLLING MOMENT COEFFICIENT IN PHASE I FLIGHT AT 20 KNOTS

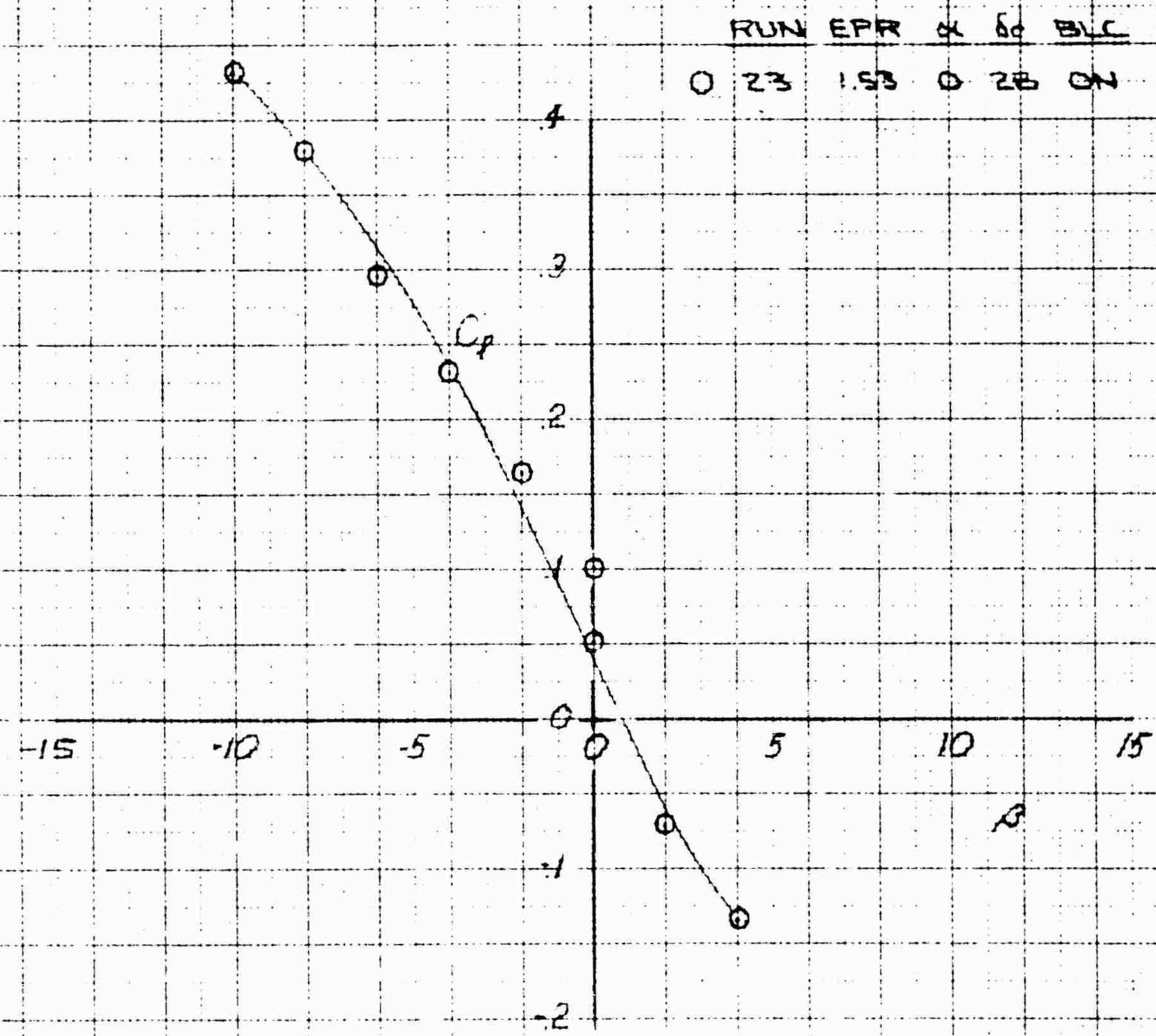

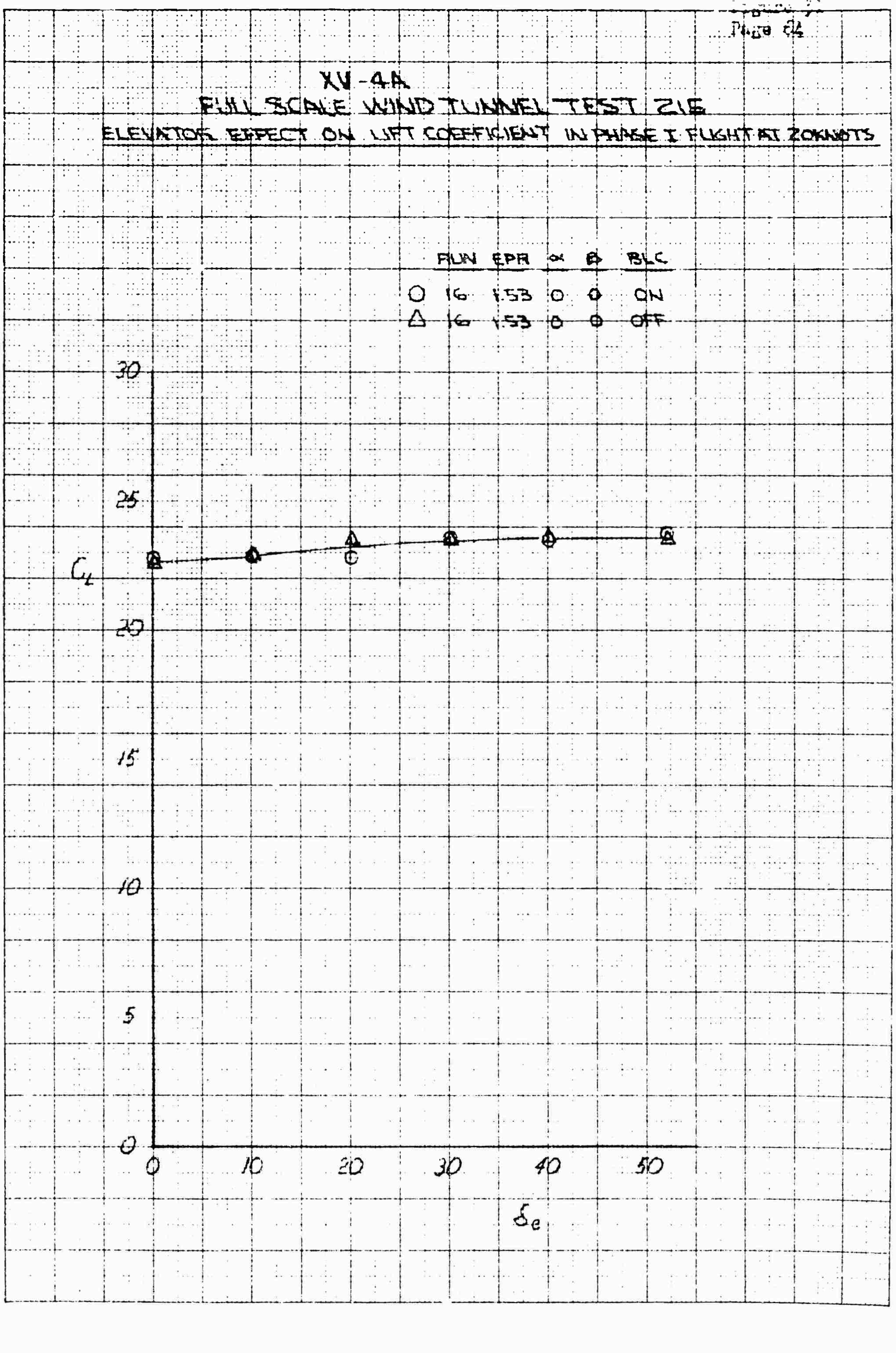

XV-4A
FULL SCALE WIND TUNNEL TEST 216
ELEVATOR EFFECT ON LIFT COEFFICIENT IN PHASE I FLIGHT AT 20KNOTS
RUN EPR α β BLC
16 1.53 0 0 ON
16 1.53 0 0 OFF
30
25
20
15
10
5
0
C_L
0
10
20
30
40
50
δ_e

XV-4A
FULL SCALE WIND TUNNEL TEST 215
ELEVATOR EFFECT ON DRAG COEFFICIENT IN PHASE I FLIGHT AT 20 KNOTS

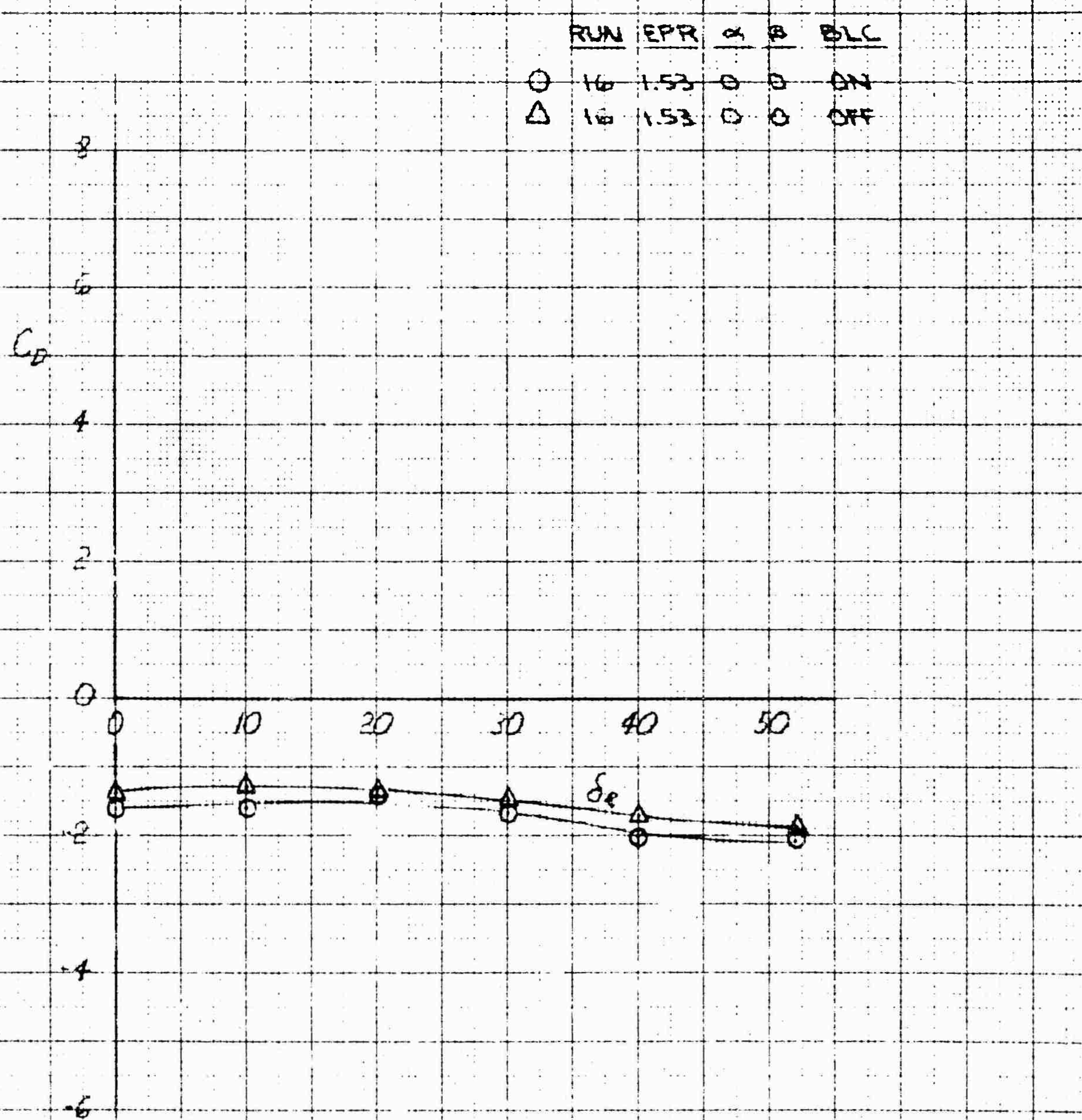

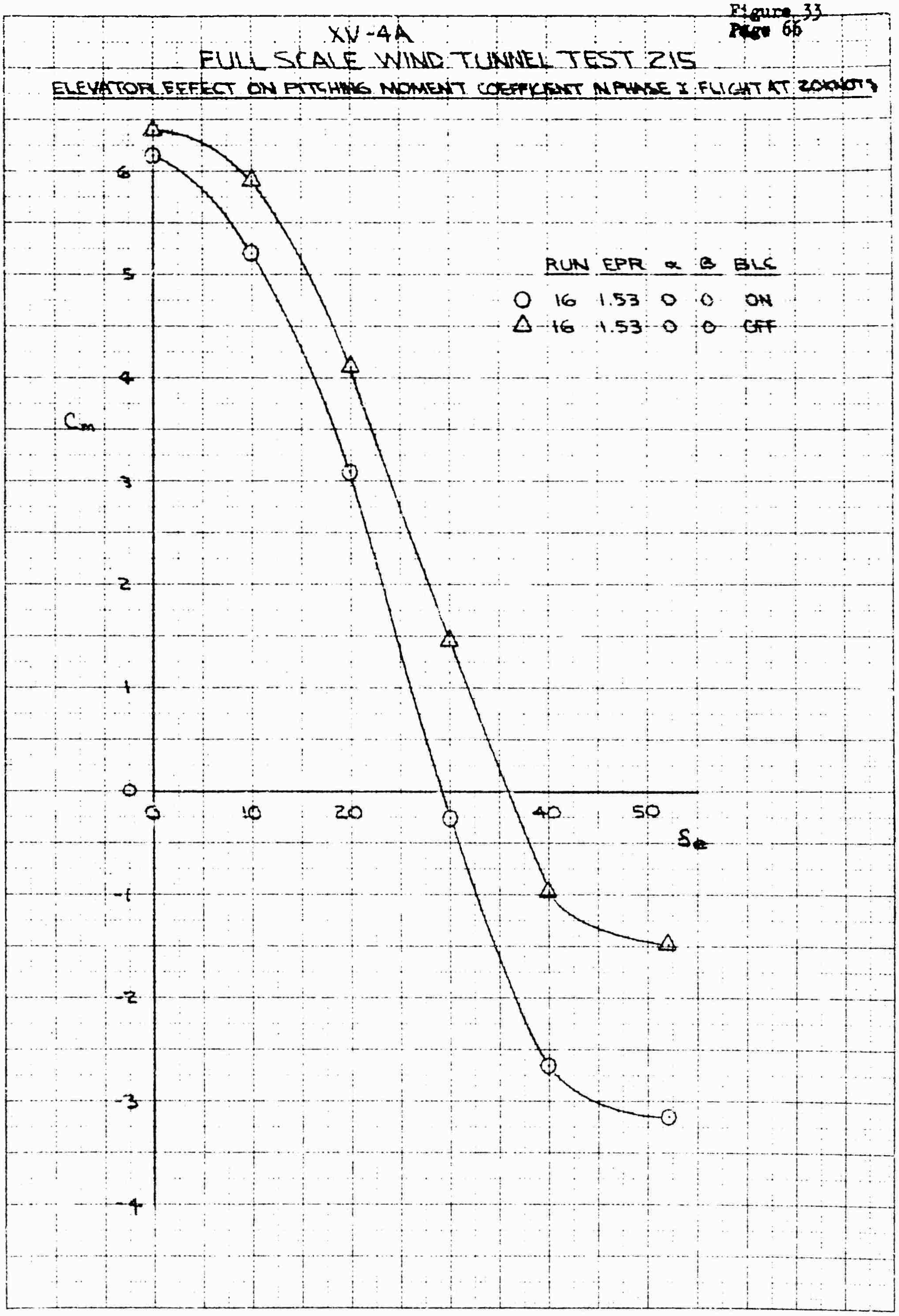
XV-4A
FULL SCALE WIND TUNNEL TEST 215
ELEVATOR EFFECT ON PITCHING MOMENT COEFFICIENT IN PHASE I FLIGHT AT 20KNOTS
RUN EPR α β BLC
16 1.53 0 0 ON
16 1.53 0 0 OFF
Cm
6
5
4
3
2
1
0
-1
-2
-3
-4
0
10
20
40
50
δe

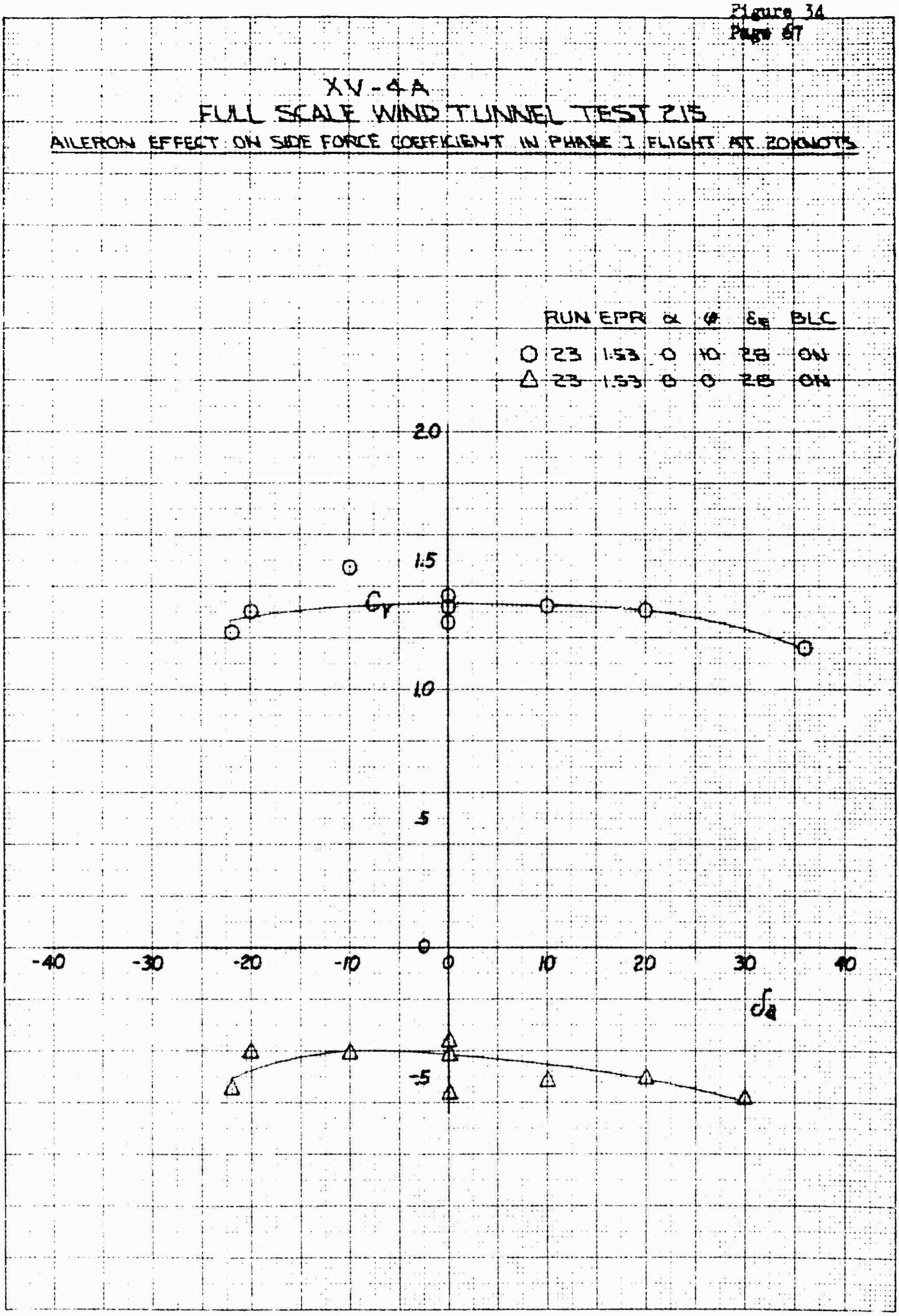
XV-4A
FULL SCALE WIND TUNNEL TEST 215
AILERON EFFECT ON SIDE FORCE COEFFICIENT IN PHASE I FLIGHT AT 20KNOTS
RUN EPR α φ δE BLC
○ 23 1.53 0 10 28 ON
△ 23 1.53 0 0 28 ON
2.0
1.5
1.0
.5
0
-.5
CY
-40 -30 -20 -10 0 10 20 30 40
δa

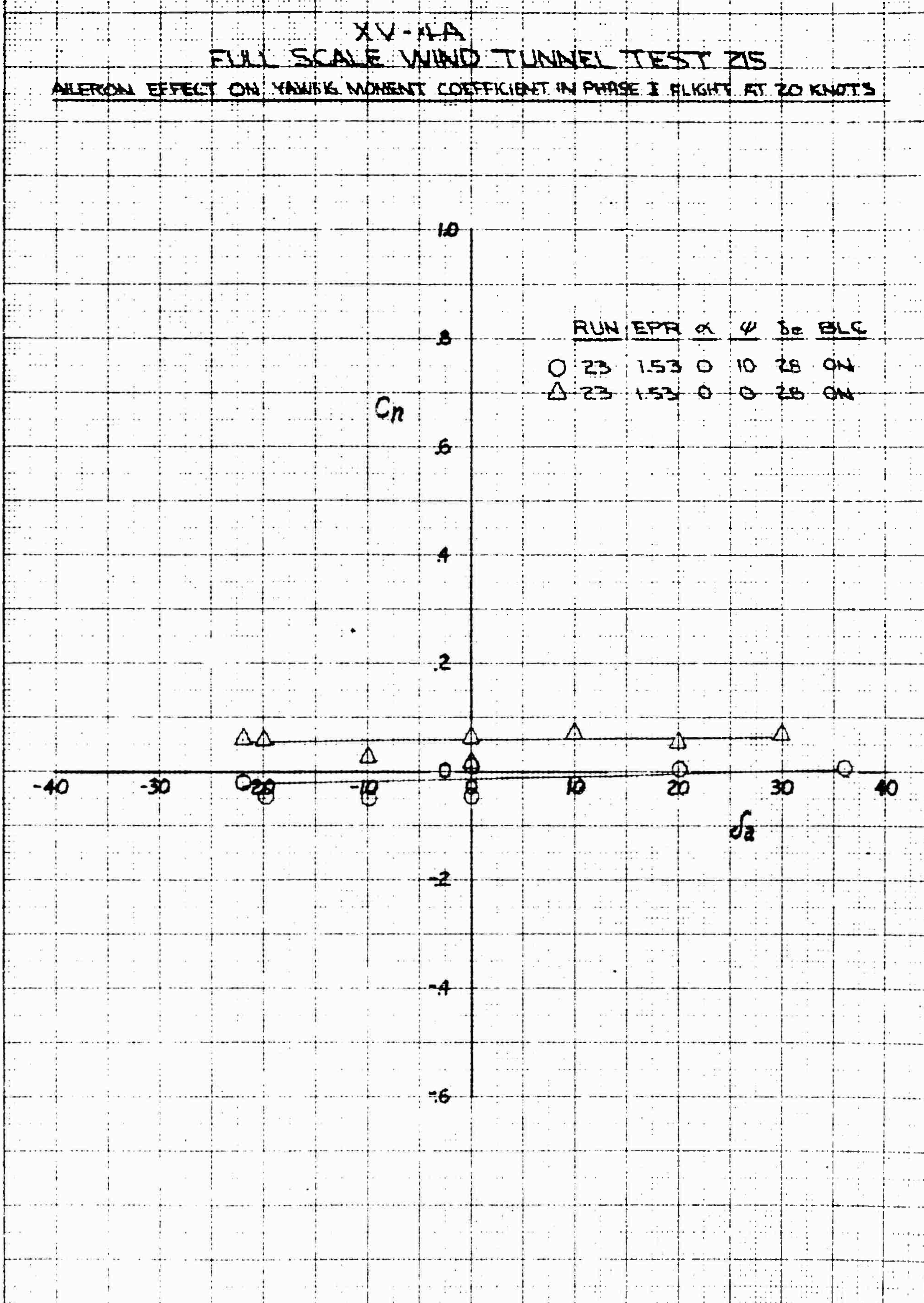
XV-4A
FULL SCALE WIND TUNNEL TEST 215
AILERON EFFECT ON YAWING MOMENT COEFFICIENT IN PHASE I FLIGHT AT 20 KNOTS
RUN EPR α ψ δe BLC
○ 23 1.53 0 10 28 ON
△ 23 1.53 0 0 28 ON
Cn
δa
1.0
.8
.6
.4
.2
0
-.2
-.4
-.6
-40
-30
-20
-10
0
10
20
30
40

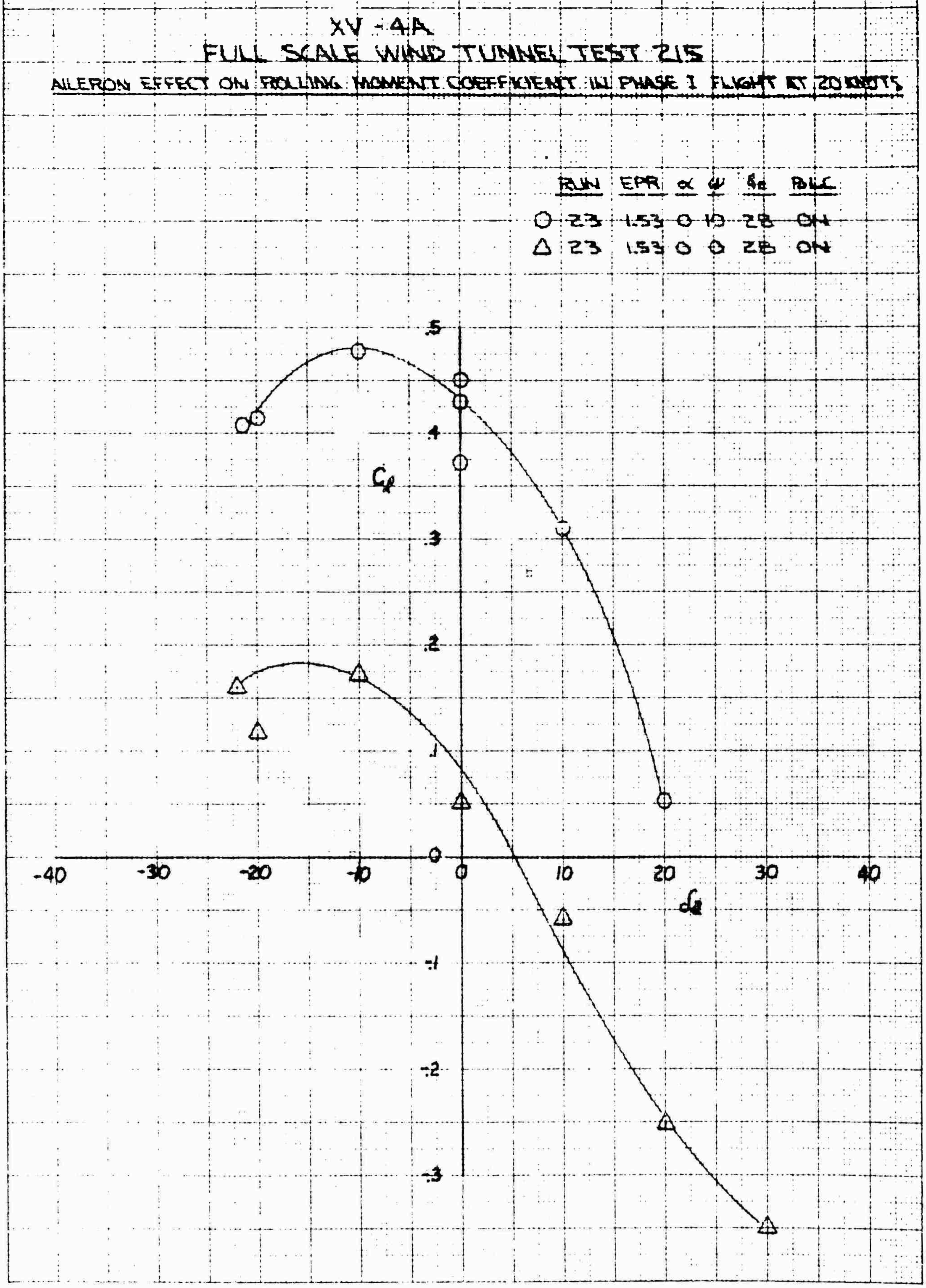
XV-4A
FULL SCALE WIND TUNNEL TEST 215
AILERON EFFECT ON ROLLING MOMENT COEFFICIENT IN PHASE I FLIGHT AT 20 KNOTS
RUN EPR α ψ δe BLC
○ 23 1.53 0 13 28 ON
△ 23 1.53 0 0 28 ON
.5
.4
.3
.2
.1
0
-.1
-.2
-.3
-40
-30
-20
-10
0
10
20
30
40

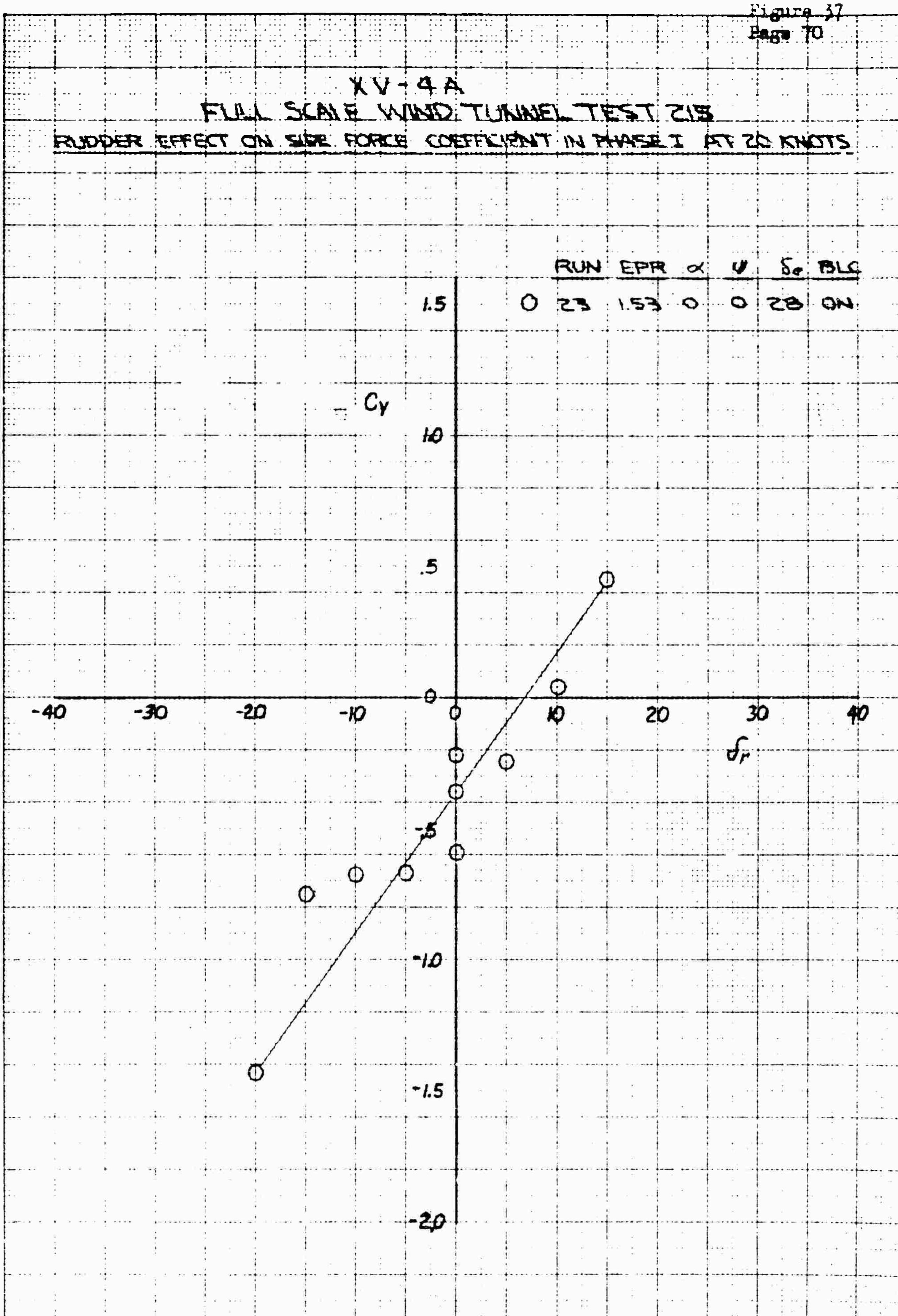
XV-4A
FULL SCALE WIND TUNNEL TEST 213
RUDDER EFFECT ON SIDE FORCE COEFFICIENT IN PHASE I AT 20 KNOTS
RUN EPR α ψ δe BLC
O 23 1.53 0 0 28 ON
Cy
1.5
1.0
.5
0
-.5
-1.0
-1.5
-2.0
-40
-30
-20
-10
0
10
20
30
40
δr

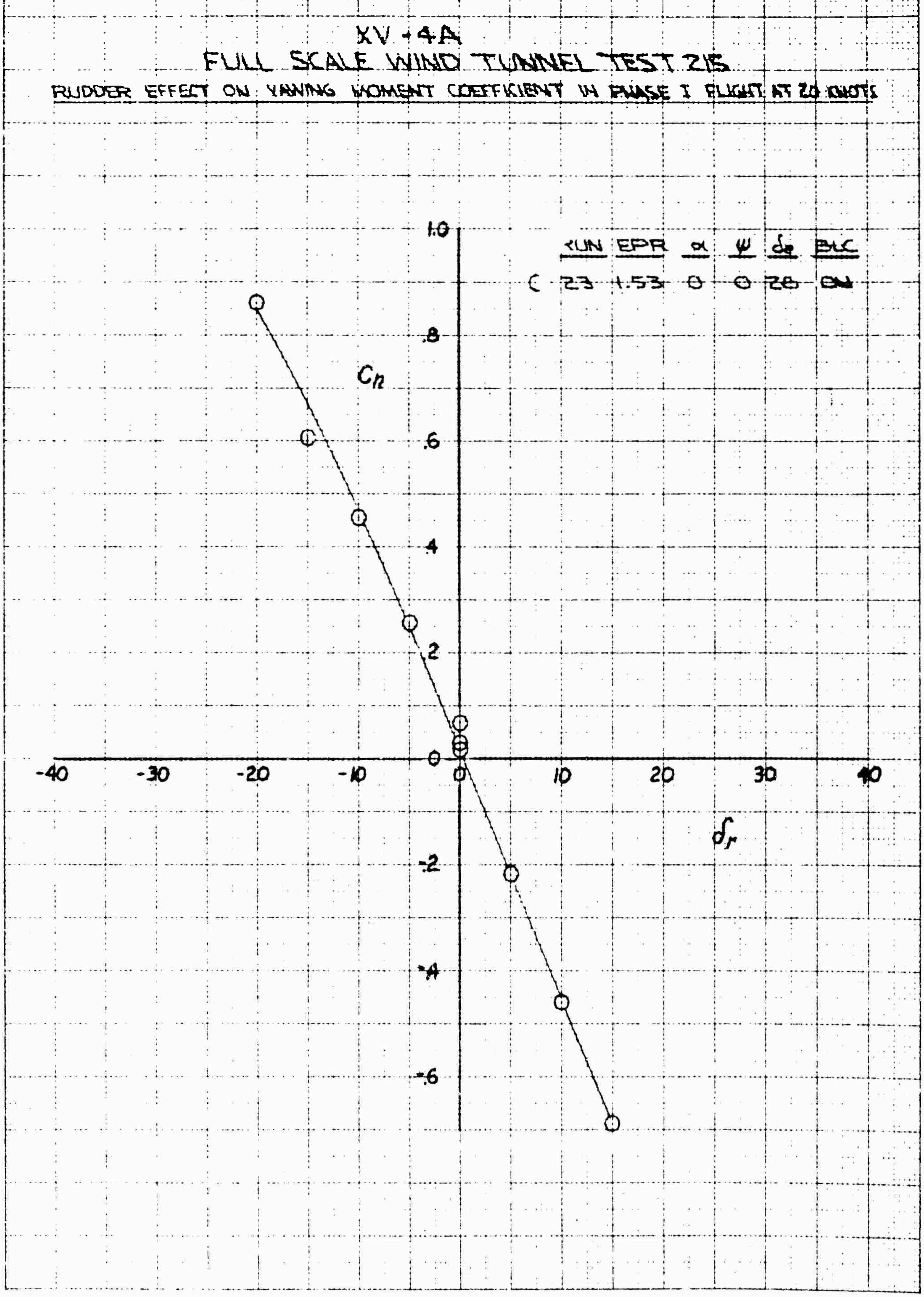
XV-4A
FULL SCALE WIND TUNNEL TEST 215
RUDDER EFFECT ON YAWING MOMENT COEFFICIENT IN PHASE I FLIGHT AT 20 KNOTS
RUN EPR α ψ δe BLC
23 1.53 0 0 28 ON
1.0
.8
.6
.4
.2
0
-.2
-.4
-.6
Cn
-40 -30 -20 -10 0 10 20 30 40
δr

XV-4A
FULL SCALE WIND TUNNEL TEST 215
RUDDER EFFECT ON ROLLING MOMENT COEFFICIENT IN PHASE I FLIGHT AT 20 KNOTS

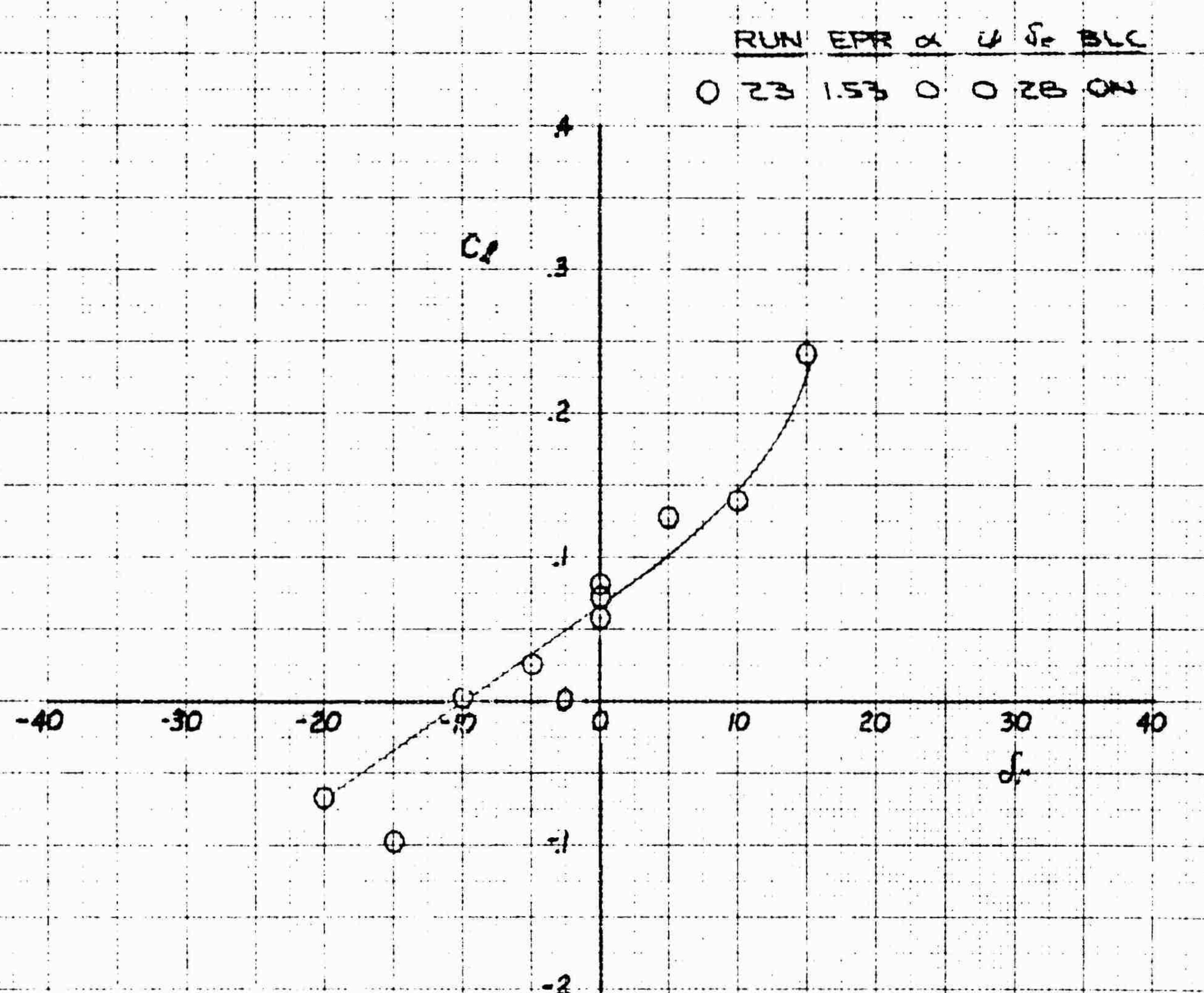

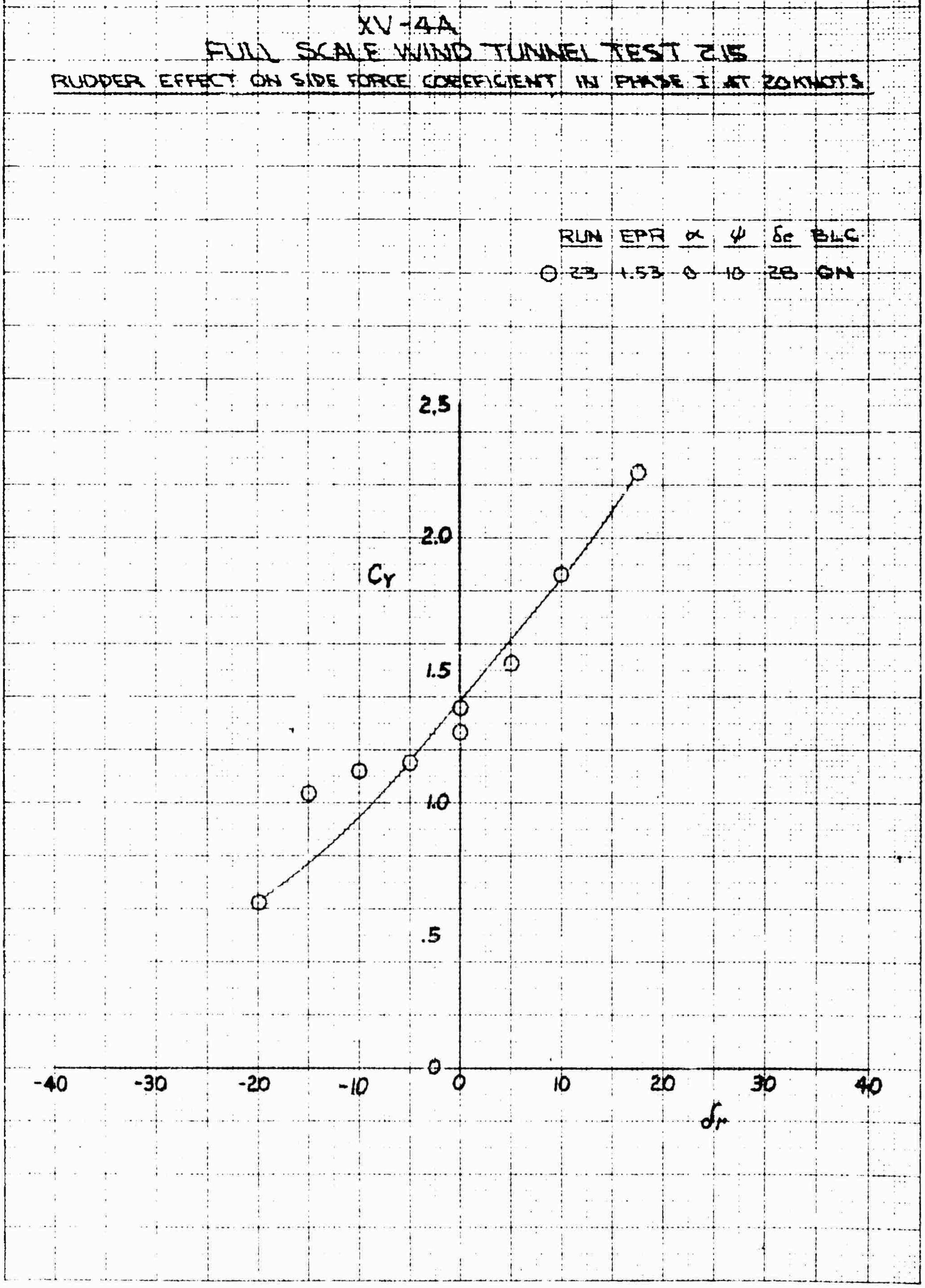
XV-4A
FULL SCALE WIND TUNNEL TEST 215
RUDDER EFFECT ON SIDE FORCE COEFFICIENT IN PHASE I AT 20KNOTS
RUN EPR α ψ δe BLC
23 1.53 0 10 28 ON
2.5
2.0
1.5
1.0
.5
0
CY
-40
-30
-20
-10
0
10
20
30
40
δr

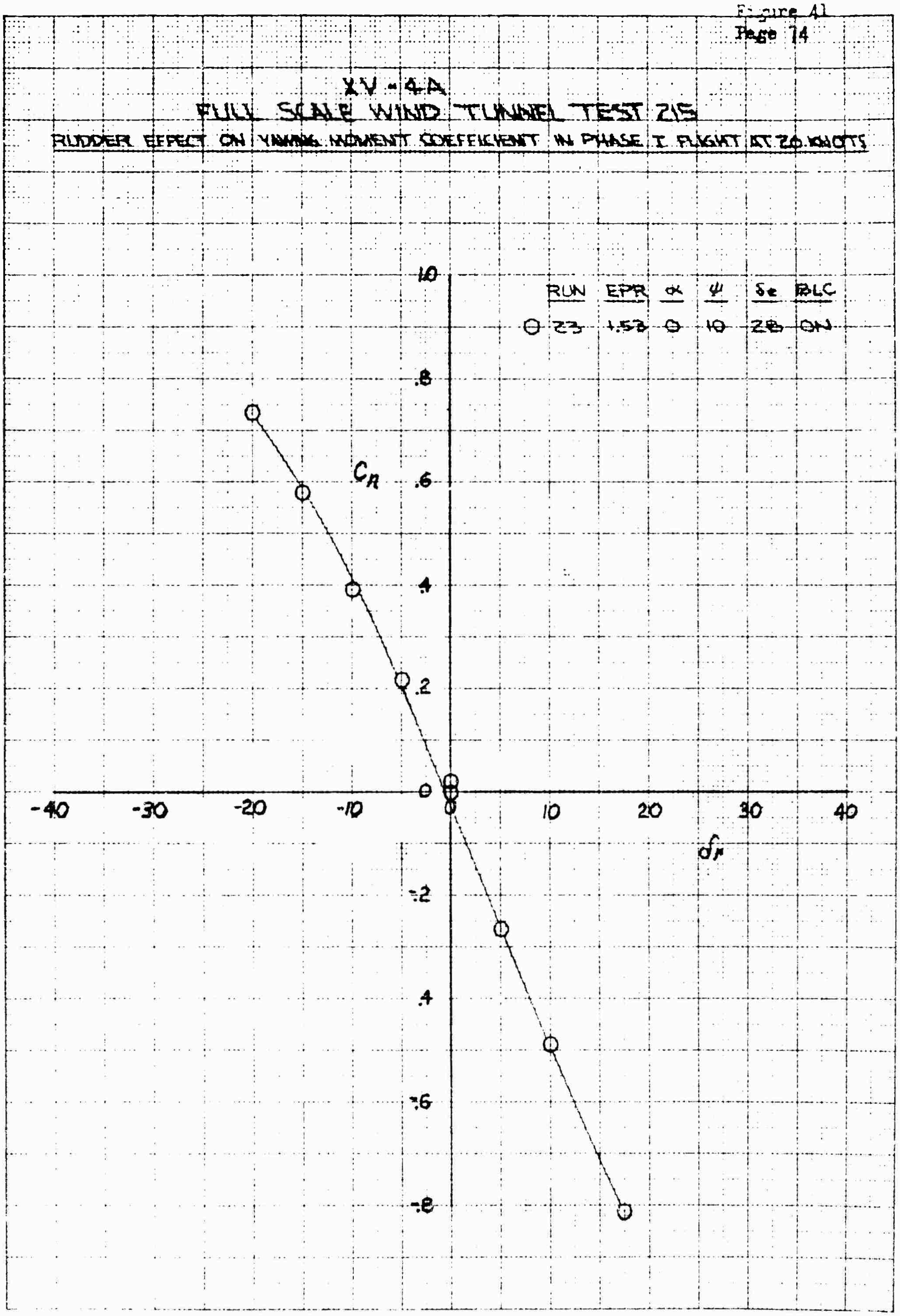
XV-4A
FULL SCALE WIND TUNNEL TEST 215
RUDDER EFFECT ON YAWING MOMENT COEFFICIENT IN PHASE I FLIGHT AT 20 KNOTS
RUN EPR α ψ δe BLC
23 1.53 0 10 28 ON
Cn
1.0
.8
.6
.4
.2
0
-.2
-.4
-.6
-.8
-40
-30
-20
-10
0
10
20
30
40
δr

XN-4A
FULL SCALE WIND TUNNEL TEST 215
RUDDER EFFECT ON ROLLING MOMENT COEFFICIENT IN PHASE I FLIGHT AT 10 KNOTS

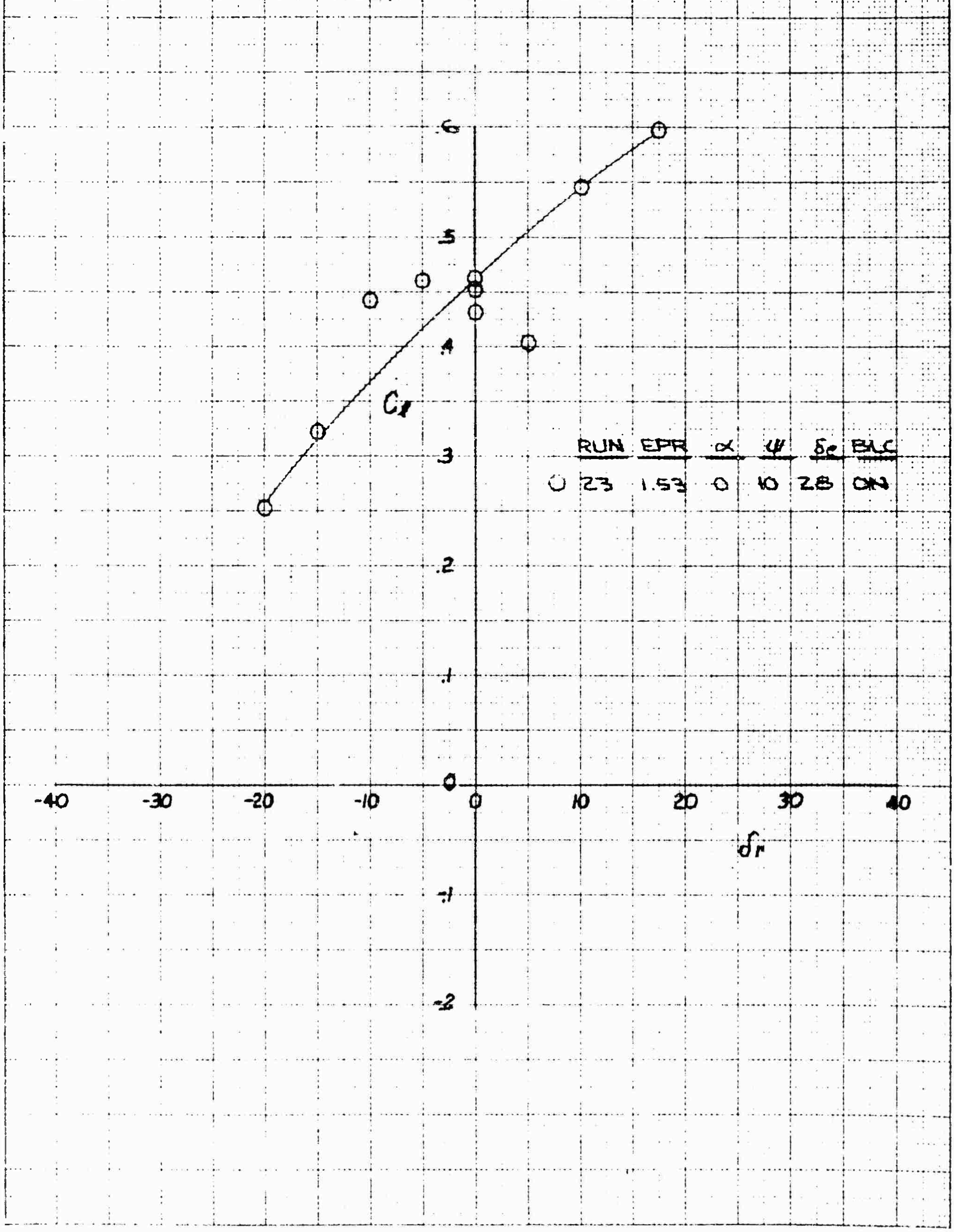

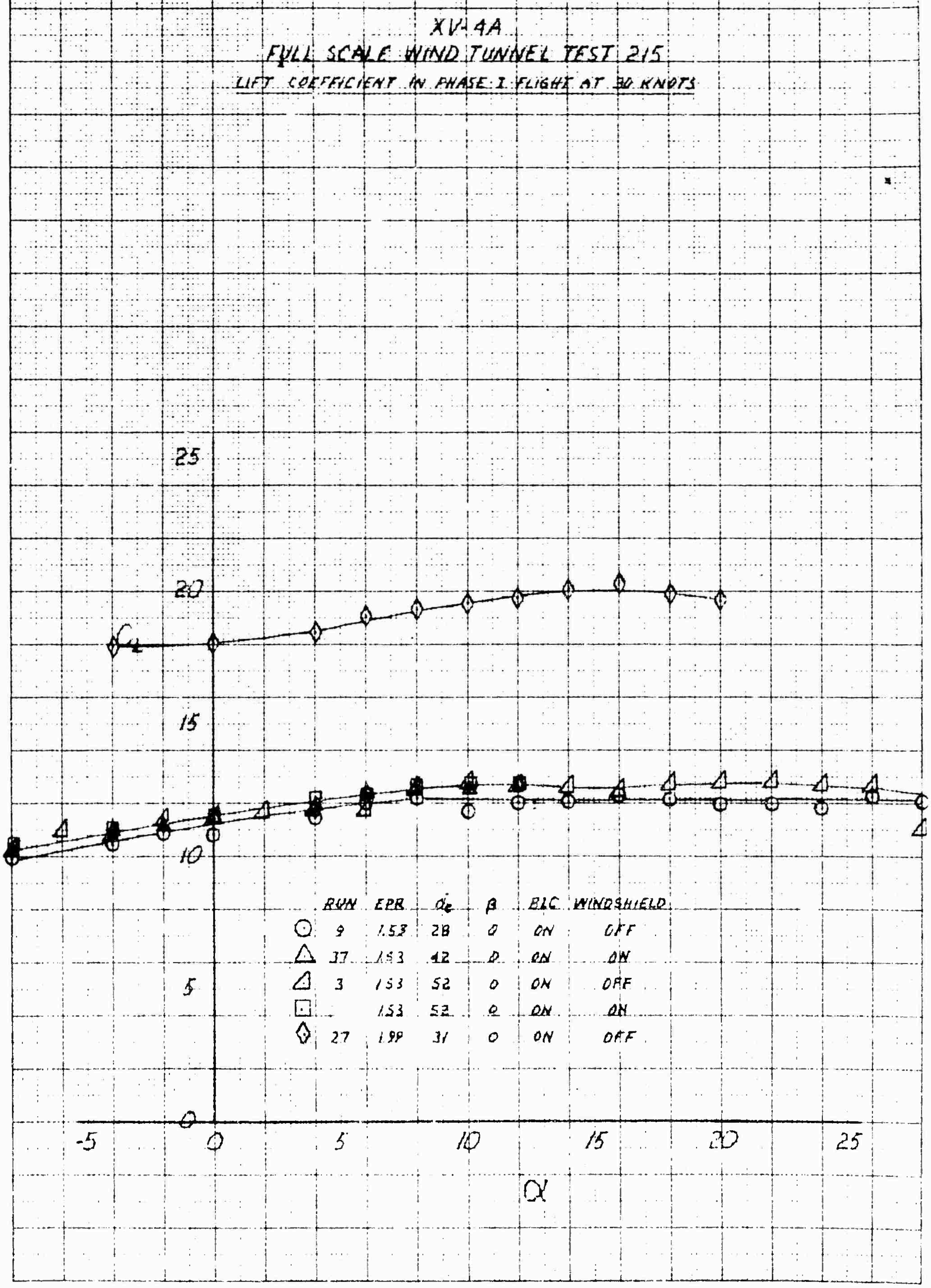
XV-4A
FULL SCALE WIND TUNNEL TEST 215
LIFT COEFFICIENT IN PHASE I FLIGHT AT 30 KNOTS
C_L
25
20
15
10
5
0
-5
0
5
10
15
20
25
α
RUN EPR α_c β BLC WINDSHIELD
○ 9 1.53 28 0 ON OFF
△ 37 1.53 42 0 ON ON
◿ 3 1.53 52 0 ON OFF
□ 1.53 52 0 ON ON
◇ 27 1.99 31 0 ON OFF

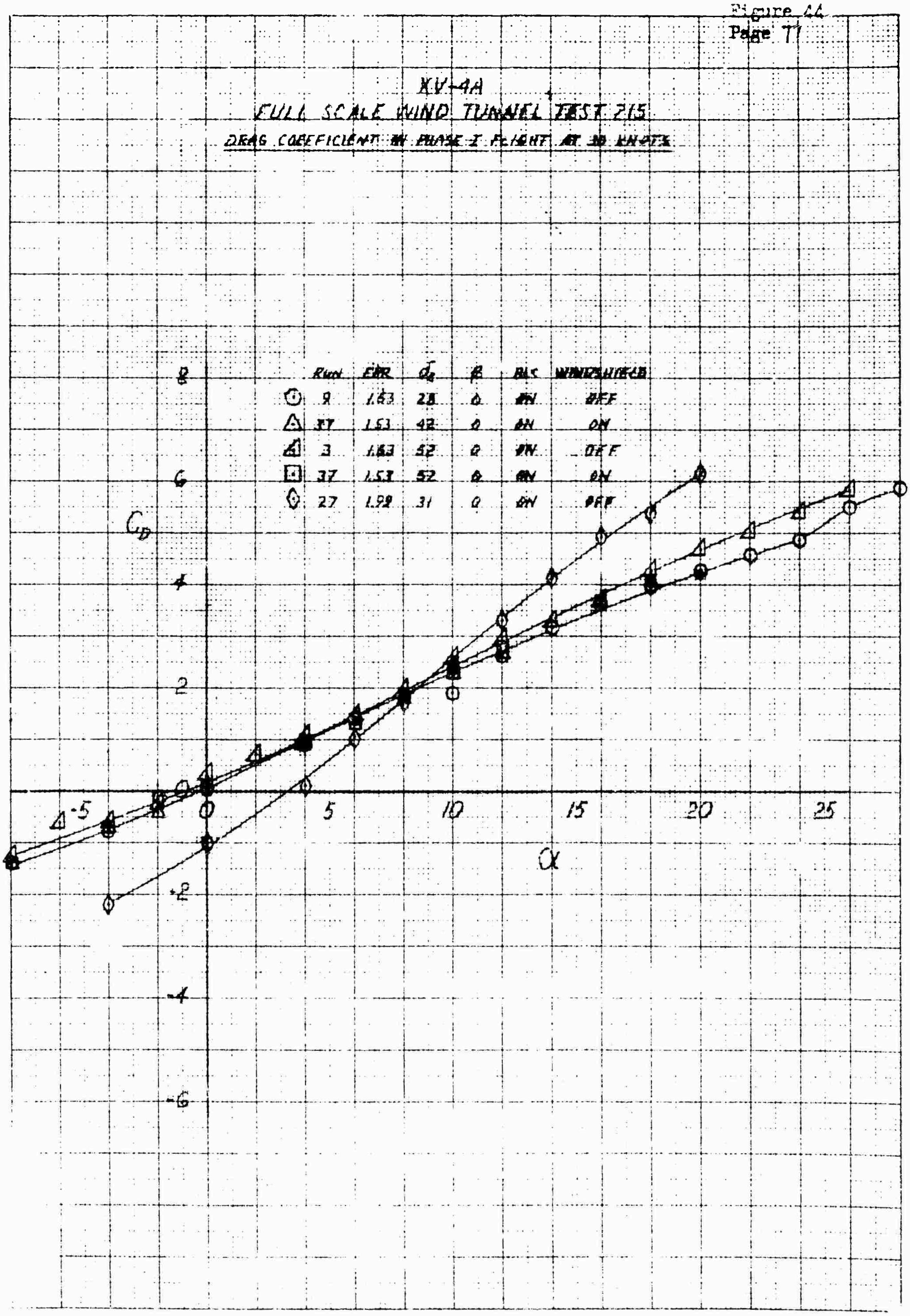
XV-4A
FULL SCALE WIND TUNNEL TEST 215
DRAG COEFFICIENT IN PHASE I FLIGHT AT 30 KNOTS
Run EPR δ β BLC WINDSHIELD
9 1.63 28 0 ON OFF
37 1.53 42 0 ON ON
3 1.63 52 0 ON OFF
37 1.53 52 0 ON ON
27 1.99 31 0 ON OFF
C_D
8
6
4
2
-2
-4
-6
-5
0
5
10
15
20
25
α

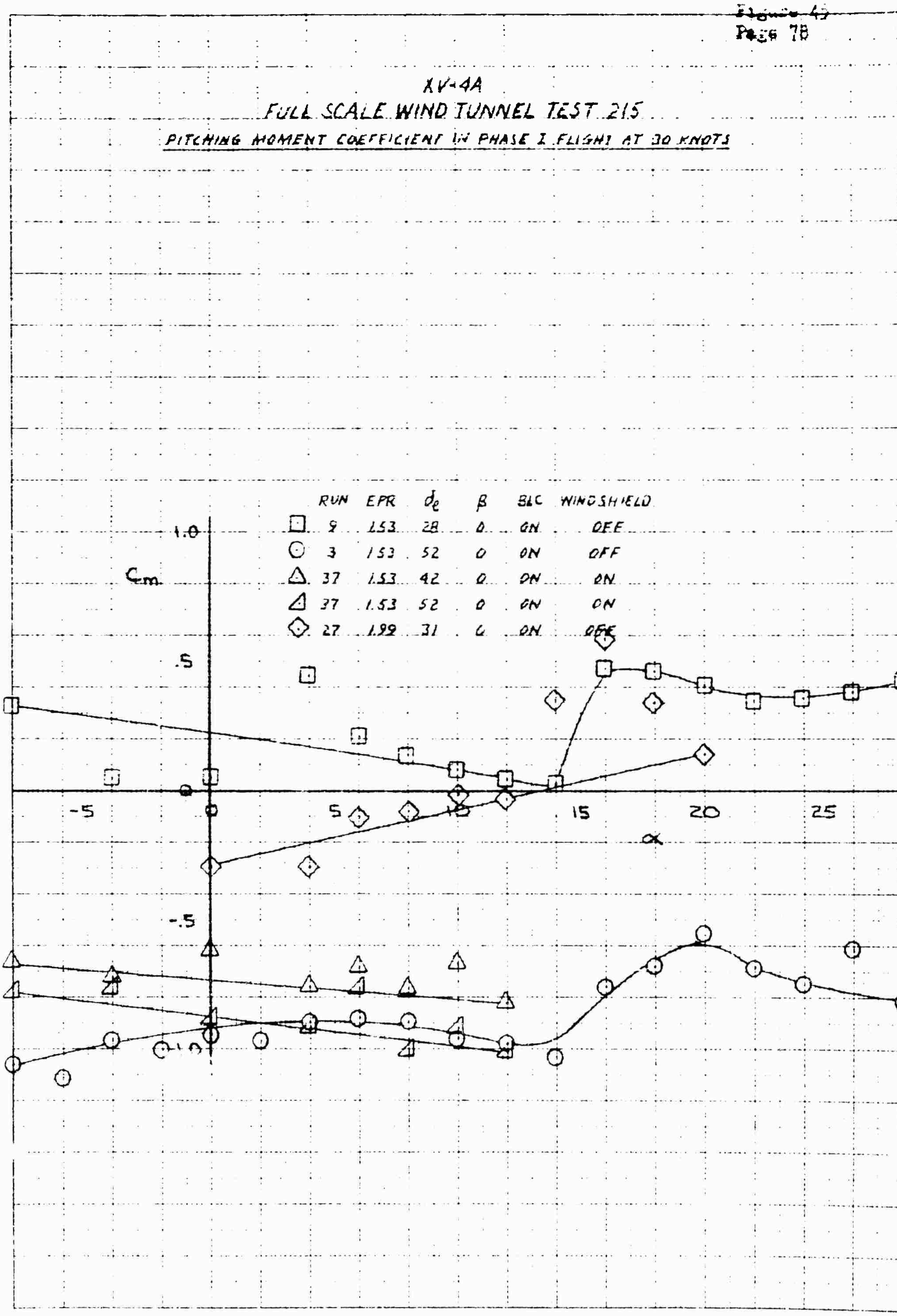
XV-4A
FULL SCALE WIND TUNNEL TEST 215
PITCHING MOMENT COEFFICIENT IN PHASE I FLIGHT AT 30 KNOTS
RUN EPR δe β BLC WINDSHIELD
9 1.53 28 0 ON OFF
3 1.53 52 0 ON OFF
37 1.53 42 0 ON ON
37 1.53 52 0 ON ON
27 1.99 31 0 ON OFF
Cm
1.0
.5
-.5
-1.0
-5
0
5
10
15
20
25
α

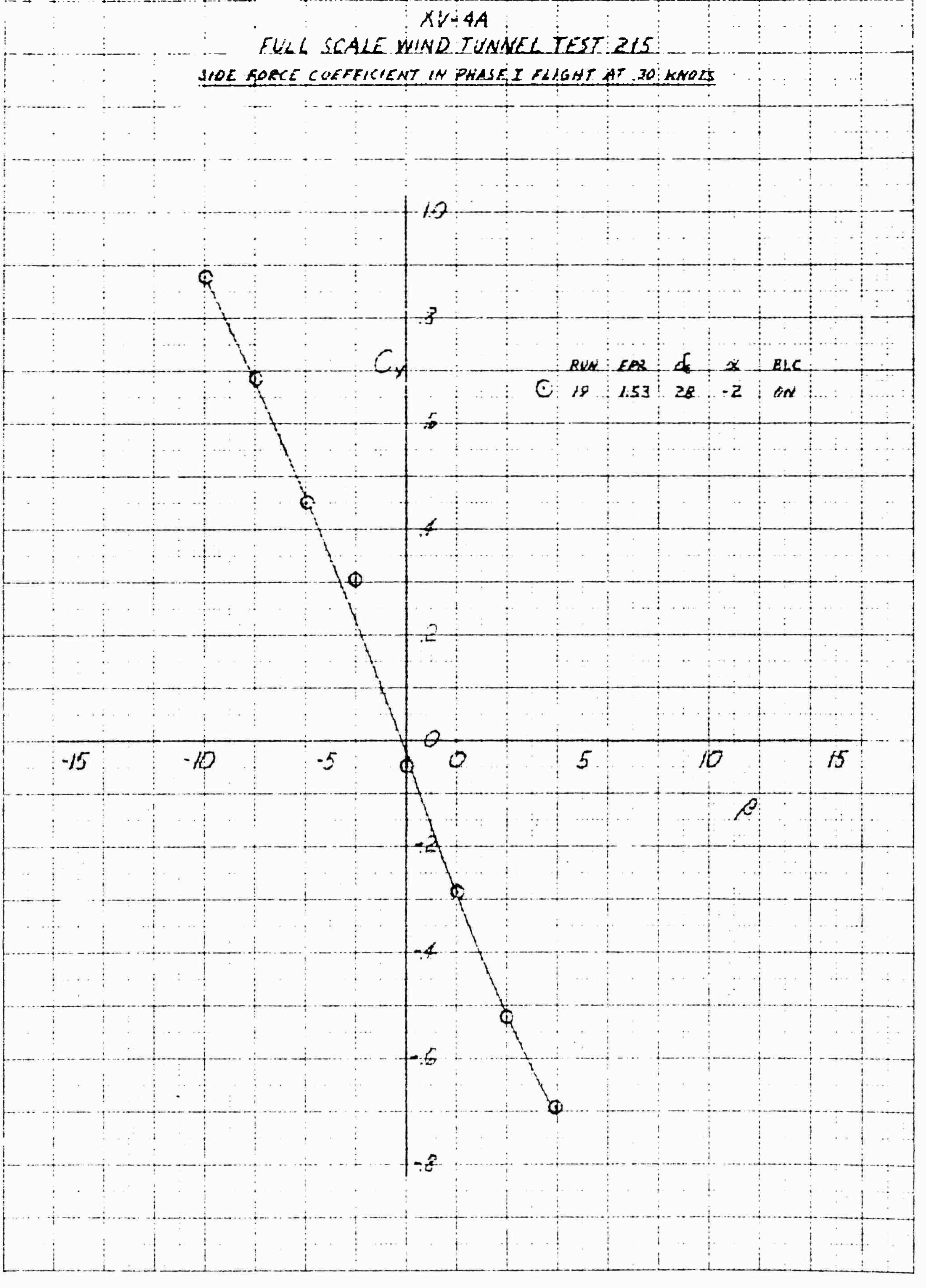
XV-4A
FULL SCALE WIND TUNNEL TEST 215
SIDE FORCE COEFFICIENT IN PHASE I FLIGHT AT 30 KNOTS
RUN EPR α BLC
19 1.53 28 -2 ON
1.0
.8
.6
.4
.2
0
-.2
-.4
-.6
-.8
-15
-10
-5
0
5
10
15
β

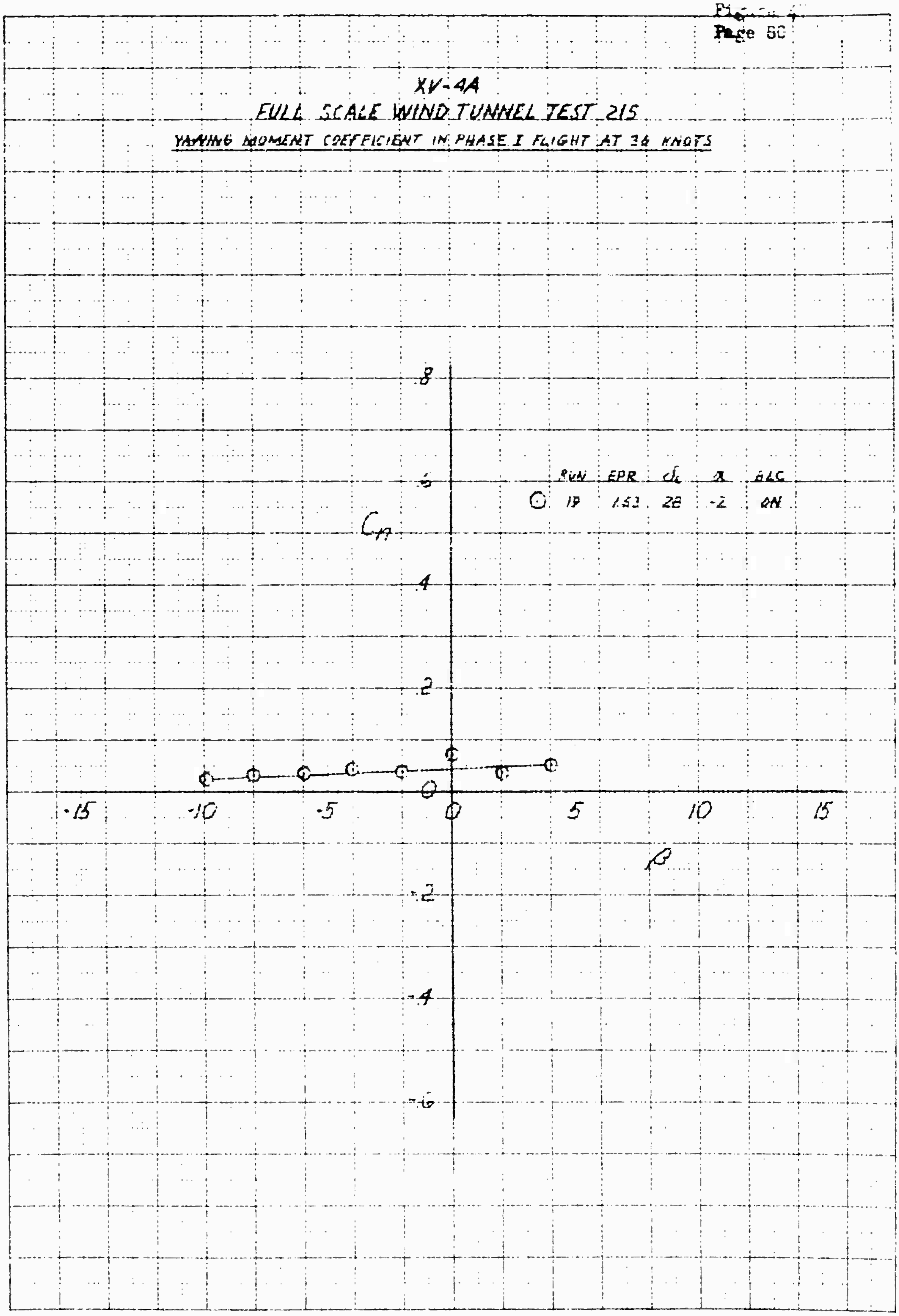
XV-4A
FULL SCALE WIND TUNNEL TEST 215
YAWING MOMENT COEFFICIENT IN PHASE I FLIGHT AT 36 KNOTS
RUN EPR δ α BLC
19 1.53 28 -2 ON
Cn
β
.8
.6
.4
.2
0
-.2
-.4
-.6
-15
-10
-5
5
10
15

XV-4A

FULL SCALE WIND TUNNEL TEST 215

ROLLING MOMENT COEFFICIENT IN PHASE 2 FLIGHT AT 30 KNOTS

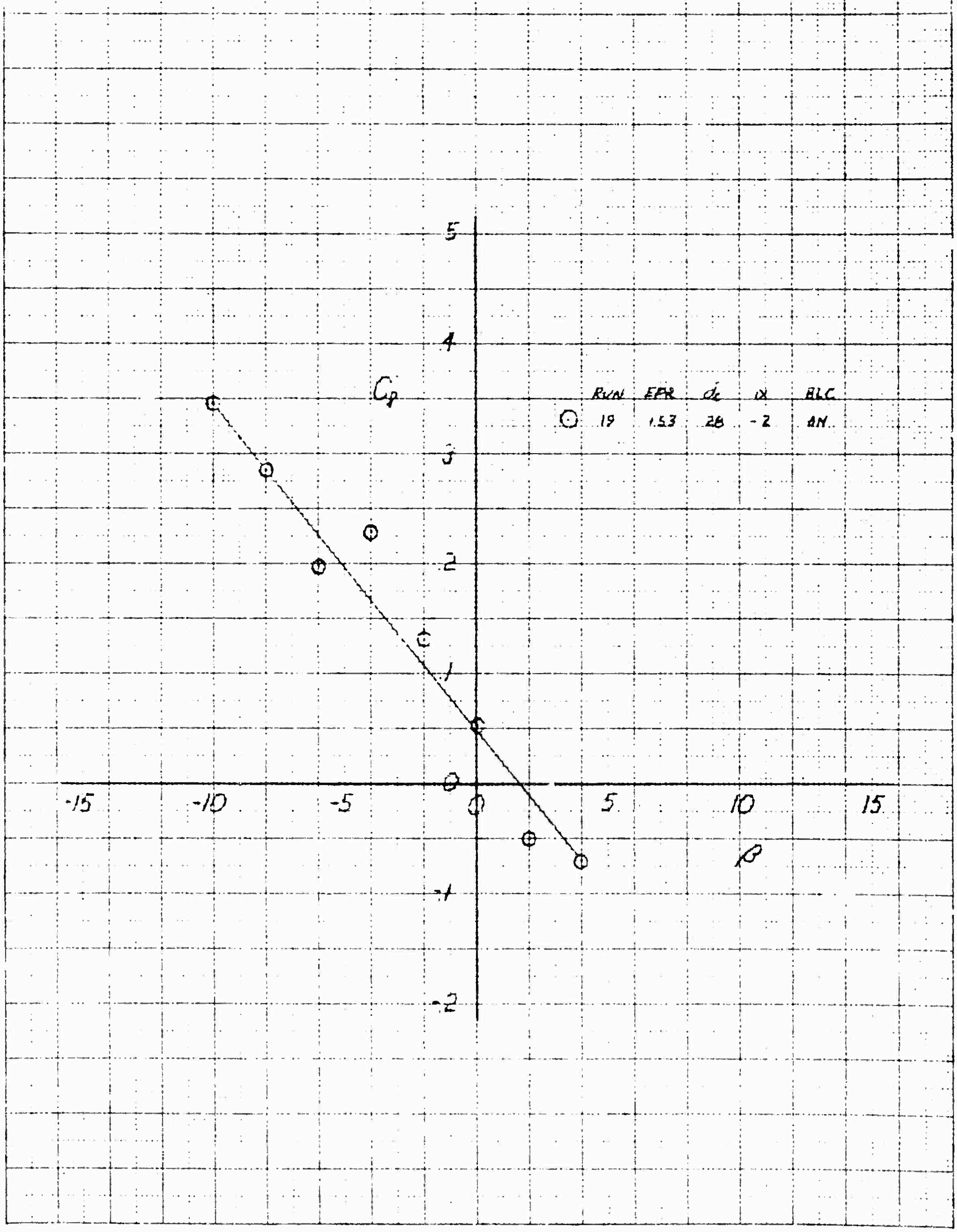

XV-4A
FULL SCALE WIND TUNNEL TEST 215

ELEVATOR EFFECT ON LIFT COEFFICIENT IN PHASE I FLIGHT AT 30 KNOTS

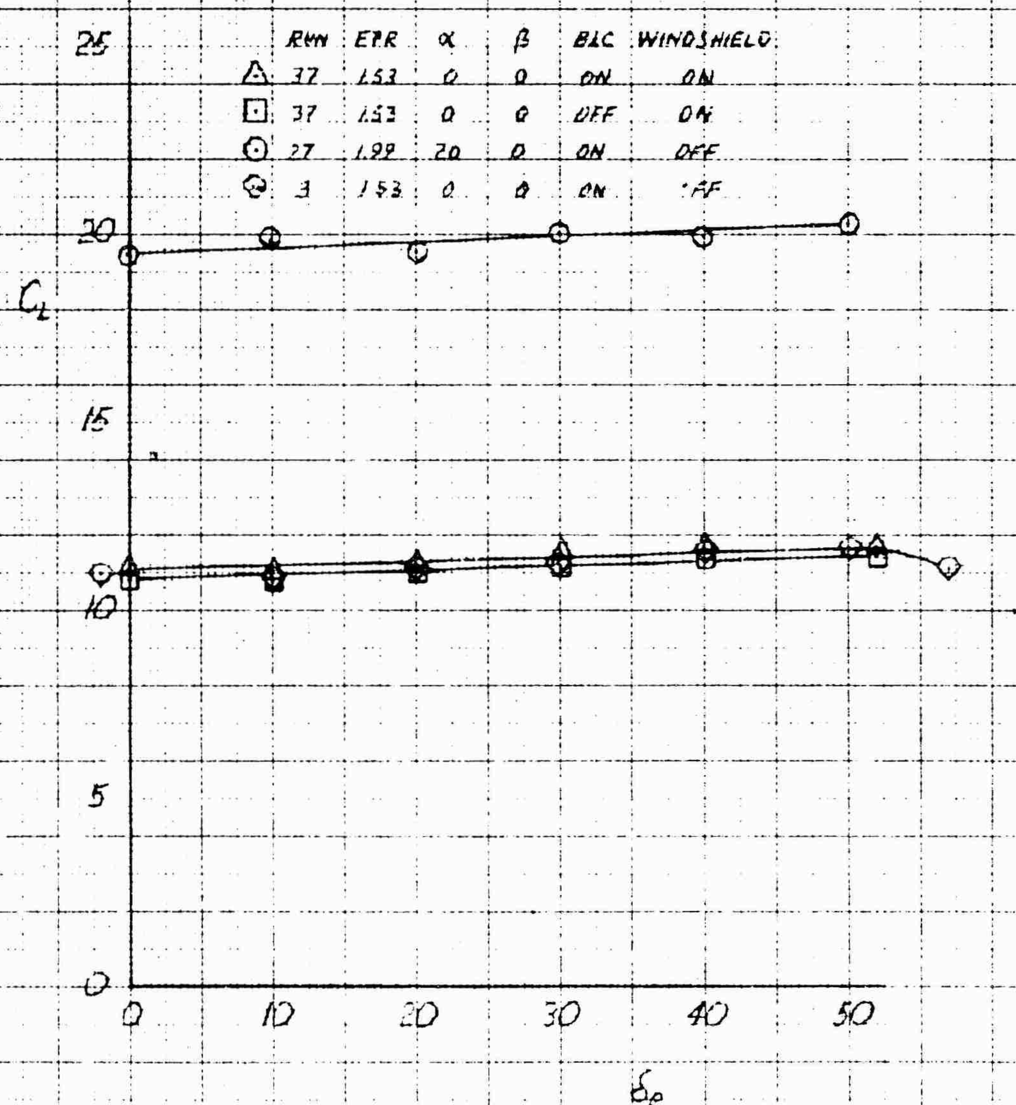

XV-4A

FULL SCALE WIND TUNNEL TEST 215

ELEVATOR EFFECT ON DRAG COEFFICIENT IN PHASE I FLIGHT AT 30 KNOTS

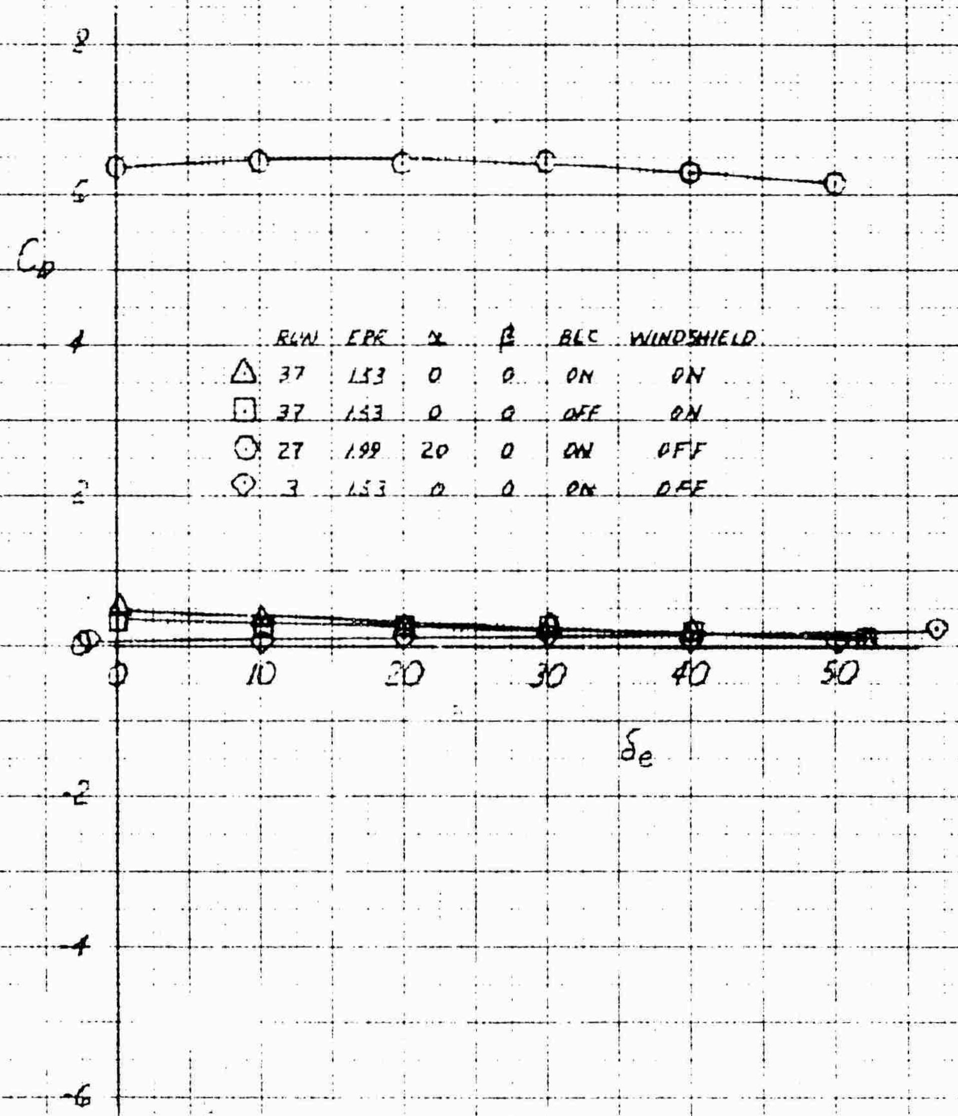

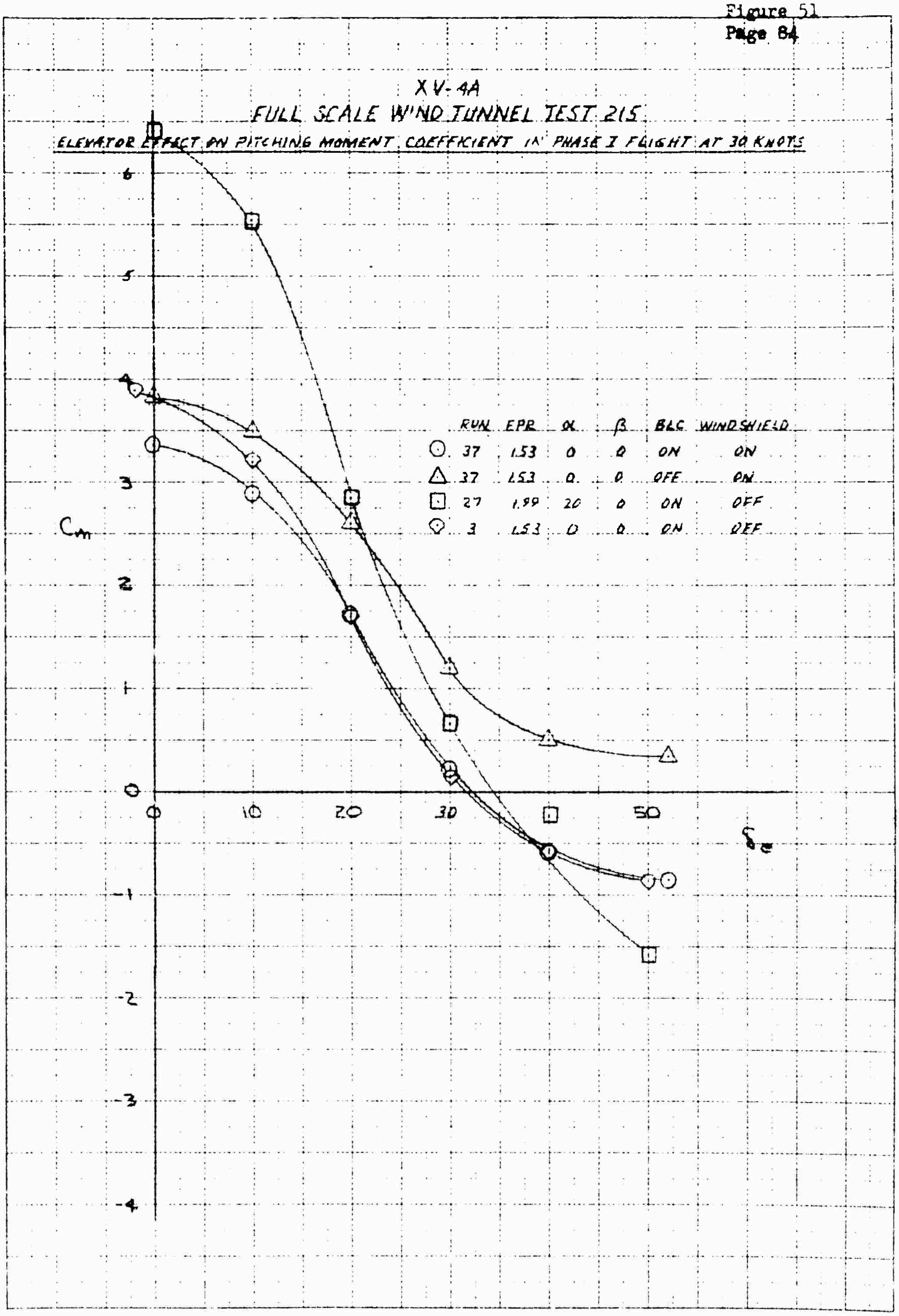
XV-4A
FULL SCALE WIND TUNNEL TEST 215
ELEVATOR EFFECT ON PITCHING MOMENT COEFFICIENT IN PHASE I FLIGHT AT 30 KNOTS
RUN EPR α β BLC WINDSHIELD
37 1.53 0 0 ON ON
37 1.53 0 0 OFF ON
27 1.99 20 0 ON OFF
3 1.53 0 0 ON OFF
C_m
δ_e
6
5
4
3
2
1
0
-1
-2
-3
-4
0
10
20
30
40
50

XV-4A
FULL SCALE WIND TUNNEL TEST 215
AILERON EFFECT ON SIDE FORCE COEFFICIENT IN PHASE I AT 30 KNOTS

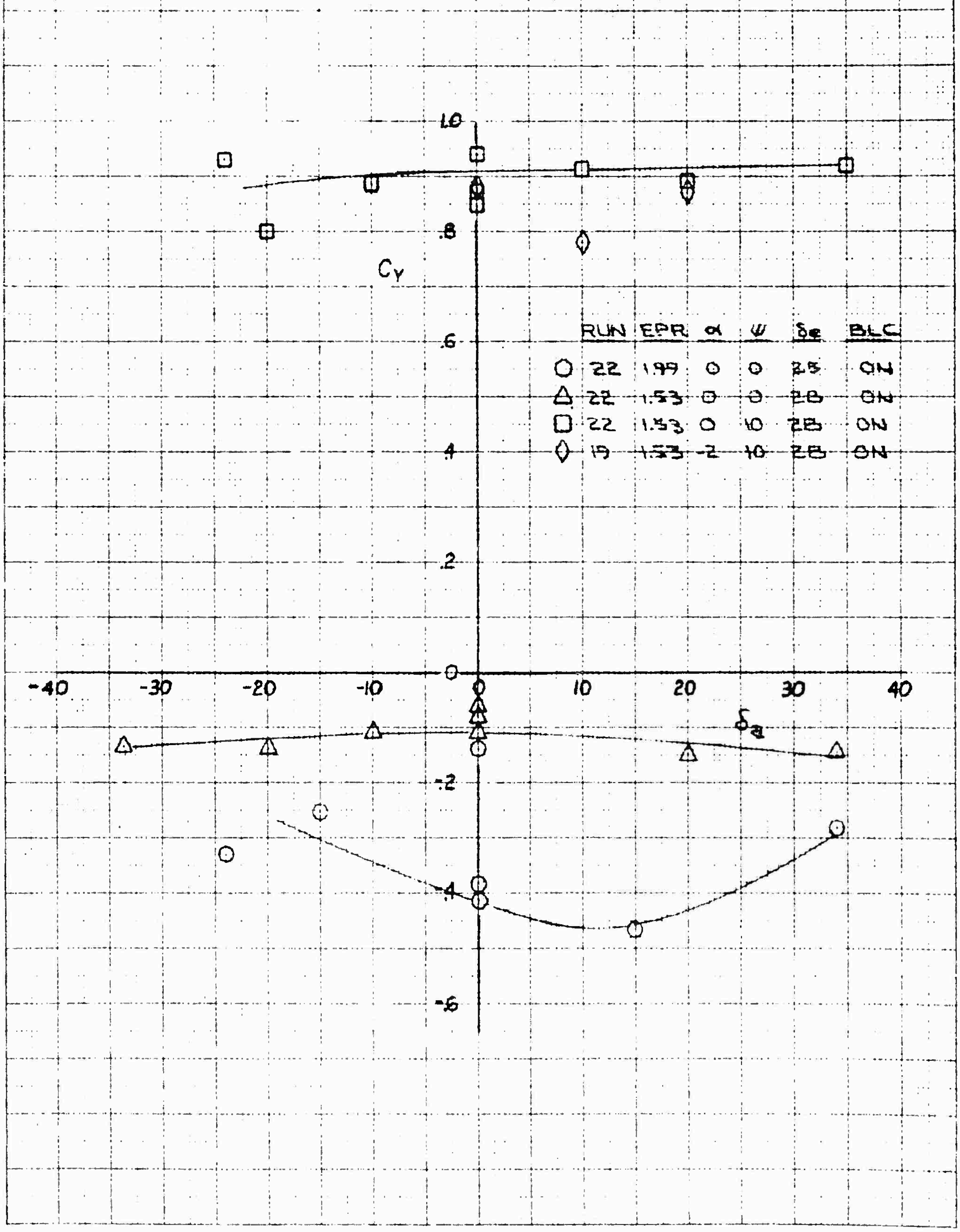

XV-4A
FULL SCALE WIND TUNNEL TEST 215
AILERON EFFECT ON YAWING MOMENT COEFFICIENT IN PHASE I AT 30 KNOTS

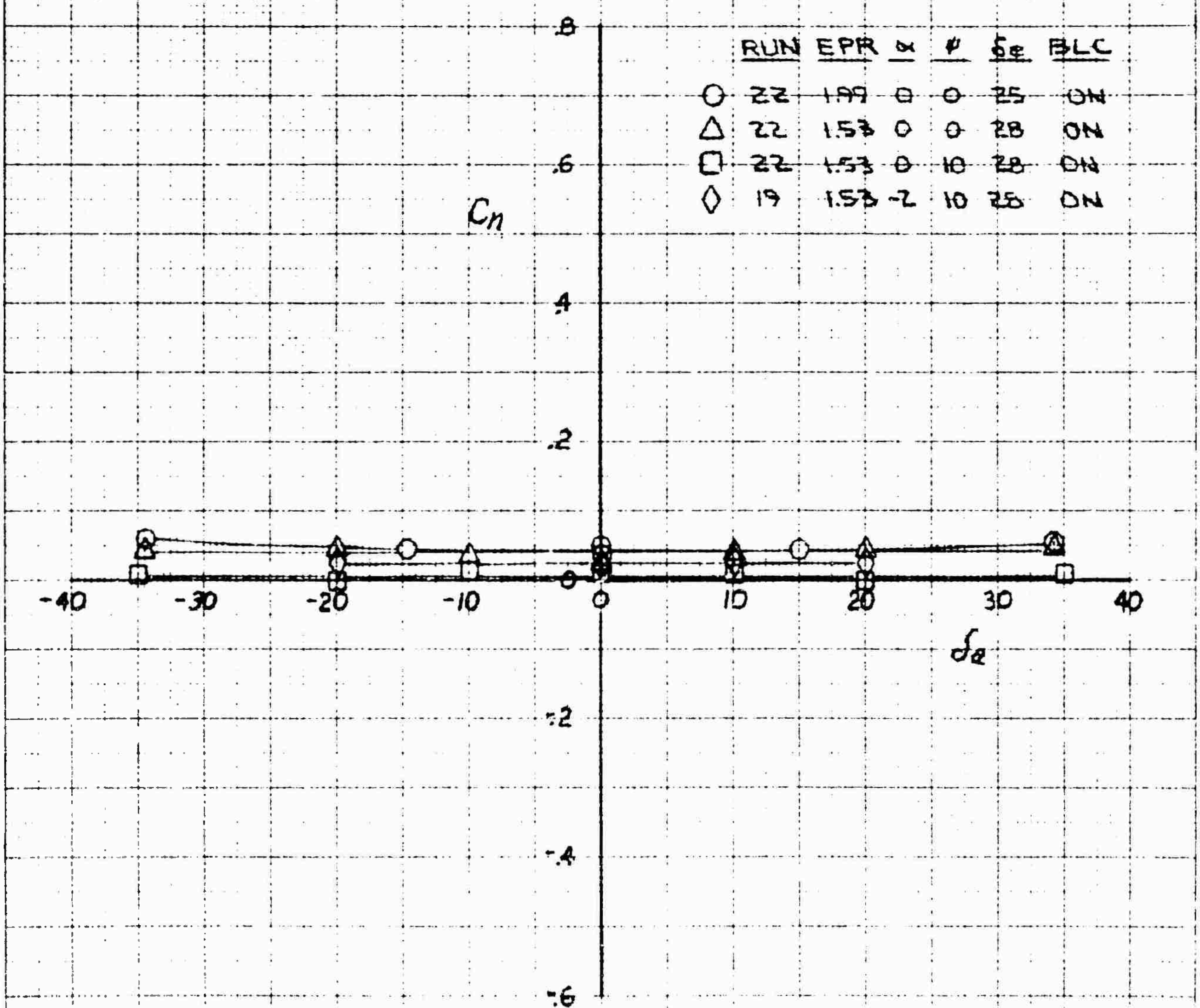

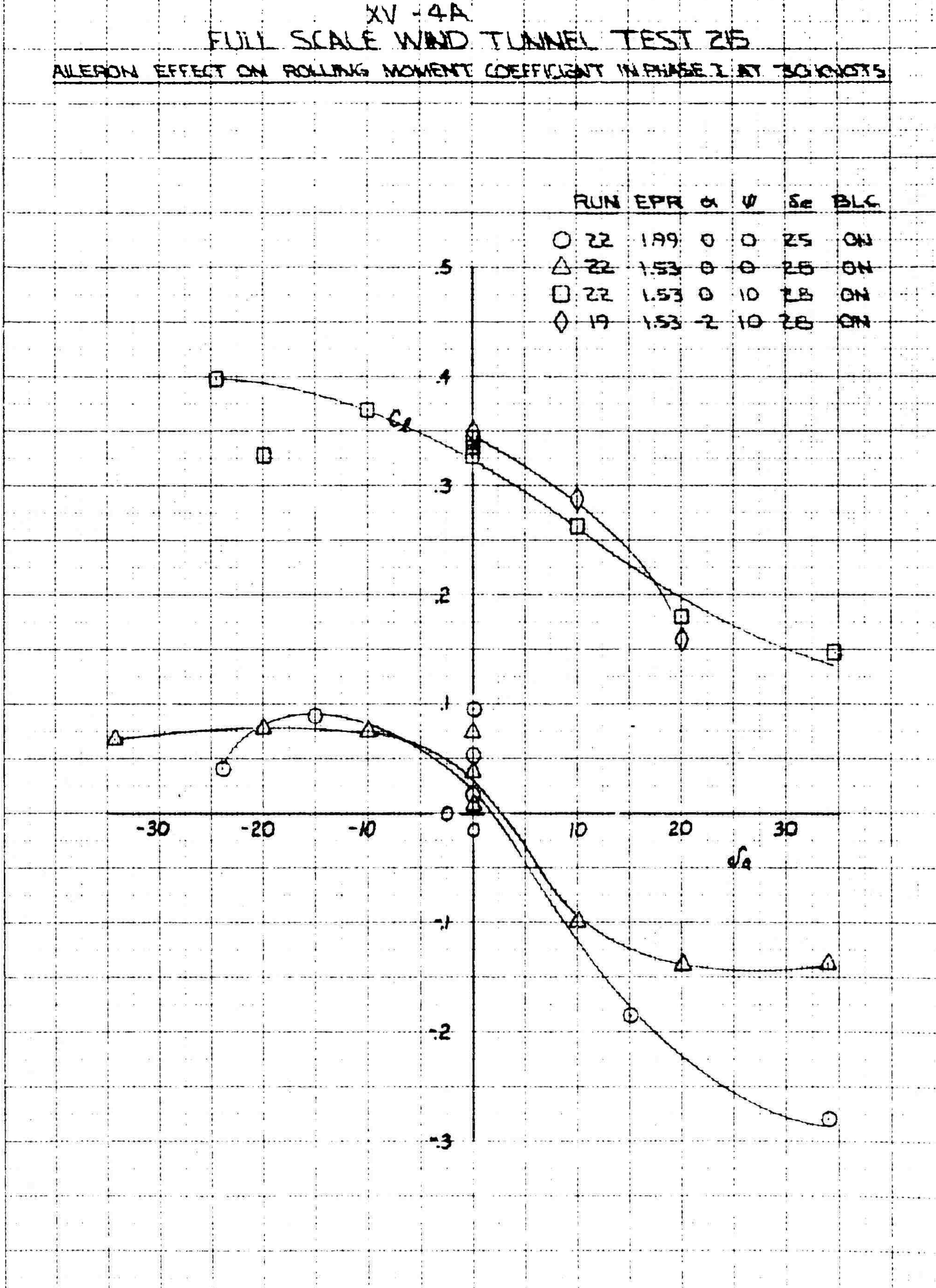
XV - 4A
FULL SCALE WIND TUNNEL TEST 215
AILERON EFFECT ON ROLLING MOMENT COEFFICIENT IN PHASE I AT 30 KNOTS
RUN EPR α ψ δe BLC
22 1.99 0 0 25 ON
22 1.53 0 0 25 ON
22 1.53 0 10 28 ON
19 1.53 -2 10 28 ON
Cl
.5
.4
.3
.2
.1
0
-.1
-.2
-.3
-30
-20
-10
0
10
20
30
δa

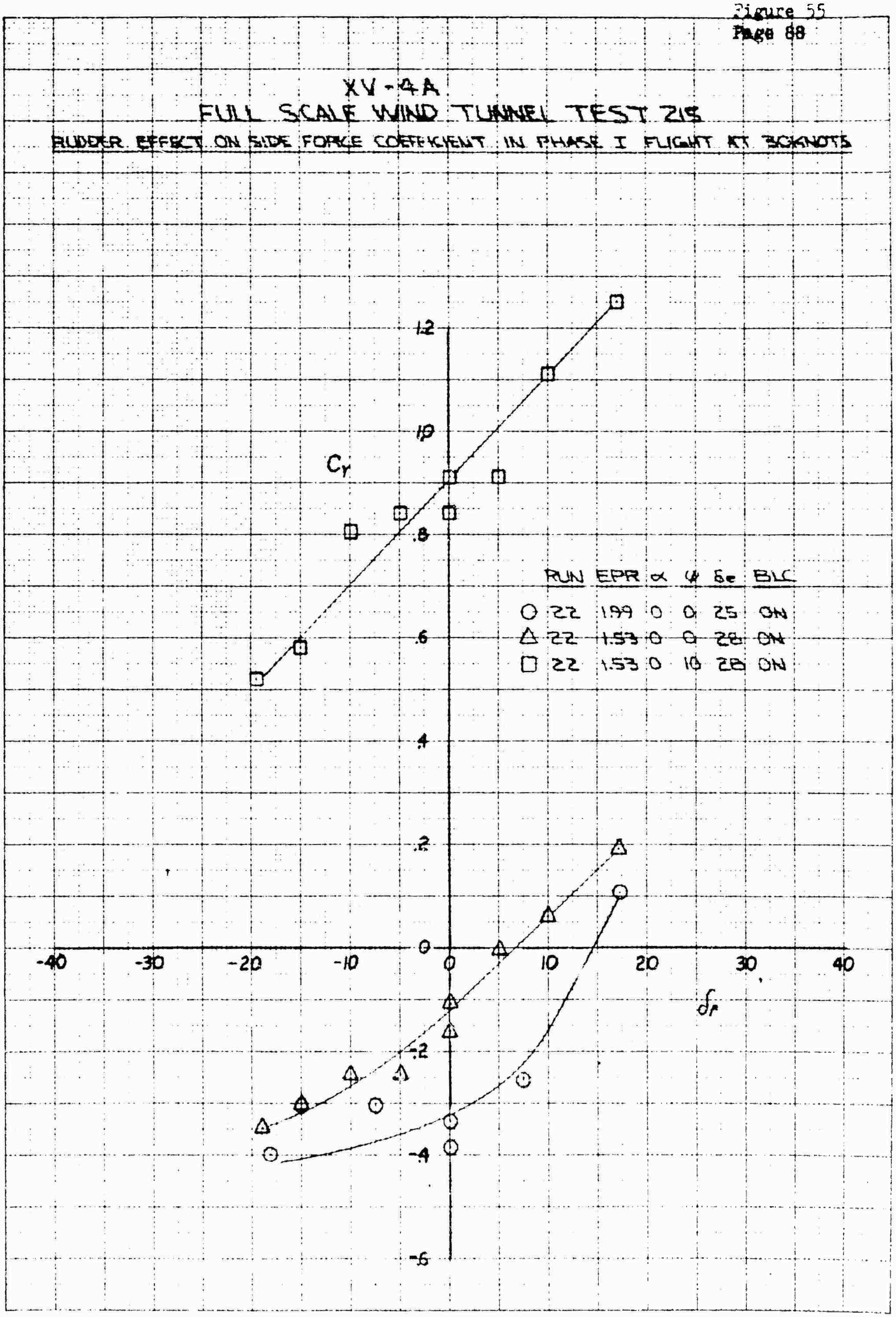
XV-4A
FULL SCALE WIND TUNNEL TEST 215
RUDDER EFFECT ON SIDE FORCE COEFFICIENT IN PHASE I FLIGHT AT 30KNOTS
C_Y
1.2
1.0
.8
.6
.4
.2
0
-.2
-.4
-.6
-40
-30
-20
-10
0
10
20
30
40
δ_r
RUN EPR α ψ δe BLC
○ 22 1.99 0 0 25 ON
△ 22 1.53 0 0 28 ON
□ 22 1.53 0 10 28 ON

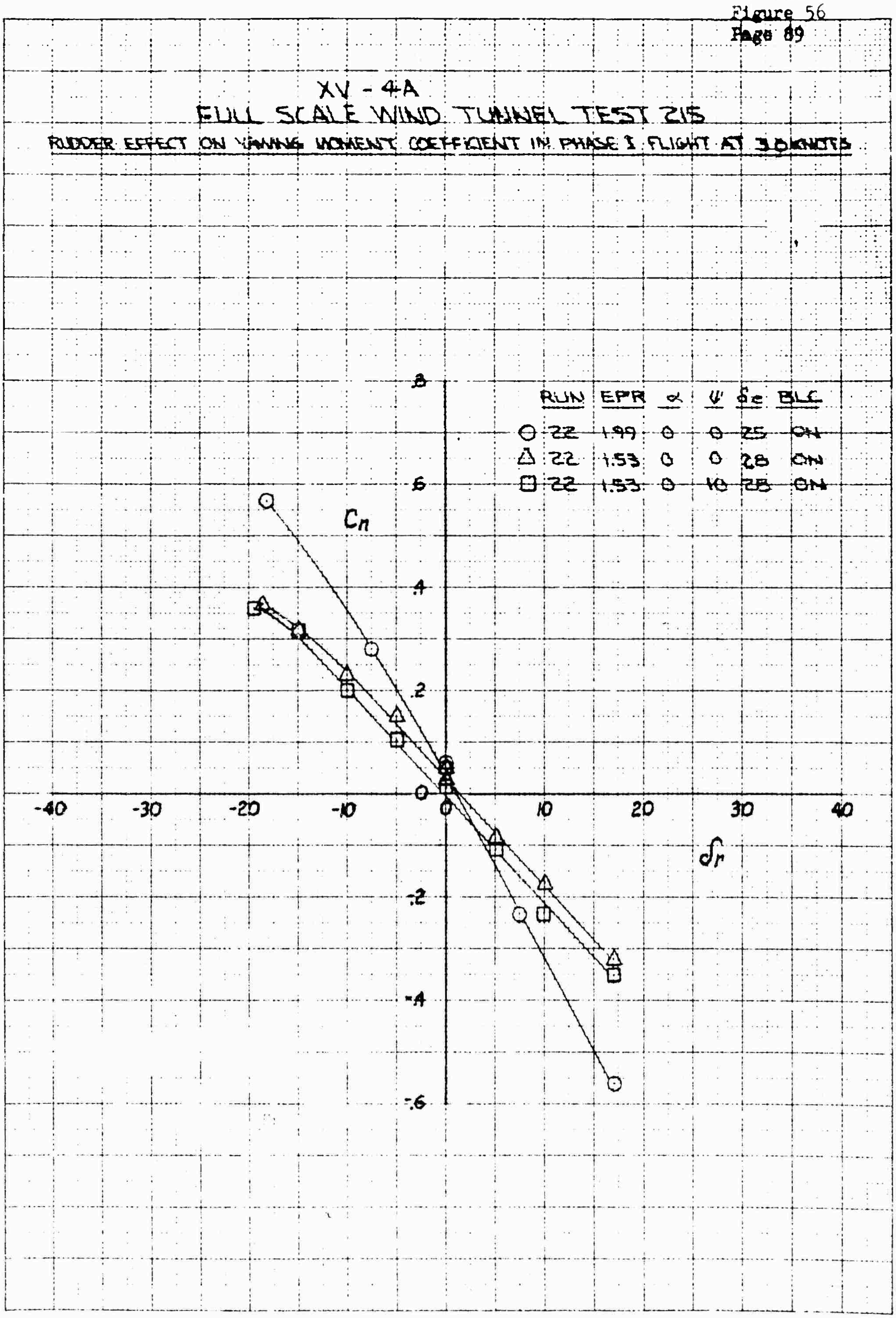
XV - 4A
FULL SCALE WIND TUNNEL TEST 215
RUDDER EFFECT ON YAWING MOMENT COEFFICIENT IN PHASE I FLIGHT AT 30 KNOTS
RUN EPR α ψ δe BLC
○ 22 1.99 0 0 25 ON
△ 22 1.53 0 0 28 ON
□ 22 1.53 0 10 25 ON
Cn
.8
.6
.4
.2
0
-.2
-.4
-.6
-40
-30
-20
-10
0
10
20
30
40
δr

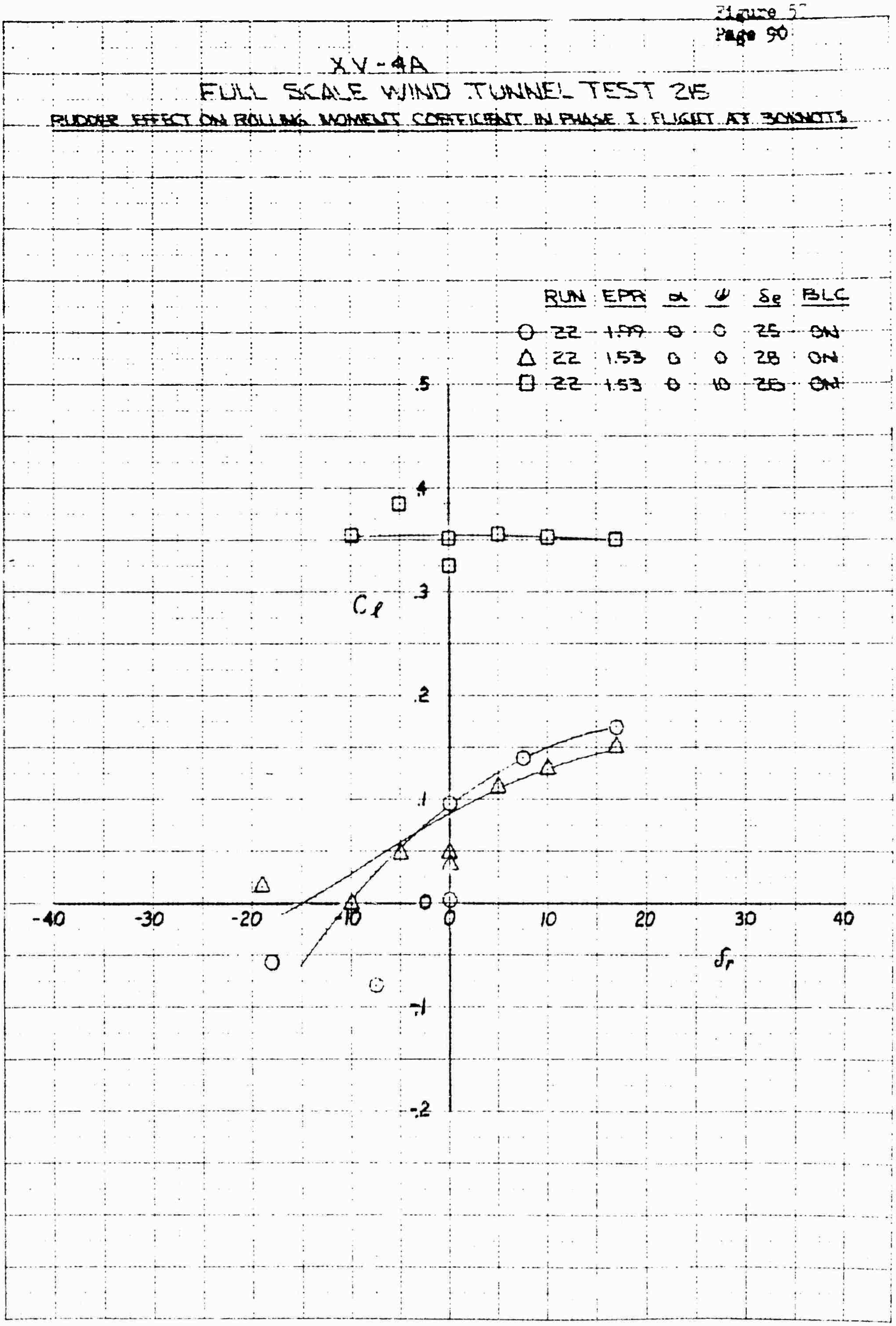
XV-4A
FULL SCALE WIND TUNNEL TEST 215
RUDDER EFFECT ON ROLLING MOMENT COEFFICIENT IN PHASE I FLIGHT AT 30 KNOTS
RUN EPR α ψ δe BLC
○ 22 1.99 0 0 25 ON
△ 22 1.53 0 0 28 ON
□ 22 1.53 0 10 25 ON
Cℓ
.5
.4
.3
.2
.1
0
-.1
-.2
-40
-30
-20
-10
0
10
20
30
40
δr

STABILITY AND CONTROL COMPARISON IN CONV

FULL SCALE DATA AMES 40' X 80'

Run No.		28	29	30	31	33	34
Ejector Doors		Closed	Closed	Closed	Closed	Closed	Cl
Flap Deflection (δ_f)	Deg.	40	40	40	0	40	40
Engines		Wind-milling	Wind-milling	Wind-milling	Wind-milling	Var. EPR	Var. EPR
Equivalent Airspeed	Knots	80	40	80	80	80	40
q	Lb/Ft^2	21.70	5.43	21.70	21.70	21.70	5.4
α	Deg.	Var.	Var.	0	Var.	Var.	0
β	Deg.	0	0	Var.	Var.	0	0
δ_e	Deg.	Var.	0	-18	Var.	Var.	0
δ_a	Deg.	Var.	0	Var.	Var.	0	0
δ_r	Deg.	Var.	0	Var.	Var.	0	0
C_{L_α}	1/Deg.	.090	.093	-	.088	.108	-
$C_{L_{\delta_e}}$	1/Deg.	+.0044	-	-	+.0048	+.0070	-
α (C_L = 0)	Deg.	-6.4	-6.5	-	-.6	-6.4	-
C_L (α = 0)		.58	.54	-	+.05	.76	-
$C_{L_{Max}}$		1.42	1.35	-	1.10	1.77	-
dC_M/dC_L		-.112	0	-	-.139	-.045	-
C_M (C_L = δ_e = 0)		-.205	-.30	-	-.160	-.33	-
$C_{M_{\delta_e}}$	1/Deg.	-.018	-	-	-.018	-.025	-

STABILITY AND CONTROL COMPARISON IN CONVENTIONAL FLIGHT

FULL SCALE DATA AMES 40' X 80'						EST. FROM SMALL SCALE DATA COMPARISON WITH RUN NO.			
29	30	31	33	34	35	28 & 30	31	33	35
Closed	Closed	Closed	Closed	Closed	Open	Closed	Closed	Closed	Open
40	40	0	40	40	40	40	0	40	40
Wind-milling	Wind-milling	Wind-milling	Var. EPR	Var. EPR	Wind-milling	Off	Off	EPR = 1.53	Off
40	80	80	80	40	80	-	-	80	-
5.43	21.70	21.70	21.70	5.43	21.70	-	-	21.70	-
Var.	0	Var.	Var.	0	Var.	-	-	21.70	-
0	Var.	Var.	0	0	Var.	-	-	-	-
0	-18	Var.	Var.	0	0	-	-	-	-
0	Var.	Var.	0	0	0	-	-	-	-
0	Var.	Var.	0	0	0	-	-	-	-
.093	-	.088	.108	-	.070	.089	.0863	.107	.070
-	-	+.0048	+.0070	-	-	+.00715	+.00715	+.00715	+.00715
-6.5	-	-.6	-6.4	-	-9.5	-6.6	+.245	-6.4	-8.35
.54	-	+.05	.76	-	.67	.60	-.021	.685	.585
1.35	-	1.10	1.77	-	1.52	1.82	1.20	1.75	1.62
0	-	-.139	-.045	-	-.432	-.078	-.147	-.0416	-.545
-.30	-	-.160	-.33	-	-.035	-.065	+.0615	.0282	.310
-	-	-.018	-.025	-	-	-.0252	-.0252	-.0252	-.0252

FULL SCALE DATA AMES 40' X 80'

Run No.		28	29	30	31	33	34
C_Y ($\delta_a = \delta_r = \beta = 0$)		-.008	-	-.018	-.008	-	-
C_{Y_β}	1/Deg.	-	-	-.020	-.020	-	-
$C_{Y_{\delta_a}}$	1/Deg.	0	-	0	0	-	-
$C_{Y_{\delta_r}}$	1/Deg.	+.0053	-	+.0053	+.0053	-	-
C_n ($\delta_a = \delta_r = \beta = 0$)		-.0020	-	-.0030	-.0020	-	-
C_{n_β}	1/Deg.	-	-	+.0045	+.0045	-	-
$C_{n_{\delta_a}}$	1/Deg.	-.00013	-	-.00013	-.00013	-	-
$C_{n_{\delta_r}}$	1/Deg.	-.0033	-	-.0033	-.0033	-	-
C_l ($\delta_a = \delta_r = \beta = 0$)		+..027	-	+.016	+.014	-	-
C_{l_β}	1/Deg.	-	-	-.0018	-.0018	-	-
$C_{l_{\delta_a}}$	1/Deg.	-.0011	-	-.0011	-.0011	-	-
$C_{l_{\delta_r}}$	1/Deg.	+.0008	-	+.0008	+.0008	-	-
$dC_M/dEPR$		-	-	-	-	+.270	+.2
$dC_L/dEPR$		-	-	-	-	+.035	-.1

A

STABILITY AND CONTROL COMPARISON IN CONVENTIONAL FLIGHT

E[illegible]-7034
Fig. [illegible] (Cont'd)
Page 190A

FULL SCALE DATA AMES 40' X 80'						EST. FROM SMALL SCALE DATA [illegible] COMPARISON WITH RUN NO.			
29	30	31	33	34	35	28 & 30	31	33	35
-	-.018	-.008	-	-	-.010	0	0	0	-
-	-.020	-.020	-	-	-.019 (α = 0) -.016 (α = 8)	-.0196	-.0196	-.0196	-
-	0	0	-	-	-	0	0	0	-
-	+.0053	+.0053	-	-	-	+.0040	+.0040	+.0040	-
-	-.0030	-.0020	-	-	+.0010	0	0	0	-
-	+.0045	+.0045	-	-	+.0014 (α = 0) -.0011 (α = 8)	+.0030	+.0030	+.0030	-
-	-.00013	-.00013	-	-	-	Neg.	Neg.	Neg.	-
-	-.0033	-.0033	-	-	-	-.00212	-.00212	-.00212	-
-	+.016	+.014	-	-	+.003	0	0	0	-
-	-.0018	-.0018	-	-	-.0026 (α = 0) -.0008 (α = 8)	-.0026	-.0026	-.0026	-
-	-.0011	-.0011	-	-	-	-.00082	-.00082	-.00082	-
-	+.0008	+.0008	-	-	-	+.00076	+.00076	+.00076	-
-	-	-	+.270	+.250	-	-	-	-	-
-	-	-	+.035	-.150	-	-	-	-	-

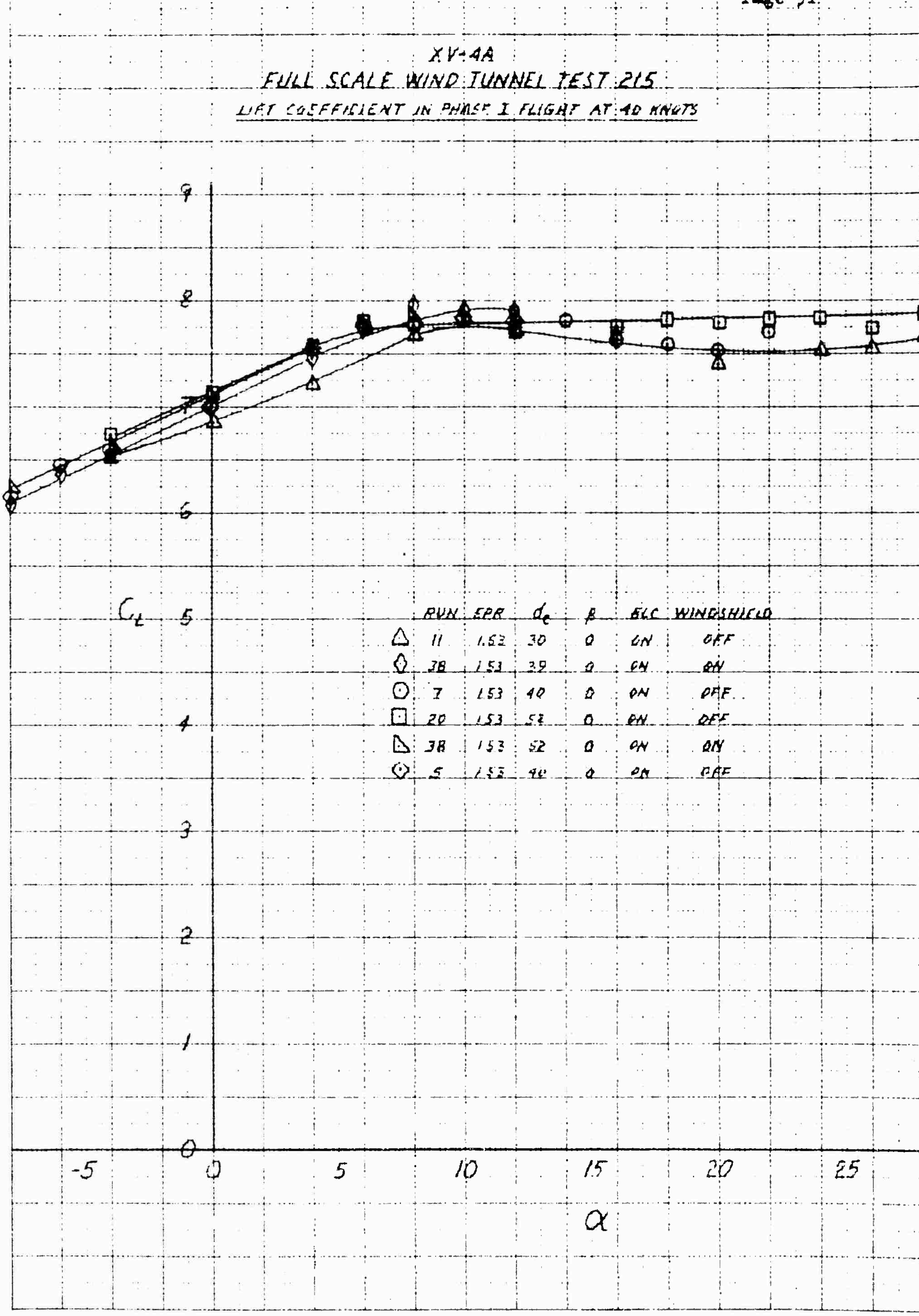
XV-4A
FULL SCALE WIND TUNNEL TEST 215
LIFT COEFFICIENT IN PHASE I FLIGHT AT 40 KNOTS
RUN EPR d_e β BLC WINDSHIELD
△ 11 1.52 30 0 ON OFF
◇ 38 1.53 39 0 ON ON
⊙ 7 1.53 40 0 ON OFF
□ 20 1.53 52 0 ON OFF
◺ 38 1.53 52 0 ON ON
◇ 5 1.53 40 0 ON OFF
C_L
0
1
2
3
4
5
6
8
9
-5
0
5
10
15
20
25
α

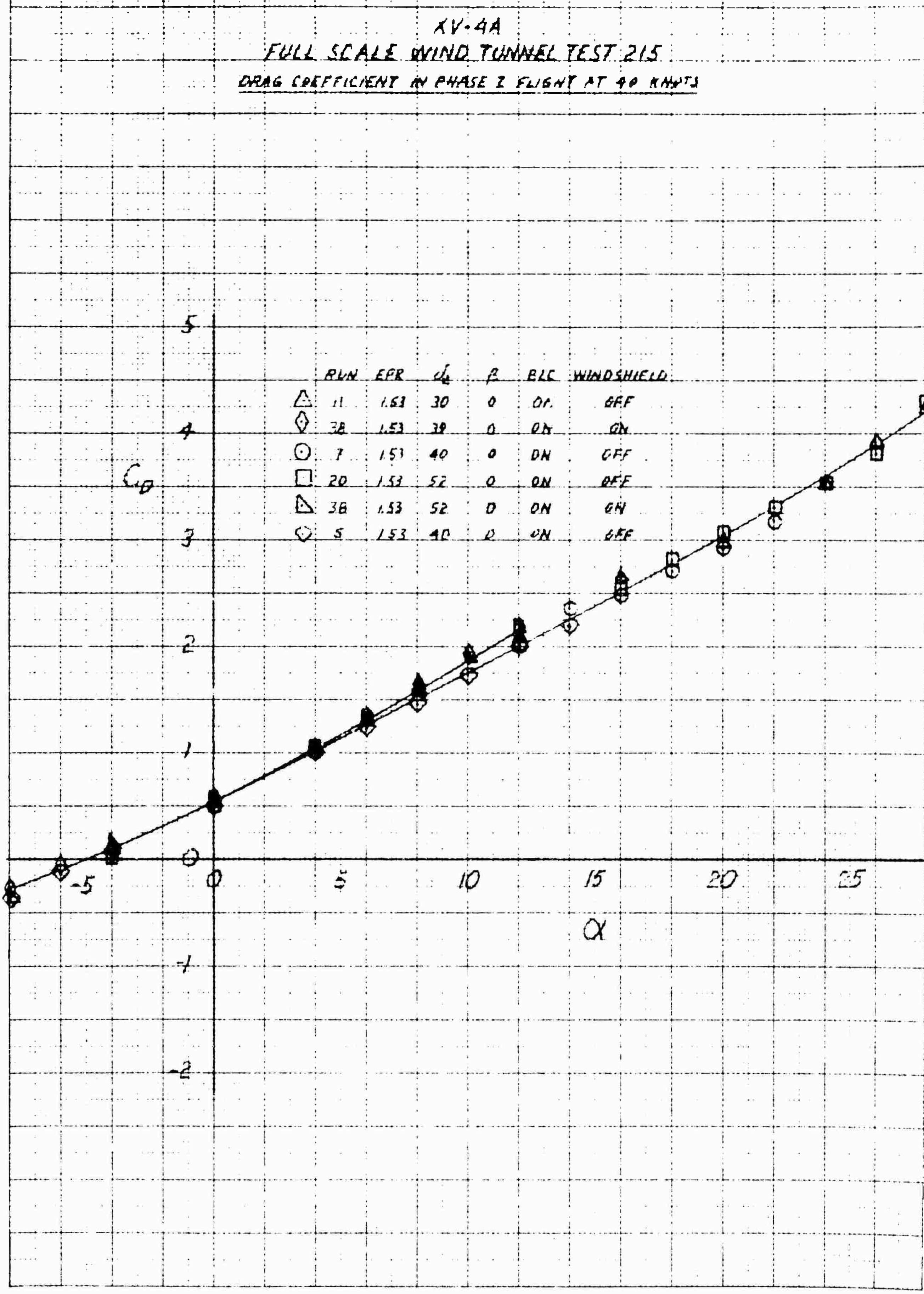
XV-4A
FULL SCALE WIND TUNNEL TEST 215
DRAG COEFFICIENT IN PHASE I FLIGHT AT 40 KNOTS
RUN EPR δ_f β BLC WINDSHIELD
11 1.53 30 0 ON OFF
38 1.53 39 0 ON ON
7 1.53 40 0 ON OFF
20 1.53 52 0 ON OFF
38 1.53 52 0 ON ON
5 1.53 40 0 ON OFF
C_D
α
5
4
3
2
1
-1
-2
-5
0
5
10
15
20
25

XV-4A

FULL SCALE WIND TUNNEL TEST 215

PITCHING MOMENT COEFFICIENT IN PHASE I FLIGHT AT 40 KNOTS

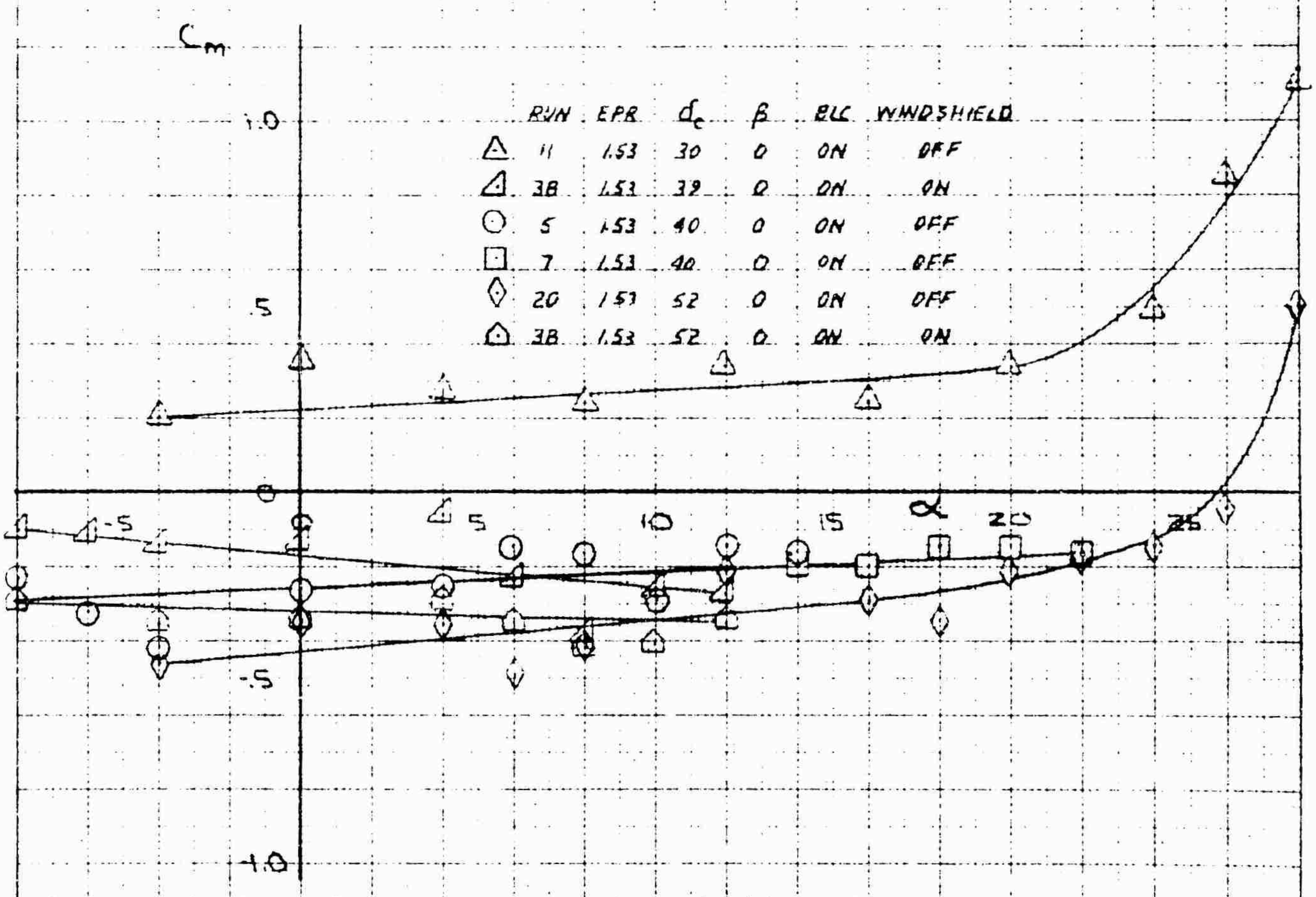

XV-4A
FULL SCALE WIND TUNNEL TEST 215
SIDE FORCE COEFFICIENT IN PHASE I FLIGHT AT 40 KNOTS

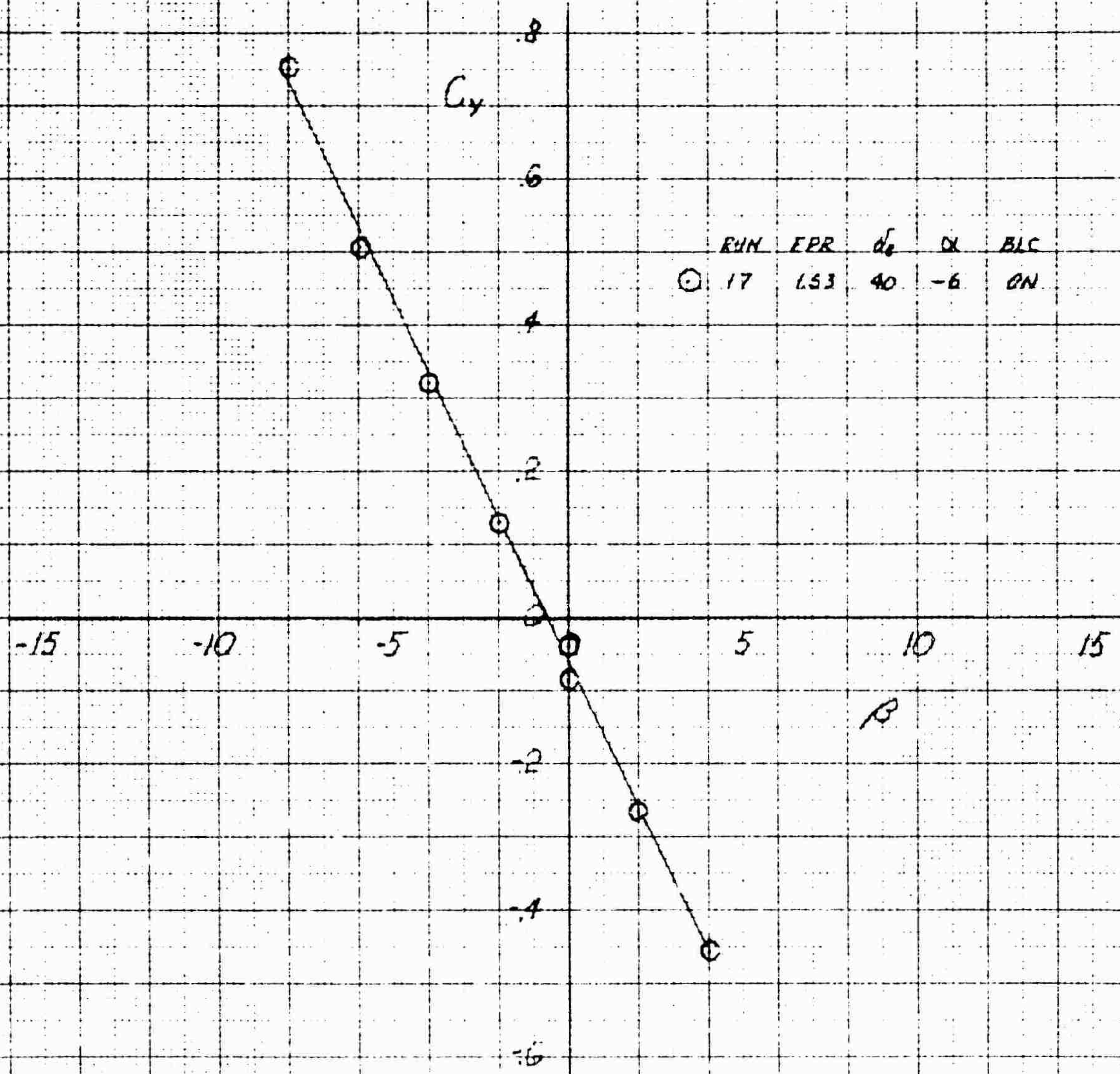

XV-4A

FULL SCALE WIND TUNNEL TEST 215

YAWING MOMENT COEFFICIENT IN PHASE I FLIGHT AT 40 KNOTS

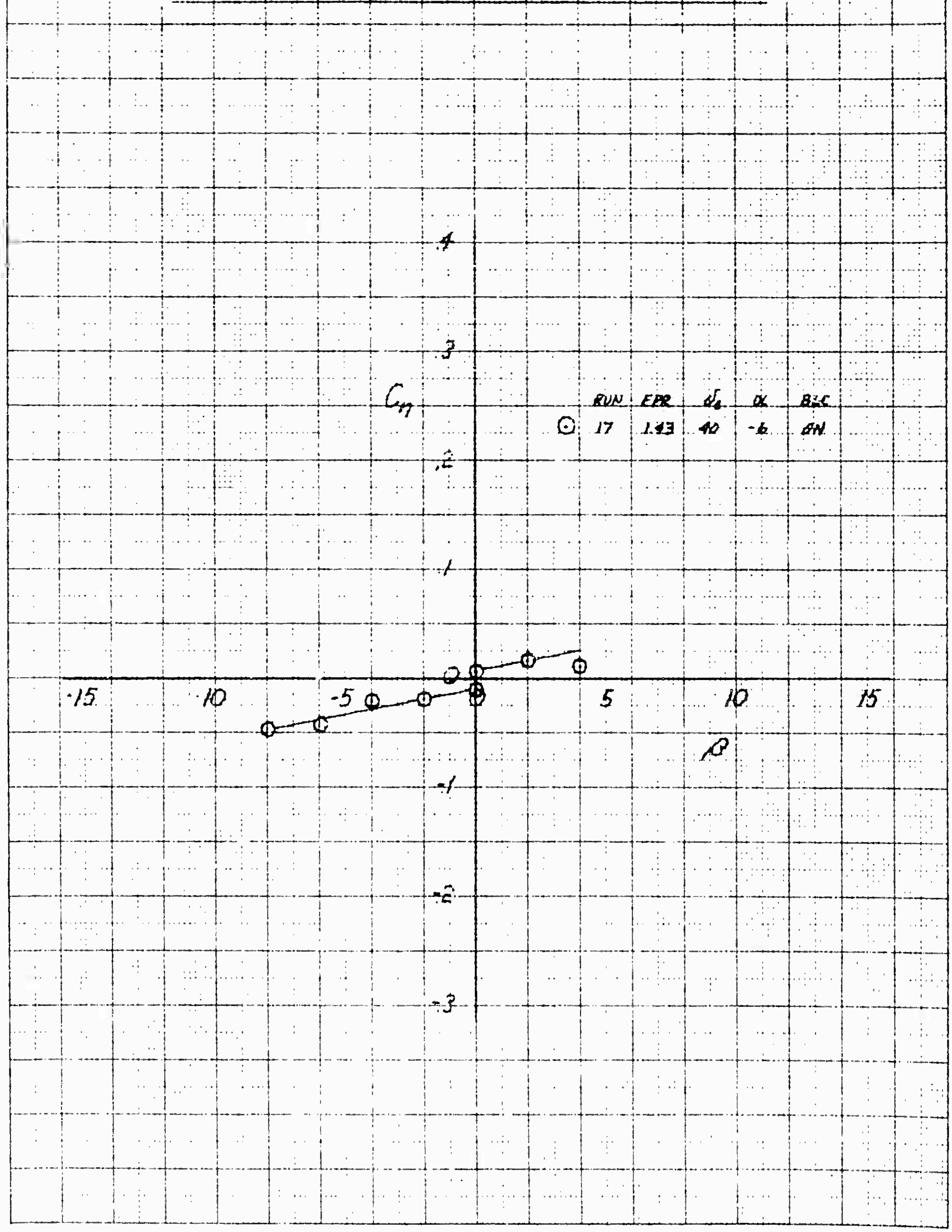

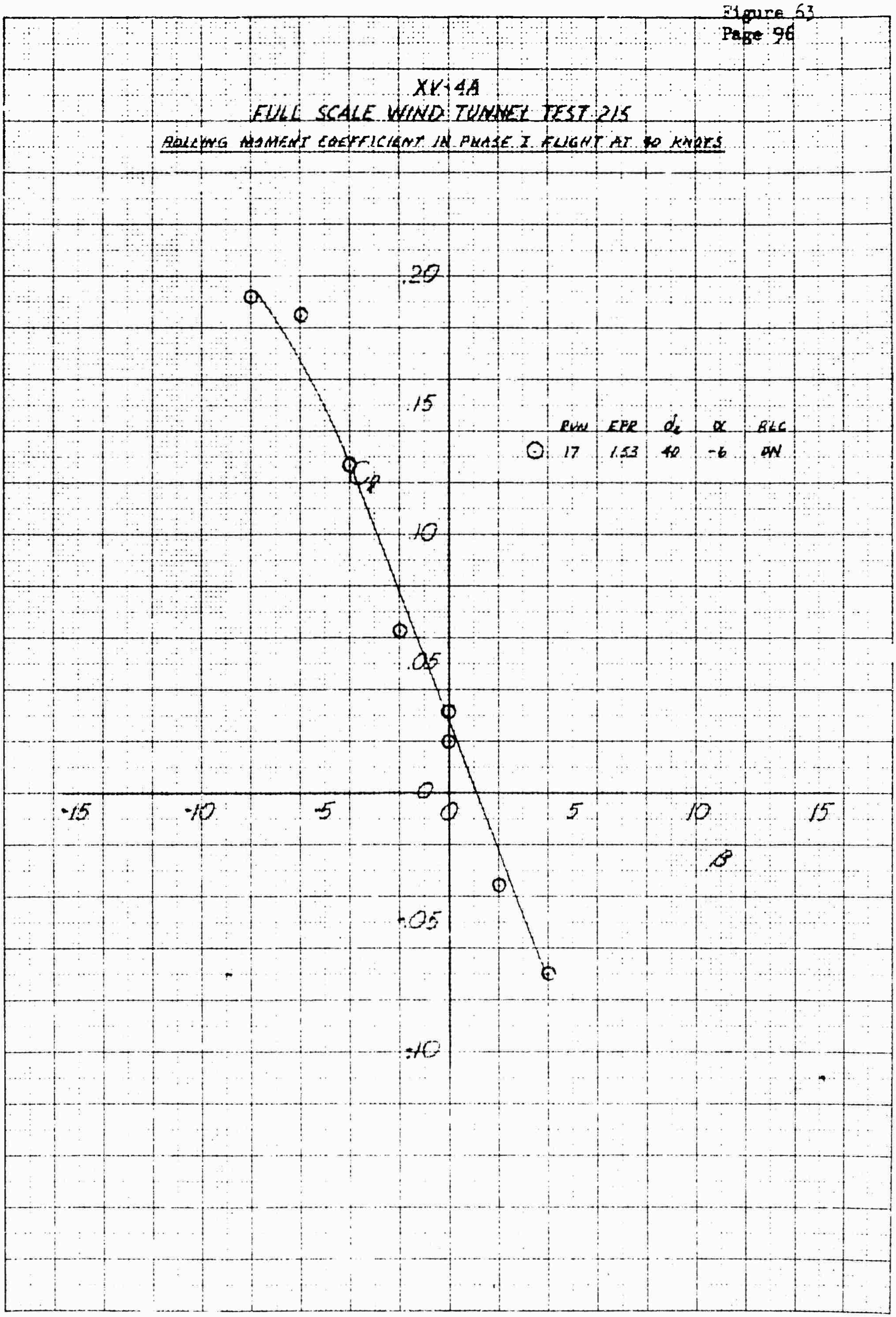
XV-4A
FULL SCALE WIND TUNNEL TEST 215
ROLLING MOMENT COEFFICIENT IN PHASE I FLIGHT AT 40 KNOTS
RUN EPR d_i α BLC
17 1.53 40 -6 ON
.20
.15
.10
.05
0
-.05
-.10
-15
-10
-5
0
5
10
15
β
C_l

XVF 4A

FULL SCALE WIND TUNNEL TEST 215

ELEVATOR EFFECT ON LIFT COEFFICIENT IN PHASE I FLIGHT AT [illegible]KNOTS

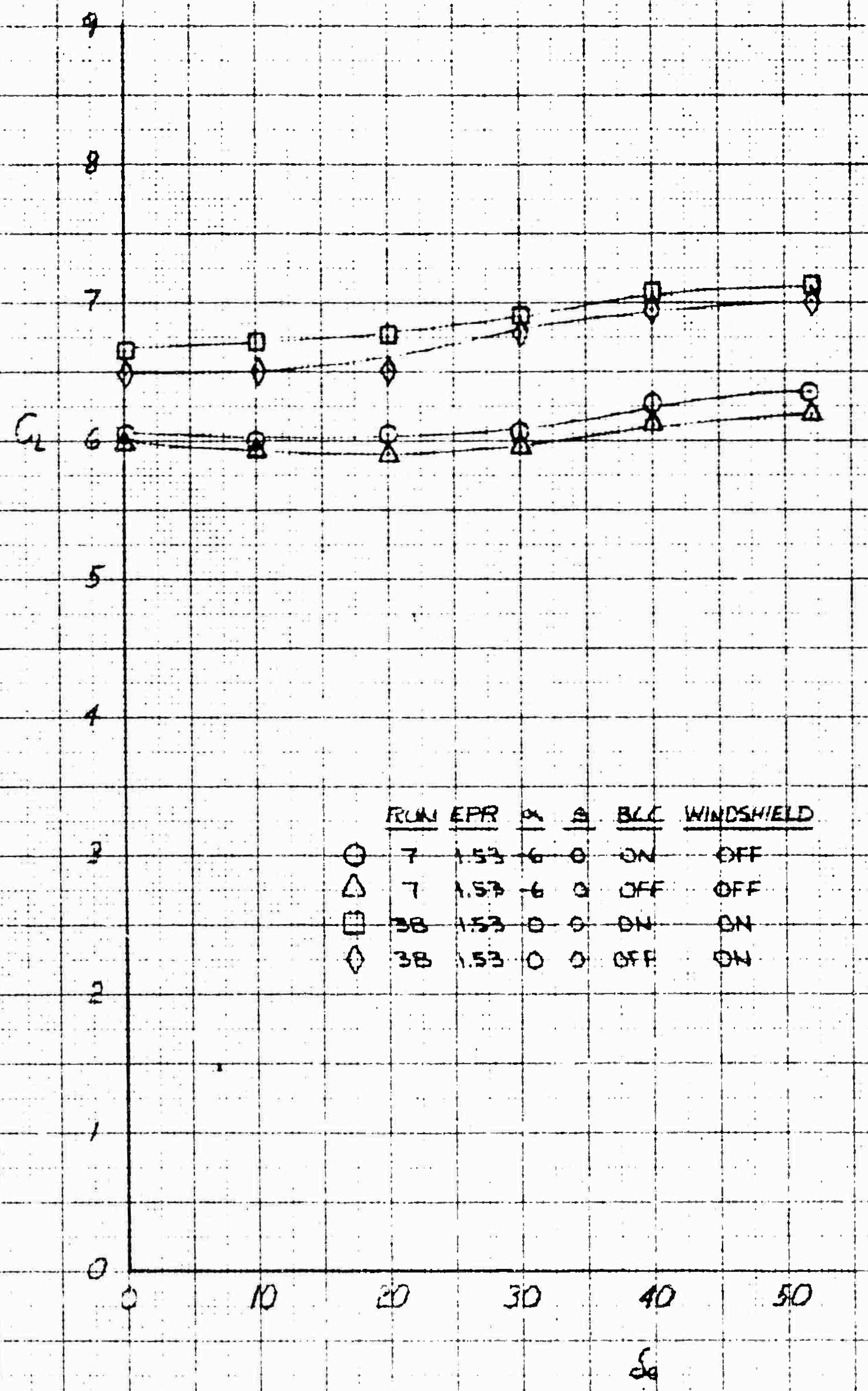

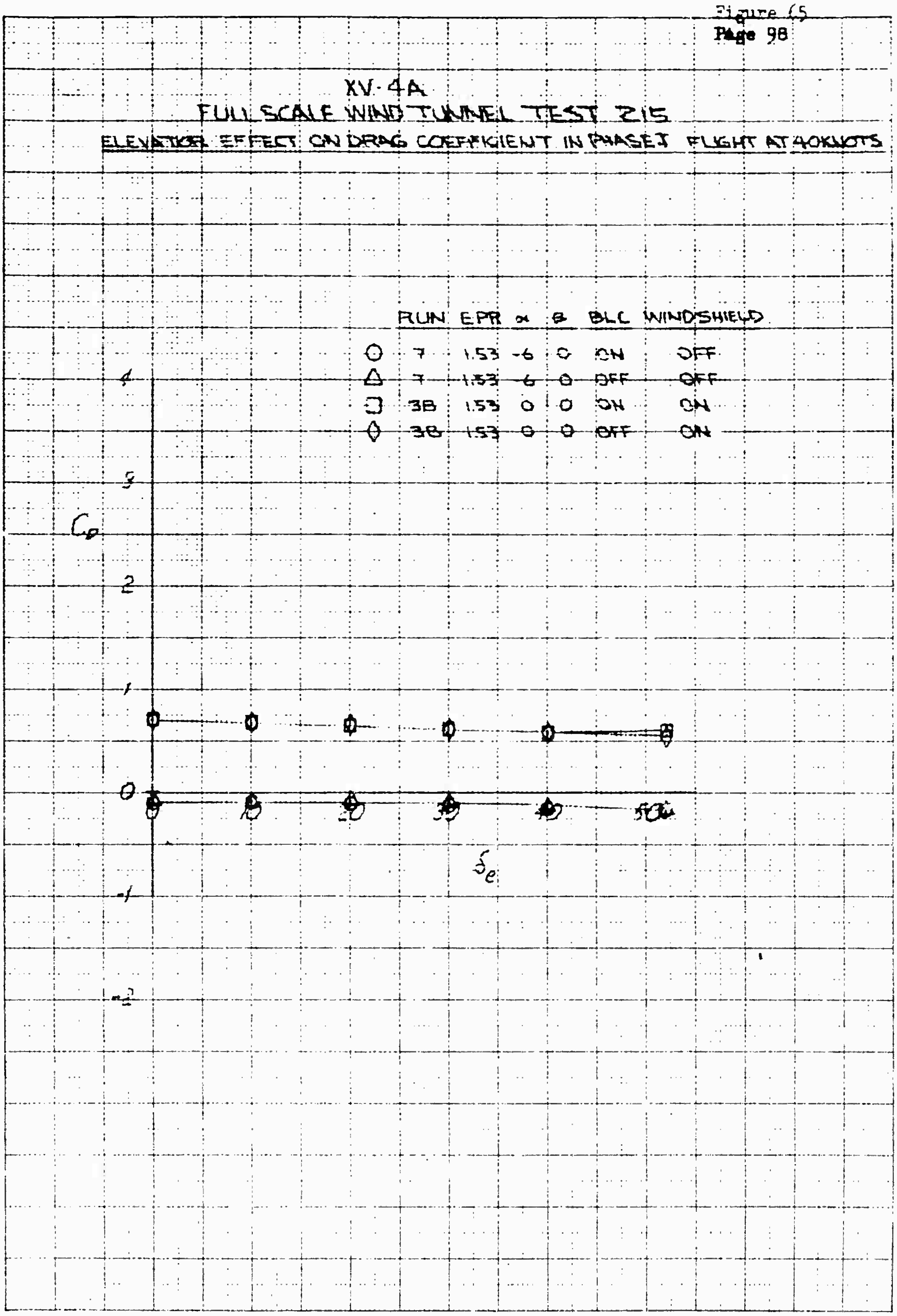
XV-4A
FULL SCALE WIND TUNNEL TEST 215
ELEVATOR EFFECT ON DRAG COEFFICIENT IN PHASE I FLIGHT AT 40KNOTS
RUN EPR α β BLC WINDSHIELD
○ 7 1.53 -6 0 ON OFF
△ 7 1.53 -6 0 OFF OFF
□ 38 1.53 0 0 ON ON
◇ 38 1.53 0 0 OFF ON
C_D
4
3
2
1
0
-1
-2
0
10
20
30
40
50
δ_e

XV-4A
FULL SCALE WIND TUNNEL TEST 215
ELEVATOR EFFECT ON PITCHING MOMENT COEFFICIENT IN PHASE I AT 40KNOTS

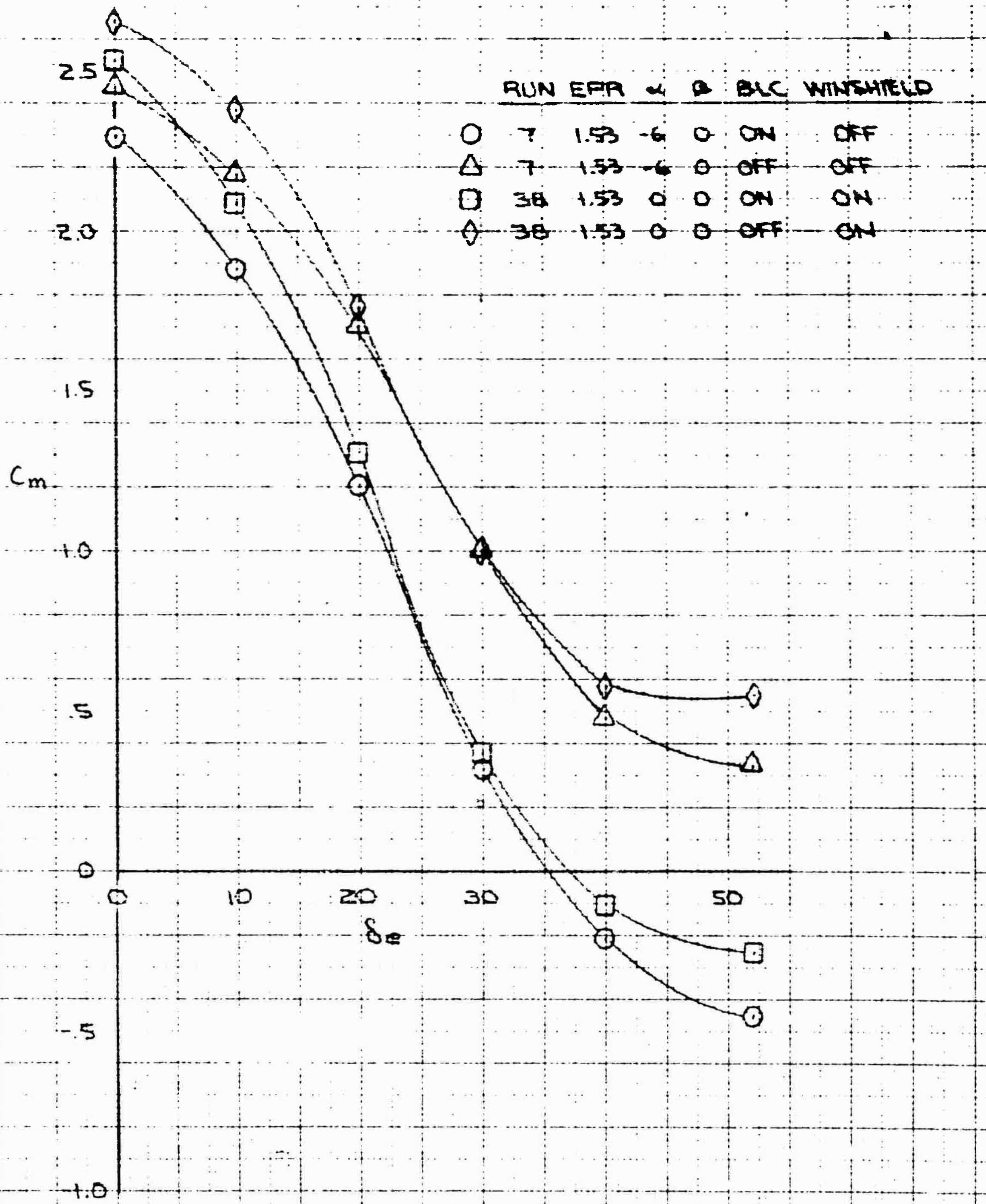

XV-4A
FULL SCALE WIND TUNNEL TEST 215
AILERON EFFECT ON SIDE FORCE COEFFICIENT IN PHASE I FLIGHT AT 40 KNOTS

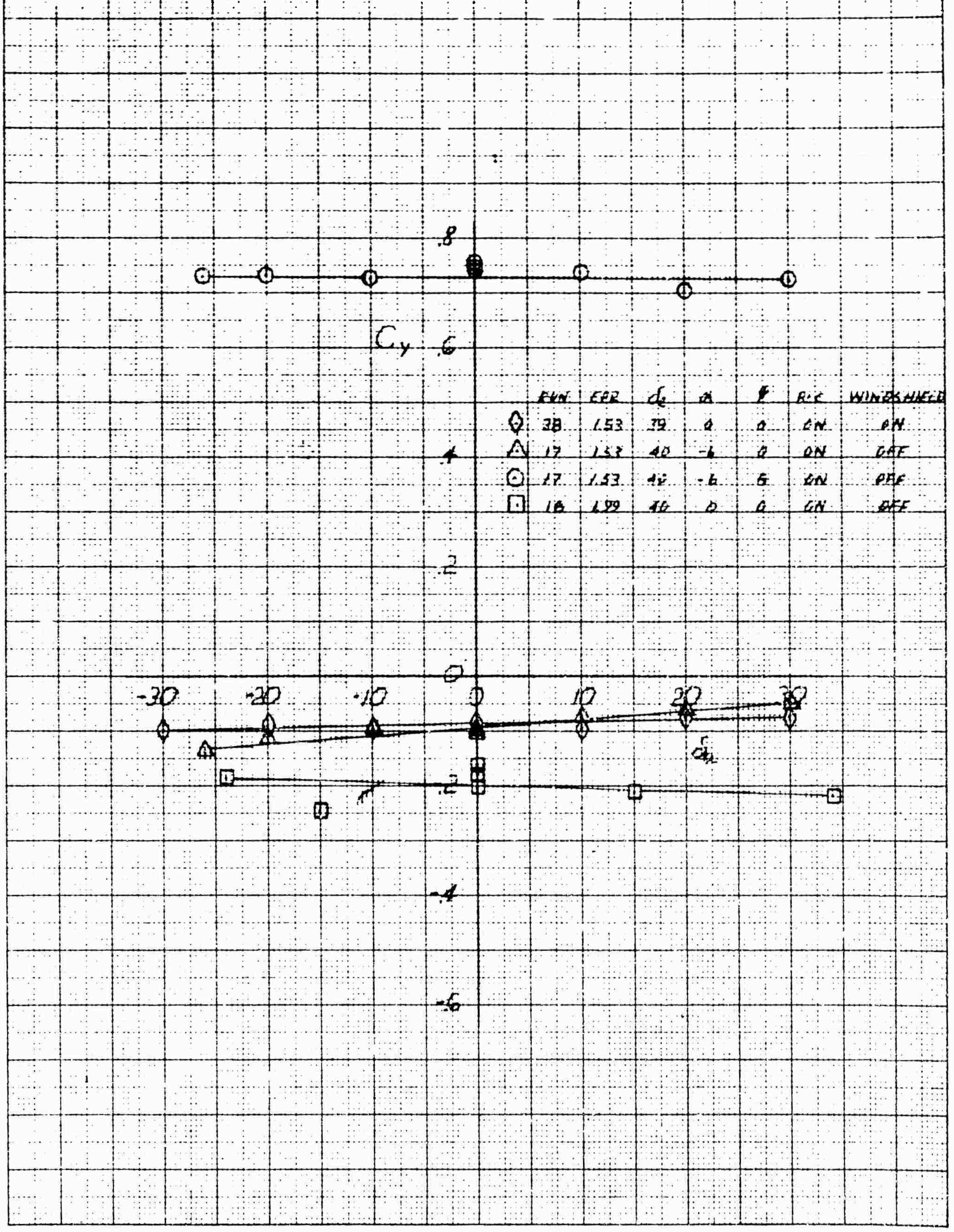

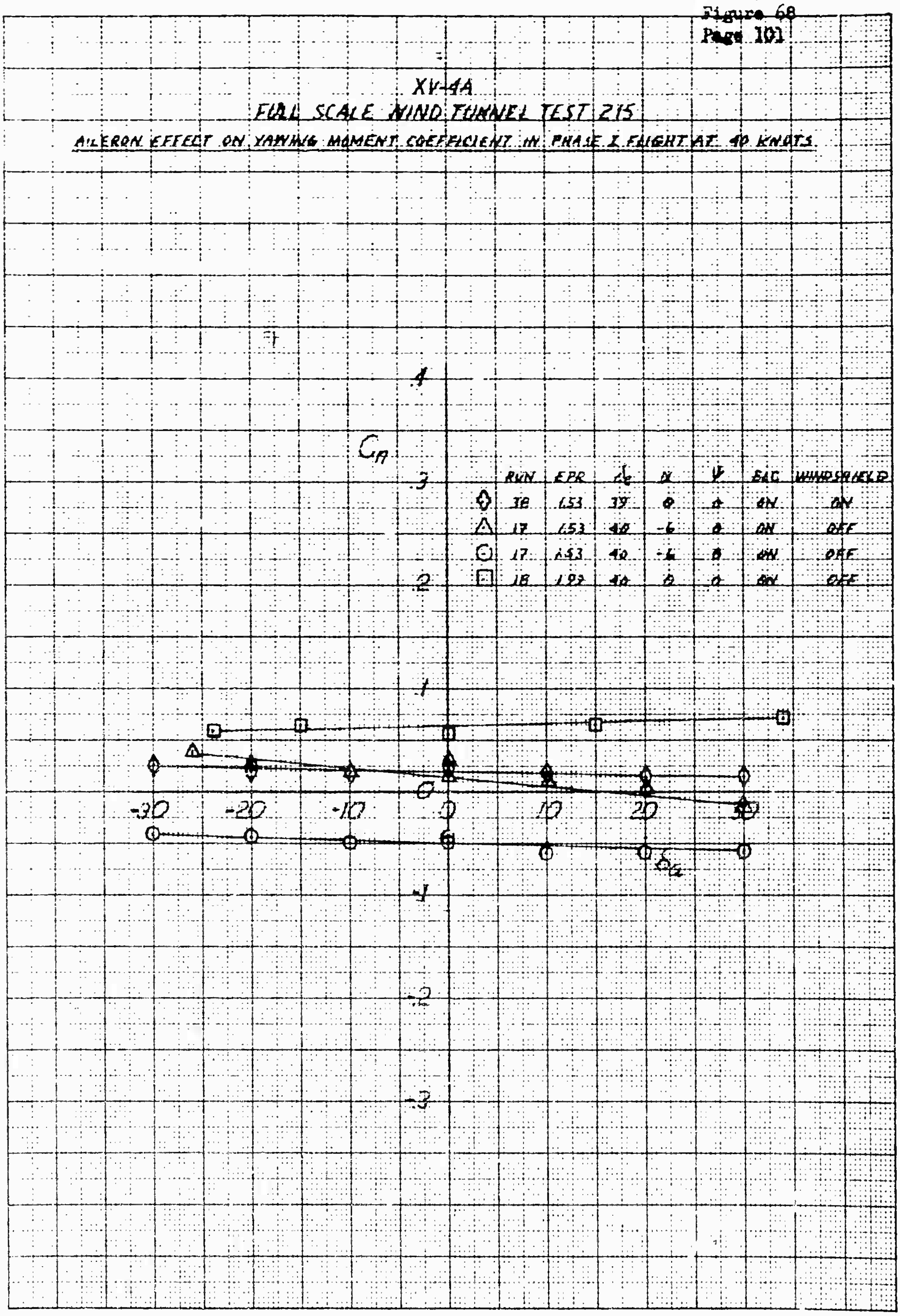
XV-4A
FULL SCALE WIND TUNNEL TEST 215
AILERON EFFECT ON YAWING MOMENT COEFFICIENT IN PHASE I FLIGHT AT 40 KNOTS
.4
.3
.2
.1
0
-.1
-.2
-.3
C_n
-30
-20
-10
0
10
20
30
δ_a
RUN EPR δ_f α ψ SAS WINDSHIELD
38 1.53 39 0 0 ON ON
17 1.53 40 -6 0 ON OFF
17 1.53 40 -6 0 ON OFF
18 1.97 40 0 0 ON OFF

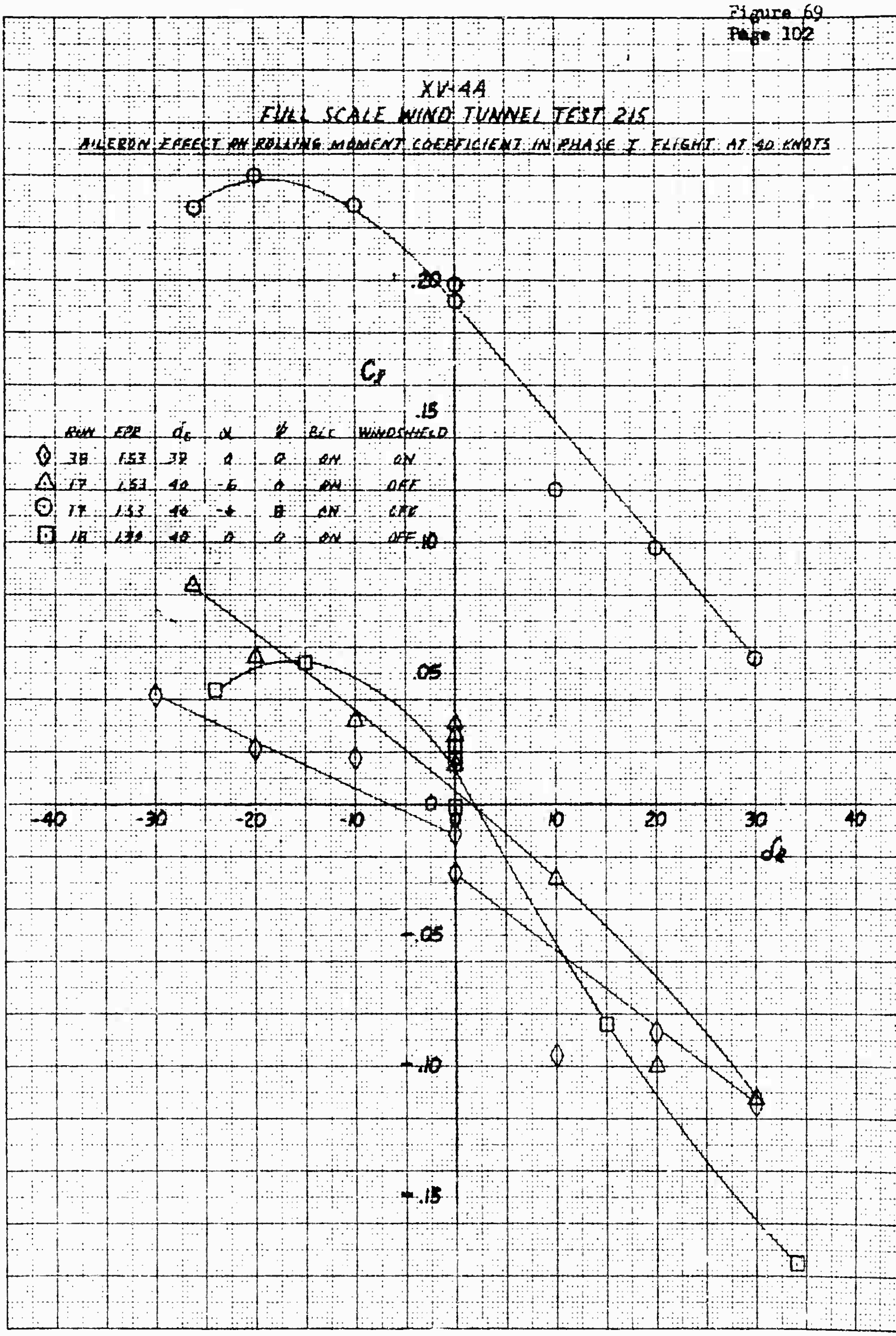
XV-4A
FULL SCALE WIND TUNNEL TEST 215
AILERON EFFECT ON ROLLING MOMENT COEFFICIENT IN PHASE I FLIGHT AT 40 KNOTS
RUN
EPR
WINDSHIELD
.20
.15
.10
.05
-.05
-.10
-.15
-40
-30
-20
-10
10
20
30
40

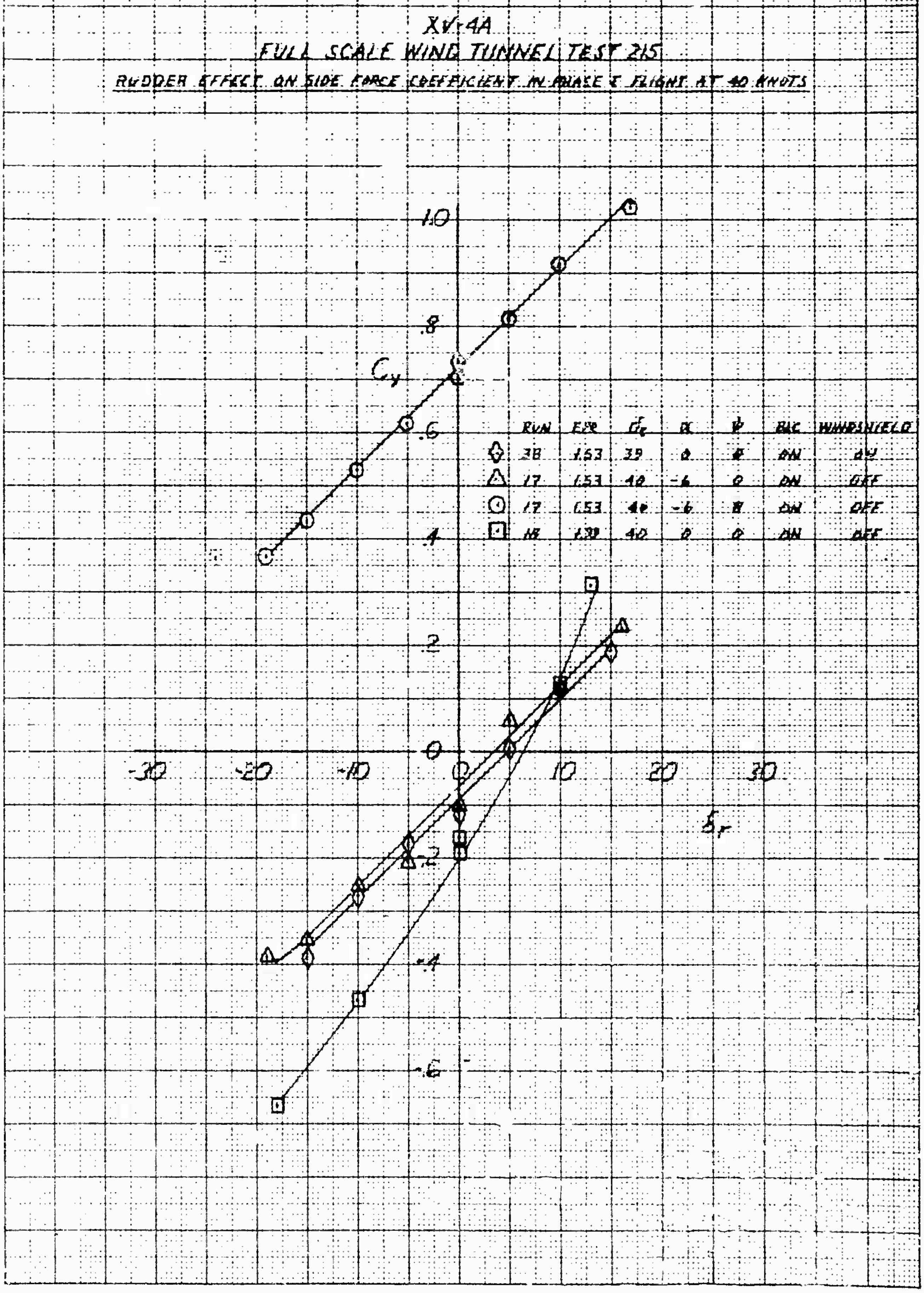
XV-4A
FULL SCALE WIND TUNNEL TEST 215
RUDDER EFFECT ON SIDE FORCE COEFFICIENT IN PHASE I FLIGHT AT 40 KNOTS
RUN EPR θ α ψ BLC WINDSHIELD
38 1.53 39 0 0 ON
17 1.53 40 -6 0 ON OFF
17 1.53 40 -6 8 ON OFF
18 1.30 40 0 0 ON OFF
C_y
1.0
.8
.6
.4
.2
0
-.2
-.4
-.6
-30 -20 -10 0 10 20 30
δ_r

XV-4A
FULL SCALE WIND TUNNEL TEST 215
RUDDER EFFECT ON YAWING MOMENT COEFFICIENT IN PHASE I FLIGHT AT 40 KNOTS

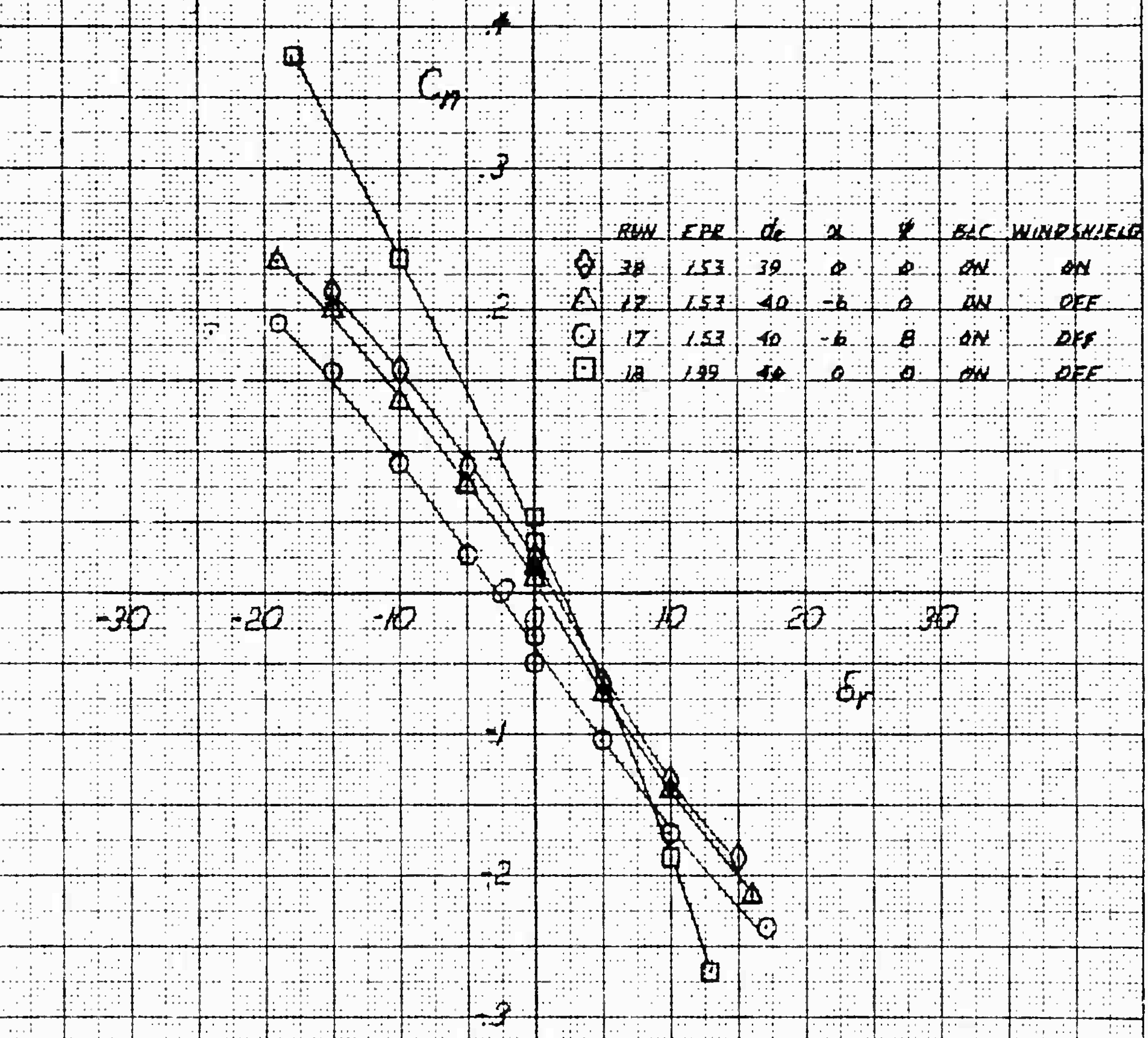

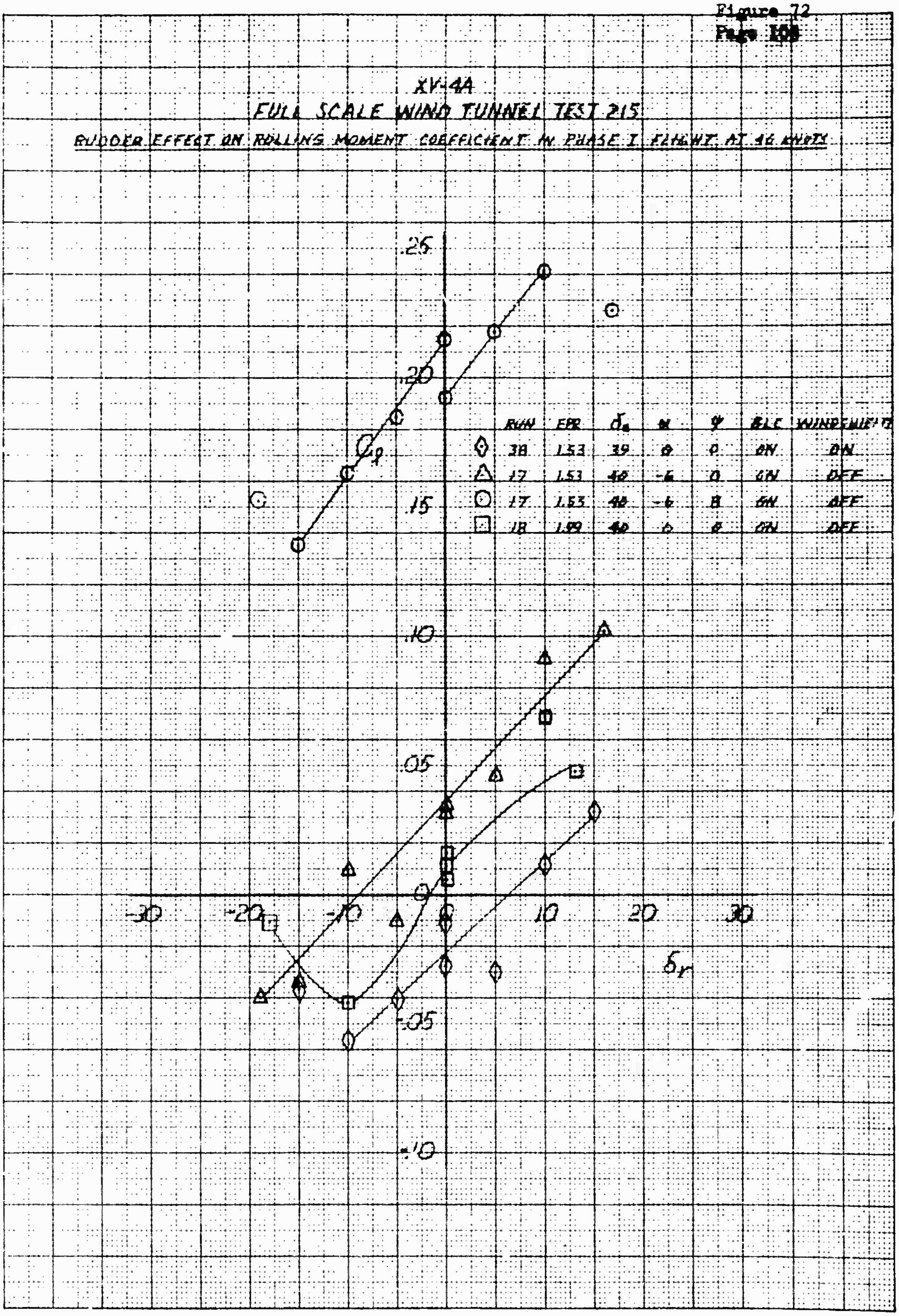
XV-4A
FULL SCALE WIND TUNNEL TEST 215
RUDDER EFFECT ON ROLLING MOMENT COEFFICIENT IN PHASE I FLIGHT AT 46 KNOTS
.25
.20
.15
.10
.05
-.05
-.10
C_ℓ
-30
-20
-10
0
10
20
30
δ_r
RUN EPR δ_a α ψ BLC WINDSHIELD
38 1.53 39 0 0 ON ON
17 1.53 40 -6 0 ON OFF
17 1.53 40 -6 8 ON OFF
18 1.99 40 0 0 ON OFF

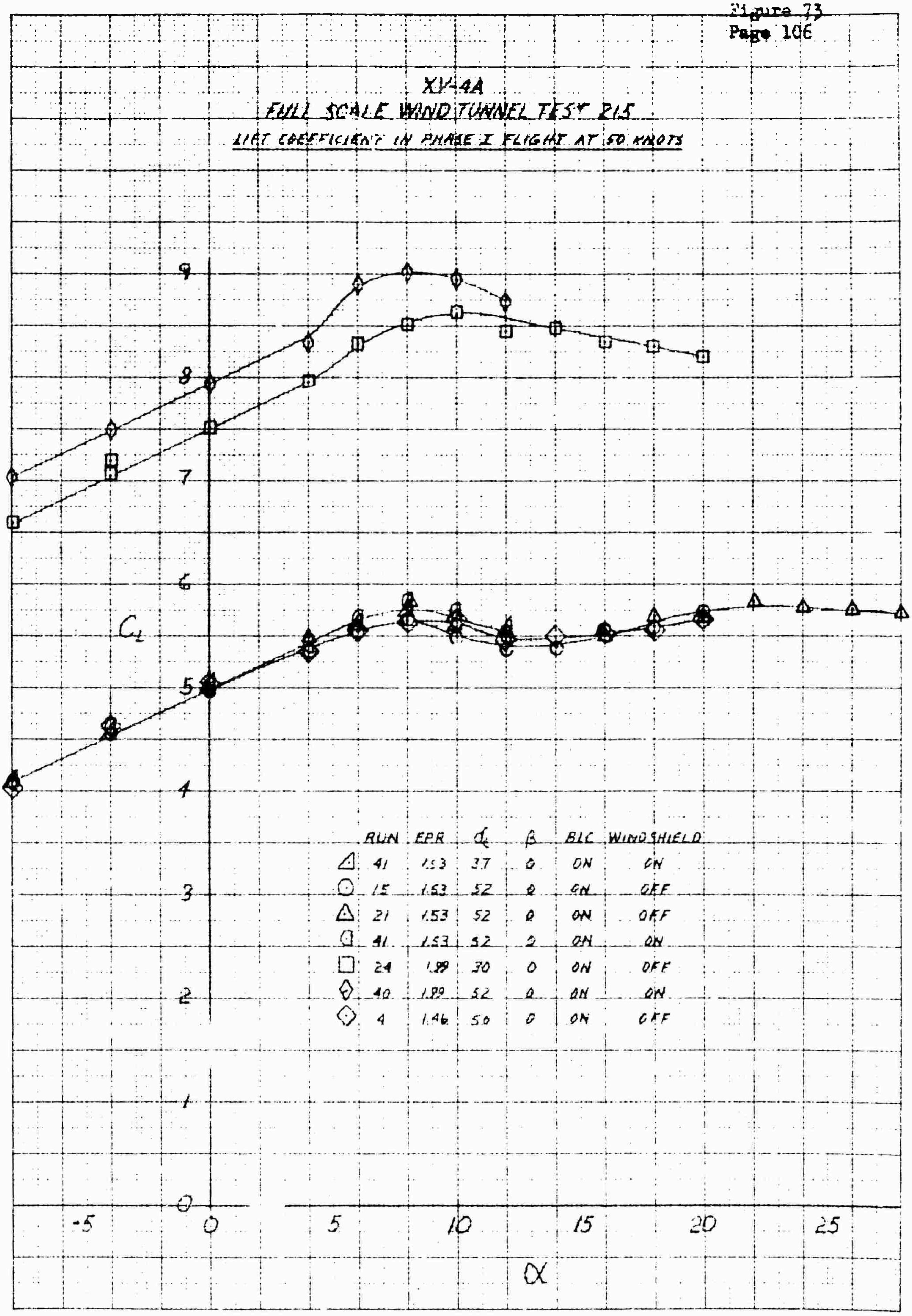
XV-4A
FULL SCALE WIND TUNNEL TEST 215
LIFT COEFFICIENT IN PHASE I FLIGHT AT 50 KNOTS
C_L
0
1
2
3
4
5
6
7
8
9
-5
0
5
10
15
20
25
α
RUN EPR α_c β BLC WINDSHIELD
41 1.53 37 0 ON ON
15 1.53 52 0 ON OFF
21 1.53 52 0 ON OFF
41 1.53 52 0 ON ON
24 1.99 30 0 ON OFF
40 1.99 52 0 ON ON
4 1.46 50 0 ON OFF

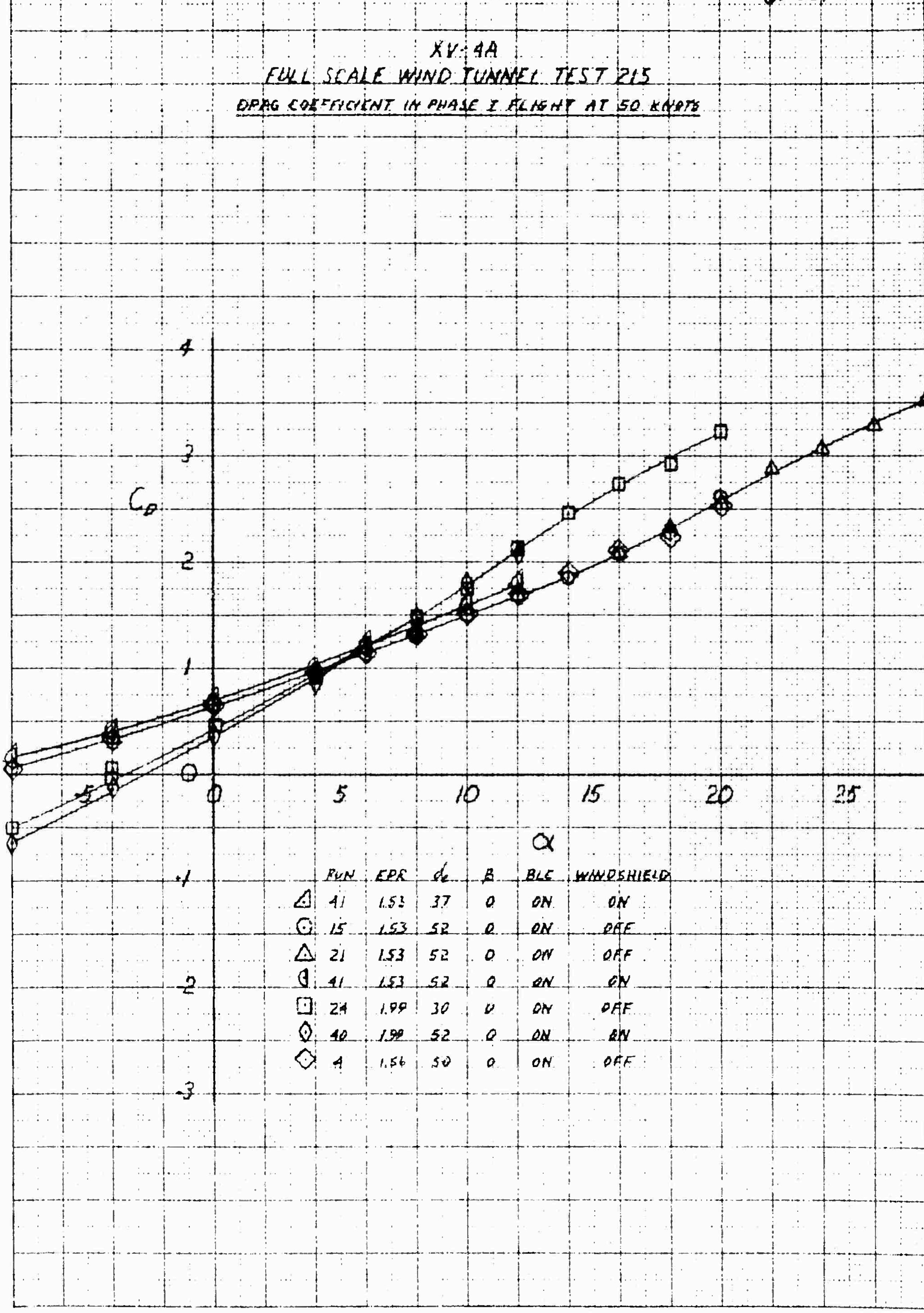
XV-4A
FULL SCALE WIND TUNNEL TEST 215
DRAG COEFFICIENT IN PHASE I FLIGHT AT 50 KNOTS
C_D
4
3
2
1
0
-1
-2
-3
-5
0
5
10
15
20
25
α
RUN EPR δ_e β BLC WINDSHIELD
41 1.53 37 0 ON ON
15 1.53 52 0 ON OFF
21 1.53 52 0 ON OFF
41 1.53 52 0 ON ON
24 1.99 30 0 ON OFF
40 1.99 52 0 ON ON
4 1.56 50 0 ON OFF

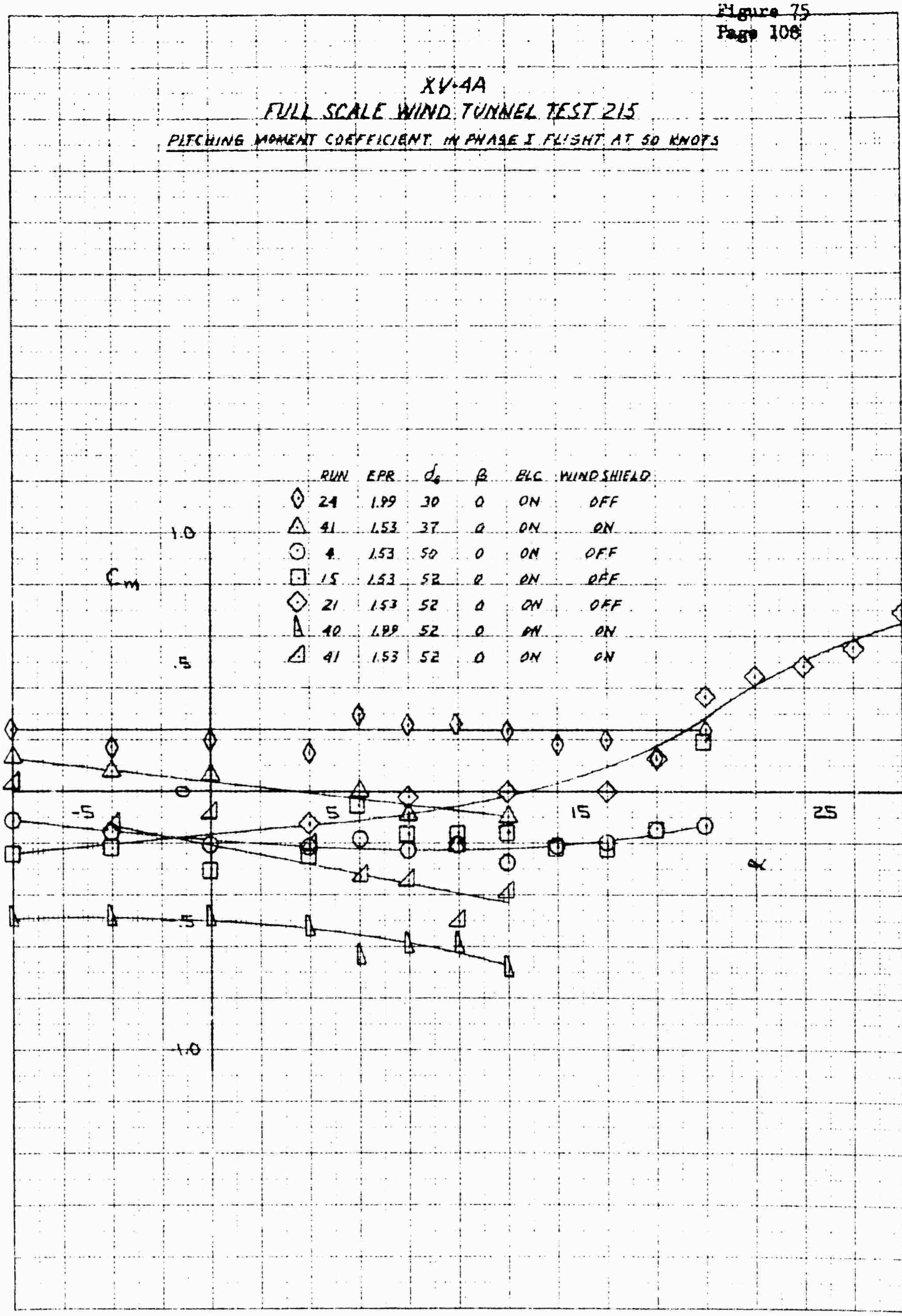
XV-4A
FULL SCALE WIND TUNNEL TEST 215
PITCHING MOMENT COEFFICIENT IN PHASE I FLIGHT AT 50 KNOTS
RUN EPR δ β BLC WINDSHIELD
24 1.99 30 0 ON OFF
41 1.53 37 0 ON ON
4 1.53 50 0 ON OFF
15 1.53 52 0 ON OFF
21 1.53 52 0 ON OFF
40 1.99 52 0 ON ON
41 1.53 52 0 ON ON
Cm
1.0
.5
-.5
-1.0
-5
5
15
25
α

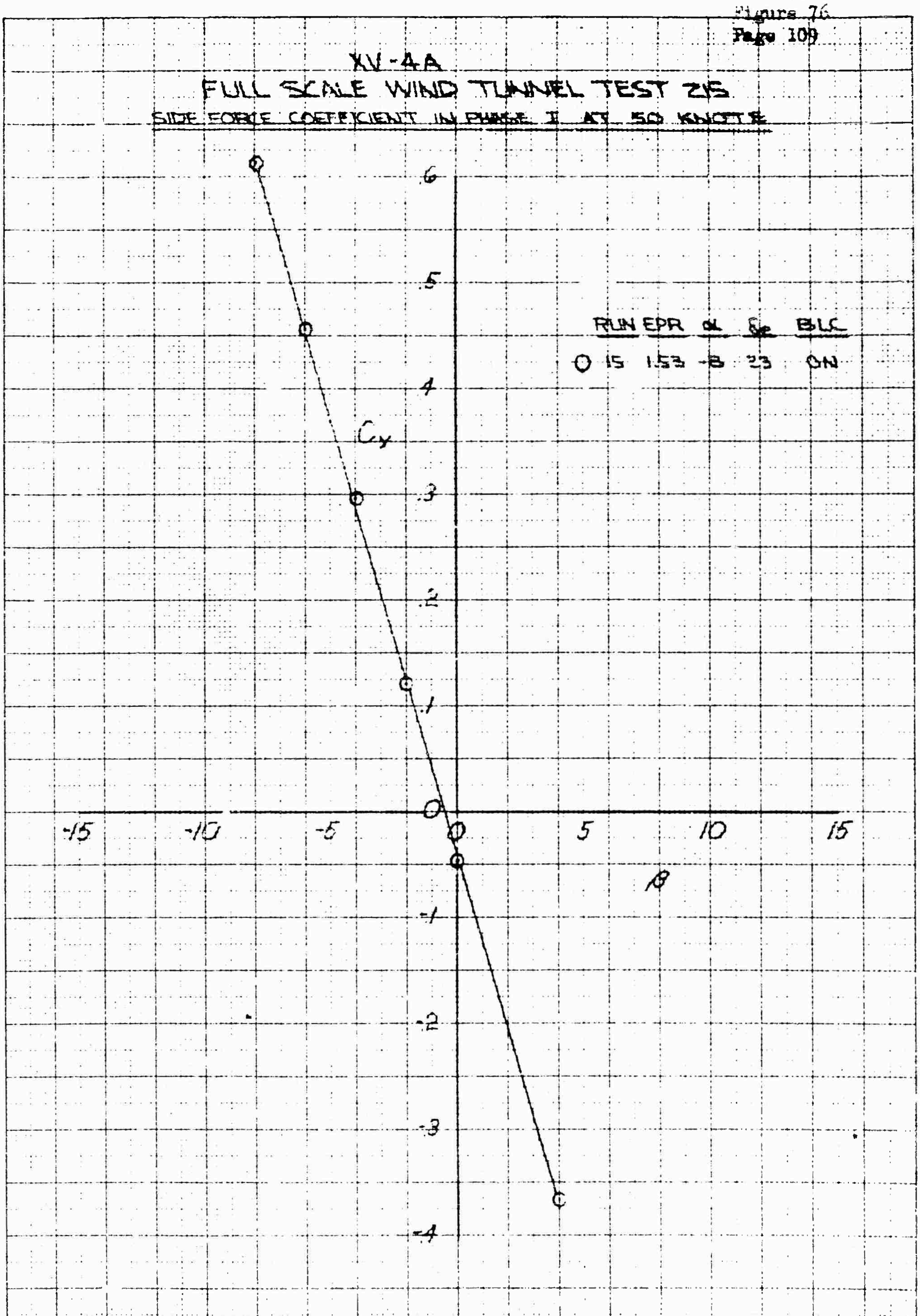

XV-4A
FULL SCALE WIND TUNNEL TEST 215
SIDE FORCE COEFFICIENT IN PHASE I AT 50 KNOTS
RUN EPR α δe BLC
15 1.53 -8 23 ON
Cy
.6
.5
.4
.3
.2
.1
0
-.1
-.2
-.3
-.4
-15
-10
-5
0
5
10
15
β

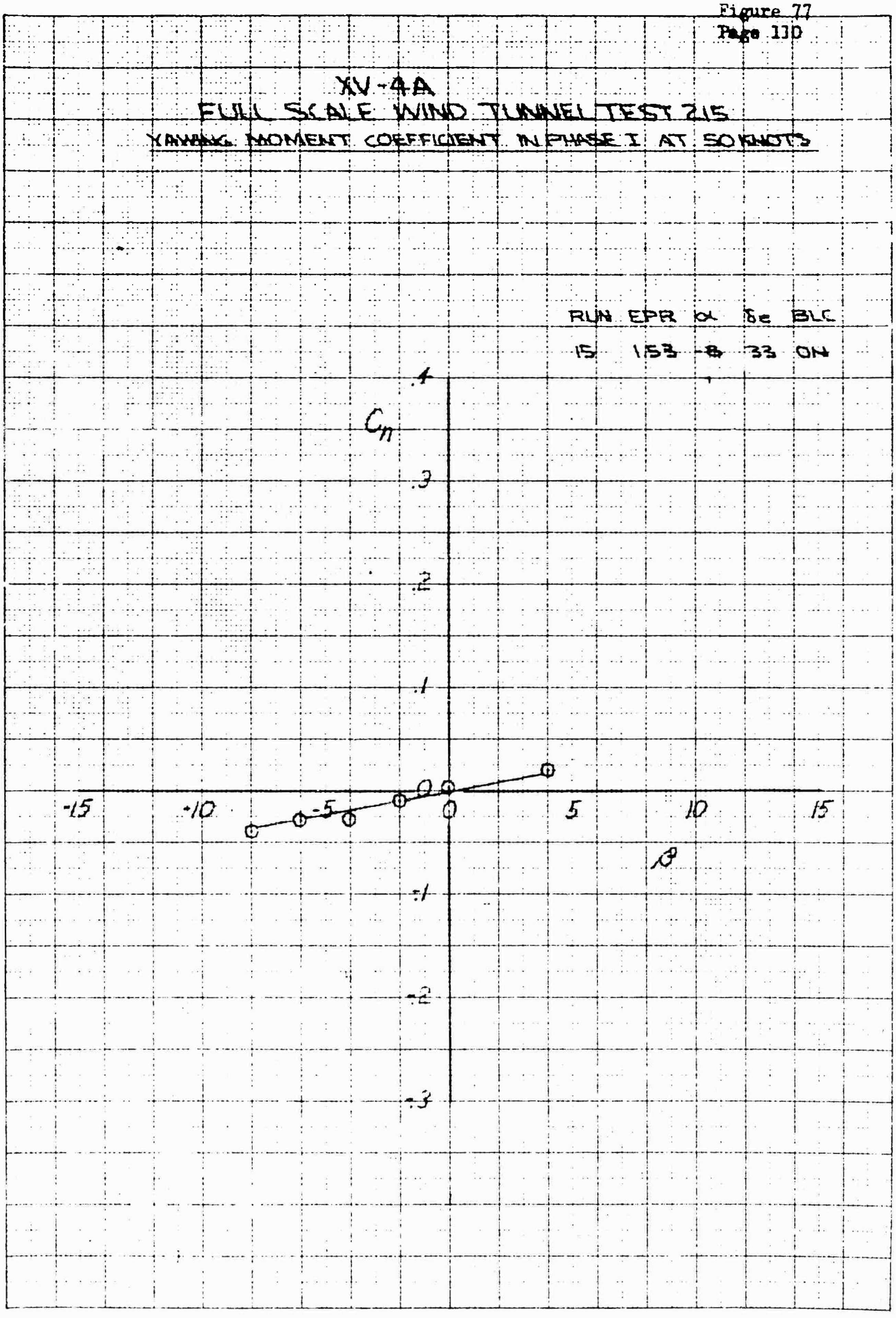
XV-4A
FULL SCALE WIND TUNNEL TEST 215
YAWING MOMENT COEFFICIENT IN PHASE I AT 50 KNOTS
RUN EPR α δe BLC
15 153 -8 33 ON
C_n
.4
.3
.2
.1
-.1
-.2
-.3
-15
-10
-5
0
5
10
15
β

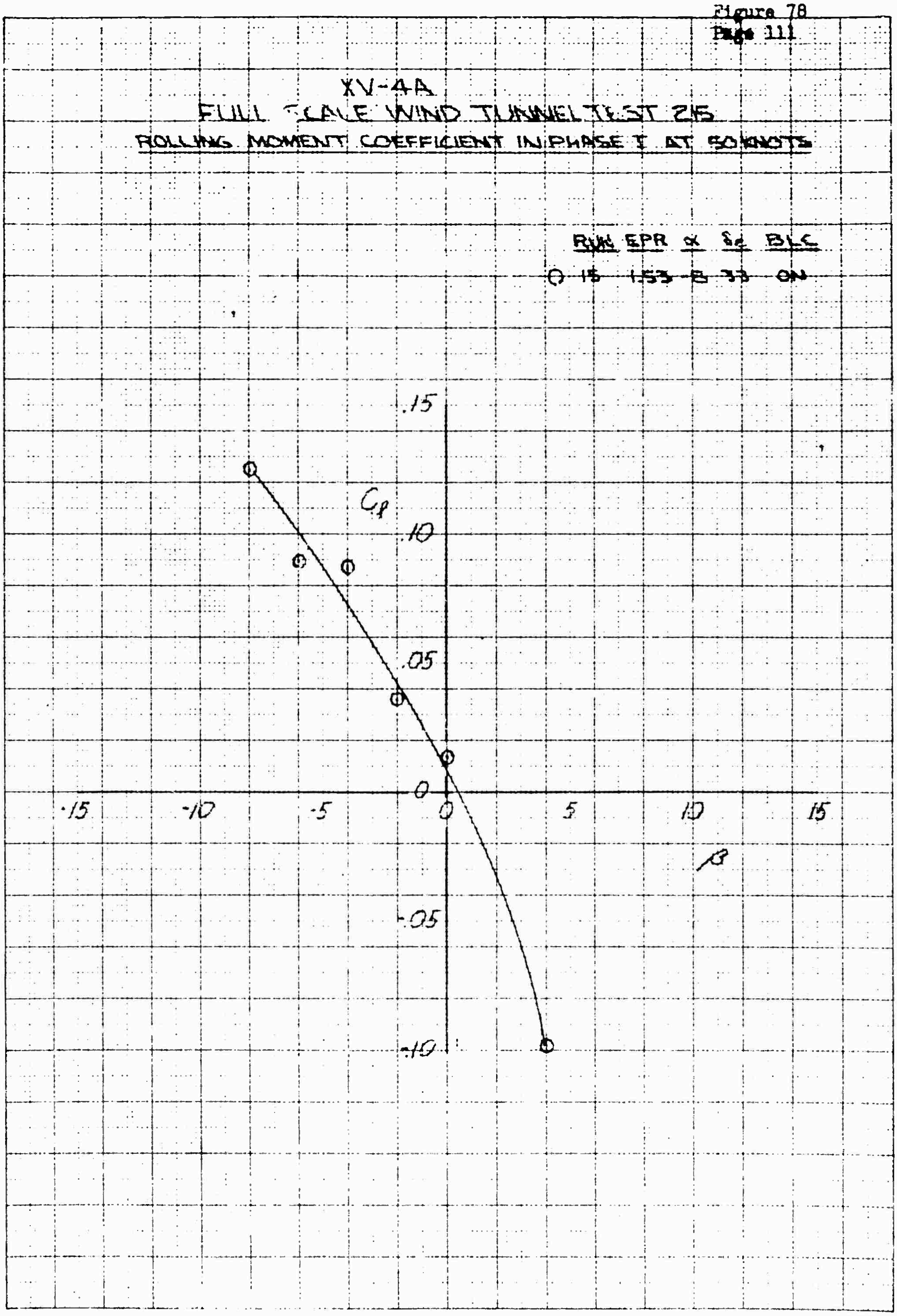
XV-4A
FULL SCALE WIND TUNNEL TEST 215
ROLLING MOMENT COEFFICIENT IN PHASE I AT 50 KNOTS
RUN EPR α δe BLC
15 1.53 -8 33 ON
.15
.10
.05
0
-.05
-.10
-15
-10
-5
0
5
10
15
β

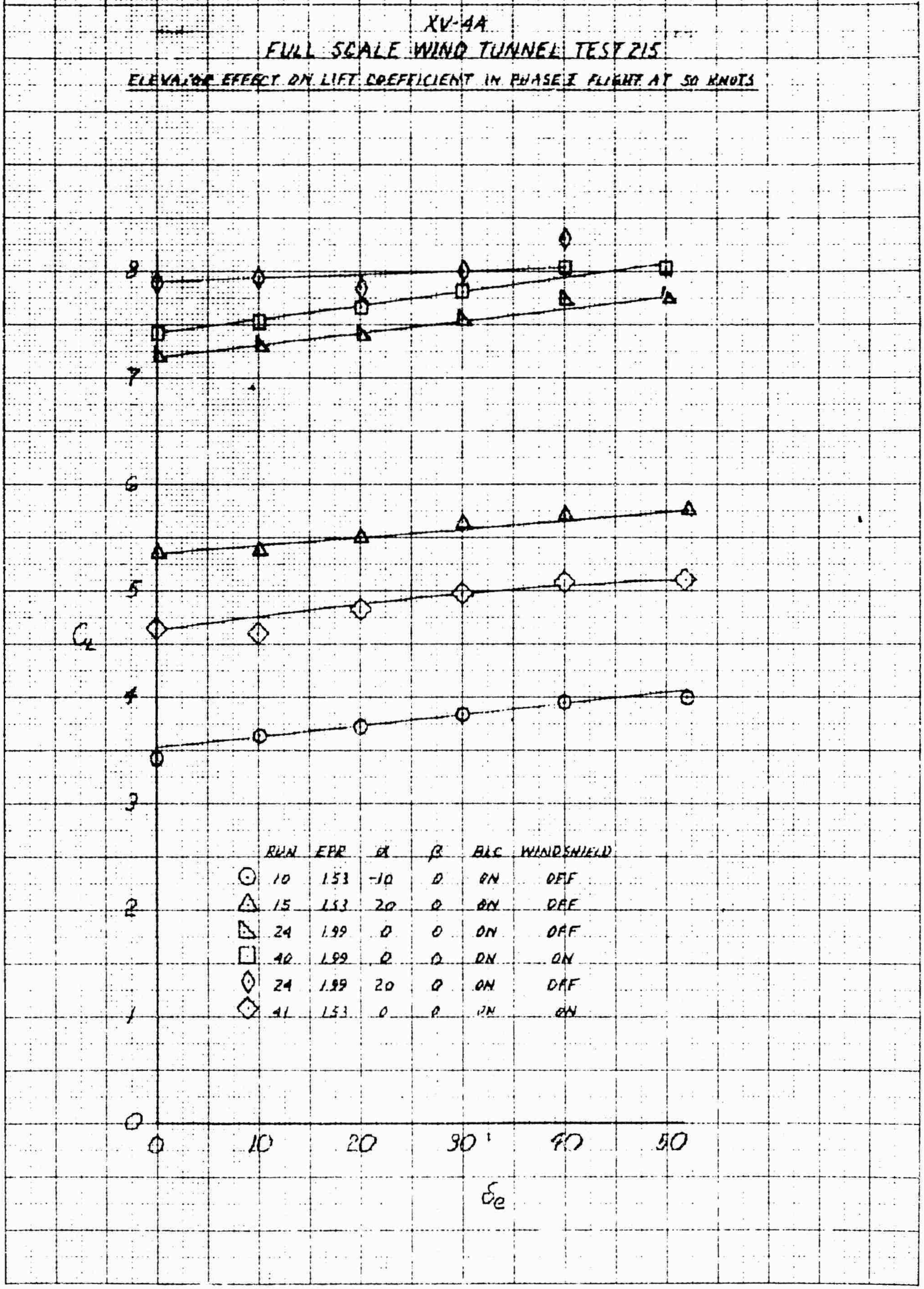
XV-4A
FULL SCALE WIND TUNNEL TEST 215
ELEVATOR EFFECT ON LIFT COEFFICIENT IN PHASE I FLIGHT AT 50 KNOTS
8
7
6
5
4
3
2
1
0
C_L
0
10
20
30
40
50
δ_e
RUN EPR α β BLC WINDSHIELD
10 1.53 -10 0 ON OFF
15 1.53 20 0 ON OFF
24 1.99 0 0 ON OFF
40 1.99 0 0 ON ON
24 1.99 20 0 ON OFF
41 1.53 0 0 ON ON

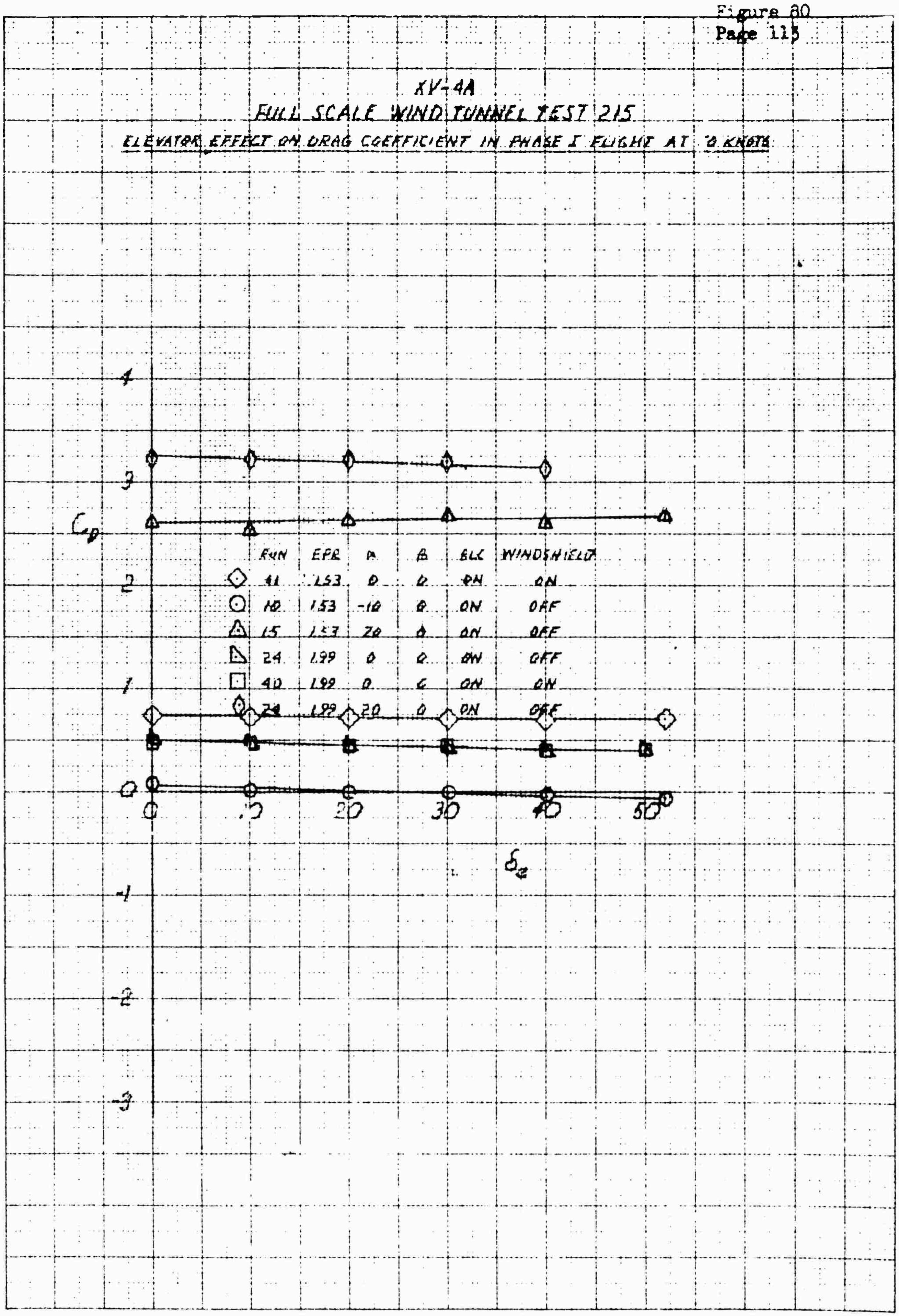
XV-4A
FULL SCALE WIND TUNNEL TEST 215
ELEVATOR EFFECT ON DRAG COEFFICIENT IN PHASE I FLIGHT AT 0 KNOTS
C_D
4
3
2
1
0
-1
-2
-3
0
10
20
30
40
50
δ_e
RUN EPR α β BLC WINDSHIELD
41 1.53 0 0 ON ON
10 1.53 -10 0 ON OFF
15 1.53 20 0 ON OFF
24 1.99 0 0 ON OFF
40 1.99 0 0 ON ON
24 1.99 20 0 ON OFF

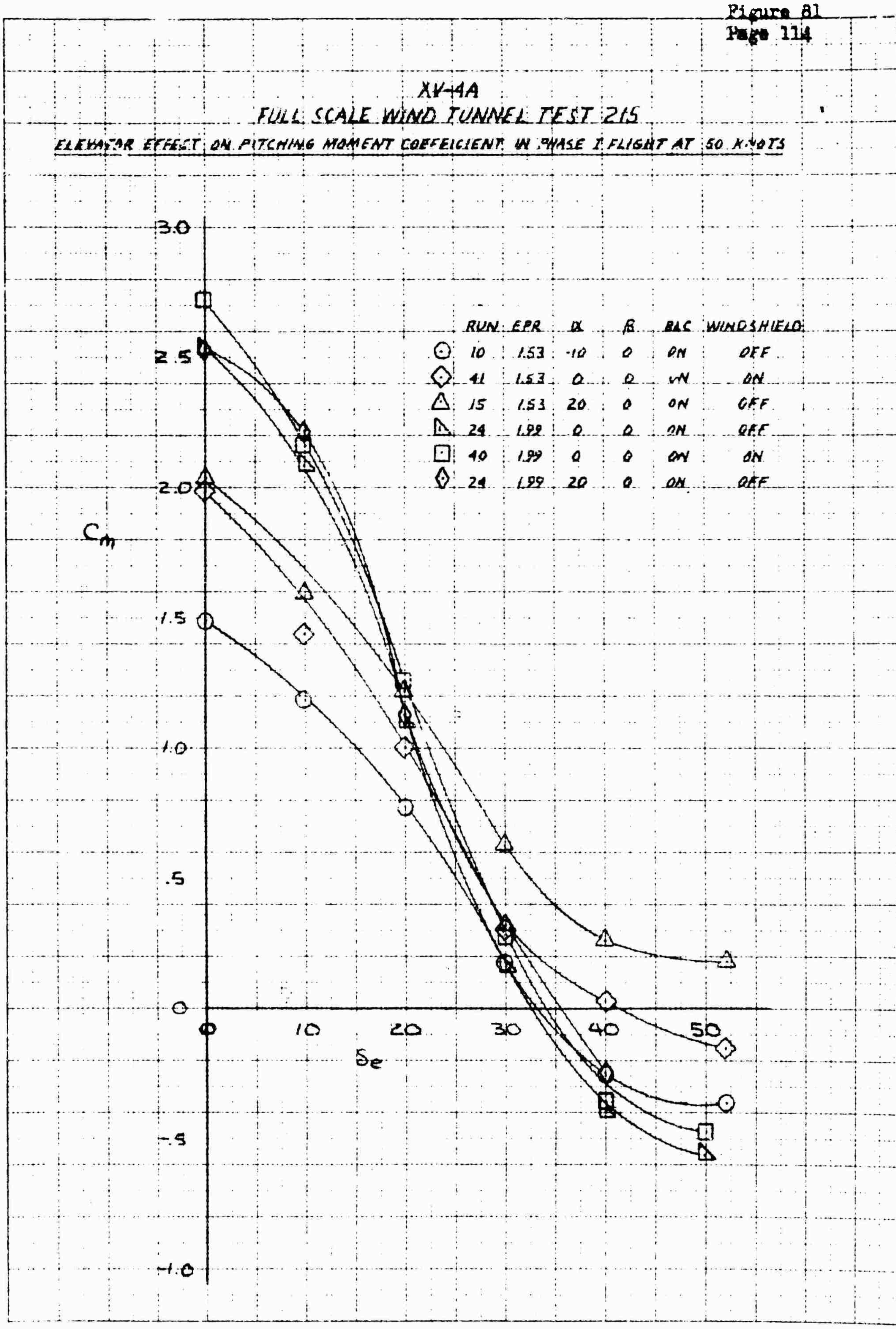
XV-4A
FULL SCALE WIND TUNNEL TEST 215
ELEVATOR EFFECT ON PITCHING MOMENT COEFFICIENT IN PHASE I FLIGHT AT 50 KNOTS
RUN EPR α β BLC WINDSHIELD
10 1.53 -10 0 ON OFF
41 1.53 0 0 ON ON
15 1.53 20 0 ON OFF
24 1.99 0 0 ON OFF
40 1.99 0 0 ON ON
24 1.99 20 0 ON OFF
C_m
3.0
2.5
2.0
1.5
1.0
.5
0
-.5
-1.0
0
10
20
30
40
50
δ_e

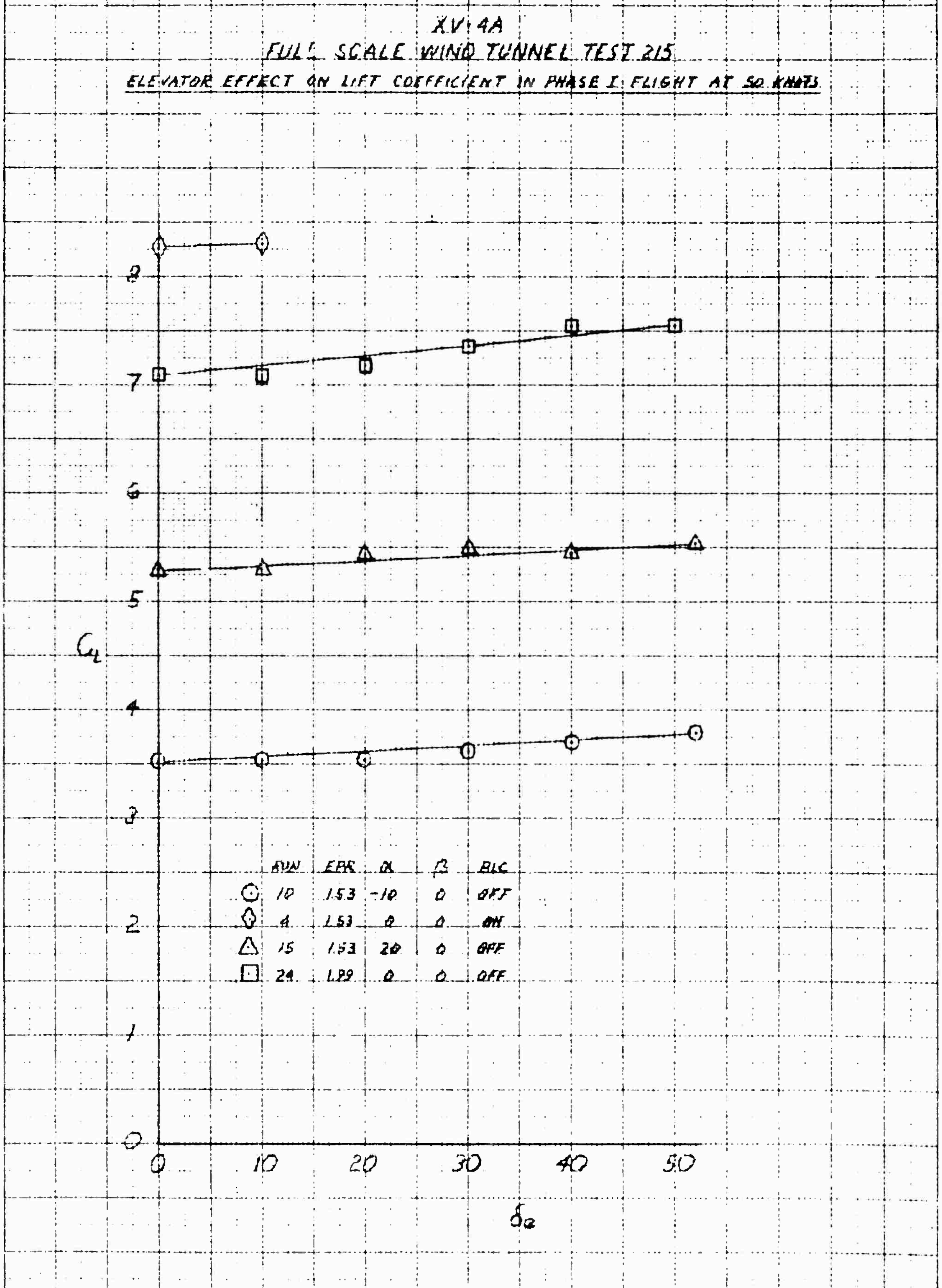
XV-4A
FULL SCALE WIND TUNNEL TEST 215
ELEVATOR EFFECT ON LIFT COEFFICIENT IN PHASE I FLIGHT AT 50 KNOTS
C_L
δ_e
0
10
20
30
40
50
1
2
3
4
5
6
7
8
RUN EPR α β BLC
10 1.53 -10 0 OFF
4 1.53 0 0 ON
15 1.53 20 0 OFF
24 1.89 0 0 OFF

XV-4A
FULL SCALE WIND TUNNEL TEST 215
ELEVATOR EFFECT ON DRAG COEFFICIENT IN PHASE I FLIGHT AT 50 KNOTS

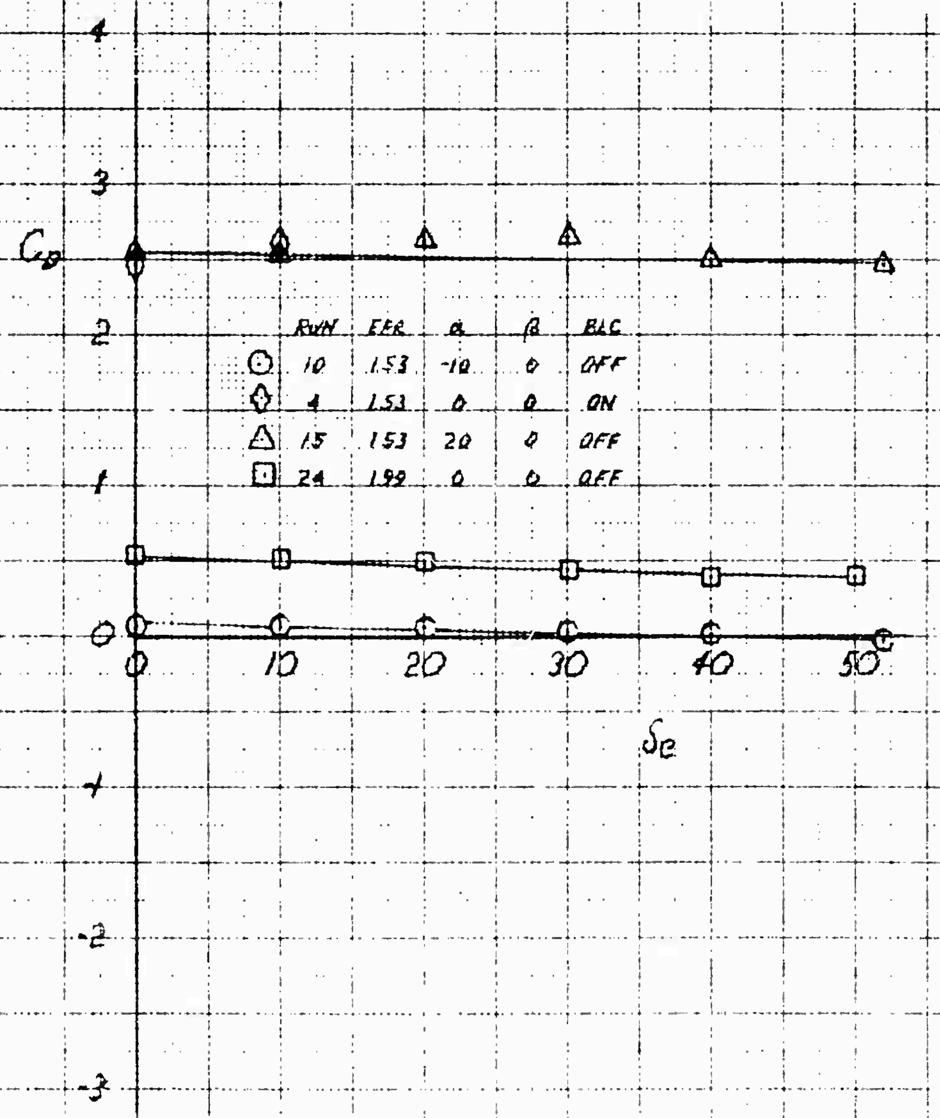

XV-4A

FULL SCALE WIND TUNNEL TEST 215

ELEVATOR EFFECT ON PITCHING MOMENT COEFFICIENT IN PHASE I FLIGHT AT 50 KNOTS

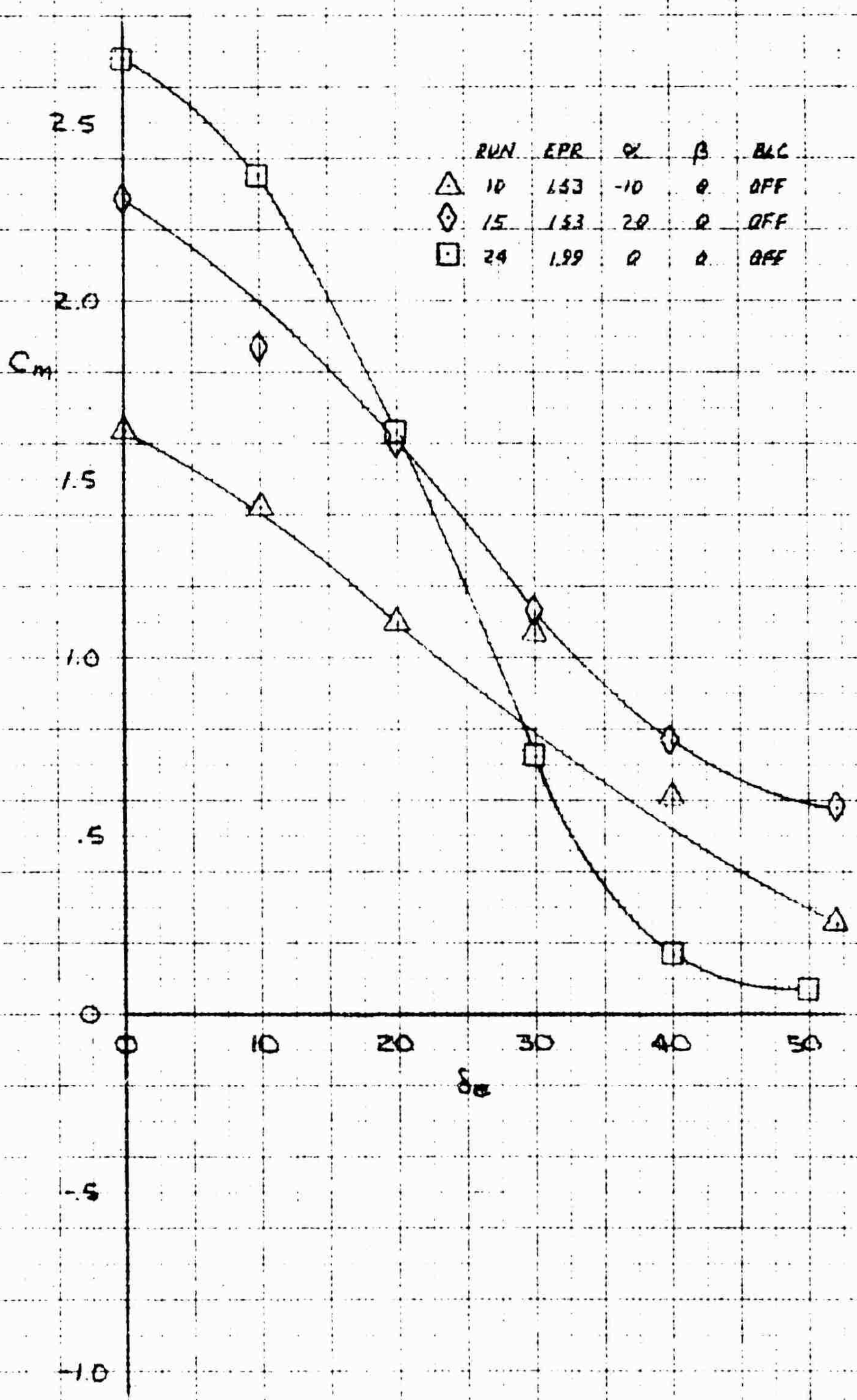

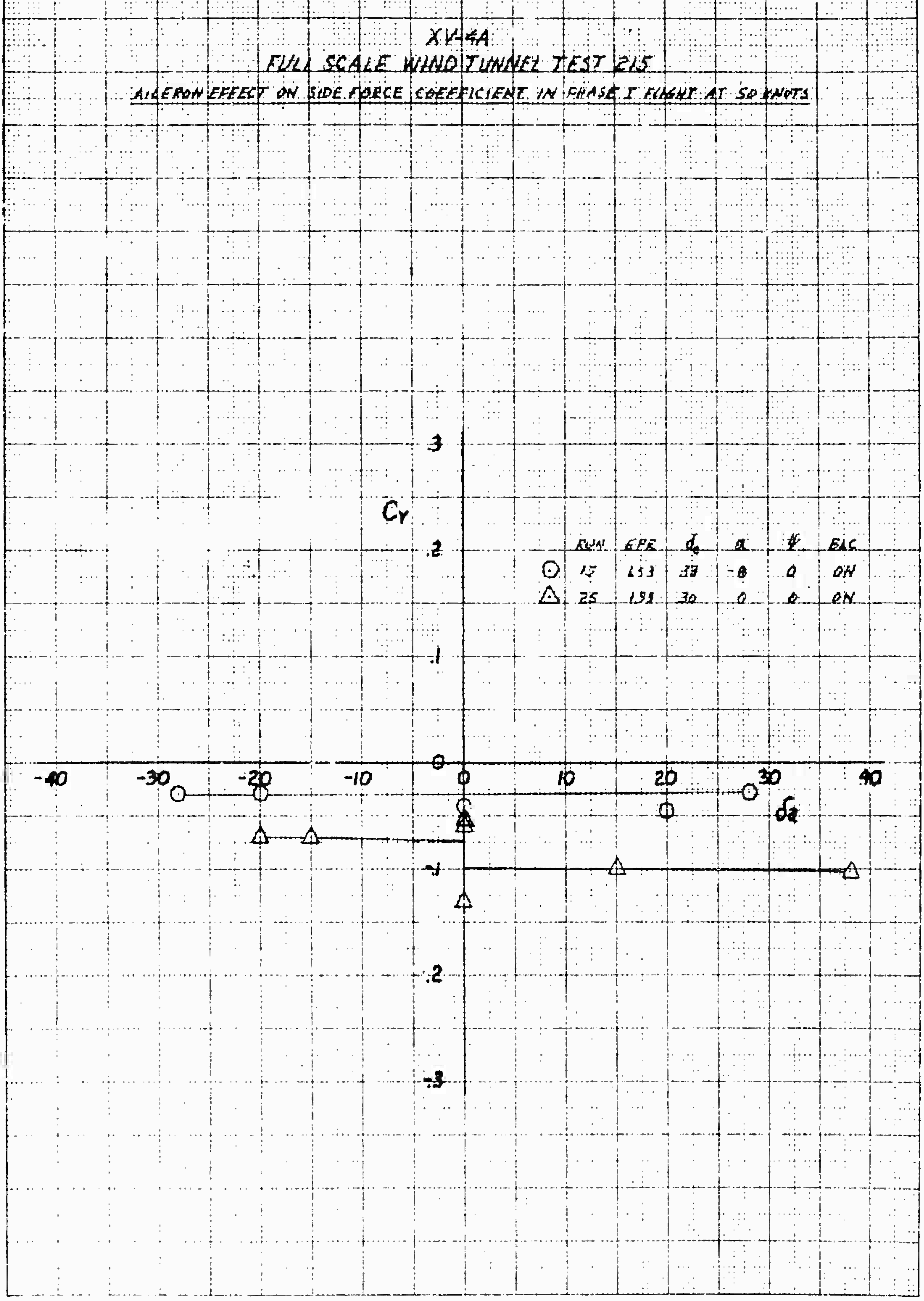
XV-4A
FULL SCALE WIND TUNNEL TEST 215
AILERON EFFECT ON SIDE FORCE COEFFICIENT IN PHASE I FLIGHT AT 50 KNOTS
C_Y
.3
.2
.1
0
-.1
-.2
-.3
-40
-30
-20
-10
0
10
20
30
40
δ_a
RUN EPE δ_f ɑ Ψ EAC
15 153 37 -8 0 ON
25 191 30 0 0 ON

XV-4A
FULL SCALE WIND TUNNEL TEST 215
AILERON EFFECT ON YAWING MOMENT COEFFICIENT IN PHASE I FLIGHT AT 50 KNOTS

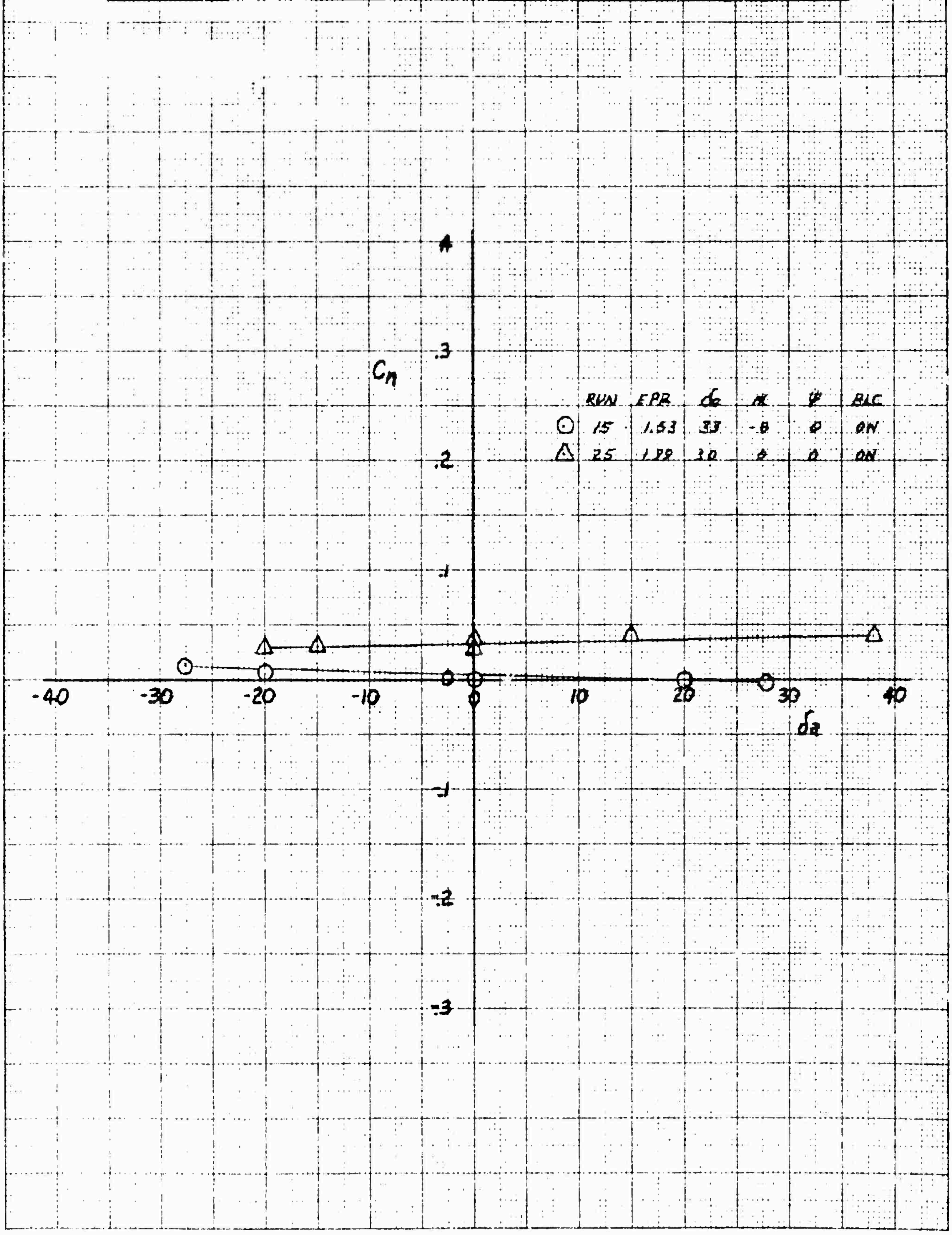

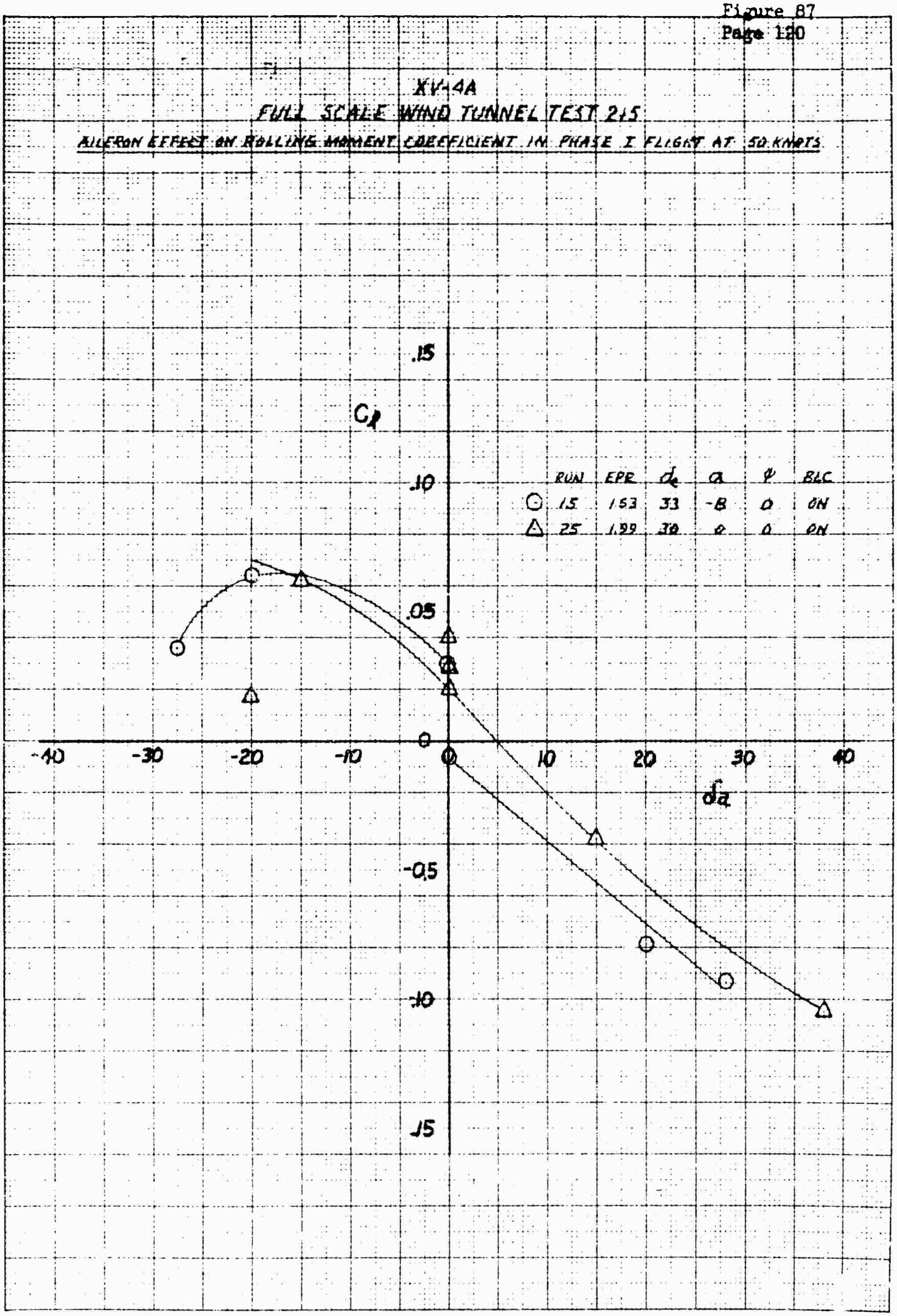
XV-4A
FULL SCALE WIND TUNNEL TEST 215
AILERON EFFECT ON ROLLING MOMENT COEFFICIENT IN PHASE I FLIGHT AT 50 KNOTS
.15
C_l
.10
.05
0
-0.5
-.10
-.15
-40
-30
-20
-10
0
10
20
30
40
δa
RUN EPE δe α ψ BLC
15 1.53 33 -8 0 ON
25 1.99 30 0 0 ON

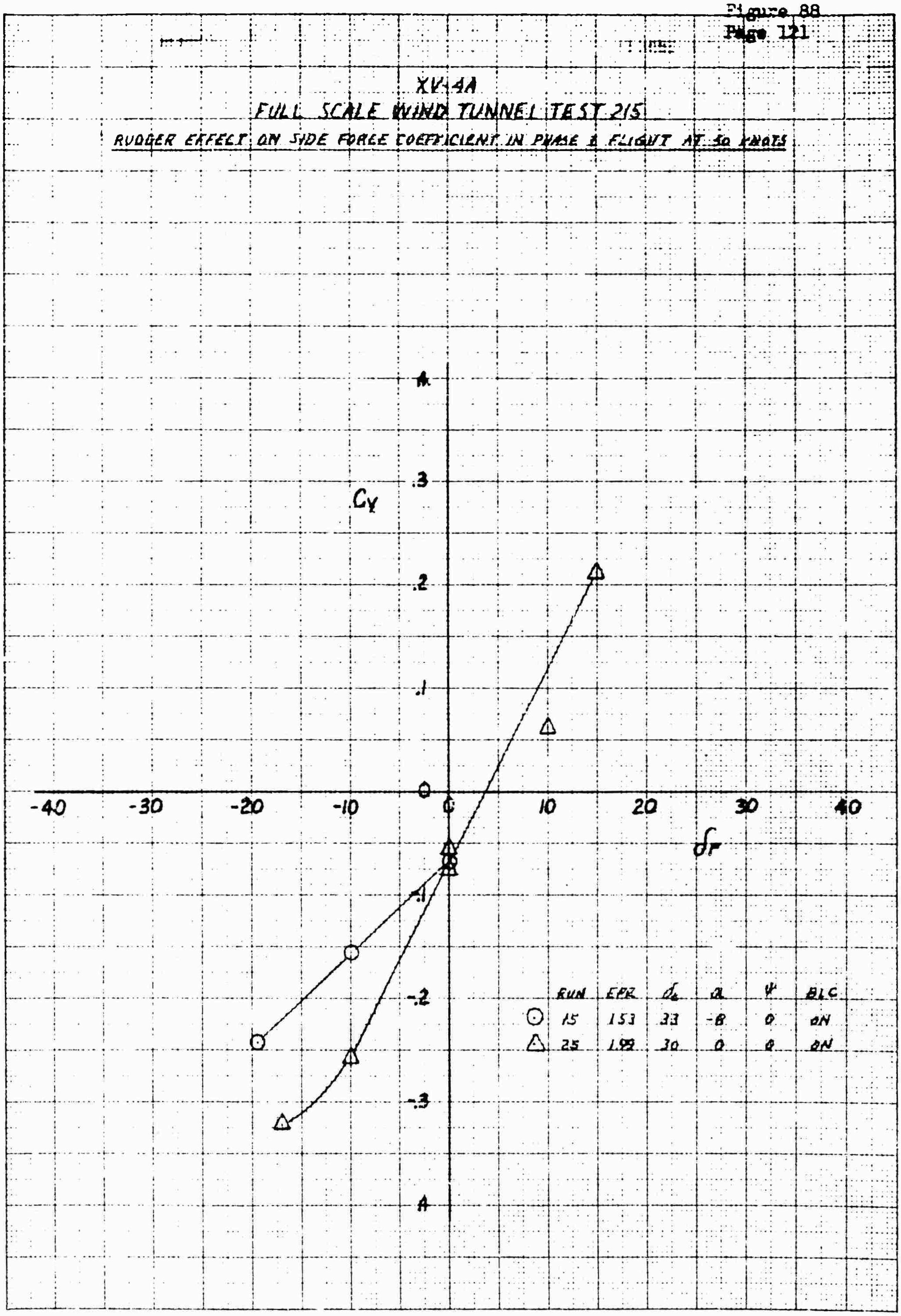
XV-4A
FULL SCALE WIND TUNNEL TEST 215
RUDDER EFFECT ON SIDE FORCE COEFFICIENT IN PHASE 1 FLIGHT AT 50 KNOTS
C_Y
.4
.3
.2
.1
0
-.1
-.2
-.3
-.4
-40
-30
-20
-10
0
10
20
30
40
δ_r
RUN EPR δ_e α ψ BLC
15 153 33 -8 0 ON
25 1.99 30 0 0 ON

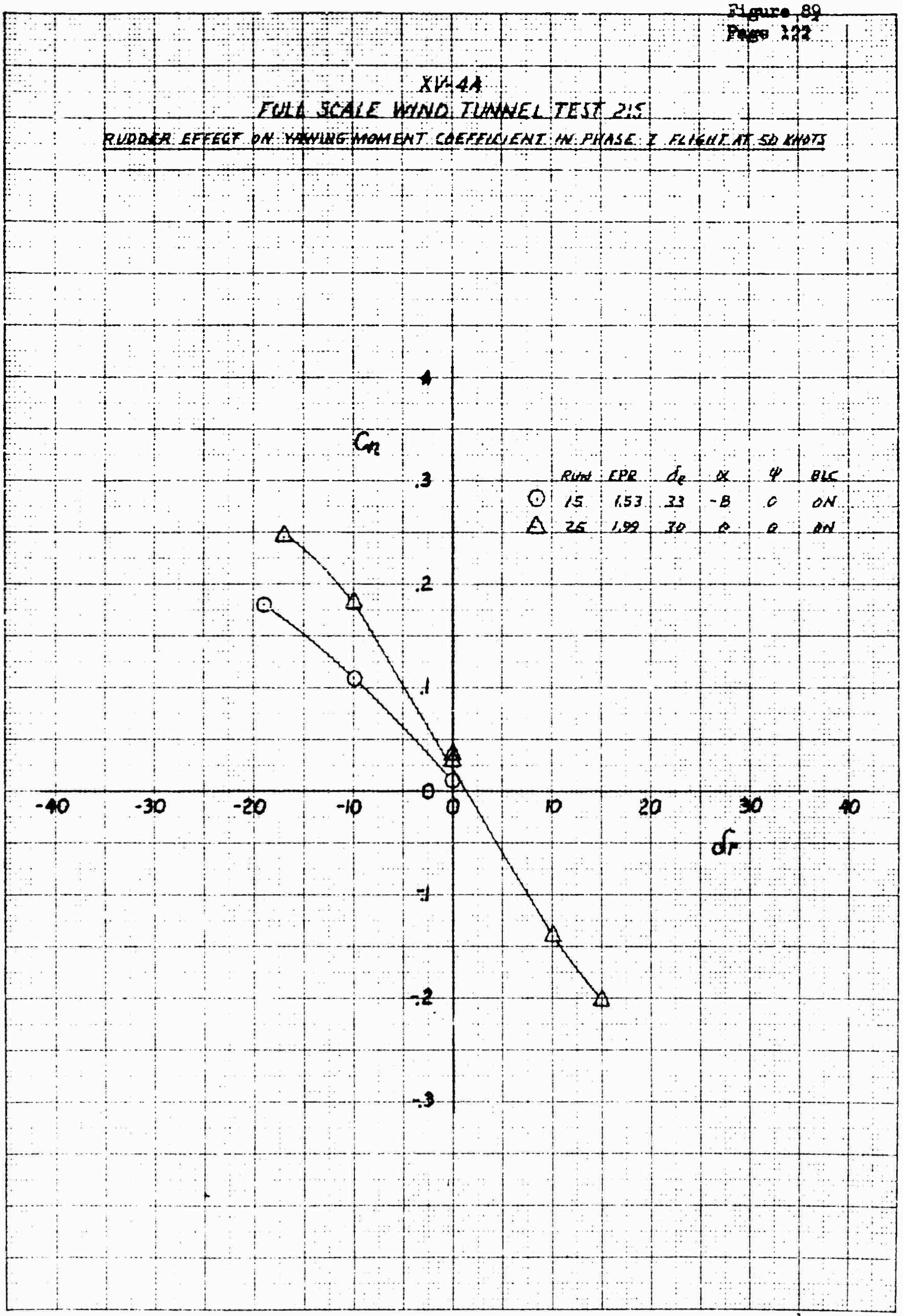
XV-4A
FULL SCALE WIND TUNNEL TEST 215
RUDDER EFFECT ON YAWING MOMENT COEFFICIENT IN PHASE I FLIGHT AT 50 KNOTS
Cn
Run EPR δe α ψ BLC
15 1.53 33 -8 0 ON
25 1.99 30 0 0 ON
.4
.3
.2
.1
0
-.1
-.2
-.3
-40
-30
-20
-10
0
10
20
30
40
δr

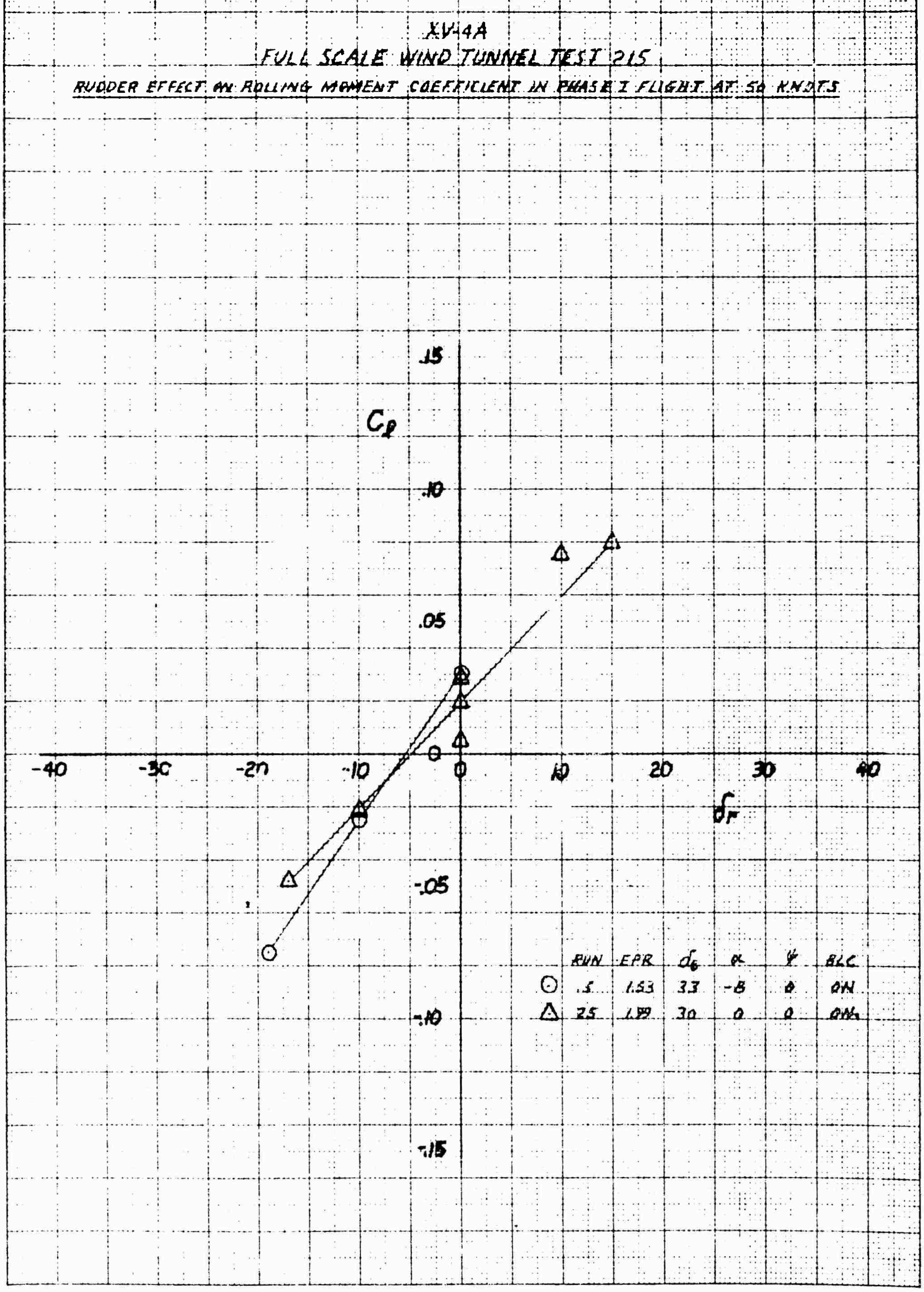
XV-4A
FULL SCALE WIND TUNNEL TEST 215
RUDDER EFFECT ON ROLLING MOMENT COEFFICIENT IN PHASE I FLIGHT AT 50 KNOTS
C_l
.15
.10
.05
-.05
-.10
-.15
-40
-30
-20
-10
0
10
20
30
40
δ_r
RUN EPR δ_6 α ψ BLC
⊙ 5 1.53 33 -8 0 ON
△ 25 1.59 30 0 0 ON

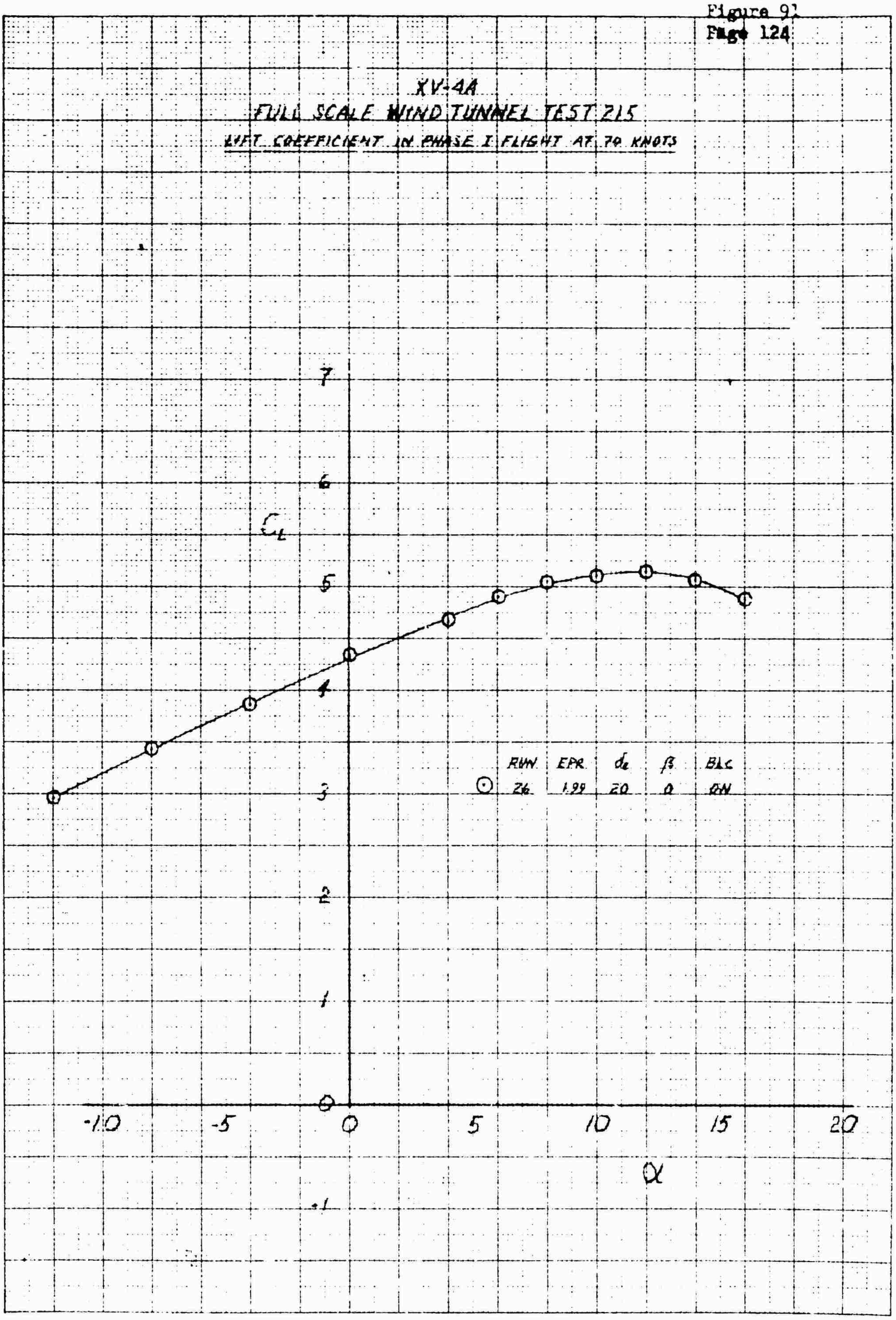
XV-4A
FULL SCALE WIND TUNNEL TEST 215
LIFT COEFFICIENT IN PHASE I FLIGHT AT 70 KNOTS
C_L
RUN EPR d_e β BLC
26 1.99 20 0 ON
α

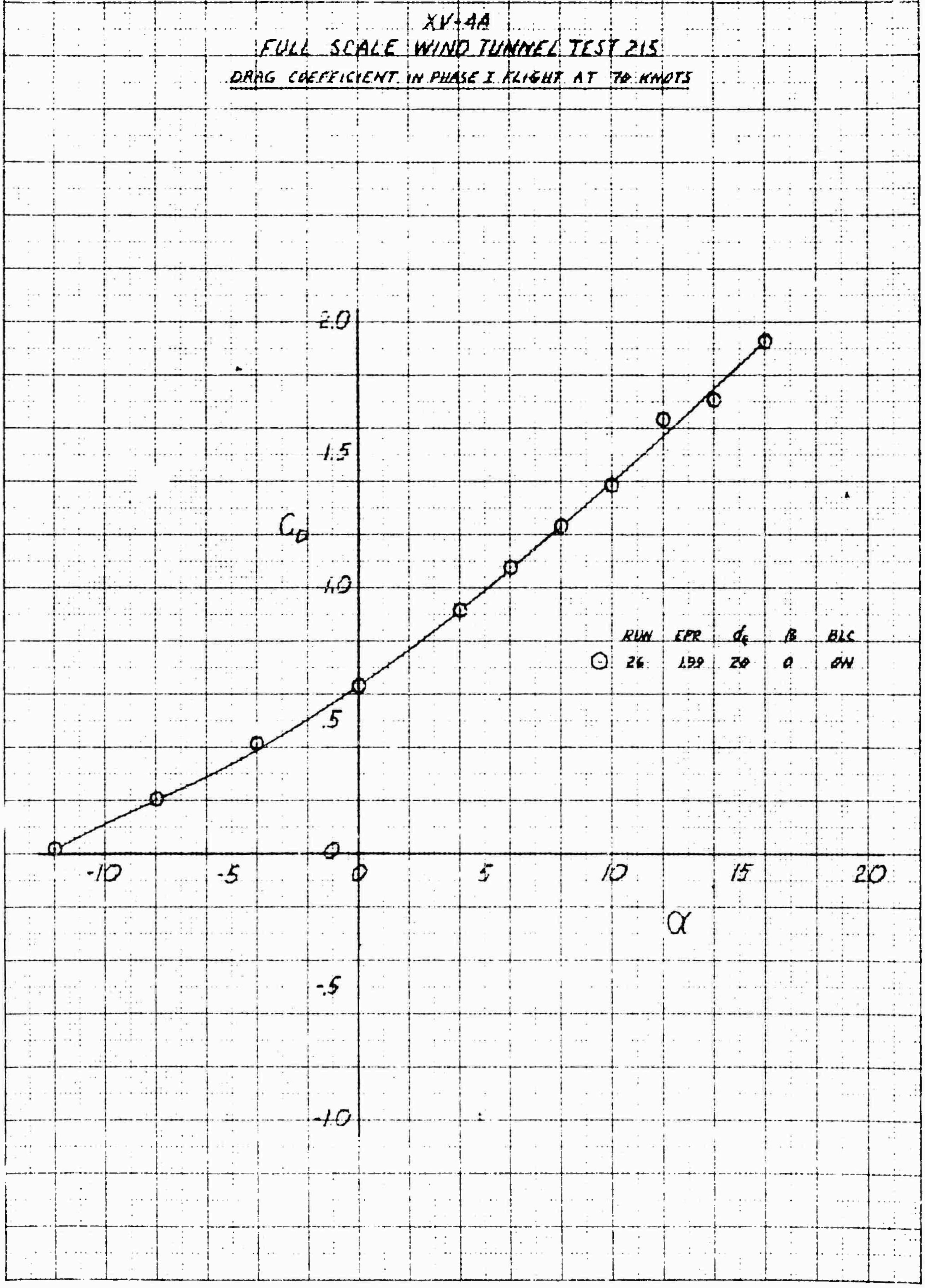
XV-4A
FULL SCALE WIND TUNNEL TEST 215
DRAG COEFFICIENT IN PHASE I FLIGHT AT 70 KNOTS
2.0
1.5
1.0
.5
0
-.5
-1.0
C_D
-10
-5
0
5
10
15
20
α
RUN
EPR
δ_F
β
BLC
26
1.99
20
0
ON

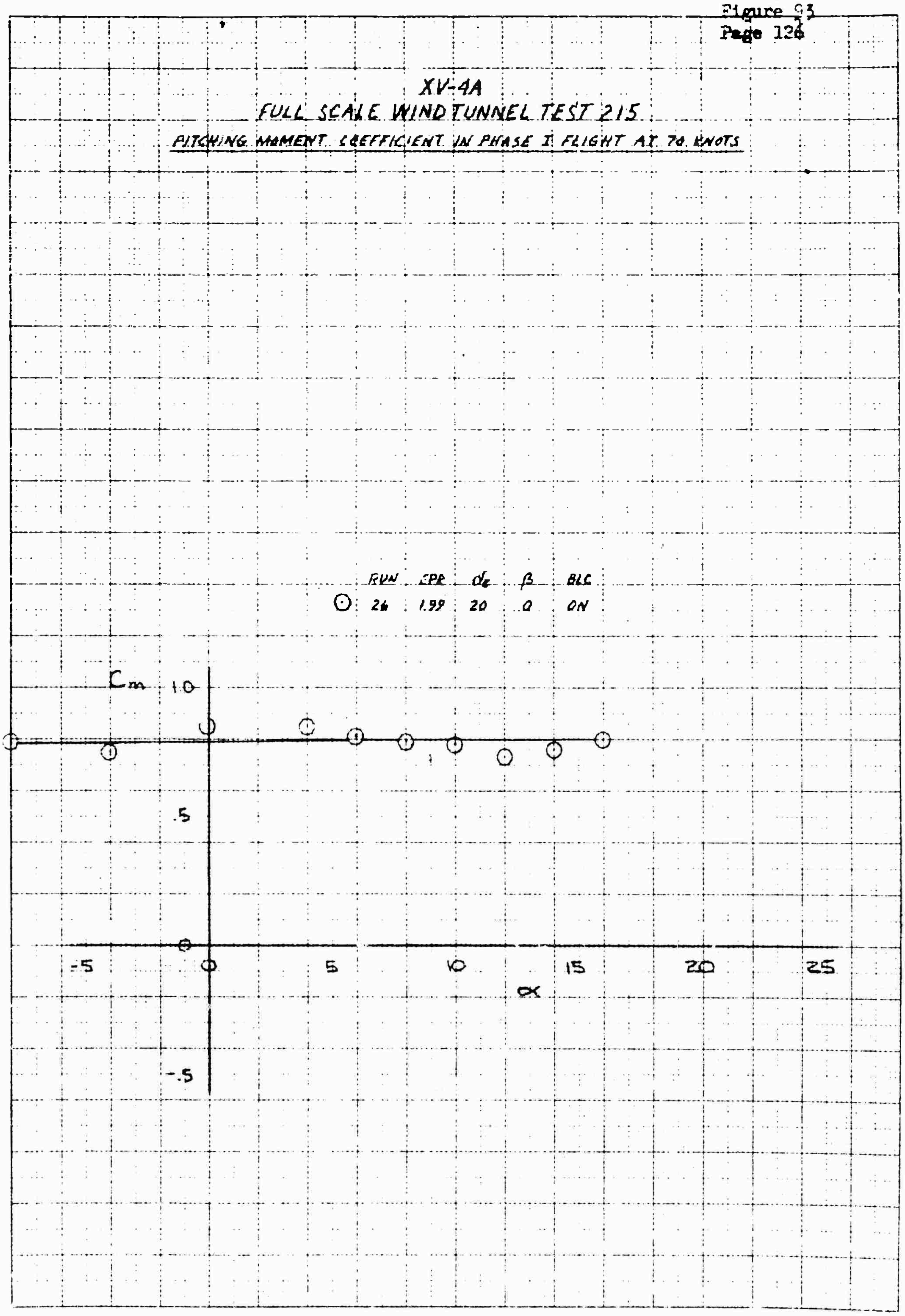
XV-4A
FULL SCALE WIND TUNNEL TEST 215
PITCHING MOMENT COEFFICIENT IN PHASE I FLIGHT AT 70 KNOTS
RUN
CPR
β
BLC
26
1.99
20
0
ON
Cm
1.0
.5
-.5
-5
0
5
10
15
20
25
α

XV-4A
FULL SCALE WIND TUNNEL TEST 215
ELEVATOR EFFECT ON LIFT COEFFICIENT IN PHASE I FLIGHT AT 70 KNOTS

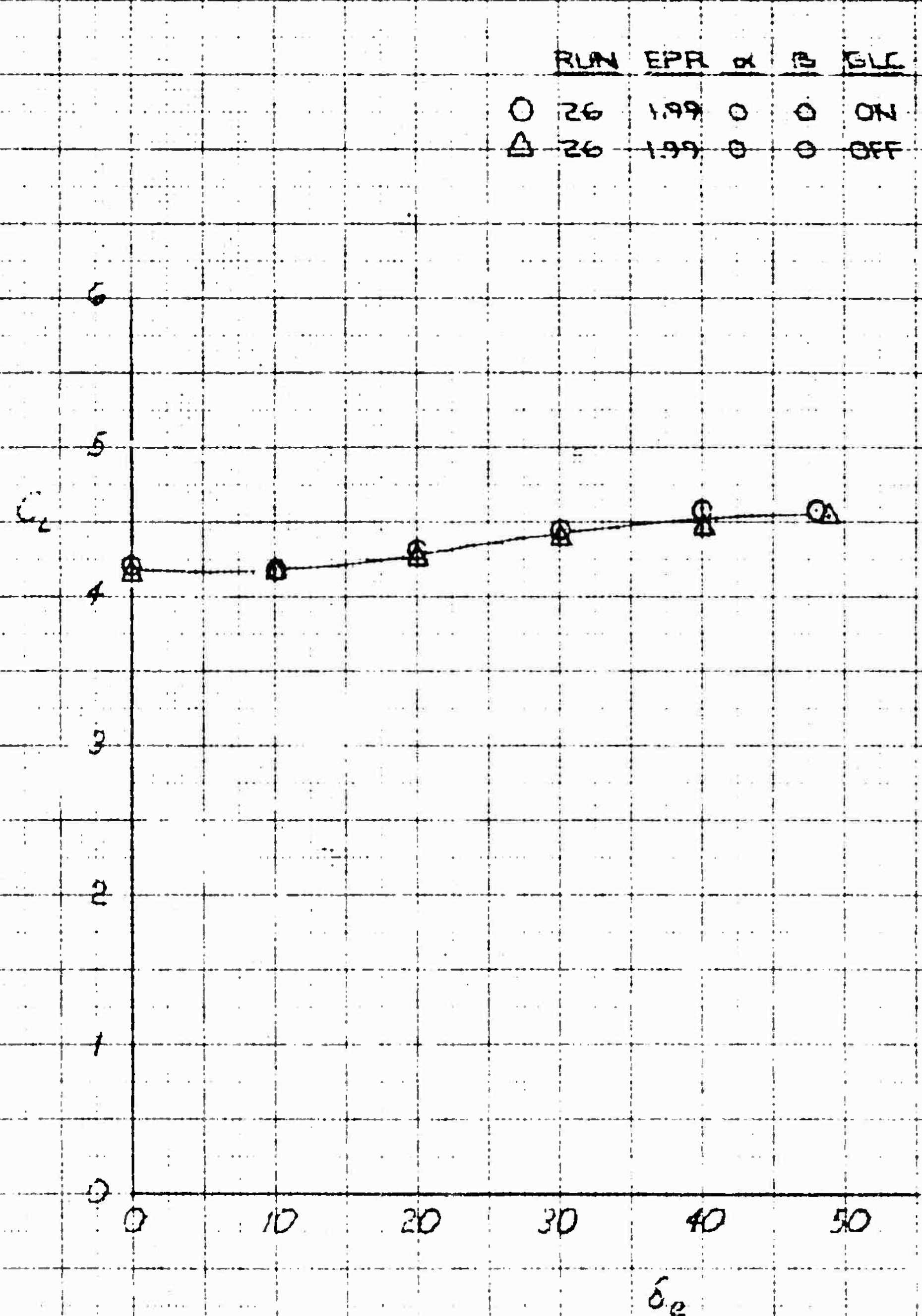

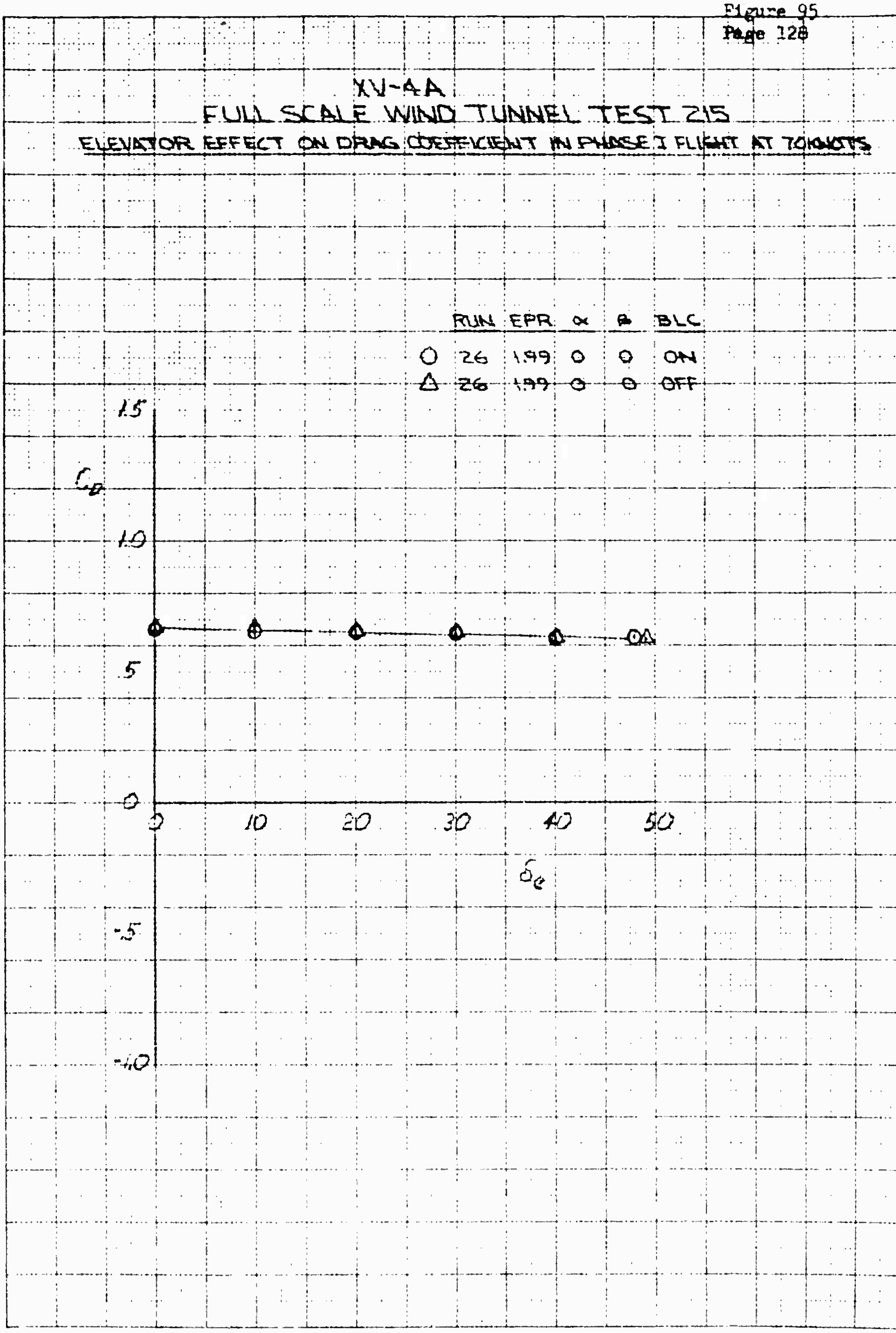
XV-4A
FULL SCALE WIND TUNNEL TEST 215
ELEVATOR EFFECT ON DRAG COEFFICIENT IN PHASE I FLIGHT AT 70 KNOTS
RUN EPR α β BLC
○ 26 1.99 0 0 ON
△ 26 1.99 0 0 OFF
1.5
C_D
1.0
.5
0
-.5
-1.0
0
10
20
30
40
50
δ_e

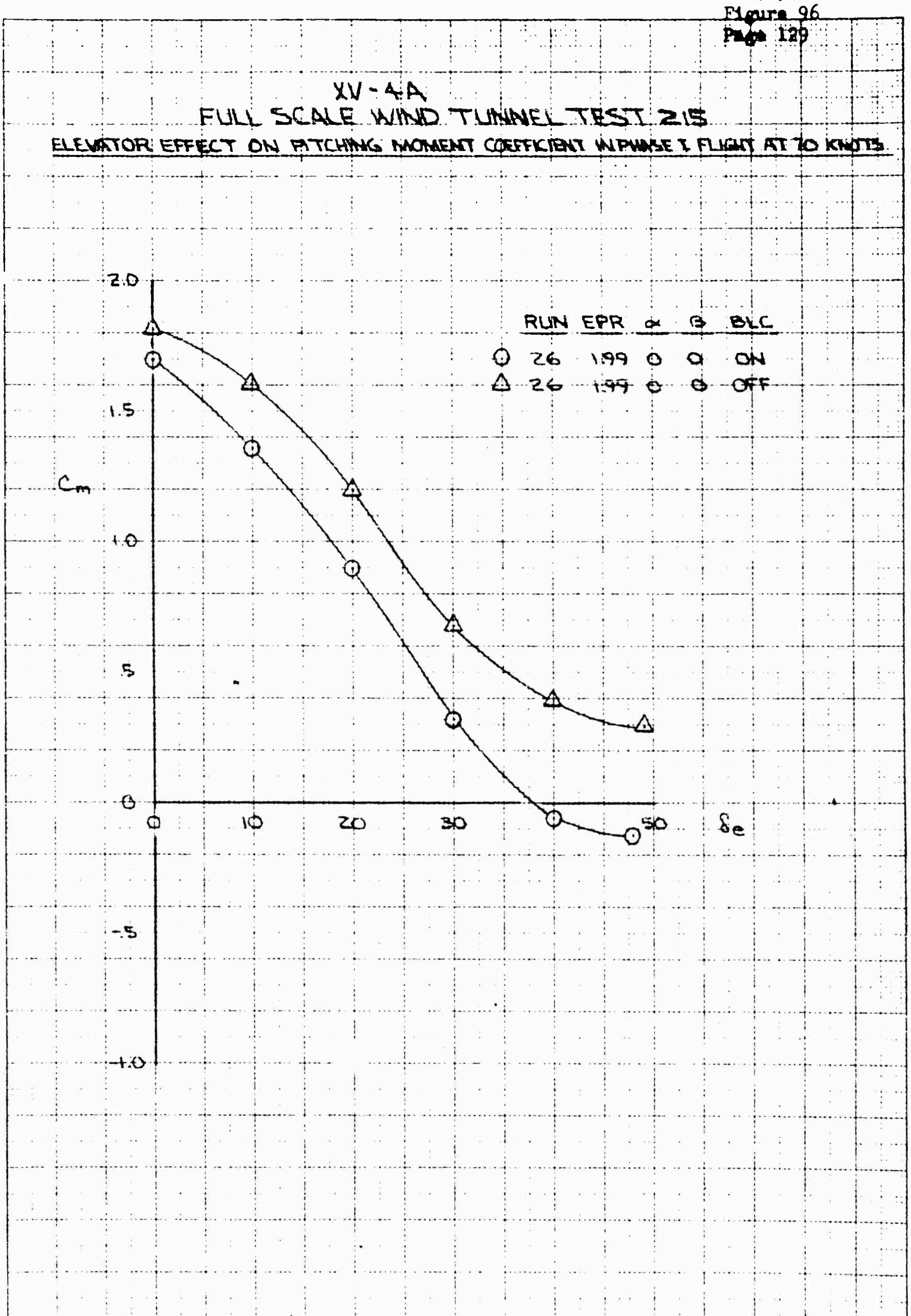
XV-4A
FULL SCALE WIND TUNNEL TEST 215
ELEVATOR EFFECT ON PITCHING MOMENT COEFFICIENT IN PHASE I FLIGHT AT 70 KNOTS
RUN EPR α β BLC
26 1.99 0 0 ON
26 1.99 0 0 OFF
Cm
2.0
1.5
1.0
.5
0
-.5
-1.0
0
10
20
30
50
δe

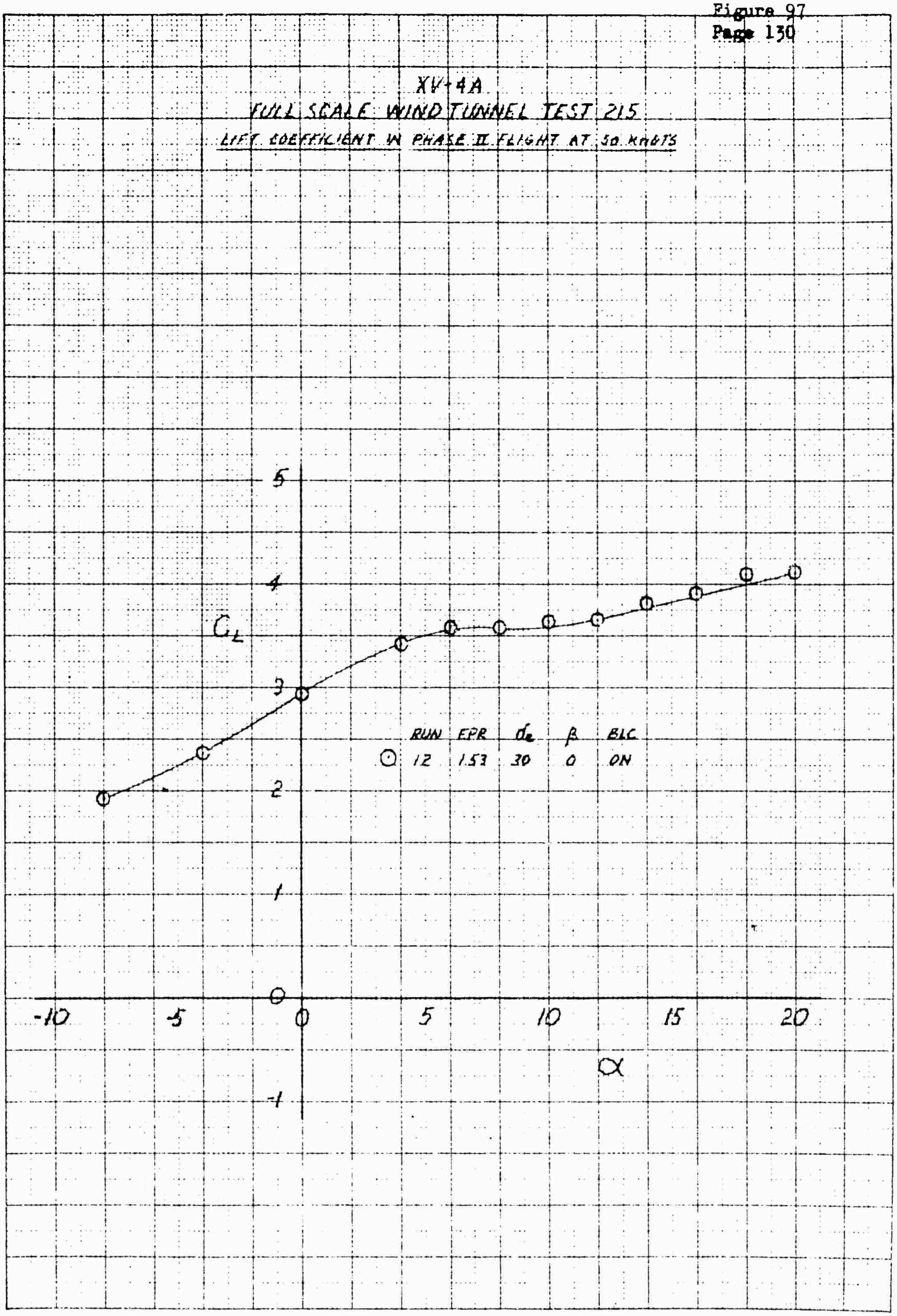
XV-4A
FULL SCALE WIND TUNNEL TEST 215
LIFT COEFFICIENT IN PHASE II FLIGHT AT 50 KNOTS
C_L
5
4
3
2
1
0
-1
-10
-5
0
5
10
15
20
α
RUN EPR δ_e β BLC
12 1.53 30 0 ON

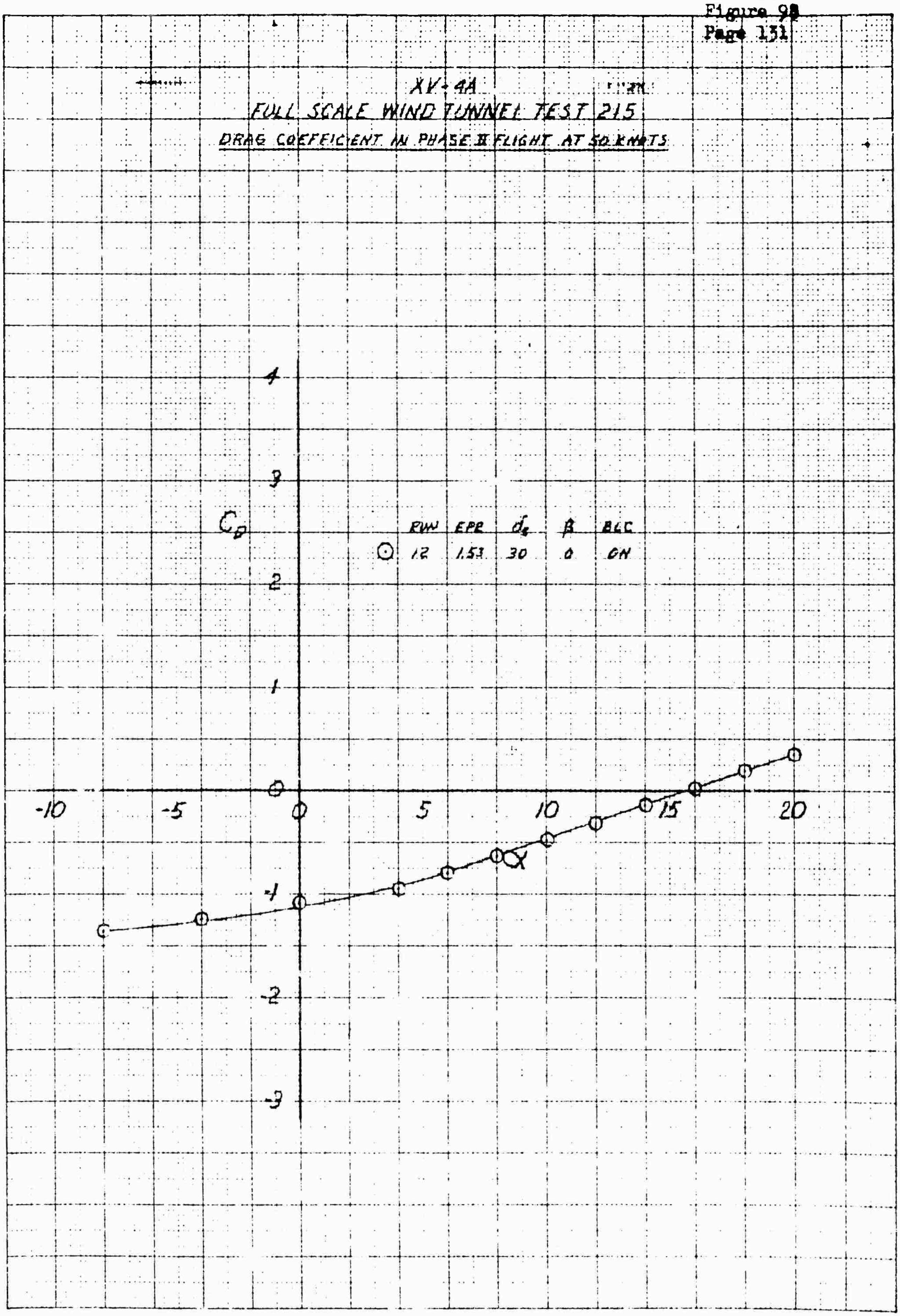
XV-4A
FULL SCALE WIND TUNNEL TEST 215
DRAG COEFFICIENT IN PHASE II FLIGHT AT 50 KNOTS
C_D
RW EPR δ_F β BLC
⊙ 12 1.53 30 0 ON
4
3
2
1
-1
-2
-3
-10
-5
0
5
10
15
20
α

XV-4A
FULL SCALE WIND TUNNEL TEST 215
PITCHING MOMENT COEFFICIENT IN PHASE II FLIGHT AT 50 KNOTS

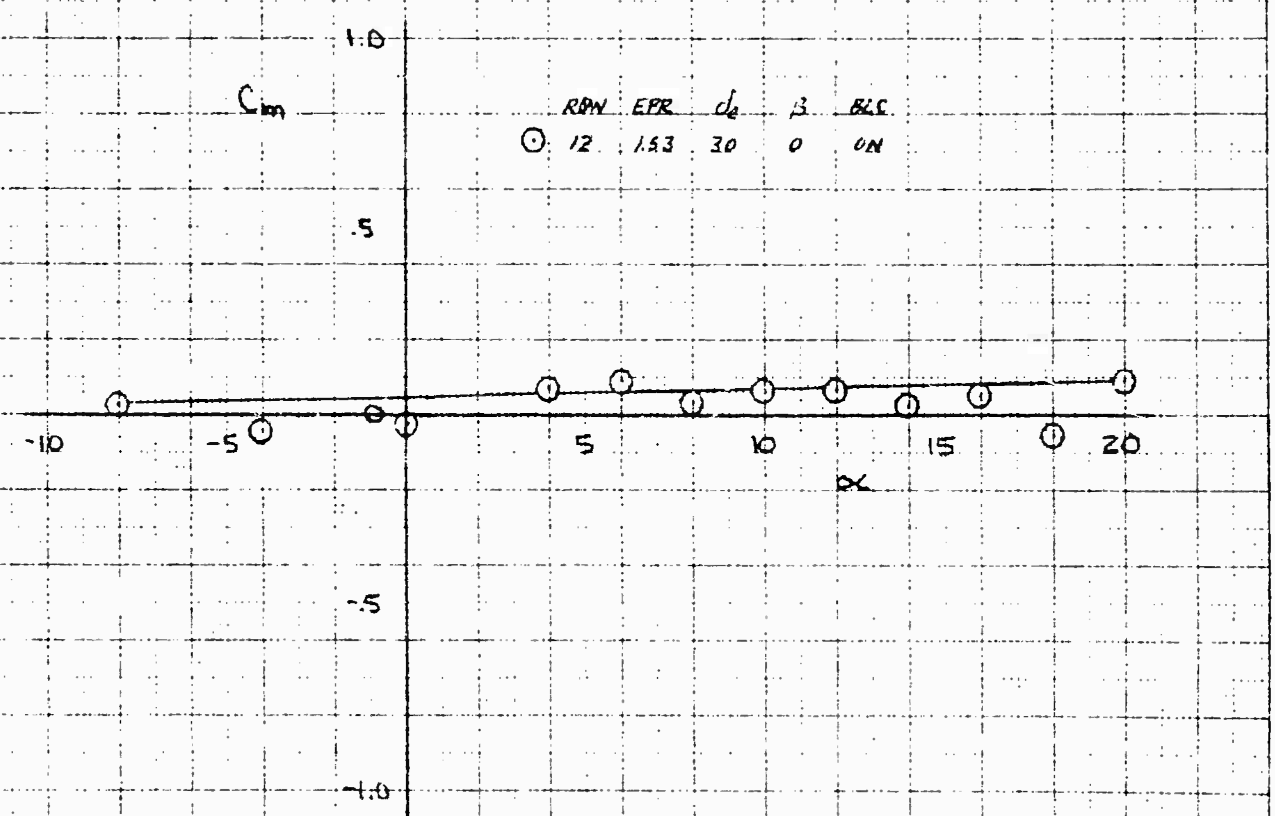

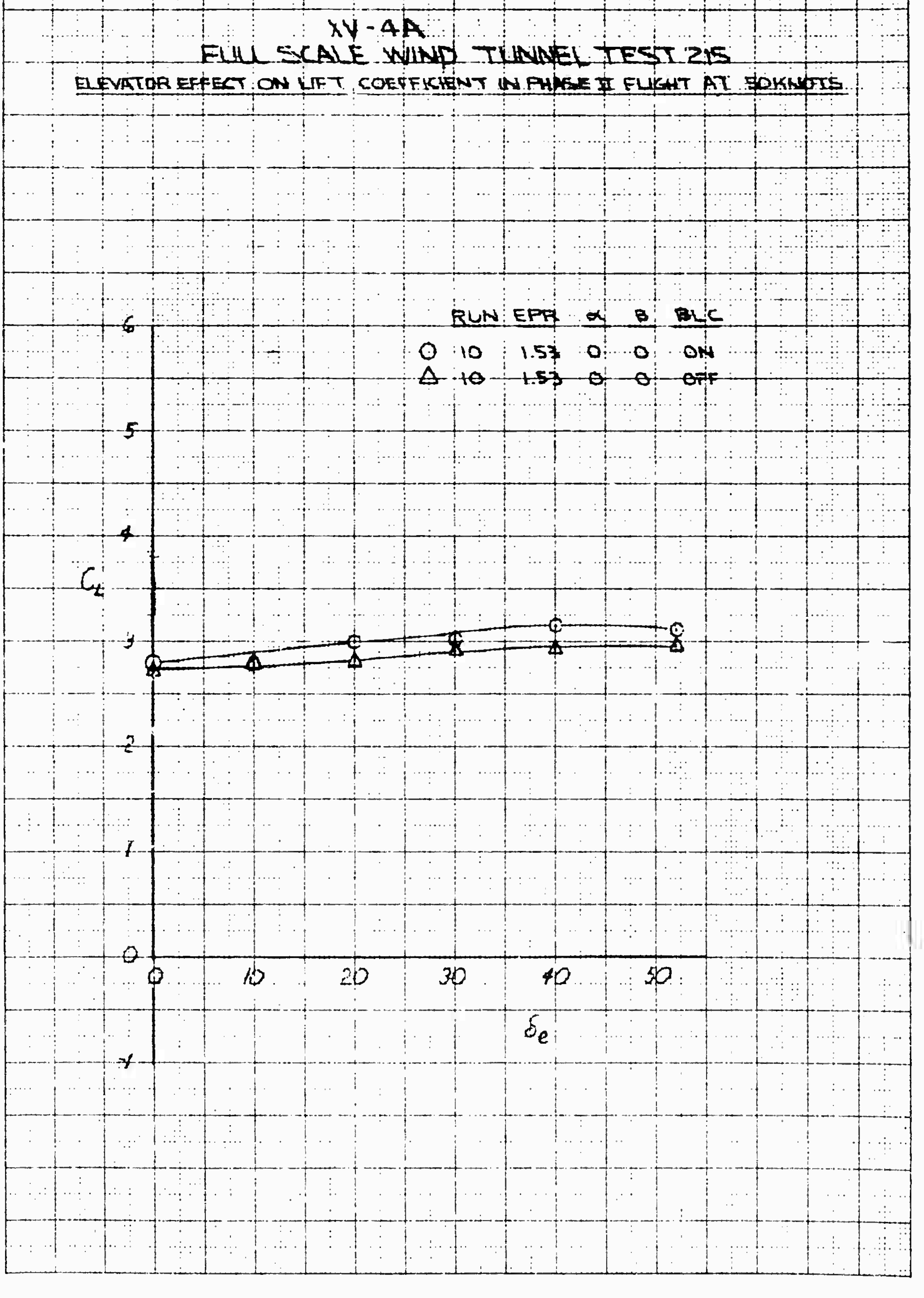
XV-4A
FULL SCALE WIND TUNNEL TEST 215
ELEVATOR EFFECT ON LIFT COEFFICIENT IN PHASE II FLIGHT AT 50 KNOTS
RUN EPR α β BLC
○ 10 1.53 0 0 ON
△ 10 1.53 0 0 OFF
C_L
6
5
4
3
2
1
0
-1
0
10
20
30
40
50
δ_e

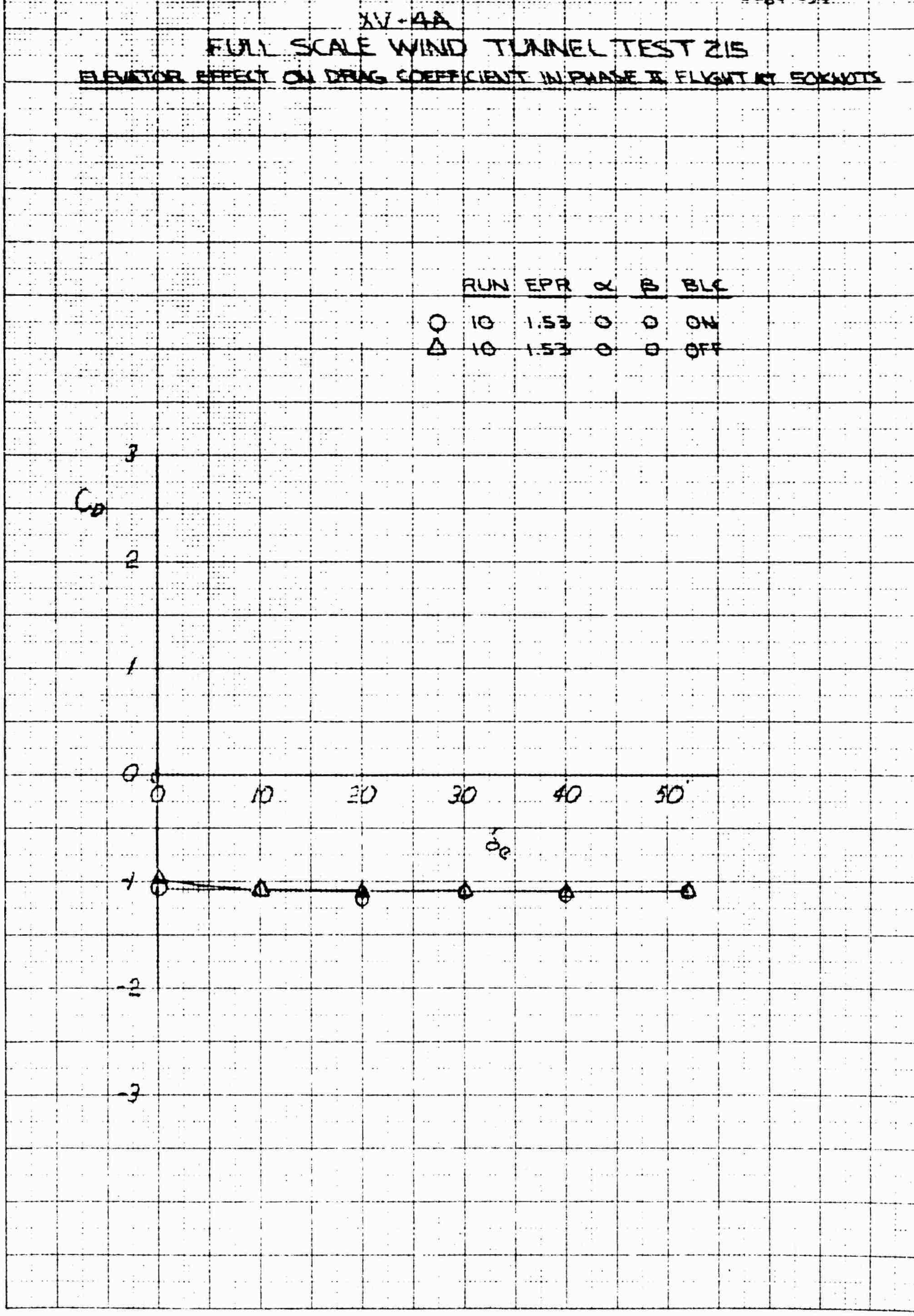

XV-4A
FULL SCALE WIND TUNNEL TEST 215
ELEVATOR EFFECT ON DRAG COEFFICIENT IN PHASE II FLIGHT AT 50 KNOTS
RUN EPR α β BLC
10 1.53 0 0 ON
10 1.53 0 0 OFF
C_D
3
2
1
0
-1
-2
-3
0
10
20
30
40
50
δ_e

XV-4A
FULL SCALE WIND TUNNEL TEST 215
ELEVATOR EFFECT ON PITCHING MOMENT COEFFICIENT IN PHASE II AT 50 KNOTS

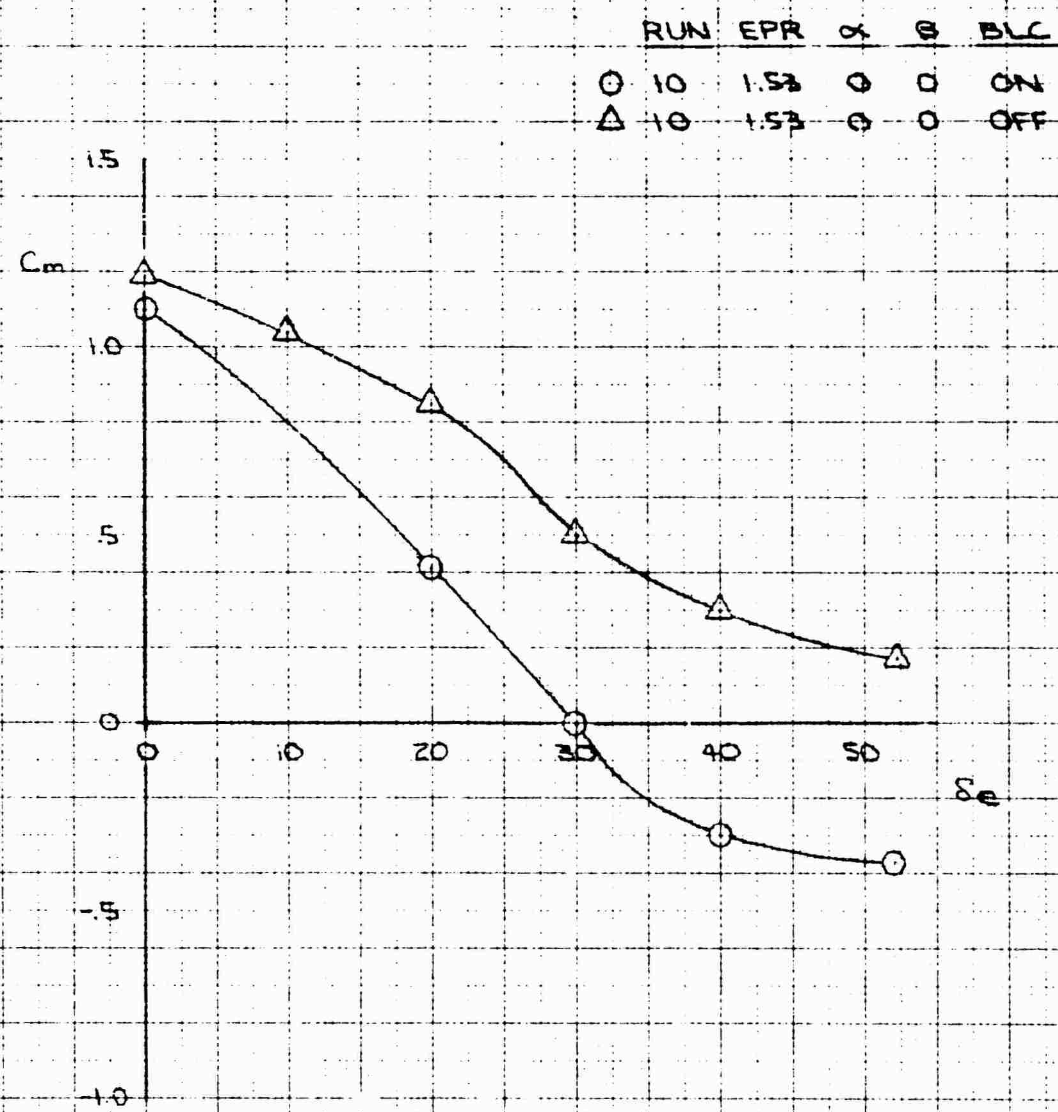

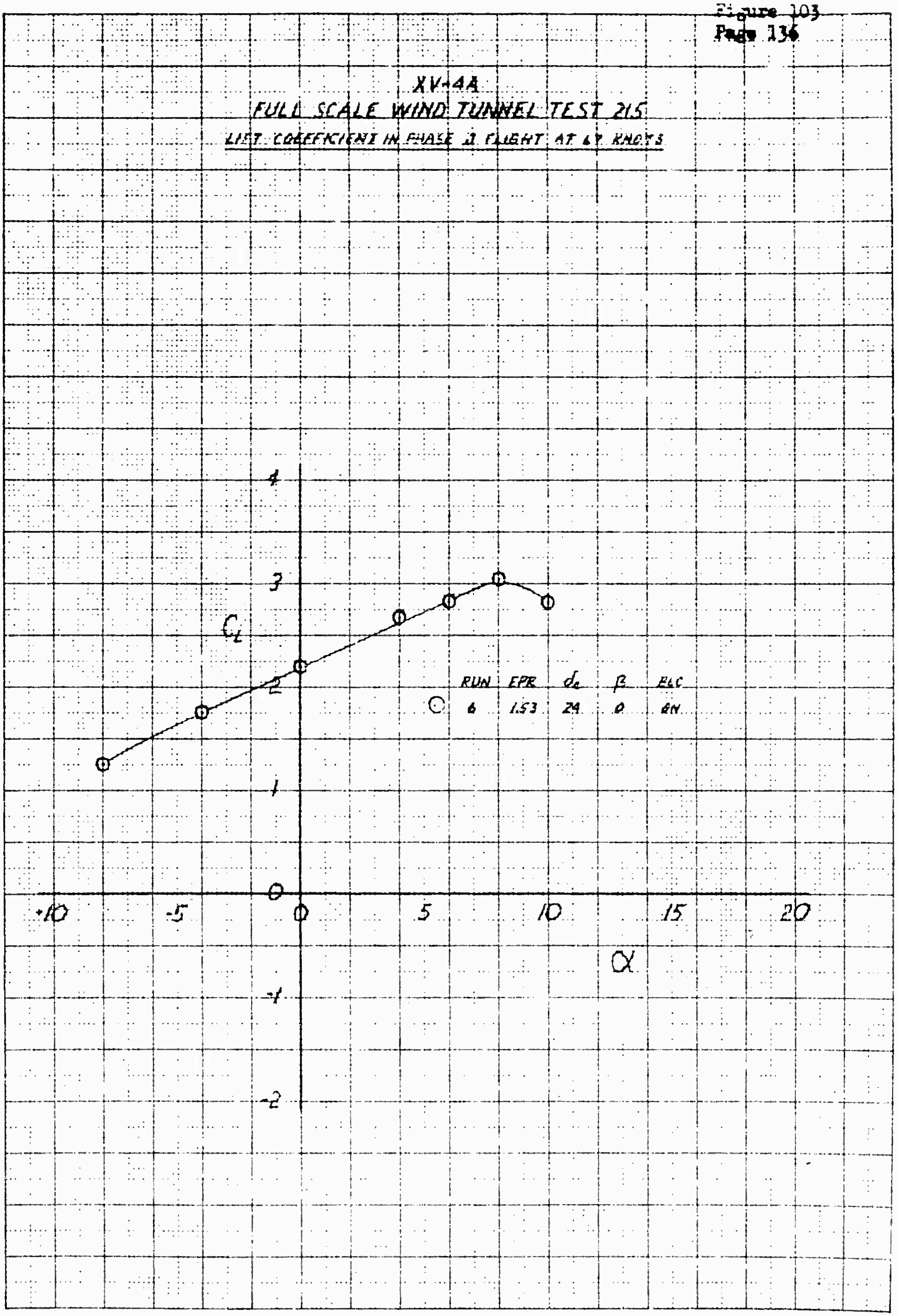
XV-4A
FULL SCALE WIND TUNNEL TEST 215
LIFT COEFFICIENT IN PHASE II FLIGHT AT 67 KNOTS
C_L
α
RUN EPR δ_e β ELC
6 1.53 24 0 ON
4
3
2
1
0
-1
-2
-10
-5
0
5
10
15
20

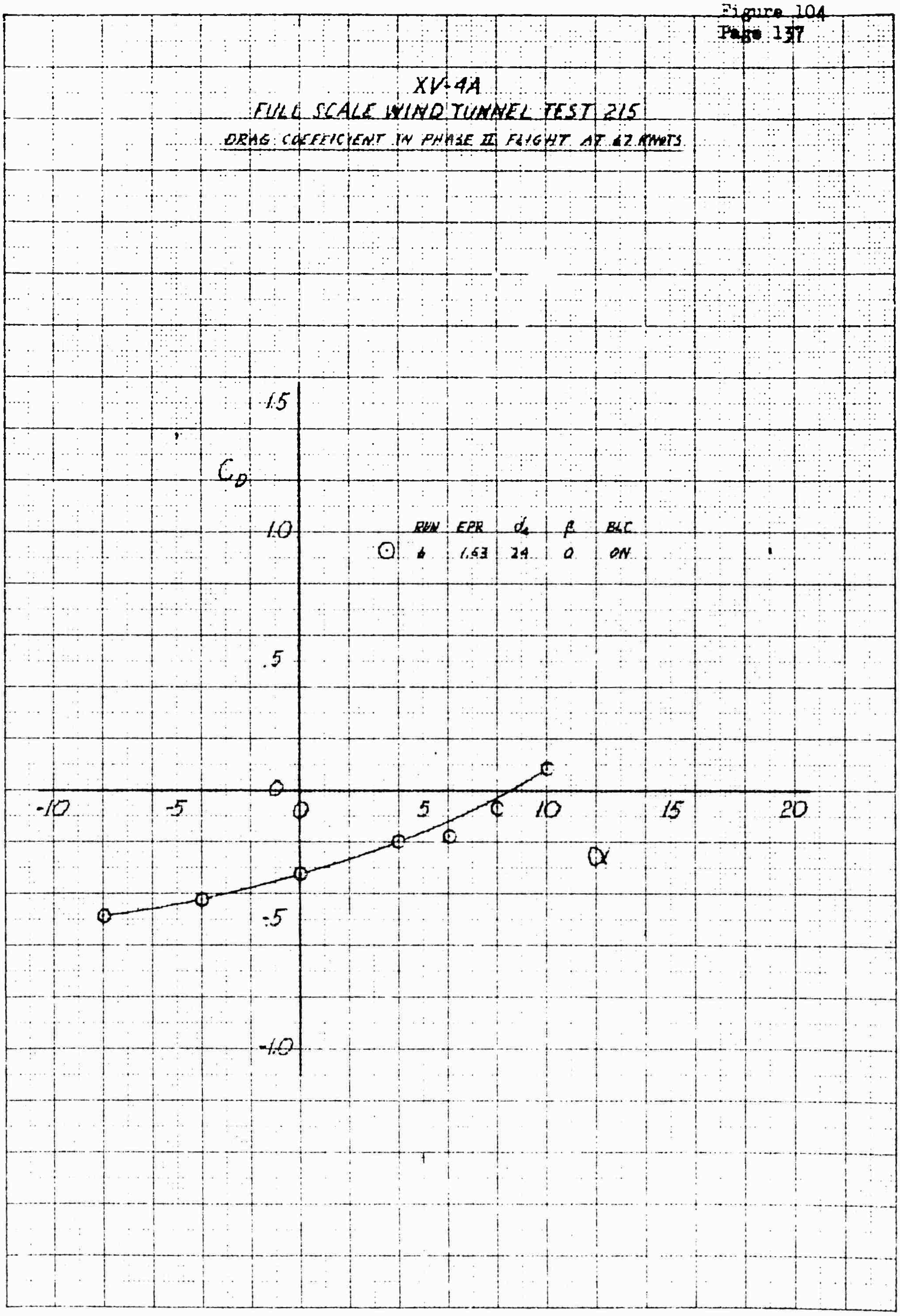
XV-4A
FULL SCALE WIND TUNNEL TEST 215
DRAG COEFFICIENT IN PHASE II FLIGHT AT
C_D
1.5
1.0
.5
0
-.5
-1.0
-10
-5
0
5
10
15
20
α
RUN EPR d_4 β BLC
6 1.63 24 0 ON

XV-4A
FULL SCALE WIND TUNNEL TEST 215
PITCHING MOMENT COEFFICIENT IN PHASE II FLIGHT AT 67 KNOTS

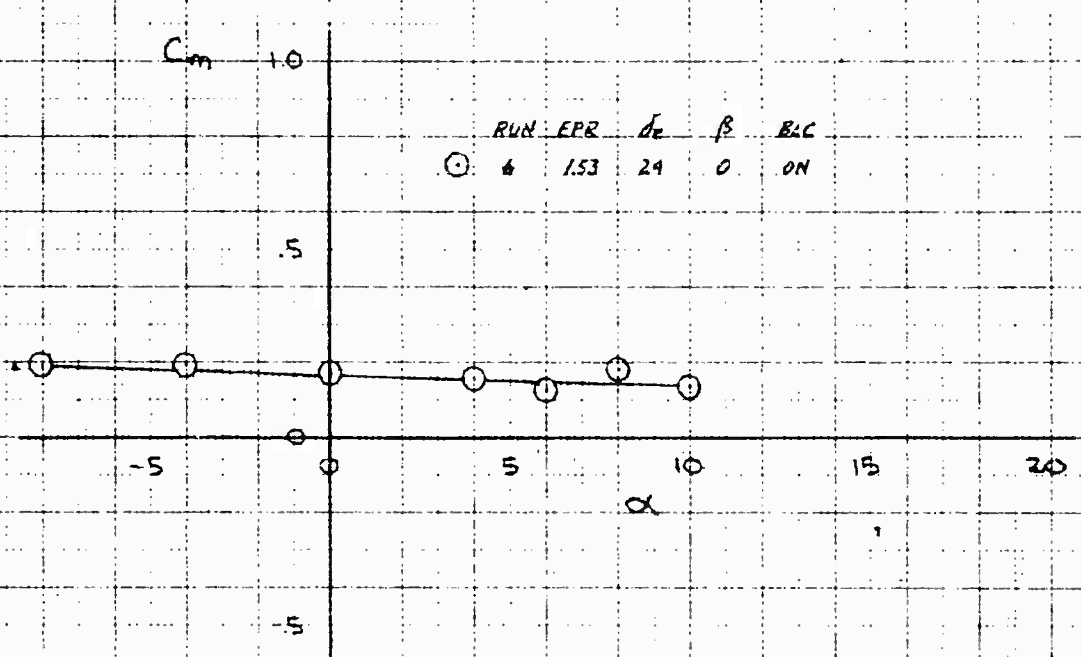

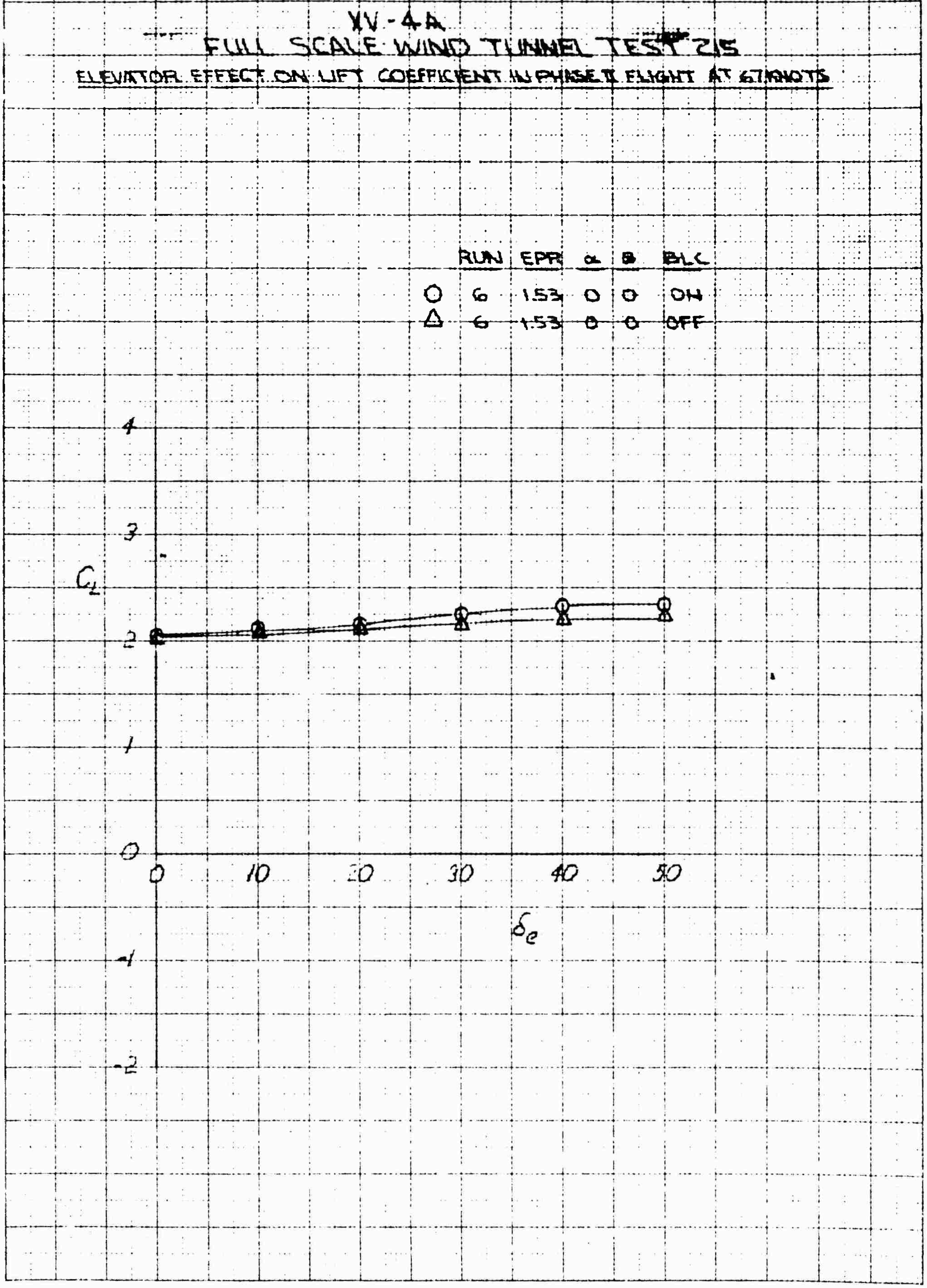
XV-4A
FULL SCALE WIND TUNNEL TEST 215
ELEVATOR EFFECT ON LIFT COEFFICIENT IN PHASE II FLIGHT AT 67 KNOTS
RUN EPR α β BLC
○ 6 1.53 0 0 ON
△ 6 1.53 0 0 OFF
4
3
2
1
0
-1
-2
C_L
0
10
20
30
40
50
δ_e

XV-4A
FULL SCALE WIND TUNNEL TEST 215
ELEVATOR EFFECT ON DRAG COEFFICIENT IN PHASE II FLIGHT AT 67 KNOTS

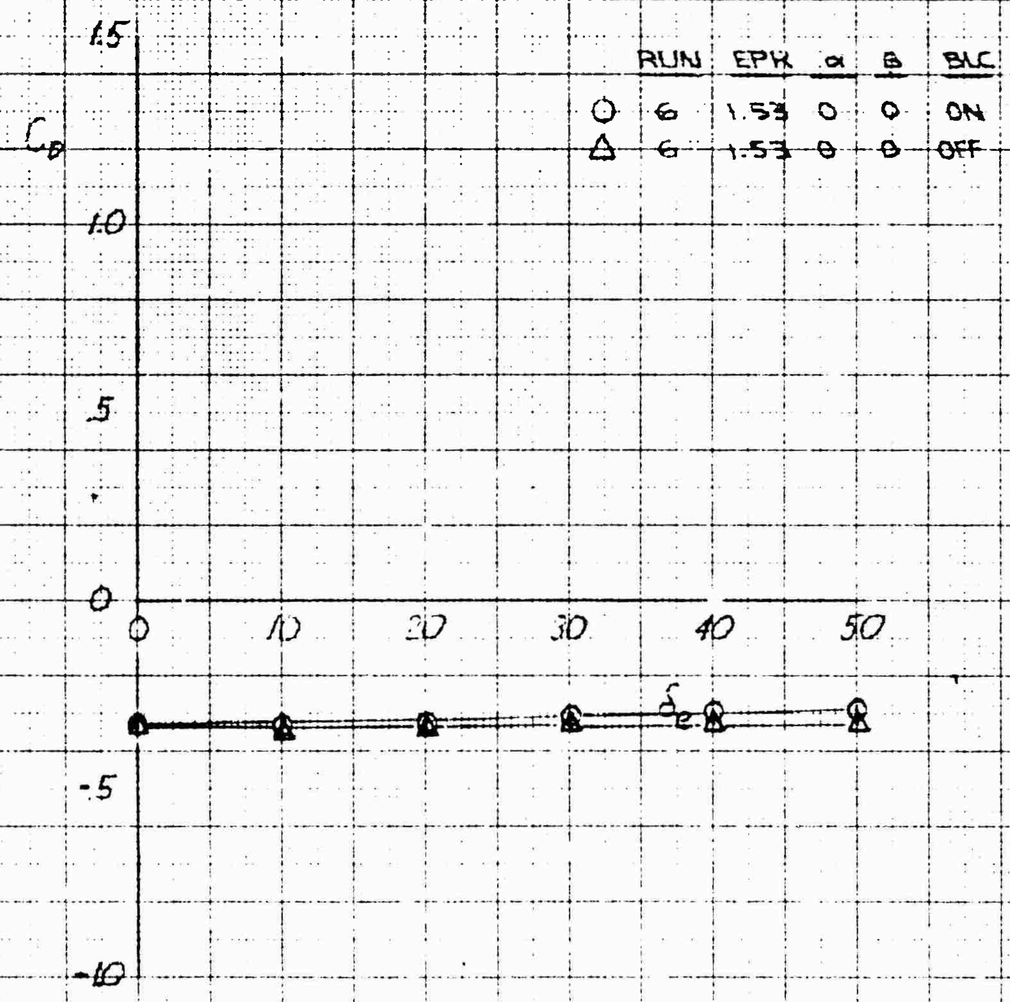

XV-4A
FULL SCALE WIND TUNNEL TEST 215
ELEVATOR EFFECT ON PITCHING MOMENT COEFFICIENT IN PHASE II FLIGHT AT 67 KNOTS

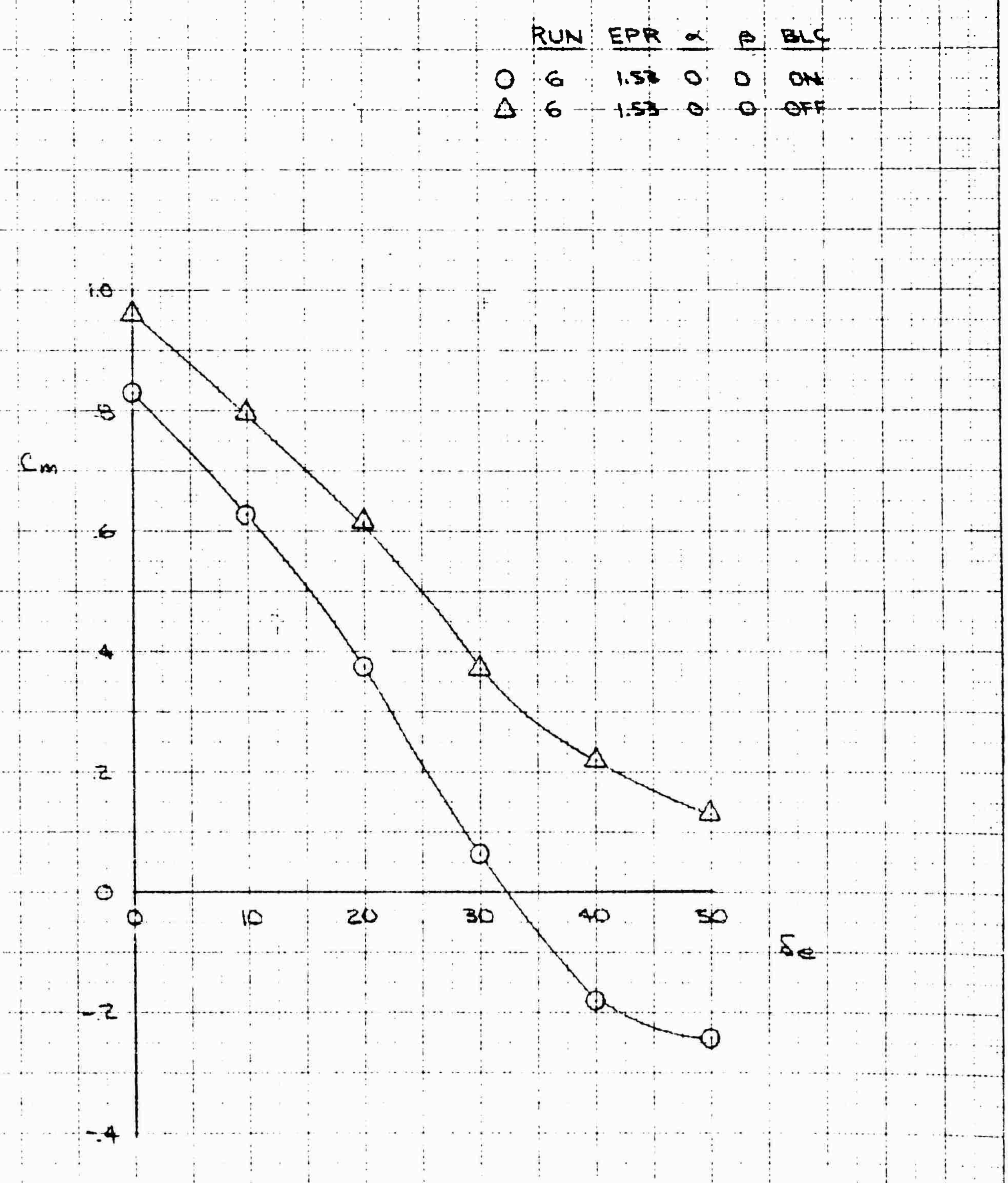

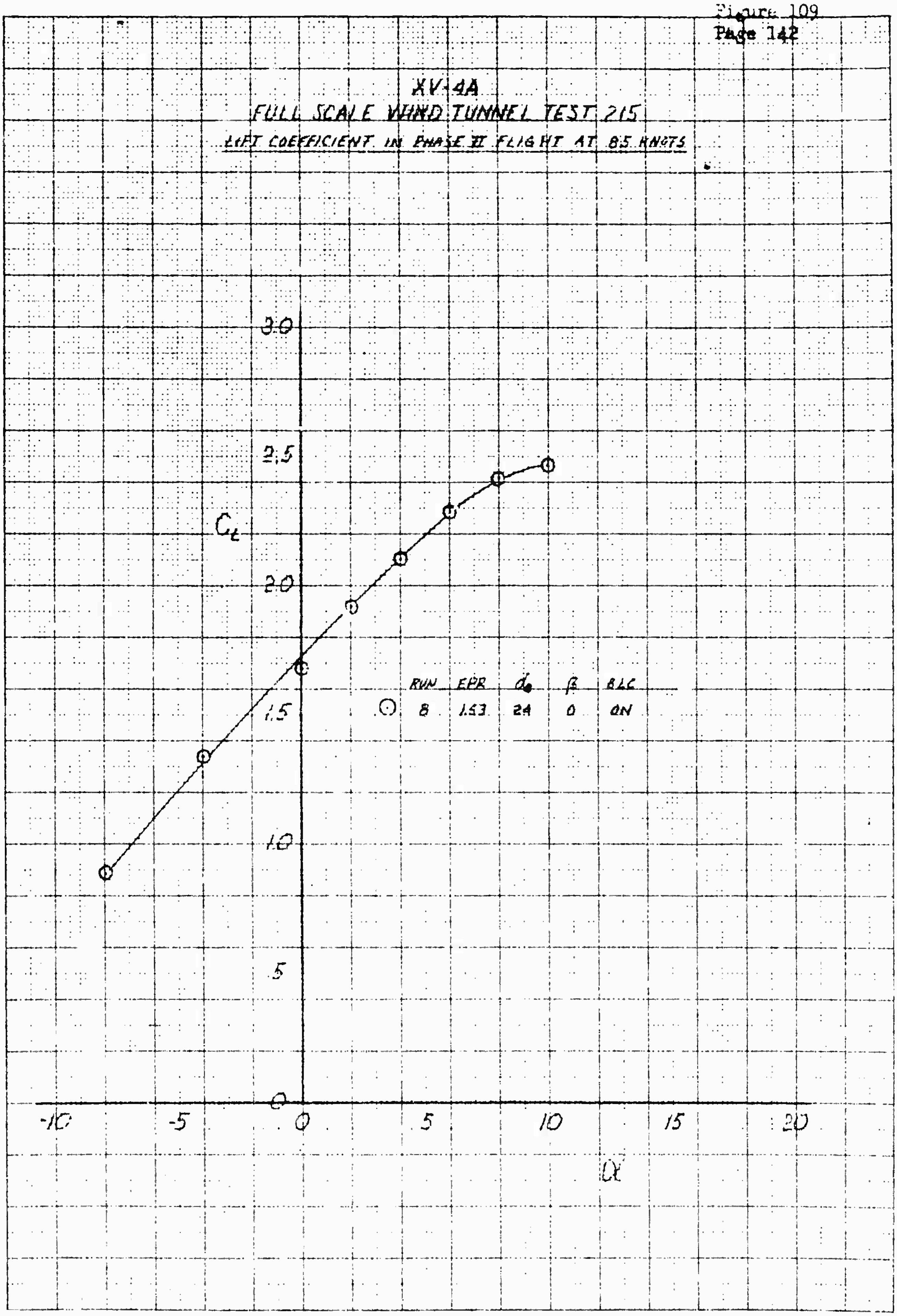
XV-4A
FULL SCALE WIND TUNNEL TEST 215
LIFT COEFFICIENT IN PHASE II FLIGHT AT 85 KNOTS
3.0
2.5
2.0
1.5
1.0
.5
0
C_L
RUN EPR α_0 β BLC
8 1.53 24 0 ON
-10
-5
0
5
10
15
20
α

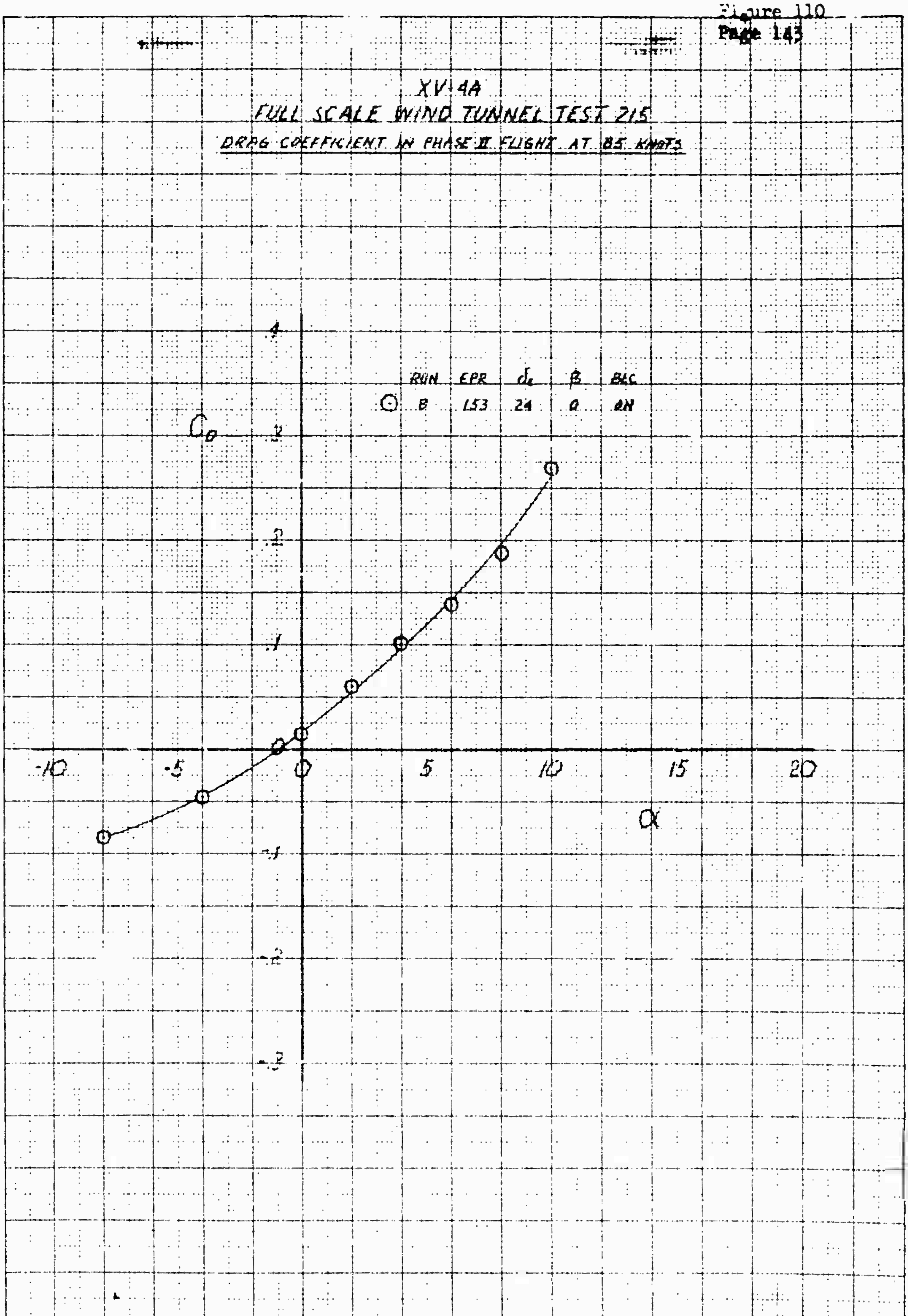
XV-4A
FULL SCALE WIND TUNNEL TEST 215
DRAG COEFFICIENT IN PHASE II FLIGHT AT 85 KNOTS
RUN EPR δ_e β BAC
8 1.53 24 0 ON
C_D
.4
.3
.2
.1
-.1
-.2
-.3
-10 -5 0 5 10 15 20
α

XV-4A
FULL SCALE WIND TUNNEL TEST 215
PITCHING MOMENT COEFFICIENT IN PHASE II FLIGHT AT 85 KNOTS

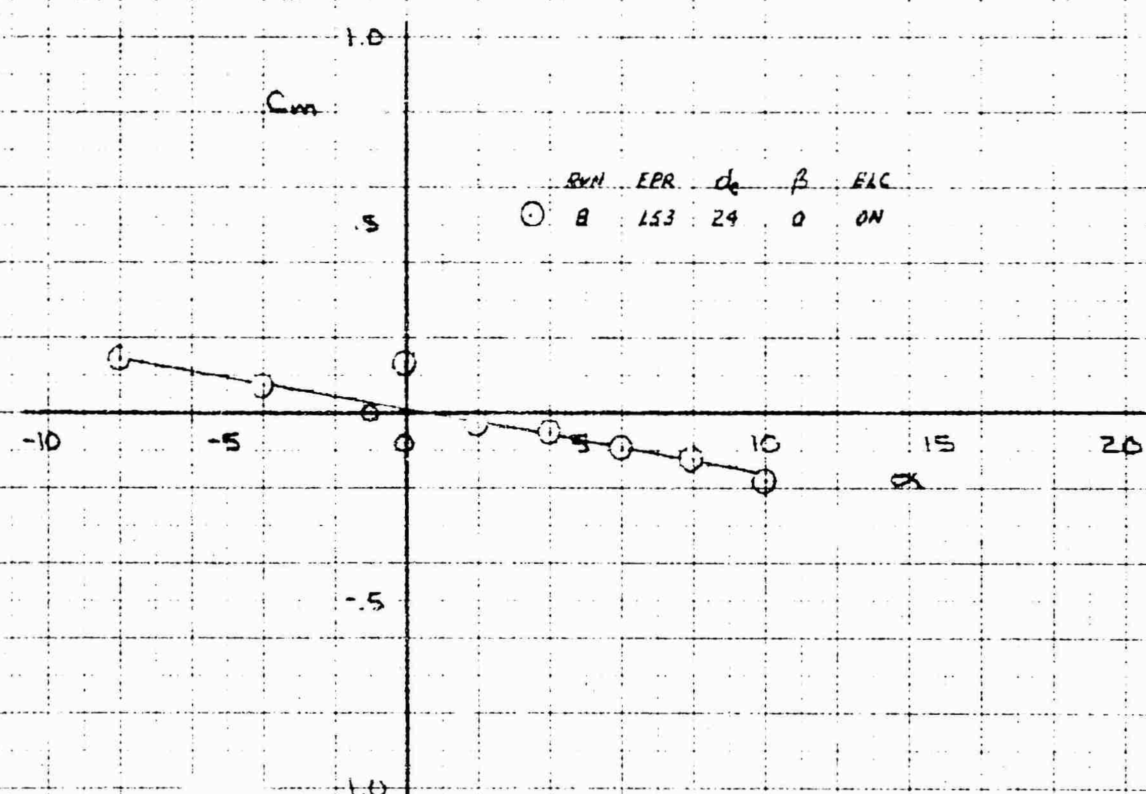

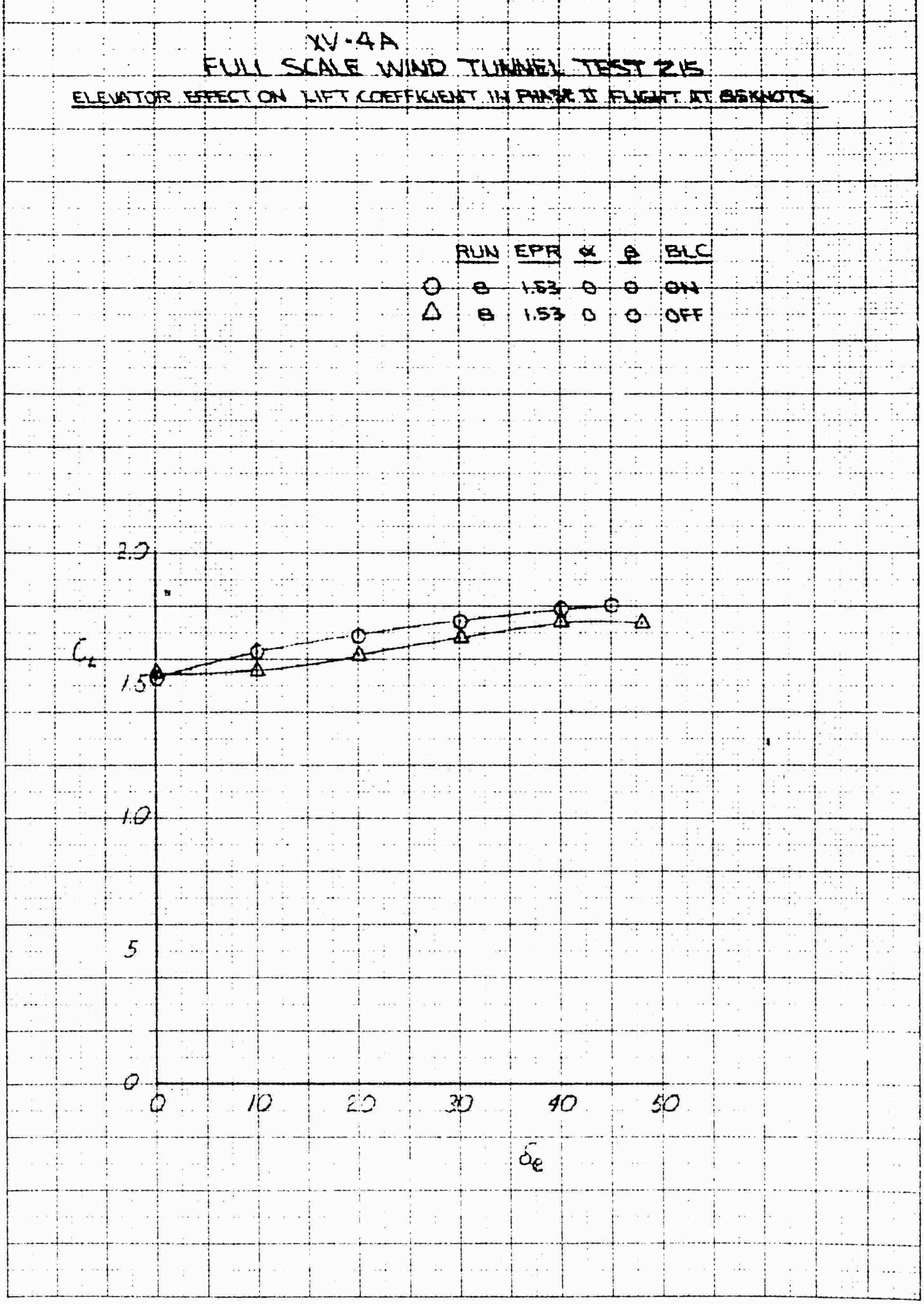
XV-4A
FULL SCALE WIND TUNNEL TEST 215
ELEVATOR EFFECT ON LIFT COEFFICIENT IN
RUN EPR α β BLC
○ 8 1.53 0 0 ON
△ 8 1.53 0 0 OFF
2.0
1.5
1.0
5
0
C_L
0
10
20
30
40
50
δ_e

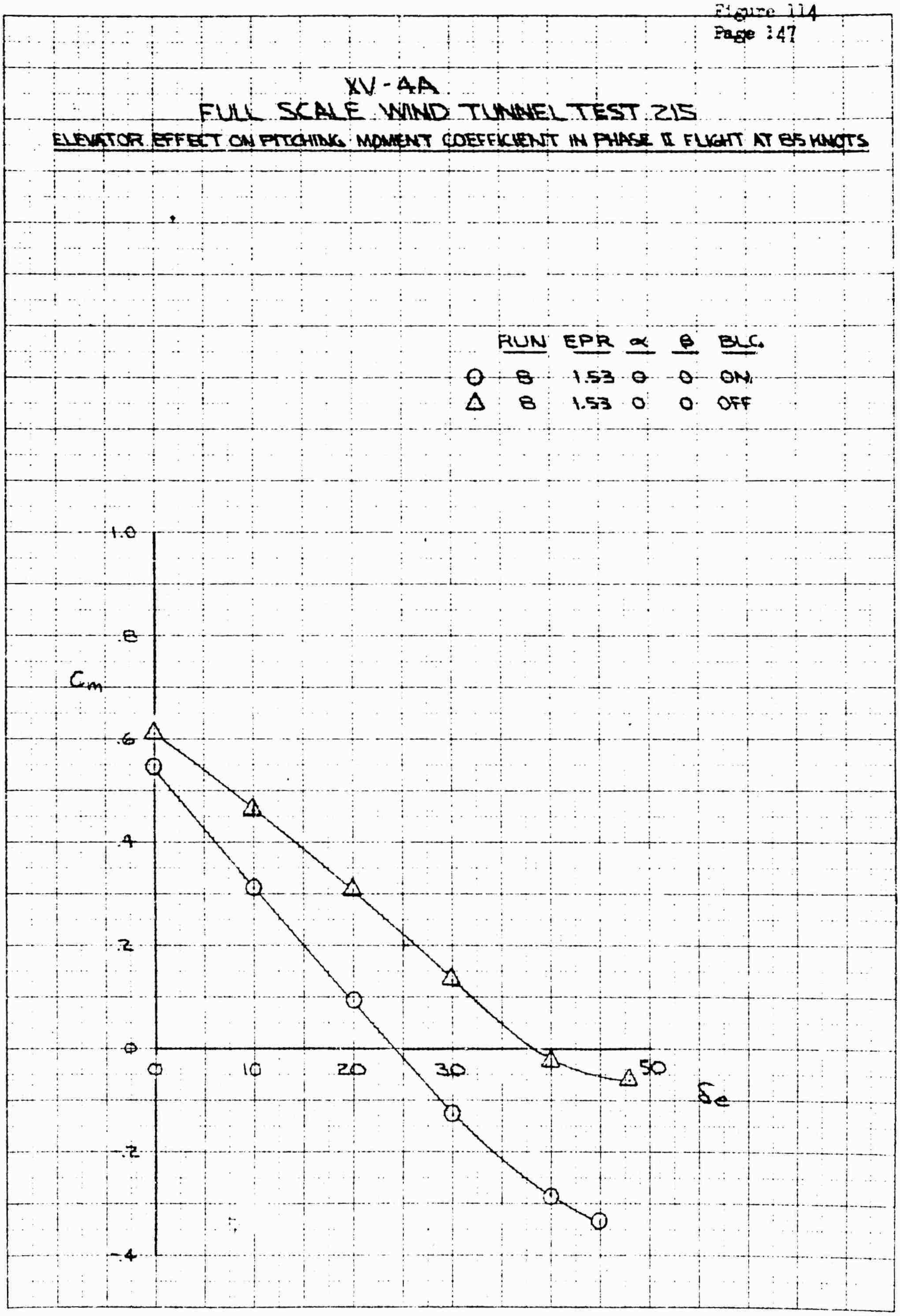
XV-4A
FULL SCALE WIND TUNNEL TEST 215
ELEVATOR EFFECT ON PITCHING MOMENT COEFFICIENT IN PHASE II FLIGHT AT 85 KNOTS
RUN EPR α β BLC
8 1.53 0 0 ON
8 1.53 0 0 OFF
1.0
.8
Cm
.6
.4
.2
0
-.2
-.4
0
10
20
30
50
δe

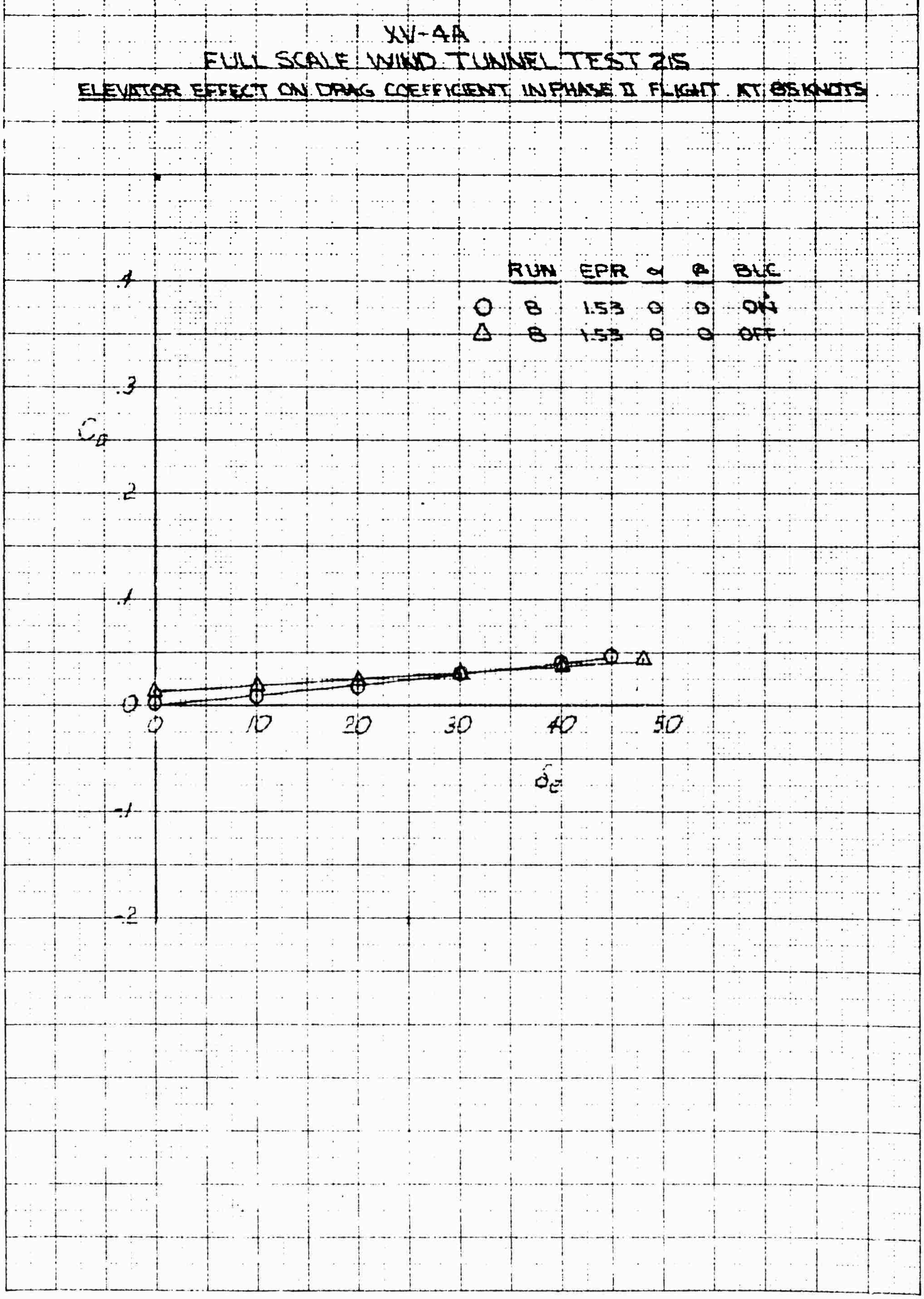
XV-4A
FULL SCALE WIND TUNNEL TEST 215
ELEVATOR EFFECT ON DRAG COEFFICIENT IN PHASE II FLIGHT AT 85 KNOTS
RUN EPR α β BLC
○ 8 1.53 0 0 ON
△ 8 1.53 0 0 OFF
.4
.3
C_D
.2
.1
0
-.1
-.2
0
10
20
30
40
50
δ_e

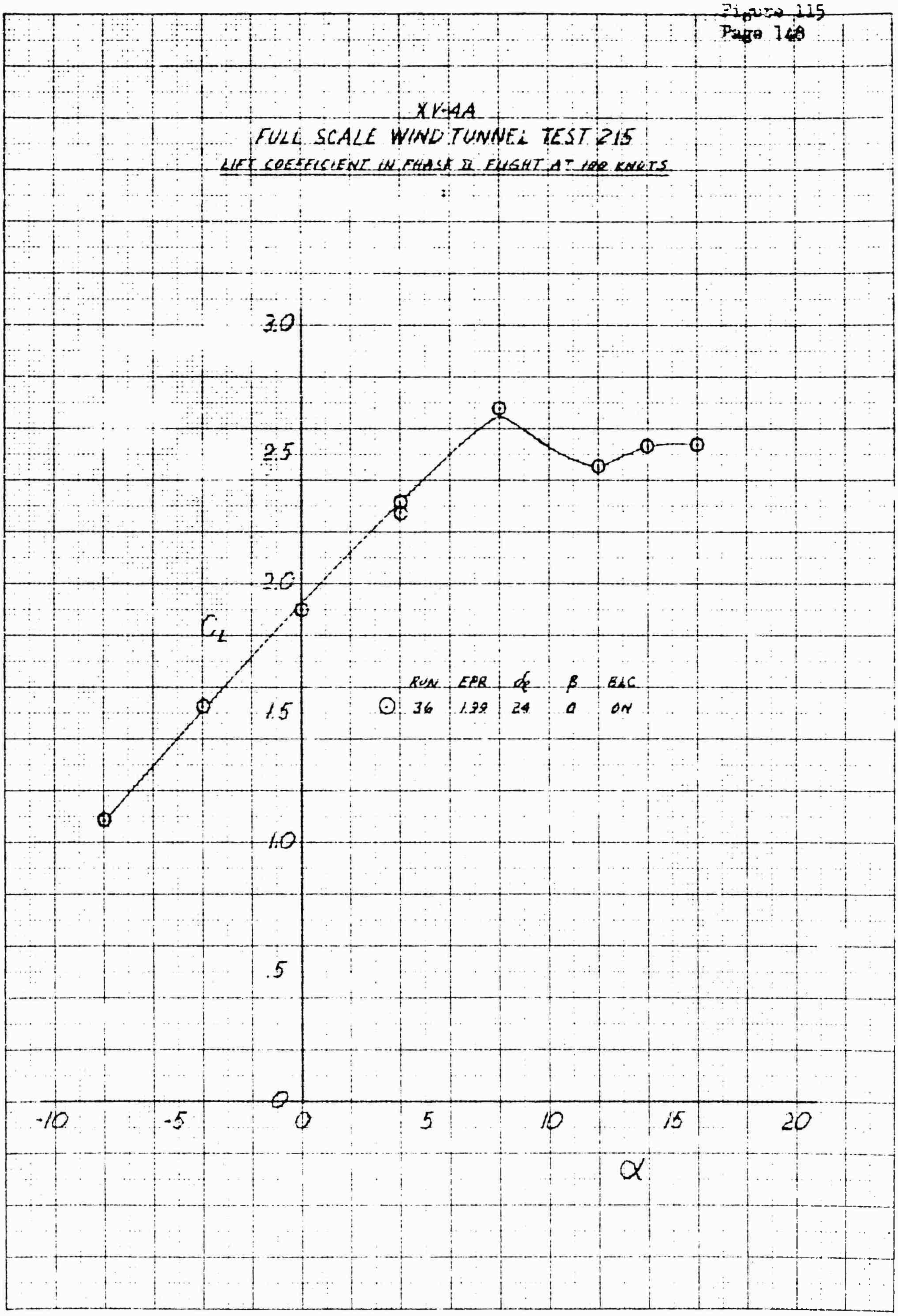
XV-4A
FULL SCALE WIND TUNNEL TEST 215
LIFT COEFFICIENT IN PHASE II FLIGHT AT 100 KNOTS
3.0
2.5
2.0
1.5
1.0
.5
0
C_L
RUN EPR δ_f β BLC
36 1.39 24 0 ON
-10
-5
0
5
10
15
20
α

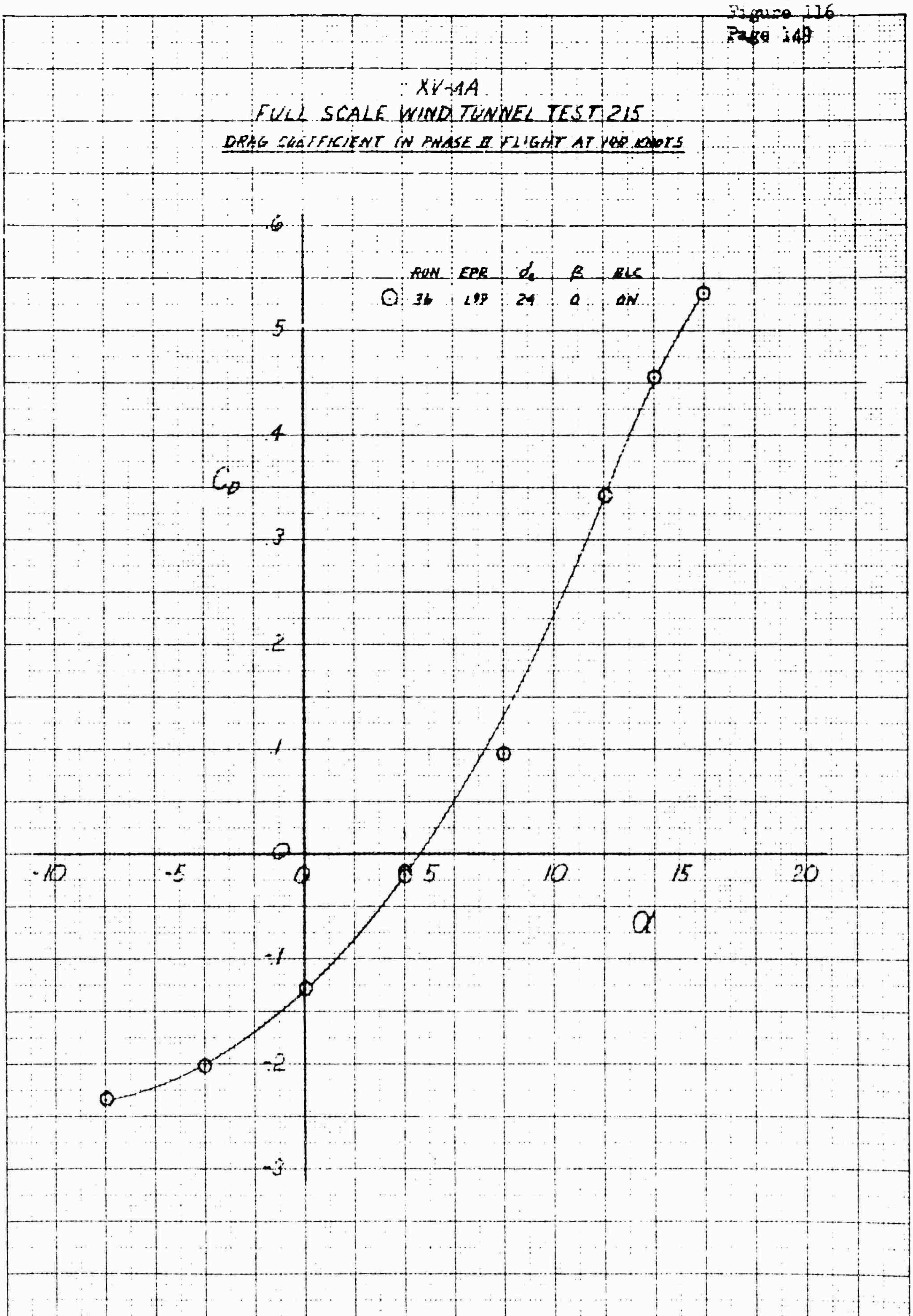
XV-4A
FULL SCALE WIND TUNNEL TEST 215
RUN EPR δe β BLC
36 24 0 ON
C_D
α
.6
5
.4
.3
.2
.1
0
-.1
-.2
-.3
-10
-5
0
5
10
15
20

XV-4A
FULL SCALE WIND TUNNEL TEST 215
PITCHING MOMENT COEFFICIENT IN PHASE II FLIGHT AT 100 KNOTS

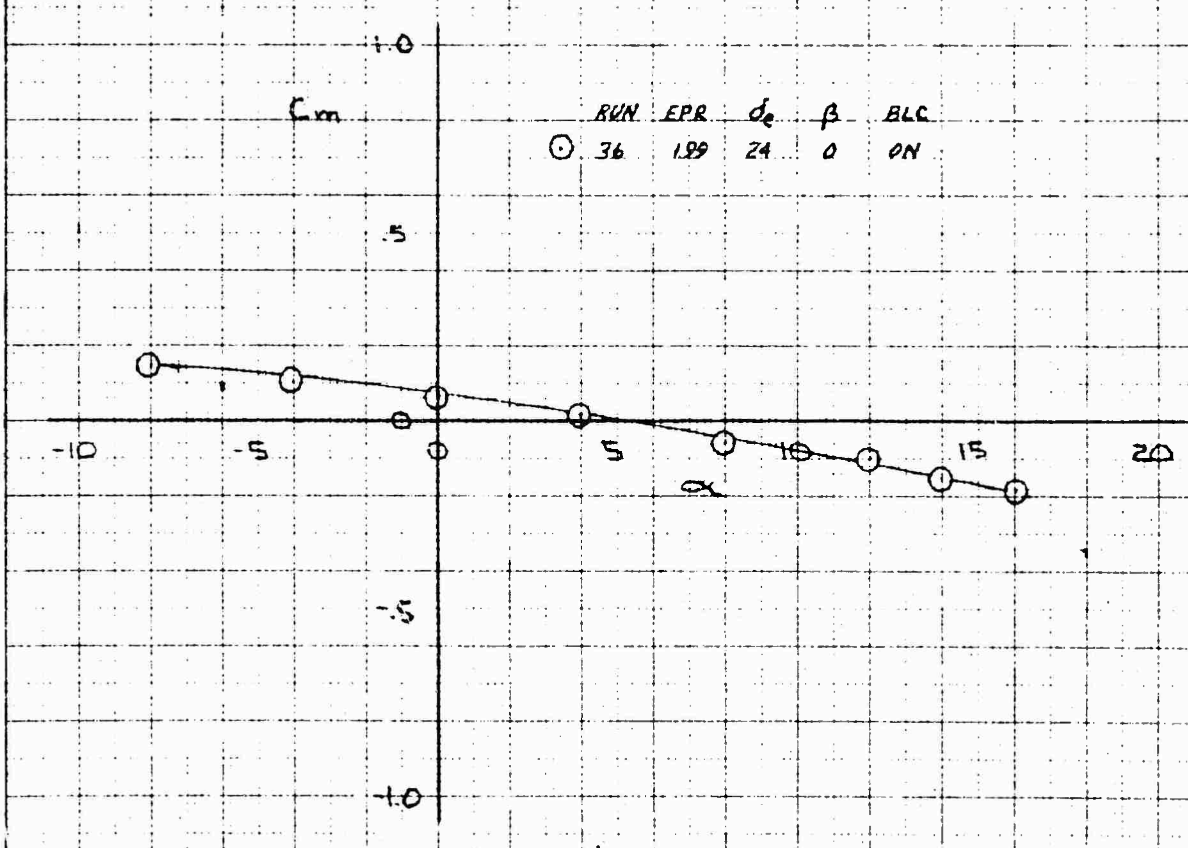

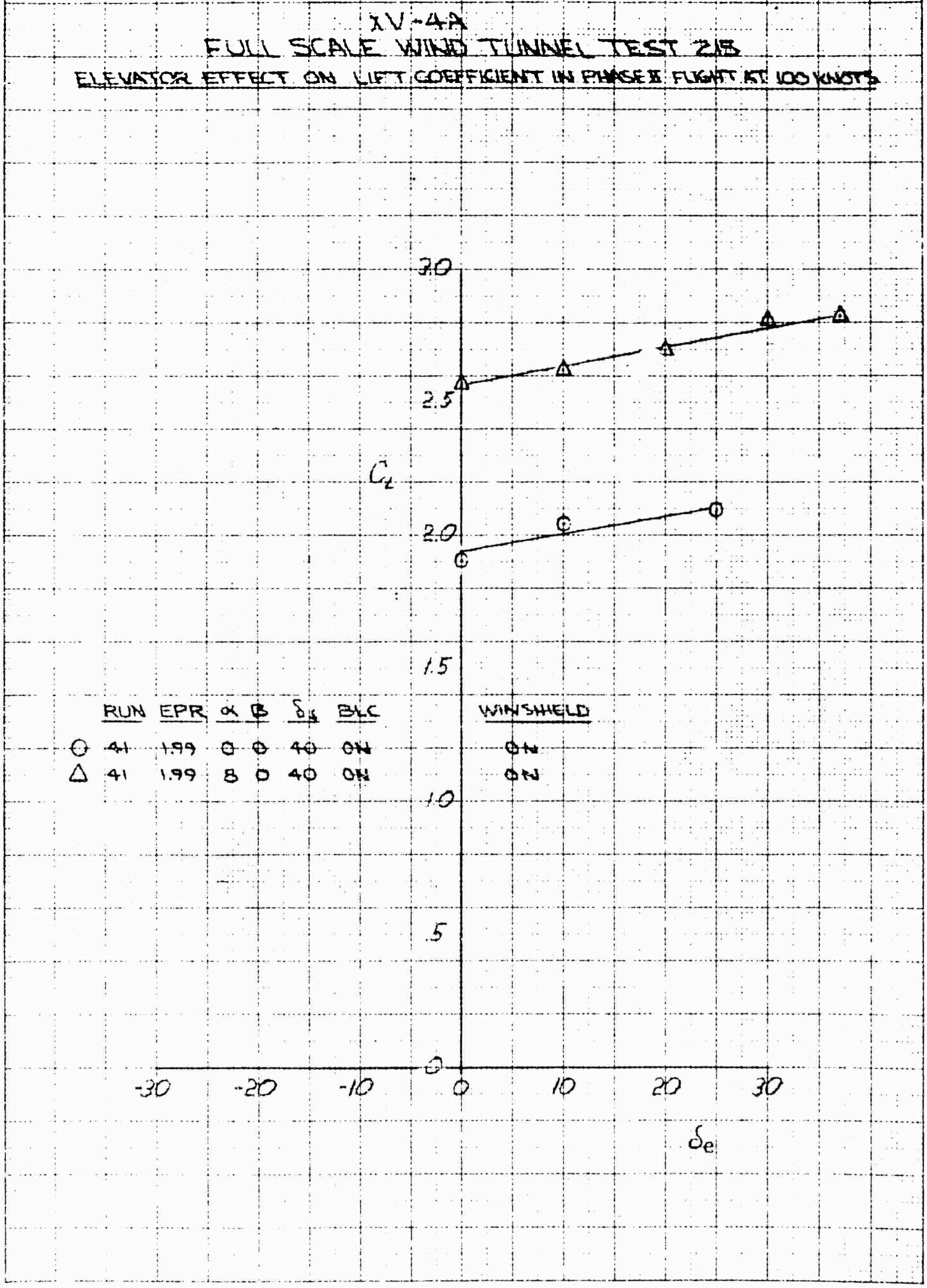
XV-4A
FULL SCALE WIND TUNNEL TEST 215
ELEVATOR EFFECT ON LIFT COEFFICIENT IN PHASE II FLIGHT AT 100 KNOTS
3.0
2.5
2.0
1.5
1.0
.5
0
C_L
-30
-20
-10
0
10
20
30
δ_e
RUN EPR α β δ_f BLC WINSHIELD
○ 41 1.99 0 0 40 ON ON
△ 41 1.99 8 0 40 ON ON

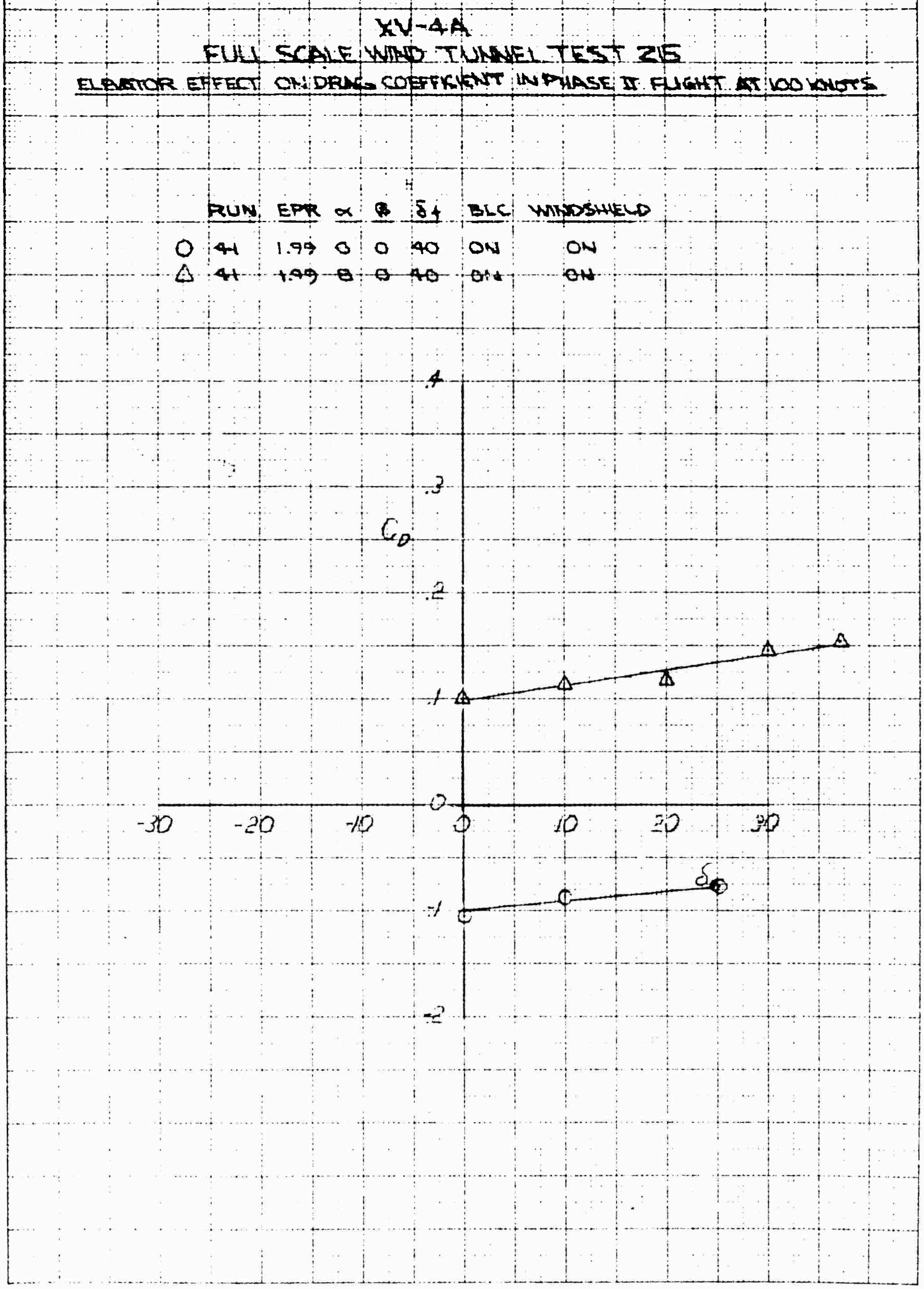
XV-4A
FULL SCALE WIND TUNNEL TEST 215
ELEVATOR EFFECT ON DRAG COEFFICIENT IN PHASE II FLIGHT AT 100 KNOTS
RUN EPR α β δf BLC WINDSHIELD
○ 41 1.99 0 0 40 ON ON
△ 41 1.99 8 0 40 ON ON
.4
.3
.2
.1
0
-.1
-.2
C_D
-30
-20
-10
0
10
20
30
δ_e

XV-4A
FULL SCALE WIND TUNNEL TEST 215
ELEVATOR EFFECT ON PITCHING MOMENT COEFFICIENT IN PHASE II FLIGHT AT 100 KNOTS

	RUN	EPR	α	β	δ_f	BLC	WINDSHIELD
○	41	1.99	0	0	40	ON	ON
△	41	1.99	8	0	40	ON	ON

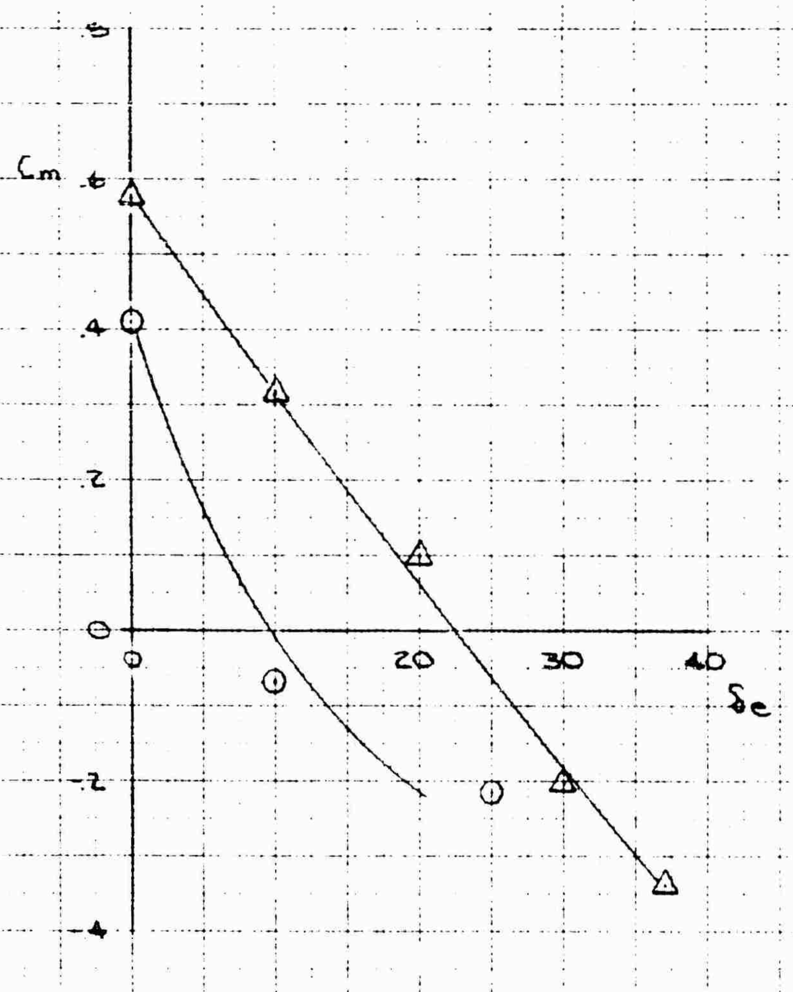

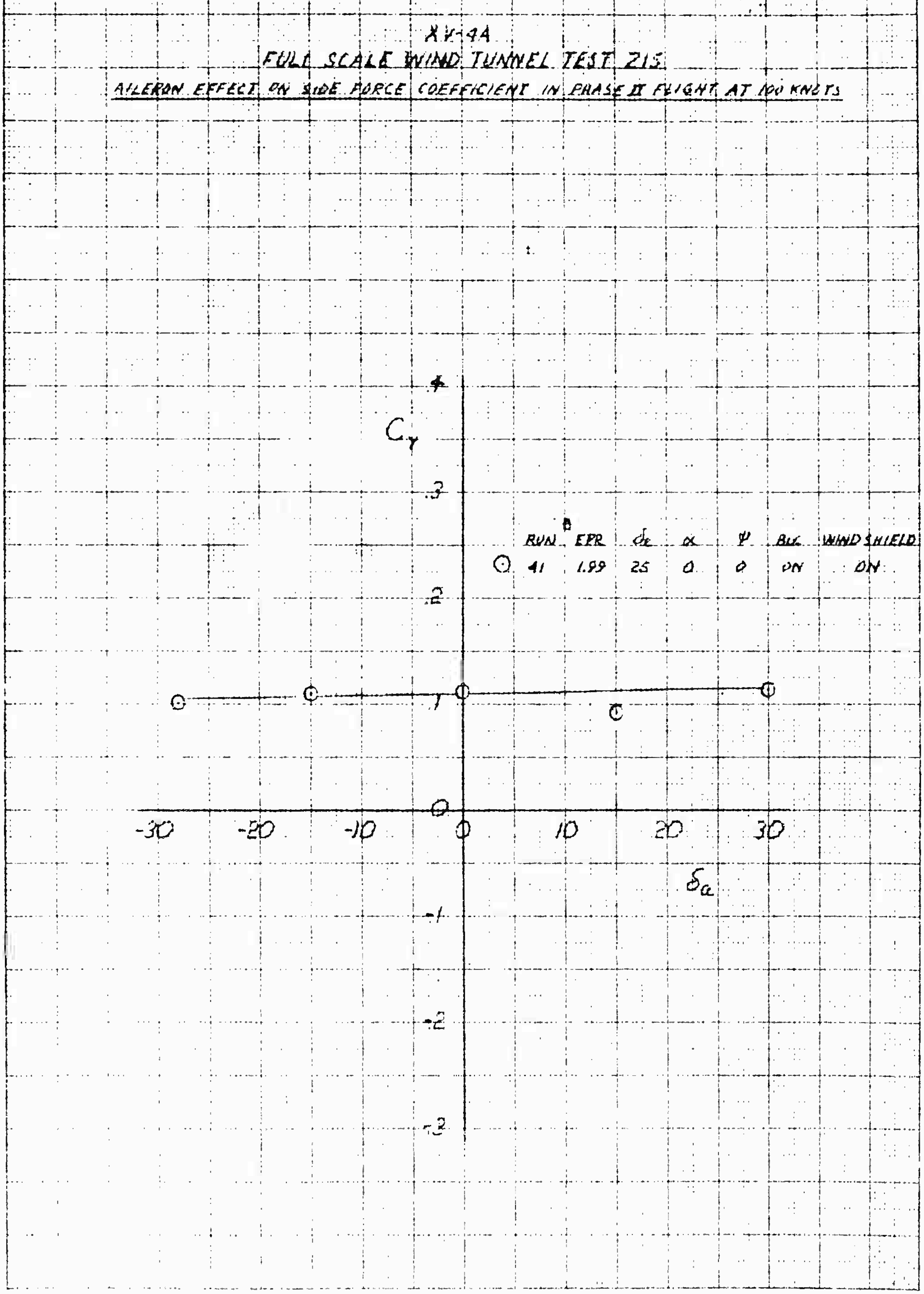

XV-4A
FULL SCALE WIND TUNNEL TEST 215
AILERON EFFECT ON SIDE FORCE COEFFICIENT IN PHASE II FLIGHT AT 100 KNOTS
C_Y
.4
.3
.2
.1
0
-.1
-.2
-.3
-30
-20
-10
0
10
20
30
δ_a
RUN EPR δ_f α ψ B.L.C. WINDSHIELD
41 1.99 25 0 0 ON ON

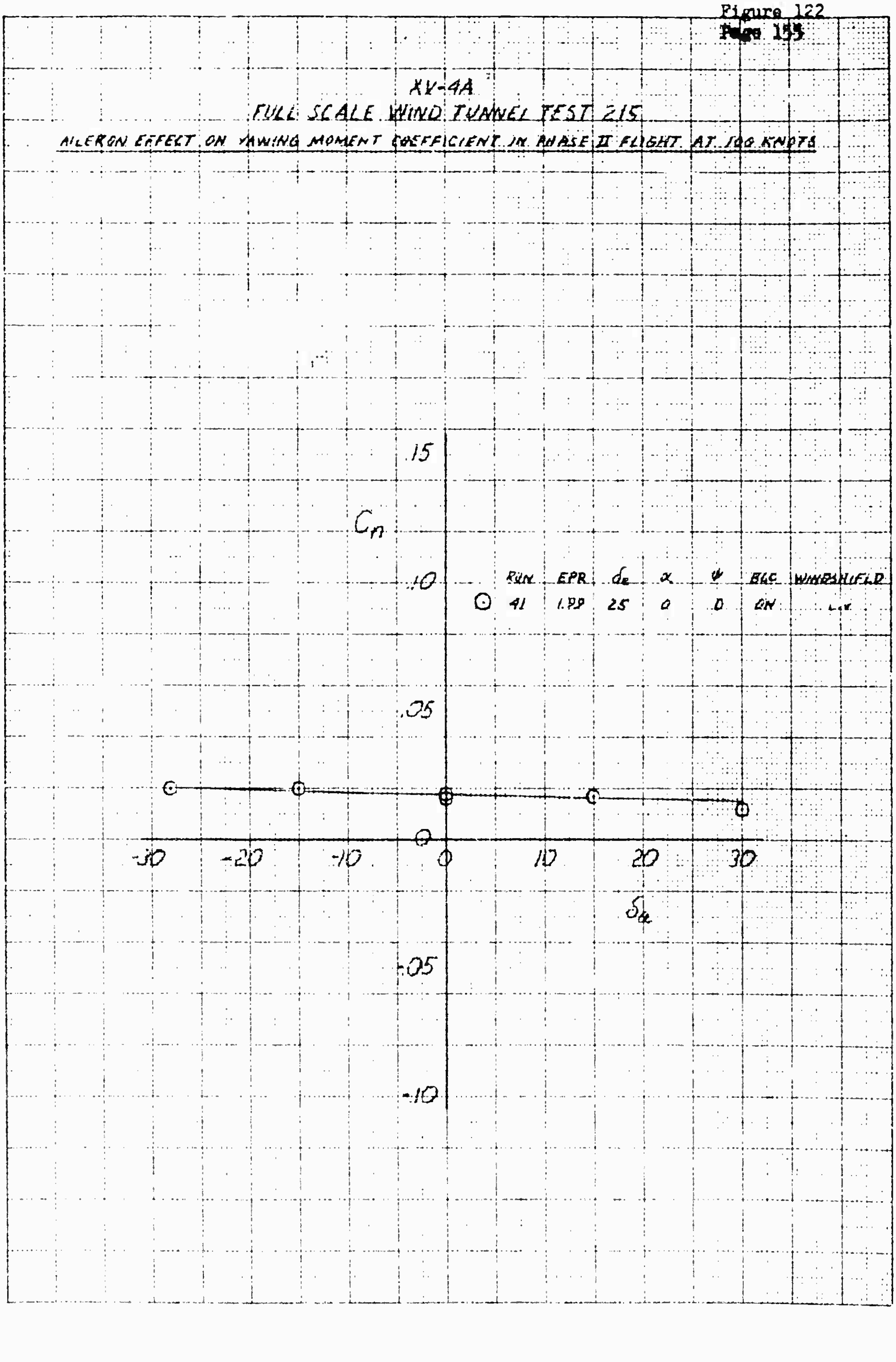
XV-4A
FULL SCALE WIND TUNNEL TEST 215
AILERON EFFECT ON YAWING MOMENT COEFFICIENT IN PHASE II FLIGHT AT 100 KNOTS
Cn
.15
.10
.05
-.05
-.10
-30
-20
-10
0
10
20
30
δa
RUN EPR δe α ψ BLC WINDSHIELD
41 1.99 25 0 0 ON

XV-4A

FULL SCALE WIND TUNNEL TEST 215

AILERON EFFECT ON ROLLING MOMENT COEFFICIENT IN PHASE II FLIGHT AT 100 KNOTS

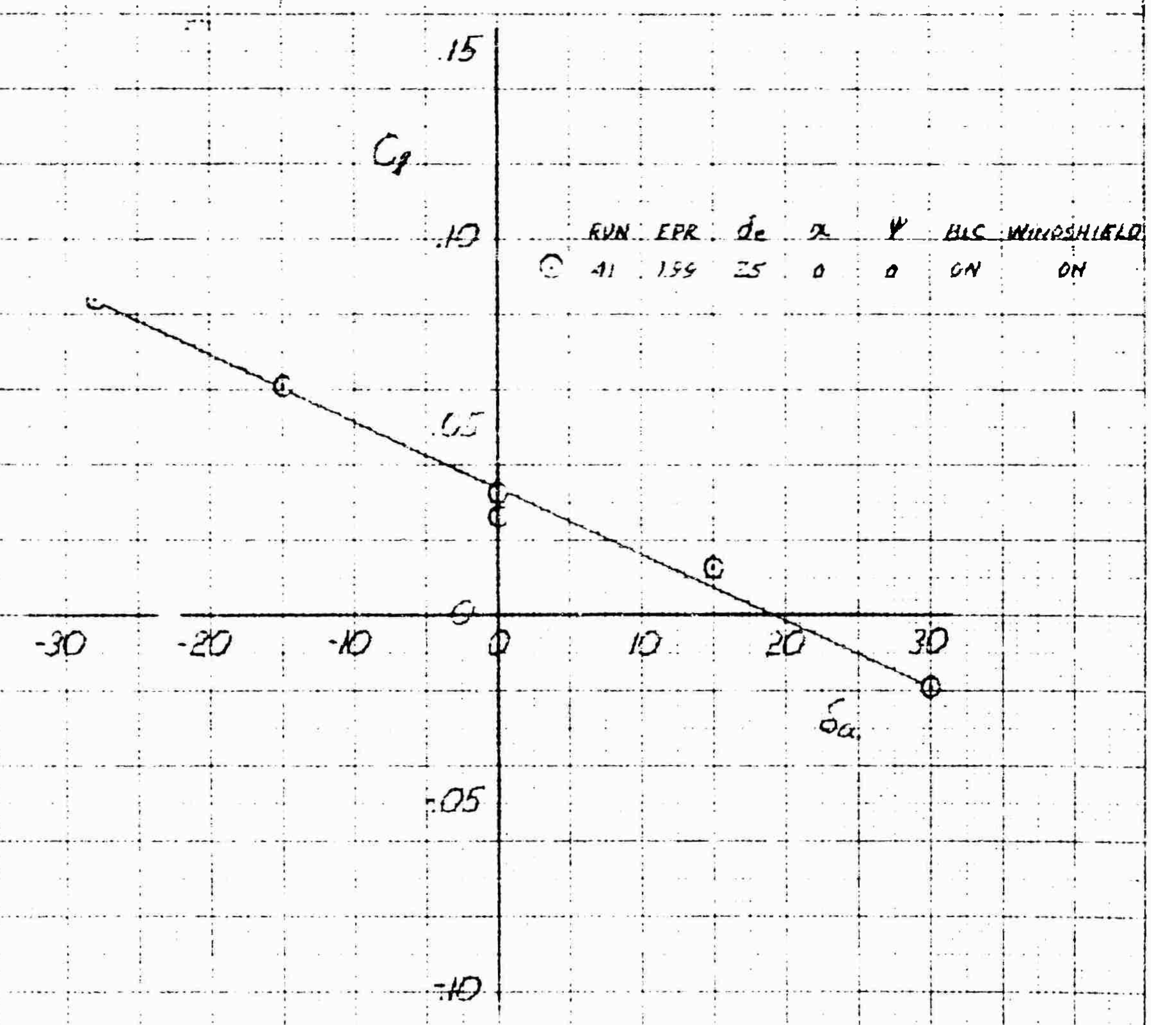

XV-4A
FULL SCALE WIND TUNNEL TEST 215
RUDDER EFFECT ON SIDE FORCE COEFFICIENT IN PHASE II FLIGHT AT 140 KNOTS

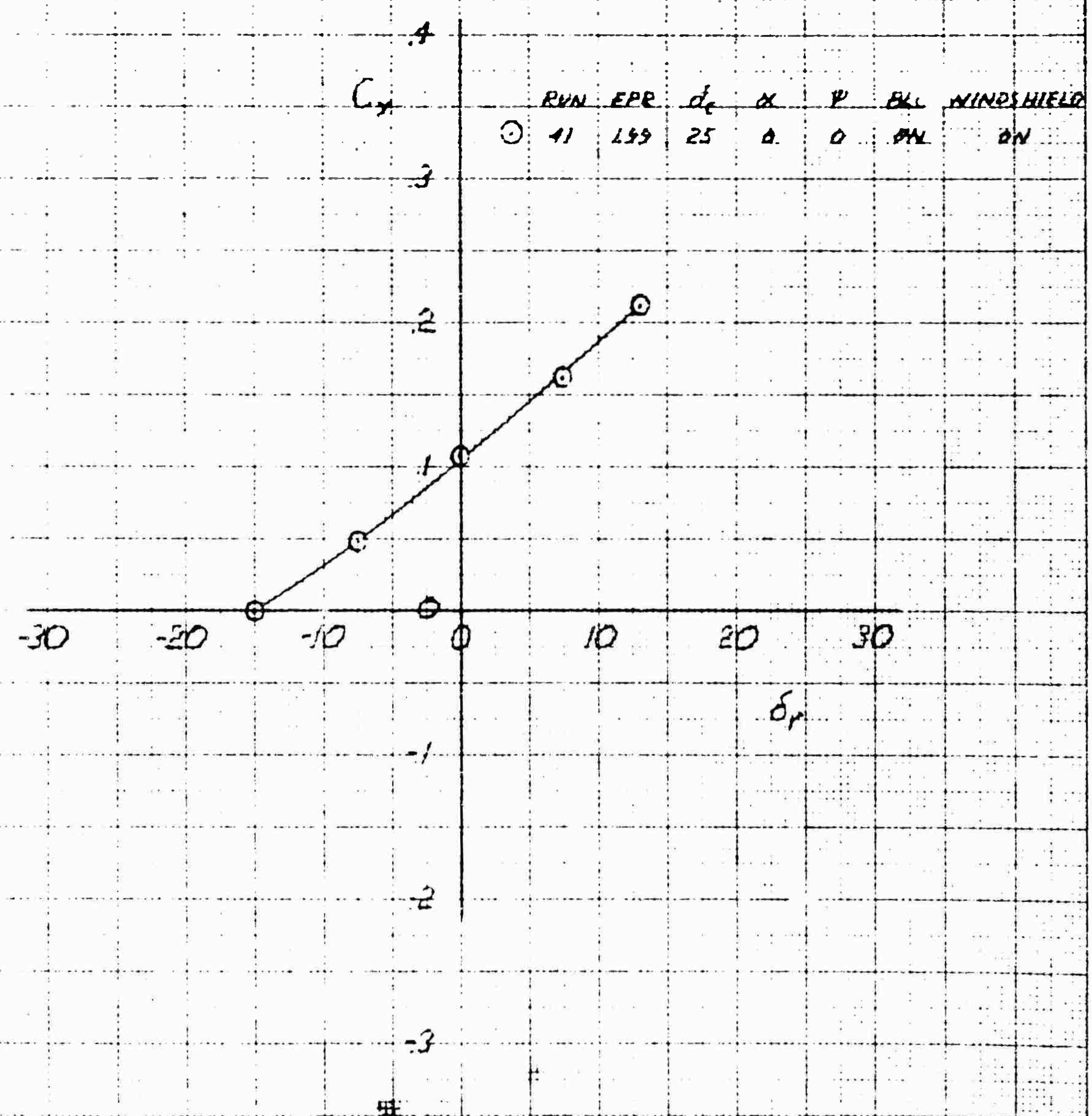

XV-4A

FULL SCALE WIND TUNNEL TEST 215

RUDDER EFFECT ON YAWING MOMENT COEFFICIENT IN PHASE II FLIGHT AT 100 KNOTS

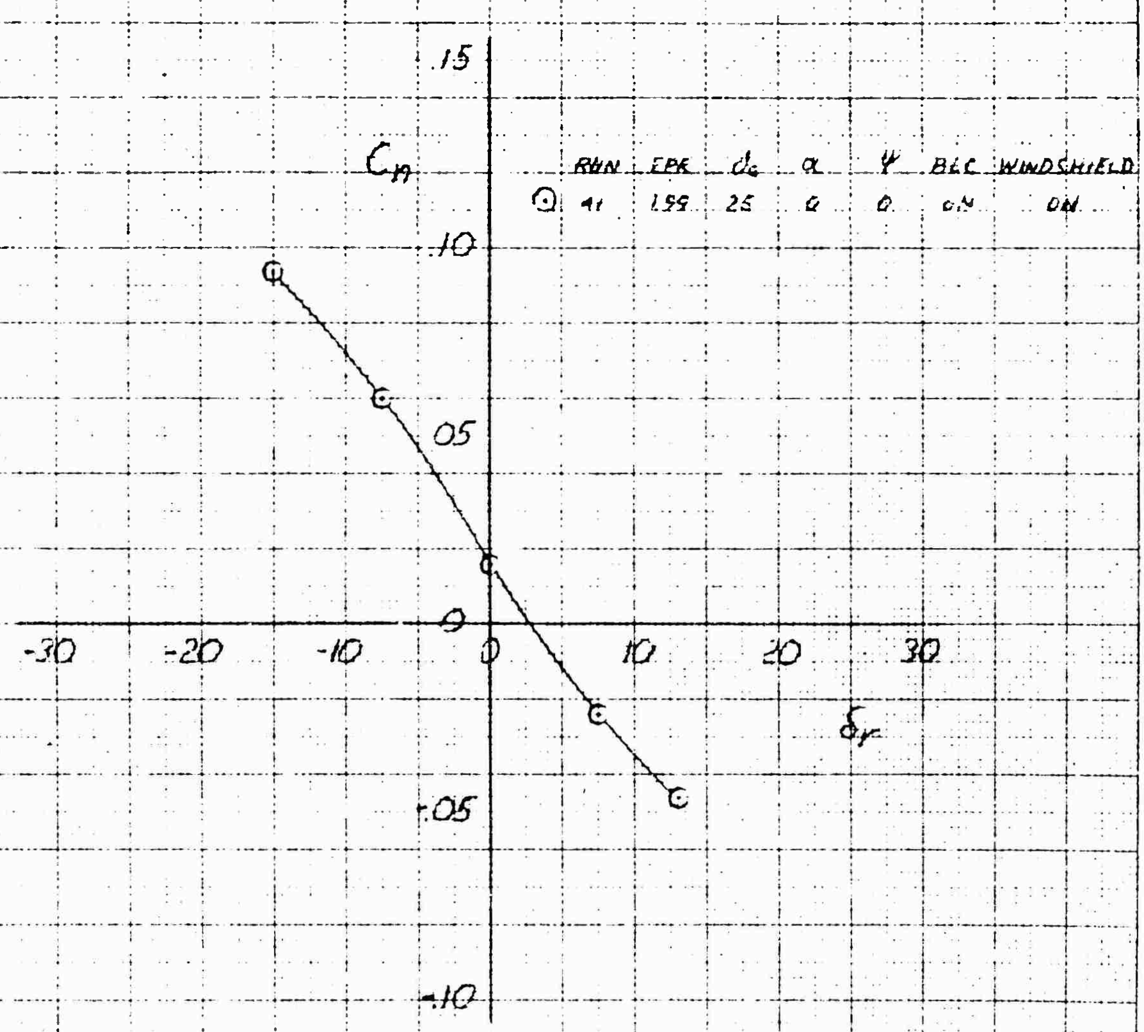

XV-4A

FULL SCALE WIND TUNNEL TEST 215

RUDDER EFFECT ON ROLLING MOMENT COEFFICIENT IN PHASE II FLIGHT AT 100 KNOTS

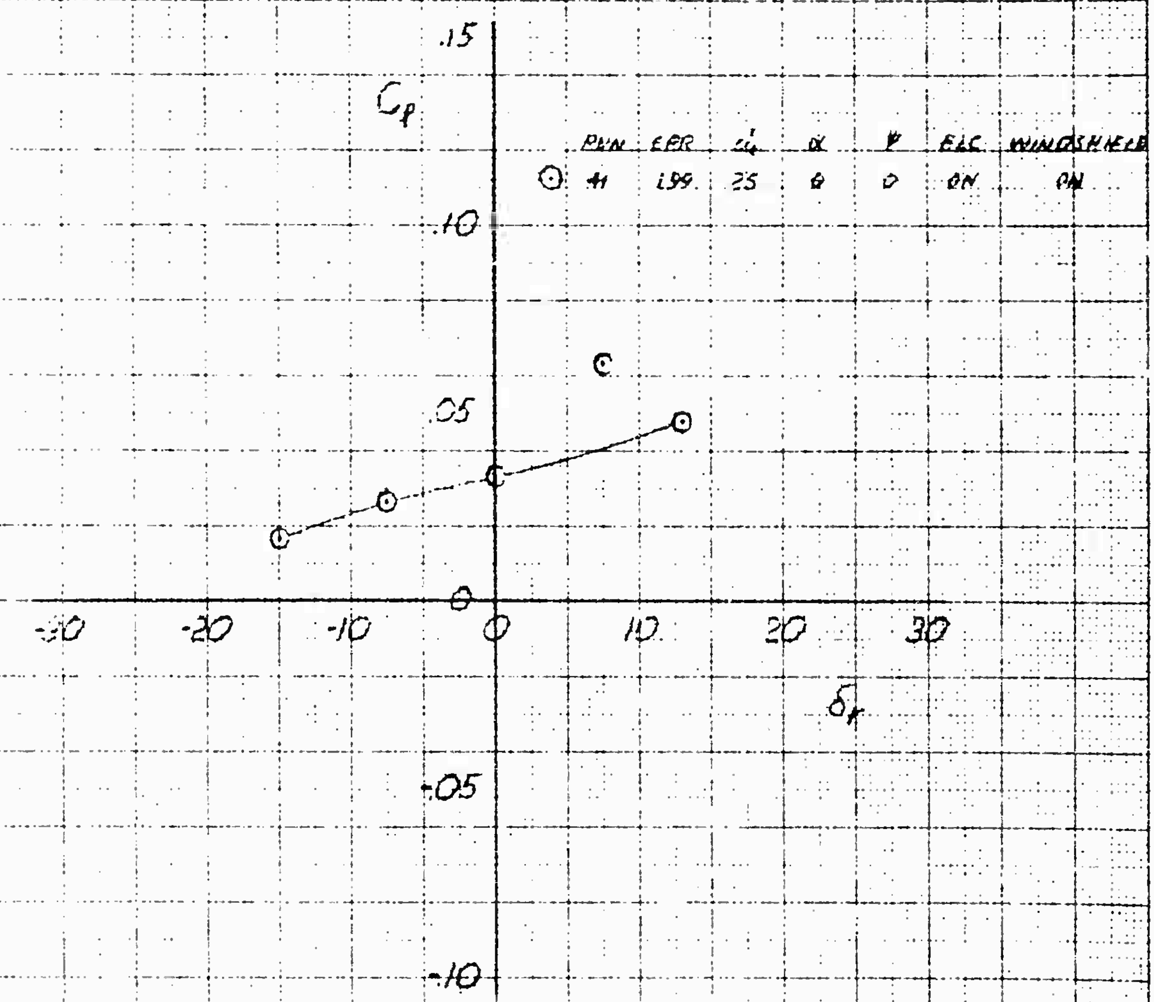

XV-4A

FULL SCALE WIND TUNNEL TEST 215

LIFT COEFFICIENT IN PHASE III FLIGHT AT 80 KNOTS

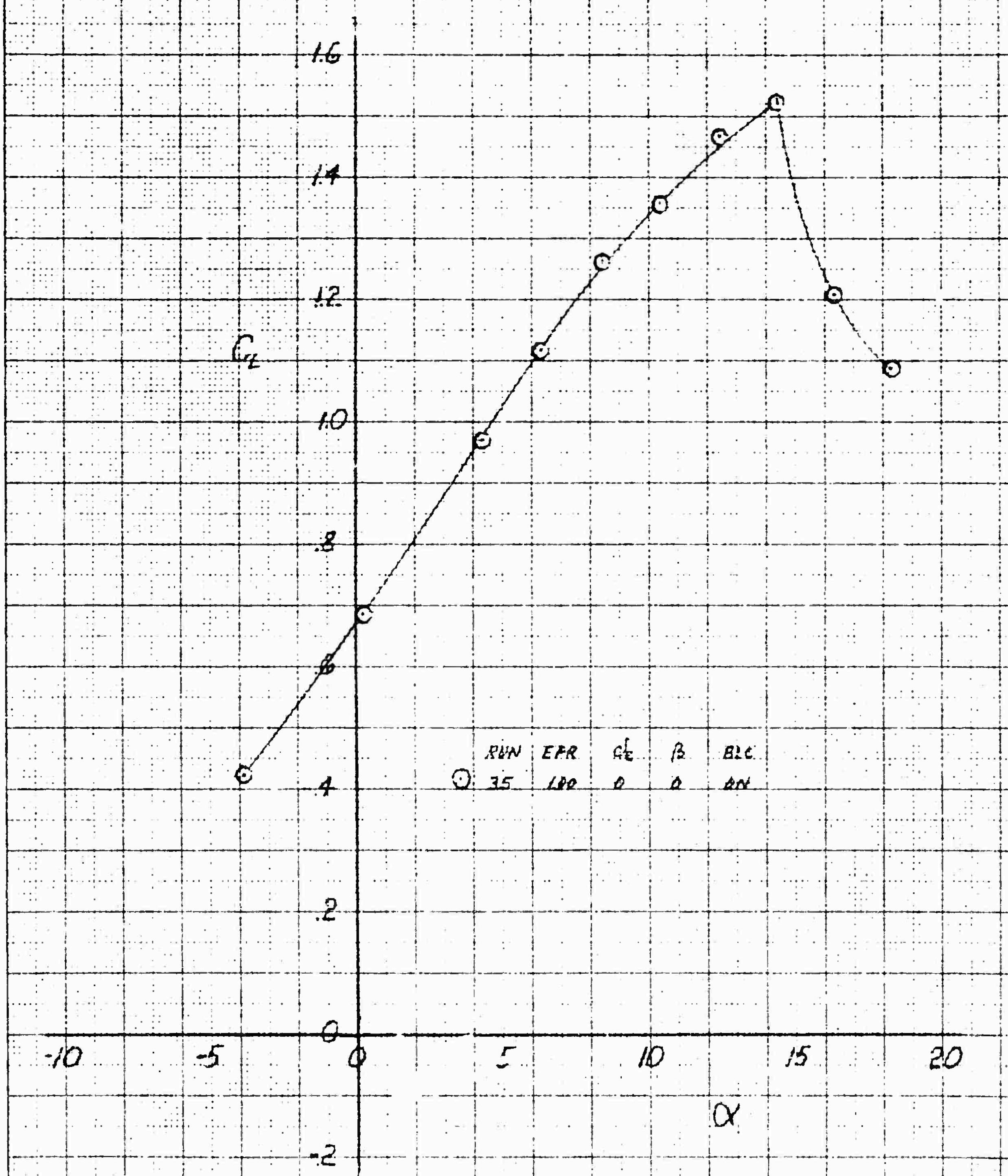

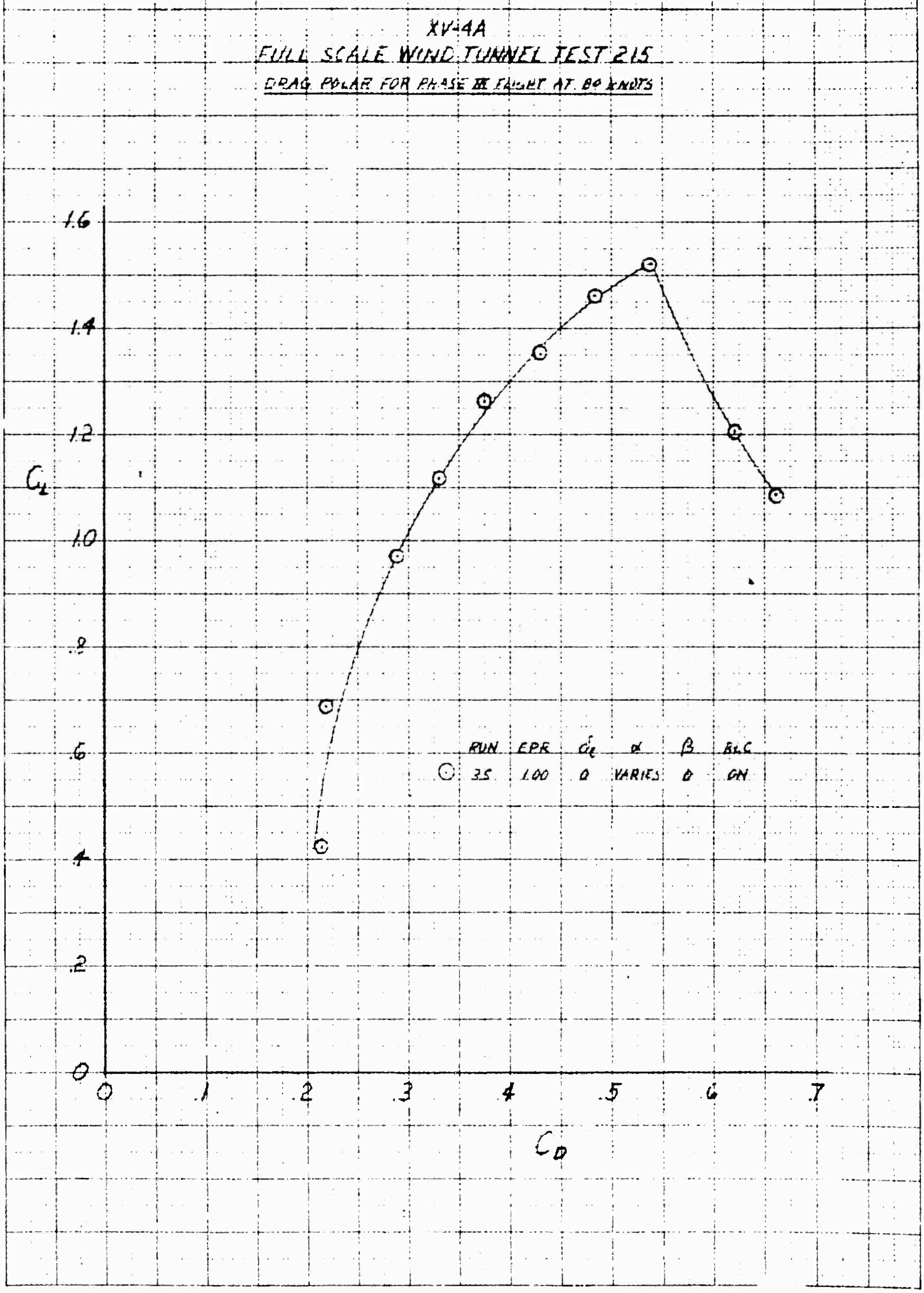
XV-4A
FULL SCALE WIND TUNNEL TEST 215
DRAG POLAR FOR PHASE III FLIGHT AT 80 KNOTS
C_L
1.6
1.4
1.2
1.0
.8
.6
.4
.2
0
0
.1
.2
.3
.4
.5
.6
.7
C_D
RUN EPR δ_f α β BLC
35 1.00 0 VARIES 0 ON

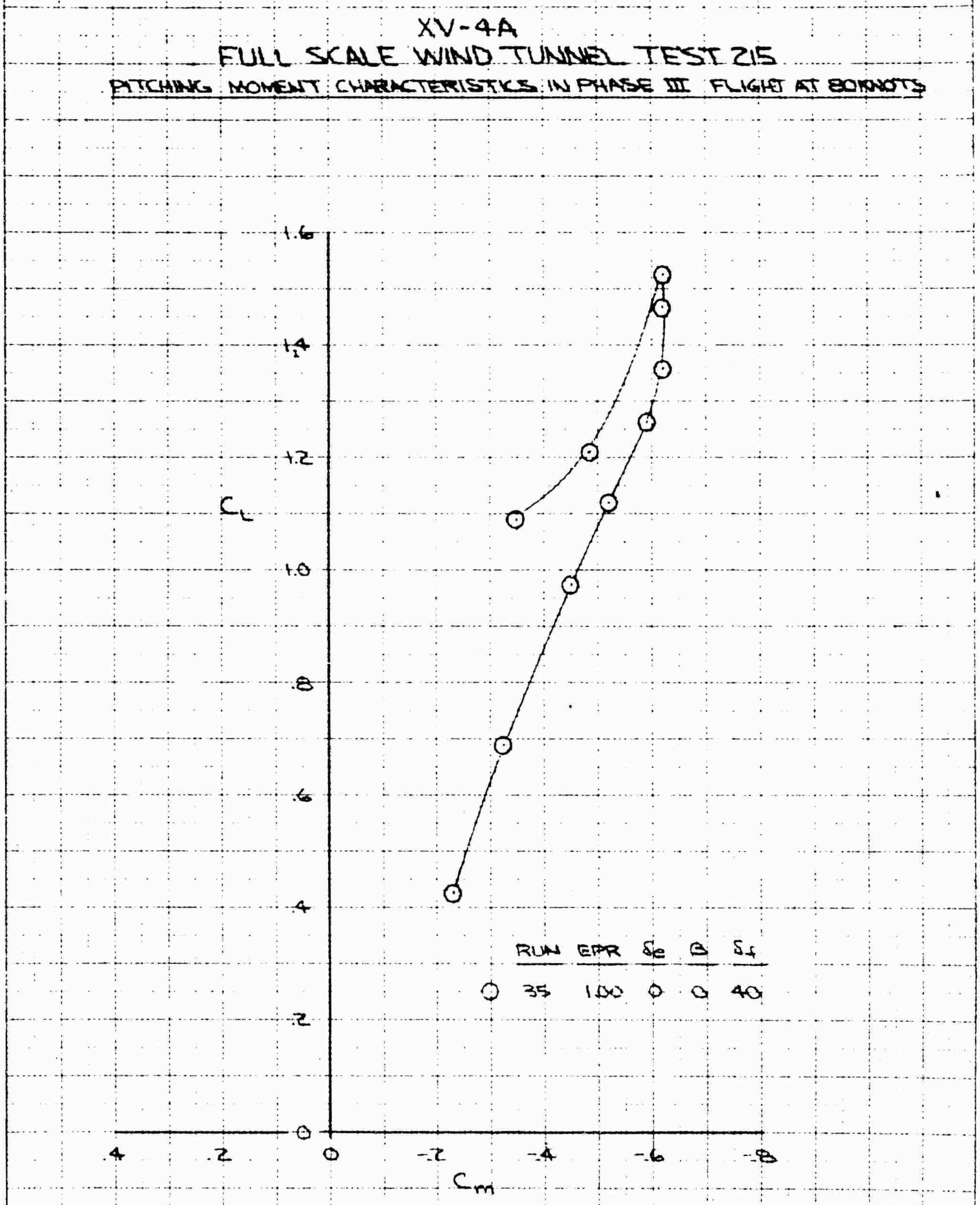
XV-4A
FULL SCALE WIND TUNNEL TEST 215
PITCHING MOMENT CHARACTERISTICS IN PHASE III FLIGHT AT 80KNOTS
1.6
1.4
1.2
1.0
.8
.6
.4
.2
0
C_L
.4
.2
0
-.2
-.4
-.6
-.8
C_m
RUN EPR δ_e β δ_f
35 1.00 0 0 40

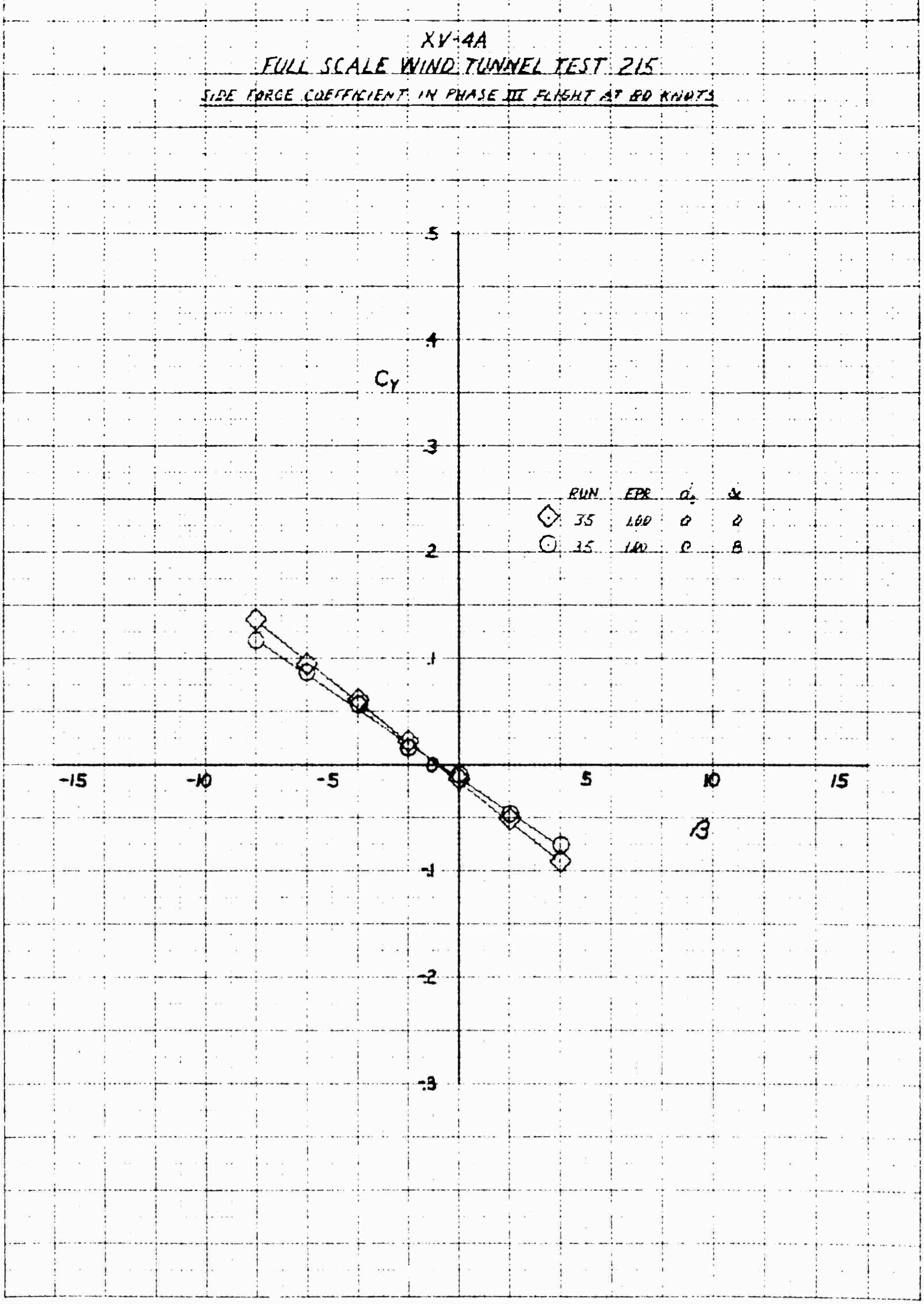
XV-4A
FULL SCALE WIND TUNNEL TEST 215
SIDE FORCE COEFFICIENT IN PHASE III FLIGHT AT 80 KNOTS
RUN EPR
35 1.00 0 0
35 1.00 0 8
CY
β
.5
.4
.3
.2
.1
-.1
-.2
-.3
-15
-10
-5
5
10
15

XV-4A

FULL SCALE WIND TUNNEL TEST 215

YAWING MOMENT COEFFICIENT IN PHASE III FLIGHT AT 80 KNOTS

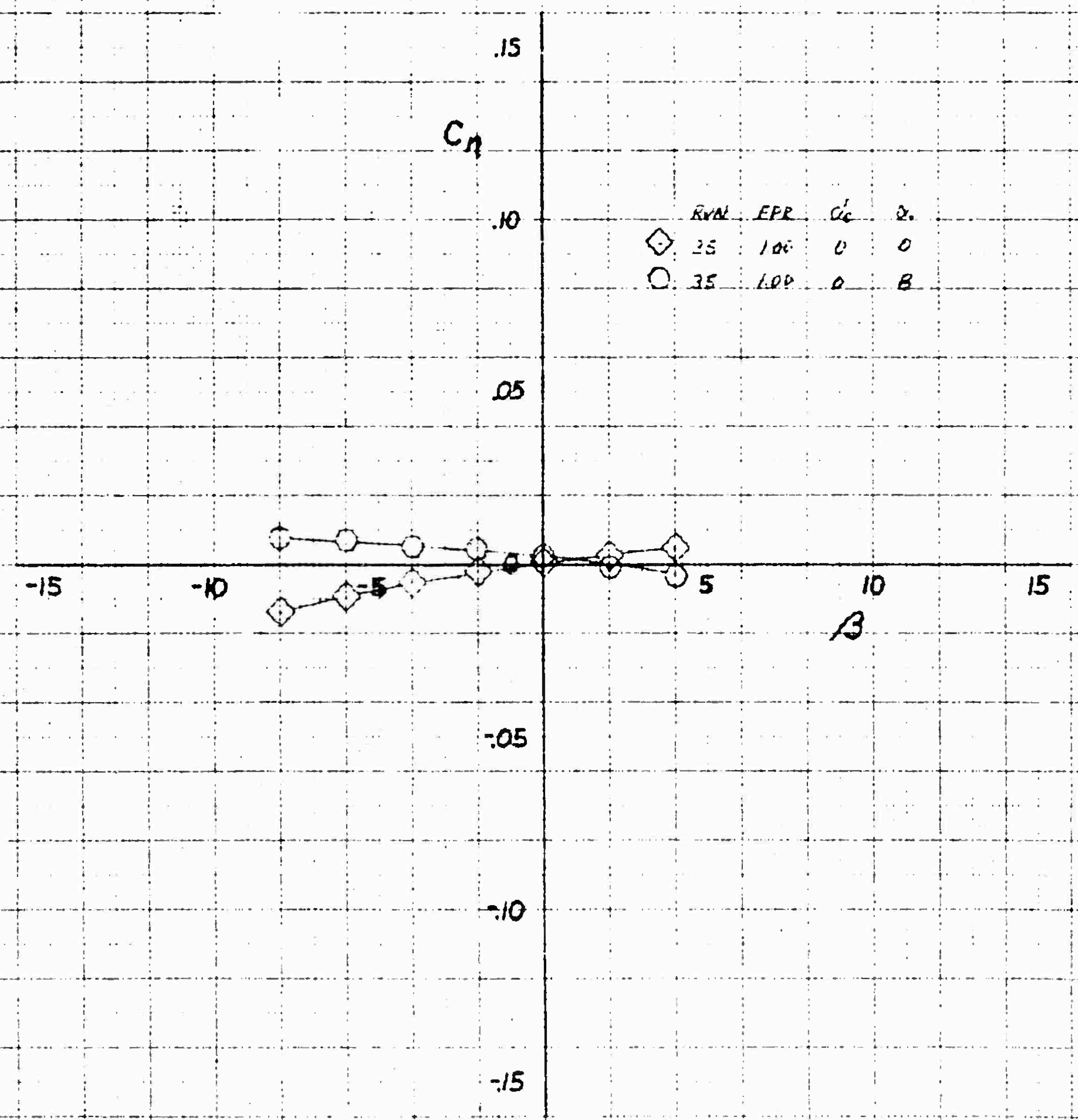

XV-4A

FULL SCALE WIND TUNNEL TEST 215

ROLLING MOMENT COEFFICIENT IN PHASE III FLIGHT AT 80 KNOTS

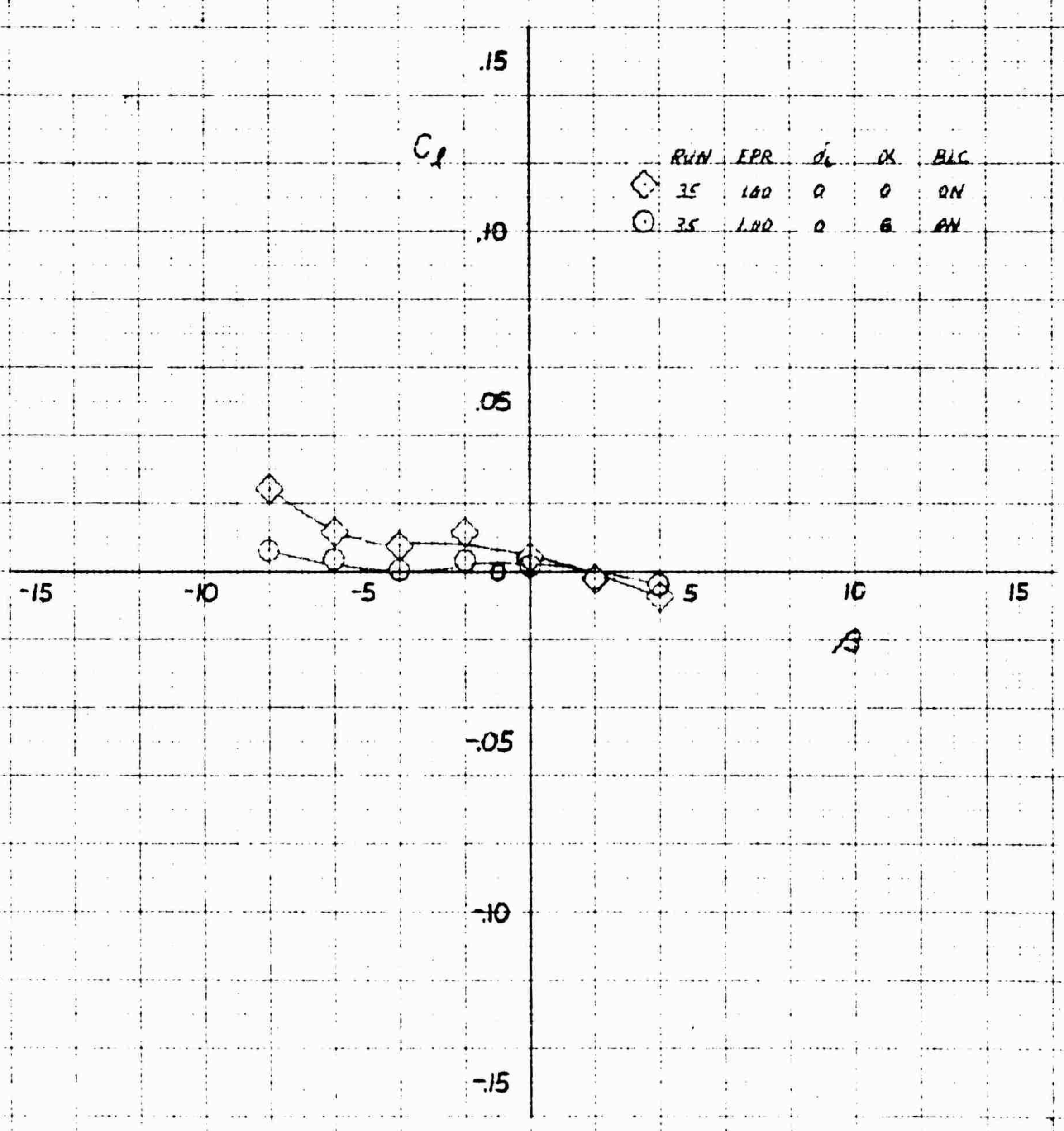

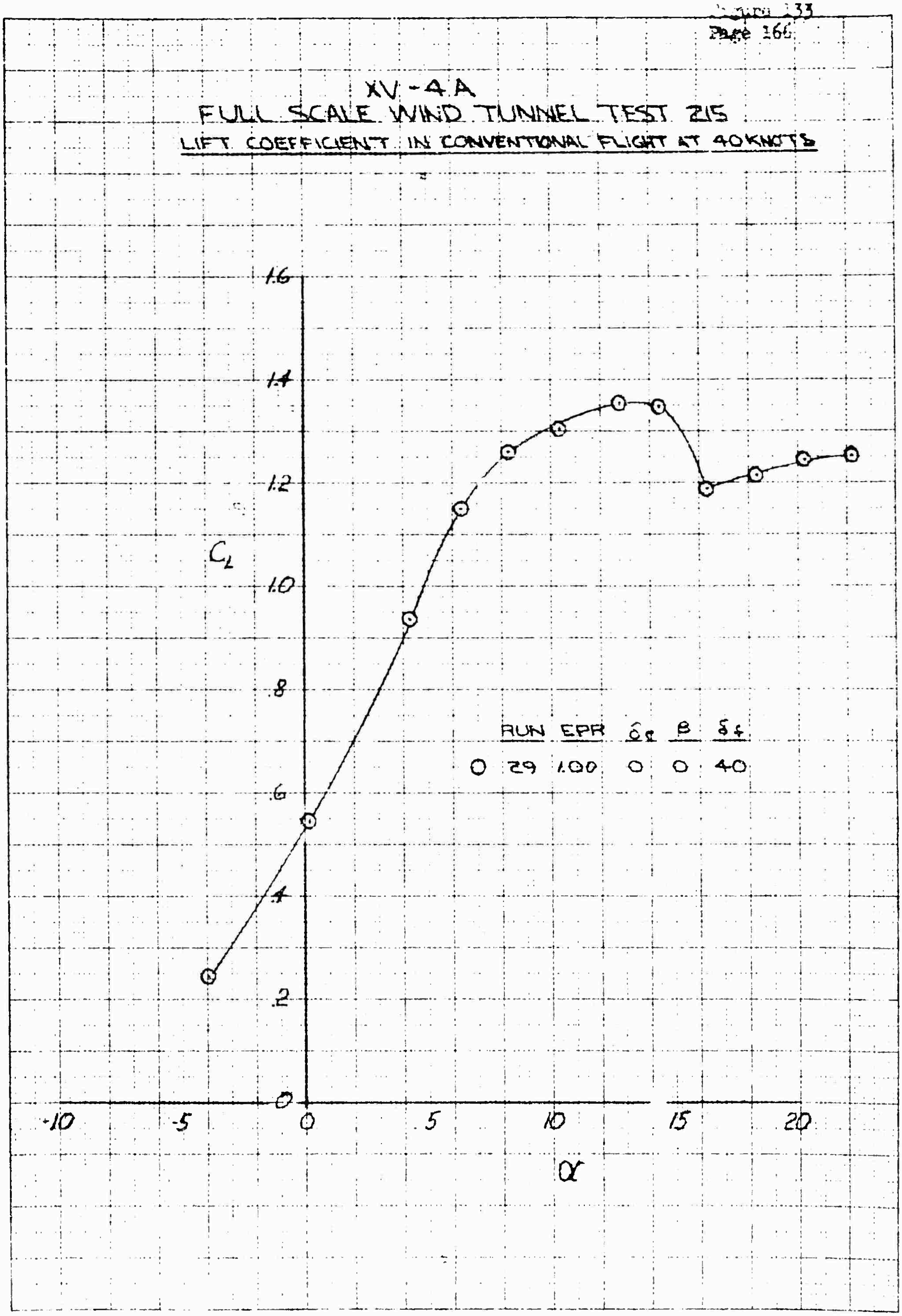

XV-4A
FULL SCALE WIND TUNNEL TEST 215
LIFT COEFFICIENT IN CONVENTIONAL FLIGHT AT 40 KNOTS
1.6
1.4
1.2
1.0
.8
.6
.4
.2
0
C_L
-10
-5
0
5
10
15
20
α
RUN EPR δ_e β δ_f
○ 29 1.00 0 0 40

XV-4A
FULL SCALE WIND TUNNEL TEST 215
DRAG POLAR IN CONVENTIONAL FLIGHT AT 40 KNOTS

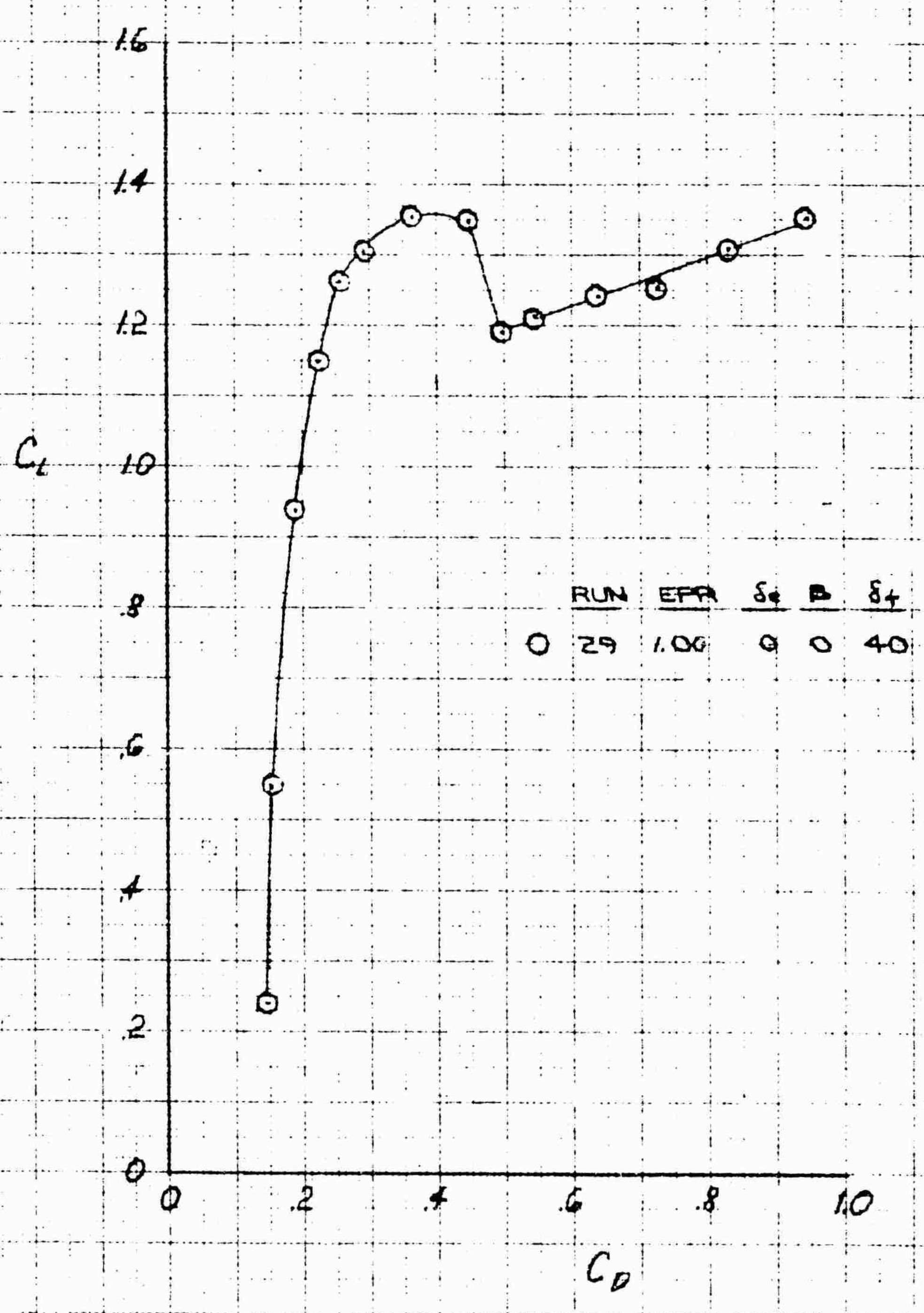

XV-4A
FULL SCALE WIND TUNNEL TEST 215
PITCHING MOMENT CHARACTERISTICS IN CONVENTIONAL FLIGHT AT 40 KNOTS

	RUN	EPR	δ_e	β	δ_f
○	29	1.00	0	0	40

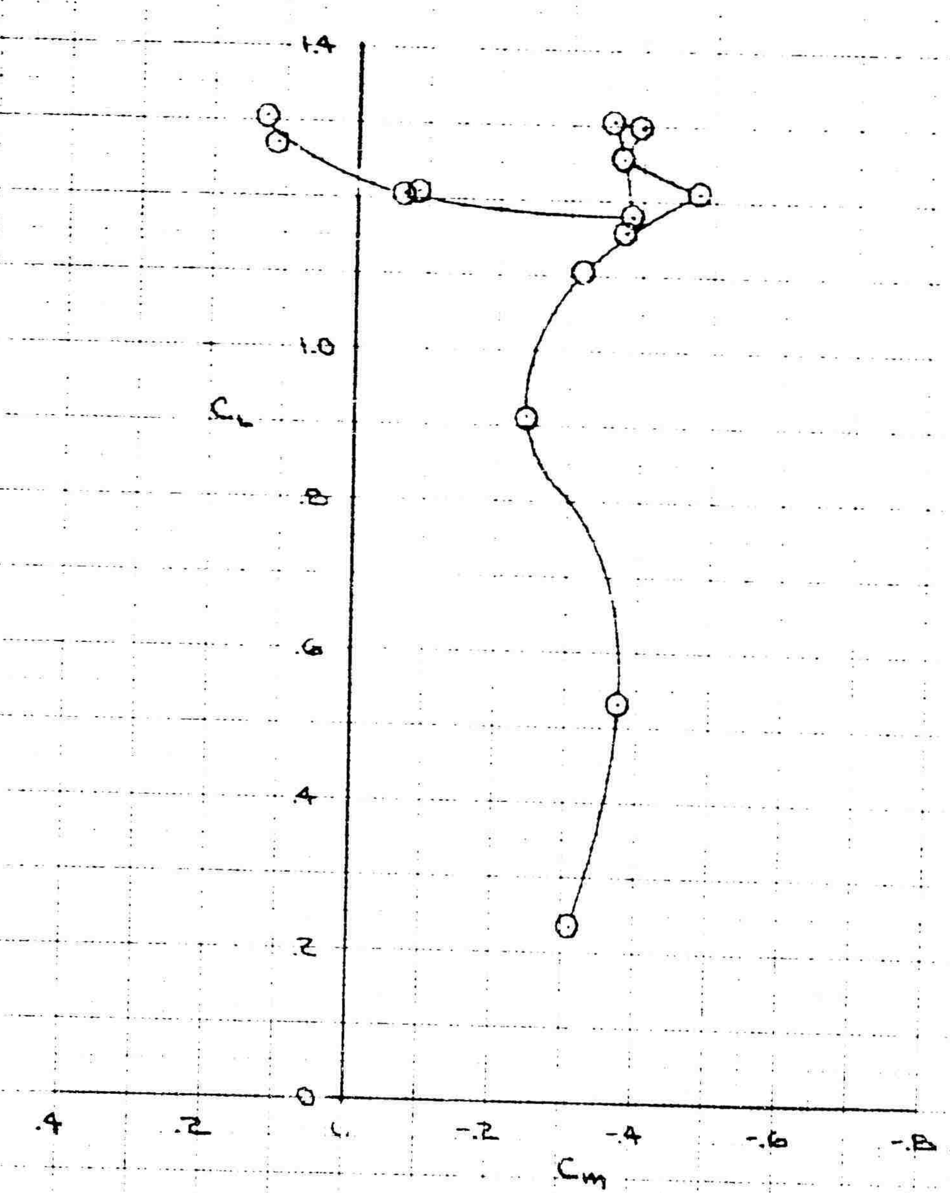

XV-4A
FULL SCALE WIND TUNNEL TEST 215
LIFT COEFFICIENT IN CONVENTIONAL FLIGHT AT 80 KNOTS

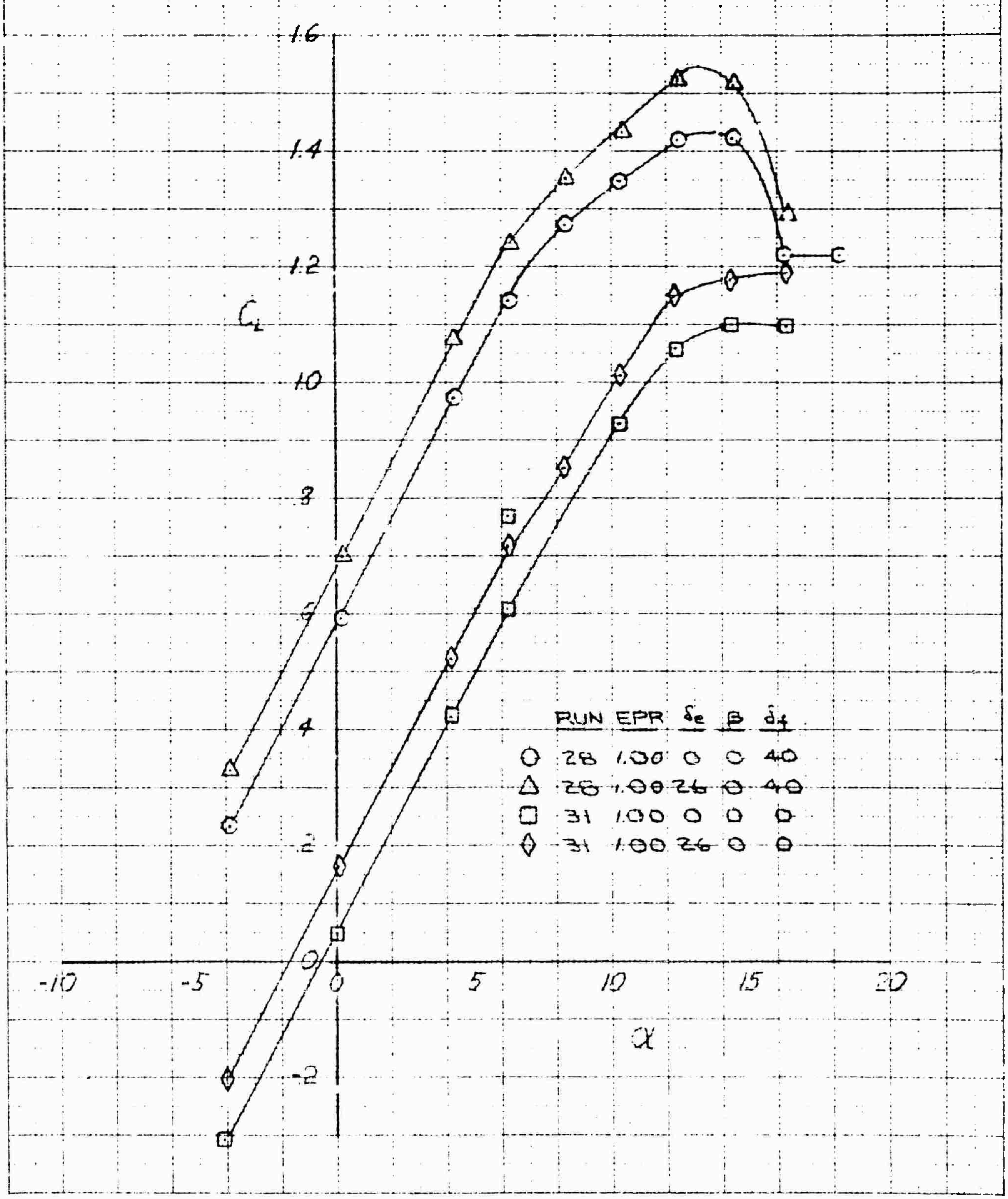

XV-4A

FULL SCALE WIND TUNNEL TEST 215

DRAG POLAR IN CONVENTIONAL FLIGHT AT 80 KNOTS

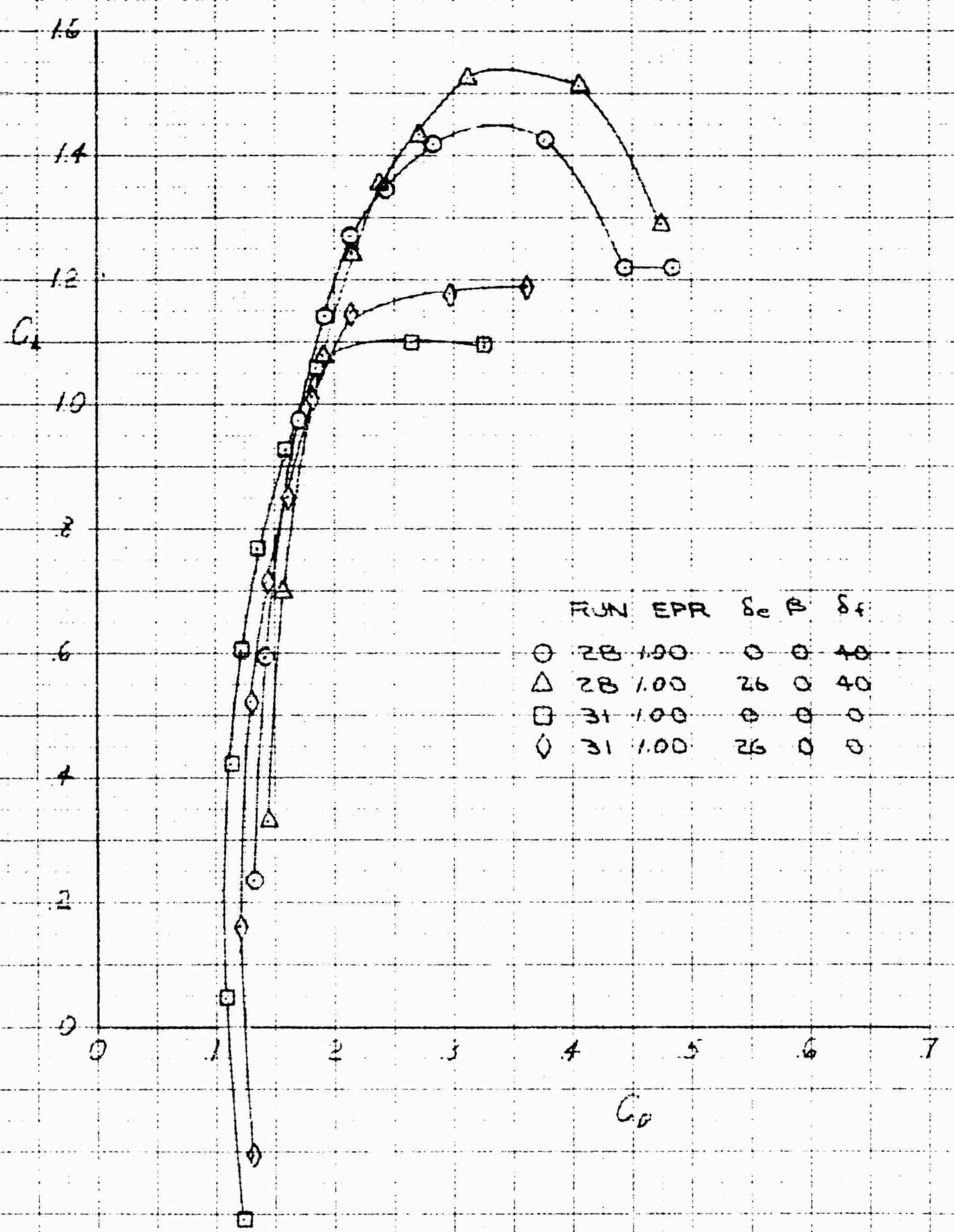

XV-4A
FULL SCALE WIND TUNNEL TEST 215
PITCHING MOMENT CHARACTERISTICS IN CONVENTIONAL FLIGHT AT 80 KNOTS

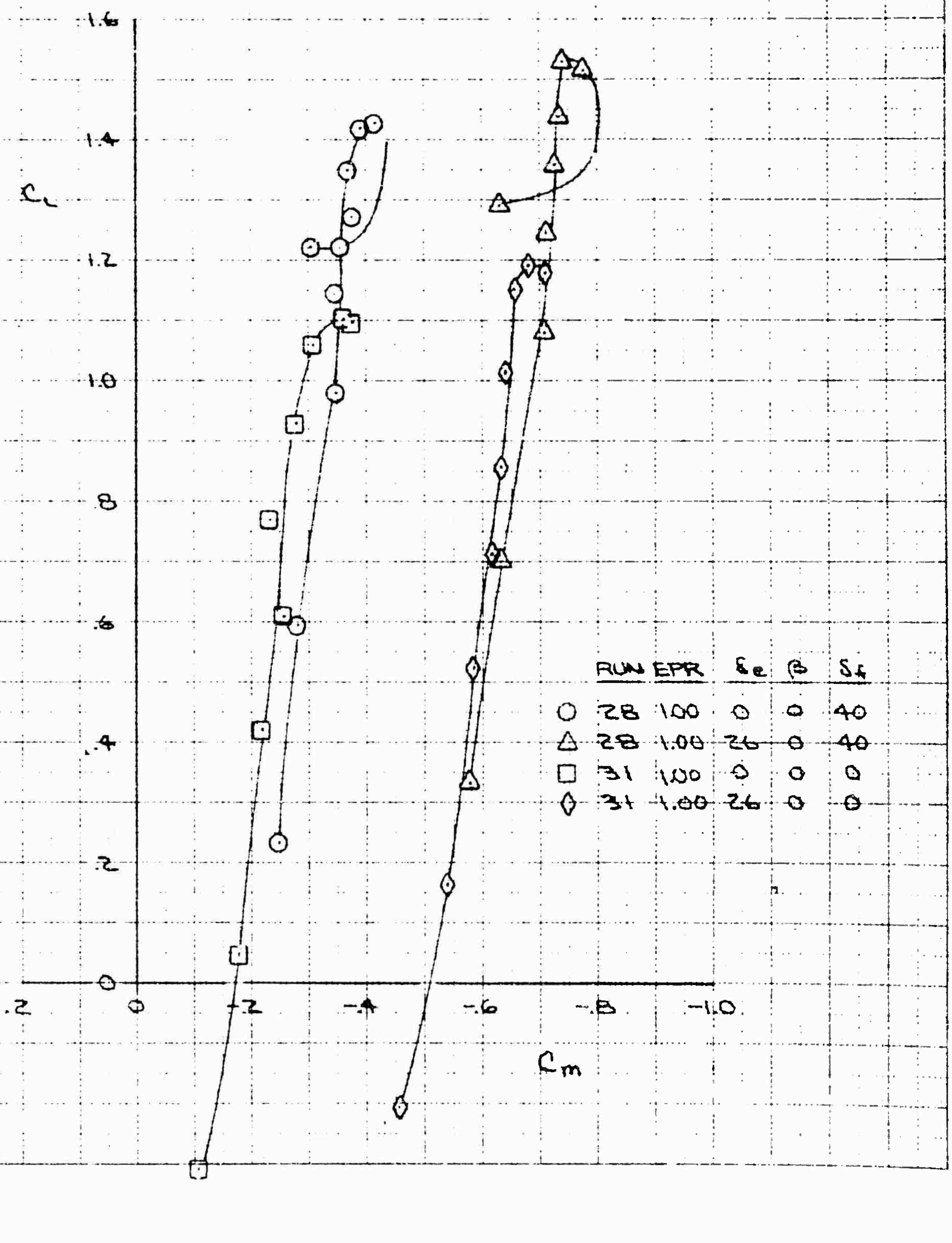

XV-4A
FULL SCALE WIND TUNNEL TEST 215
SIDE FORCE COEFFICIENT IN CONVENTIONAL FLIGHT AT 80 KNOTS

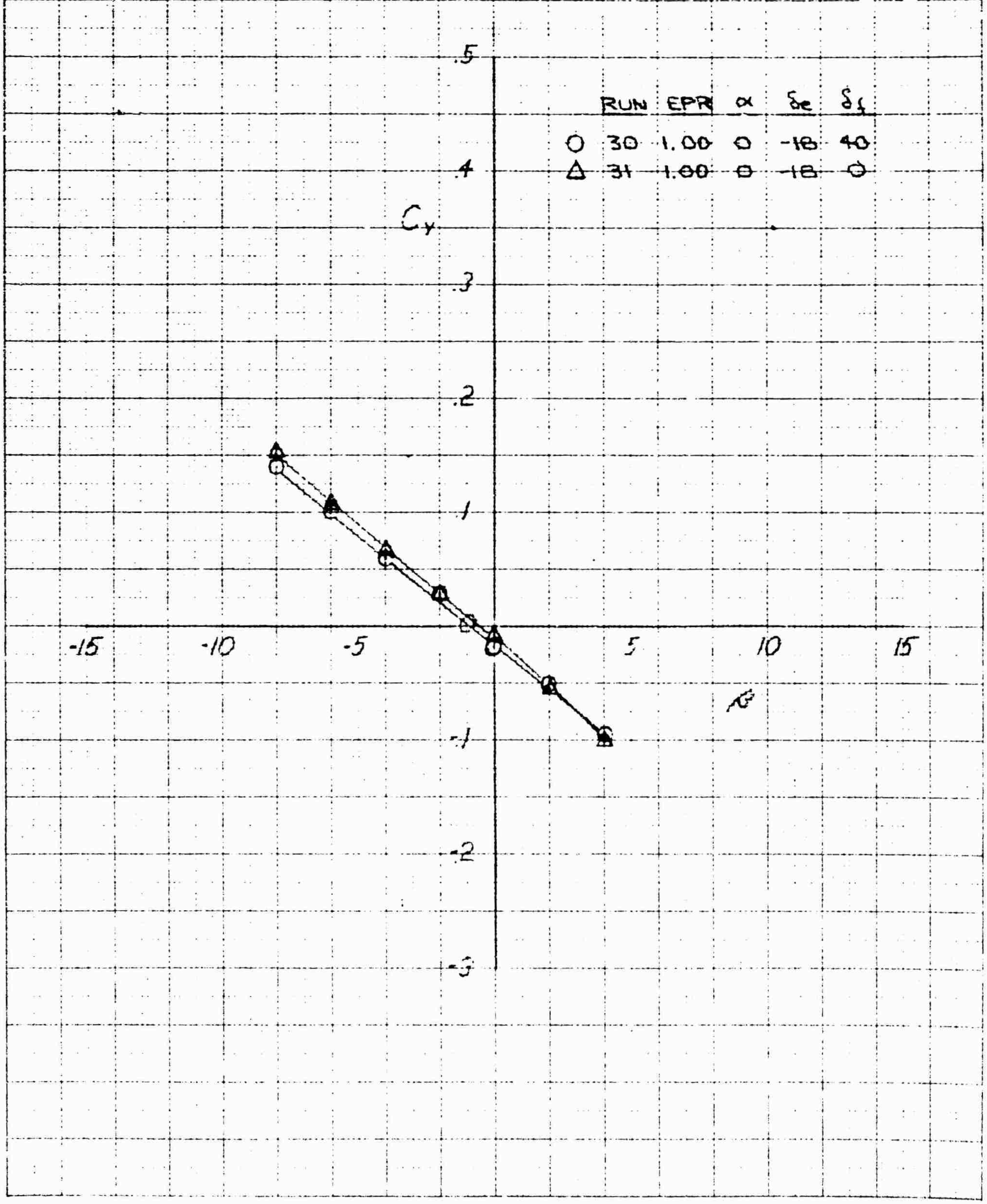

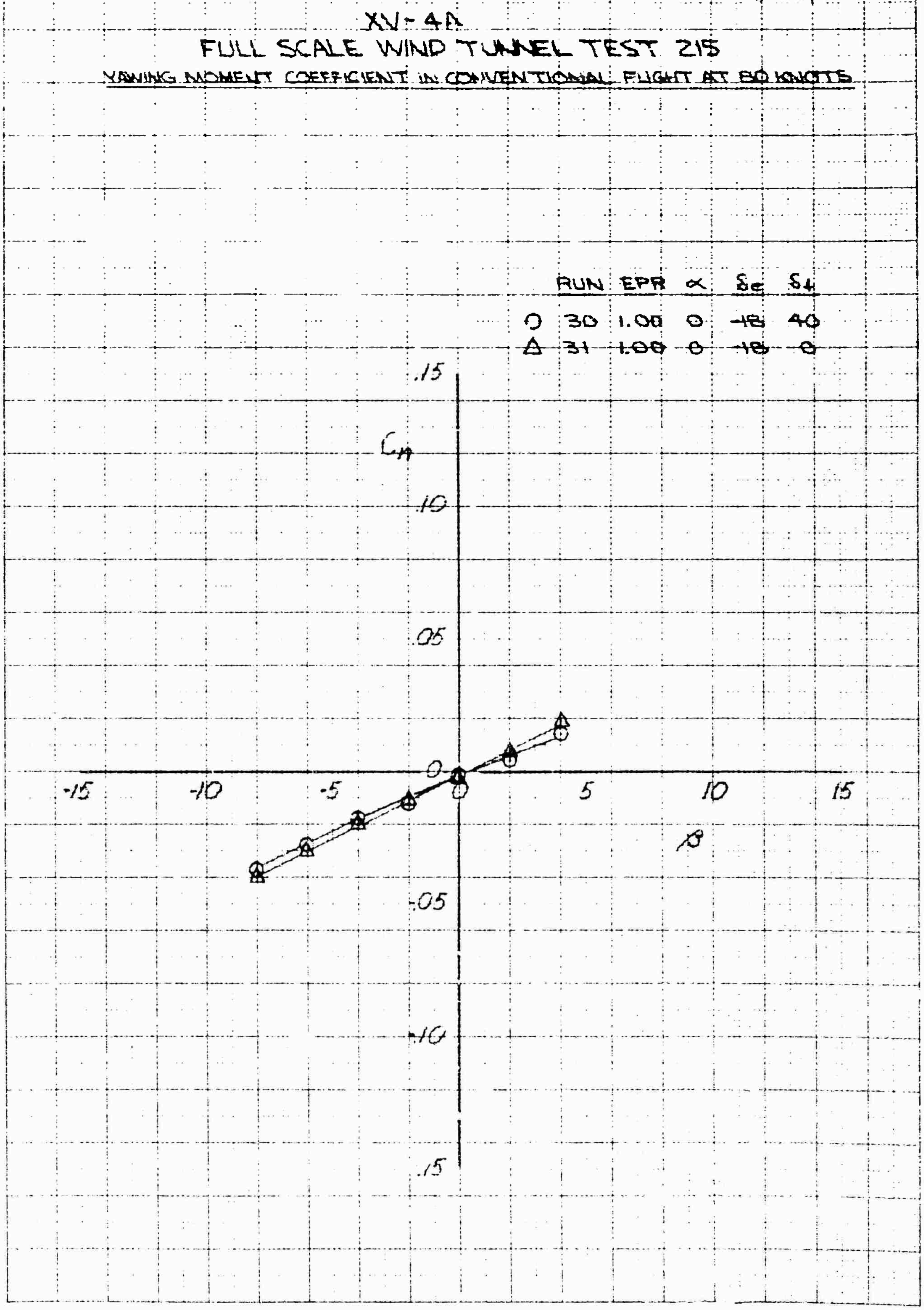
XV-4A
FULL SCALE WIND TUNNEL TEST 215
YAWING MOMENT COEFFICIENT IN CONVENTIONAL FLIGHT AT 80 KNOTS
RUN EPR α δe δf
○ 30 1.00 0 -18 40
△ 31 1.00 0 -18 0
Cn
.15
.10
.05
0
-.05
-.10
.15
-15
-10
-5
5
10
15
β

XV-4A
FULL SCALE WIND TUNNEL TEST 215
ROLLING MOMENT COEFFICIENT IN CONVENTIONAL FLIGHT AT 80 KNOTS

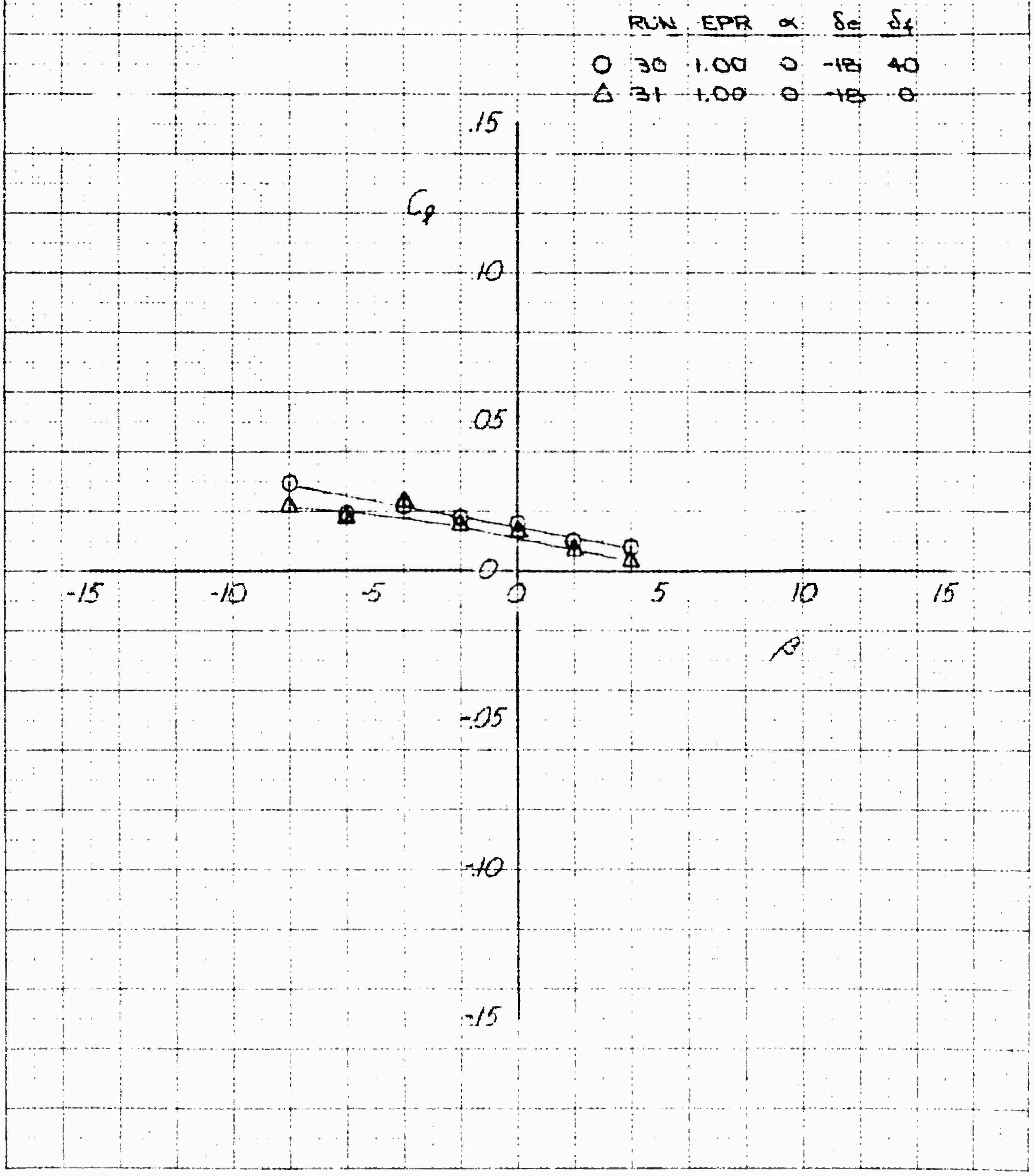

XV-4A
FULL SCALE WIND TUNNEL TEST 215
ELEVATOR EFFECT ON LIFT COEFFICIENT IN CONVENTIONAL FLIGHT AT 80KNOTS

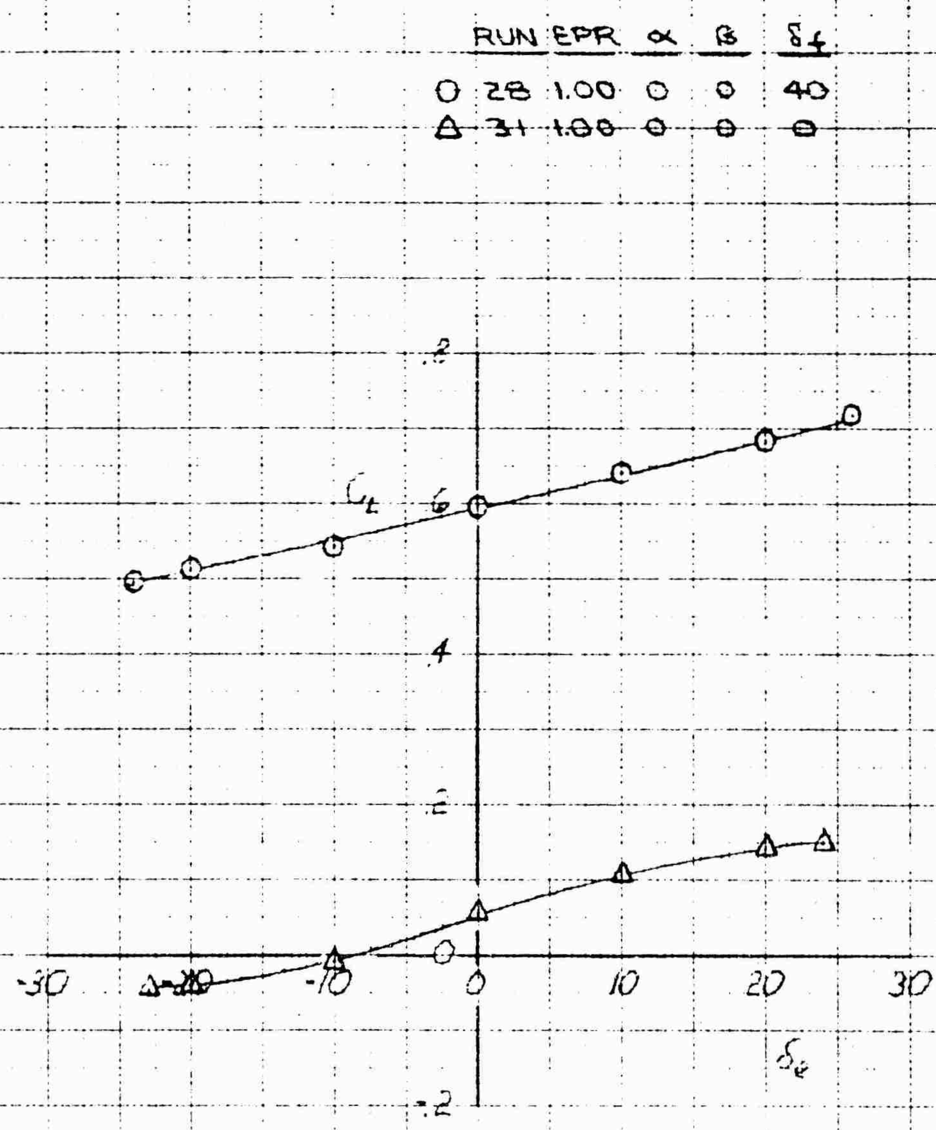

XV-4A
FULL SCALE WIND TUNNEL TEST 215
ELEVATOR EFFECT ON DRAG COEFFICIENT IN CONVENTIONAL FLIGHT AT 80 KNOTS

	RUN	EPR	α	β	δ_f
○	28	1.00	0	0	40
△	31	1.00	0	0	0

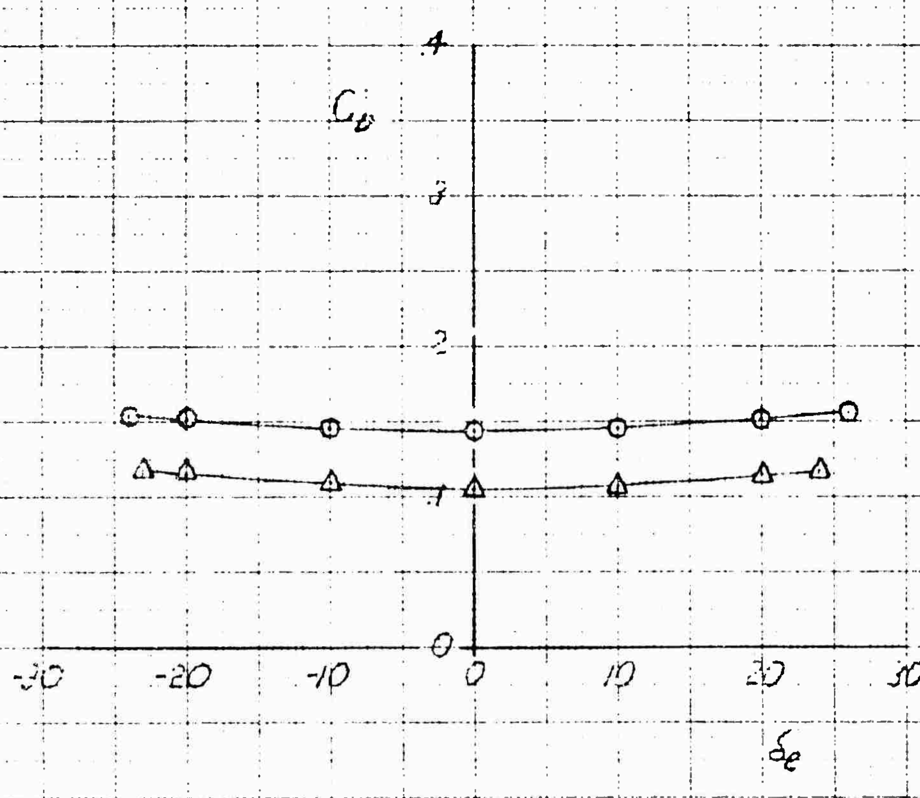

XV-4A
FULL SCALE WIND TUNNEL TEST 215
ELEVATOR EFFECT ON PITCHING MOMENT COEFFICIENT IN CONVENTIONAL FLIGHT AT 80 KNOTS

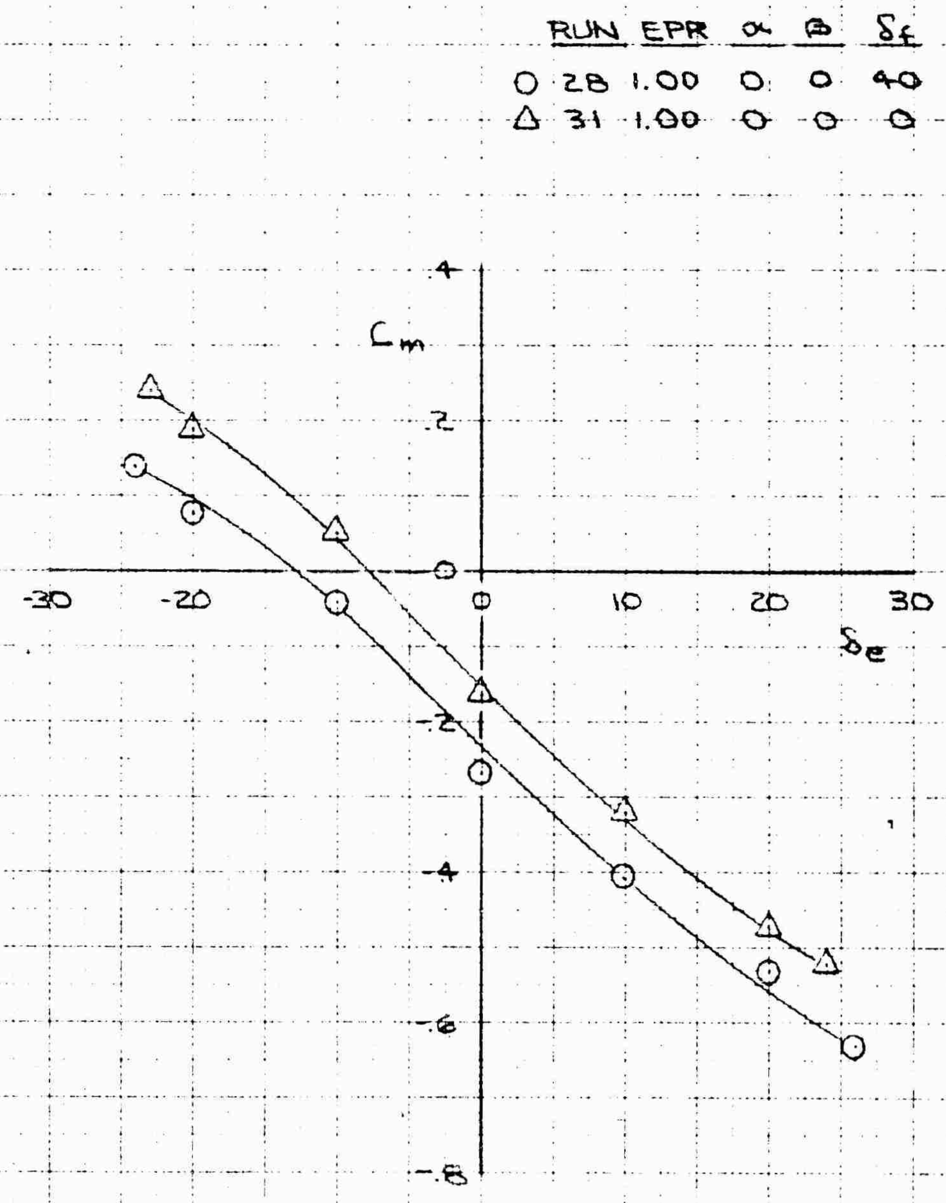

XV-4A
FULL SCALE WIND TUNNEL TEST 215
AILERON EFFECT ON SIDE FORCE COEFFICIENT IN CONVENTIONAL FLIGHT AT 60 KNOTS

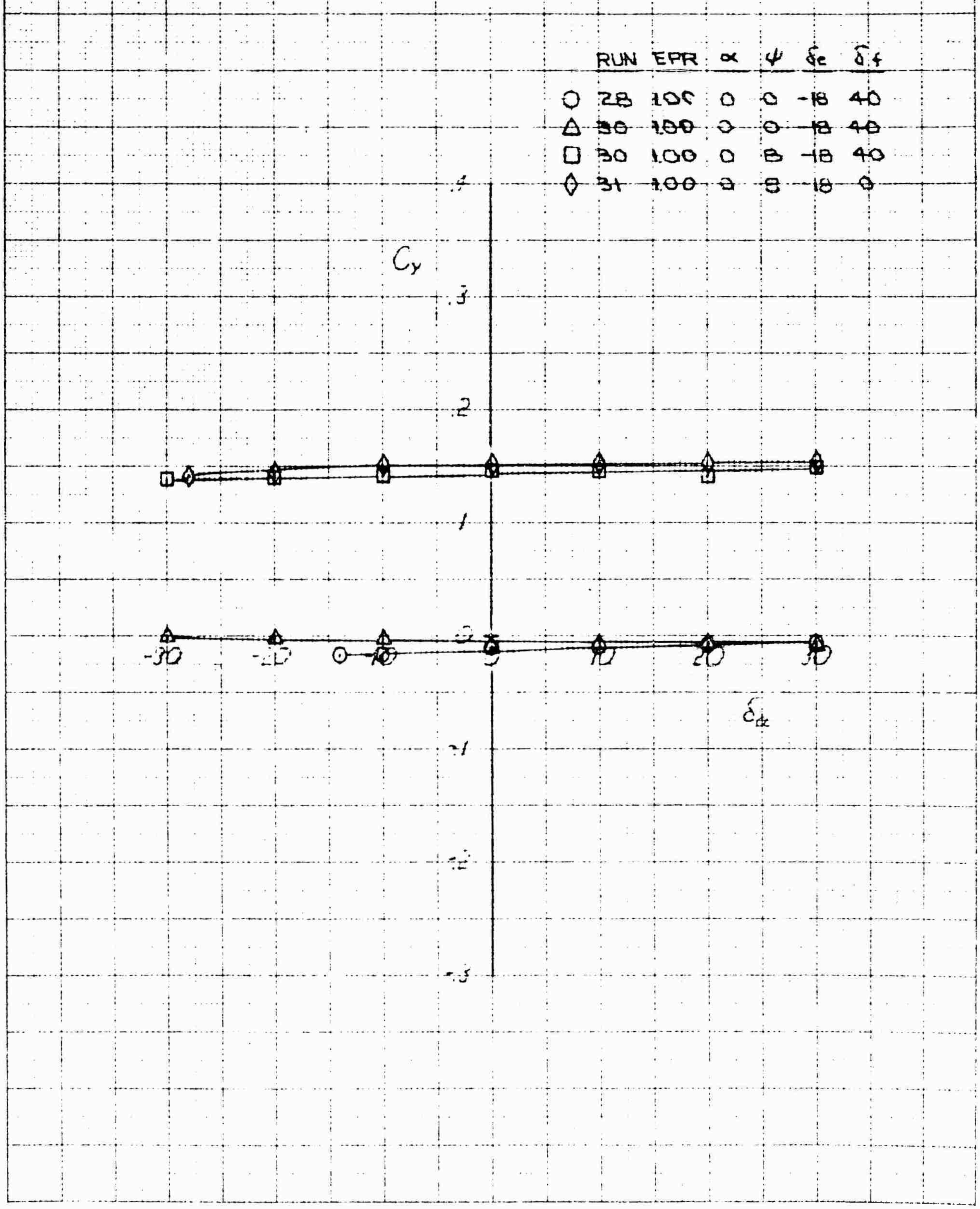

XV-4A
FULL SCALE WIND TUNNEL TEST 215
AILERON EFFECT ON YAWING MOMENT COEFFICIENT IN CONVENTIONAL FLIGHT AT 80 KNOTS

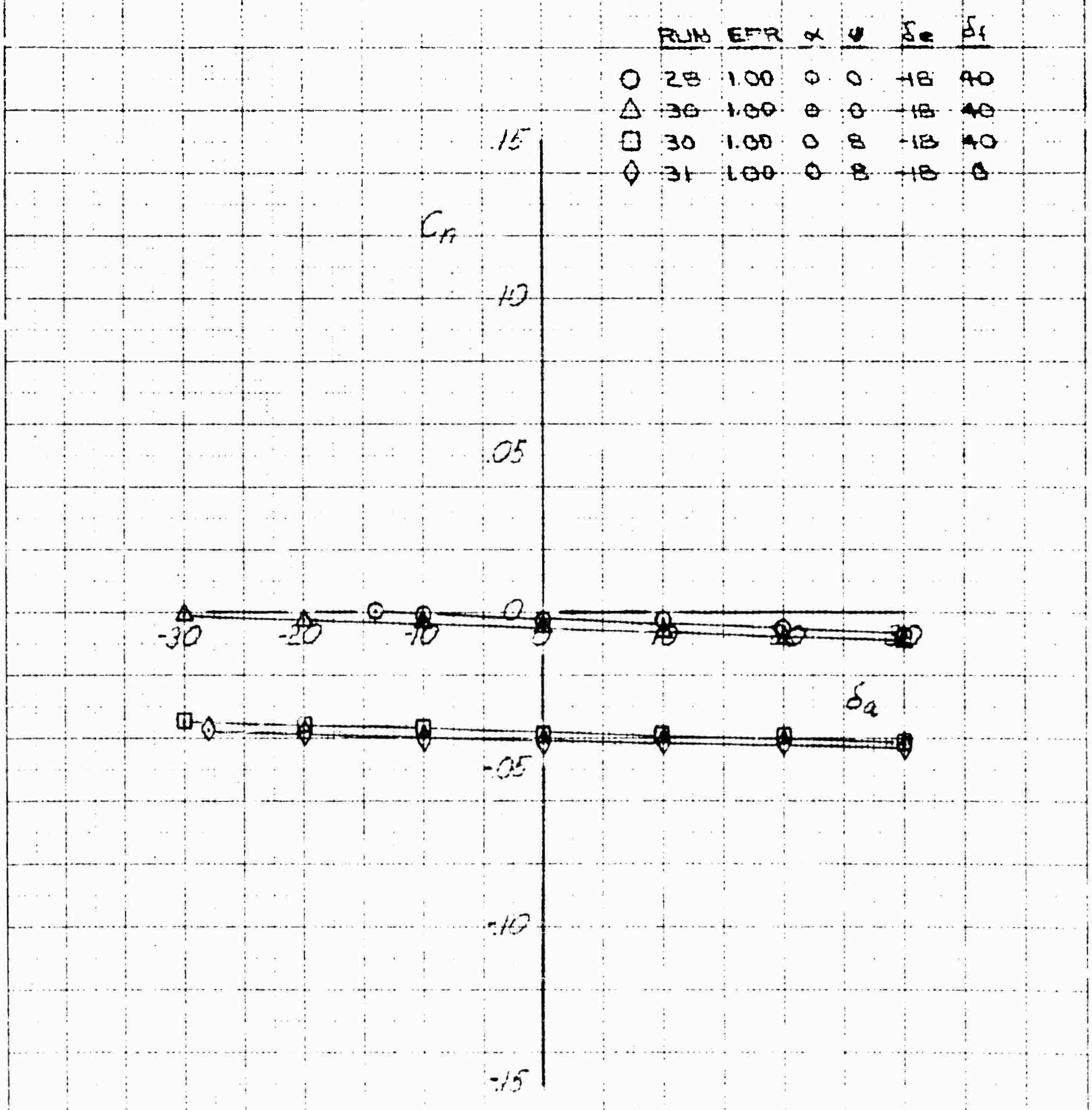

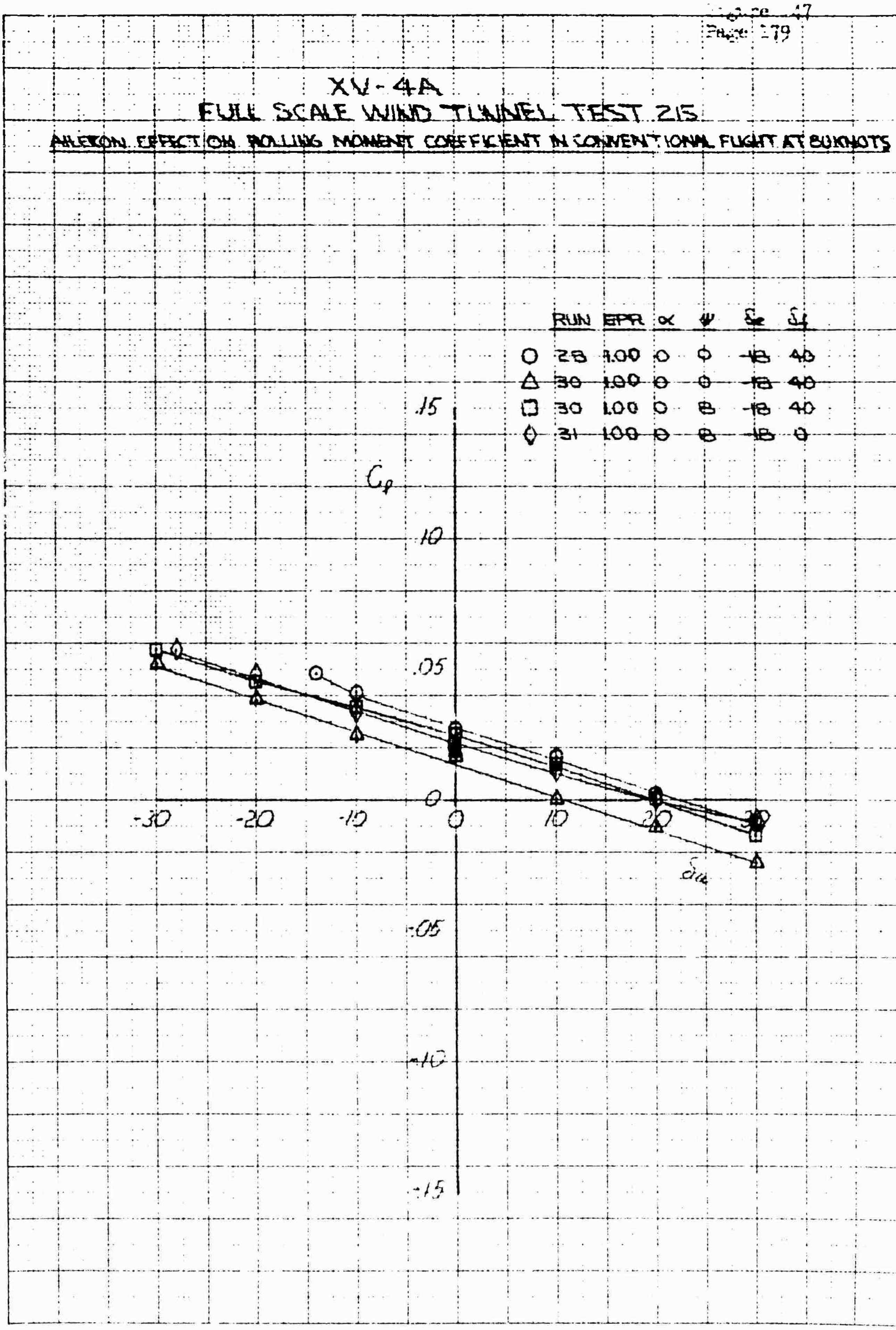

XV-4A
FULL SCALE WIND TUNNEL TEST 215
AILERON EFFECT ON ROLLING MOMENT COEFFICIENT IN CONVENTIONAL FLIGHT AT 80 KNOTS
RUN EPR α ψ δe δf
O 28 1.00 0 0 -18 40
Δ 30 1.00 0 0 -18 40
□ 30 1.00 0 8 -18 40
◊ 31 1.00 0 8 -18 0
.15
.10
.05
0
-.05
-.10
-.15
-30
-20
-10
0
10
20
30
δa

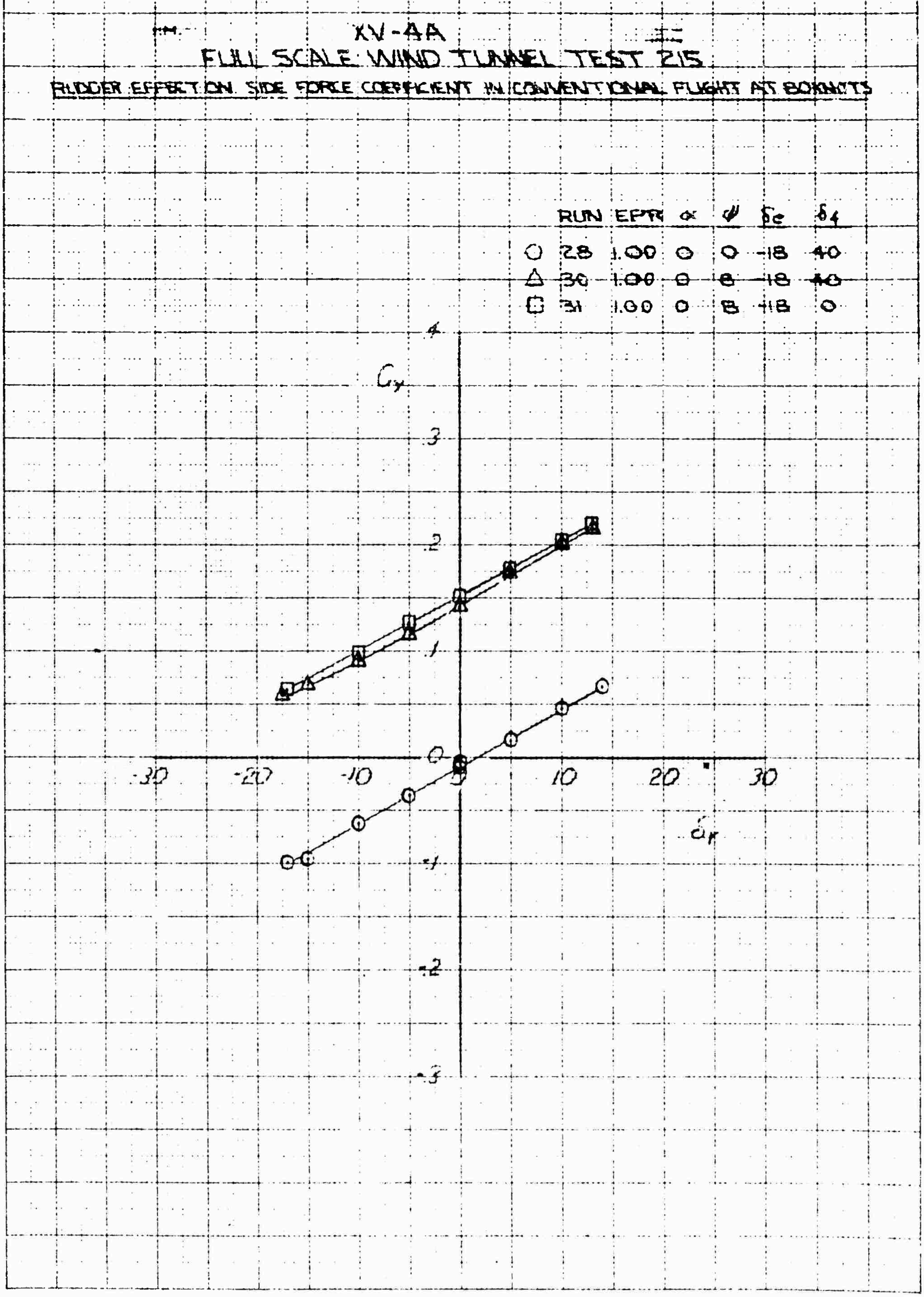
XV-4A
FULL SCALE WIND TUNNEL TEST 215
RUDDER EFFECT ON SIDE FORCE COEFFICIENT IN CONVENTIONAL FLIGHT AT 80KNOTS
RUN EPR α ψ δe δf
○ 28 1.00 0 0 -18 40
△ 30 1.00 0 8 -18 40
□ 31 1.00 0 8 +18 0
Cy
.4
.3
.2
.1
0
-.1
-.2
-.3
-30
-20
-10
0
10
20
30
δr

XV-4A
FULL SCALE WIND TUNNEL TEST 215
RUDDER EFFECT ON YAWING MOMENT COEFFICIENT IN CONVENTIONAL FLIGHT AT 80 KNOTS

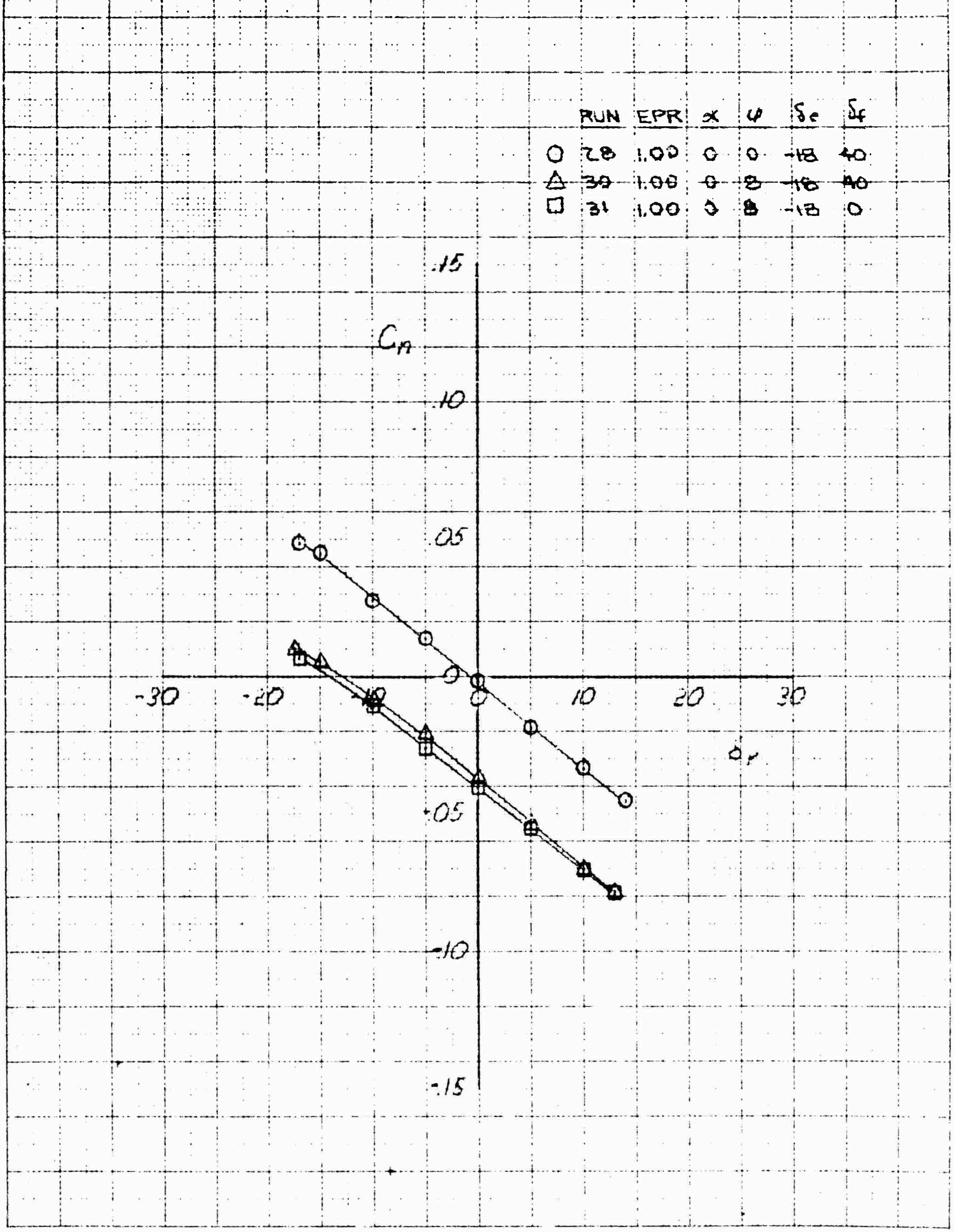

XV-4A
FULL SCALE WIND TUNNEL TEST 215
RUDDER EFFECT ON ROLLING MOMENT COEFFICIENT IN CONVENTIONAL FLIGHT AT 80 KNOTS

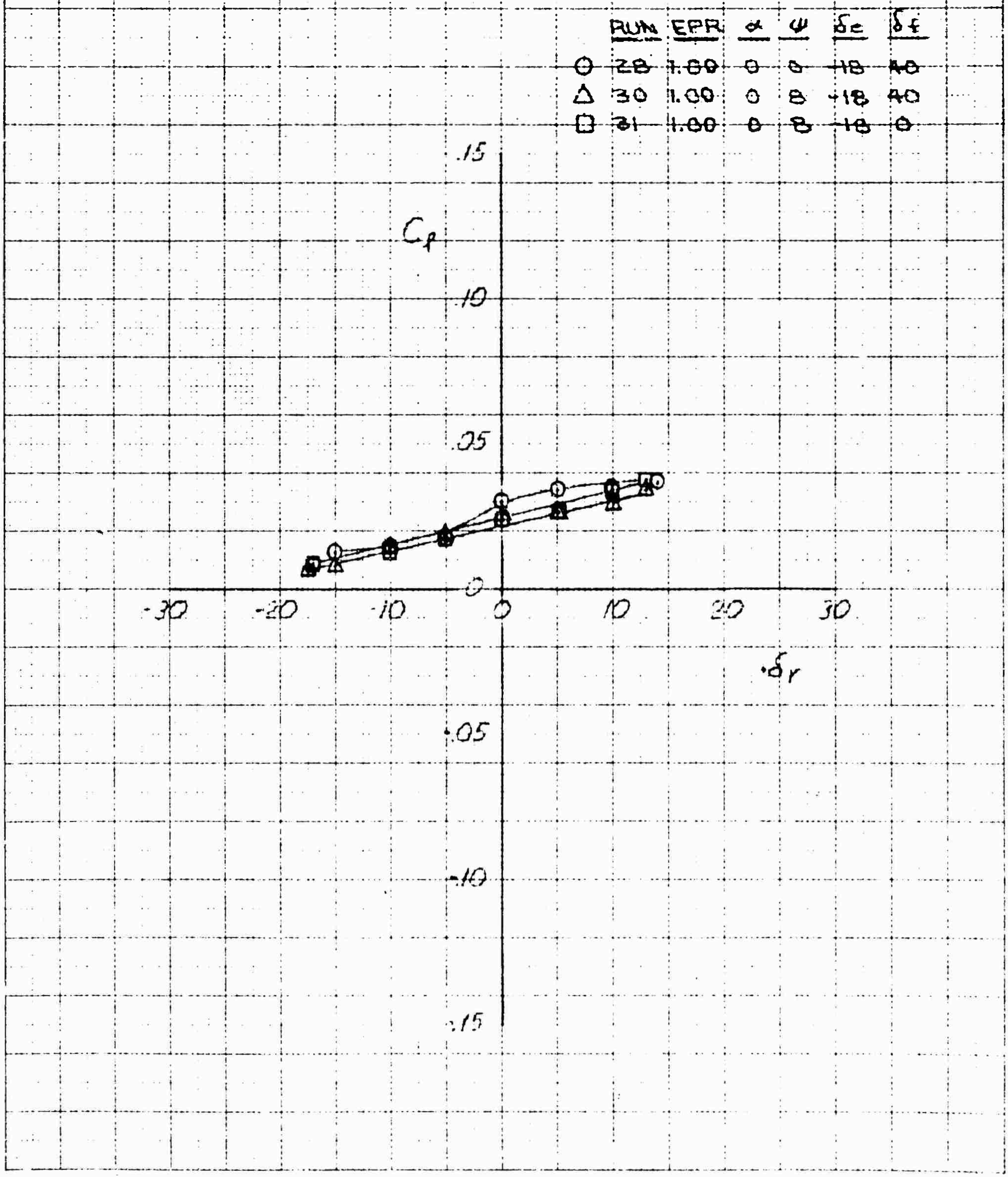

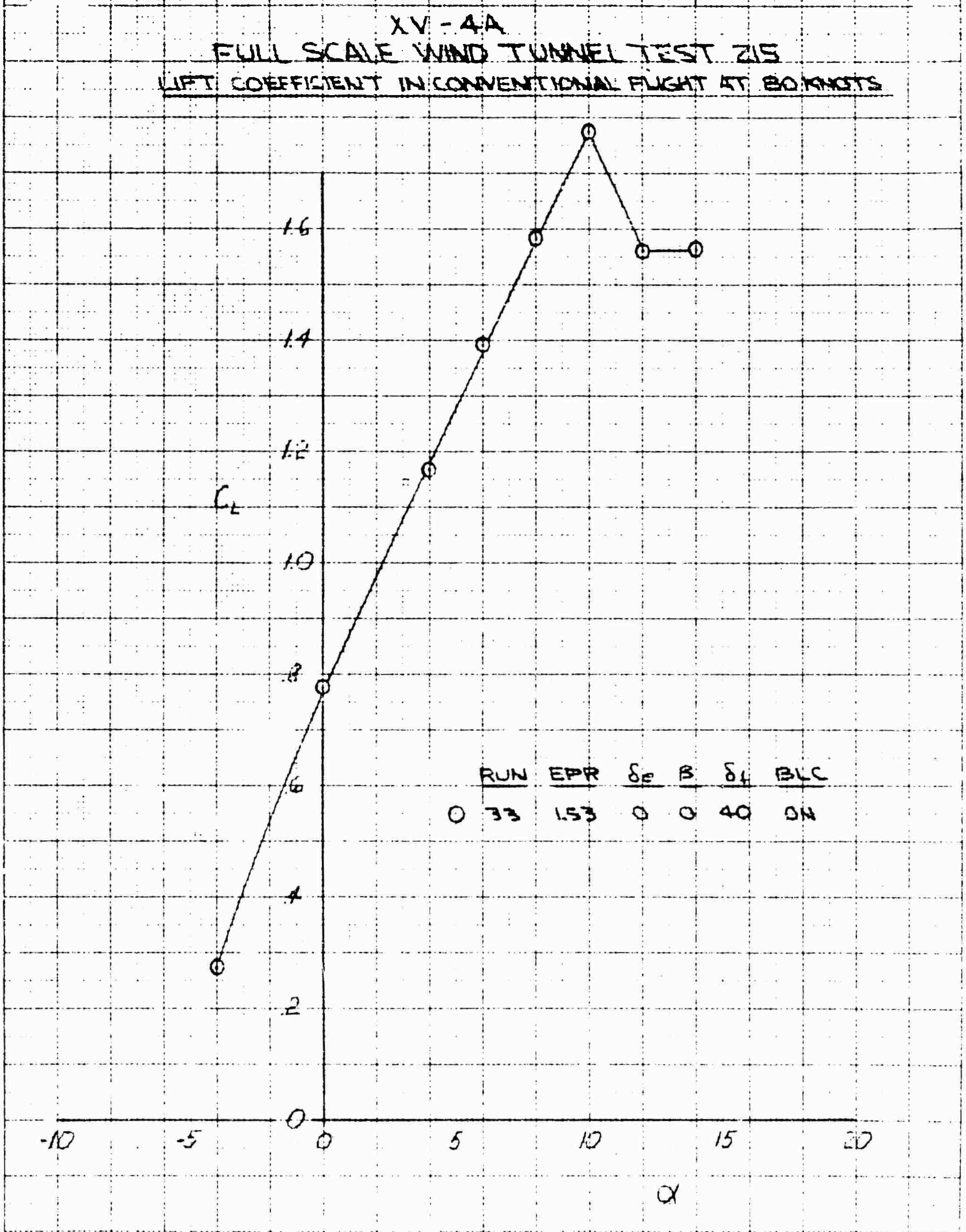
XV - 4A
FULL SCALE WIND TUNNEL TEST 215
LIFT COEFFICIENT IN CONVENTIONAL FLIGHT AT 80 KNOTS
1.6
1.4
1.2
1.0
.8
.6
.4
.2
0
C_L
-10
-5
0
5
10
15
20
α
RUN EPR δ_E β δ_f BLC
33 1.53 0 0 40 ON

XV-4A
FULL SCALE WIND TUNNEL TEST 215
DRAG POLAR IN CONVENTIONAL FLIGHT AT 80 KNOTS

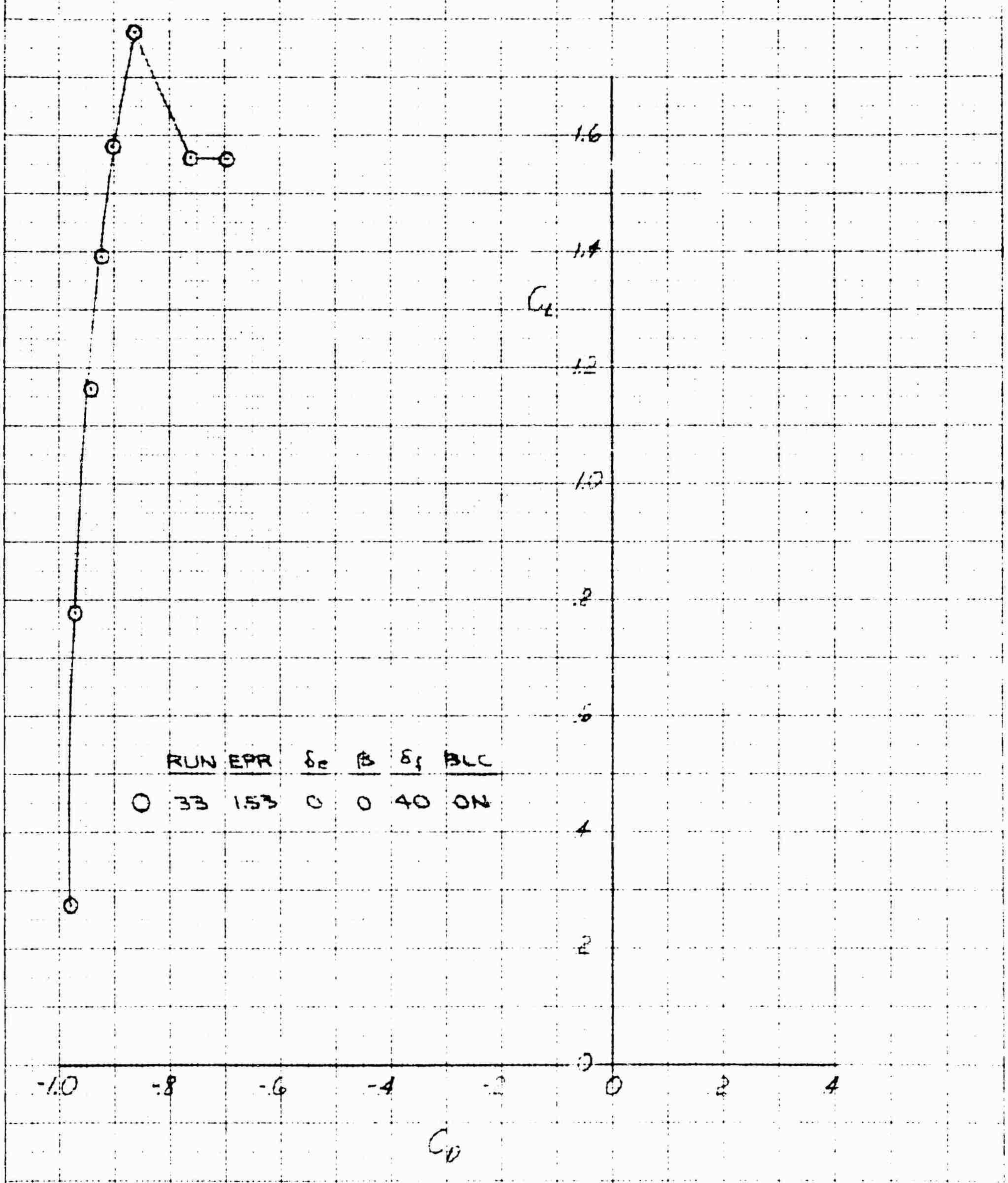

XV-4A
FULL SCALE WIND TUNNEL TEST 215
PITCHING MOMENT CHARACTERISTICS IN CONVENTIONAL FLIGHT AT 80 KNOTS

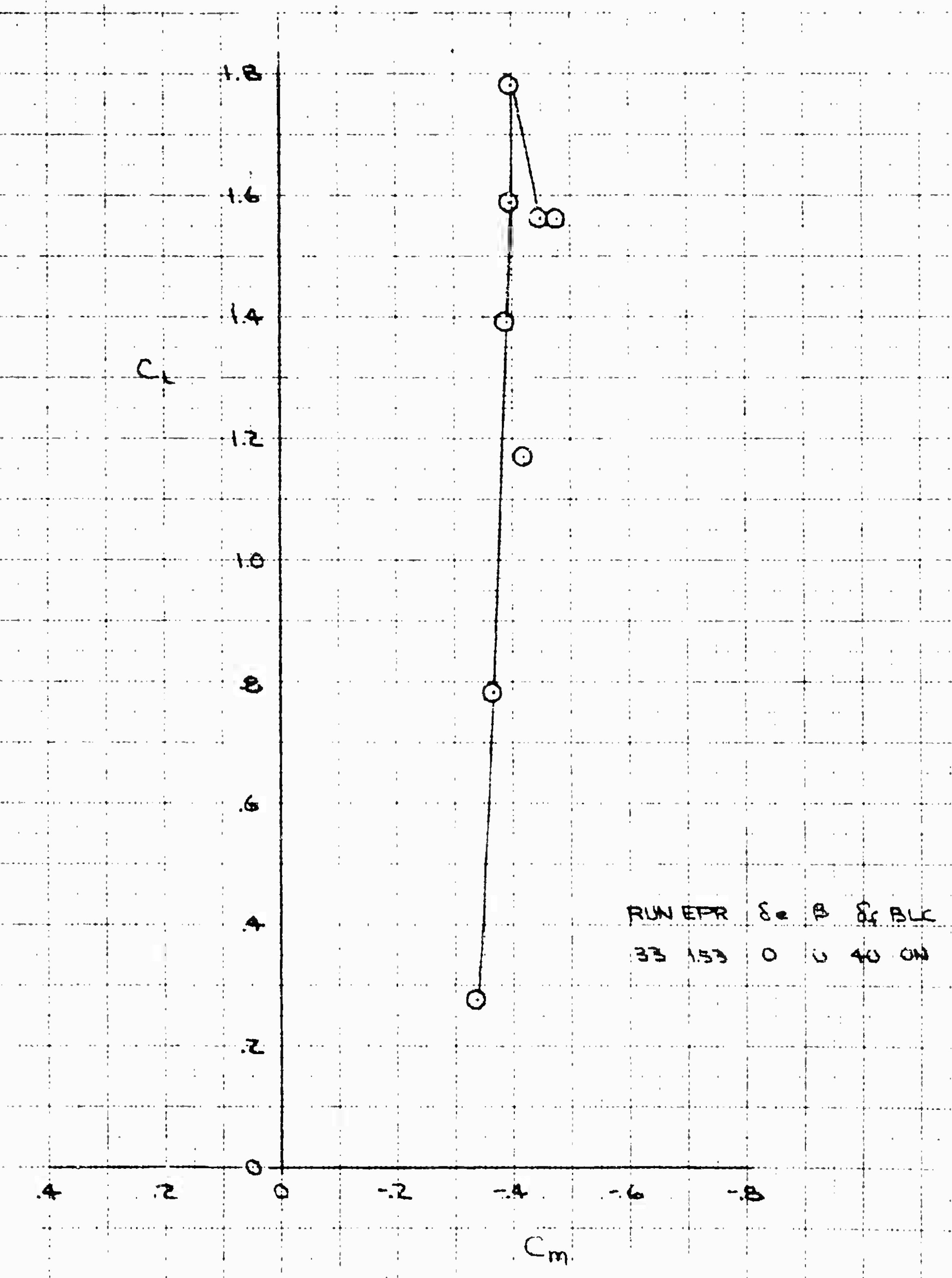

XV-4A
FULL SCALE WIND TUNNEL TEST 215
ELEVATOR EFFECT ON LIFT COEFFICIENT IN CONVENTIONAL FLIGHT AT 80 KNOTS

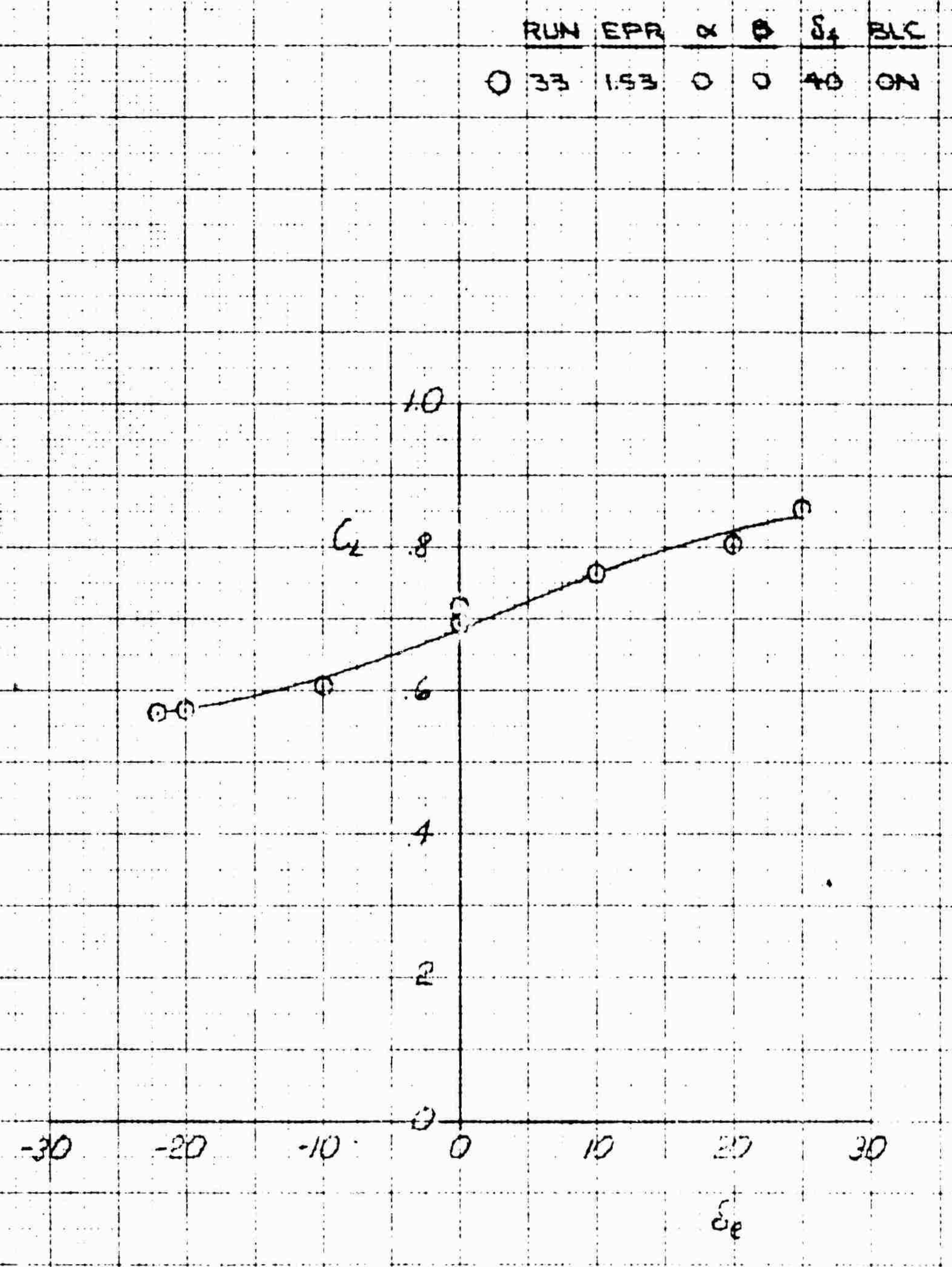

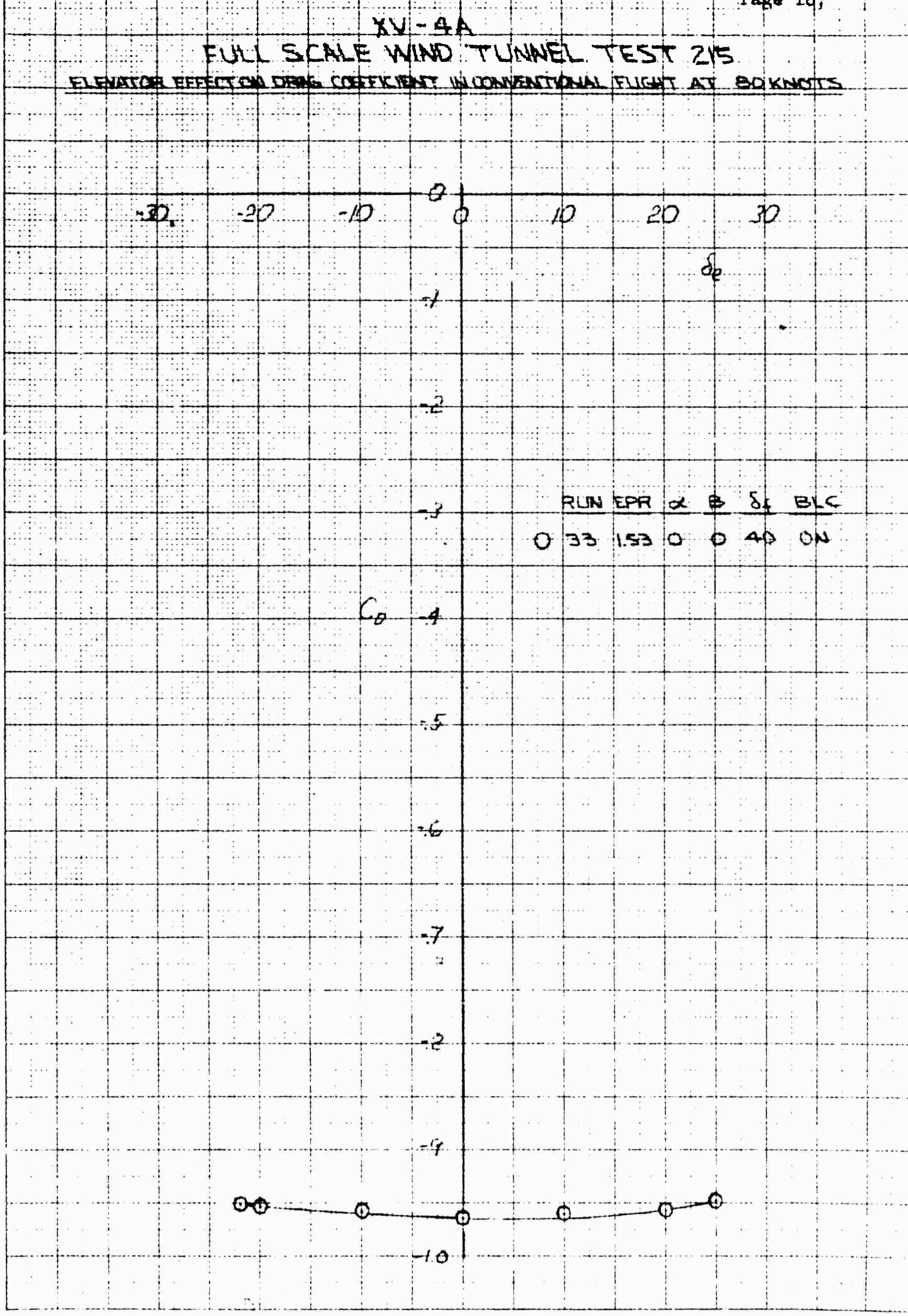
XV-4A
FULL SCALE WIND TUNNEL TEST 215
ELEVATOR EFFECT ON DRAG COEFFICIENT IN CONVENTIONAL FLIGHT AT 80 KNOTS
-30
-20
-10
0
10
20
30
δ_e
C_D
RUN EPR α β δ_f BLC
33 1.53 0 0 40 ON

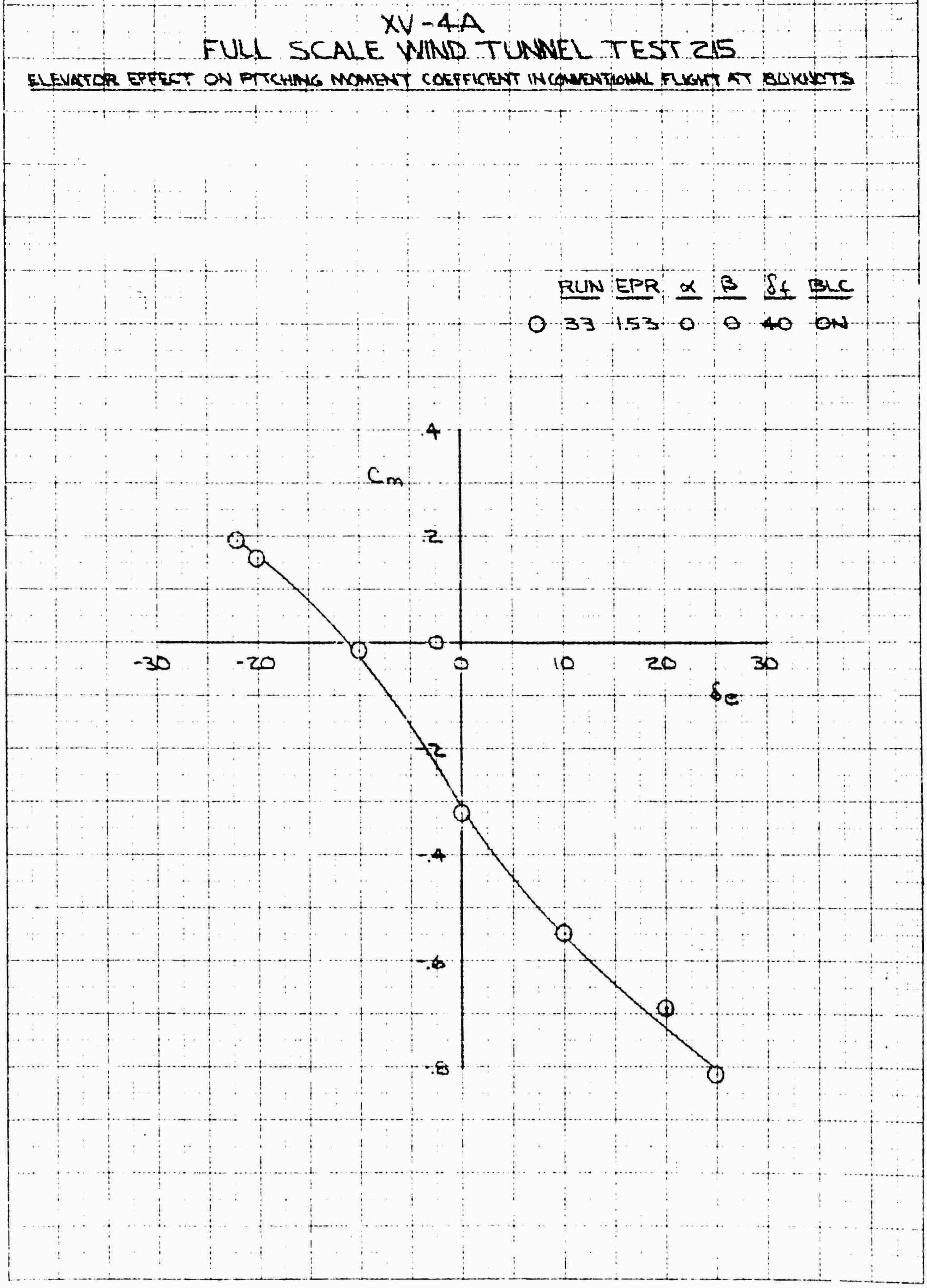
XV-4A
FULL SCALE WIND TUNNEL TEST 215
ELEVATOR EFFECT ON PITCHING MOMENT COEFFICIENT IN CONVENTIONAL FLIGHT AT 80 KNOTS
RUN EPR α β δf BLC
33 1.53 0 0 40 ON
Cm
.4
.2
-.2
-.4
-.6
-.8
-30
-20
0
10
20
30
δe

XV-4A
FULL SCALE WIND TUNNEL TEST 215
TUNNEL DYNAMIC PRESSURE EFFECT ON DATA PRESENTATION

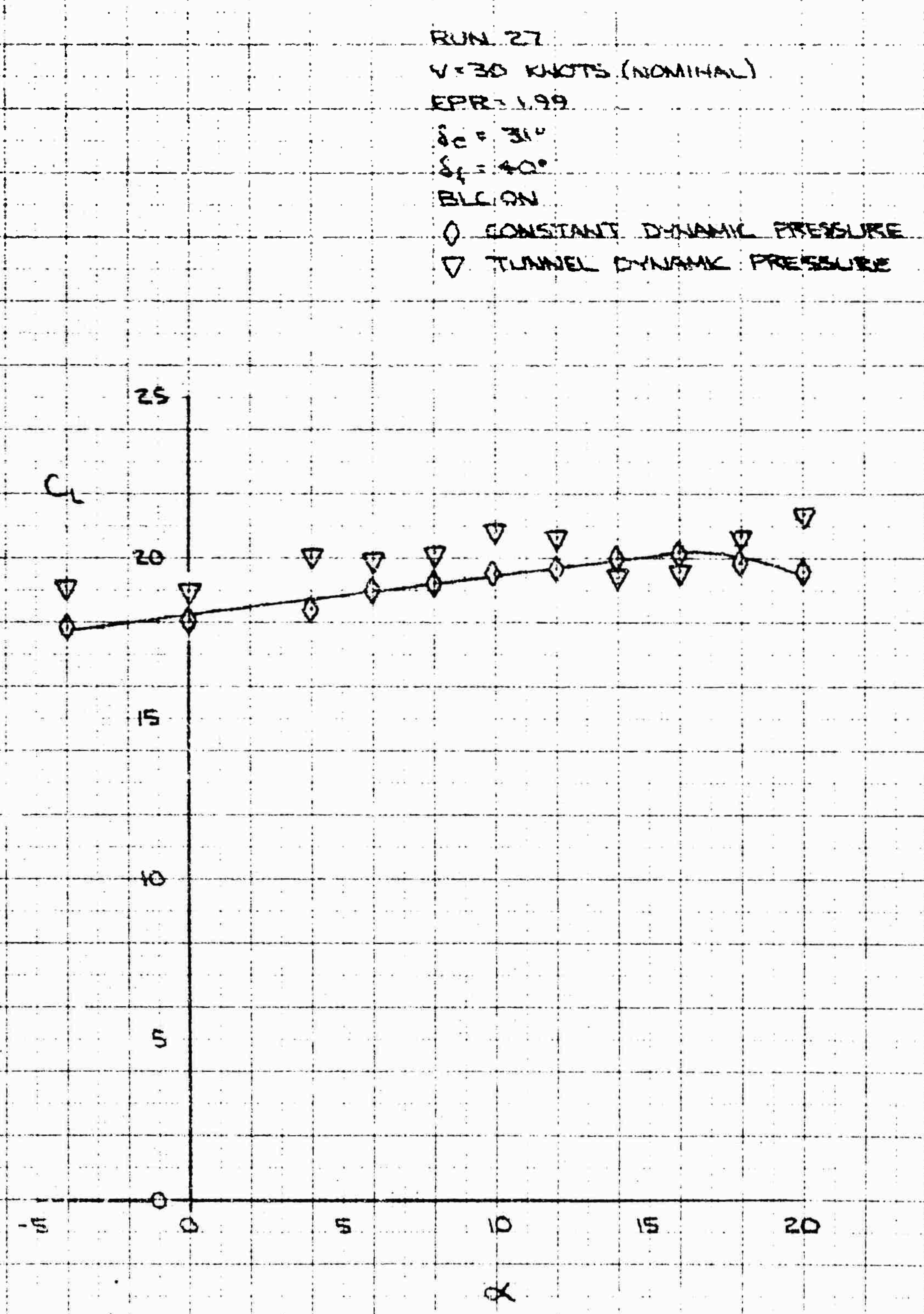

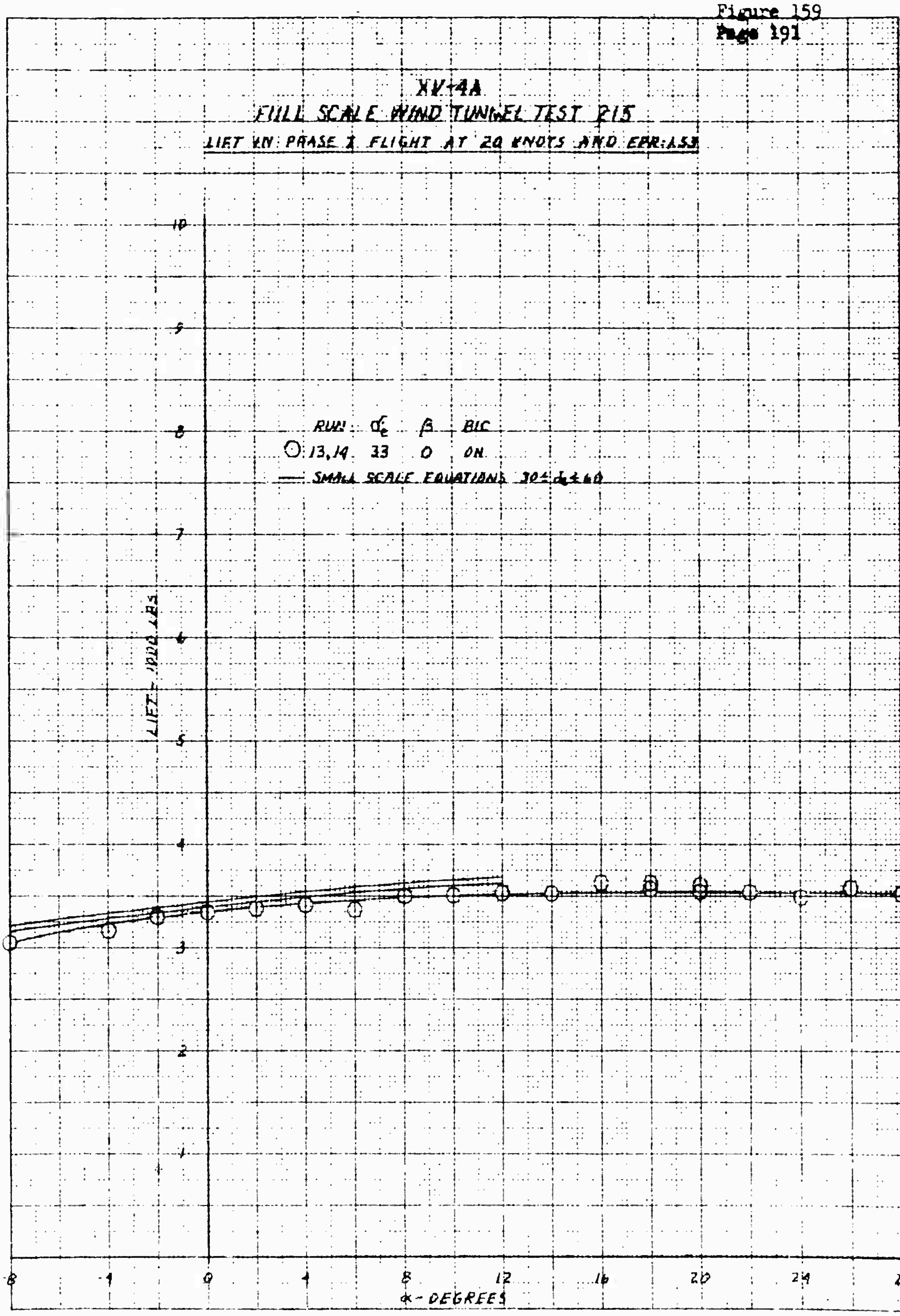
XV-4A
FULL SCALE WIND TUNNEL TEST 215
LIFT VN: PHASE 1 FLIGHT AT 20 KNOTS AND EPR:1.53
RUN: δ_c β BIC
13,14 33 0 ON
SMALL SCALE EQUATIONS
LIFT - 1000 LBS
α - DEGREES

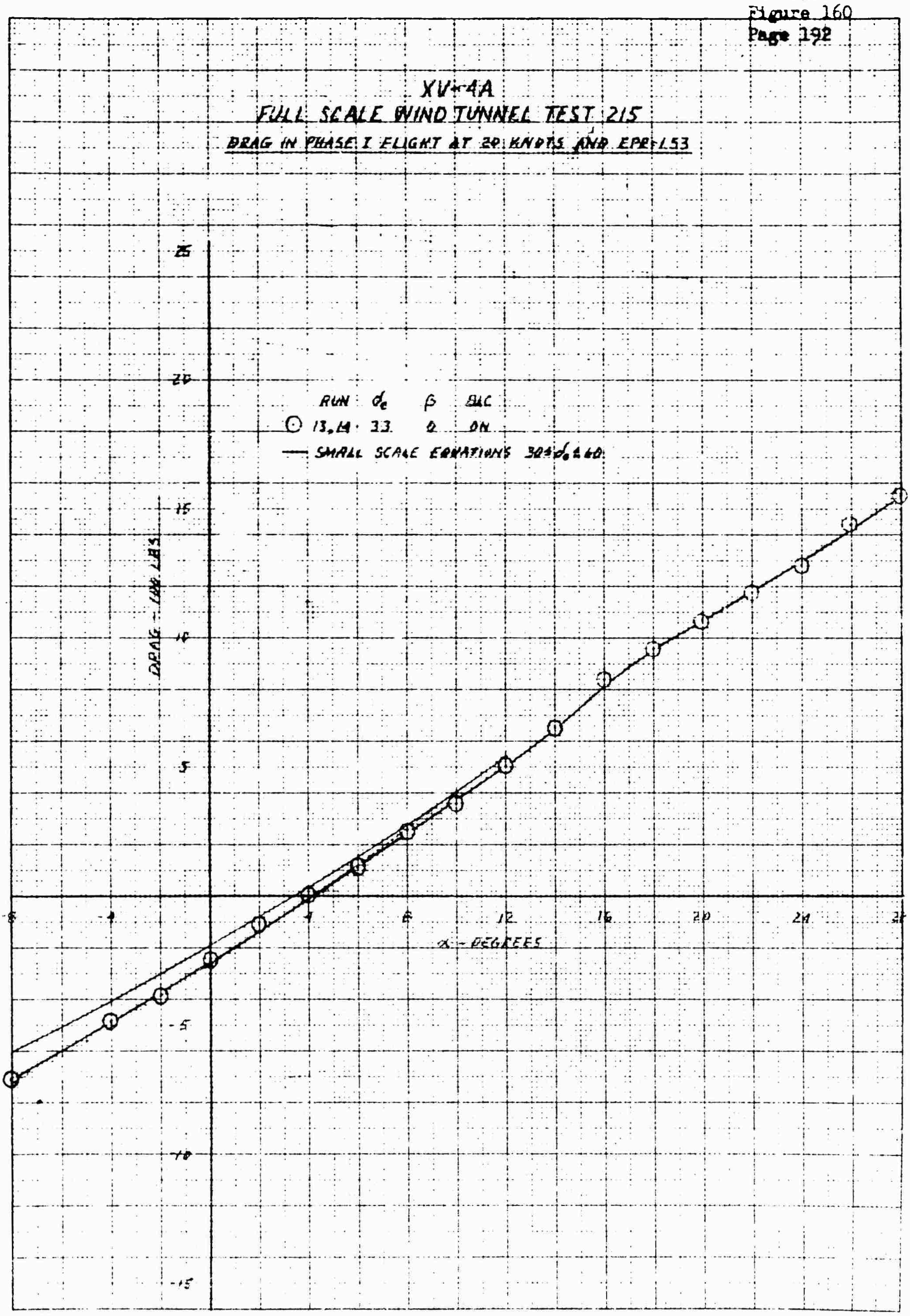
XV-4A
FULL SCALE WIND TUNNEL TEST 215
DRAG IN PHASE I FLIGHT AT 20 KNOTS AND EPR=1.53
RUN δe β BLC
13,14 33 0 ON
SMALL SCALE EQUATIONS
DRAG - 100 LBS
α - DEGREES
25
20
15
10
5
-5
-10
-15
-8
-4
4
8
12
16
20
24

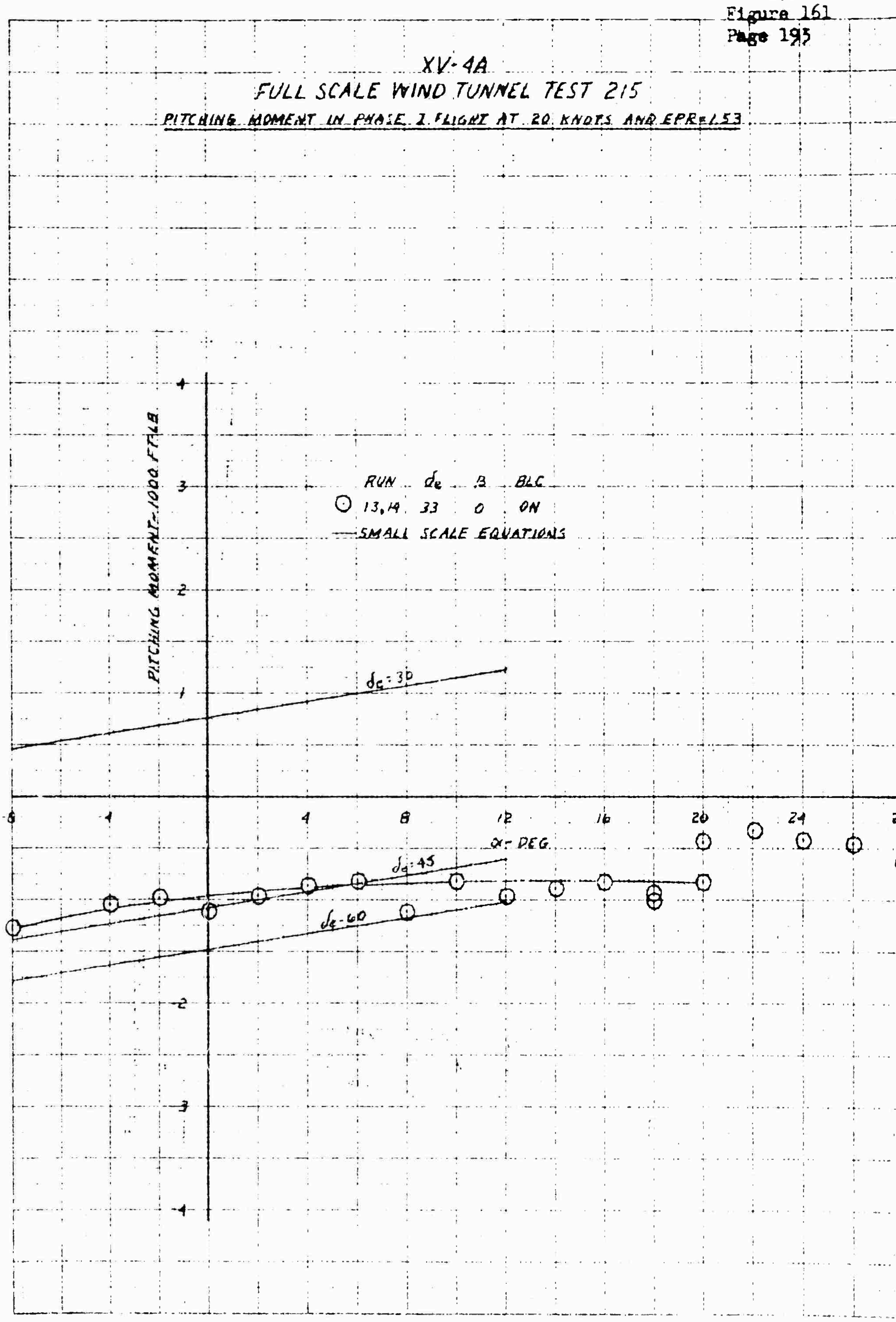
XV-4A
FULL SCALE WIND TUNNEL TEST 215
PITCHING MOMENT IN PHASE 2 FLIGHT AT 20 KNOTS AND EPR=1.53
RUN δe β BLC
13,14 33 0 ON
SMALL SCALE EQUATIONS
PITCHING MOMENT-1000 FT-LB
α - DEG
δe=30
δe=45
δe=60

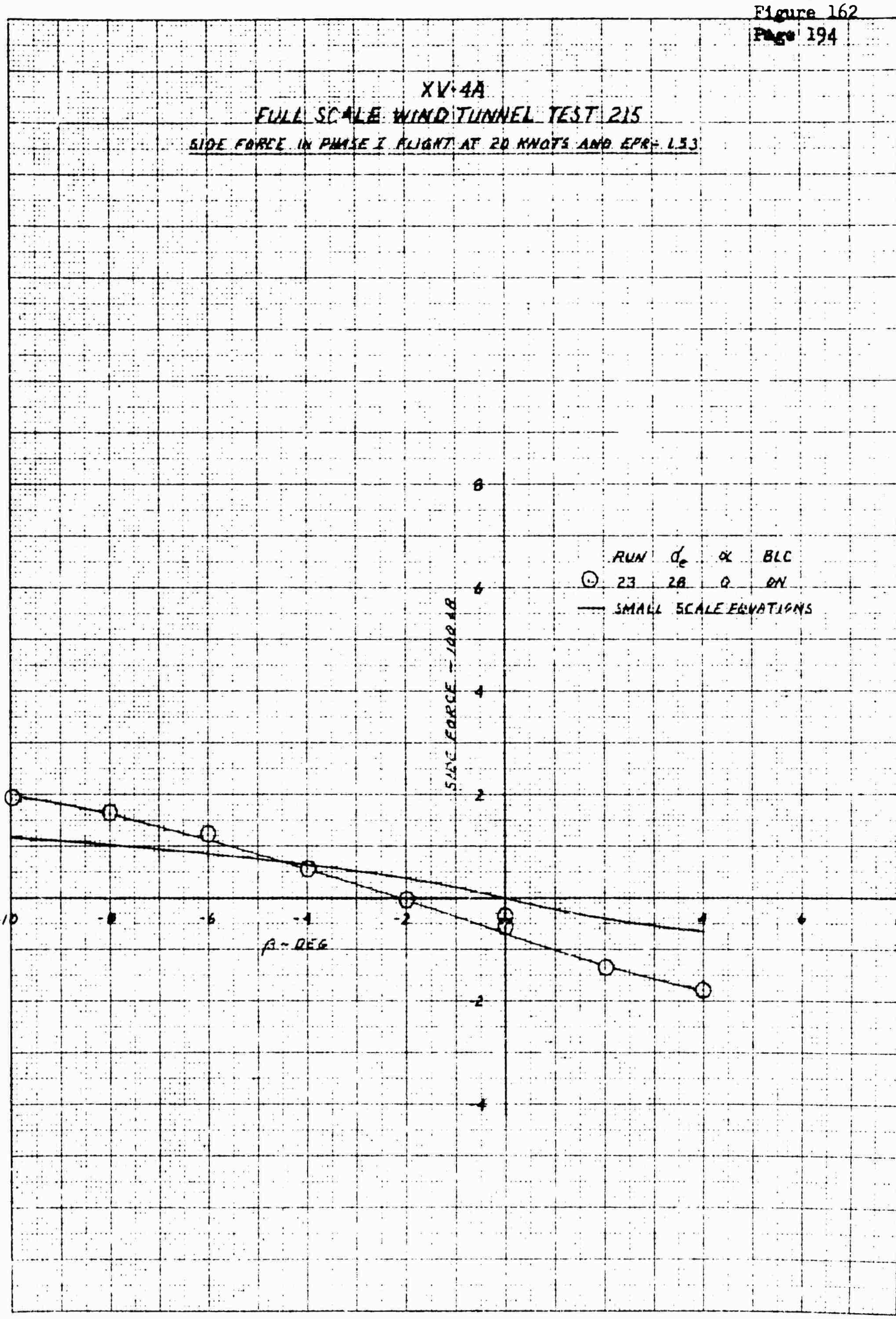
XV-4A
FULL SCALE WIND TUNNEL TEST 215
SIDE FORCE IN PHASE I FLIGHT AT 20 KNOTS AND EPR = 1.53
RUN δe α BLC
23 28 0 ON
SMALL SCALE EQUATIONS
SIDE FORCE — 100 LB
β ~ DEG
-10
-8
-6
-4
-2
4
6
8
2
-2
-4

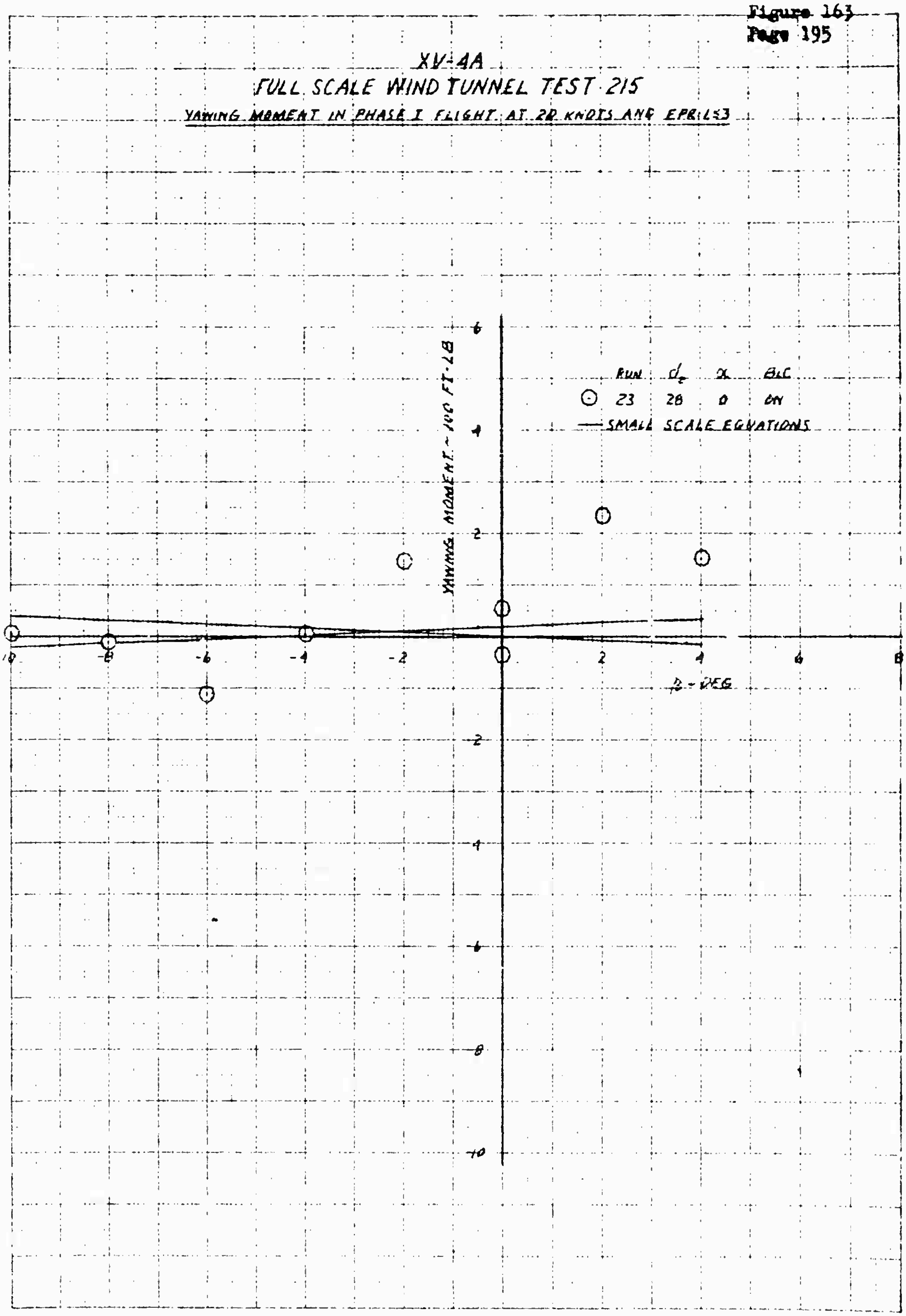
XV-4A
FULL SCALE WIND TUNNEL TEST 215
YAWING MOMENT IN PHASE I FLIGHT AT 20 KNOTS AND EPR≤3
RUN δ α BLC
23 28 0 ON
SMALL SCALE EQUATIONS
YAWING MOMENT ~ 100 FT-LB
β - DEG
6
4
2
-2
-4
-6
-8
-10
-10
-8
-6
-4
-2
2
4
6
8

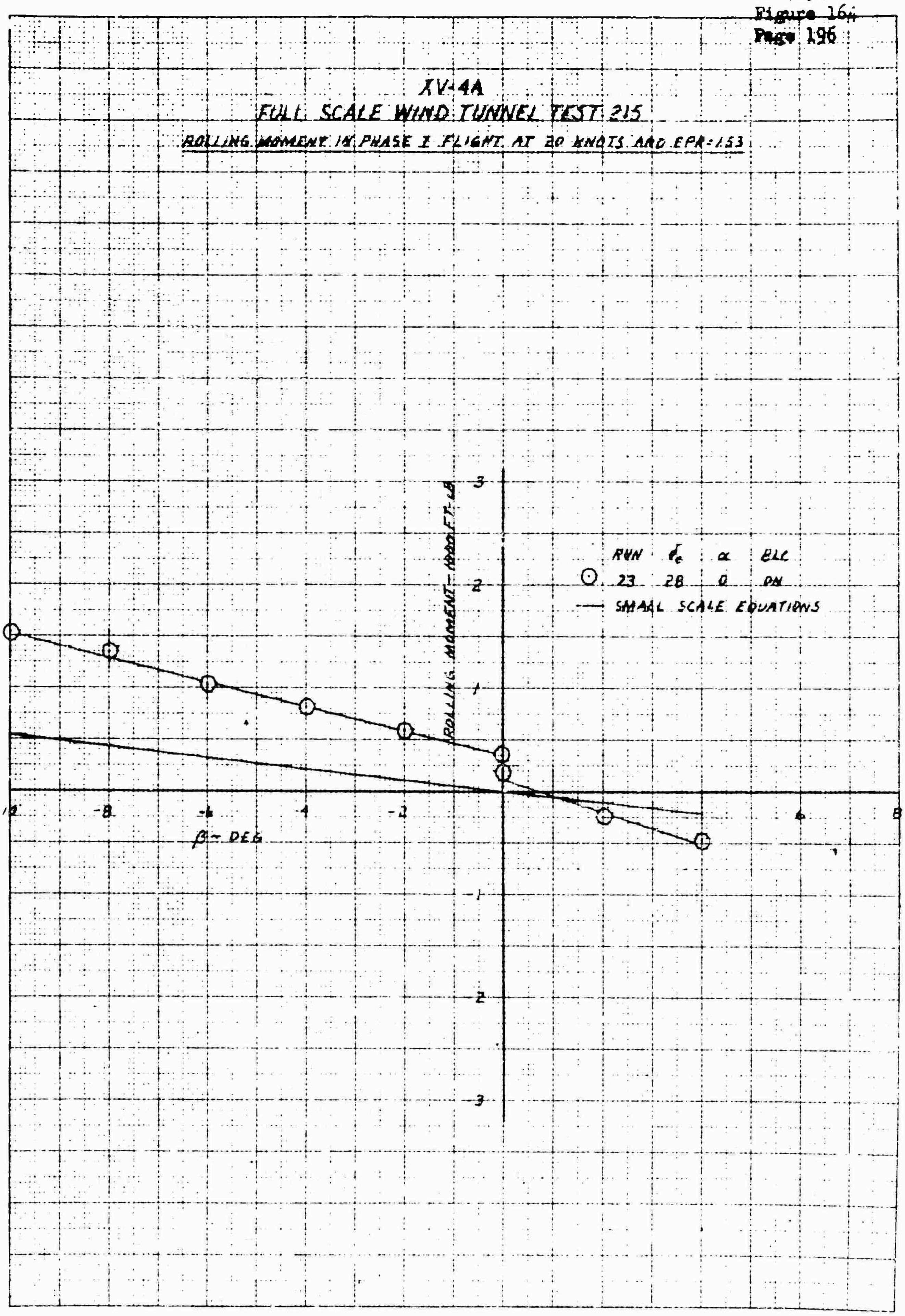
XV-4A
FULL SCALE WIND TUNNEL TEST 215
ROLLING MOMENT IN PHASE I FLIGHT AT 20 KNOTS AND EPR=1.53
ROLLING MOMENT-1000 FT-LB
RUN
α
BLC
23
28
0
ON
SMALL SCALE EQUATIONS
β ~ DEG
3
2
1
-1
-2
-3
-12
-8
-6
-4
-2
4
6
8

XV-4A

FULL SCALE WIND TUNNEL TEST 215

ELEVATOR EFFECTIVENESS IN PHASE I FLIGHT AT 20 KNOTS AND EPR=1.53

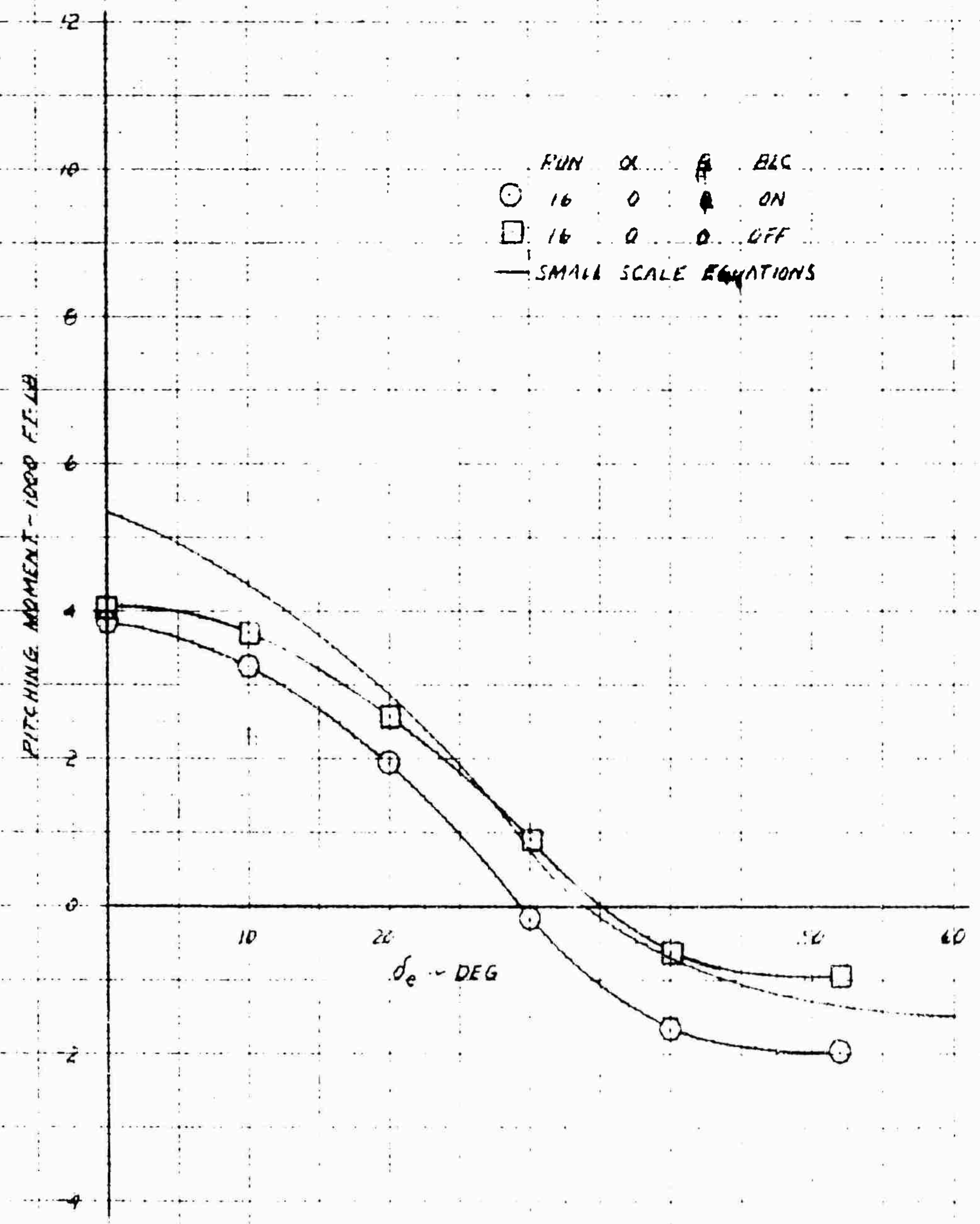

XV-4A
FULL SCALE WIND TUNNEL TEST 215
AILERON EFFECT ON SIDE FORCE IN PHASE I FLIGHT AT 20 KNOTS AND EPR = 1.53

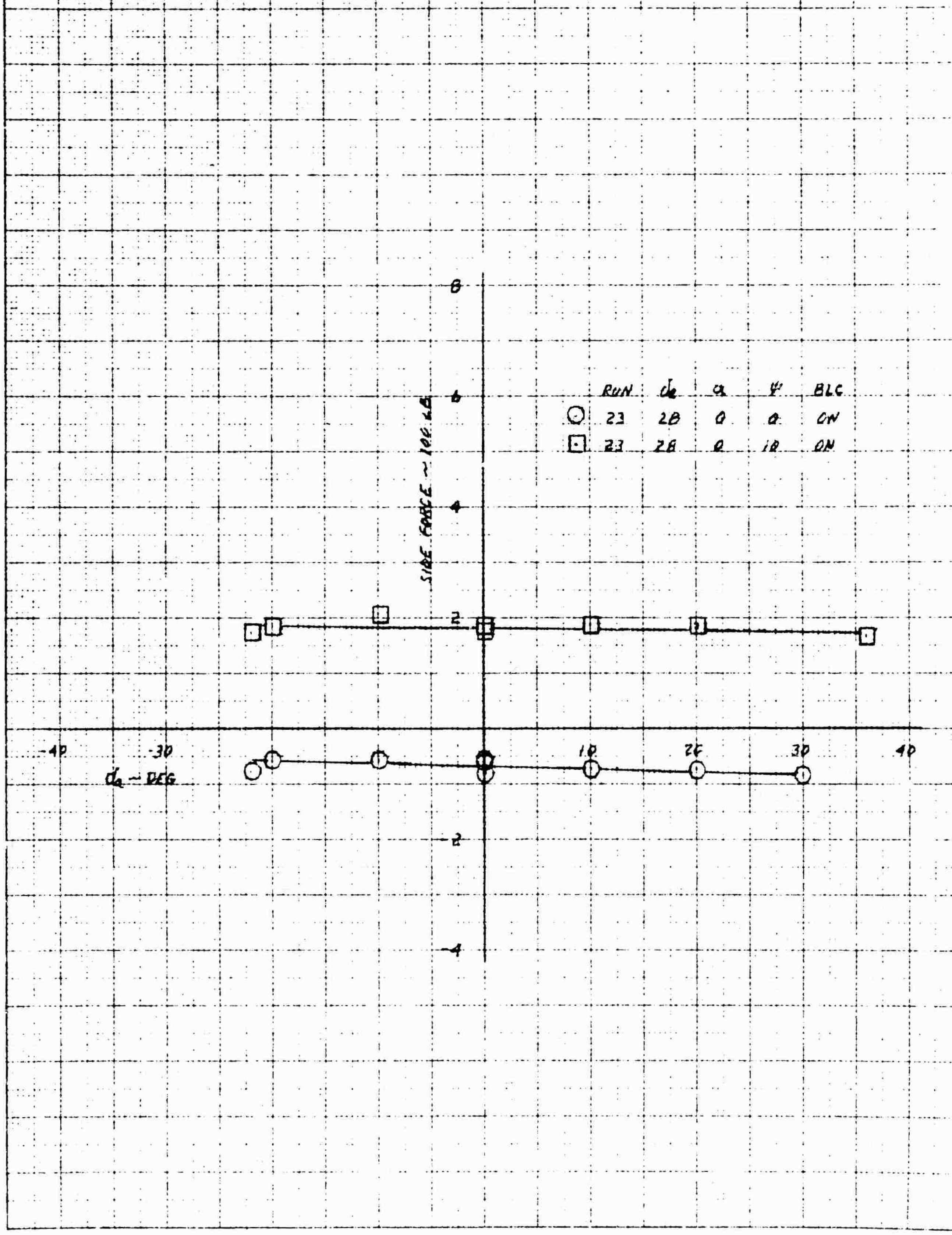

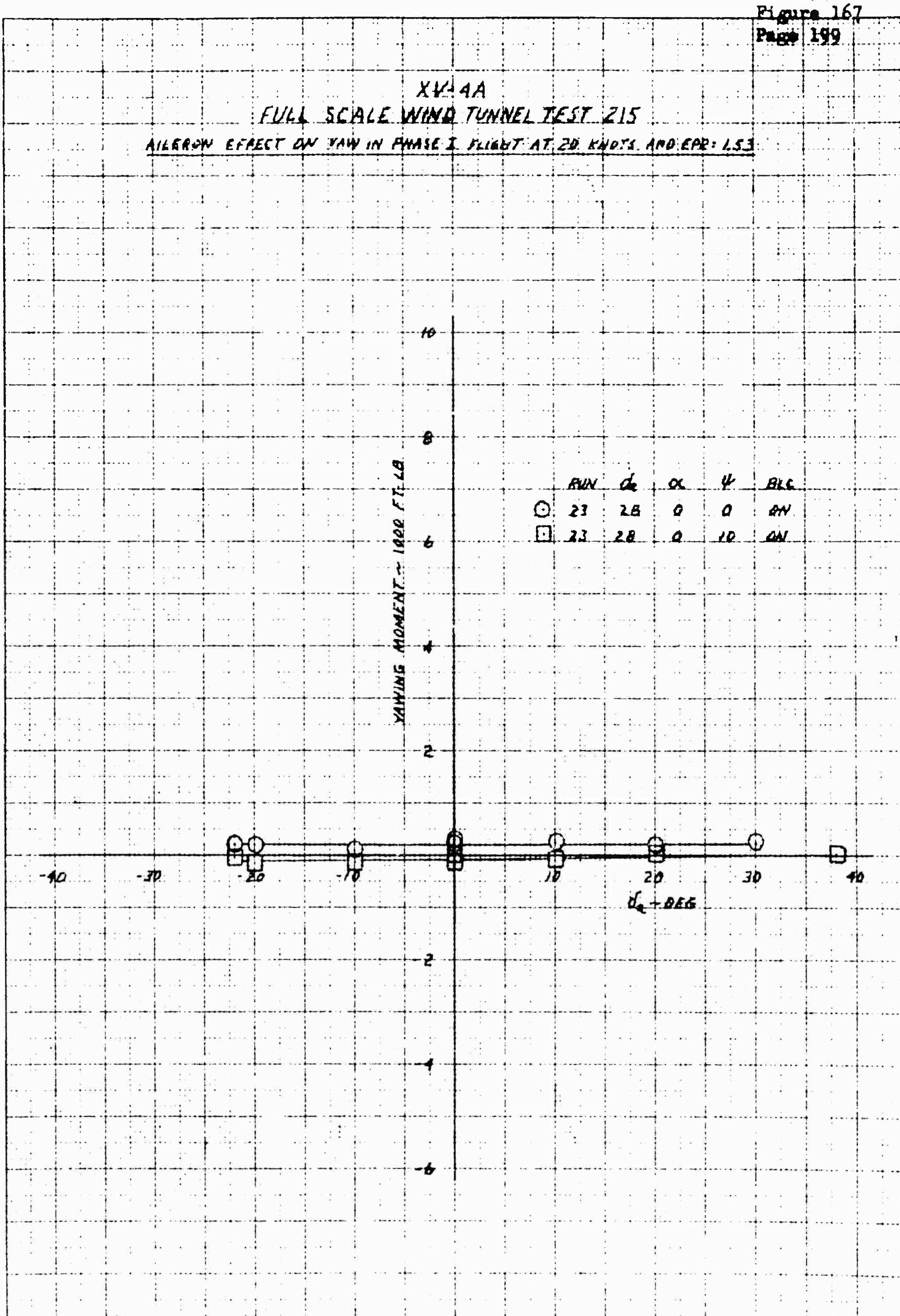
XV-4A
FULL SCALE WIND TUNNEL TEST 215
AILERON EFFECT ON YAW IN PHASE I FLIGHT AT 20 KNOTS AND EPR: 1.53
RUN δe α ψ BLC
23 28 0 0 ON
23 28 0 10 ON
YAWING MOMENT ~ 1000 FT-LB
10
8
6
4
2
-2
-4
-6
-40
-30
-20
-10
10
20
30
40
δa ~ DEG

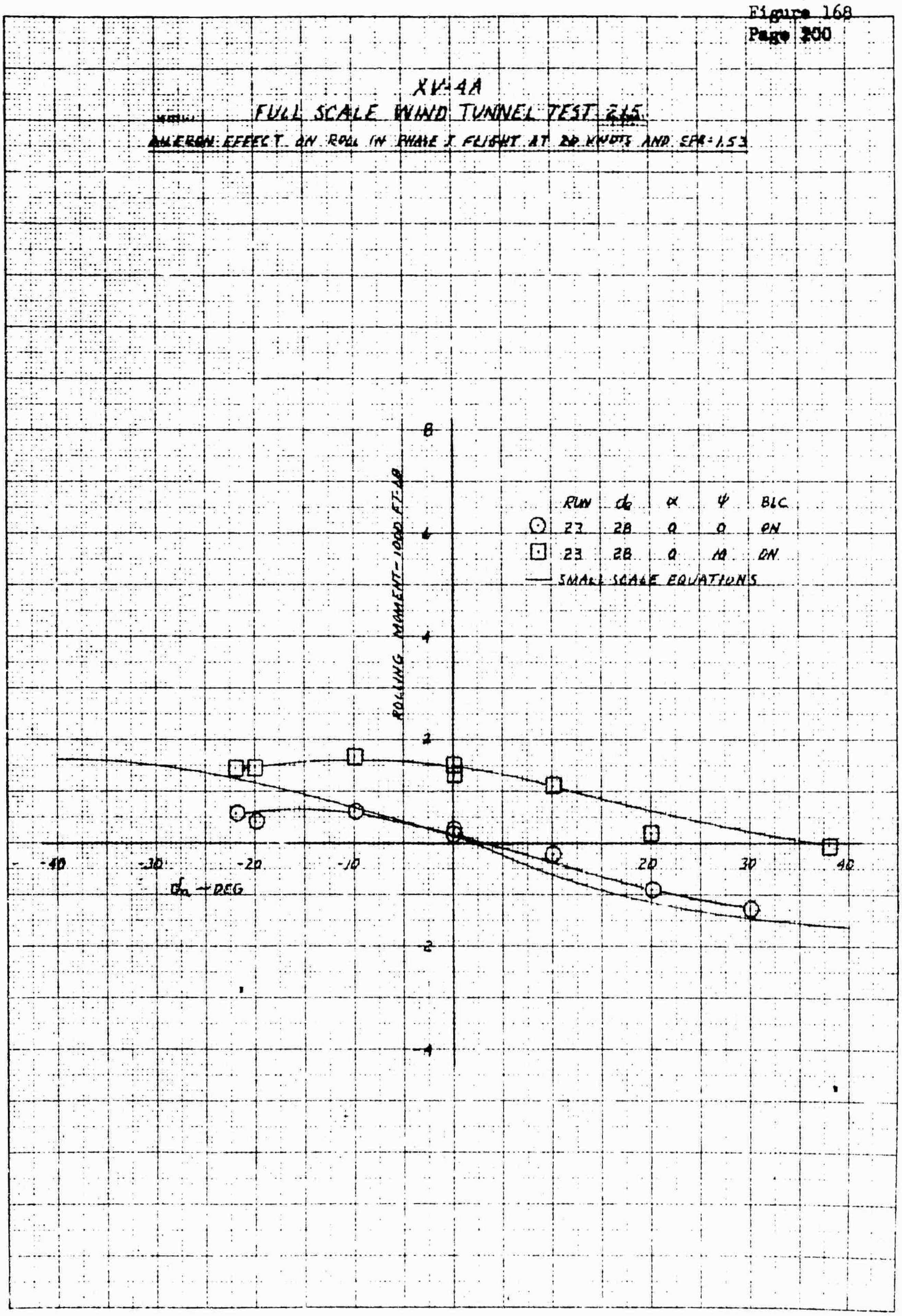
XV-4A
FULL SCALE WIND TUNNEL TEST 215
AILERON EFFECT ON ROLL IN PHASE I FLIGHT AT 20 KNOTS AND EPR=1.53
ROLLING MOMENT - 1000 FT-LB
δa - DEG
RUN δc α ψ BLC
23 28 0 0 ON
23 28 0 10 ON
SMALL SCALE EQUATIONS
8
6
4
2
-2
-4
-40
-30
-20
-10
20
30
40

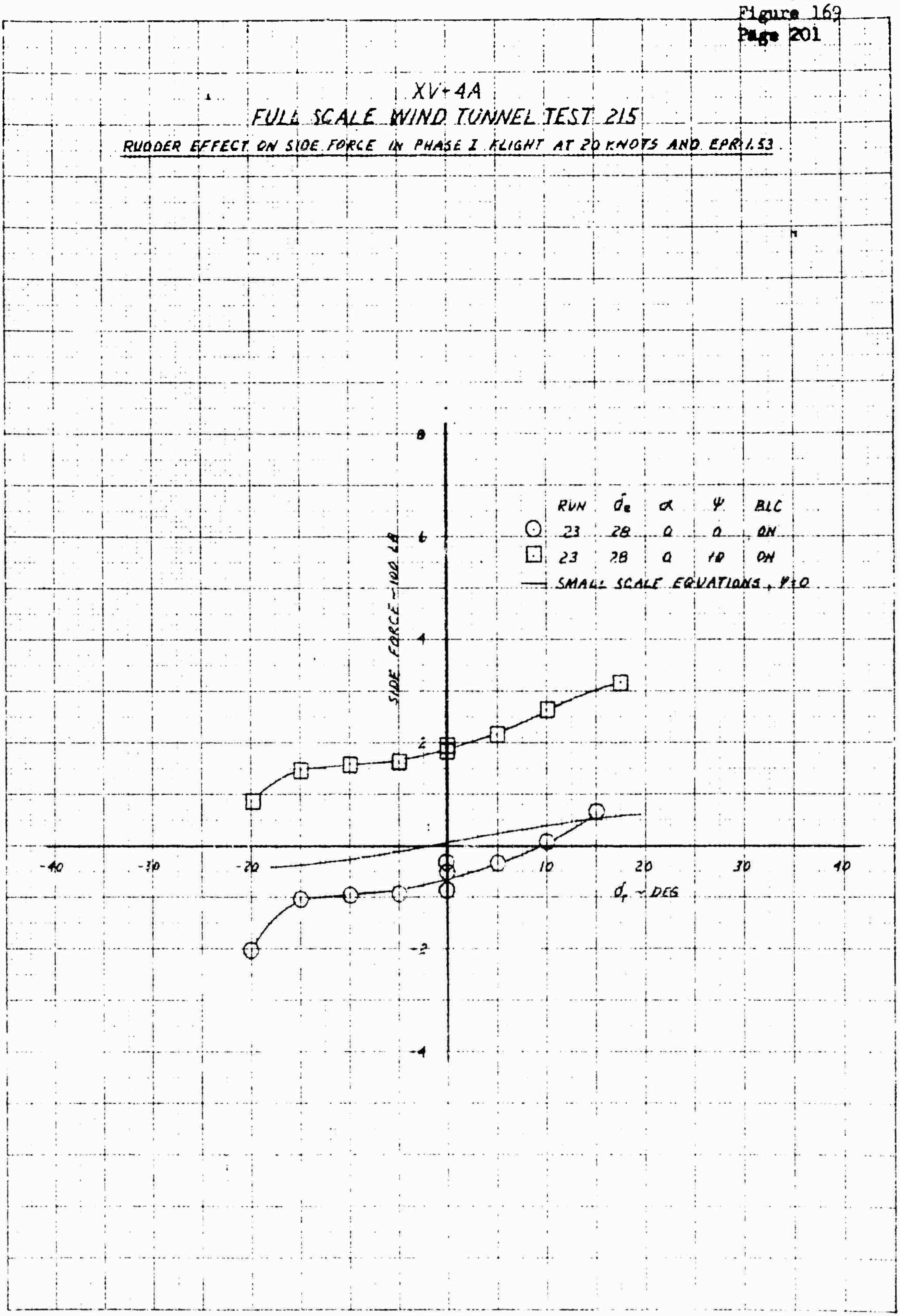
XV-4A
FULL SCALE WIND TUNNEL TEST 215
RUDDER EFFECT ON SIDE FORCE IN PHASE I FLIGHT AT 20 KNOTS AND EPR 1.53
RUN | δ_e | α | ψ | BLC
23 | 28 | 0 | 0 | ON
23 | 28 | 0 | 10 | ON
SMALL SCALE EQUATIONS, ψ=0
SIDE FORCE ~ 100 LB
δ_r ~ DEG
-40
-30
-20
10
20
30
40
8
6
4
2
-2
-4

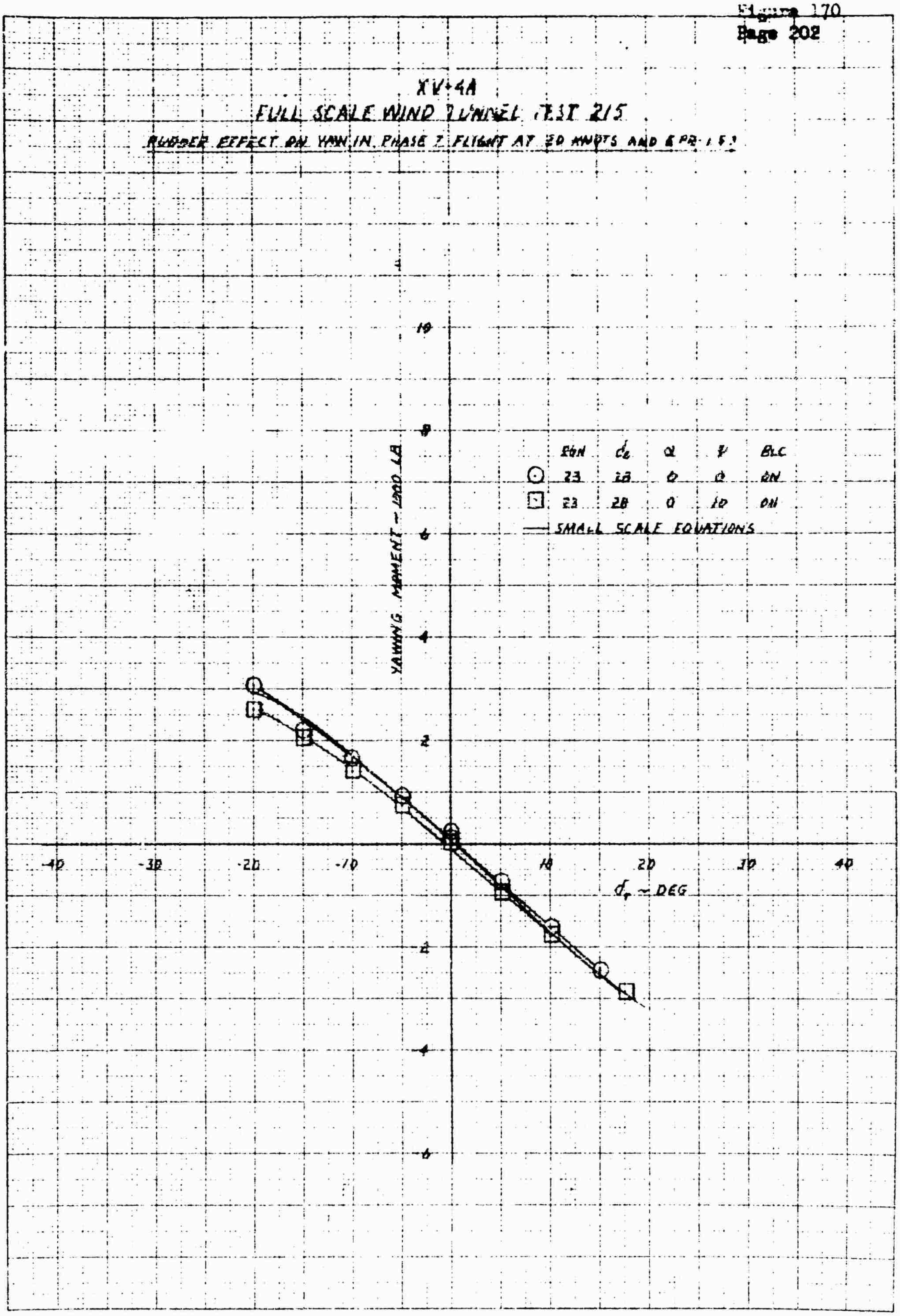
XV-4A
FULL SCALE WIND TUNNEL TEST 215
RUDDER EFFECT ON YAW IN PHASE 2 FLIGHT AT 30 KNOTS AND EPR 1.5
YAWING MOMENT ~ 1000 LB
d_r ~ DEG
RPM d_e α ψ BLC
23 28 0 0 ON
23 28 0 10 ON
SMALL SCALE EQUATIONS
-40 -30 -20 -10 10 20 30 40
10 8 6 4 2 -2 -4 -6

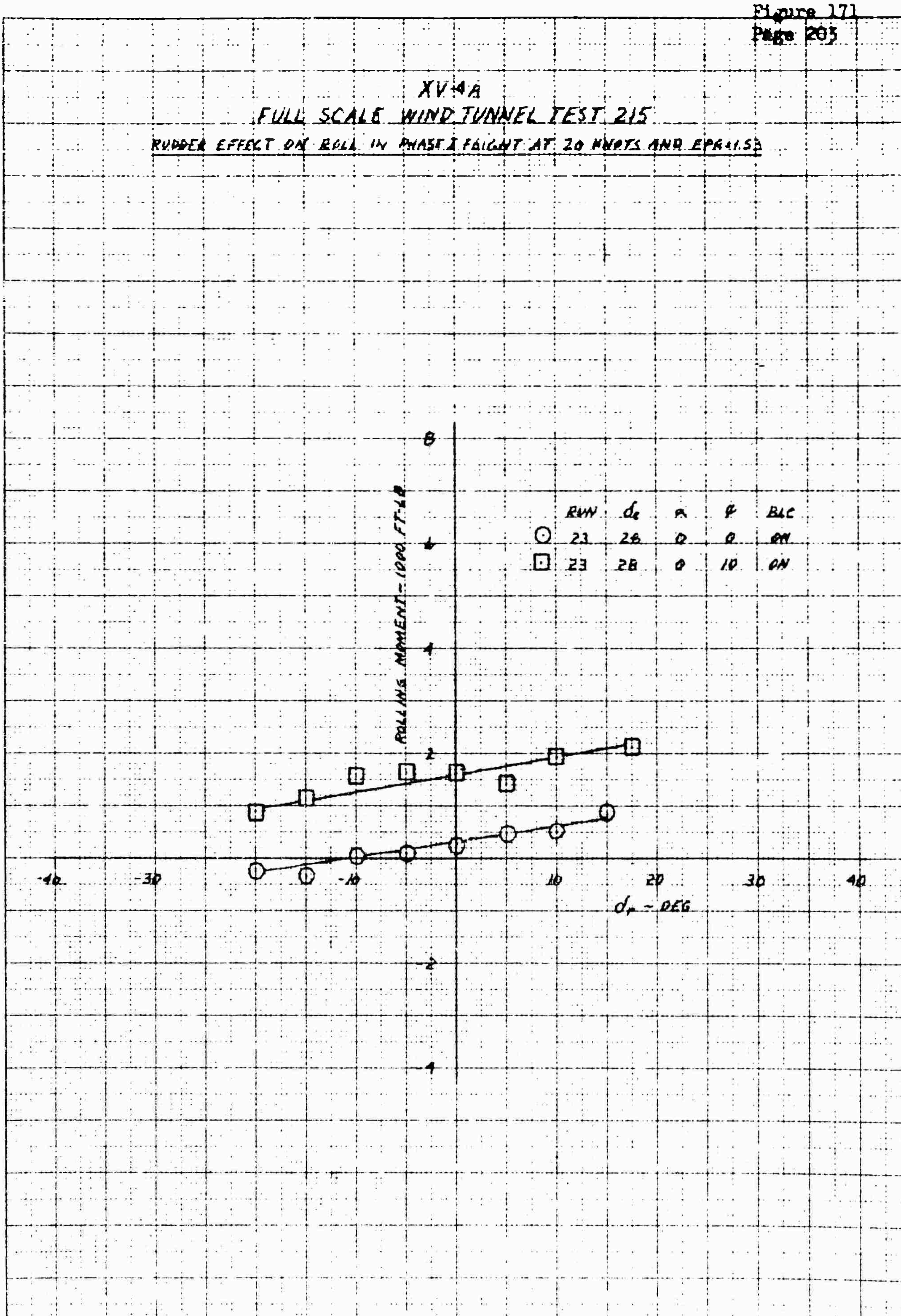
XV-4A
FULL SCALE WIND TUNNEL TEST 215
RUDDER EFFECT ON ROLL IN PHASE I FLIGHT AT 20 KNOTS AND EPR=1.53
RUN
23
23
BLC
ON
ON
ROLLING MOMENT – 1000 FT-LB
8
6
4
2
-2
-4
-40
-30
-10
10
20
30
40
– DEG

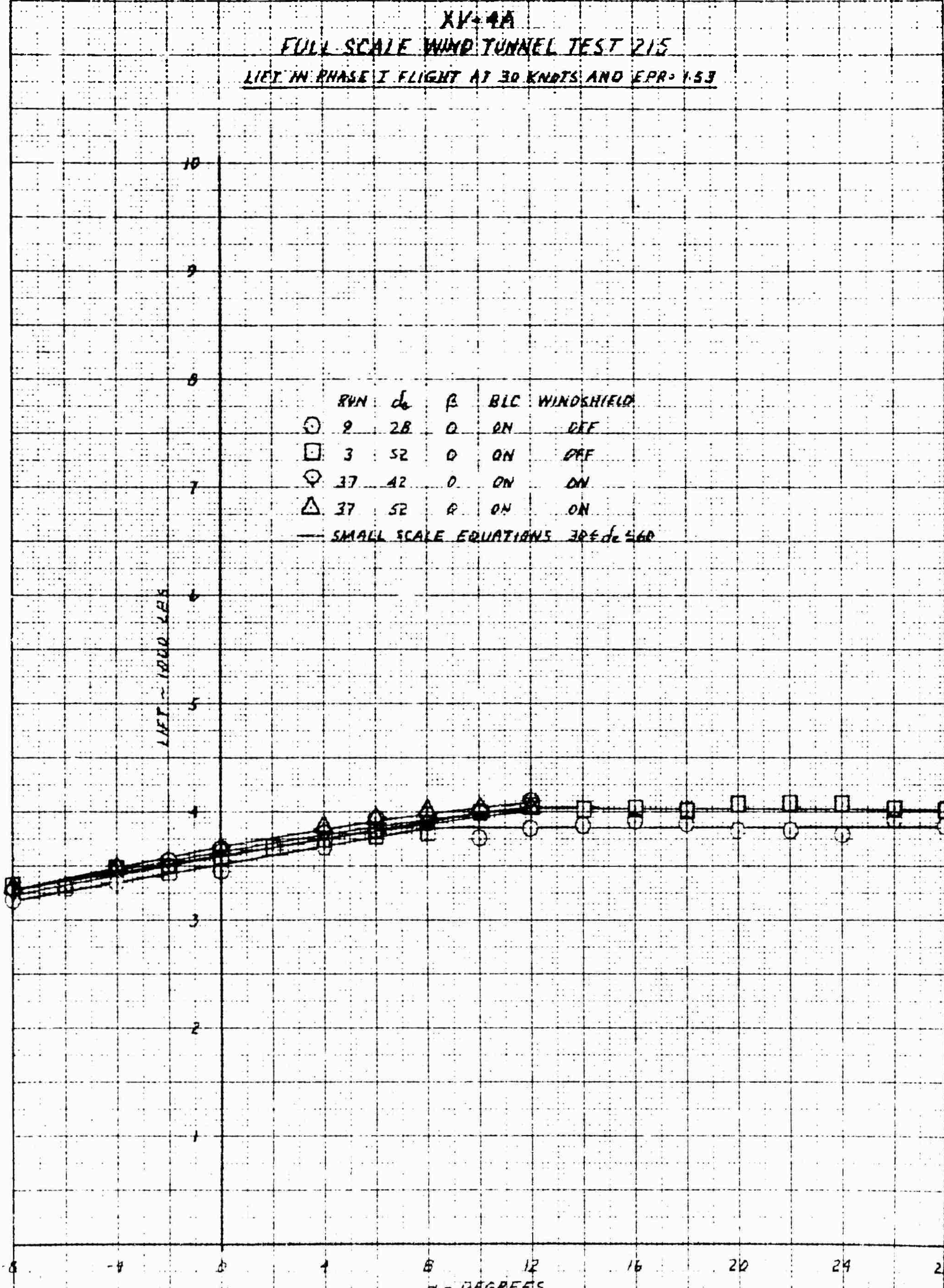
XV-4A
FULL SCALE WIND TUNNEL TEST 215
LIFT IN PHASE I FLIGHT AT 30 KNOTS AND EPR = 1.53
RUN
δ_e
β
BLC
WINDSHIELD
9
28
0
ON
OFF
3
52
0
ON
OFF
37
42
0
ON
ON
37
52
0
ON
ON
SMALL SCALE EQUATIONS 38 ≤ δ_e ≤ 60
LIFT ~ 1000 LBS
α - DEGREES

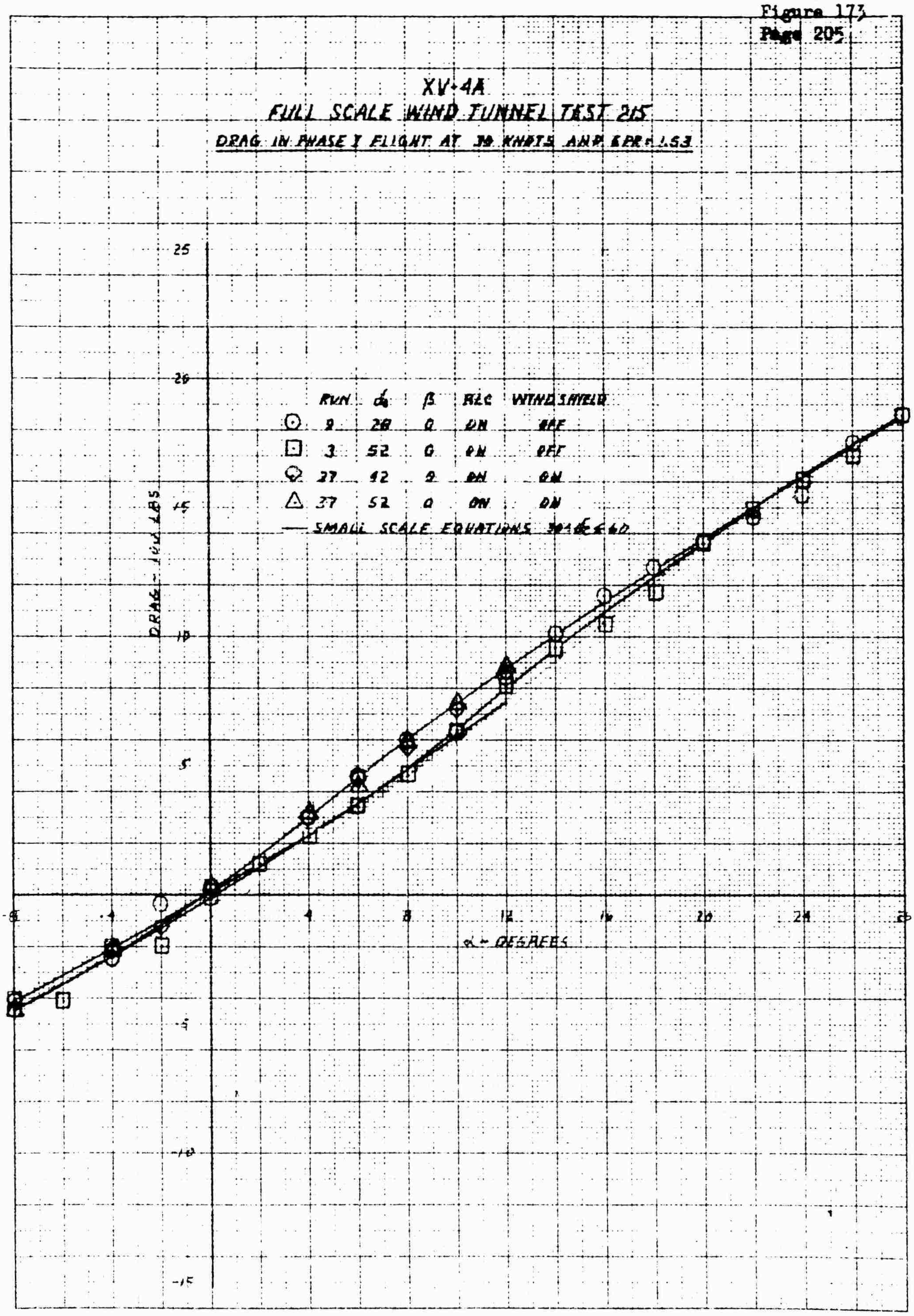
XV-4A
FULL SCALE WIND TUNNEL TEST 215
DRAG IN PHASE I FLIGHT AT 30 KNOTS AND EPR=1.53
RUN α β BLC WINDSHIELD
9 28 0 ON OFF
3 52 0 ON OFF
37 42 0 ON ON
37 52 0 ON ON
SMALL SCALE EQUATIONS
DRAG - 100 LBS
25
20
15
10
5
-5
-10
-15
-8
-4
4
8
12
16
20
24
α - DEGREES

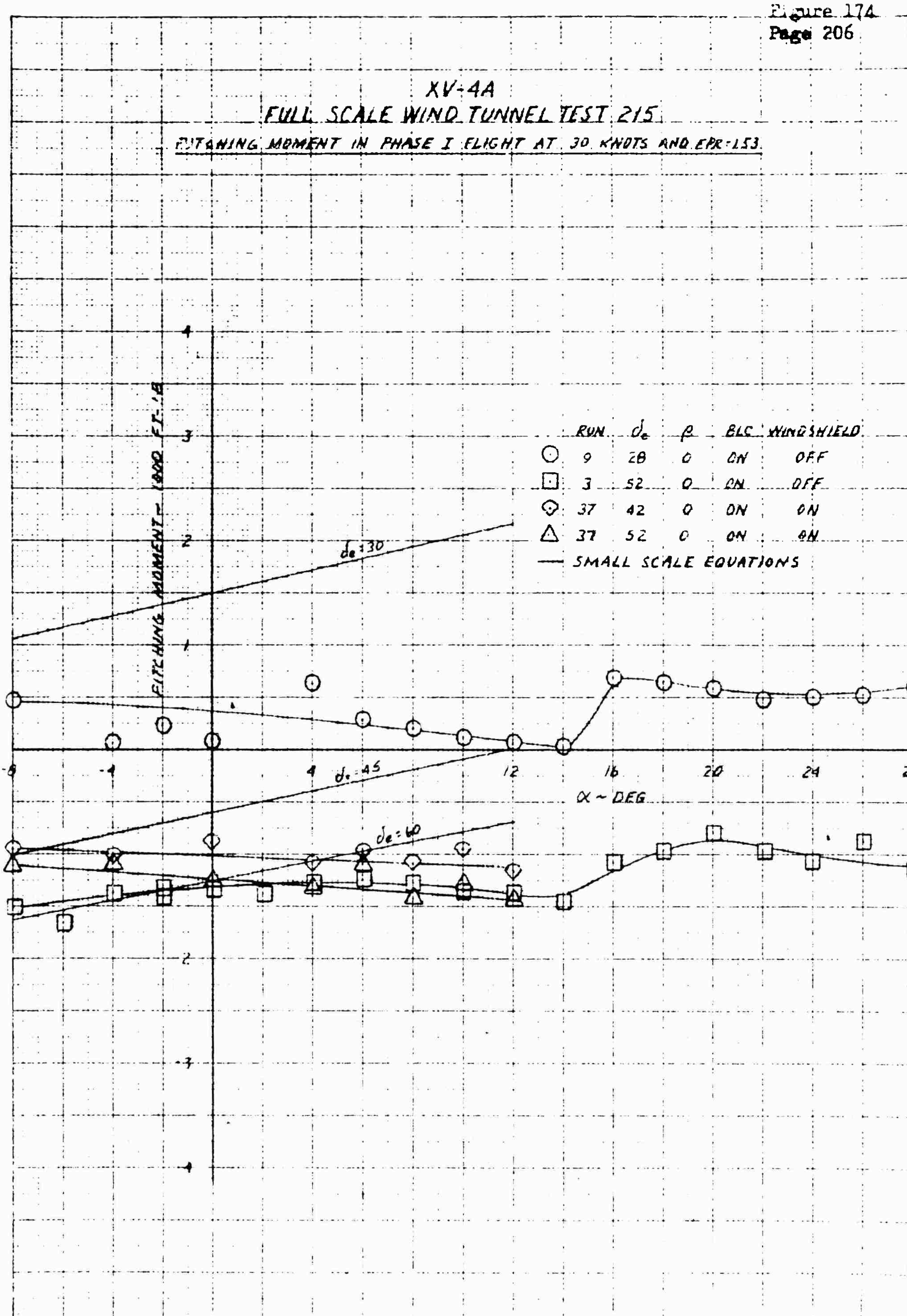
XV-4A
FULL SCALE WIND TUNNEL TEST 215
PITCHING MOMENT IN PHASE I FLIGHT AT 30 KNOTS AND EPR-1.53
PITCHING MOMENT - 1000 FT-LB
α ~ DEG
RUN δe β BLC WINDSHIELD
9 28 0 ON OFF
3 52 0 ON OFF
37 42 0 ON ON
37 52 0 ON ON
— SMALL SCALE EQUATIONS
δe = 30
δe = 45
δe = 60

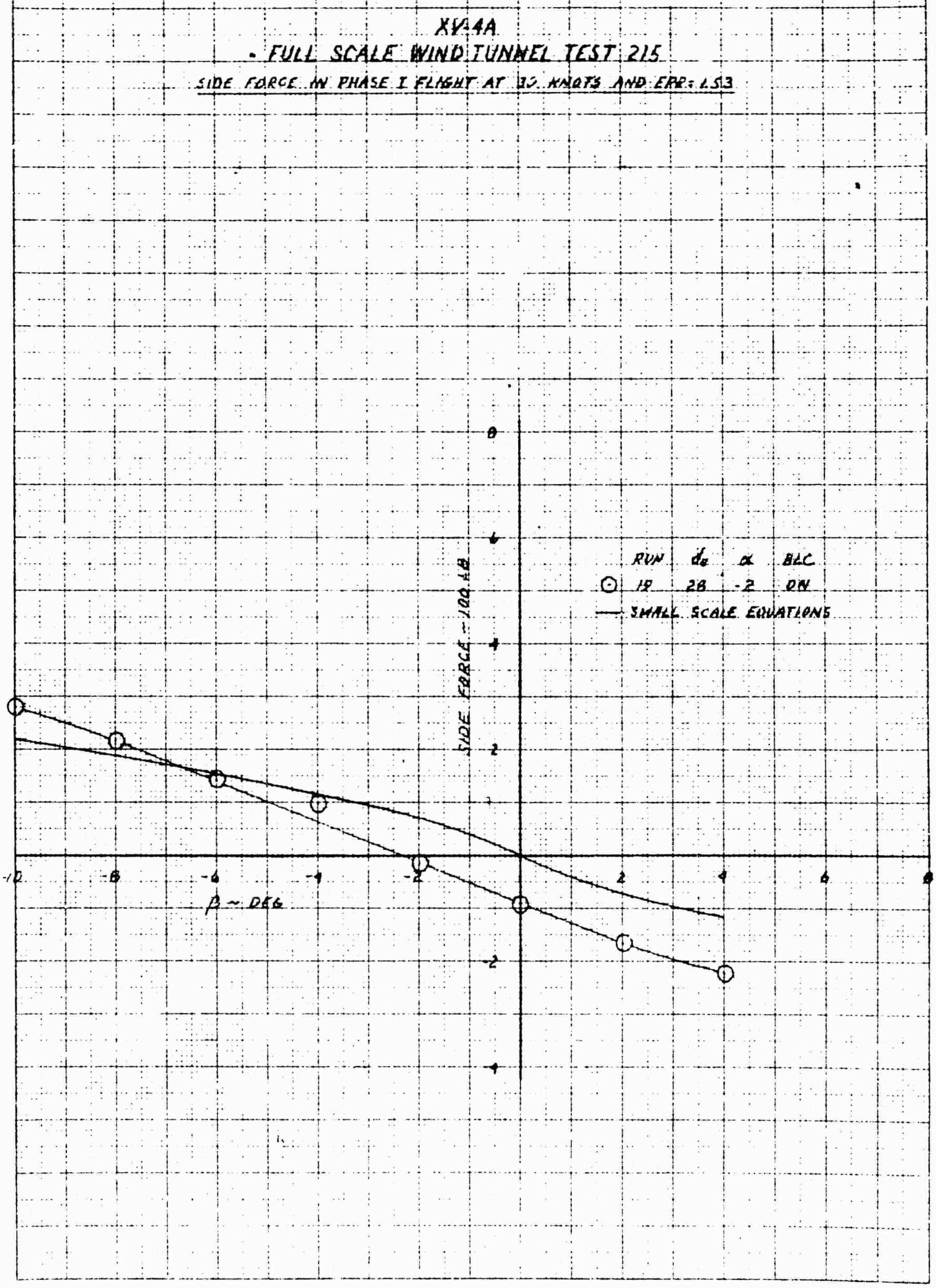
XV-4A
FULL SCALE WIND TUNNEL TEST 215
SIDE FORCE IN PHASE I FLIGHT AT 30 KNOTS AND EPR = 1.53
SIDE FORCE ~ 100 LB
β ~ DEG
RUN
BLC
19
28
-2
ON
SMALL SCALE EQUATIONS

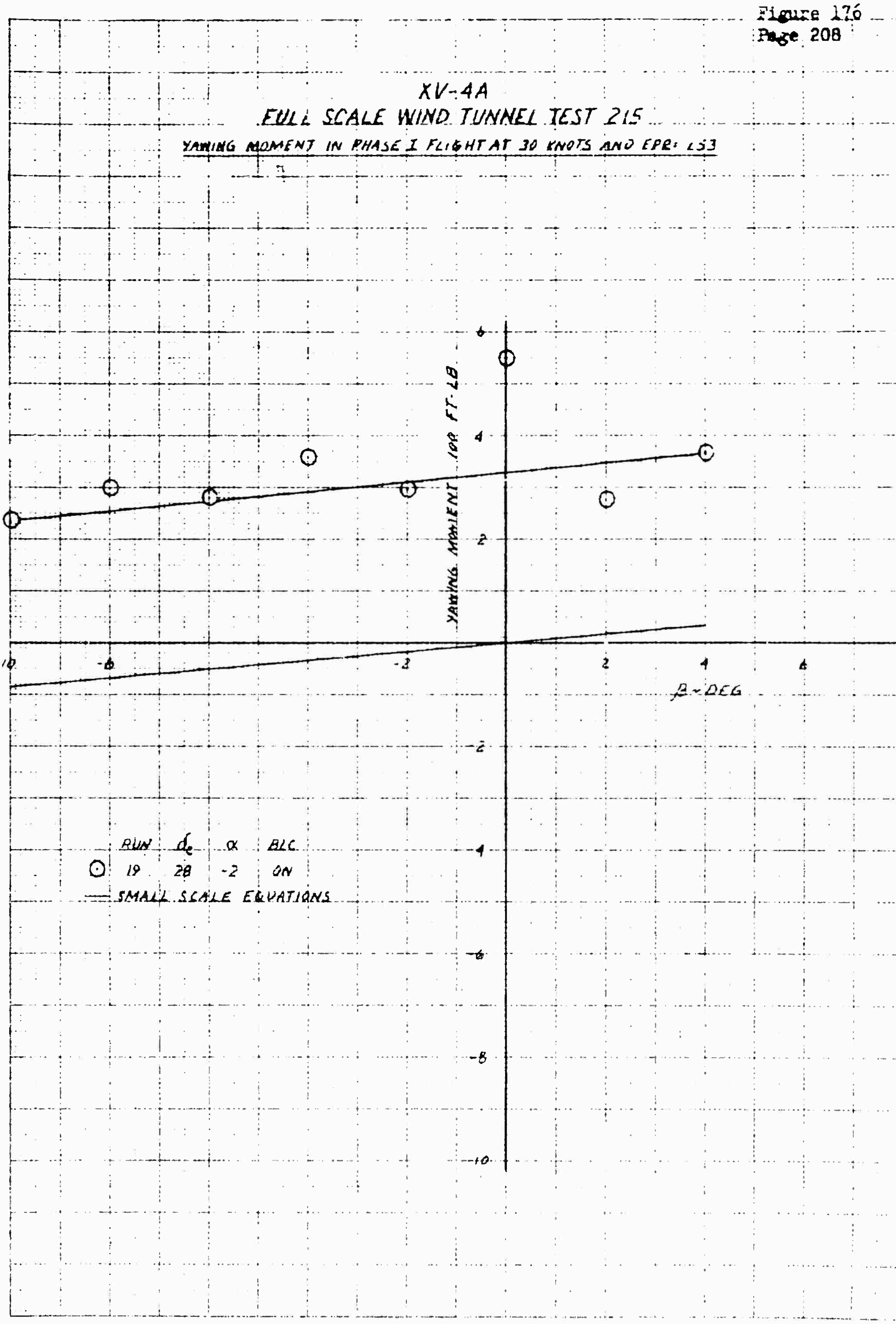
XV-4A
FULL SCALE WIND TUNNEL TEST 215
YAWING MOMENT IN PHASE I FLIGHT AT 30 KNOTS AND EPR: 1.53
YAWING MOMENT 100 FT-LB
β ~ DEG
RUN δe α BLC
19 28 -2 ON
SMALL SCALE EQUATIONS

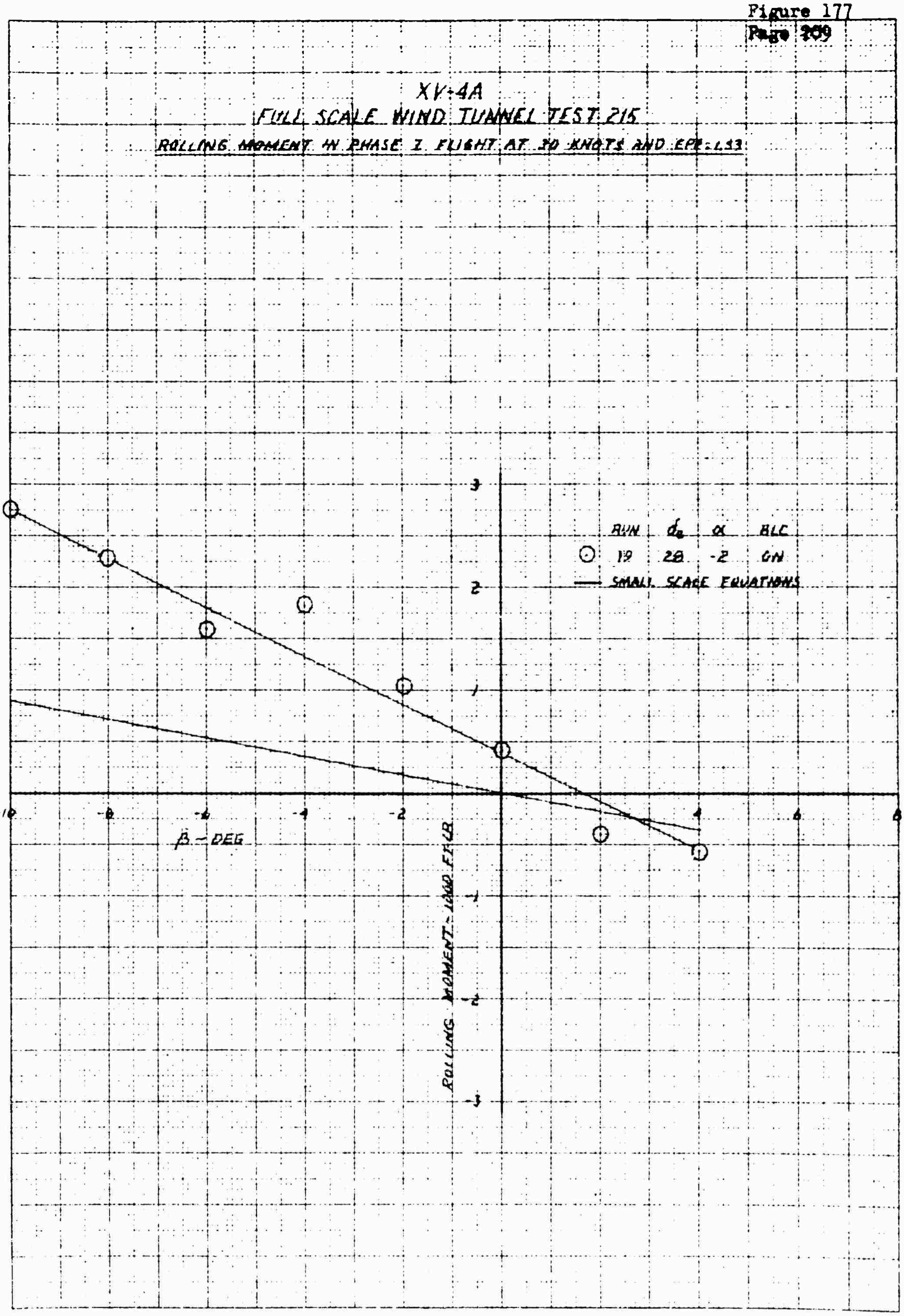
XV-4A
FULL SCALE WIND TUNNEL TEST 215
ROLLING MOMENT IN PHASE I FLIGHT AT 30 KNOTS AND EPR=1.53
RUN δ α BLC
19 28 -2 ON
SMALL SCALE EQUATIONS
β – DEG
ROLLING MOMENT – 1000 FT-LB
-10
-8
-6
-4
-2
4
6
8
3
2
1
-1
-2
-3

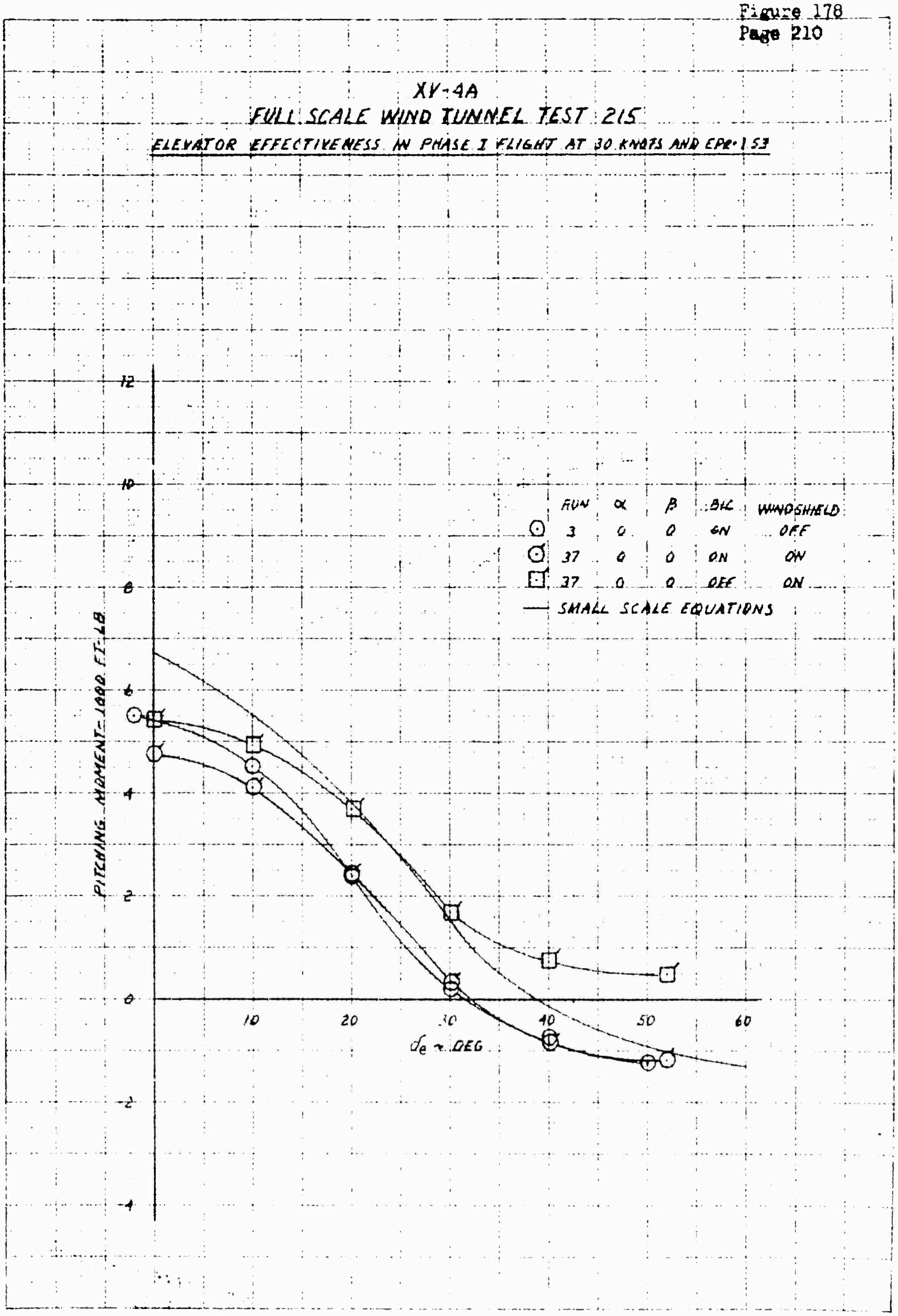
XV-4A
FULL SCALE WIND TUNNEL TEST 215
ELEVATOR EFFECTIVENESS IN PHASE I FLIGHT AT 30 KNOTS AND EPR 1.53
RUN α β BLC WINDSHIELD
3 0 0 ON OFF
37 0 0 ON ON
37 0 0 OFF ON
SMALL SCALE EQUATIONS
PITCHING MOMENT - 1000 FT-LB
δe ~ DEG

XV-4A
FULL SCALE WIND TUNNEL TEST 215
AILERON EFFECT ON SIDE FORCE IN PHASE I FLIGHT AT 30 KNOTS AND EPR = 1.53

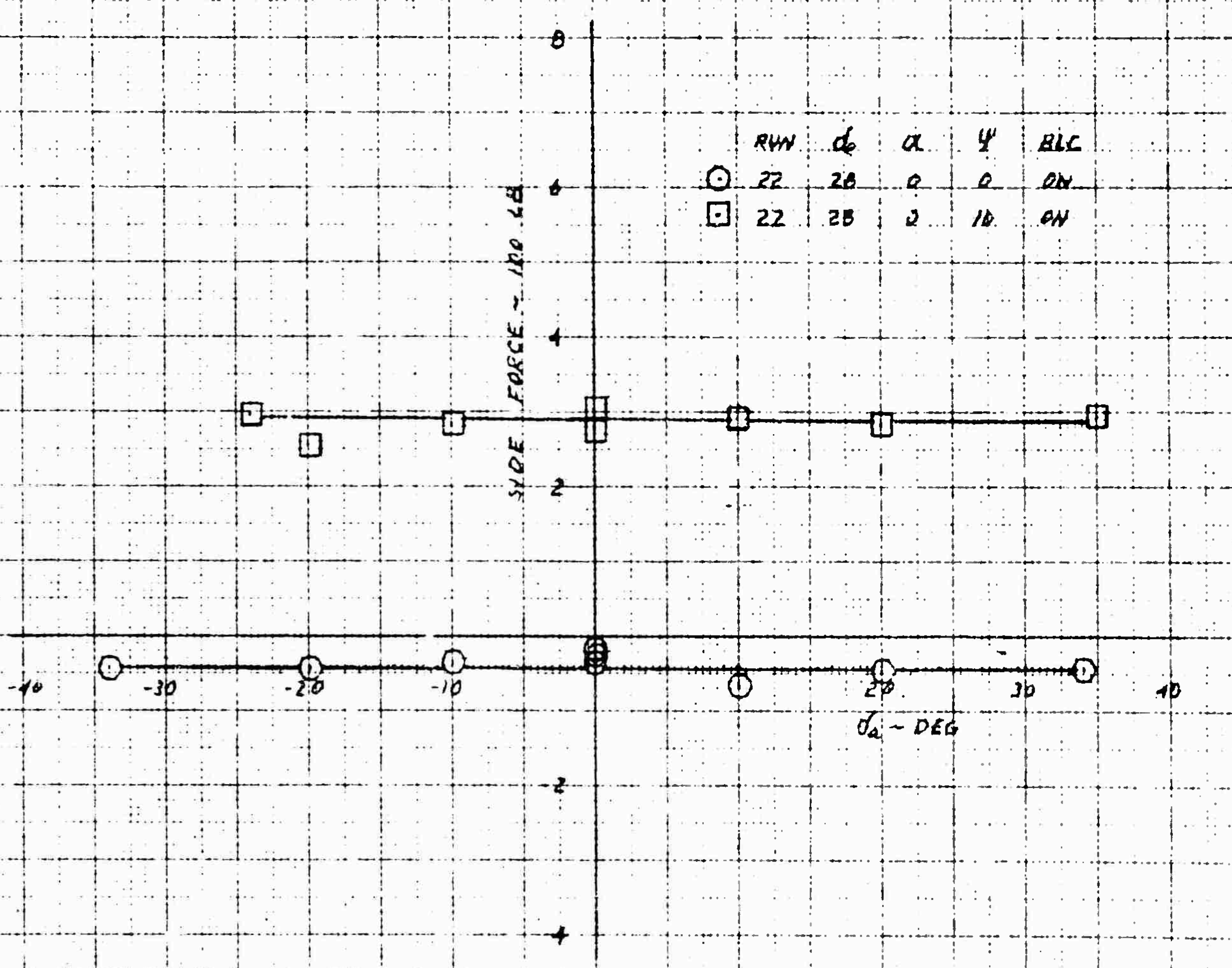

XV-4A
FULL SCALE WIND TUNNEL TEST 215
AILERON EFFECT ON YAW IN PHASE I FLIGHT AT 30 KNOTS AND EPR=1.53

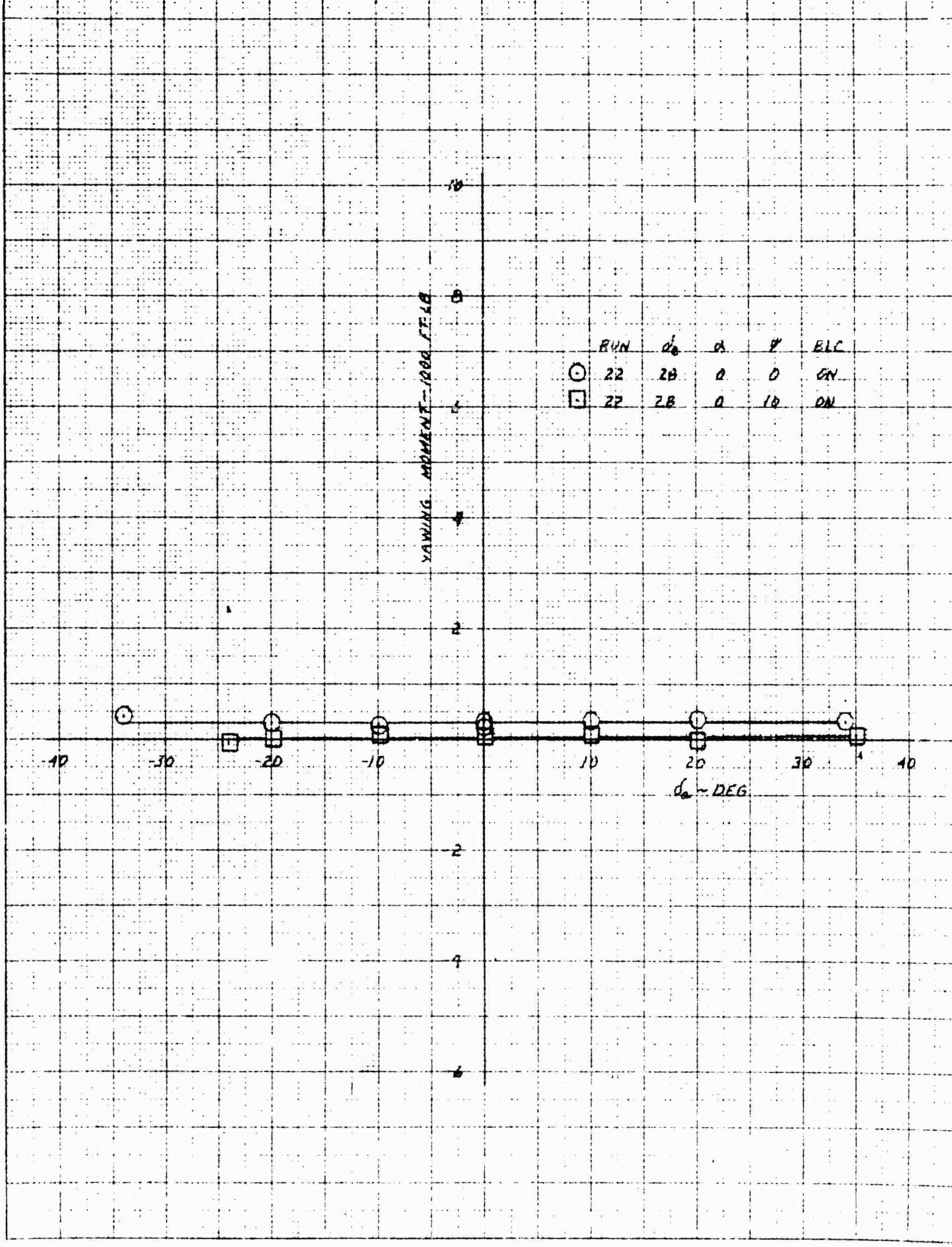

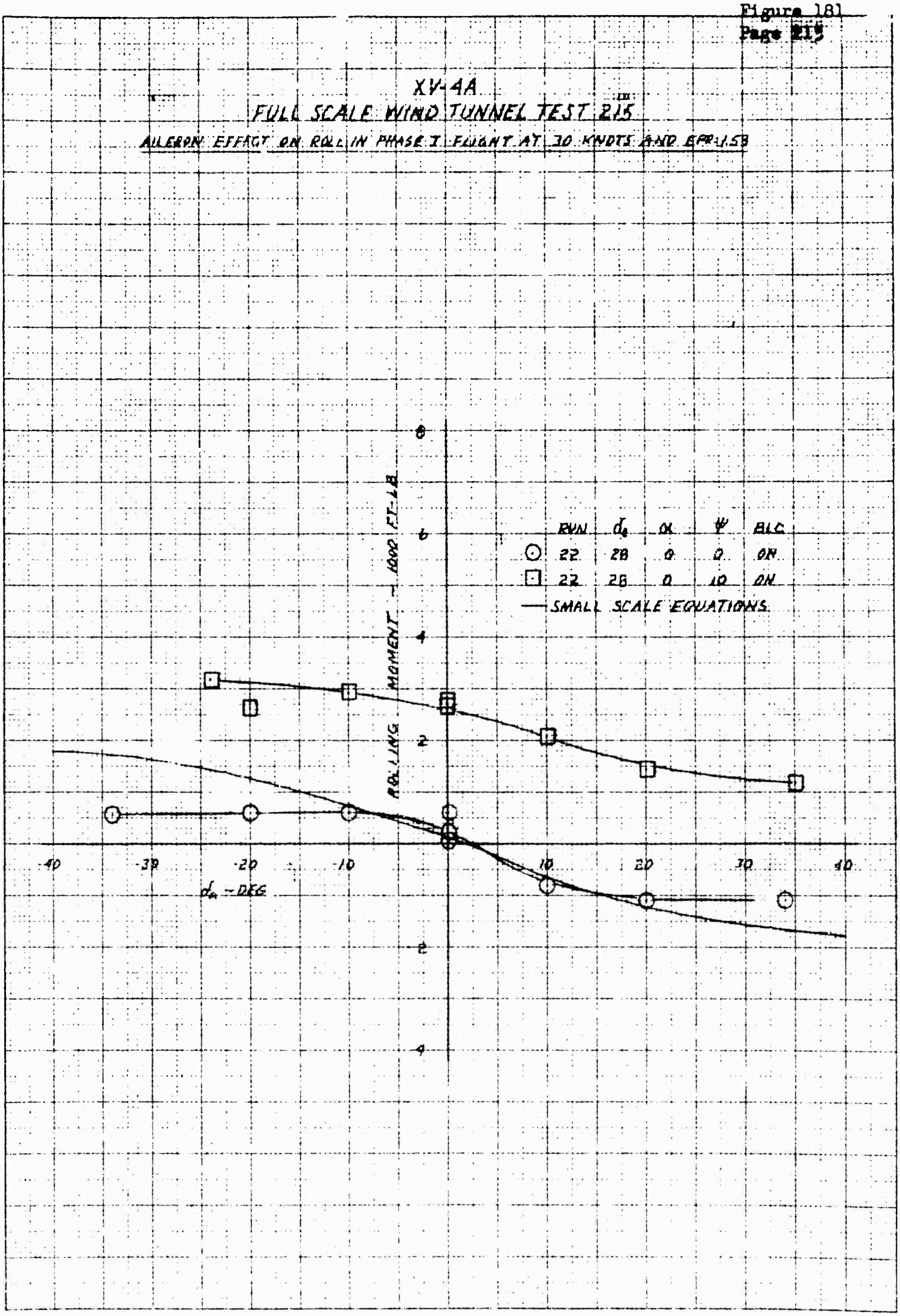
XV-4A
FULL SCALE WIND TUNNEL TEST 215
AILERON EFFECT ON ROLL IN PHASE I FLIGHT AT 30 KNOTS AND EPR=1.58
ROLLING MOMENT ~ 1000 FT-LB
RUN
22
22
ON
ON
SMALL SCALE EQUATIONS
-40
-30
-20
-10
10
20
30
40
8
6
4
2
-2
-4

XV-4A
FULL SCALE WIND TUNNEL TEST 215
RUDDER EFFECT ON SIDE FORCE IN PHASE I FLIGHT AT 30 KNOTS AND EPR=1.53

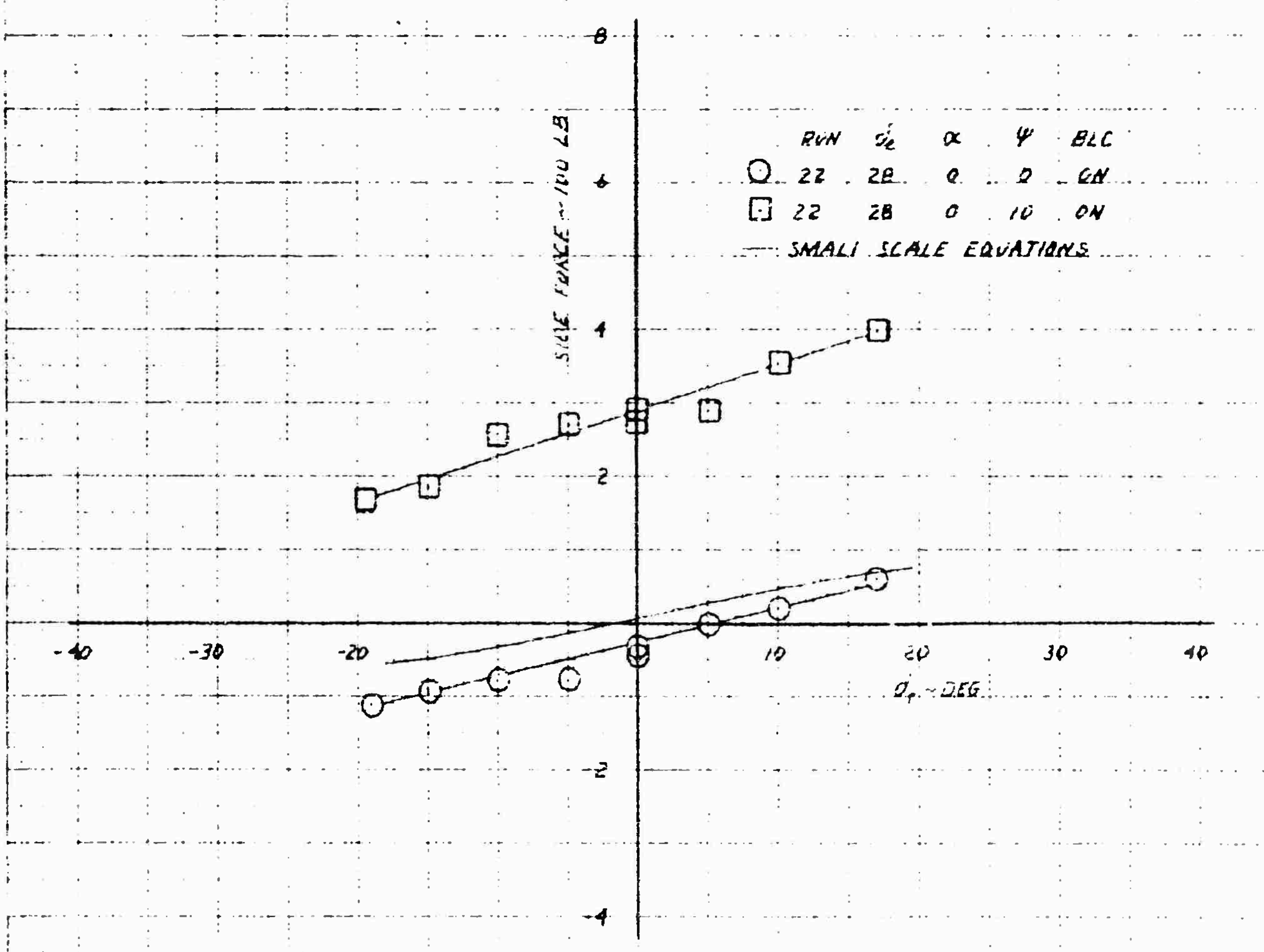

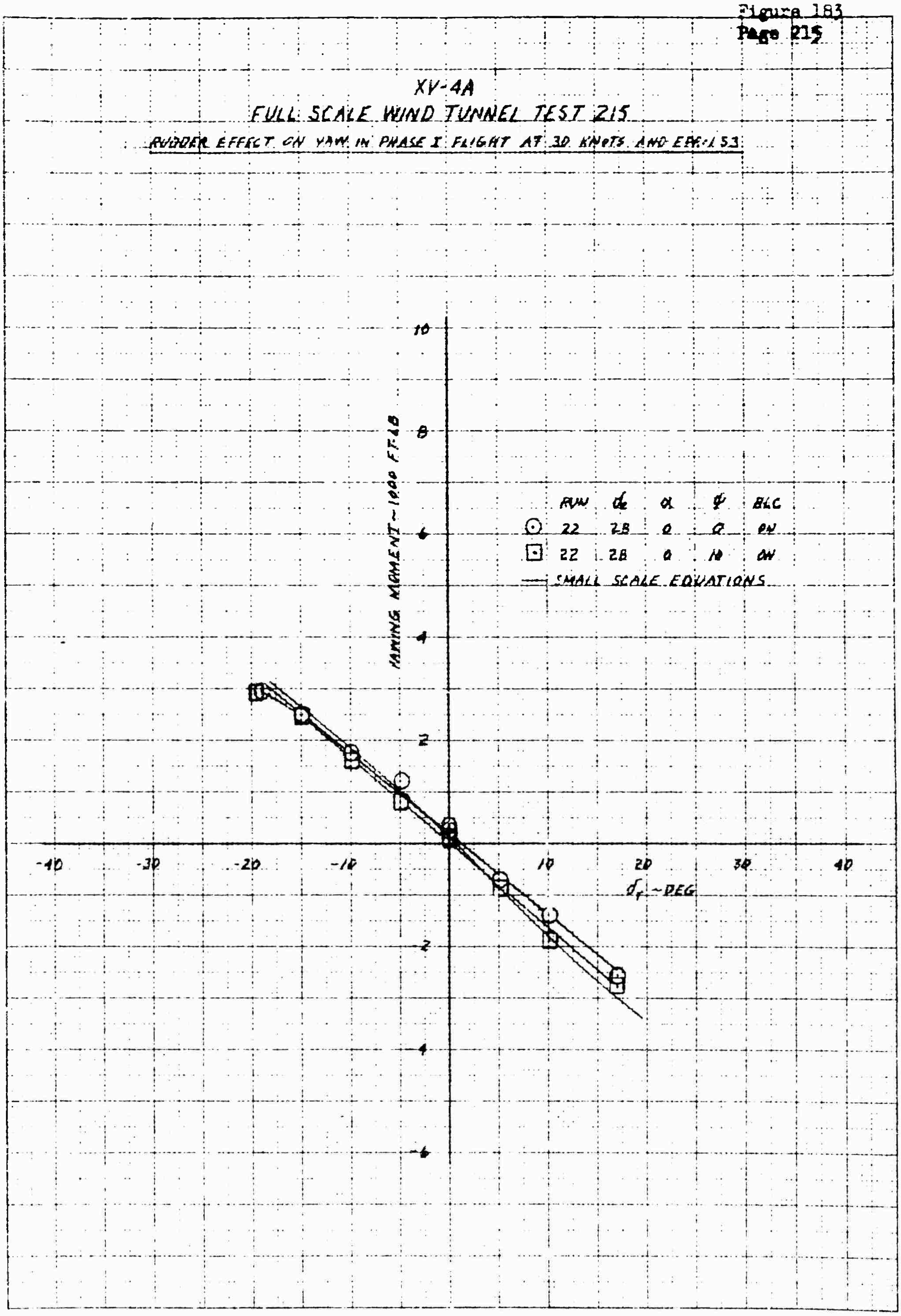
XV-4A
FULL SCALE WIND TUNNEL TEST 215
RUDDER EFFECT ON YAW IN PHASE I FLIGHT AT 30 KNOTS AND EPR=1.53
YAWING MOMENT ~ 1000 FT-LB
10
8
6
4
2
-2
-4
-6
-40
-30
-20
-10
10
20
30
40
δ_r ~ DEG
RUN
22
22
28
28
0
0
0
10
BLC
ON
ON
SMALL SCALE EQUATIONS

XV-4A

FULL SCALE WIND TUNNEL TEST 215

RUDDER EFFECT ON ROLL IN PHASE I FLIGHT AT 30 KNOTS AND EPS LS3

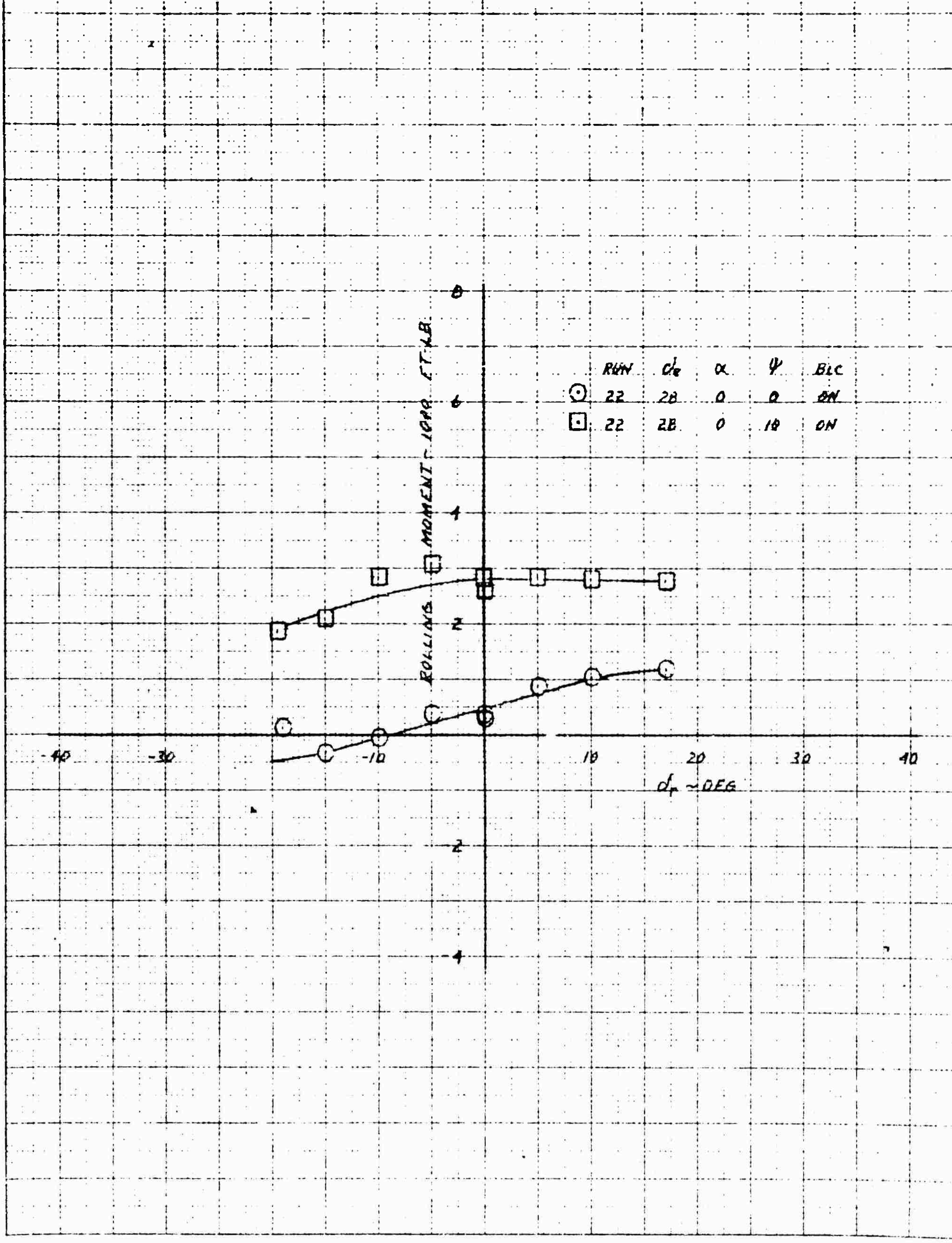

XV-4A
FULL SCALE WIND TUNNEL TEST 215
LIFT IN PHASE I FLIGHT AT 40 KNOTS AND EPR = 1.55

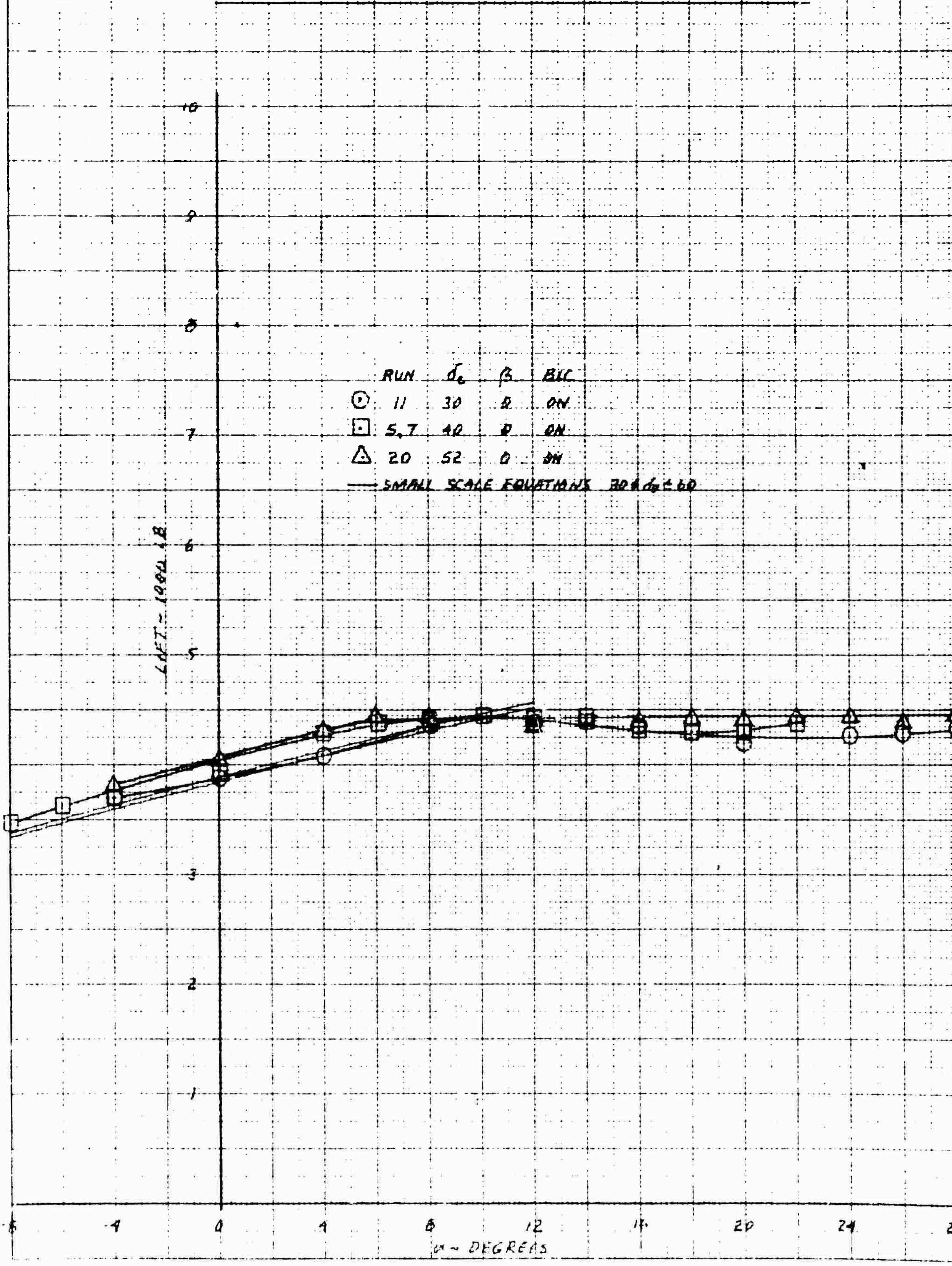

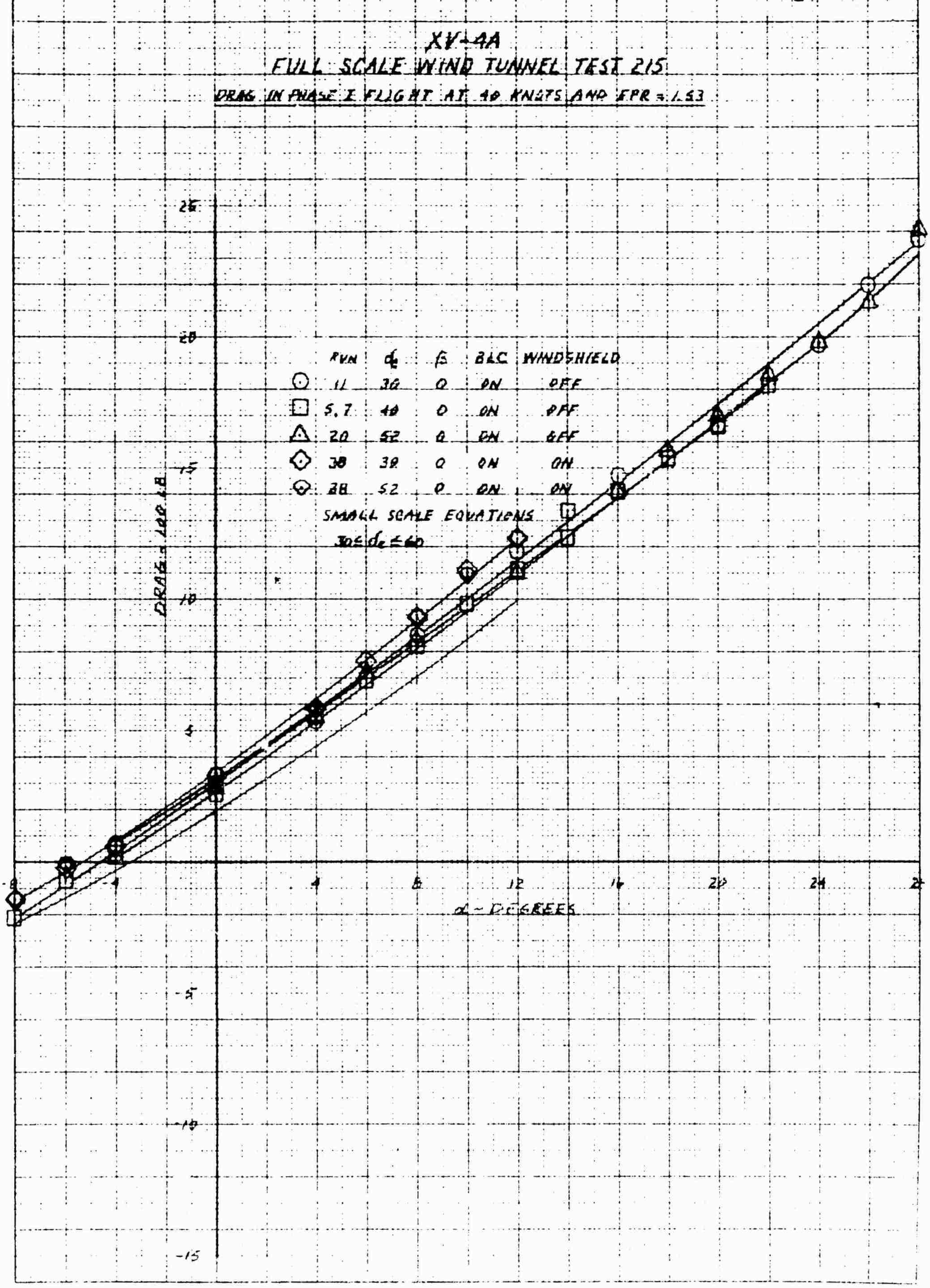
XV-4A
FULL SCALE WIND TUNNEL TEST 215
DRAG IN PHASE I FLIGHT AT 40 KNOTS AND EPR = 1.53
RUN δe β BLC WINDSHIELD
11 30 0 ON OFF
5,7 40 0 ON OFF
20 52 0 ON OFF
38 30 0 ON ON
38 52 0 ON ON
SMALL SCALE EQUATIONS
30≤δe≤60
DRAG ~ 100 LB
α ~ DEGREES

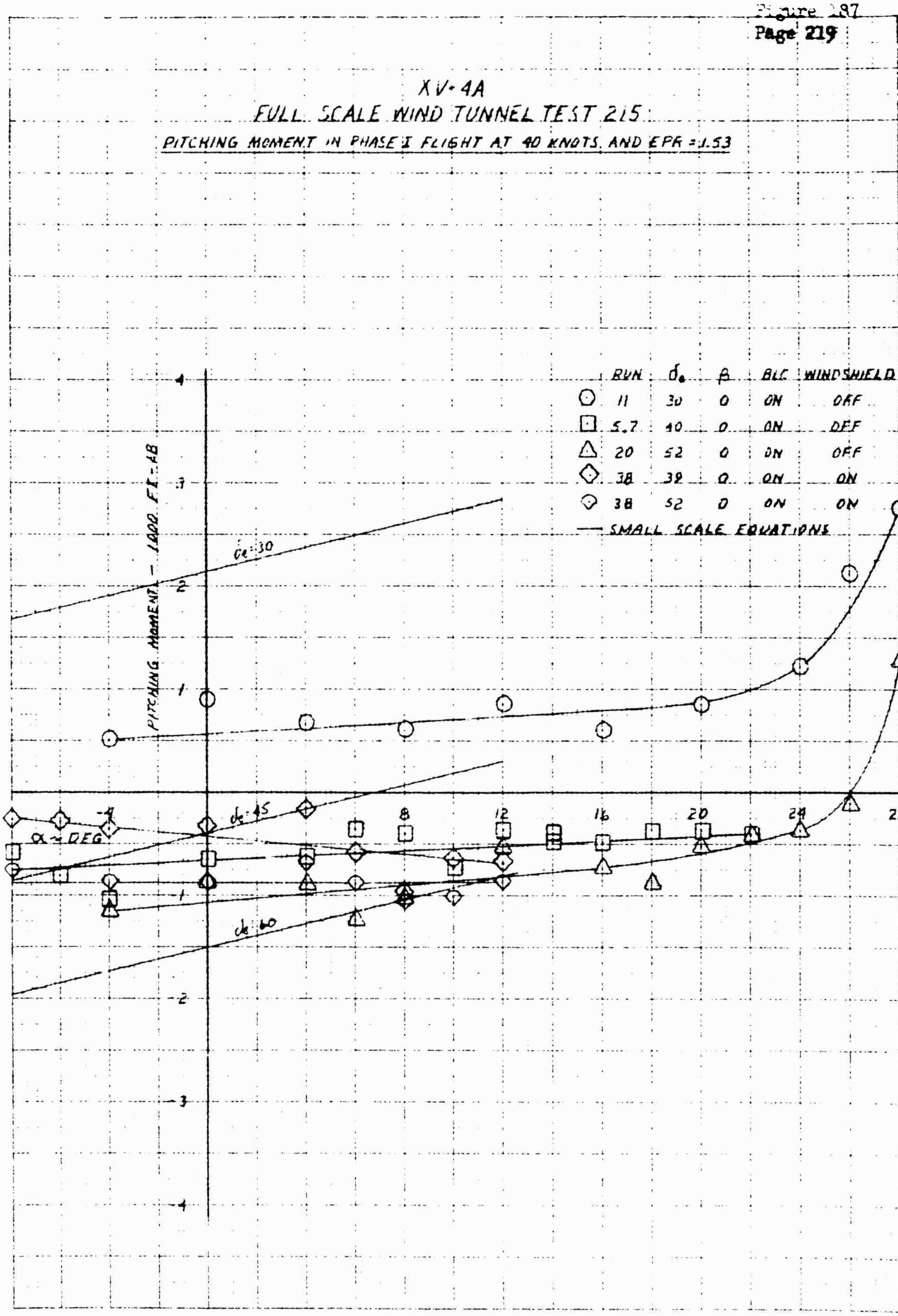
XV-4A
FULL SCALE WIND TUNNEL TEST 215
PITCHING MOMENT IN PHASE I FLIGHT AT 40 KNOTS AND EPR = 1.53
RUN δe β BLC WINDSHIELD
11 30 0 ON OFF
5,7 40 0 ON OFF
20 52 0 ON OFF
38 39 0 ON ON
38 52 0 ON ON
SMALL SCALE EQUATIONS
PITCHING MOMENT - 1000 FT-LB
α ~ DEG
δe=30
δe=45
δe=60

XV-4A
FULL SCALE WIND TUNNEL TEST 215
SIDE FORCE IN PHASE I FLIGHT AT 40 KNOTS AND EPR = 1.53

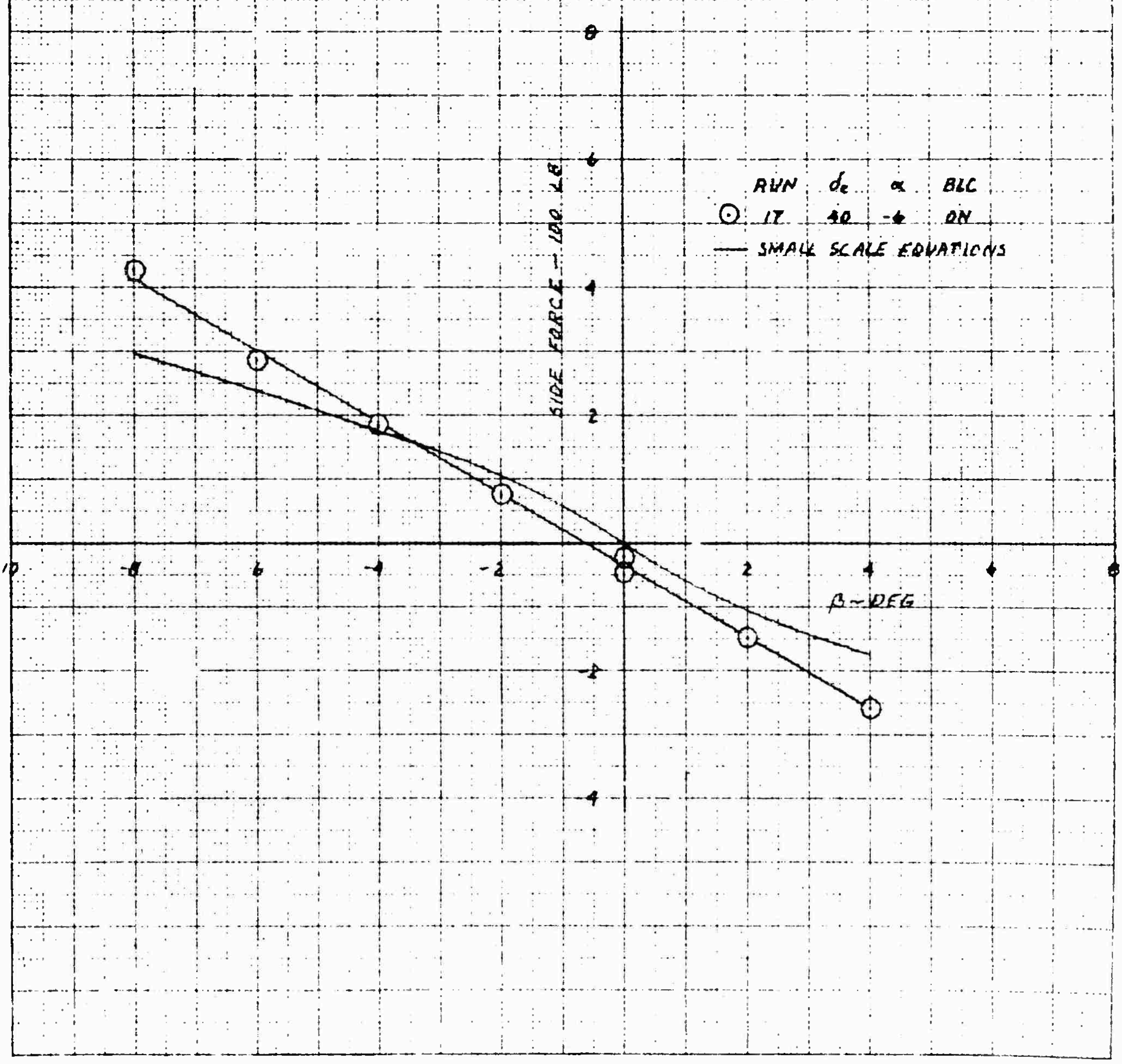

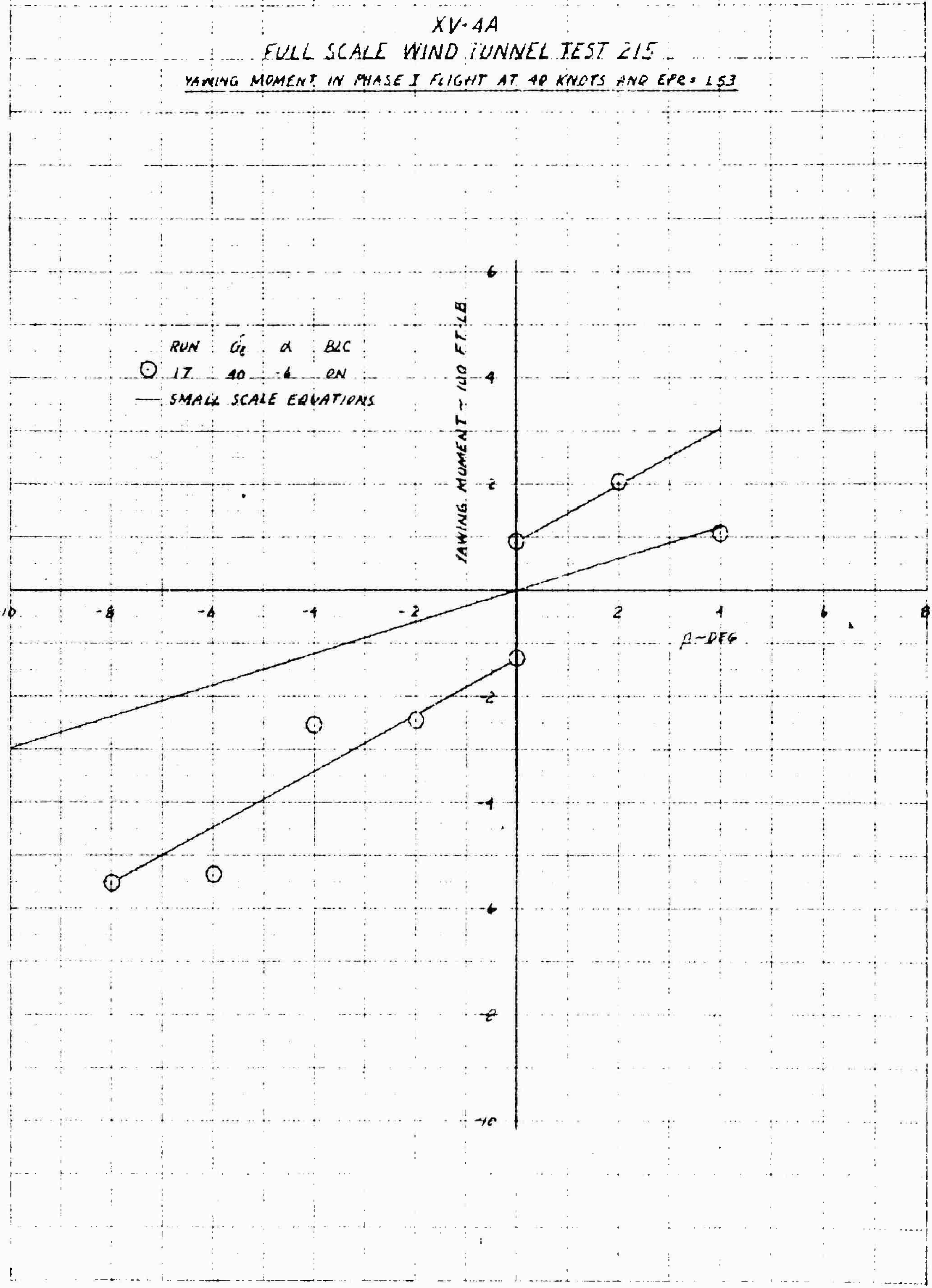
XV-4A
FULL SCALE WIND TUNNEL TEST 215
YAWING MOMENT IN PHASE I FLIGHT AT 40 KNOTS AND EPR = 1.53
RUN
α
BLC
17
40
-6
ON
— SMALL SCALE EQUATIONS
YAWING MOMENT ~ 100 FT-LB
β ~ DEG
6
4
2
-2
-4
-6
-8
-10
-8
-6
-4
-2
2
4
6
8

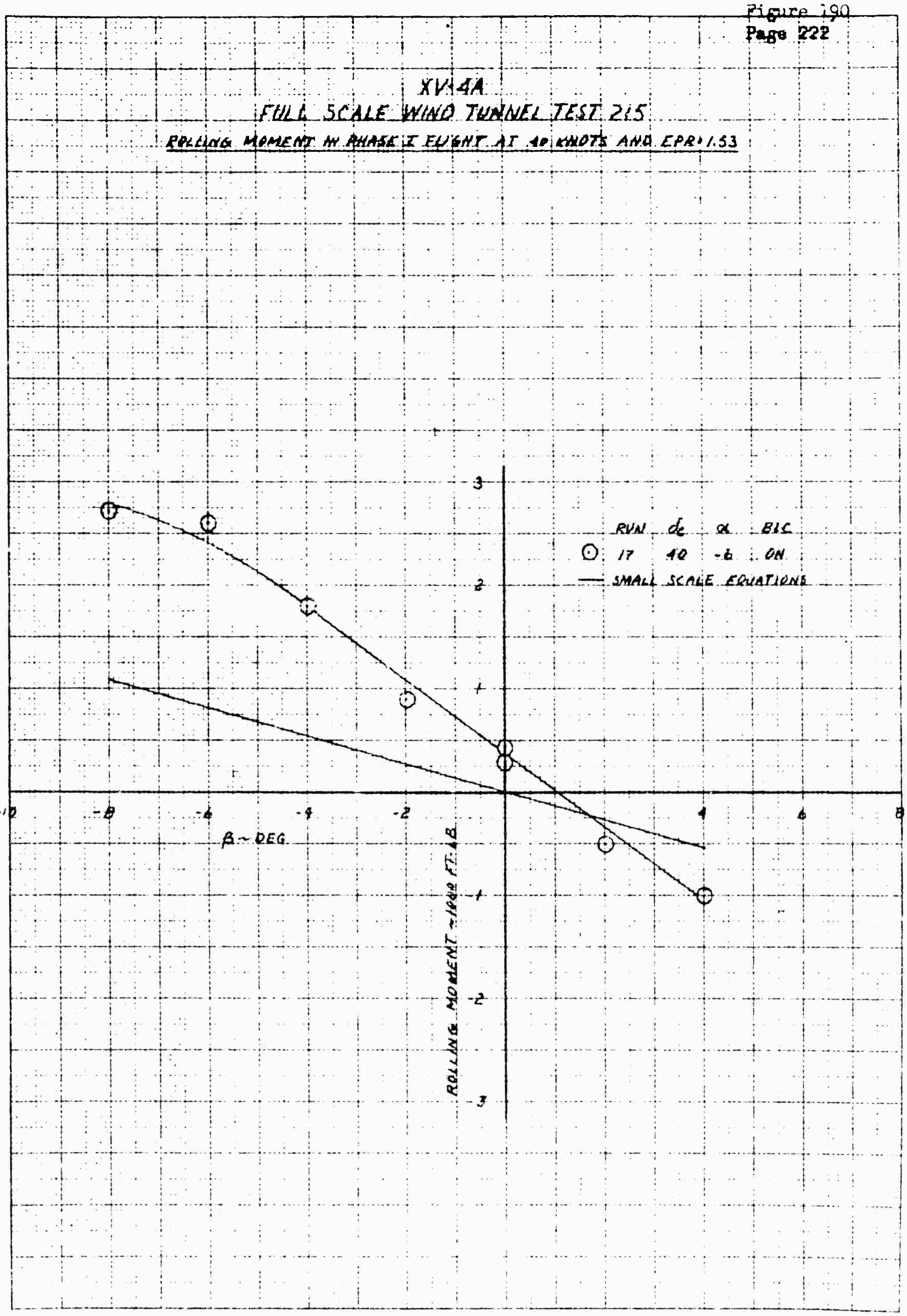
XV-4A
FULL SCALE WIND TUNNEL TEST 215
ROLLING MOMENT IN PHASE I FLIGHT AT 40 KNOTS AND EPR 1.53
RUN
17
40
-6
ON
SMALL SCALE EQUATIONS
β ~ DEG
ROLLING MOMENT ~1000 FT-LB

XV-4A
FULL SCALE WIND TUNNEL TEST 215
ELEVATOR EFFECTIVENESS IN PHASE I FLIGHT AT 40 KNOTS AND EPR=1.53

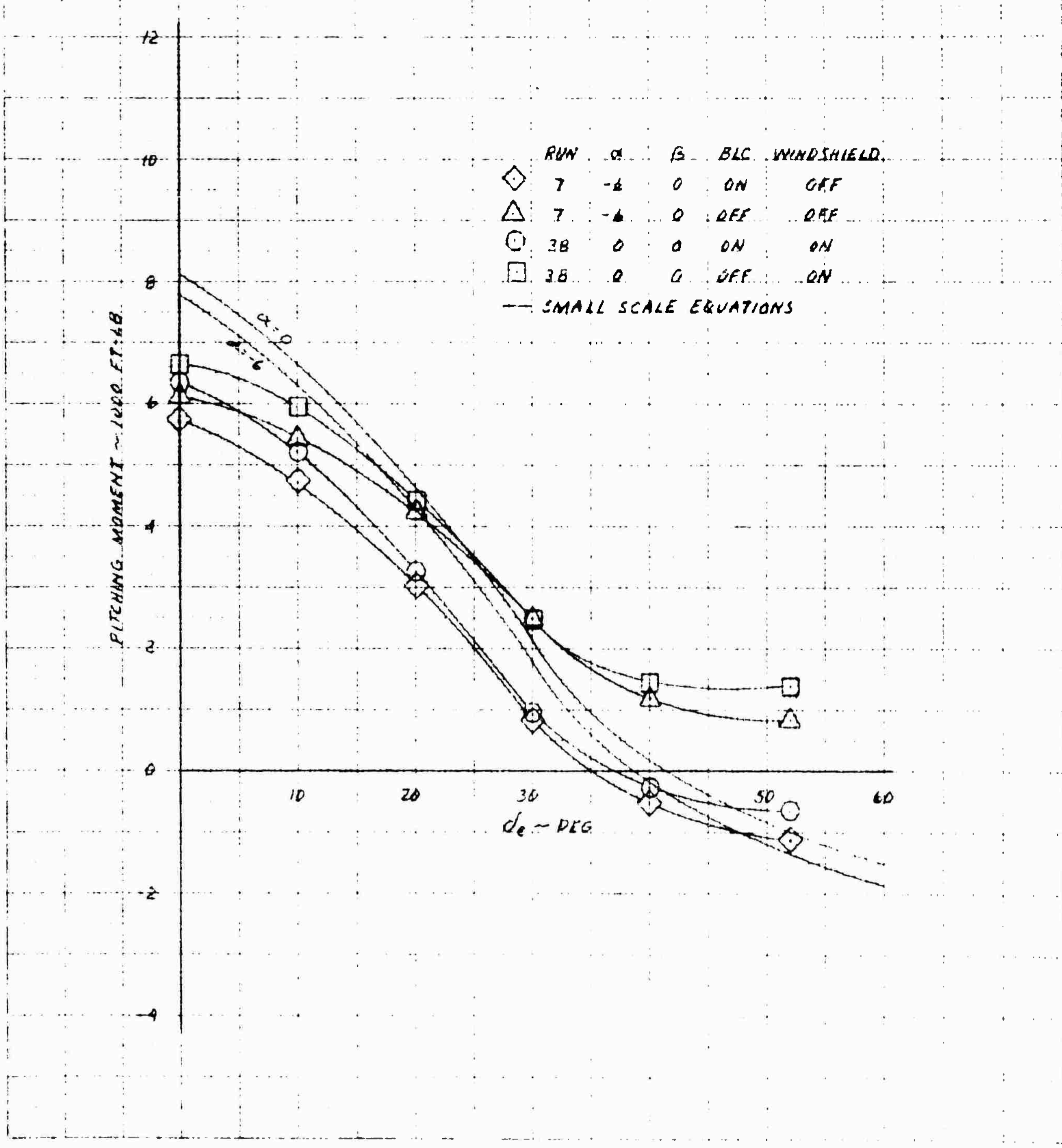

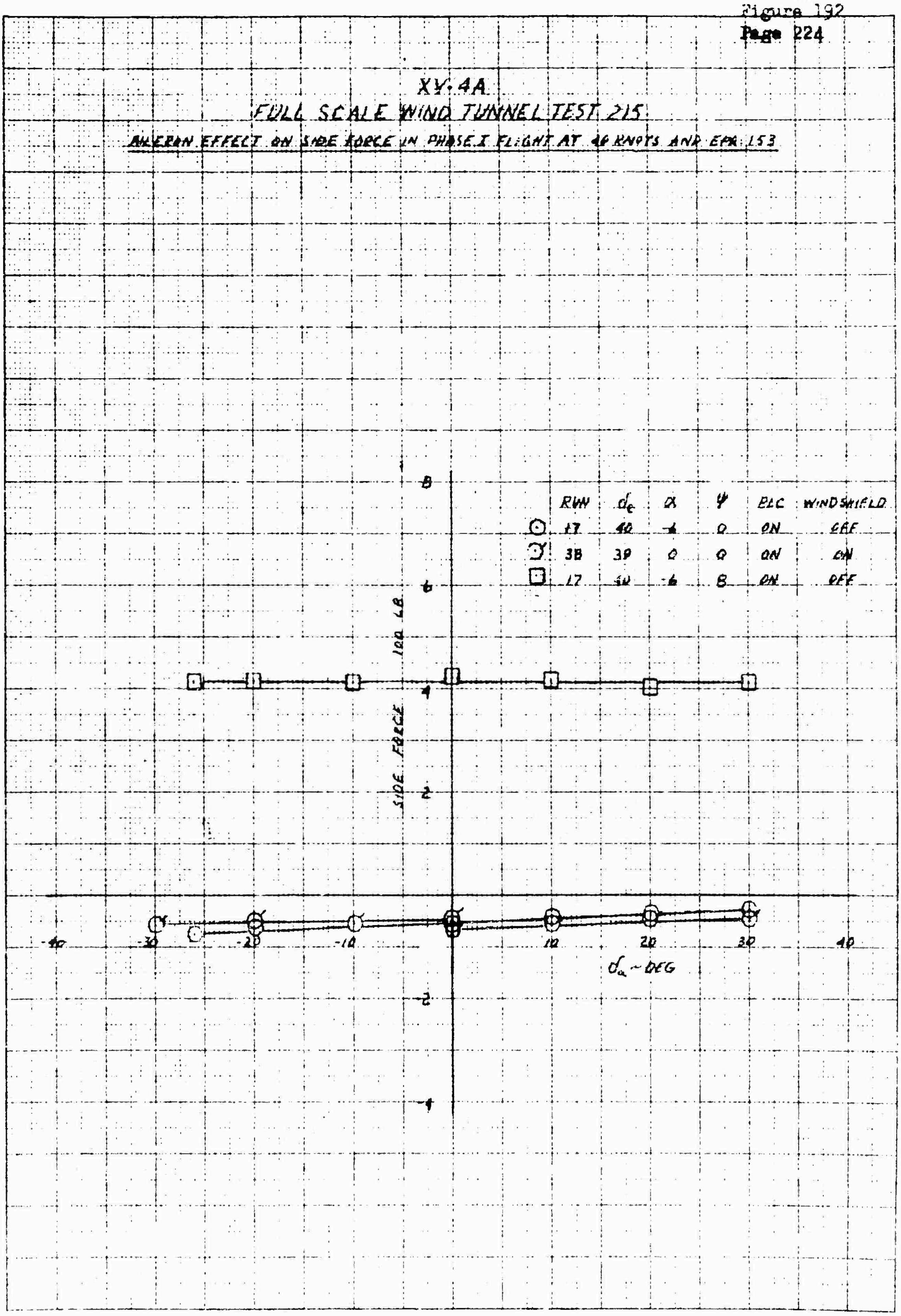
XV-4A
FULL SCALE WIND TUNNEL TEST 215
AILERON EFFECT ON SIDE FORCE IN PHASE I FLIGHT AT 40 KNOTS AND EPR 1.53
RUN
δ_e
α
ψ
ELC
WINDSHIELD
17
40
-6
0
ON
OFF
38
39
0
0
ON
ON
17
40
-6
8
ON
OFF
SIDE FORCE 100 LB
8
6
4
2
-2
-4
-40
-30
-20
-10
10
20
30
40
δ_a ~ DEG

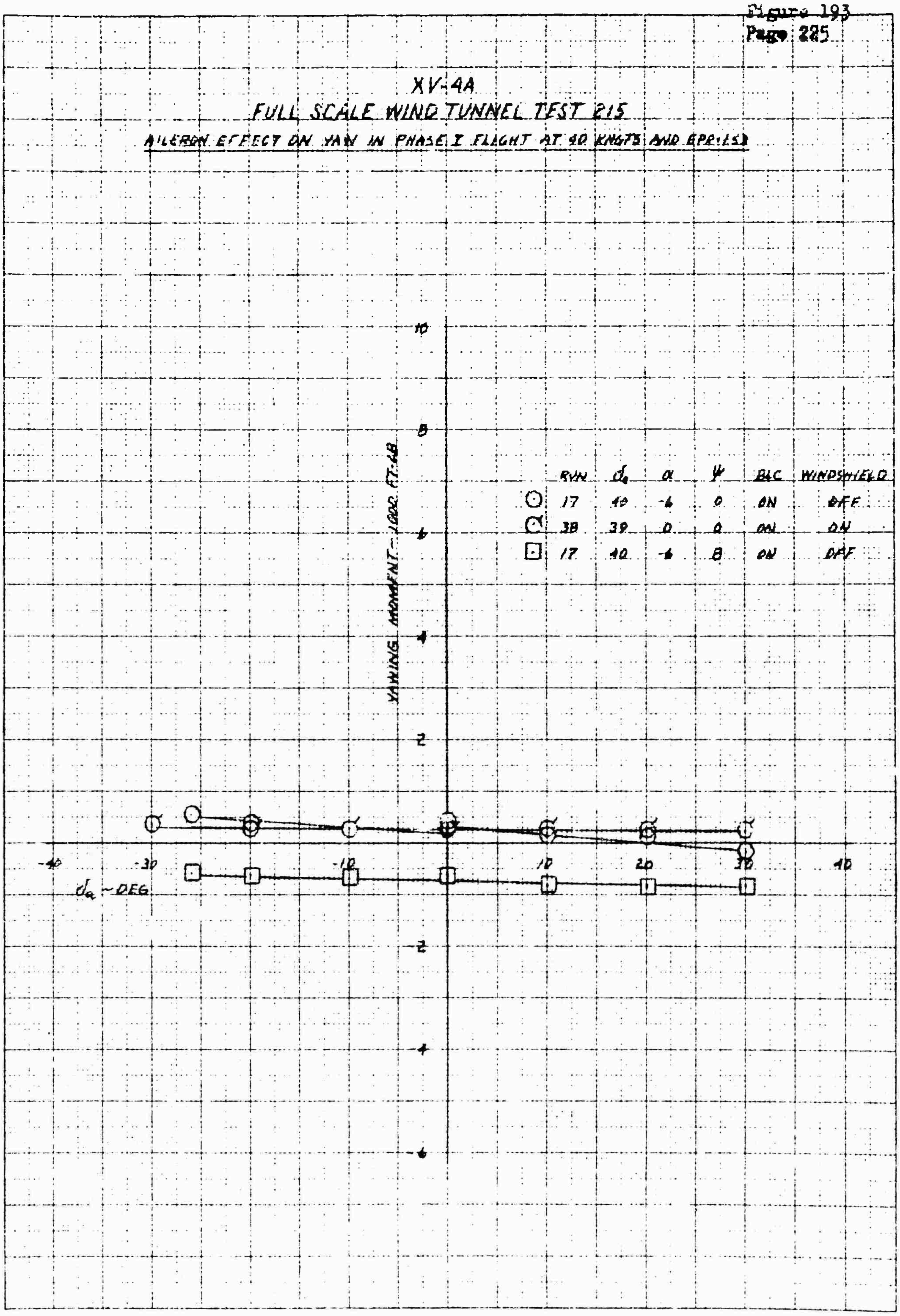
XV-4A
FULL SCALE WIND TUNNEL TEST 215
AILERON EFFECT ON YAW IN PHASE I FLIGHT AT 40 KNOTS AND EPR(ES)
YAWING MOMENT ~ 1000 FT-LB
10
8
6
4
2
-2
-4
-6
-40
-30
-10
10
20
30
40
δ_a ~ DEG
RUN δ_e α ψ BLC WINDSHIELD
17 40 -6 0 ON OFF
38 39 0 0 ON ON
17 40 -6 8 ON OFF

XV-4A
FULL SCALE WIND TUNNEL TEST 215
AILERON EFFECT ON ROLL IN PHASE I FLIGHT AT 40 KNOTS AND EFR 153

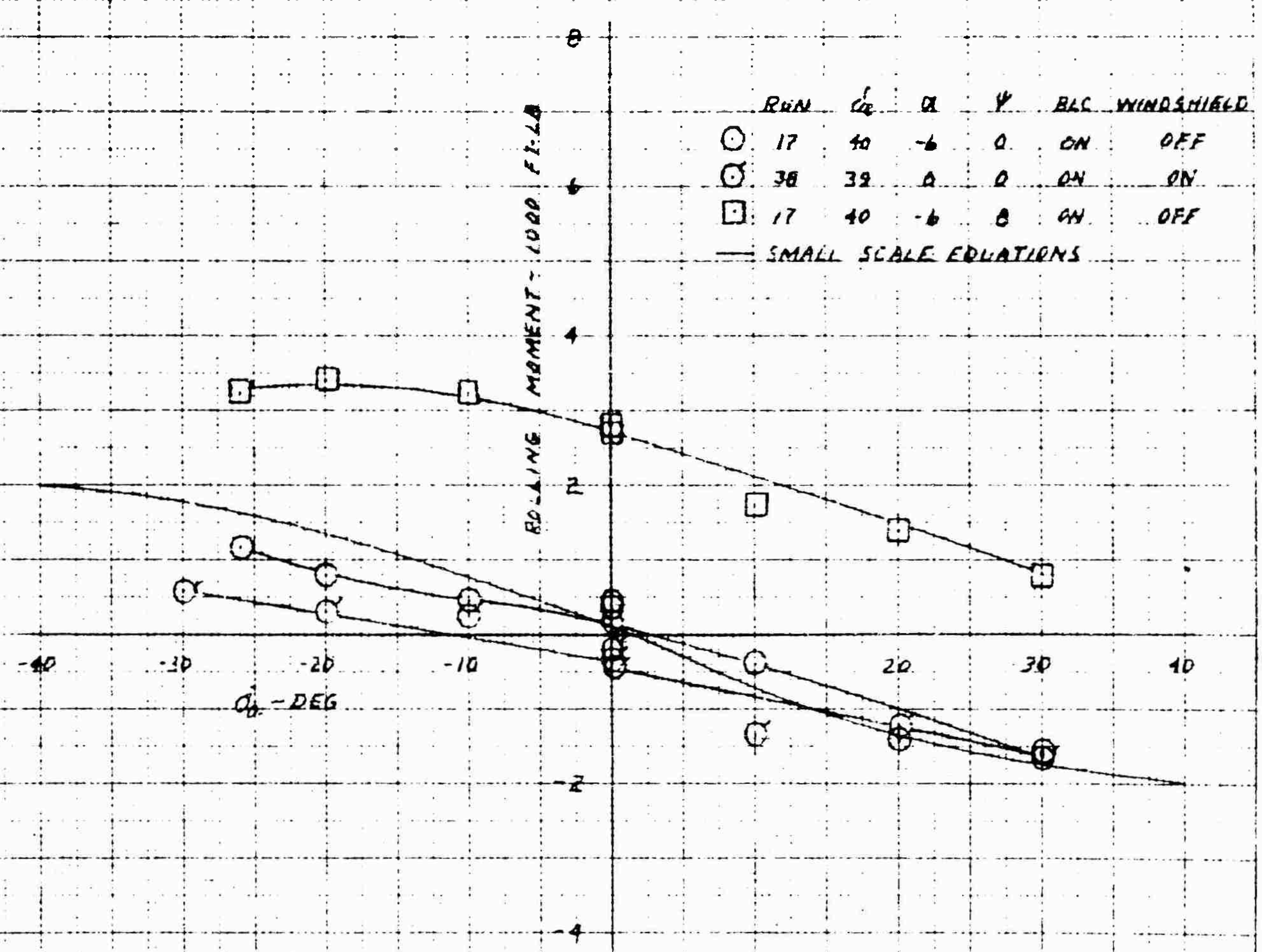

XV-4A

FULL SCALE WIND TUNNEL TEST 215

RUDDER EFFECT ON SIDE FORCE IN PHASE I FLIGHT AT 40 KNOTS AND EPR 1.53

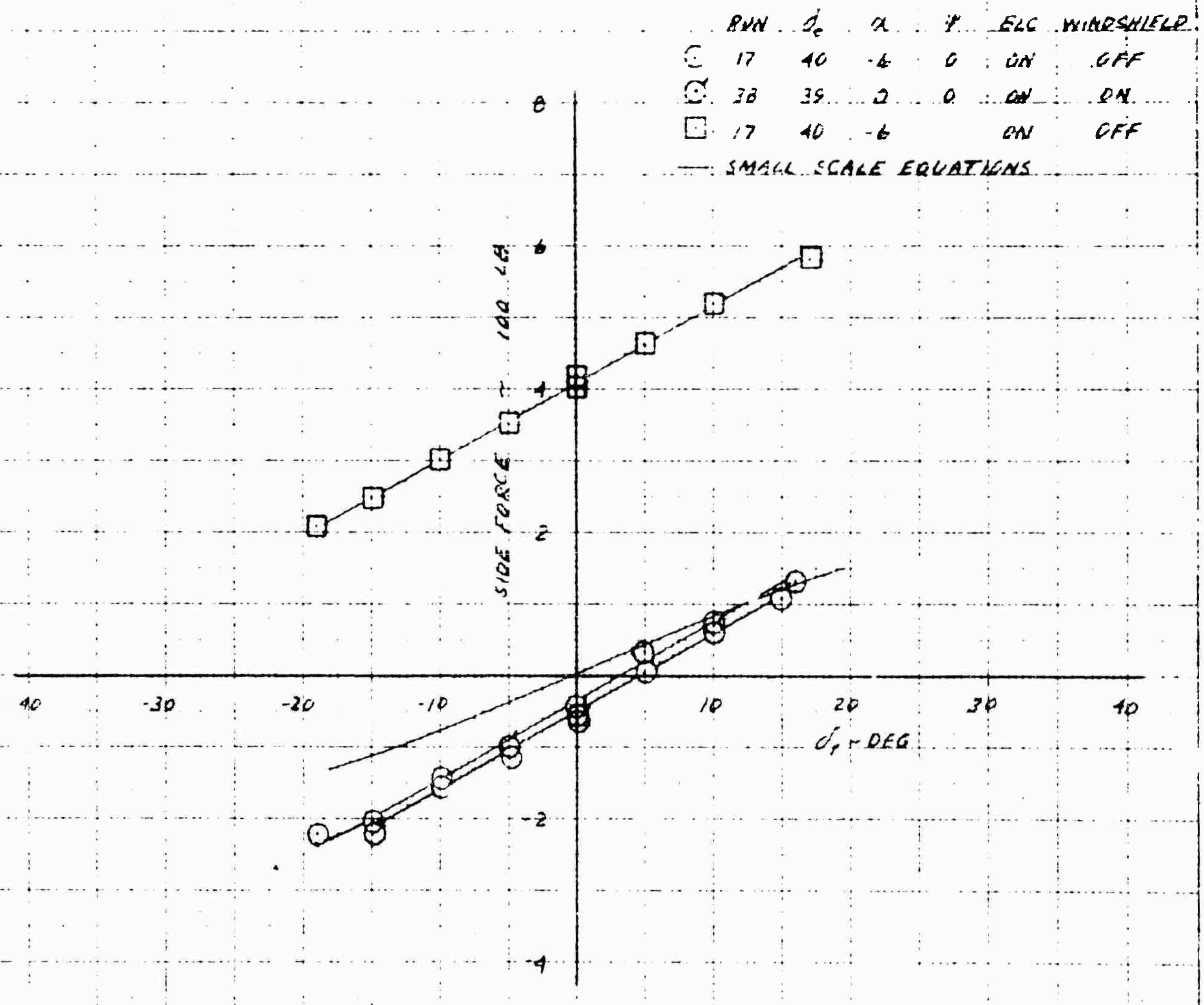

XV-4A

FULL SCALE WIND TUNNEL TEST 215

RUDDER EFFECT ON YAW IN PHASE I FLIGHT AT 40 KNOTS AND EPR = 1.53

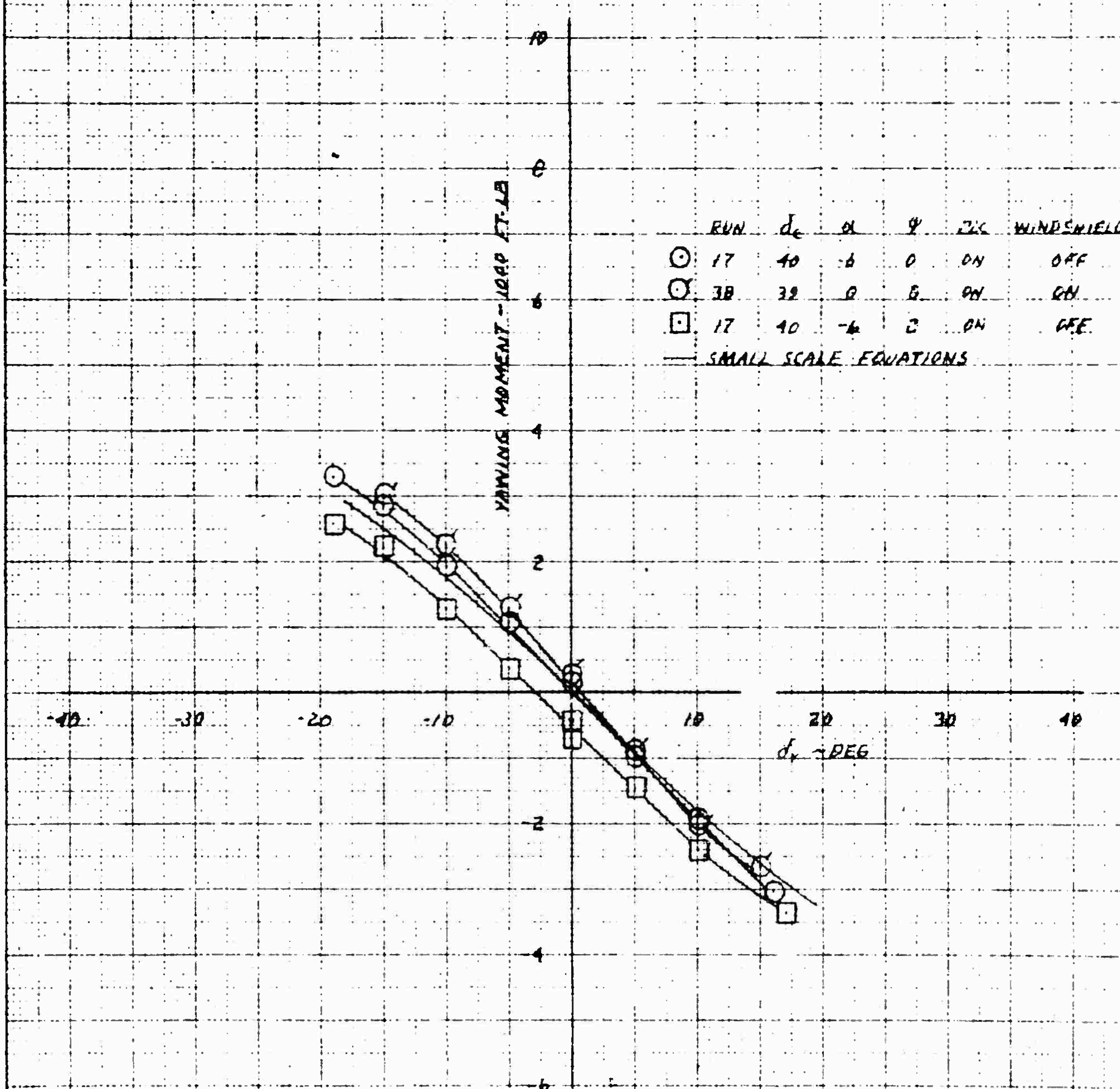

XV-4A
FULL SCALE WIND TUNNEL TEST 215
RUDDER EFFECT ON ROLL IN PHASE I FLIGHT AT 40 KNOTS AND EPR 1.53

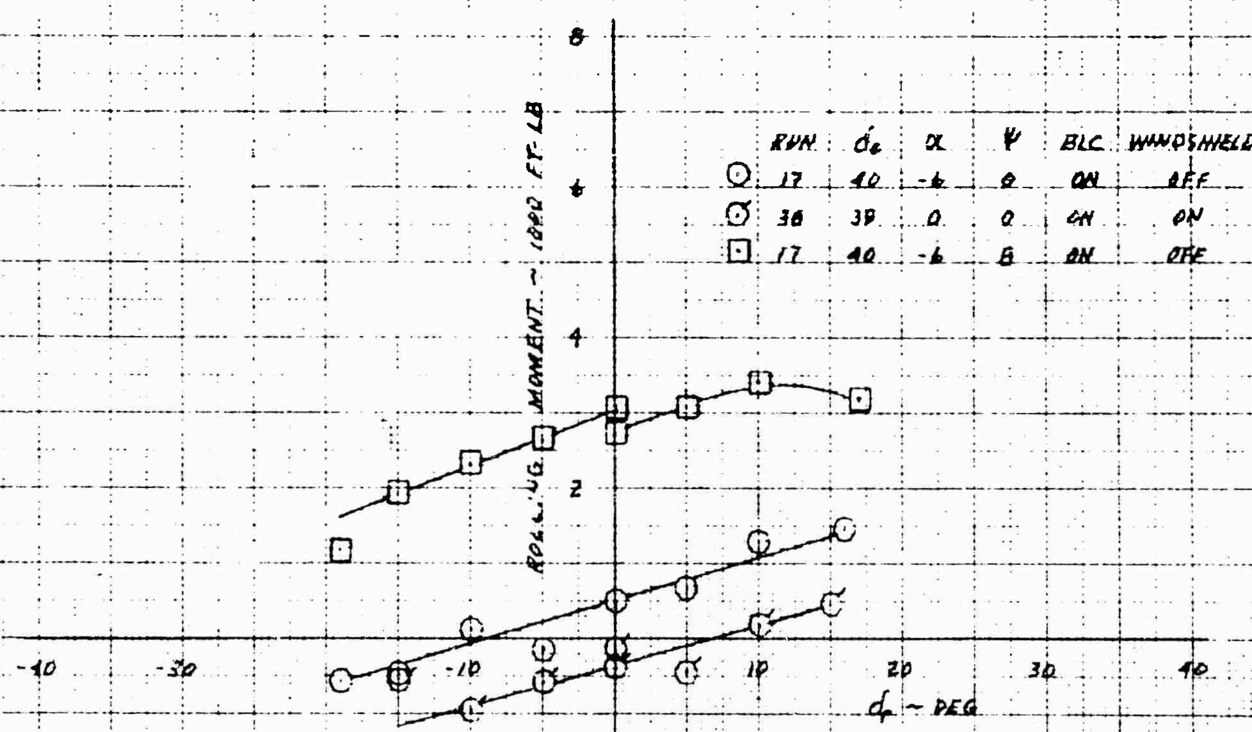

XV-4A

FULL SCALE WIND TUNNEL TEST 215

LIFT IN PHASE I FLIGHT AT 50 KNOTS AND EPR = 1.53

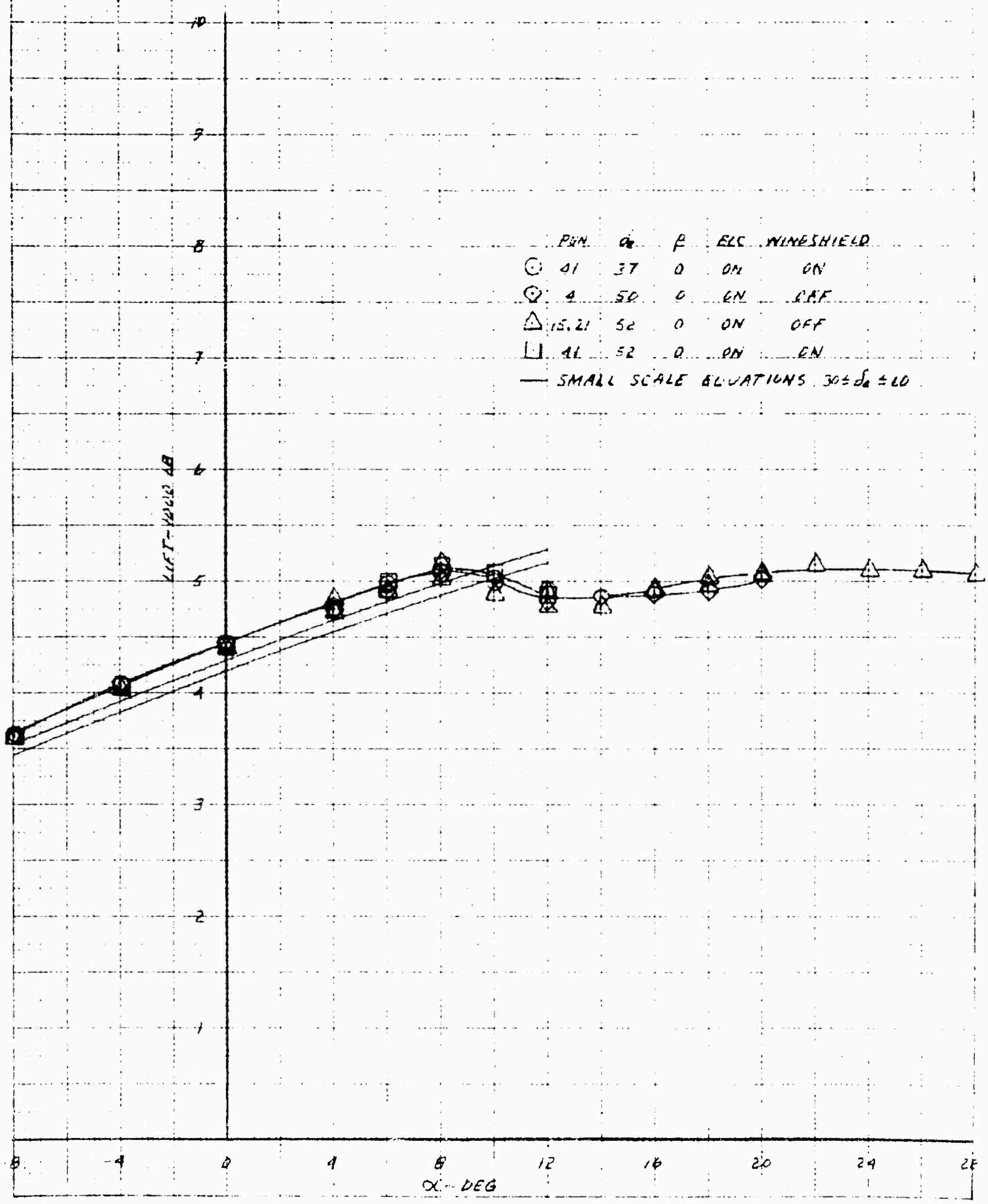

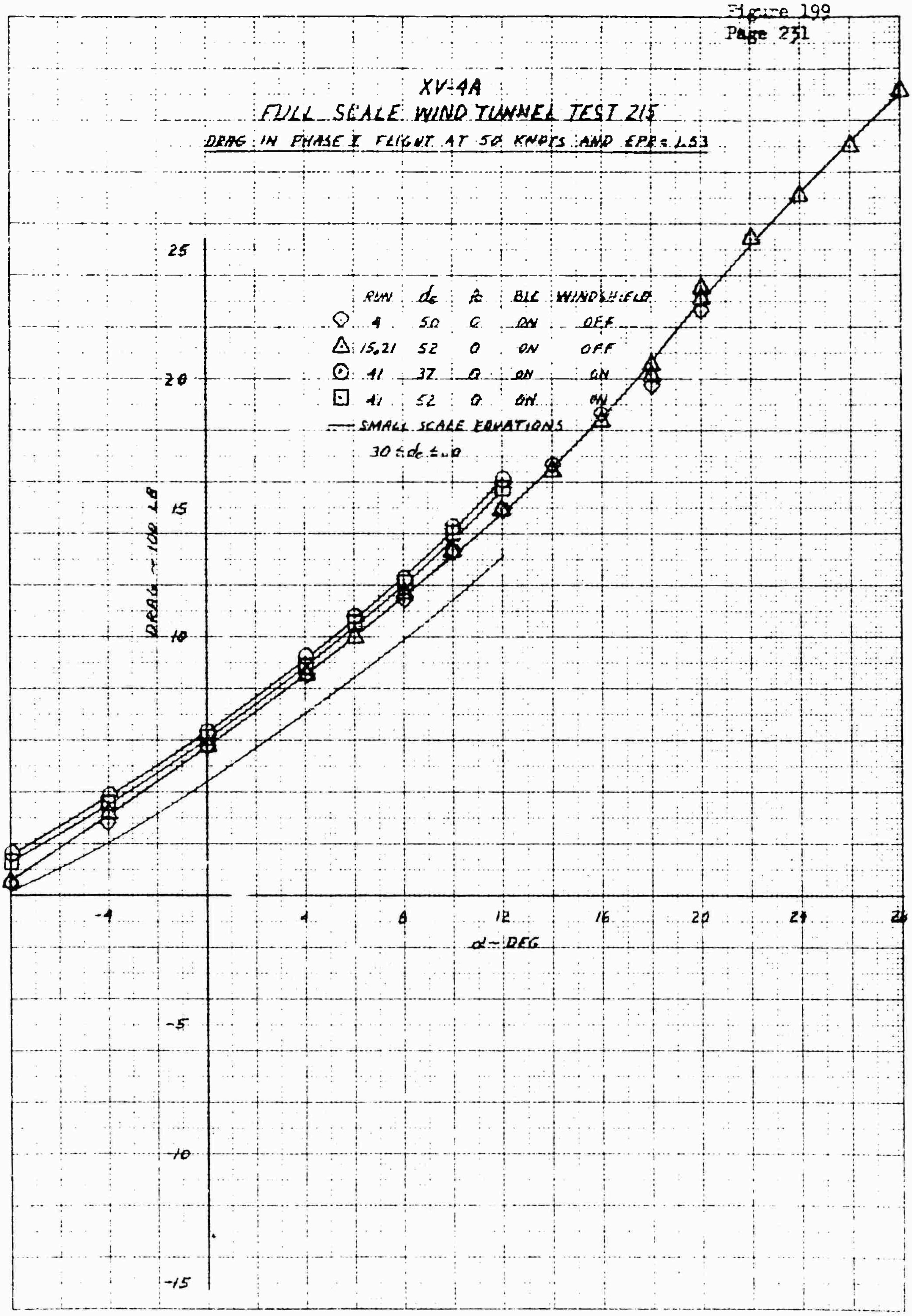
XV-4A
FULL SCALE WIND TUNNEL TEST 215
DRAG IN PHASE I FLIGHT AT 50 KNOTS AND EPR = 1.53
RUN
δ_E
BLC
WINDSHIELD
4
50
ON
OFF
15, 21
52
0
ON
OFF
41
37
0
ON
ON
41
52
0
ON
ON
SMALL SCALE EQUATIONS
DRAG ~ 100 LB
25
20
15
10
-5
-10
-15
-4
4
8
12
16
20
24
α ~ DEG

XV-4A
FULL SCALE WIND TUNNEL TEST 215
PITCHING MOMENT IN PHASE I FLIGHT AT 50 KNOTS AND EPR = 1.53

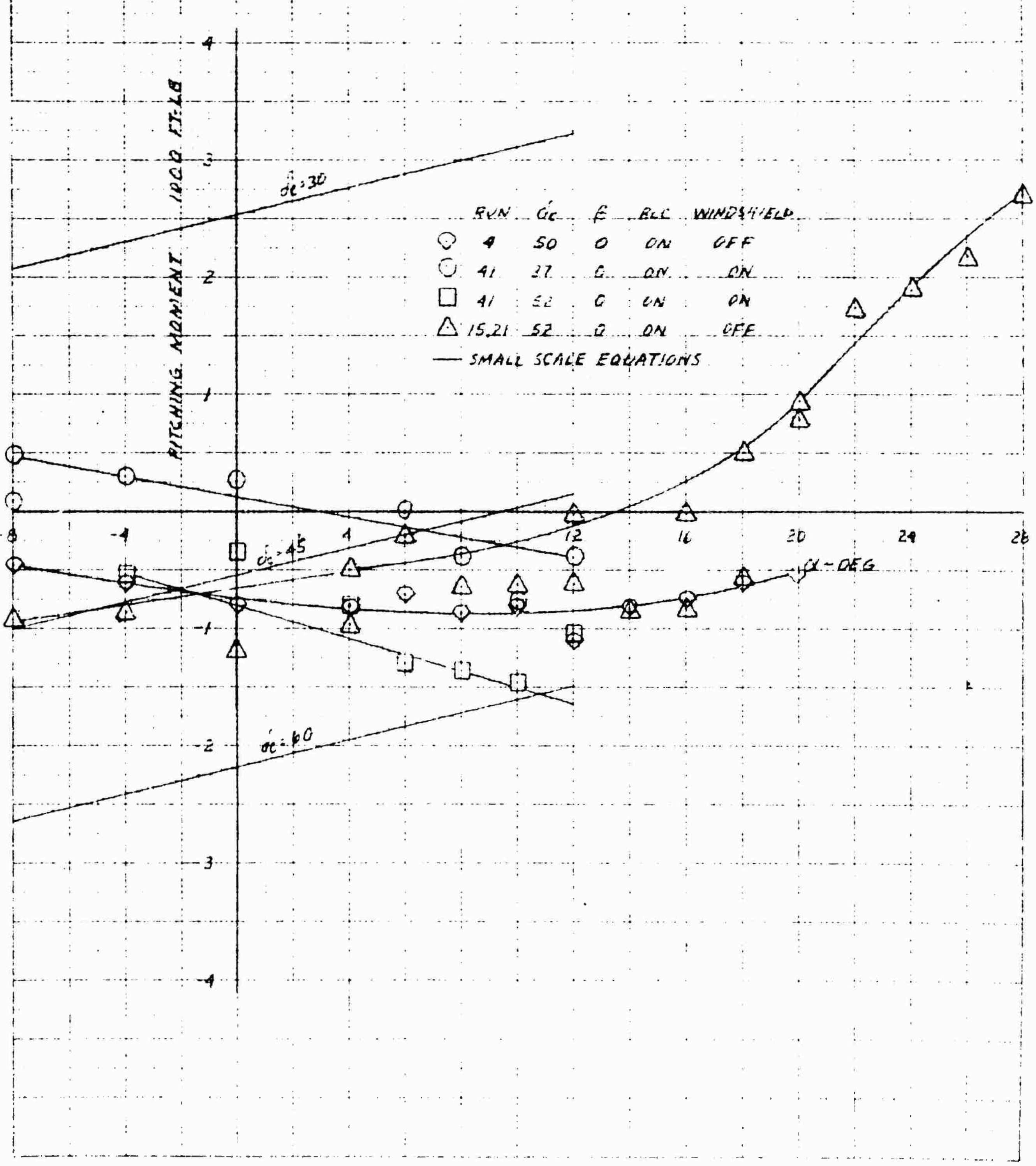

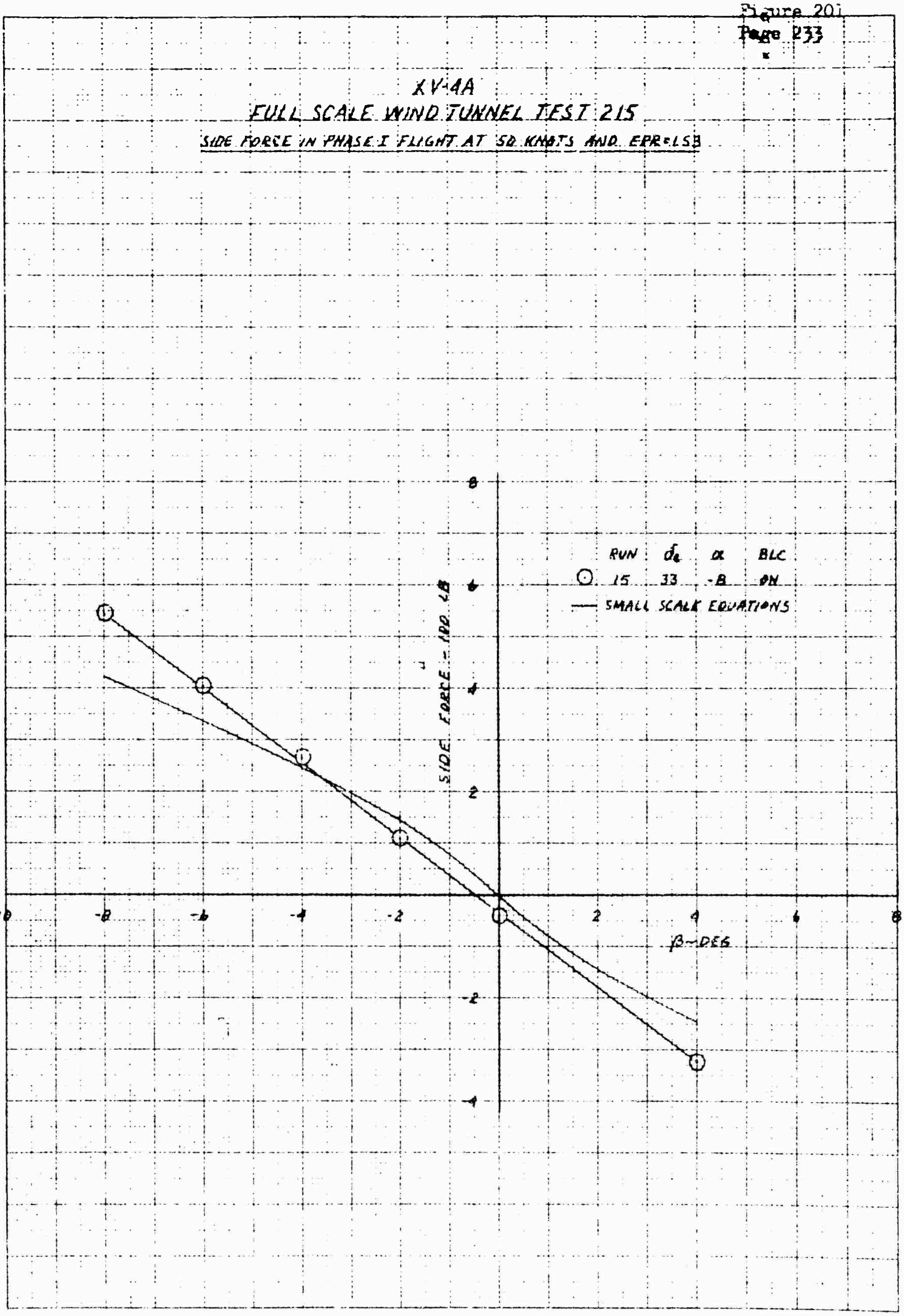
XV-4A
FULL SCALE WIND TUNNEL TEST 215
SIDE FORCE IN PHASE I FLIGHT AT 50 KNOTS AND EPR=1.53
RUN δe α BLC
⊙ 15 33 -8 ON
— SMALL SCALE EQUATIONS
SIDE FORCE - 100 LB
β~DEG
8
6
4
2
-2
-4
-10
-8
-6
-4
-2
2
4
6
8

XV-4A

FULL SCALE WIND TUNNEL TEST 215

YAWING MOMENT IN PHASE I FLIGHT AT 50 KNOTS AND EPR=1.53

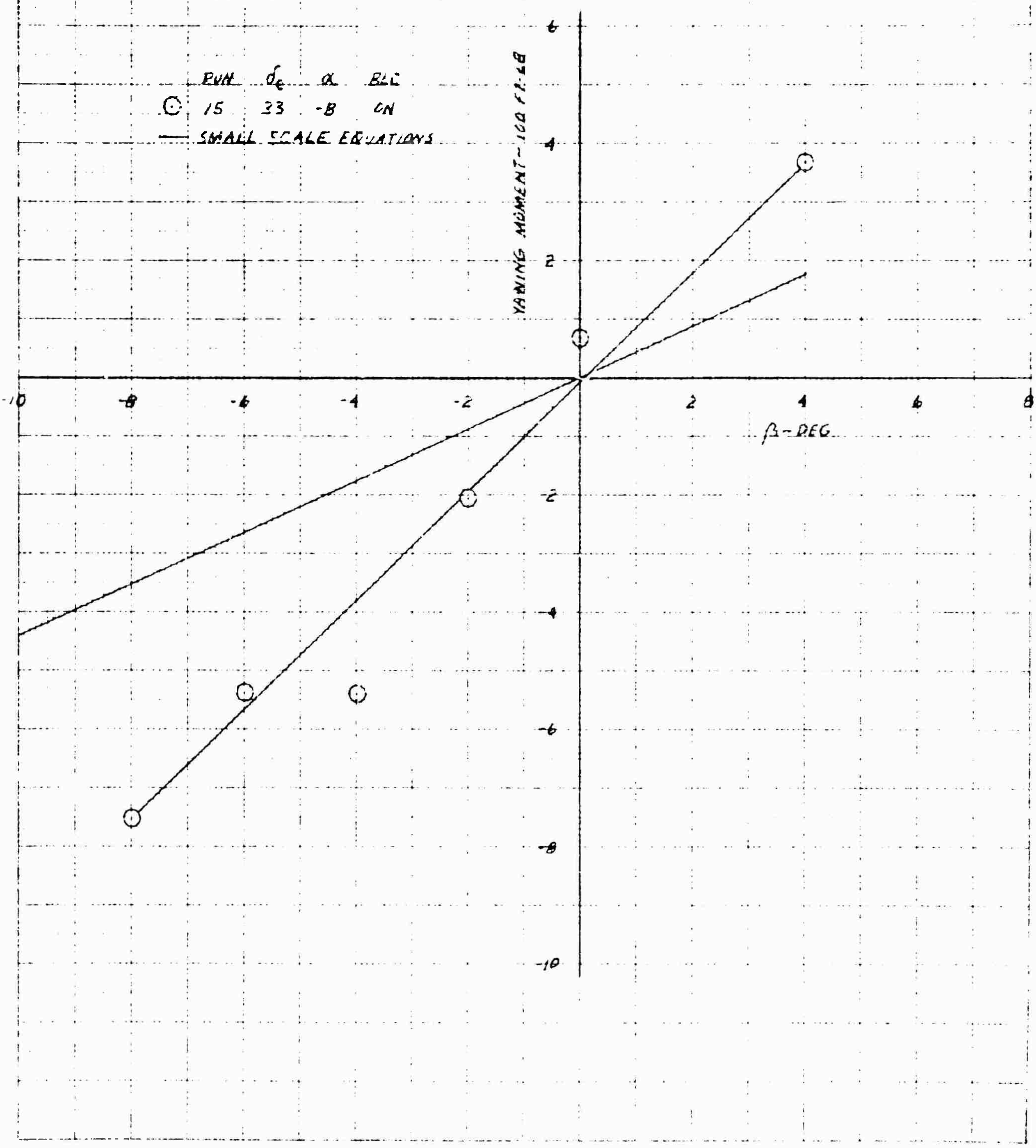

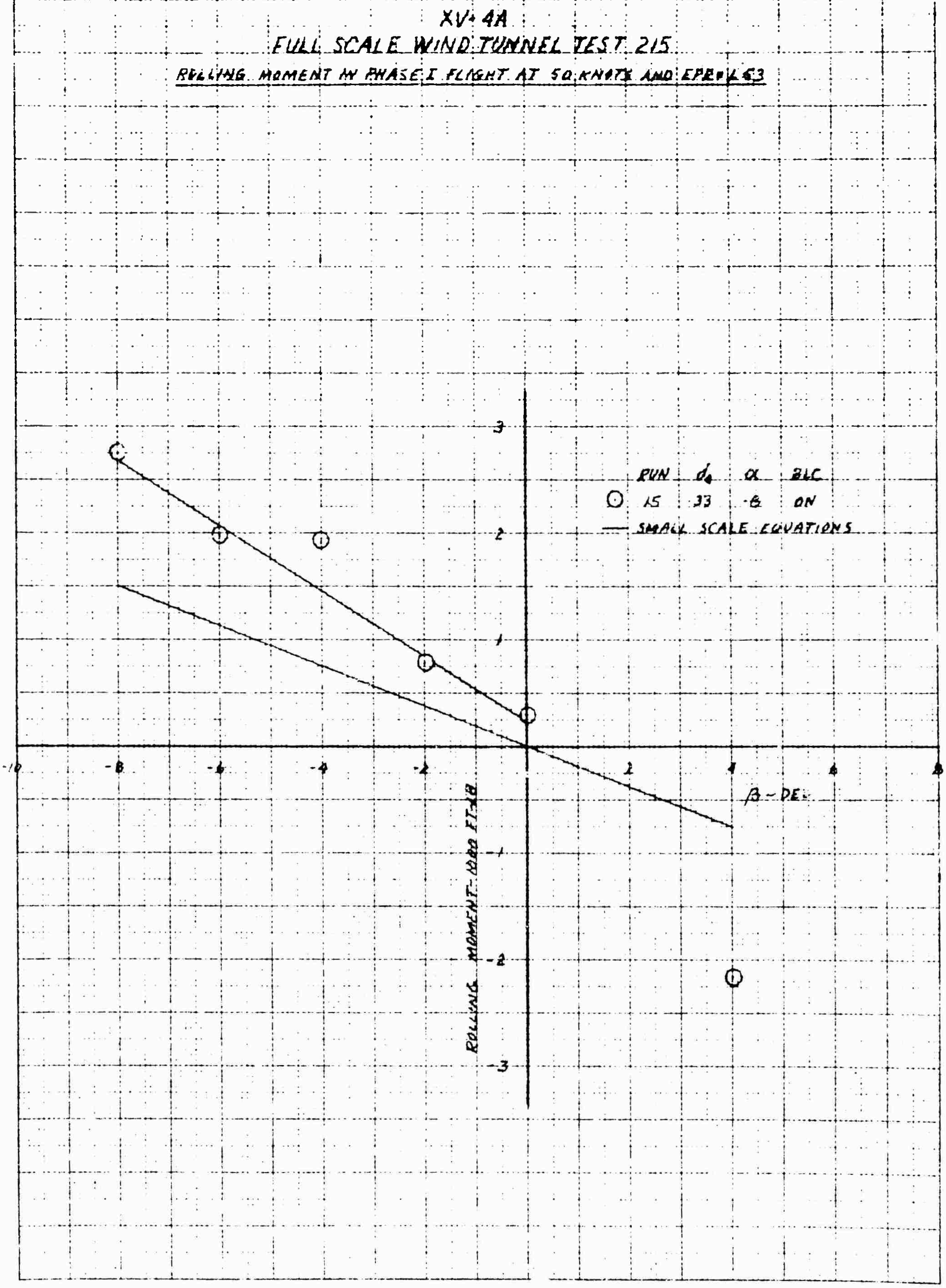
XV-4A
FULL SCALE WIND TUNNEL TEST 215
ROLLING MOMENT IN PHASE I FLIGHT AT 50 KNOTS AND EPR = 1.63
RUN
15
33
-6
BLC
ON
SMALL SCALE EQUATIONS
β ~ DEG
ROLLING MOMENT - 1000 FT-LB
-10
-8
-6
-4
-2
2
4
6
8
3
2
1
-1
-2
-3

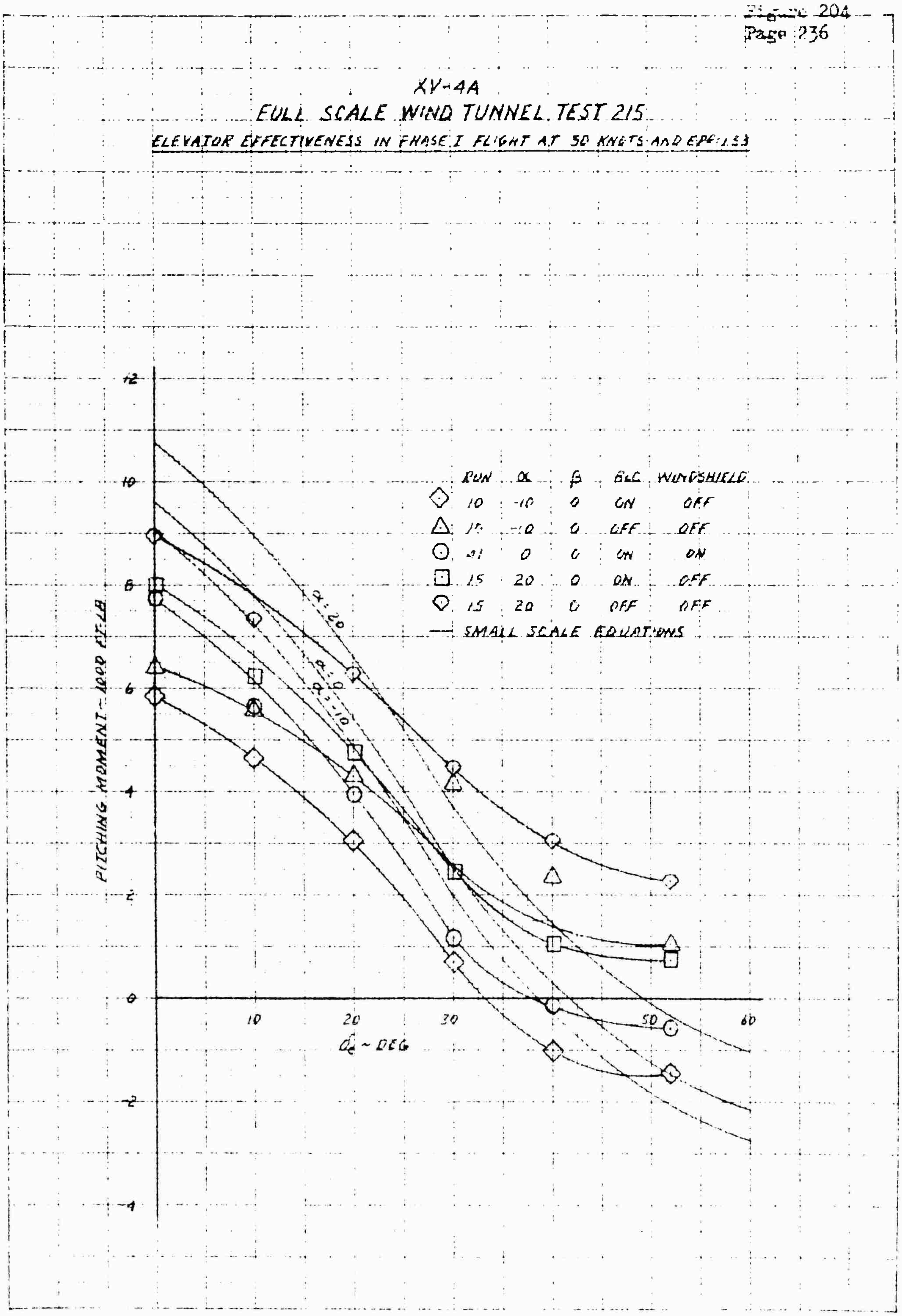
XV-4A
FULL SCALE WIND TUNNEL TEST 215
ELEVATOR EFFECTIVENESS IN PHASE I FLIGHT AT 50 KNOTS AND EPF:1.33
PITCHING MOMENT ~ 1000 FT-LB
δe ~ DEG
RUN α β BLC WINDSHIELD
10 -10 0 ON OFF
-10 0 OFF OFF
0 0 ON ON
15 20 0 ON OFF
15 20 0 OFF OFF
SMALL SCALE EQUATIONS
α = 20
α = 0
α = -10

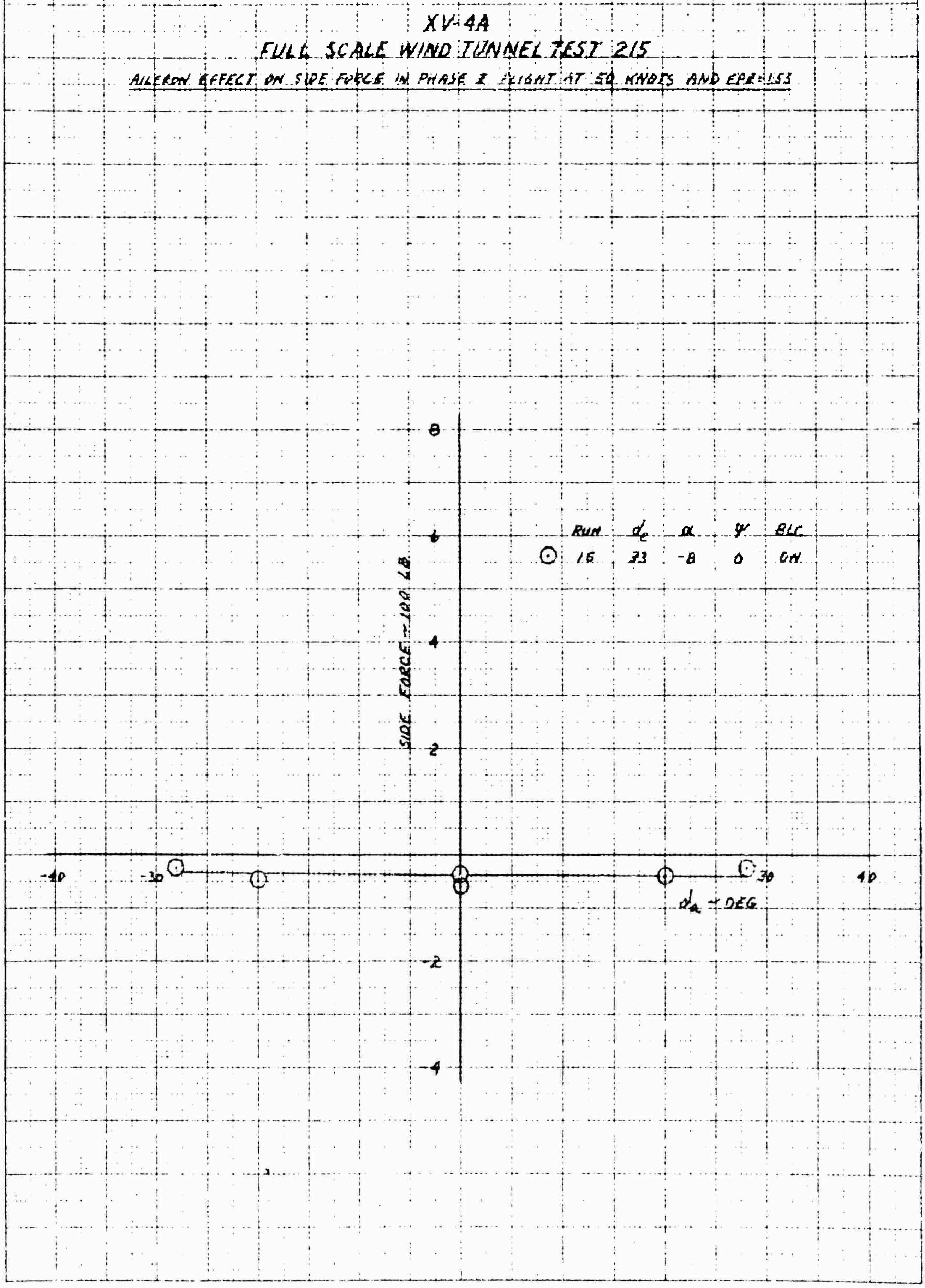
XV-4A
FULL SCALE WIND TUNNEL TEST 215
AILERON EFFECT ON SIDE FORCE IN PHASE I FLIGHT AT 50 KNOTS AND EPR=1.53
RUN
α
BLC
16
33
-8
0
ON
SIDE FORCE ~ 100 LB
8
6
4
2
-2
-4
-40
-30
30
40
DEG

XV-4A
FULL SCALE WIND TUNNEL TEST 215
AILERON EFFECT ON YAW IN PHASE I FLIGHT AT 50 KNOTS AND EPR=1.53

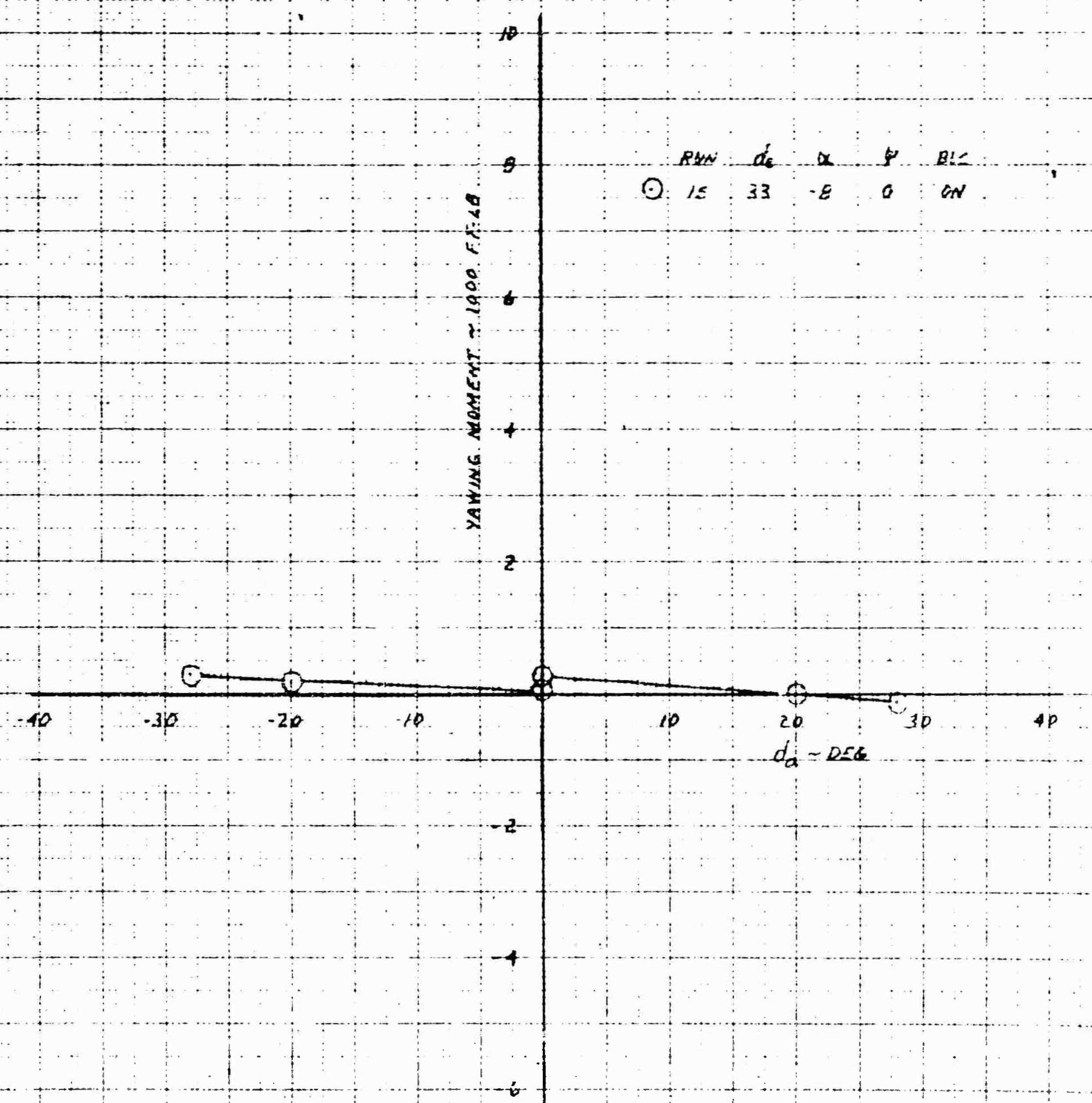

XY-4A

FULL SCALE WIND TUNNEL TEST 215

AILERON EFFECT ON ROLL IN PHASE I FLIGHT AT 50 KNOTS AND EPR=1.53

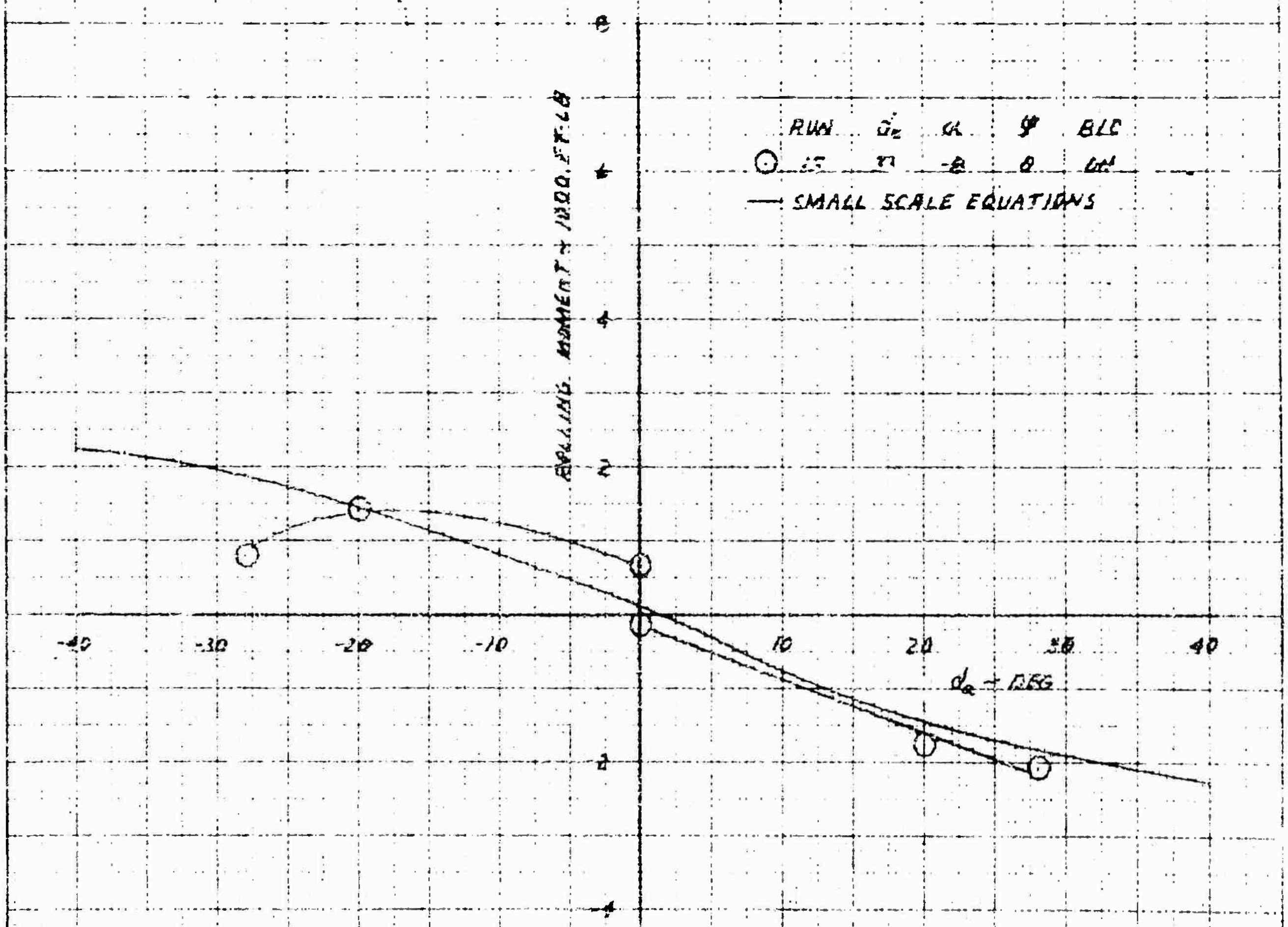

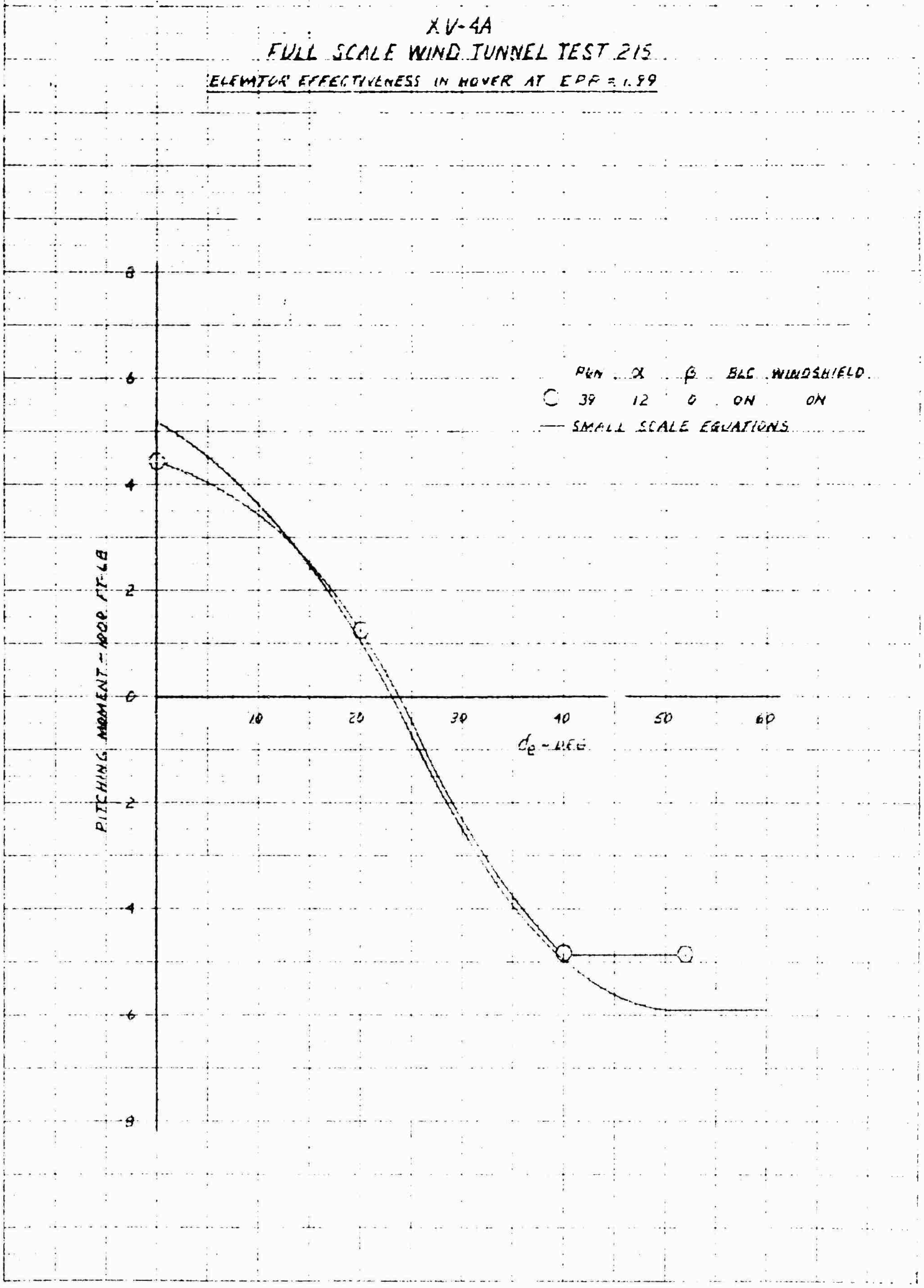
XV-4A
FULL SCALE WIND TUNNEL TEST 215
ELEVATOR EFFECTIVENESS IN HOVER AT EPR = 1.99
RUN α β BLC WINDSHIELD
39 12 0 ON ON
SMALL SCALE EQUATIONS
PITCHING MOMENT - 1000 FT-LB
8
6
4
2
0
-2
-4
-6
-8
10
20
30
40
50
60
δ_e - DEG

XV-4A
FULL SCALE WIND TUNNEL TEST 215
AILERON EFFECT ON SIDE FORCE IN HOVER AT EPR = 1.99

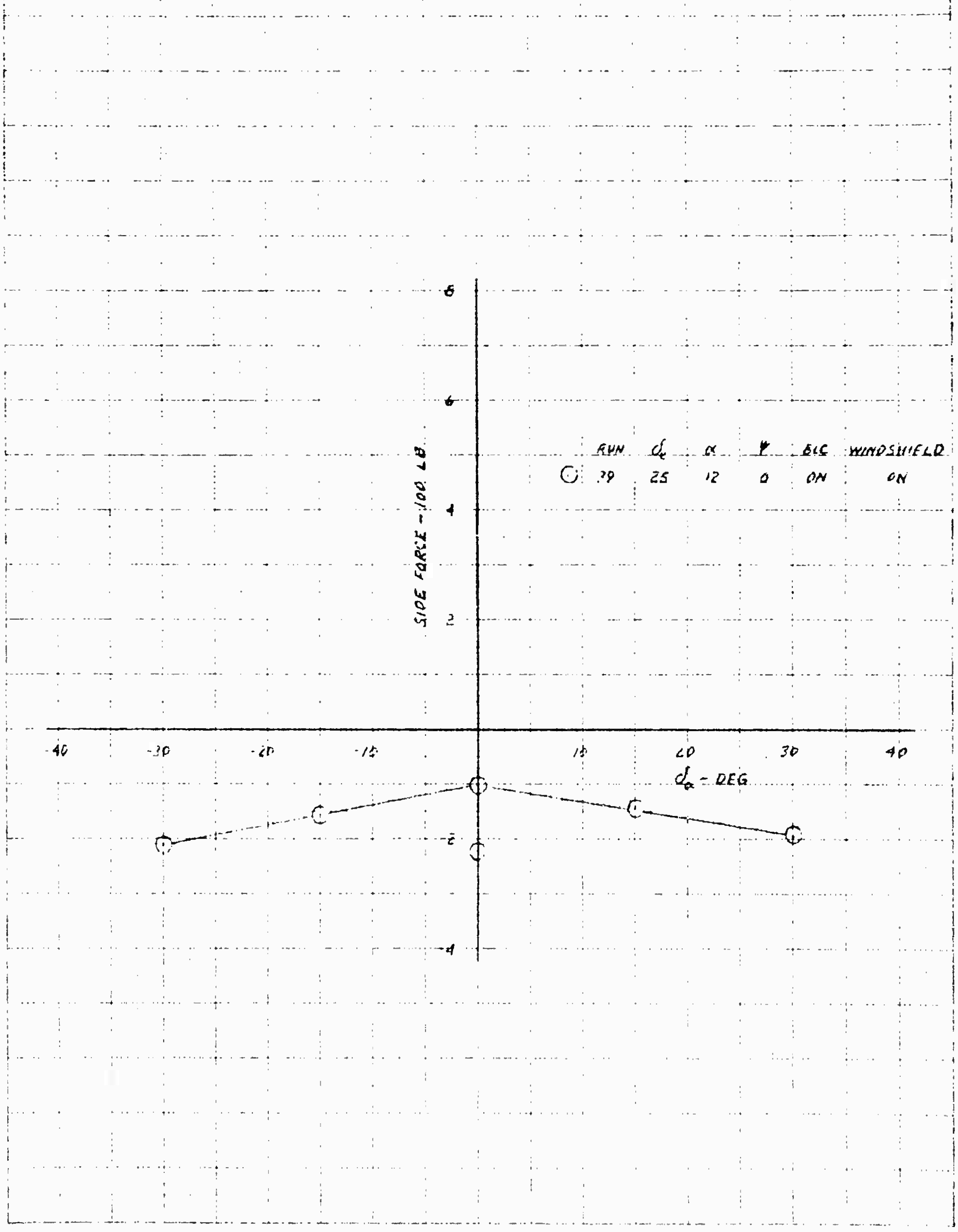

XV-4A

FULL SCALE WIND TUNNEL TEST 215

AILERON EFFECT ON YAW IN HOVER AT EPR: 1.99

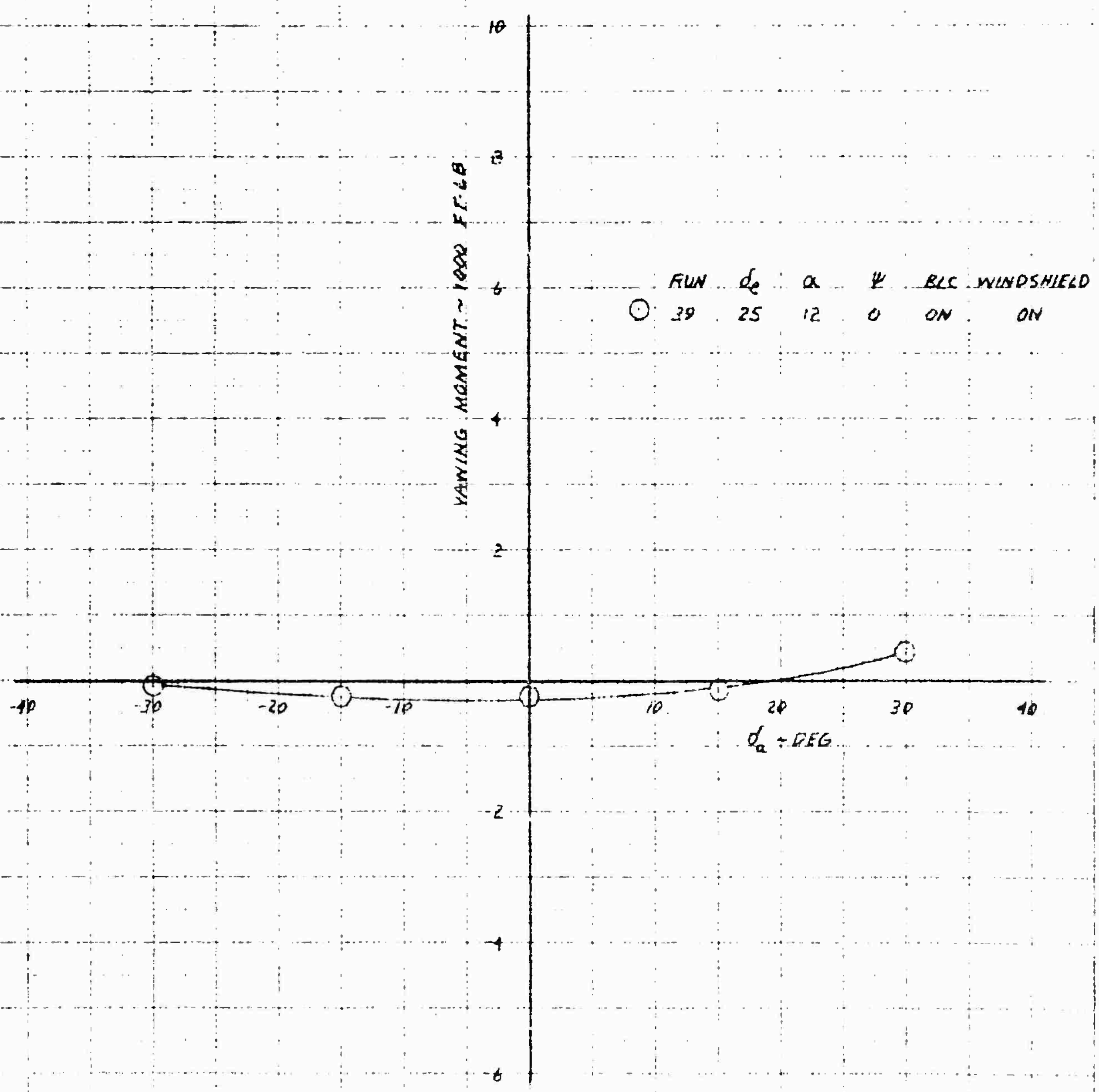

XV-4A

FULL SCALE WIND TUNNEL TEST 215

AILERON EFFECT ON ROLL IN HOVER AT EPR=1.99

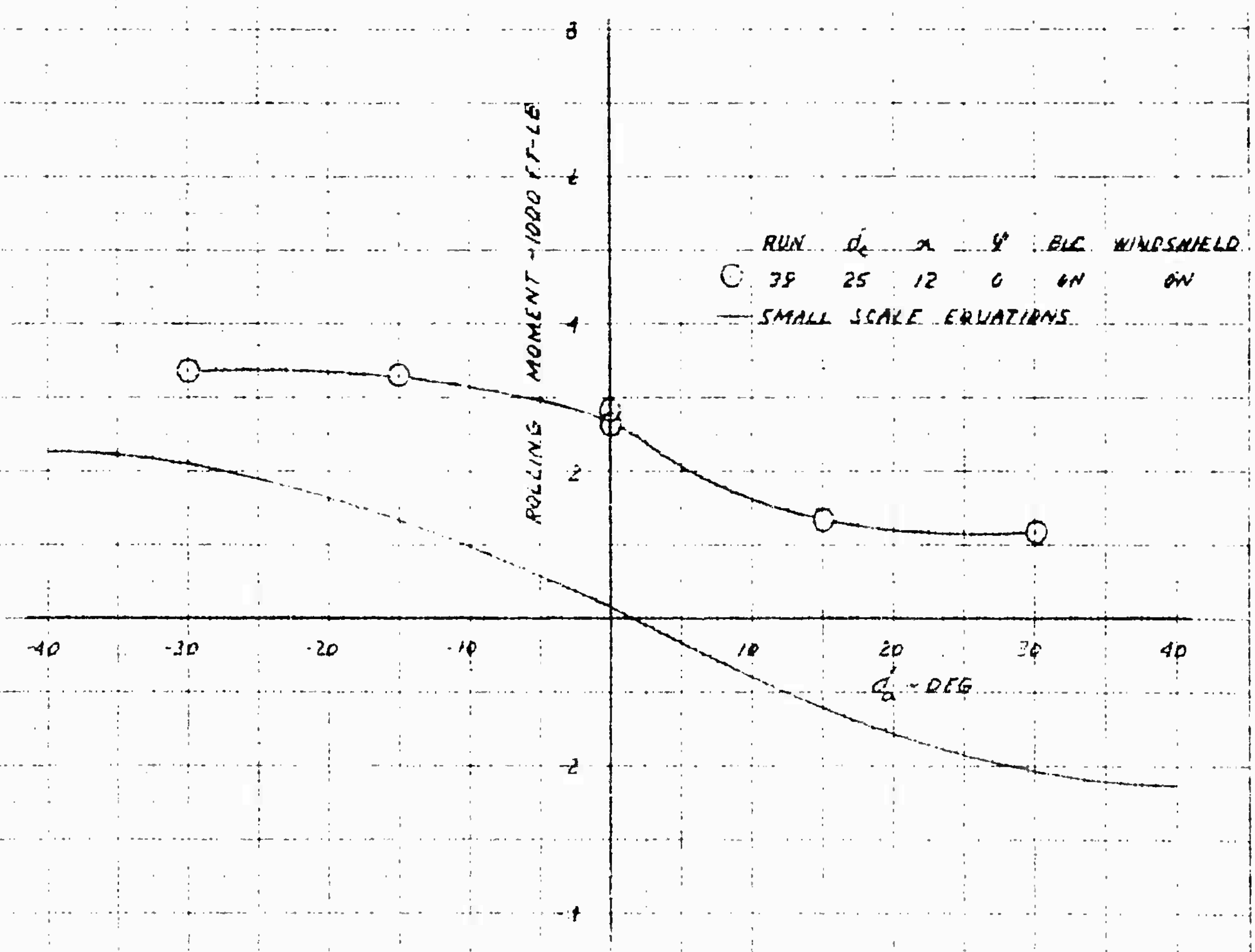

XV-4A
FULL SCALE WIND TUNNEL TEST 215
RUDDER EFFECT ON SIDE FORCE IN HOVER AT EPR=1.99

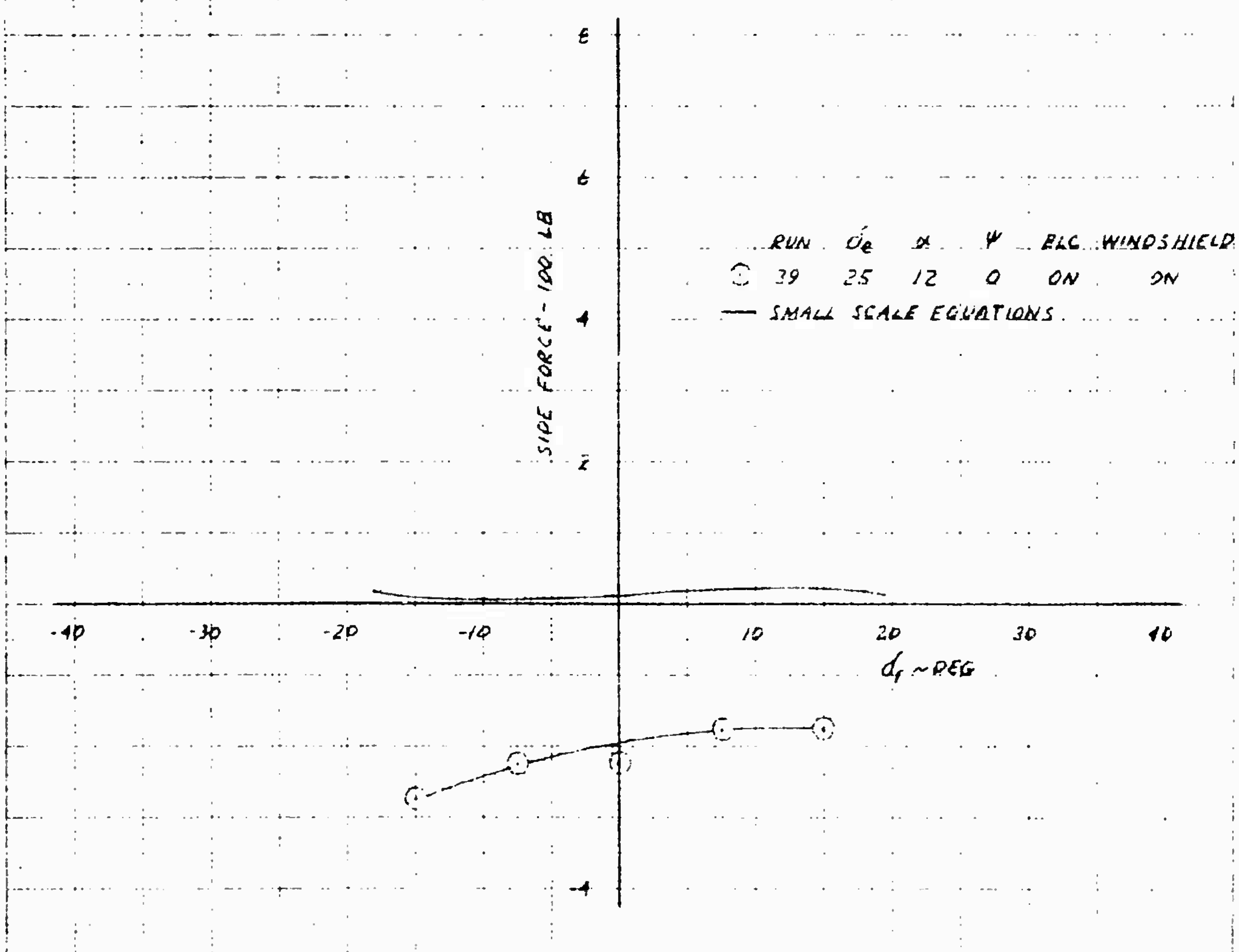

XV-4A

FULL SCALE WIND TUNNEL TEST 215

RUDDER EFFECT ON YAW IN HOVER AT EPR=199

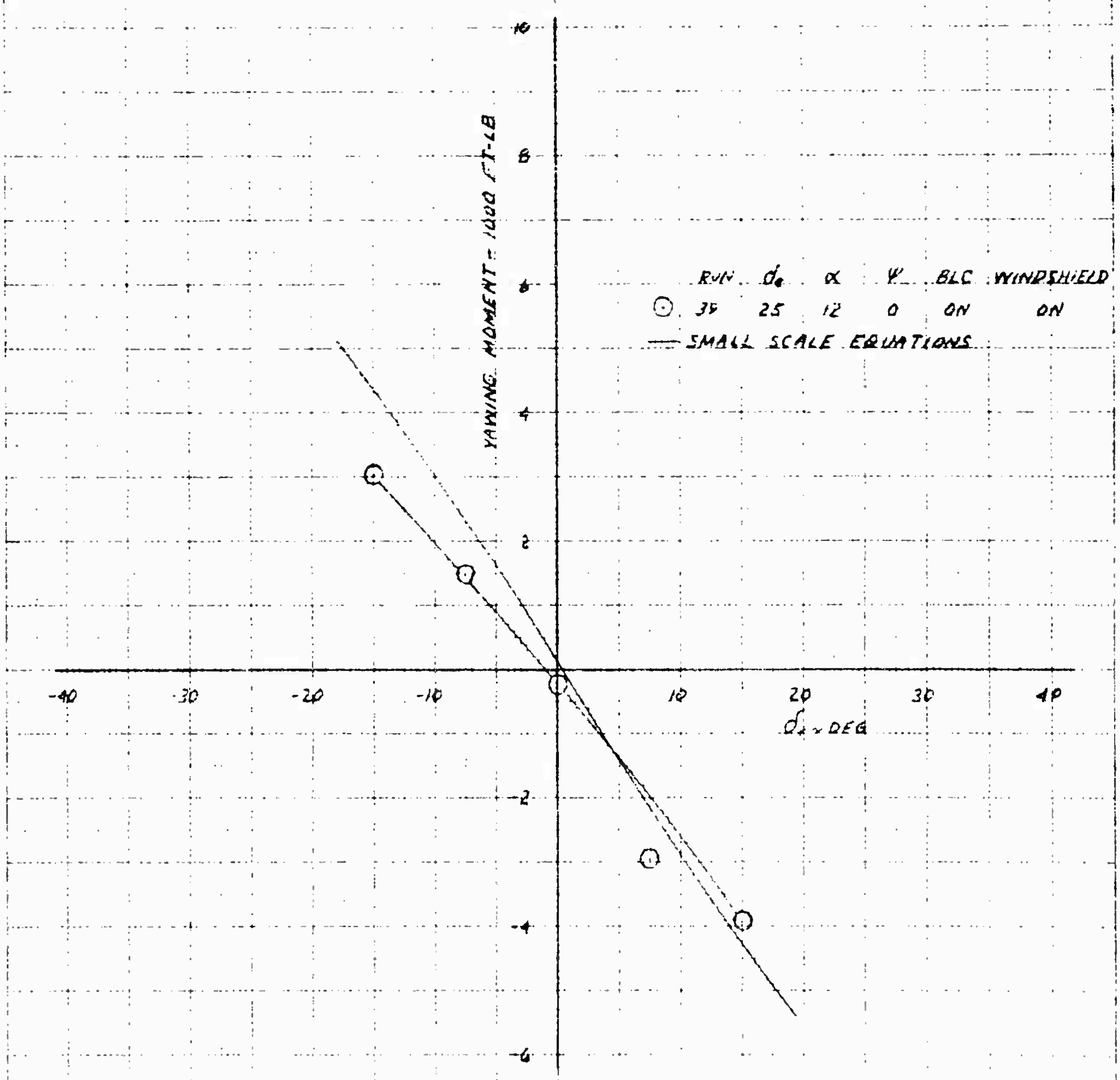

XV-4A

FULL SCALE WING TUNNEL TEST 215

LIFT IN PHASE I FLIGHT AT 80 KNOTS AND EPE = 1.99

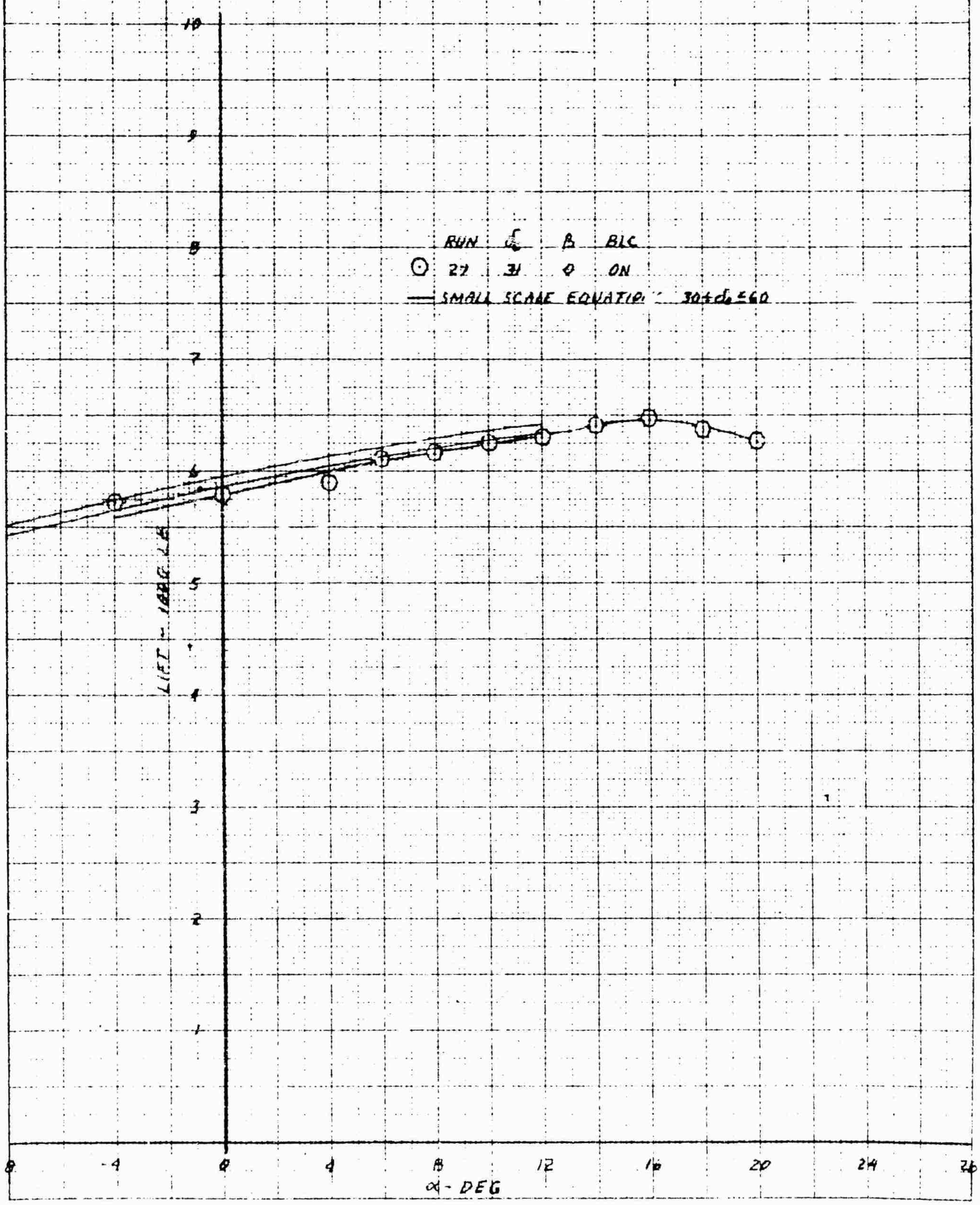

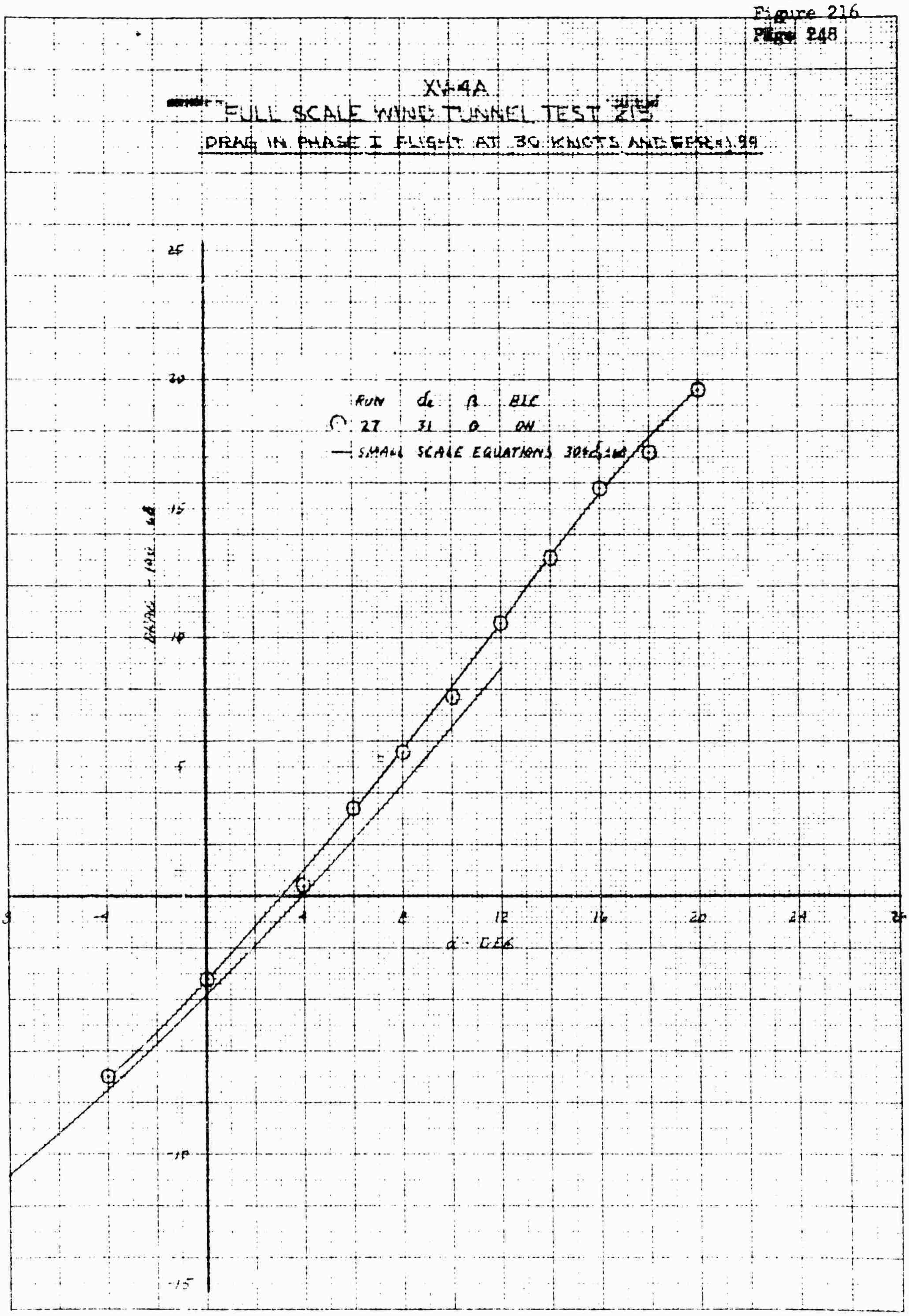
XV-4A
FULL SCALE WIND TUNNEL TEST 215
DRAG IN PHASE I FLIGHT AT 30 KNOTS AND EPR=1.99
RUN
27
31
0
ON
SMALL SCALE EQUATIONS
-4
4
8
12
16
20
24
α - DEG
25
20
15
10
5
-10
-15

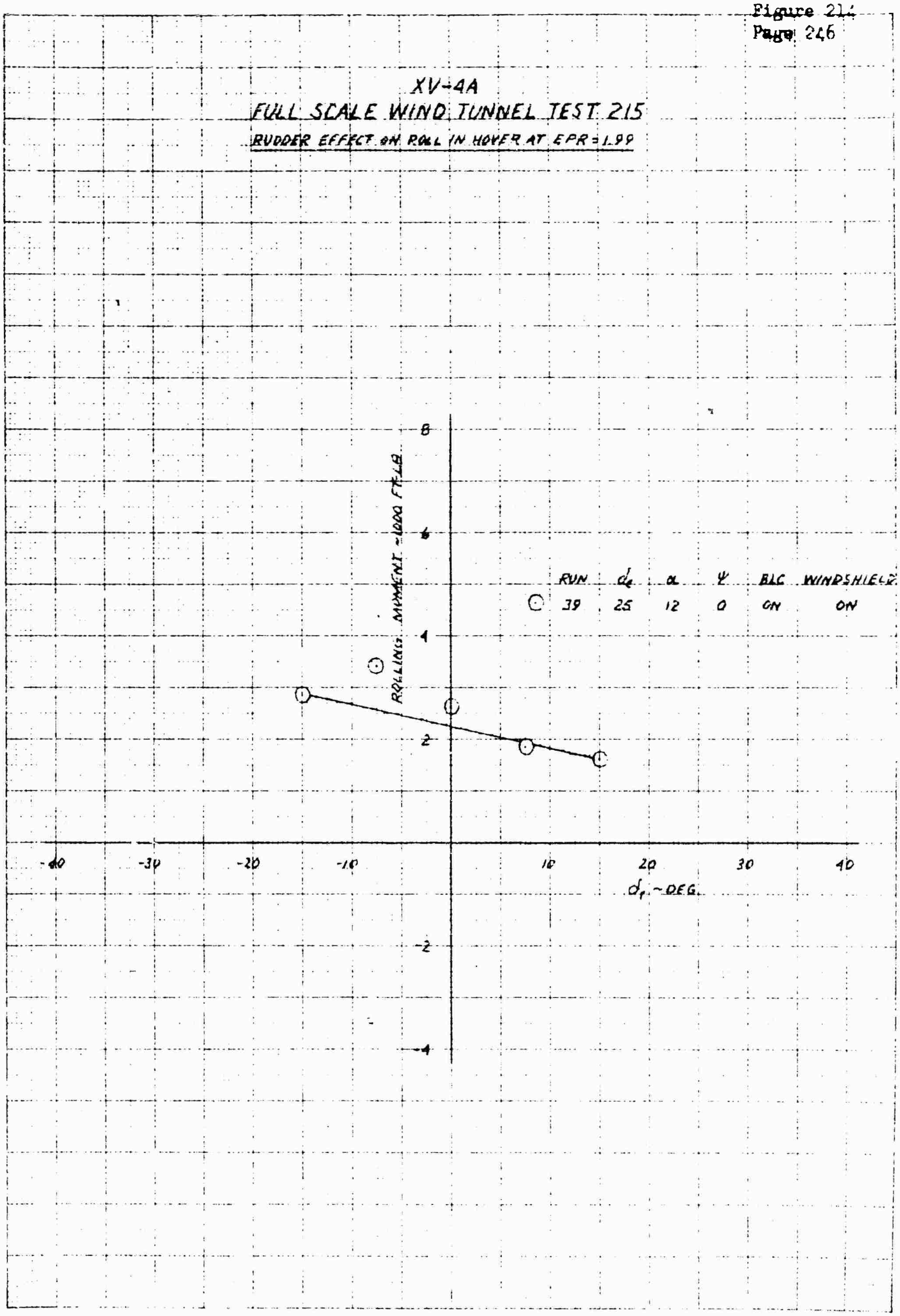
XV-4A
FULL SCALE WIND TUNNEL TEST 215
RUDDER EFFECT ON ROLL IN HOVER AT EPR = 1.99
ROLLING MOMENT ~1000 FT-LB
8
6
4
2
-2
-4
RUN
39
25
α
12
ψ
0
BLC
ON
WINDSHIELD
ON
-40
-30
-20
-10
10
20
30
40
δ_r ~ DEG.

XV-4A
FULL SCALE WIND TUNNEL TEST 215
PITCHING MOMENT IN PHASE I FLIGHT AT 30 KNOTS AND EPR = 1.99

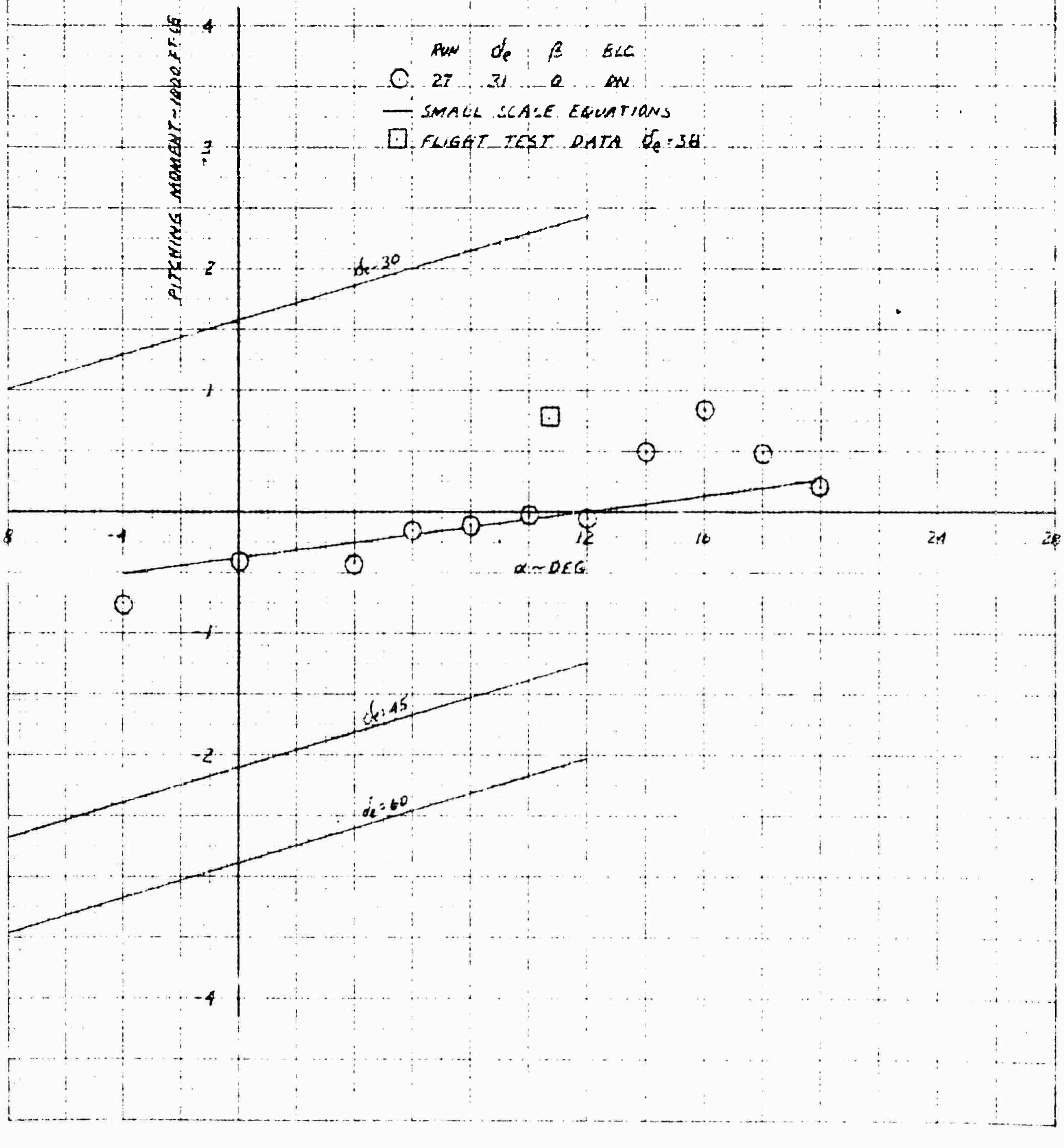

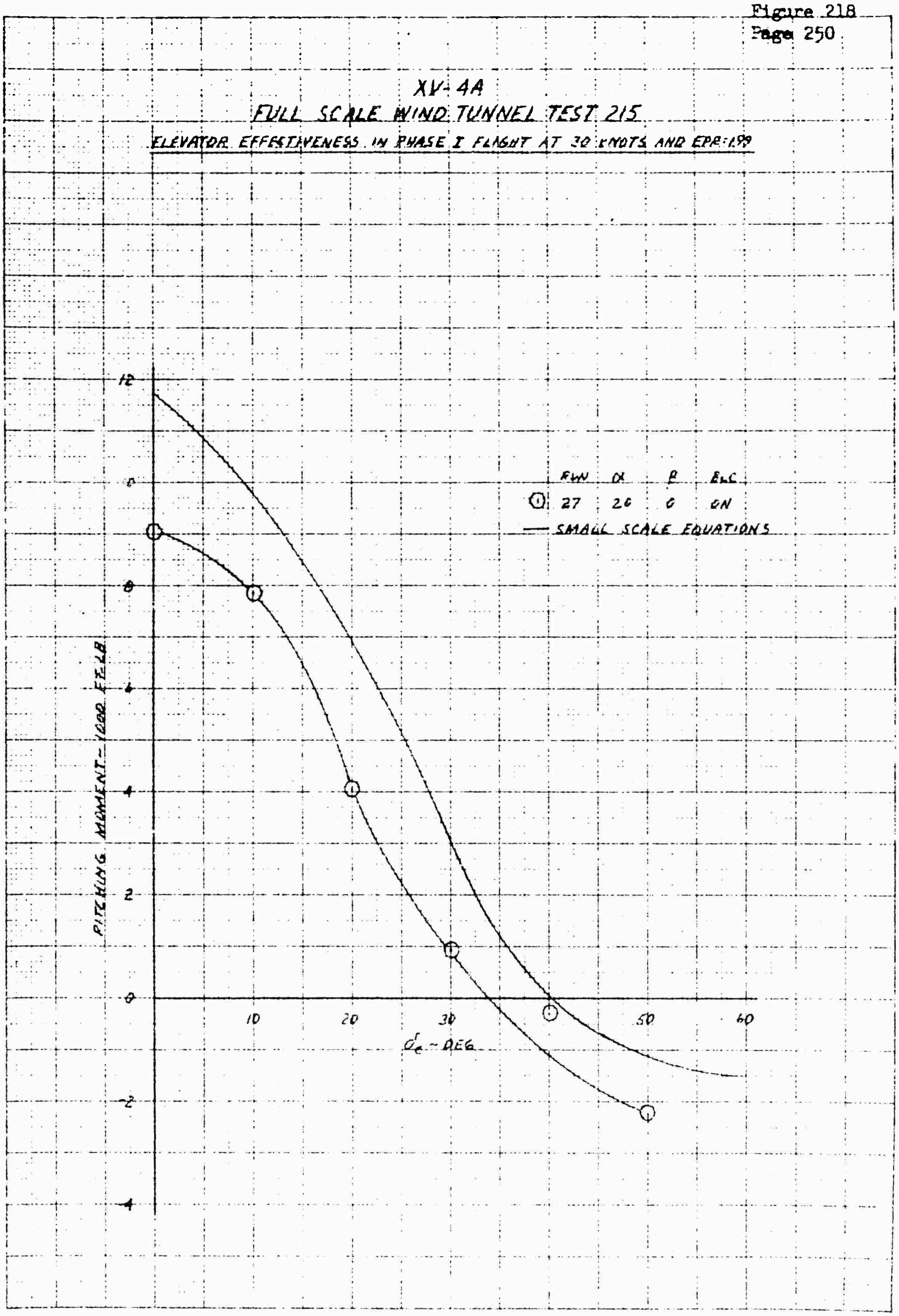
XV-4A
FULL SCALE WIND TUNNEL TEST 215
ELEVATOR EFFECTIVENESS IN PHASE I FLIGHT AT 30 KNOTS AND EPR=1.99
RUN α β ELC
27 20 0 ON
SMALL SCALE EQUATIONS
PITCHING MOMENT - 1000 FT-LB
δe ~ DEG
12
8
4
2
0
-2
-4
10
20
30
50
60

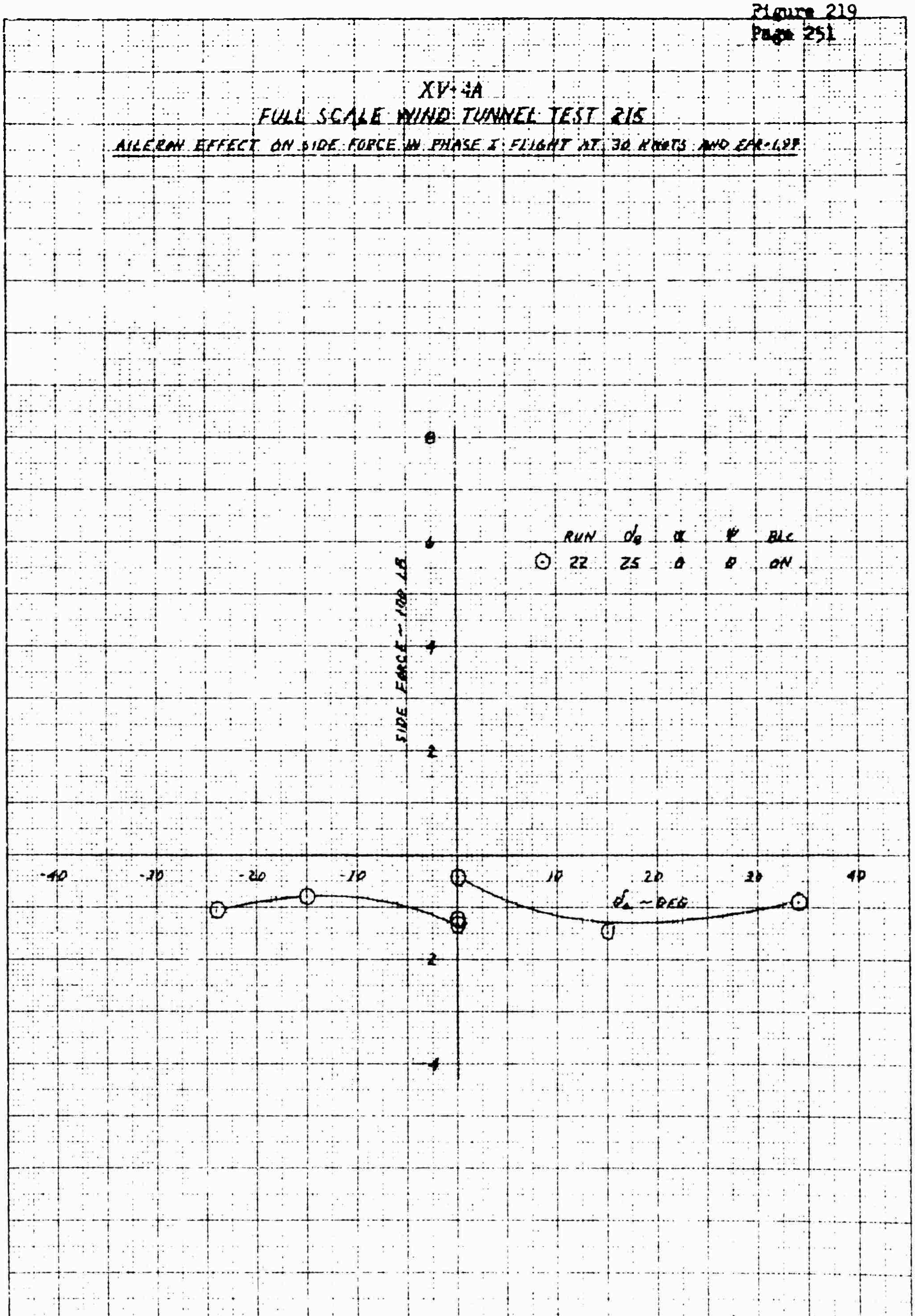
XV-4A
FULL SCALE WIND TUNNEL TEST 215
AILERON EFFECT ON SIDE FORCE IN PHASE I FLIGHT AT 30 KNOTS AND EPR-1.97
RUN
22
25
0
0
BLC
ON
SIDE FORCE ~ 100 LB
8
6
4
2
2
4
-40
-30
-20
-10
10
20
30
40
δa ~ DEG

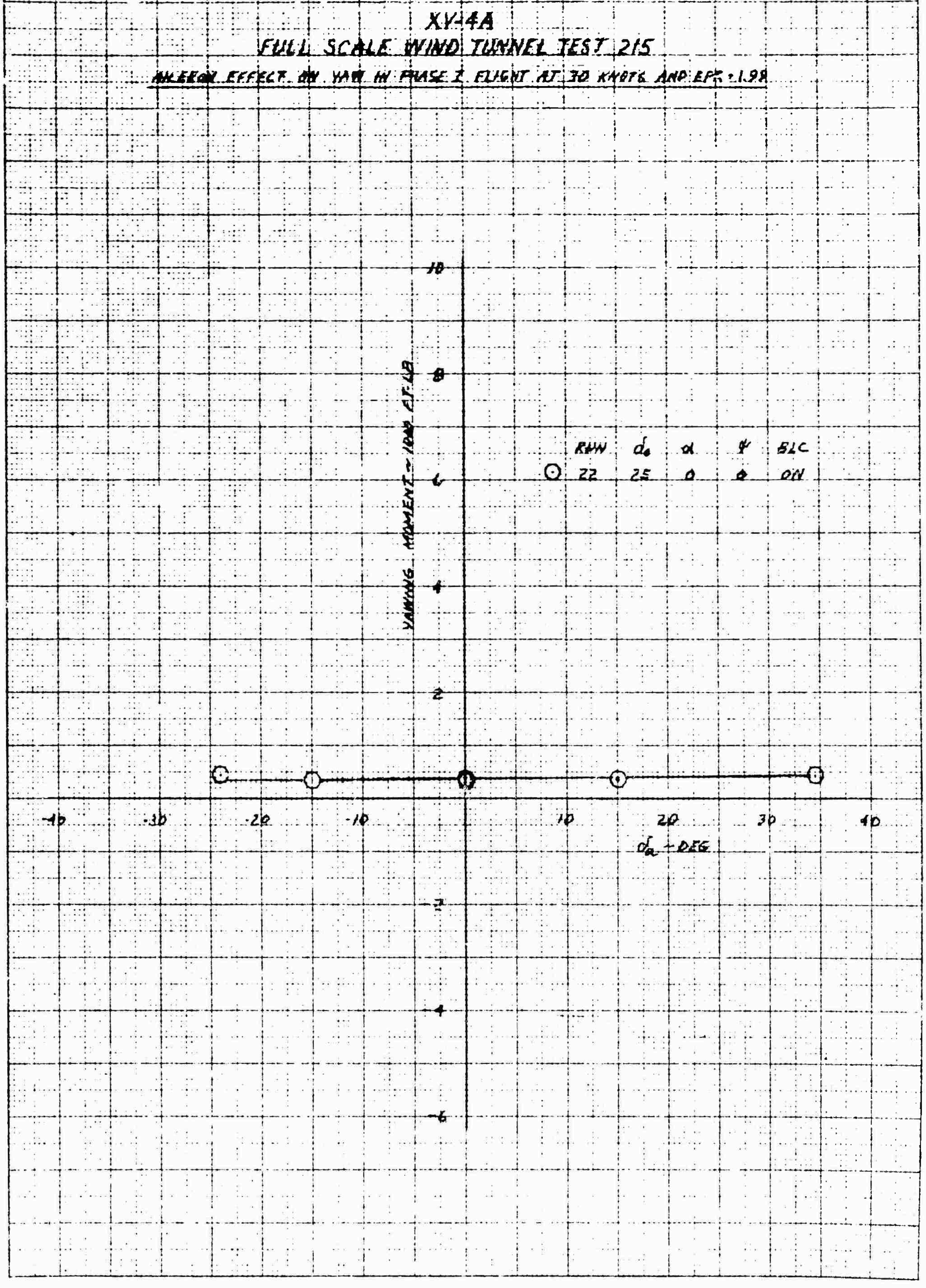
XV-4A
FULL SCALE WIND TUNNEL TEST 215
AILERON EFFECT ON YAW IN PHASE I FLIGHT AT 30 KNOTS AND EPR 1.98
YAWING MOMENT ~ 1000 FT-LB
10
8
6
4
2
-2
-4
-6
-40
-30
-20
-10
10
20
30
40
δ_a ~ DEG
RUN δ_e α ψ BLC
22 25 0 0 ON

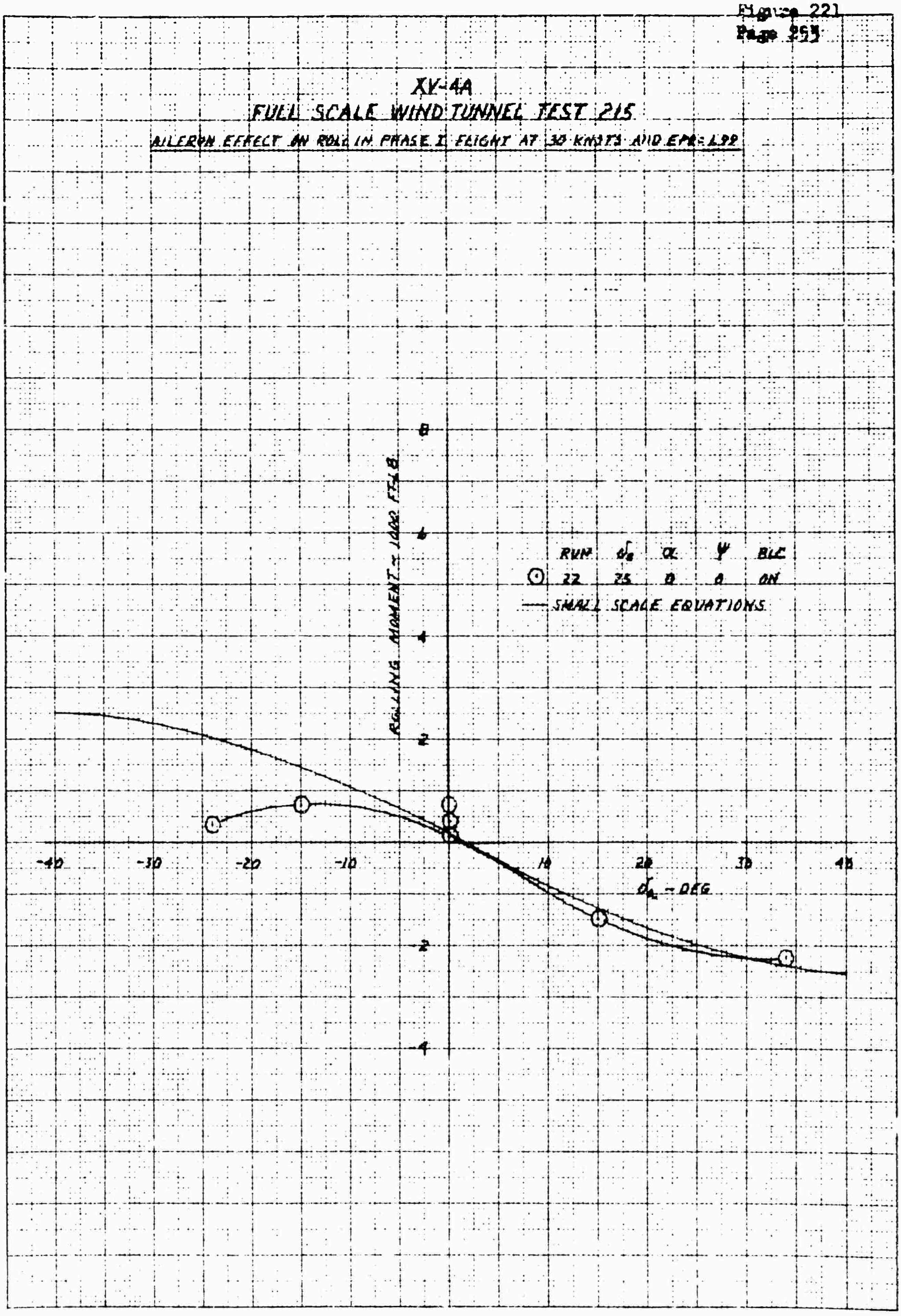
XV-4A
FULL SCALE WIND TUNNEL TEST 215
AILERON EFFECT ON ROLL IN PHASE I FLIGHT AT 30 KNOTS AND EPR=1.99
ROLLING MOMENT ~ 1000 FT-LB
δ_a ~ DEG
RUN δ_f α ψ BLC
22 75 0 0 ON
SMALL SCALE EQUATIONS
-40
-30
-20
-10
10
20
30
40
8
6
4
2
-2
-4

XV-4A
FULL SCALE WIND TUNNEL TEST 215
RUDDER EFFECT ON SIDE FORCE IN PHASE I FLIGHT AT 30 KNOTS AND EPR = 1.99

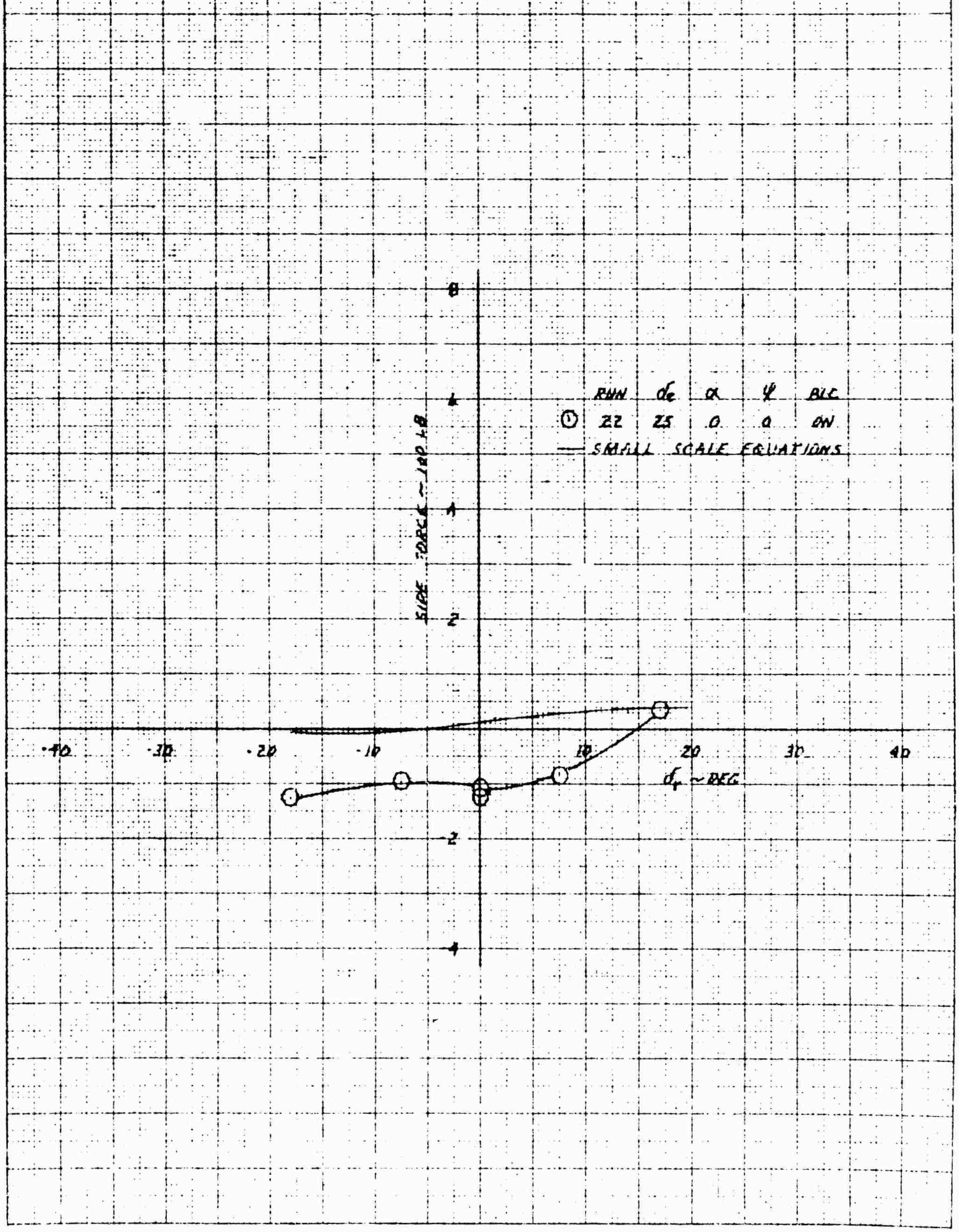

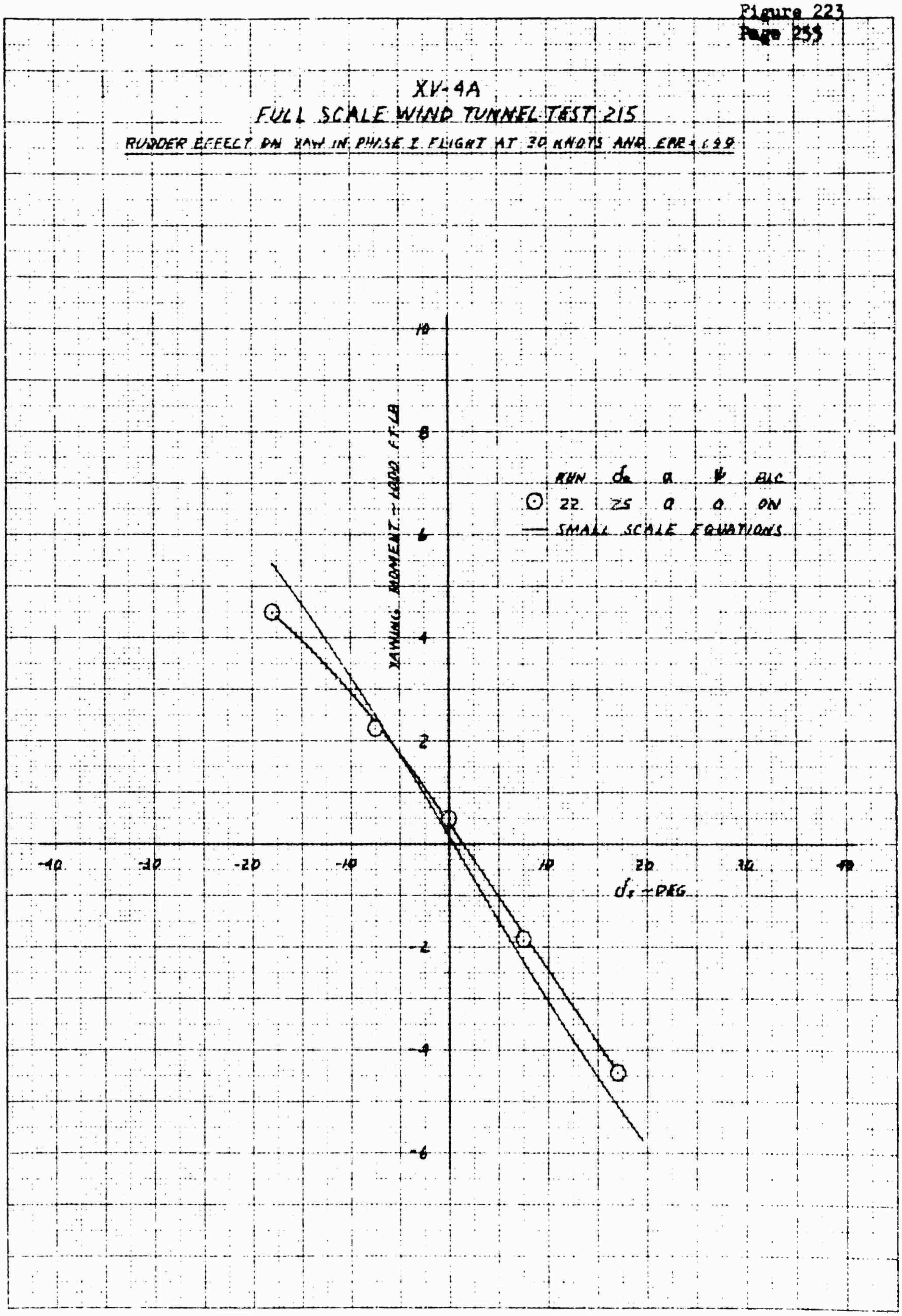
XV-4A
FULL SCALE WIND TUNNEL TEST 215
RUDDER EFFECT ON YAW IN PHASE I FLIGHT AT 30 KNOTS AND EPR 1.99
YAWING MOMENT - 1000 FT-LB
10
8
6
4
2
-2
-4
-6
-40
-30
-20
-10
10
20
30
40
δr - DEG
RUN δe α ψ BLC
22 25 0 0 ON
SMALL SCALE EQUATIONS

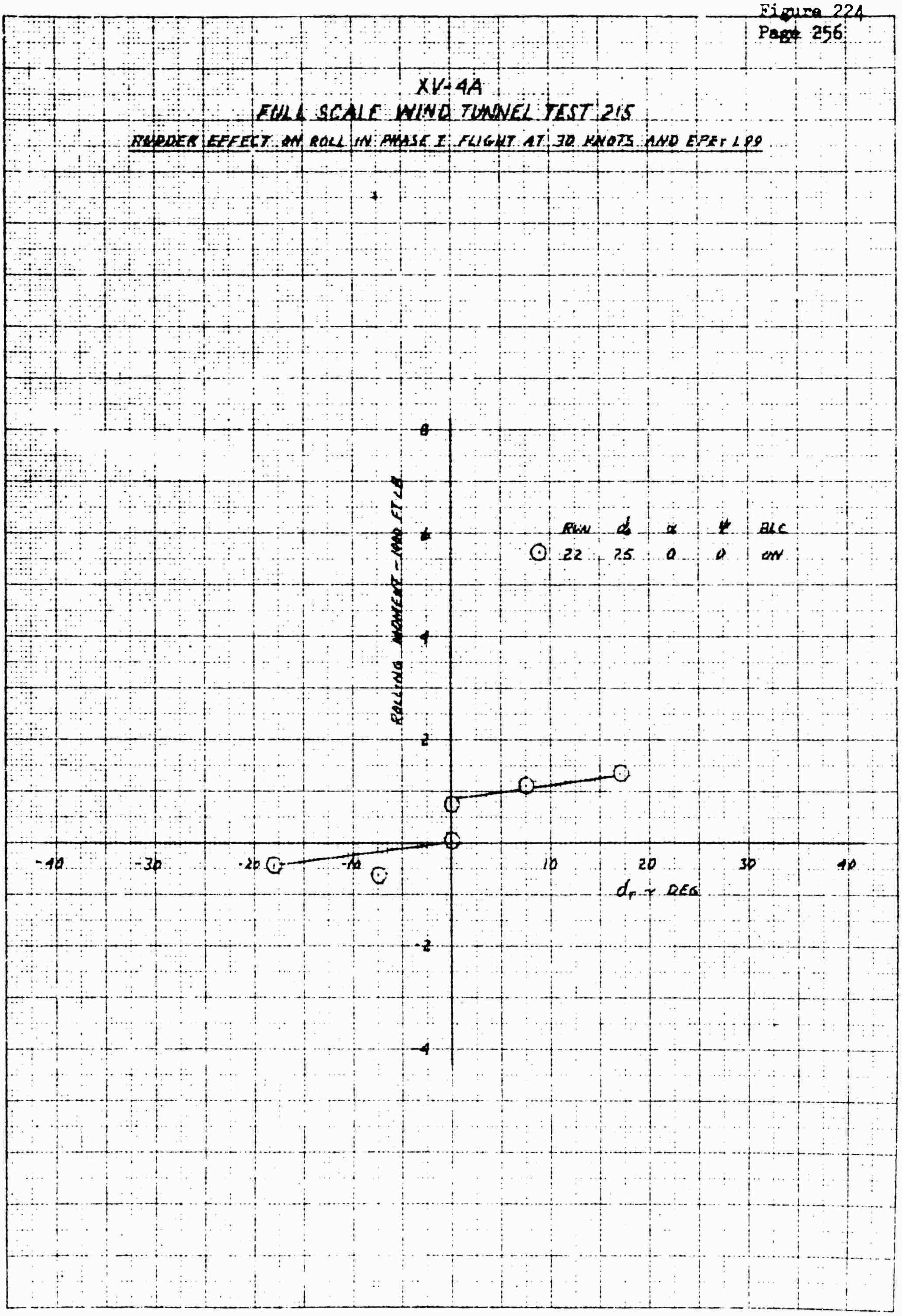
XV-4A
FULL SCALE WIND TUNNEL TEST 215
RUDDER EFFECT ON ROLL IN PHASE I FLIGHT AT 30 KNOTS AND EPE = L99
ROLLING MOMENT - 1000 FT LB
RUN
22
d_r ~ DEG
-40
-30
-20
-10
10
20
30
40
8
6
4
2
-2
-4
α
0
ψ
0
BLC
ON

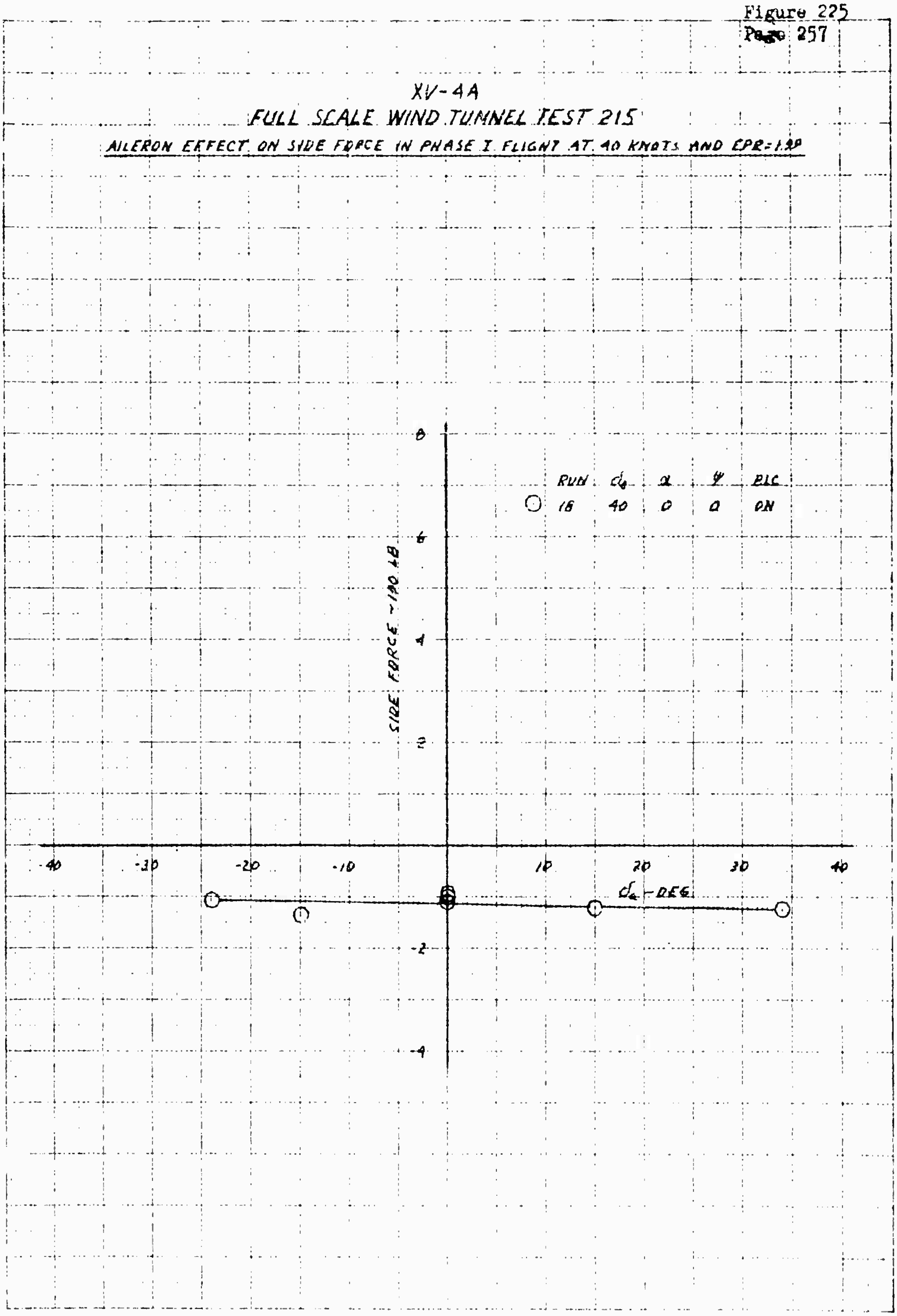
XV-4A
FULL SCALE WIND TUNNEL TEST 215
AILERON EFFECT ON SIDE FORCE IN PHASE I FLIGHT AT 40 KNOTS AND EPR=1.20
SIDE FORCE ~100 LB
8
6
4
2
-2
-4
RUN
δ_a
α
ψ
BLC
16
40
0
0
ON
-40
-30
-20
-10
10
20
30
40
δ_a - DEG

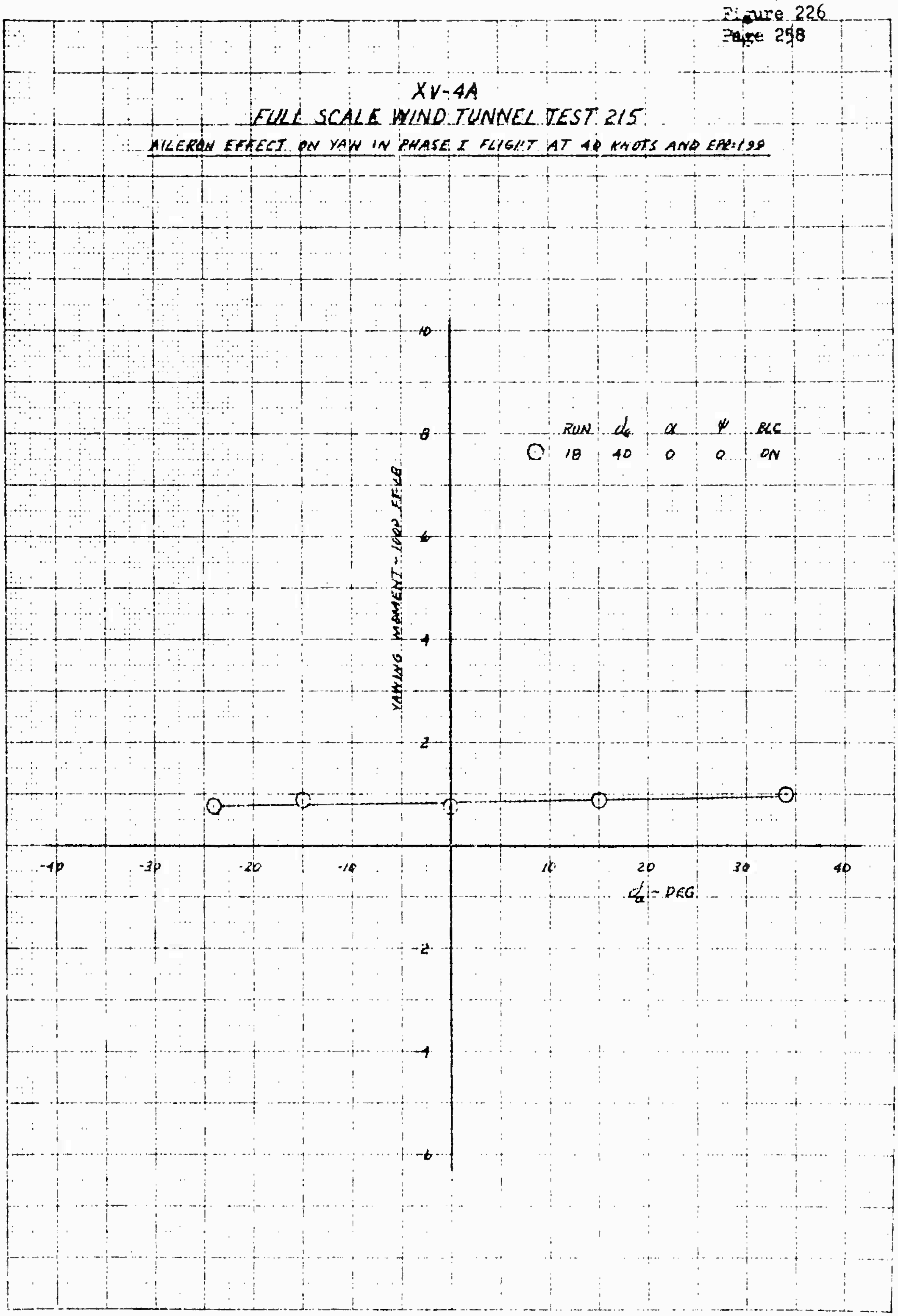
XV-4A
FULL SCALE WIND TUNNEL TEST 215
AILERON EFFECT ON YAW IN PHASE I FLIGHT AT 40 KNOTS AND EPR=1.99
RUN
18
40
0
0
BLC
ON
YAWING MOMENT ~ 1000 FT-LB
10
8
6
4
2
-2
-4
-6
-40
-30
-20
-10
10
20
30
40
DEG

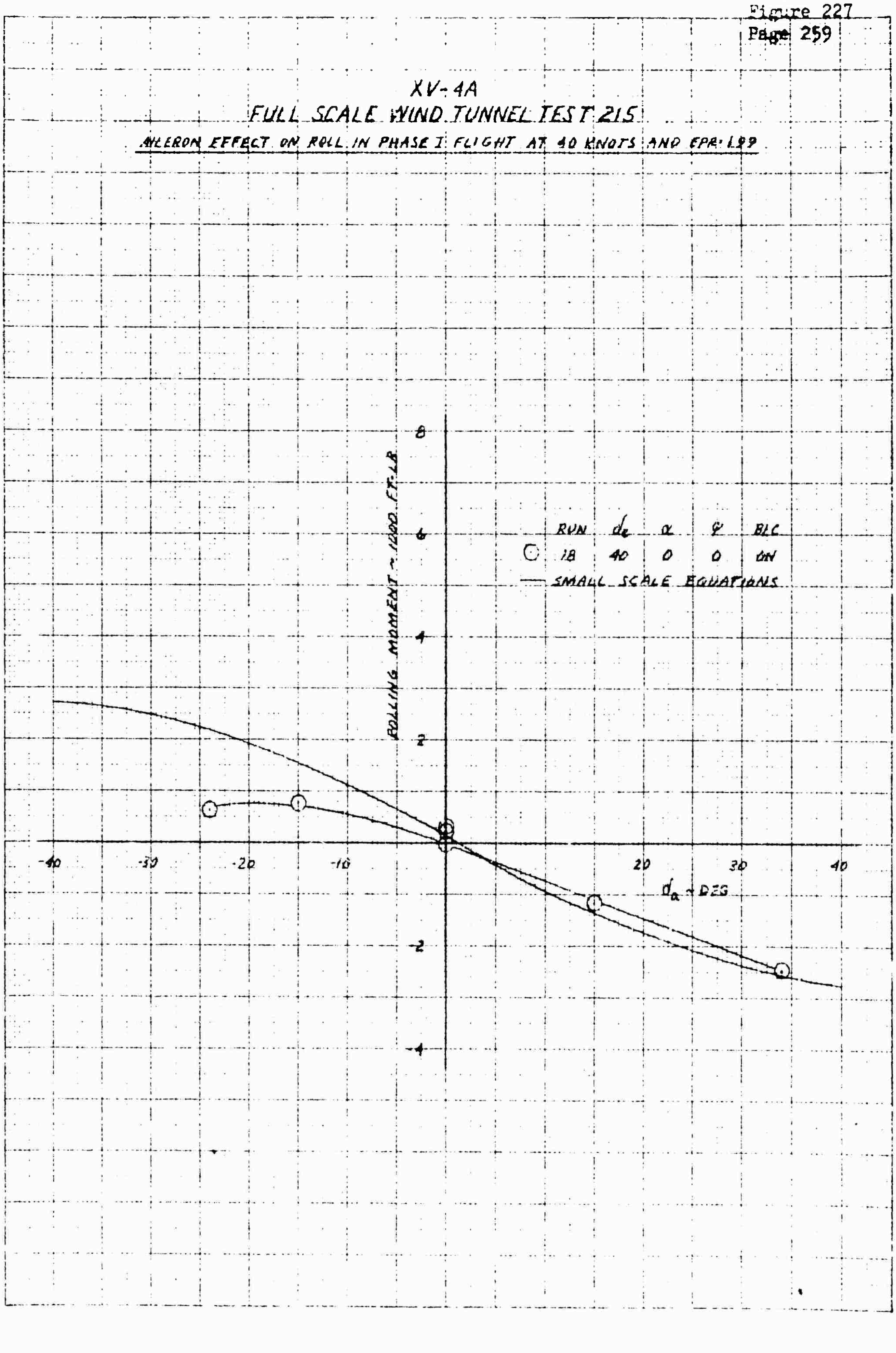
XV-4A
FULL SCALE WIND TUNNEL TEST 215
AILERON EFFECT ON ROLL IN PHASE I FLIGHT AT 40 KNOTS AND EPR: 1.99
ROLLING MOMENT ~ 1000 FT-LB
8
6
4
2
-2
-4
-40
-30
-20
-10
20
30
40
δ_a ~ DEG
RUN δ_e α ψ BLC
18 40 0 0 ON
SMALL SCALE EQUATIONS

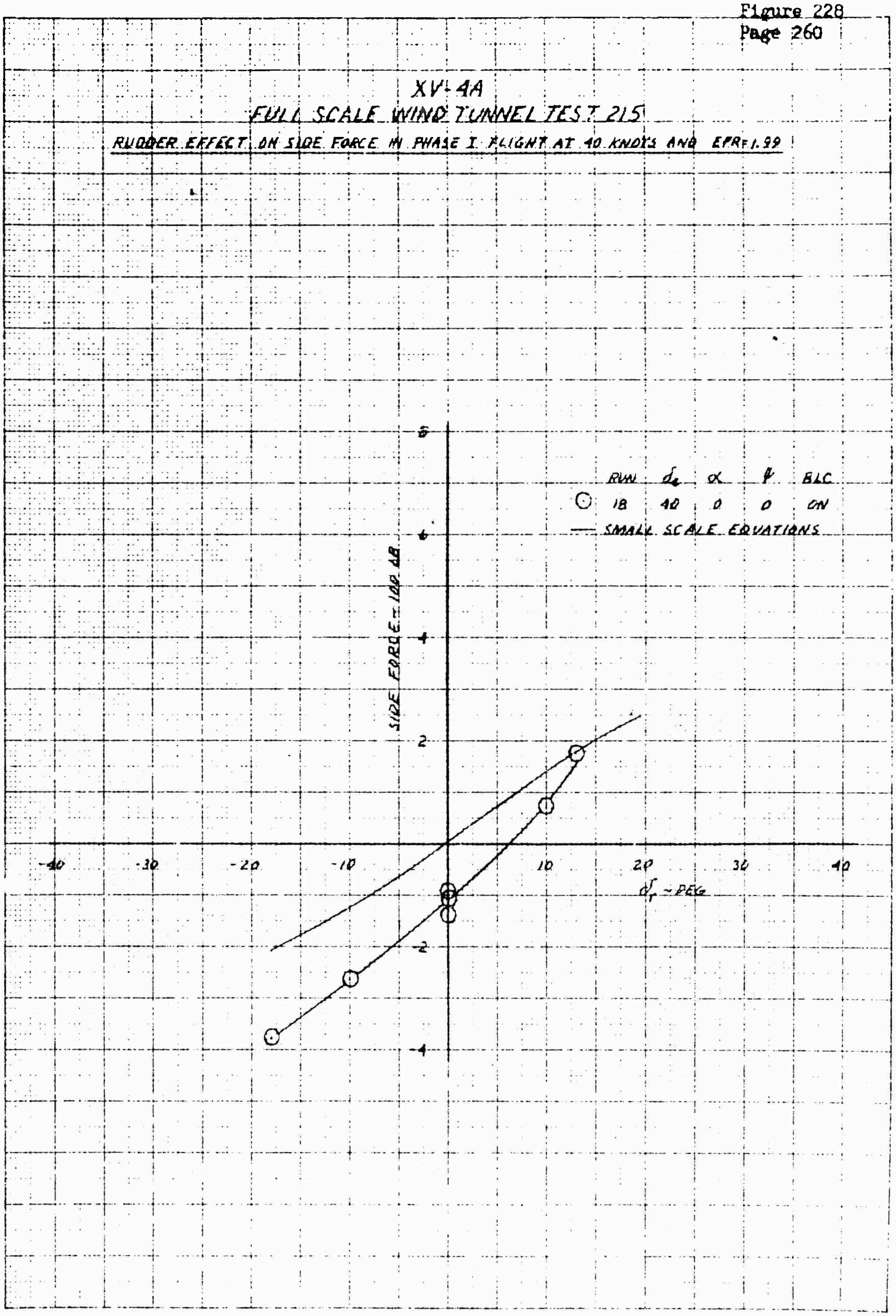
XV-4A
FULL SCALE WIND TUNNEL TEST 215
RUDDER EFFECT ON SIDE FORCE IN PHASE I FLIGHT AT 40 KNOTS AND EPR=1.99
RUN δ α ψ BLC
18 40 0 0 ON
SMALL SCALE EQUATIONS
SIDE FORCE ~ 100 LB
δr ~ DEG
-40 -30 -20 -10 10 20 30 40
6 4 2 -2 -4

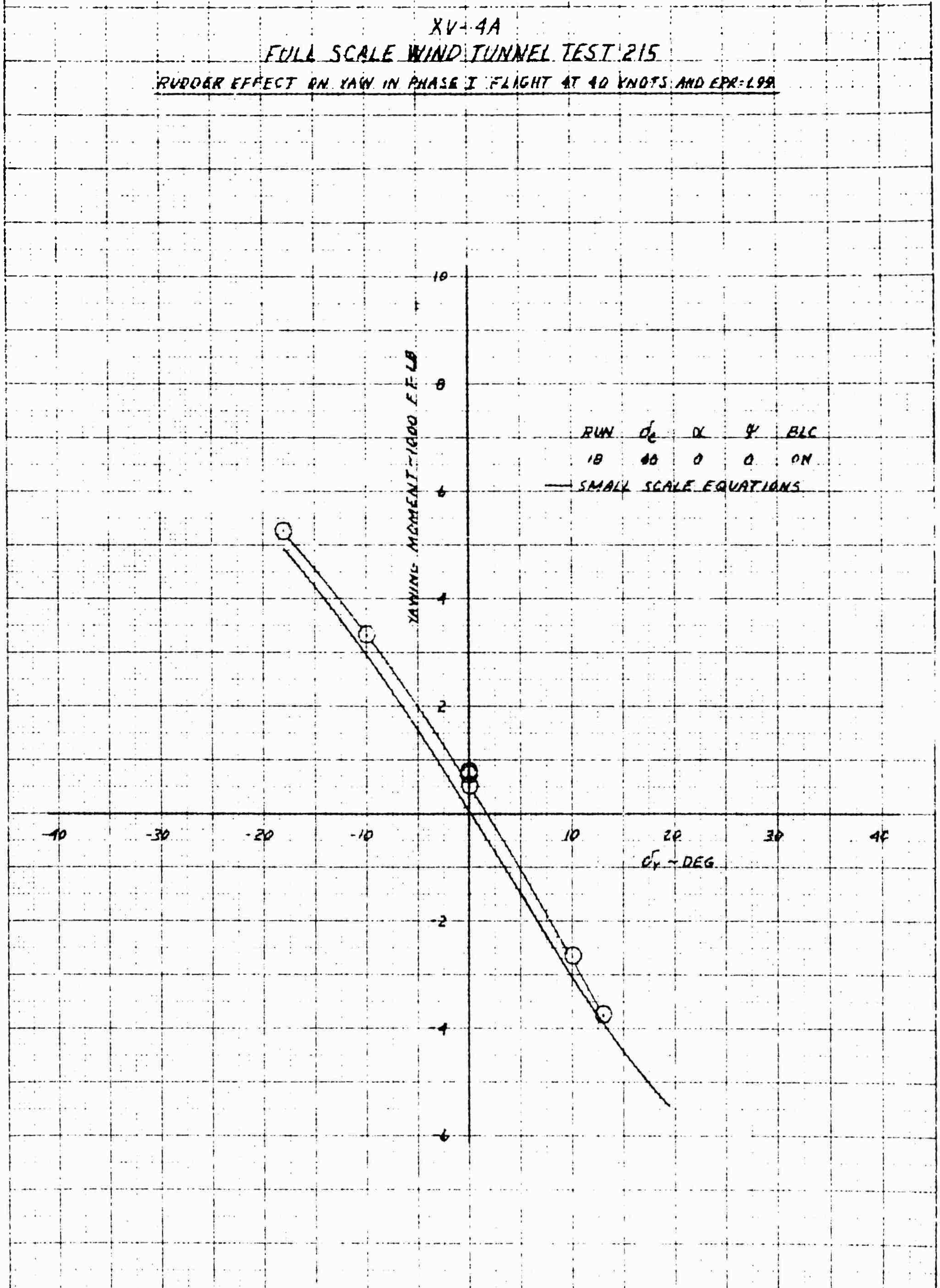
XV-4A
FULL SCALE WIND TUNNEL TEST 215
RUDDER EFFECT ON YAW IN PHASE I FLIGHT AT 40 KNOTS AND EPR=1.98
YAWING MOMENT ~1000 FT-LB
10
8
6
4
2
-2
-4
-6
-40
-30
-20
-10
10
20
30
40
δ_r ~ DEG
RUN δ_c α ψ BLC
18 40 0 0 ON
— SMALL SCALE EQUATIONS

XV-4A
FULL SCALE WIND TUNNEL TEST 215
RUDDER EFFECT ON ROLL IN PHASE I FLIGHT AT 40 KNOTS AND EPR = 1.99

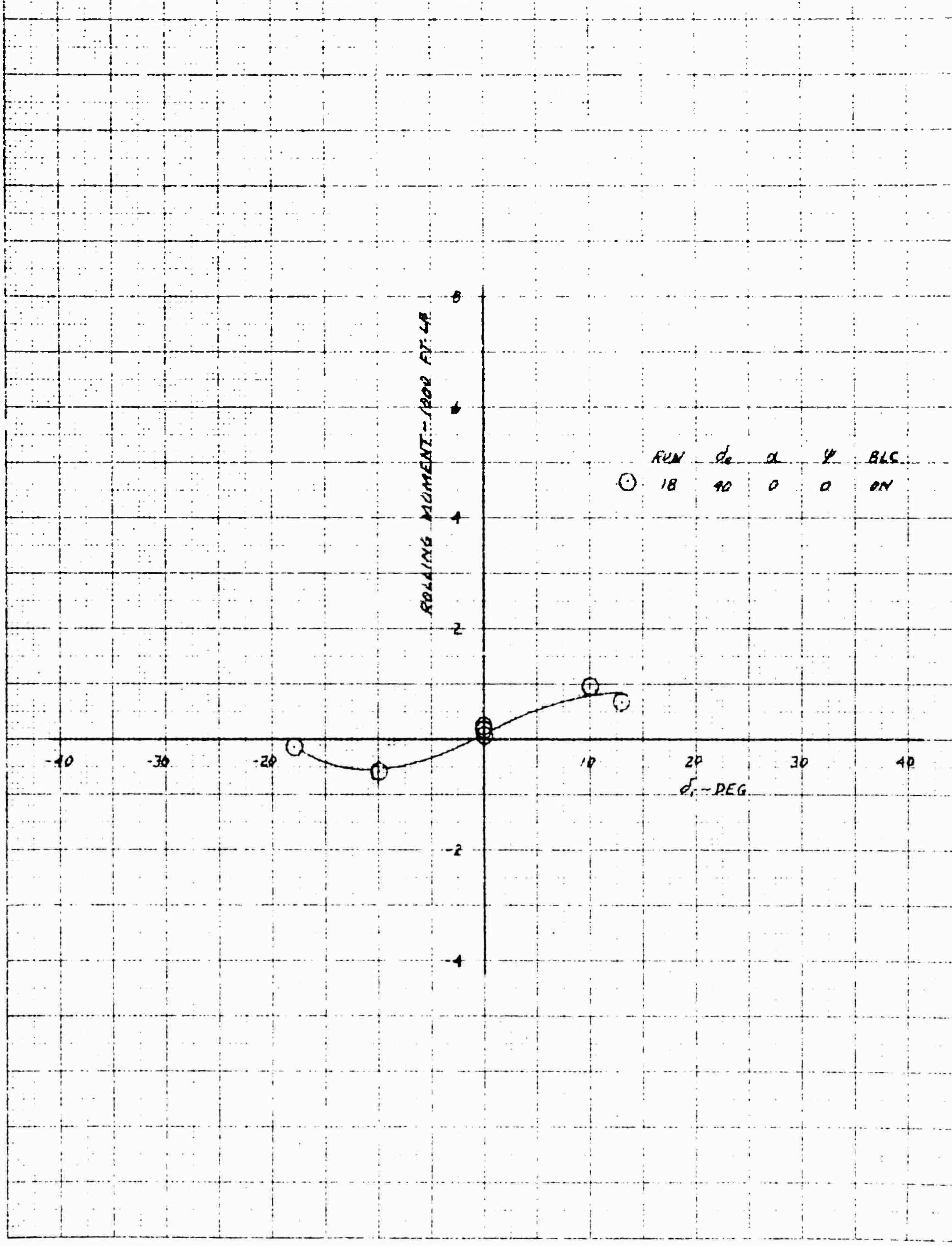

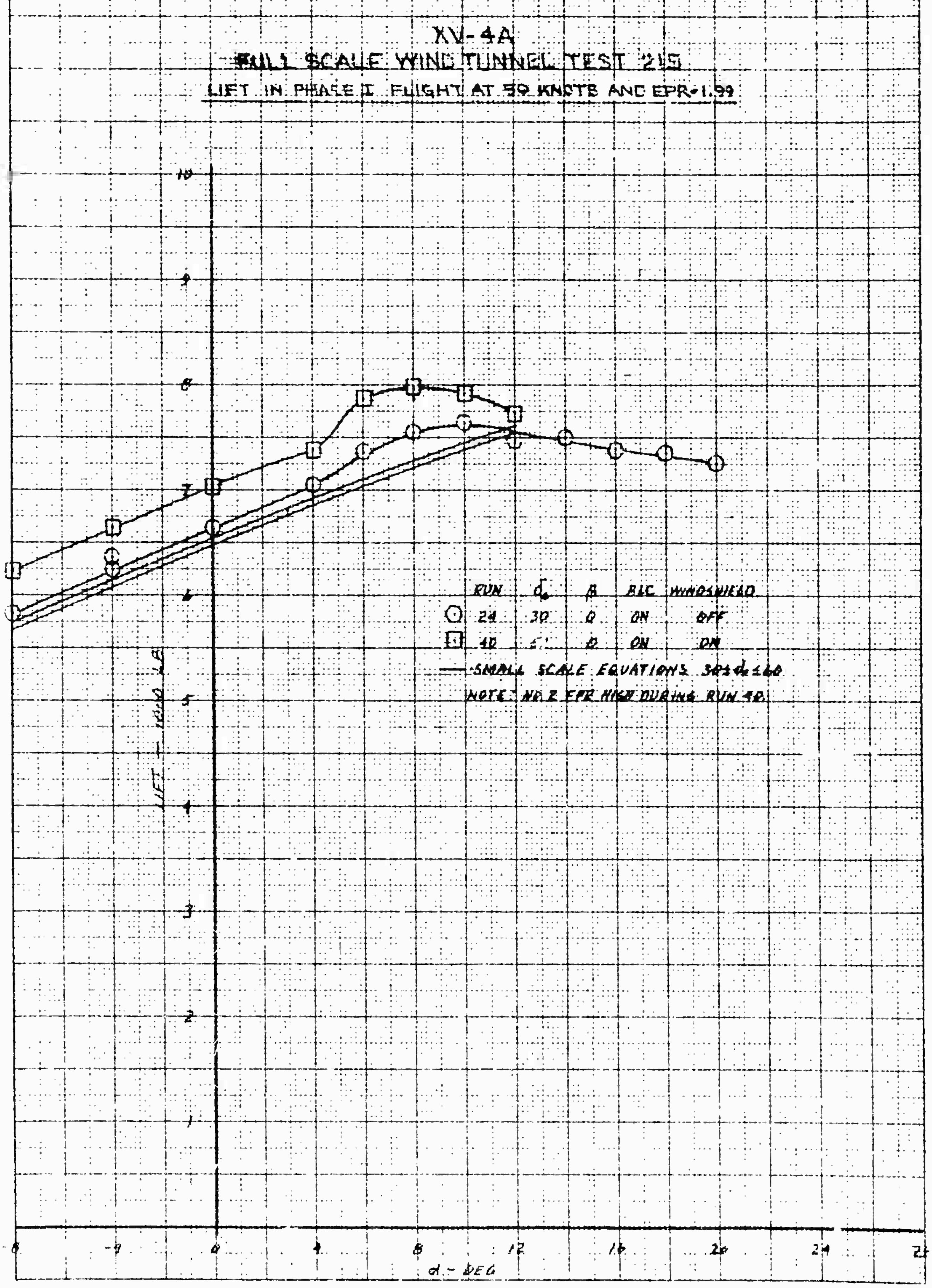
XV-4A
FULL SCALE WIND TUNNEL TEST 215
LIFT IN PHASE II FLIGHT AT 59 KNOTS AND EPR=1.99
RUN
BLC
WINDSHIELD
24
30
ON
OFF
40
ON
ON
SMALL SCALE EQUATIONS
NOTE: NO. 2 EPR HIGH DURING RUN 40.
LIFT — 1000 LB
α — DEG
10
9
8
7
6
5
4
3
2
1
-8
-4
0
4
8
12
16
20
24

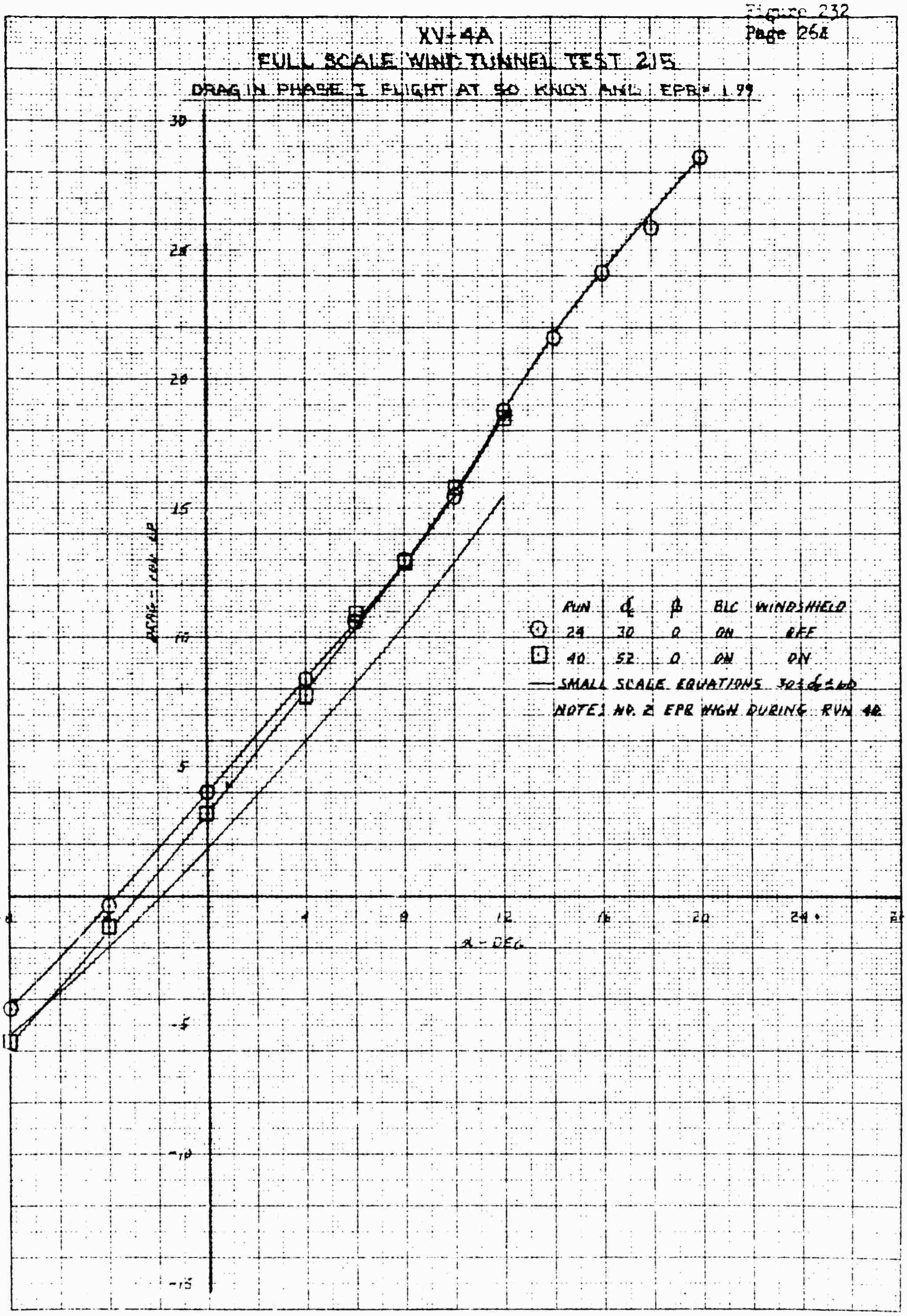
XV-4A
FULL SCALE WIND TUNNEL TEST 215
DRAG IN PHASE I FLIGHT AT 50 KNOTS AND EPR = 1.99
30
25
20
15
10
5
-5
-10
-15
DRAG - 1000 LB
-8
4
8
12
16
20
24
α - DEG
RUN δf β BLC WINDSHIELD
24 30 0 ON OFF
40 52 0 ON ON
SMALL SCALE EQUATIONS [illegible]
NOTE: NO. 2 EPR HIGH DURING RUN 40

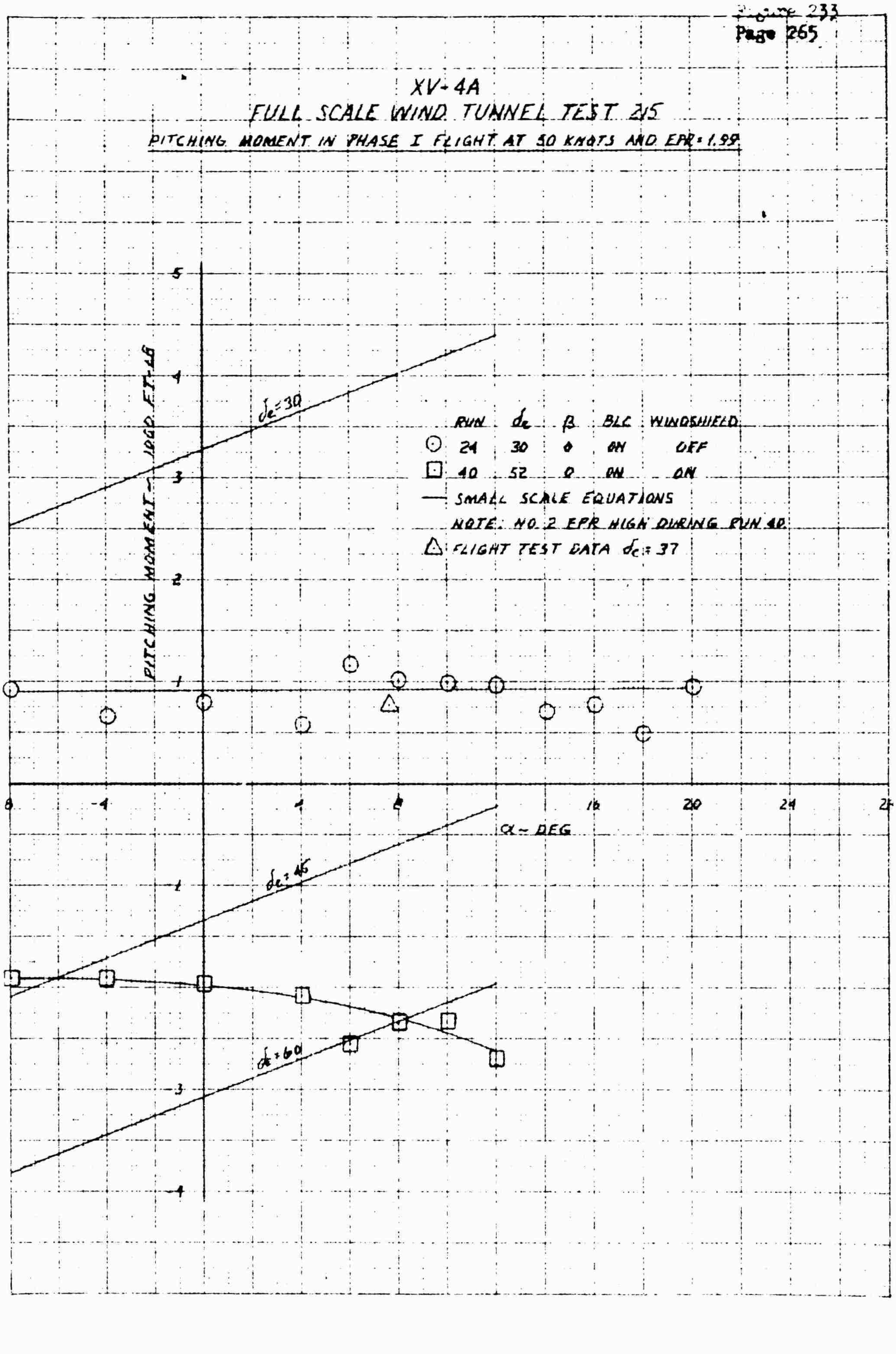

XV-4A
FULL SCALE WIND TUNNEL TEST 215
PITCHING MOMENT IN PHASE I FLIGHT AT 50 KNOTS AND EPR = 1.99
PITCHING MOMENT ~ 1000 FT-LB
α ~ DEG
δe = 30
δe = 45
δe = 60
RUN δe β BLC WINDSHIELD
24 30 0 ON OFF
40 52 0 ON ON
SMALL SCALE EQUATIONS
NOTE: NO. 2 EPR HIGH DURING RUN 40
FLIGHT TEST DATA δe = 37

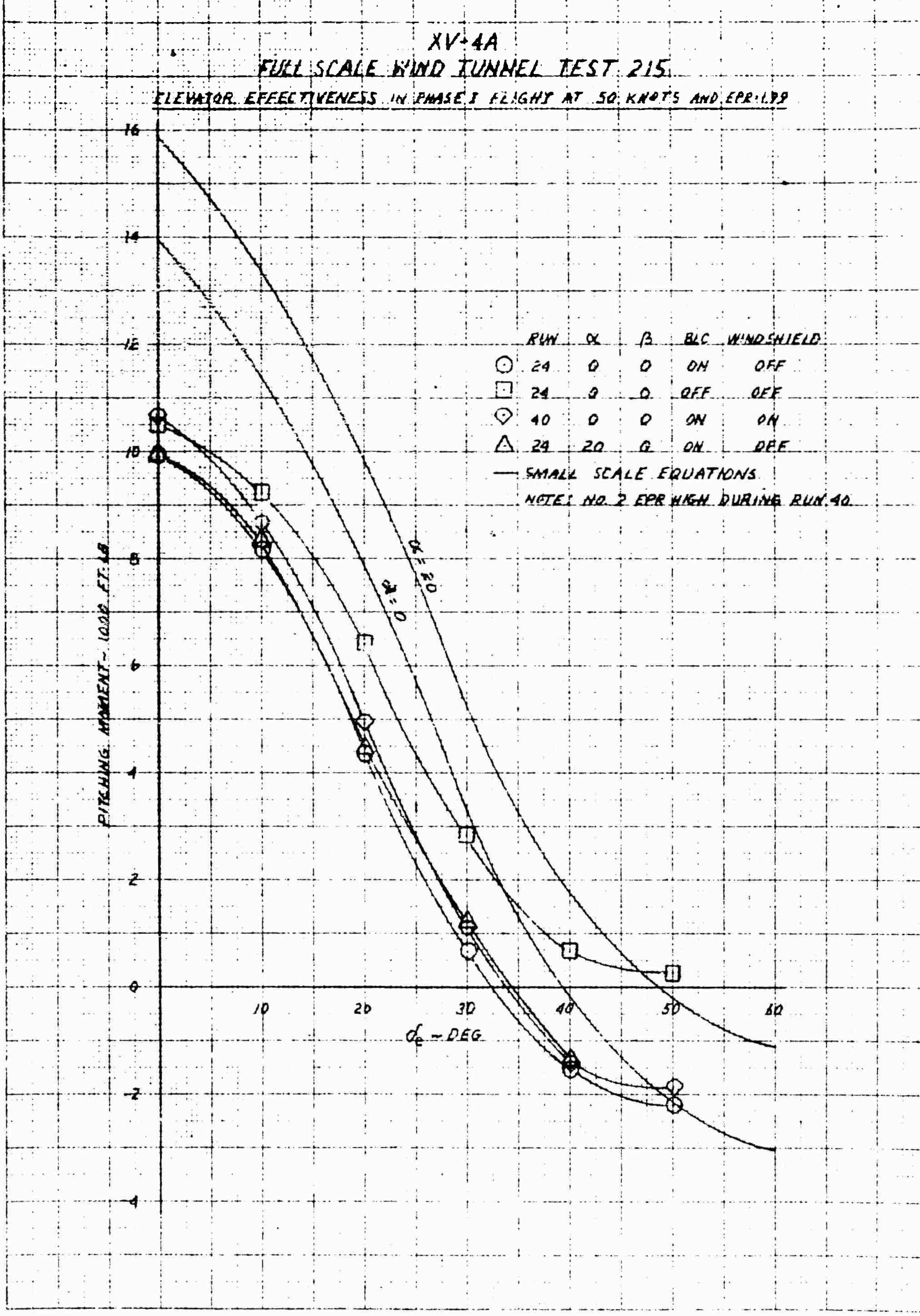
XV-4A
FULL SCALE WIND TUNNEL TEST 215
ELEVATOR EFFECTIVENESS IN PHASE I FLIGHT AT 50 KNOTS AND EPR 1.79
RUN α β BLC WINDSHIELD
24 0 0 ON OFF
24 0 0 OFF OFF
40 0 0 ON ON
24 20 0 ON OFF
SMALL SCALE EQUATIONS
NOTE: NO. 2 EPR HIGH DURING RUN 40
α = 20
α = 0
PITCHING MOMENT ~ 1000 FT-LB
δ_e ~ DEG
16
14
12
10
8
6
4
2
0
-2
-4
10
20
30
40
50
60

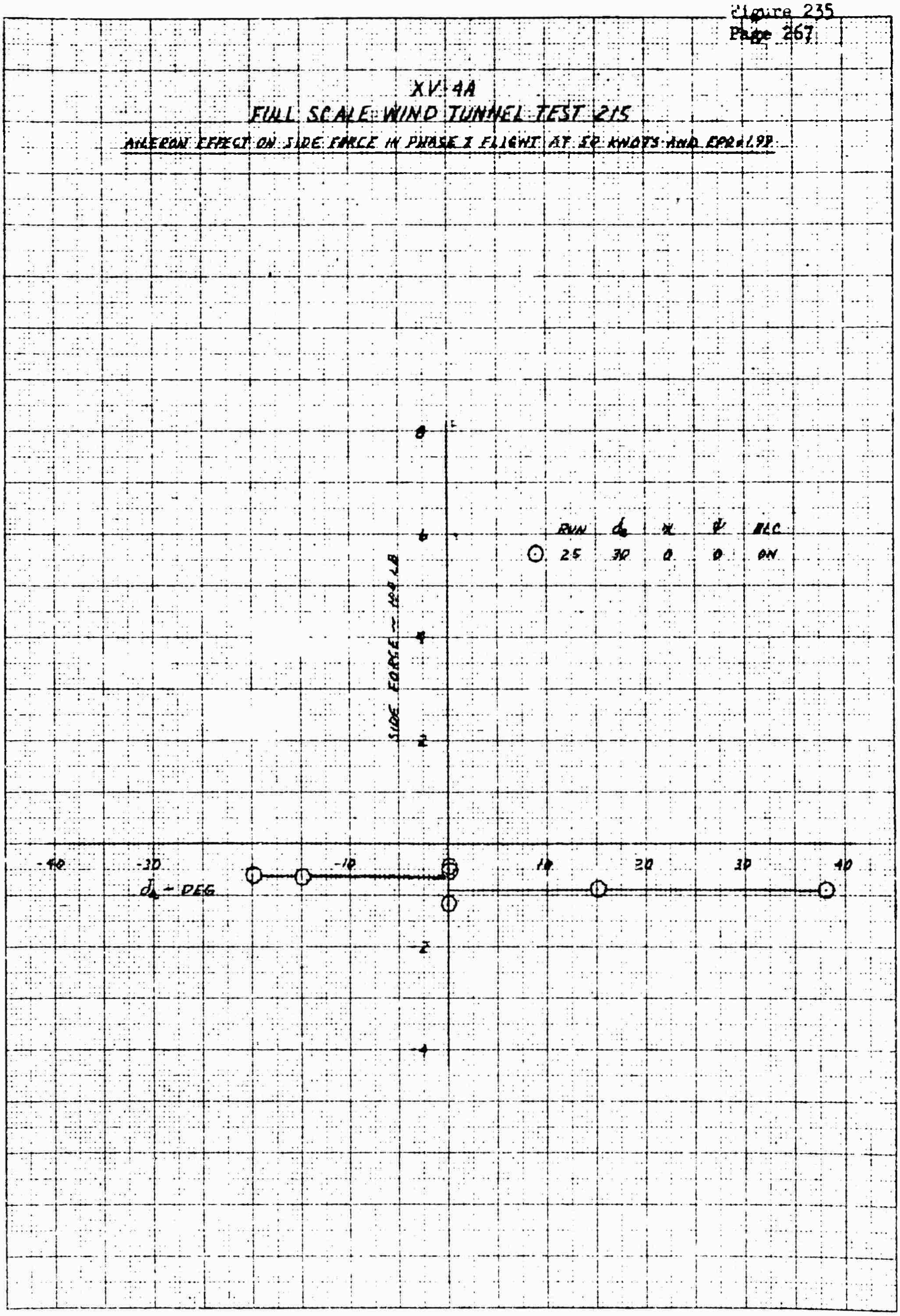
XV-4A
FULL SCALE WIND TUNNEL TEST 215
AILERON EFFECT ON SIDE FORCE IN PHASE I FLIGHT AT 50 KNOTS AND EPR=1.99
RUN
25
30
0
0
ON
SIDE FORCE ~ 100 LB
-40
-30
-10
10
20
30
40
δa ~ DEG

XV-4A

FULL SCALE WIND TUNNEL TEST 215

AILERON EFFECT ON YAW IN PHASE I FLIGHT AT 50 KNOTS AND EPR=1.99

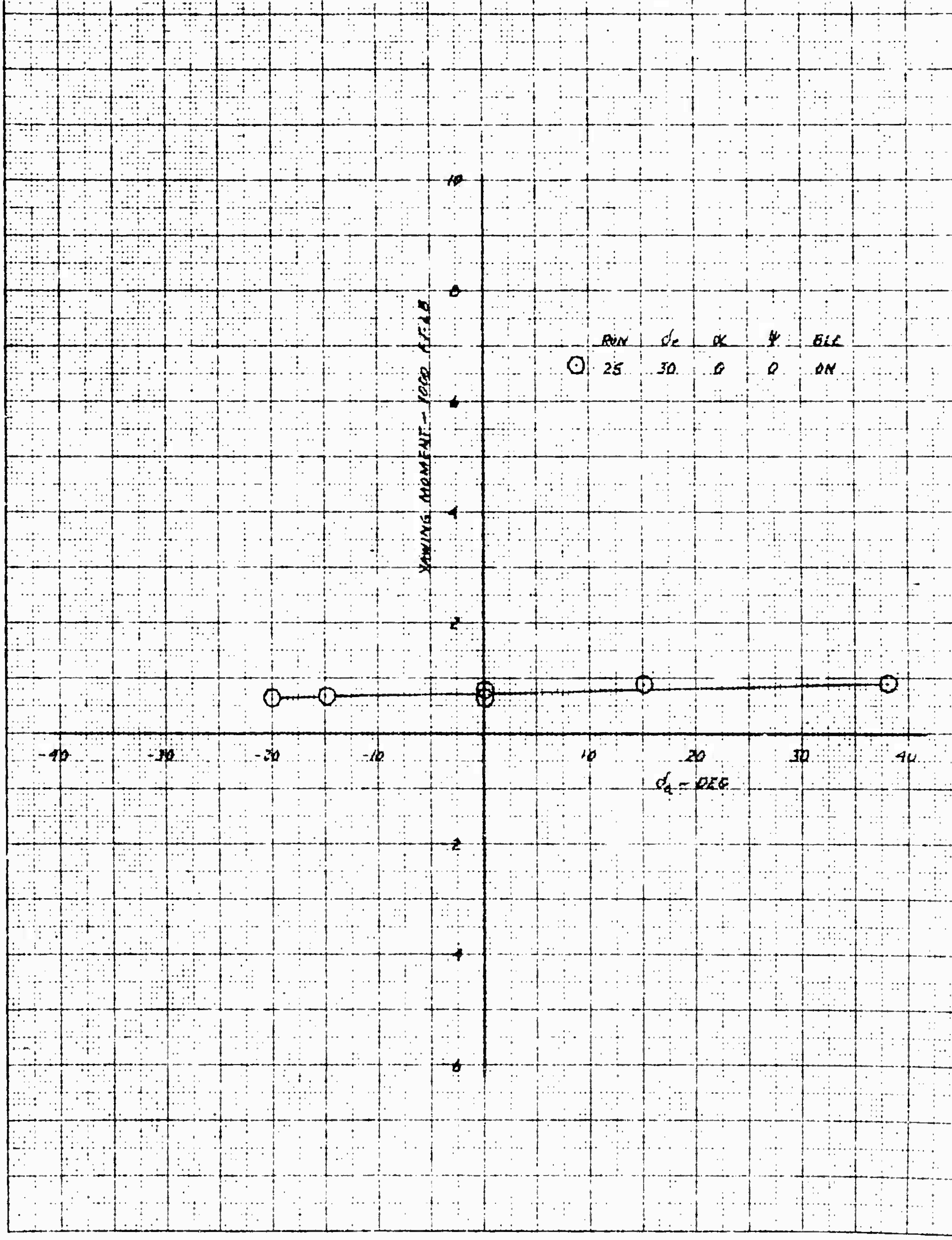

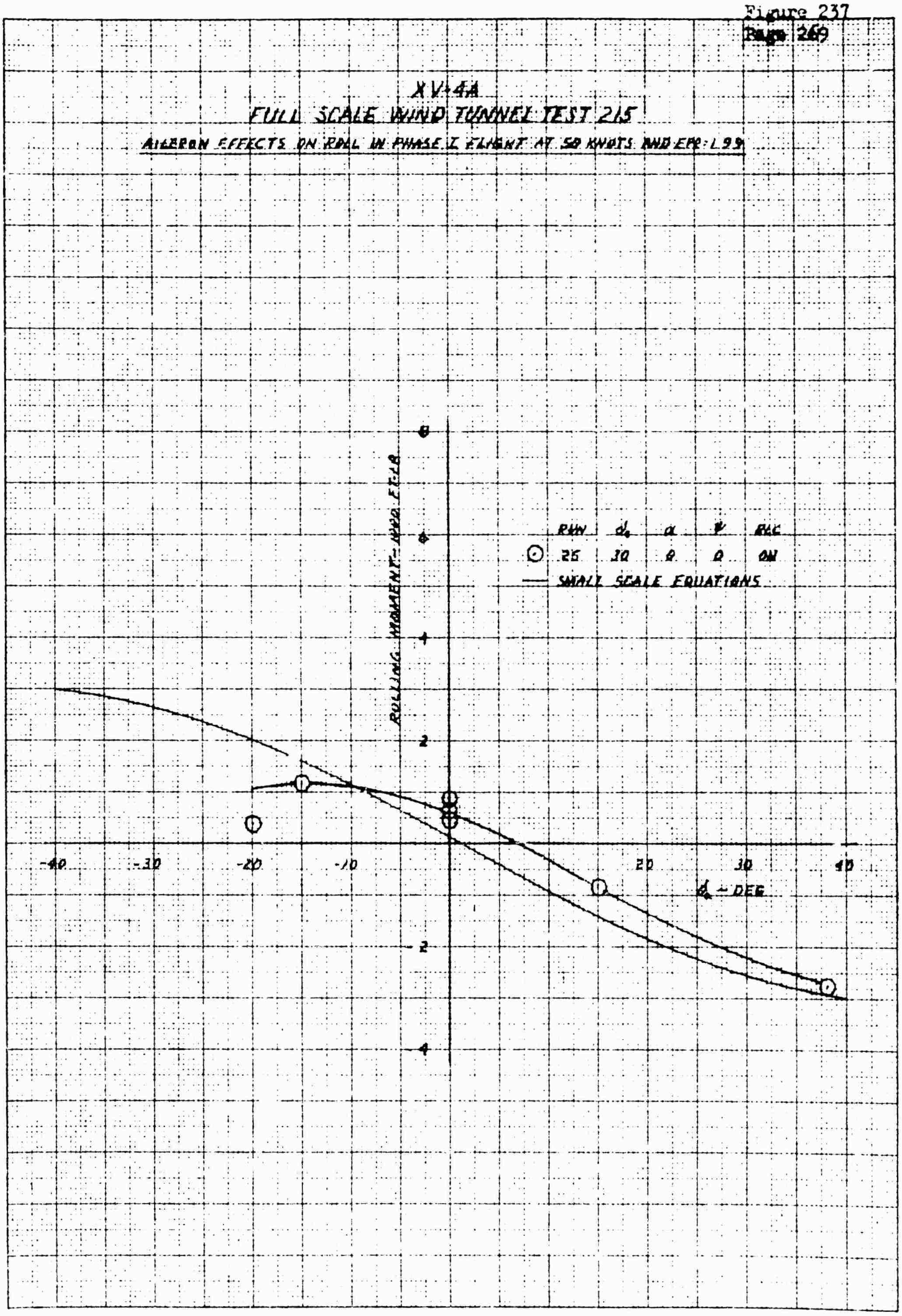
XV-4A
FULL SCALE WIND TUNNEL TEST 215
AILERON EFFECTS ON ROLL IN PHASE I FLIGHT AT 50 KNOTS AND EPR: 1.93
ROLLING MOMENT - 1000 FT-LB
RUN
25
30
0
0
ON
SMALL SCALE EQUATIONS
-40
-30
-20
-10
20
30
40
- DEG
8
6
4
2
2
4

XV-4A
FULL SCALE WIND TUNNEL TEST 215
RUDDER EFFECT ON SIDE FORCE IN PHASE I FLIGHT AT 50 KNOTS AND EPR=1.99

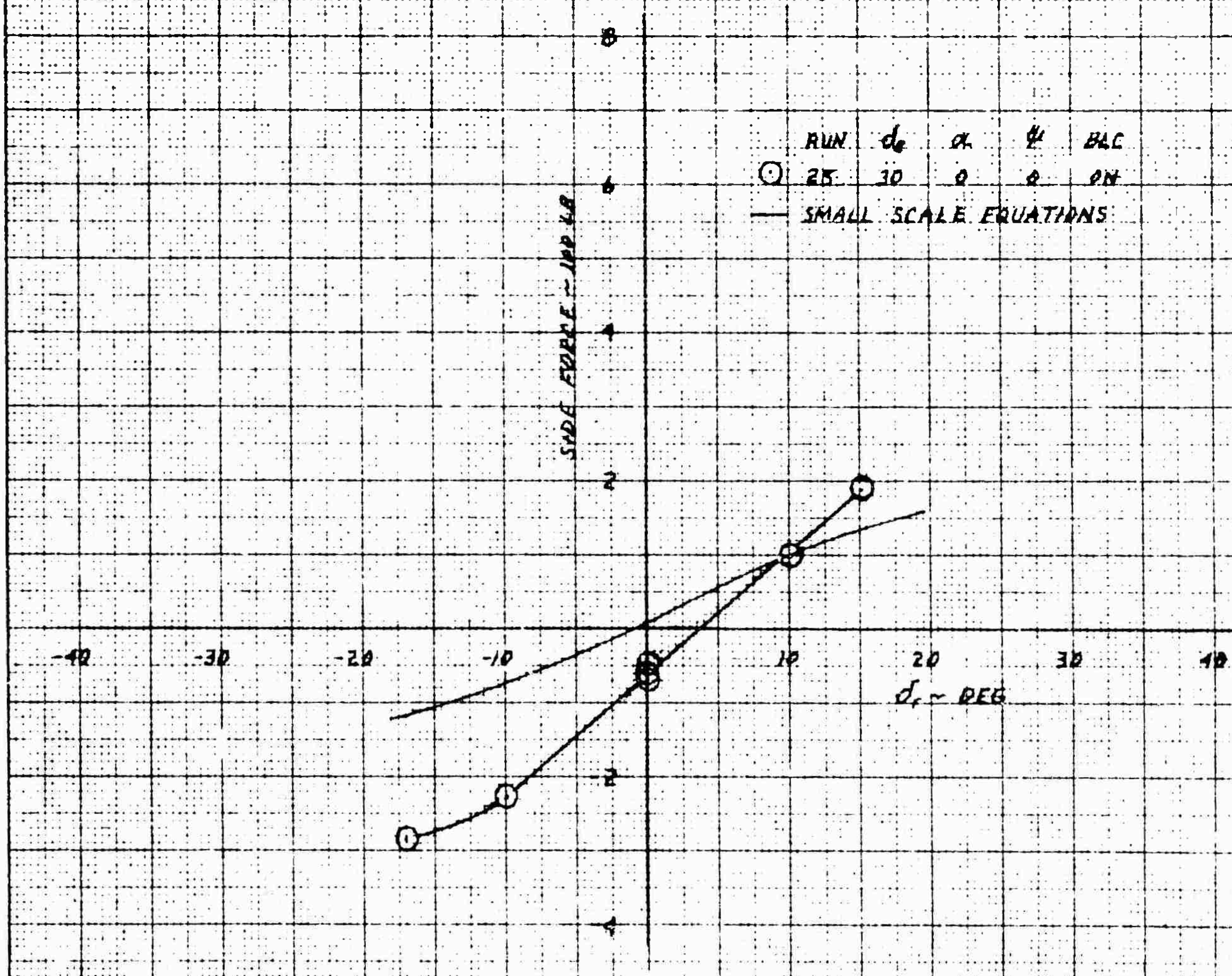

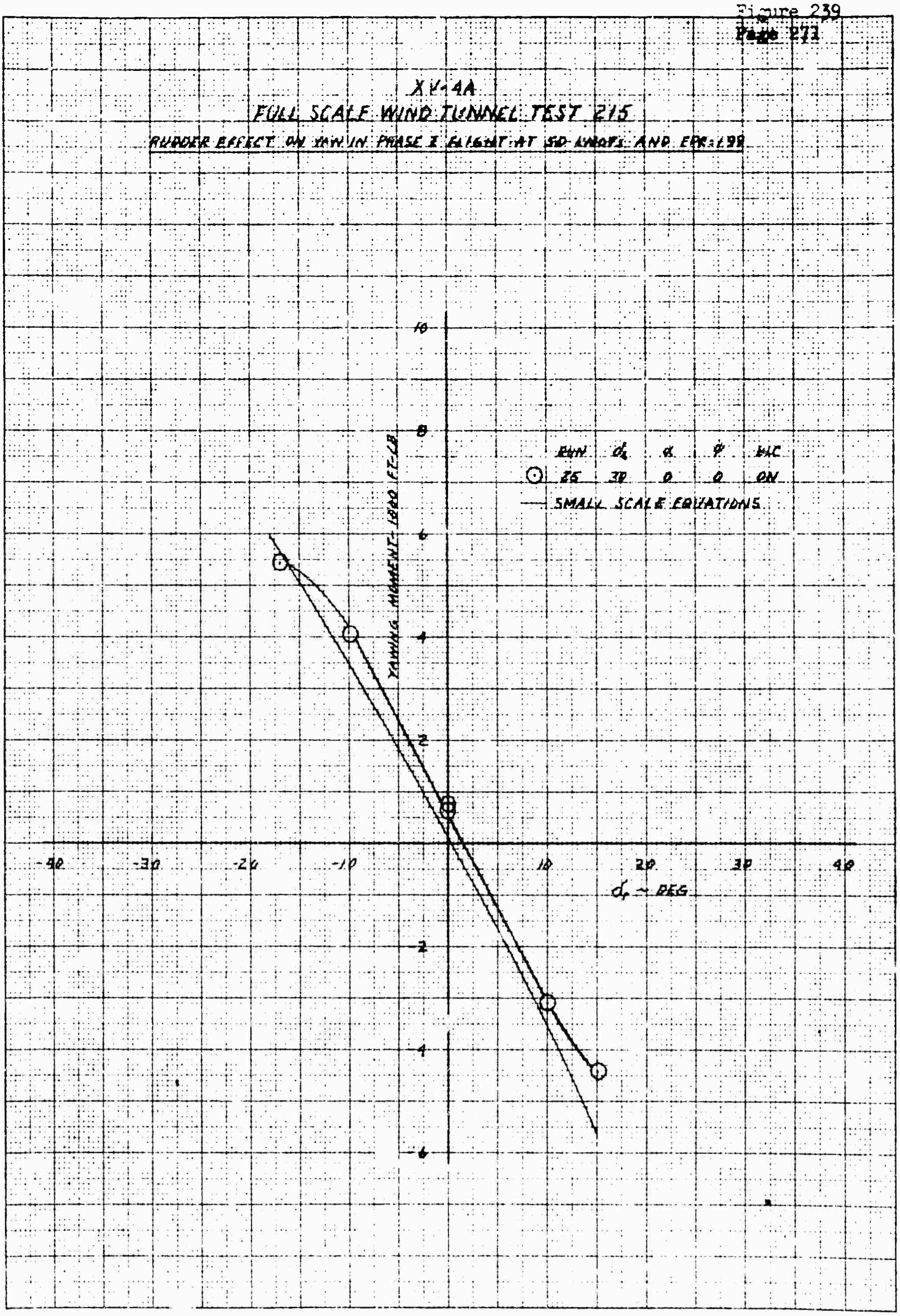
XV-4A
FULL SCALE WIND TUNNEL TEST 215
RUDDER EFFECT ON YAW IN PHASE I FLIGHT AT 50 KNOTS AND EPR=1.99
RUN
25
SMALL SCALE EQUATIONS
YAWING MOMENT-1000 FT-LB
10
8
6
4
2
-2
-4
-6
-40
-30
-20
-10
10
20
30
40
DEG

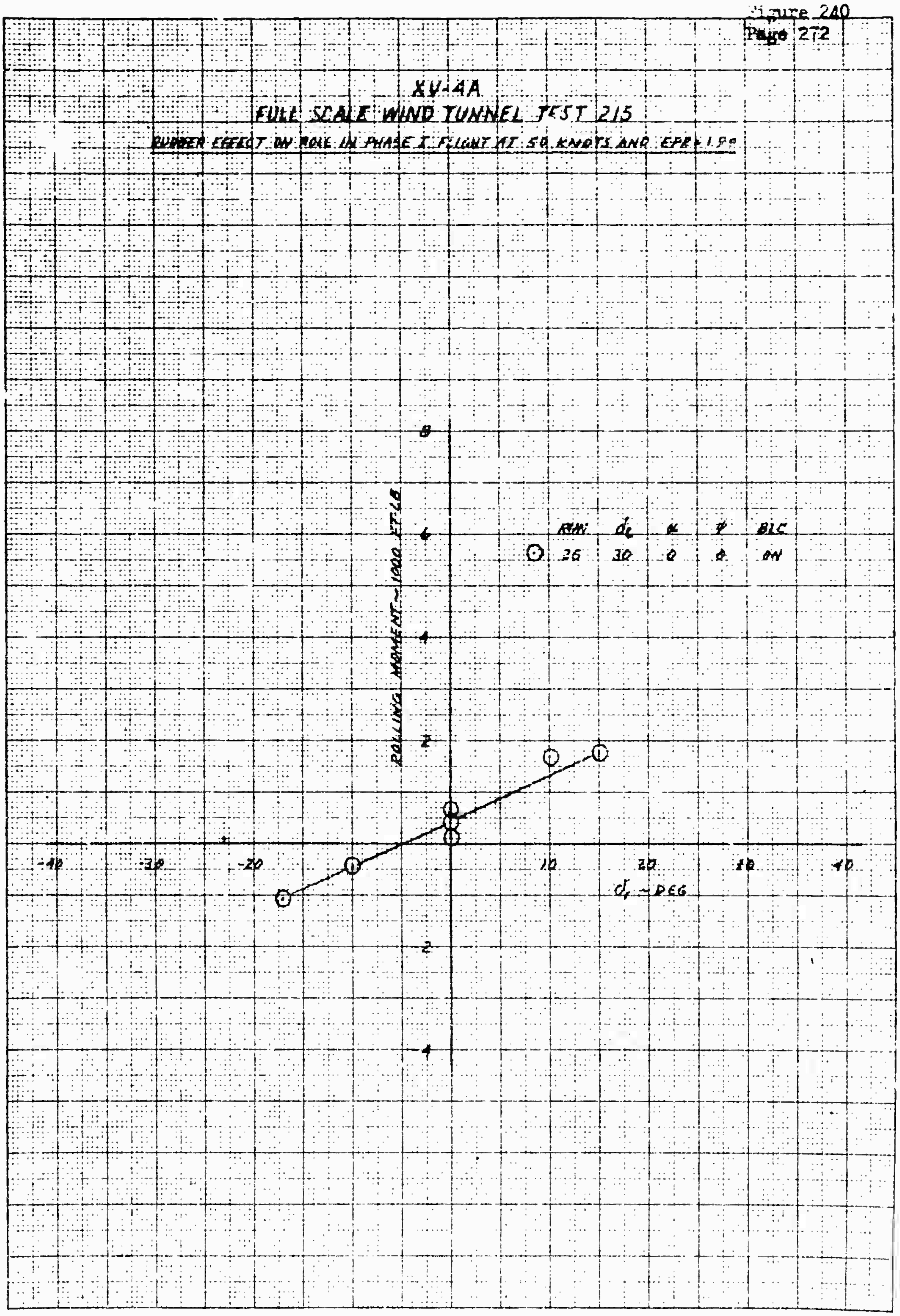
XV-4A
FULL SCALE WIND TUNNEL TEST 215
RUDDER EFFECT ON ROLL IN PHASE I FLIGHT AT 50 KNOTS AND EPR=1.9
RPM
26
30
0
0
BLC
ON
ROLLING MOMENT ~ 1000 FT-LB
8
6
4
2
2
4
-40
-30
-20
10
20
30
40
~ DEG

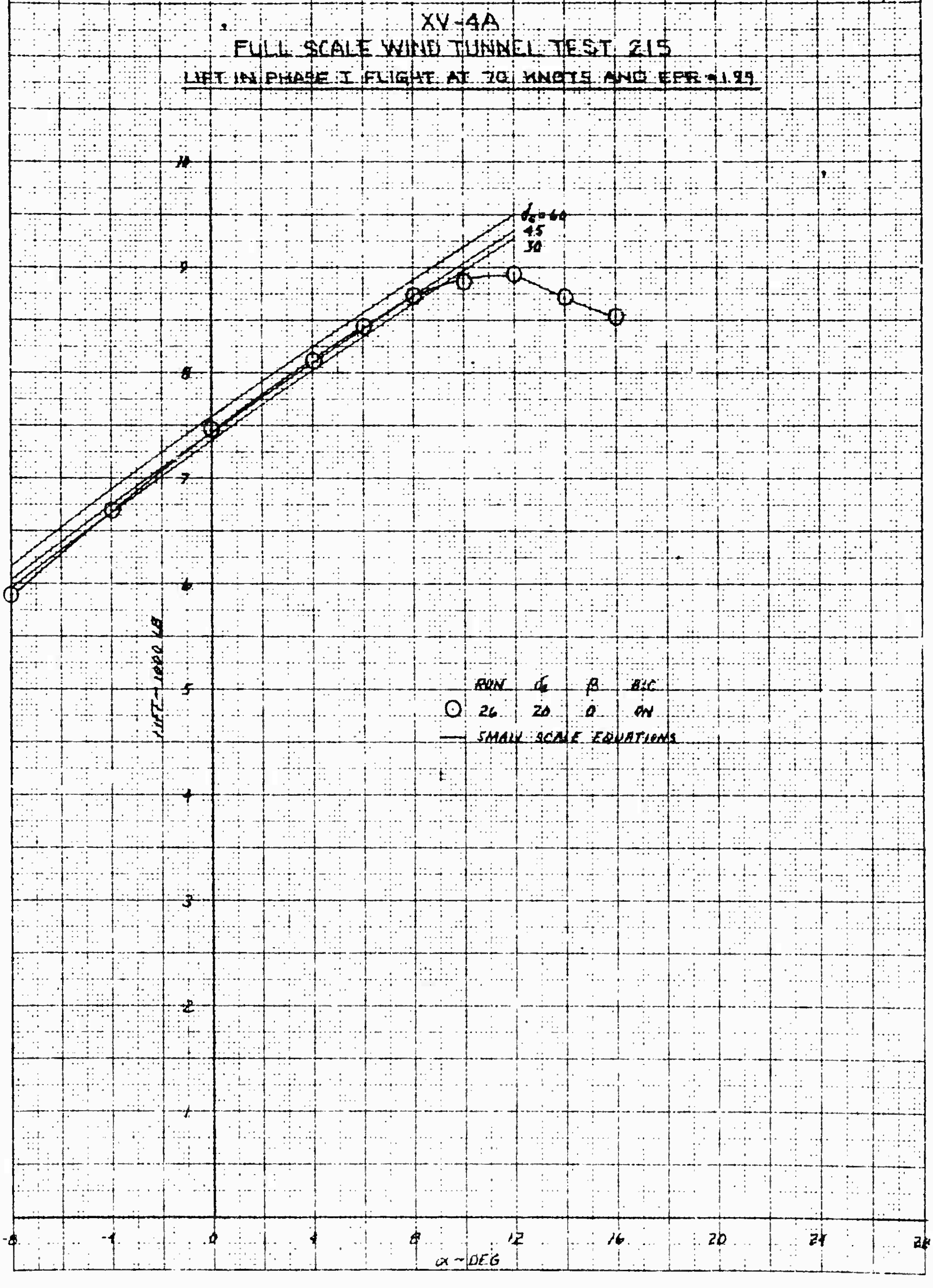
XV-4A
FULL SCALE WIND TUNNEL TEST 215
LIFT IN PHASE I FLIGHT AT 70 KNOTS AND EPR =1.95
δ=60
45
30
RUN δ β B/C
26 20 0 ON
SMALL SCALE EQUATIONS
LIFT ~ 1000 LB
α ~ DEG

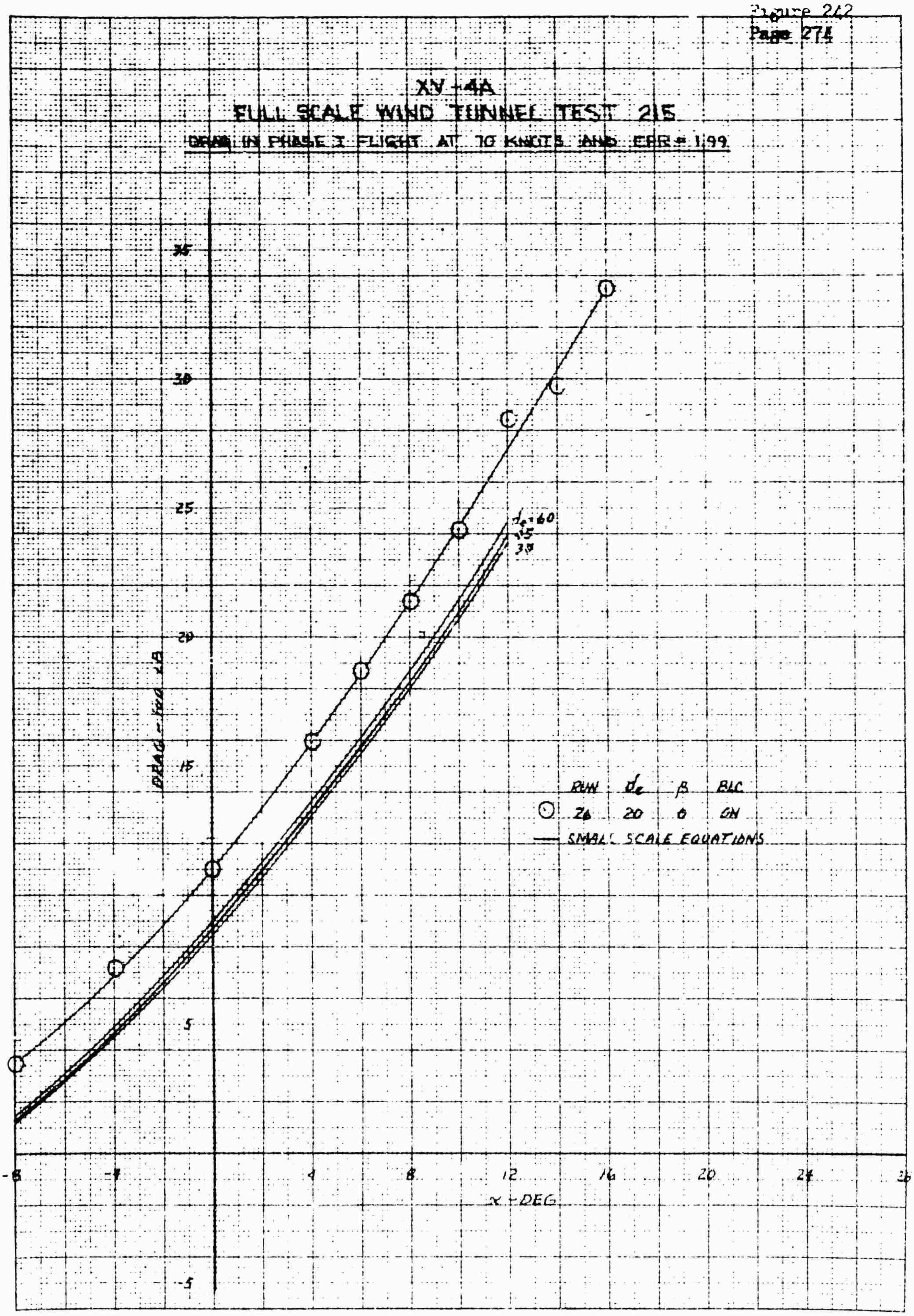
XV-4A
FULL SCALE WIND TUNNEL TEST 215
DRAG IN PHASE I FLIGHT AT 10 KNOTS AND EPR = 1.99
DRAG - 100 LB
α - DEG
RUN
δe
β
BLC
26
20
0
ON
SMALL SCALE EQUATIONS
δe = 60
45
30

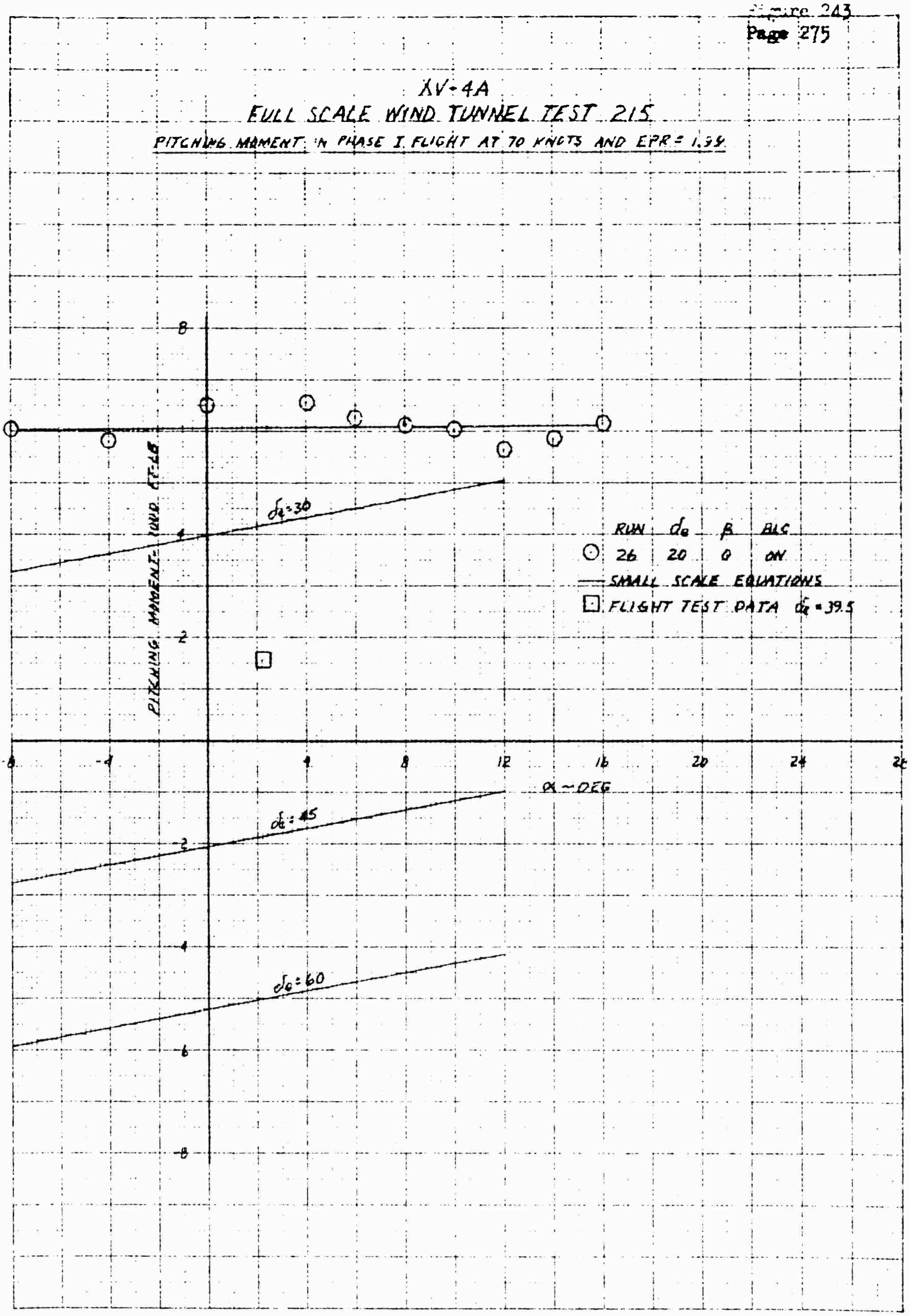
XV-4A
FULL SCALE WIND TUNNEL TEST 215
PITCHING MOMENT IN PHASE I FLIGHT AT 70 KNOTS AND EPR = 1.39
PITCHING MOMENT - 1000 FT-LB
α ~ DEG
δ_e=30
δ_e=45
δ_e=60
RUN δ_e β BLC
26 20 0 ON
SMALL SCALE EQUATIONS
FLIGHT TEST DATA δ_e = 39.5

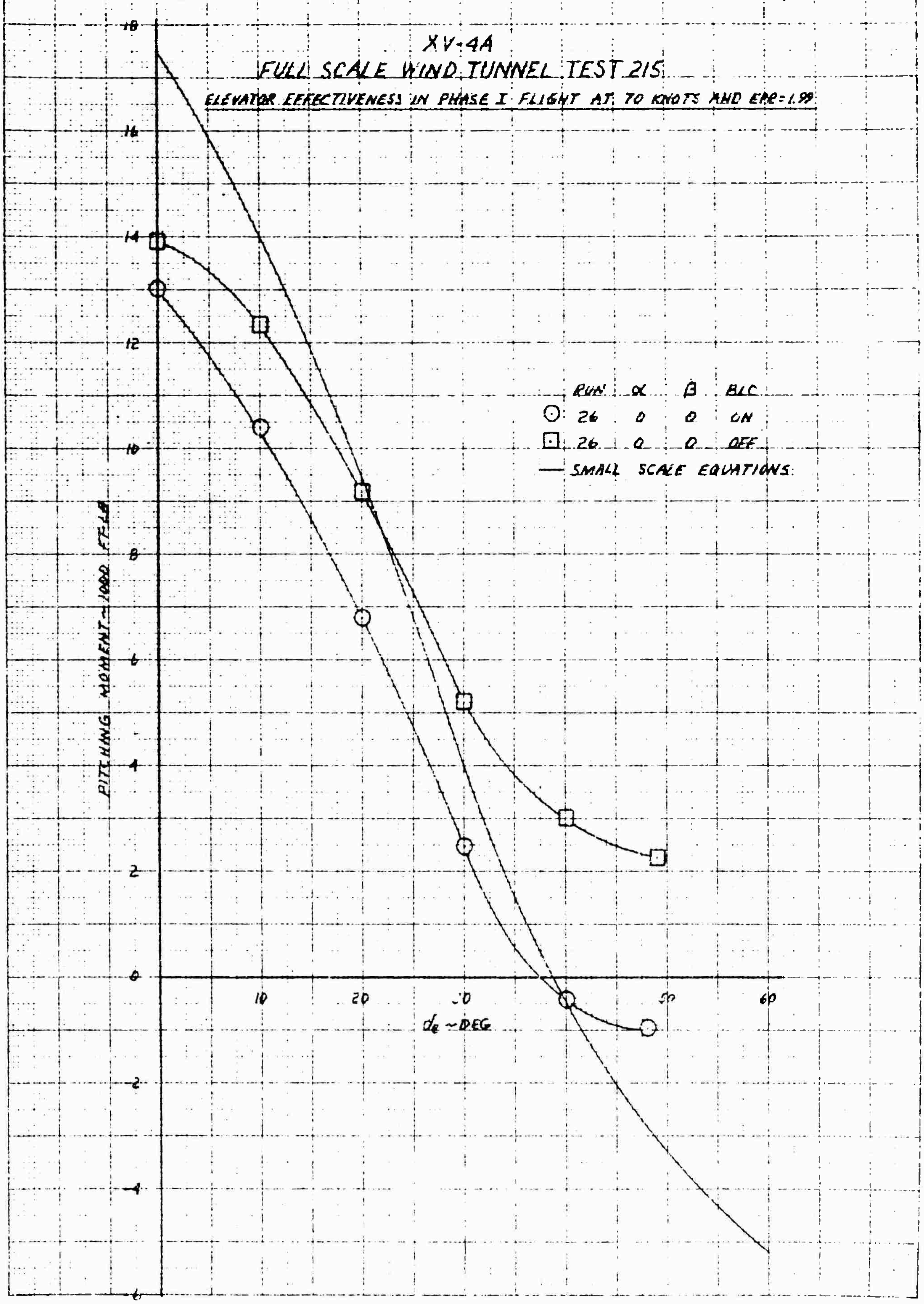
XV-4A
FULL SCALE WIND TUNNEL TEST 215
ELEVATOR EFFECTIVENESS IN PHASE I FLIGHT AT 70 KNOTS AND EPR=1.99
RUN α β BLC
26 0 0 ON
26 0 0 OFF
SMALL SCALE EQUATIONS
PITCHING MOMENT ~ 1000 FT-LB
δ_e ~ DEG
18
16
14
12
10
8
6
4
2
0
-2
-4
-6
10
20
30
40
50
60

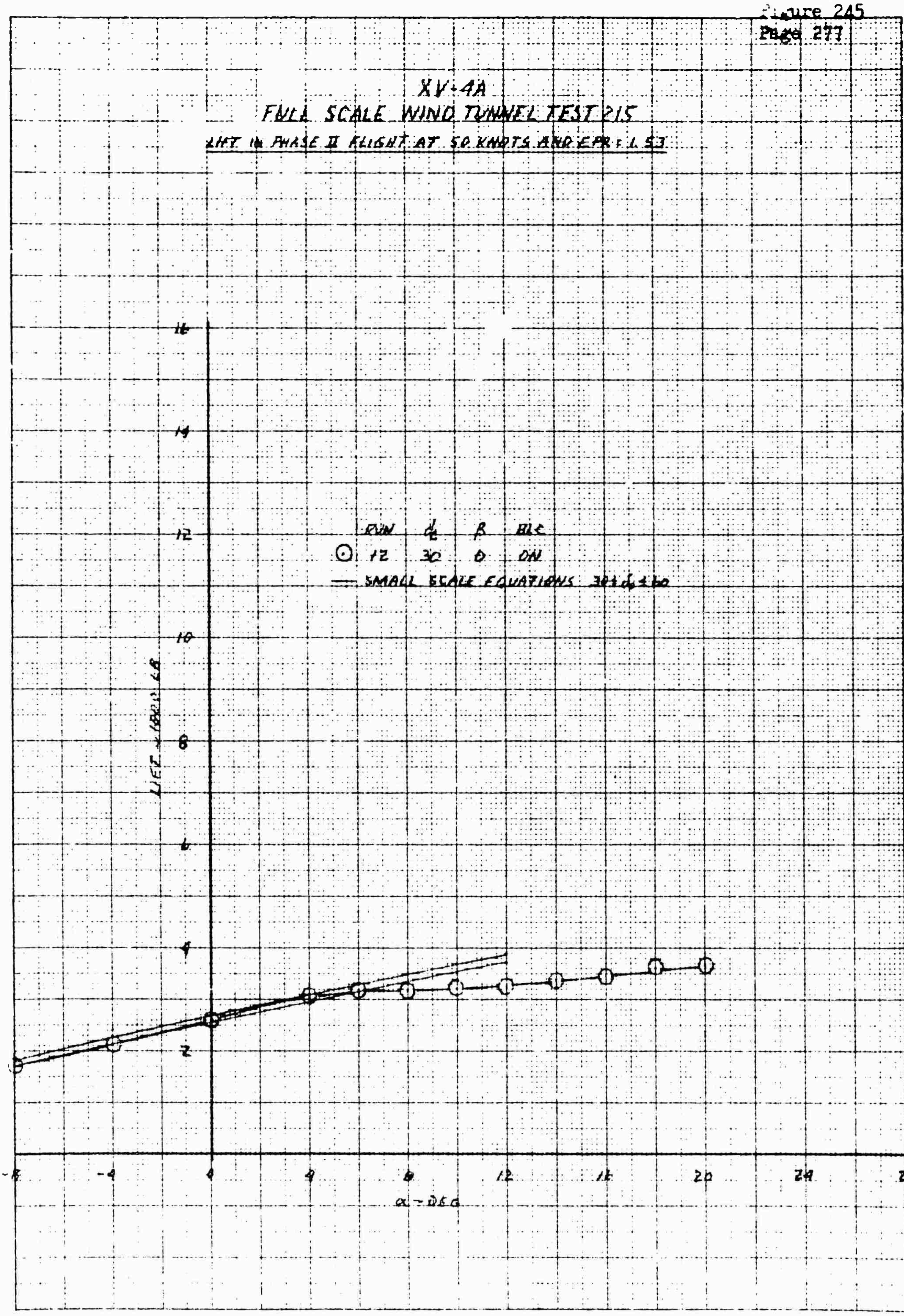
XV-4A
FULL SCALE WIND TUNNEL TEST 215
LIFT IN PHASE II FLIGHT AT 50 KNOTS AND EPR = 1.53
RUN
β
BLC
12
30
0
ON
SMALL SCALE EQUATIONS
LIFT × 1000 LB
α ~ DEG
16
14
12
10
8
6
4
2
-8
-4
0
4
8
12
16
20
24
28

XV-4A
FULL SCALE WIND TUNNEL TEST 215
DRAG IN PHASE II FLIGHT AT 52 KNOTS AND EPR=1.53

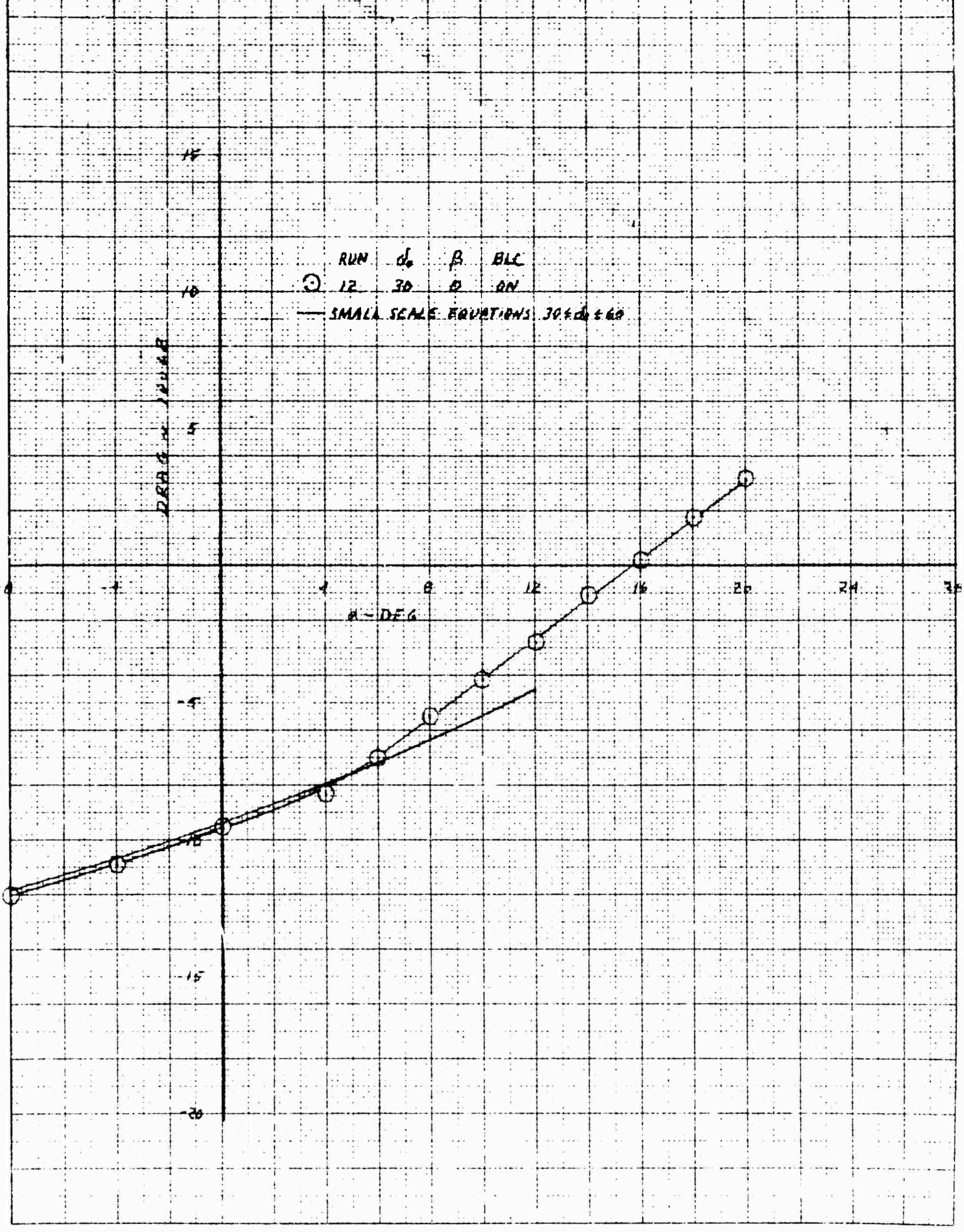

XV-4A
FULL SCALE WIND TUNNEL TEST 215
PITCHING MOMENT IN PHASE II FLIGHT AT 50 KNOTS AND EPR = 1.53

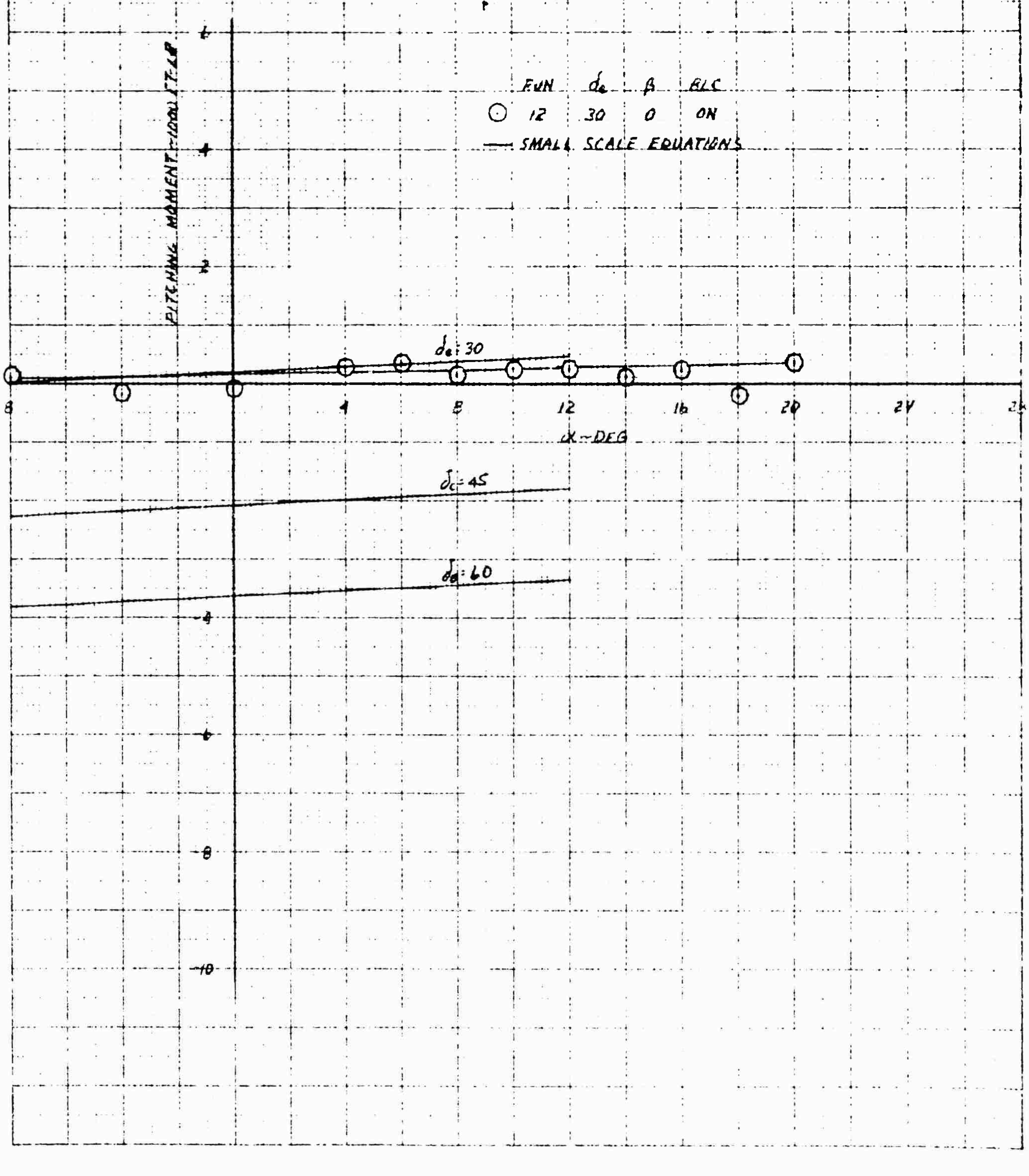

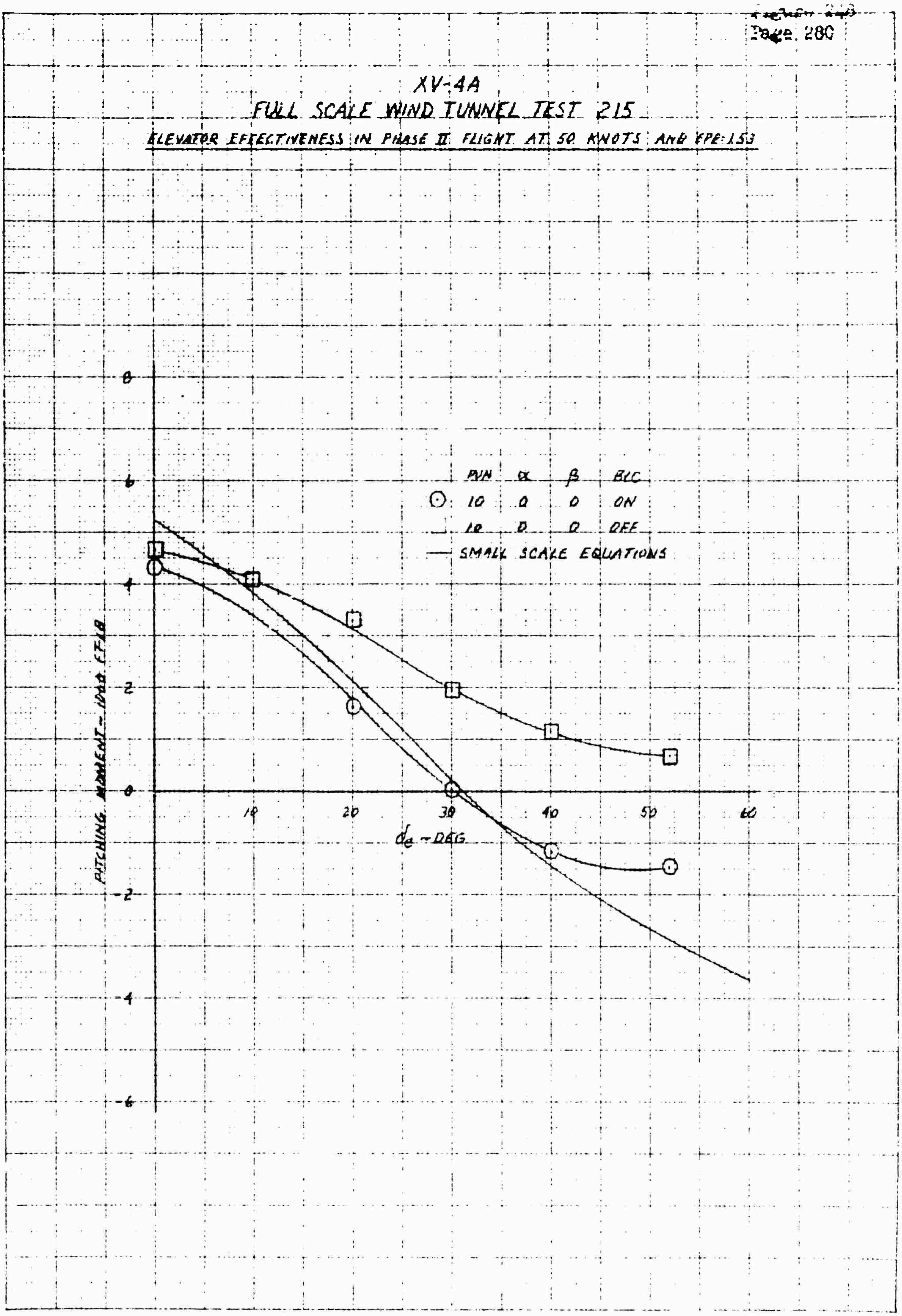
XV-4A
FULL SCALE WIND TUNNEL TEST 215
ELEVATOR EFFECTIVENESS IN PHASE II FLIGHT AT 50 KNOTS AND FPE 153
RUN α β BLC
10 0 0 ON
10 0 0 OFF
SMALL SCALE EQUATIONS
PITCHING MOMENT - 1000 FT-LB
δe ~ DEG
8
6
4
2
0
-2
-4
-6
10
20
30
40
50
60

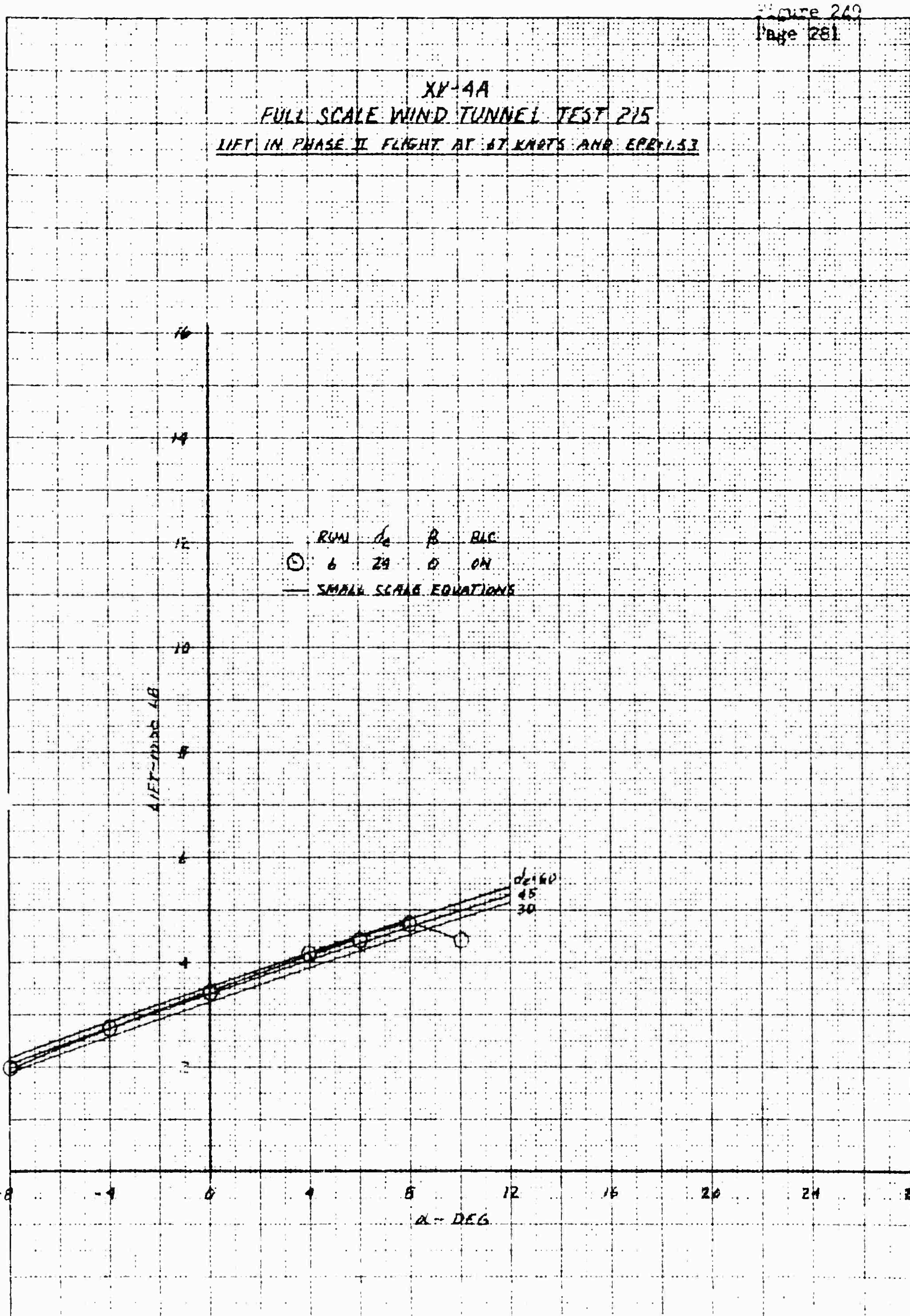
XV-4A
FULL SCALE WIND TUNNEL TEST 215
LIFT IN PHASE II FLIGHT AT 67 KNOTS AND EPR=1.53
RUN
6
29
0
ON
SMALL SCALE EQUATIONS
LIFT-1000 LB
α - DEG

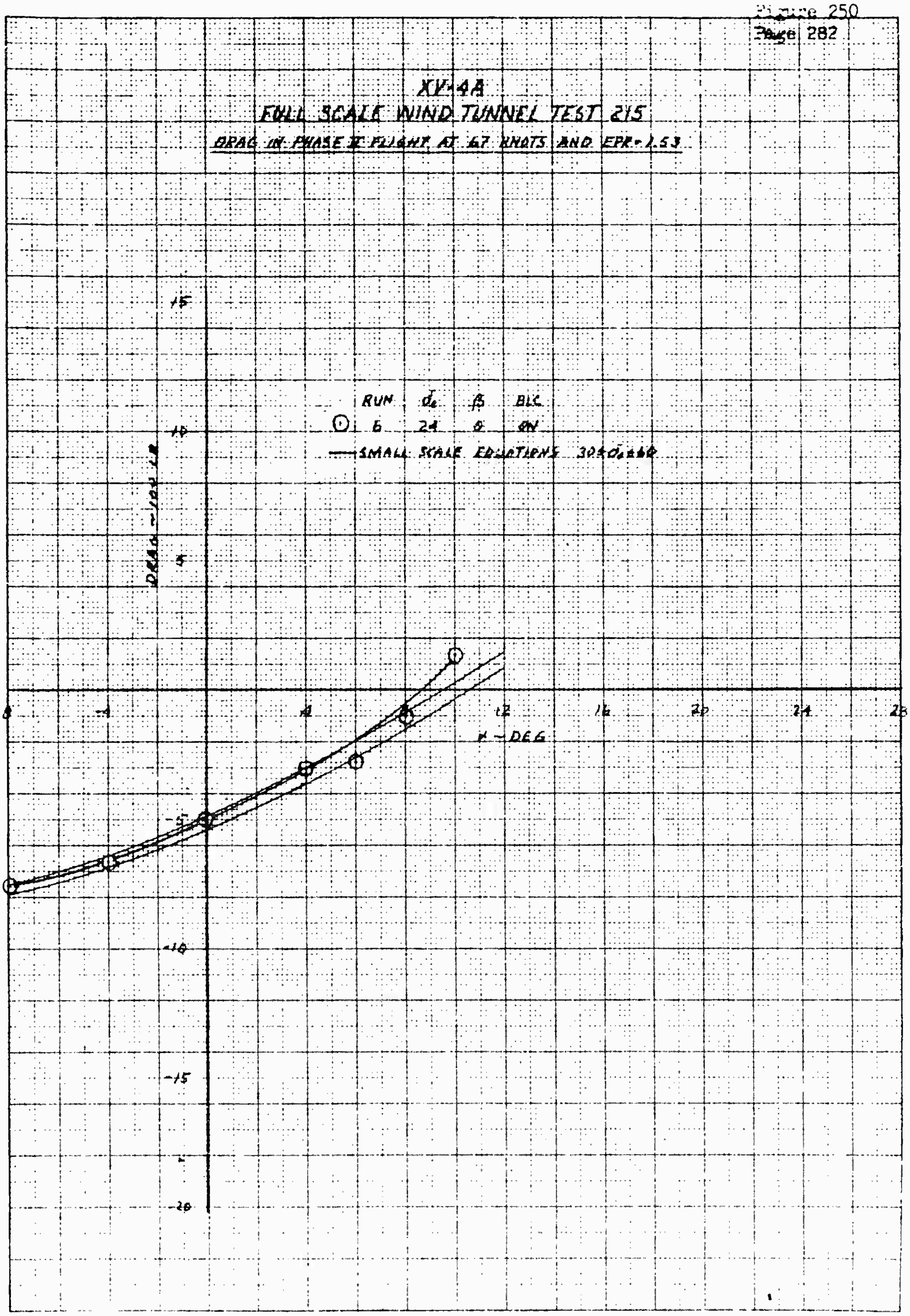
XV-4A
FULL SCALE WIND TUNNEL TEST 215
DRAG IN PHASE II FLIGHT AT 67 KNOTS AND EPR = 1.53
RUN δ_e β BLC
6 24 0 ON
SMALL SCALE EQUATIONS 30 ≤ δ_e ≤ 60
DRAG ~ 100 LB
α ~ DEG
15
10
5
-5
-10
-15
-20
-8
-4
4
8
12
16
20
24
28

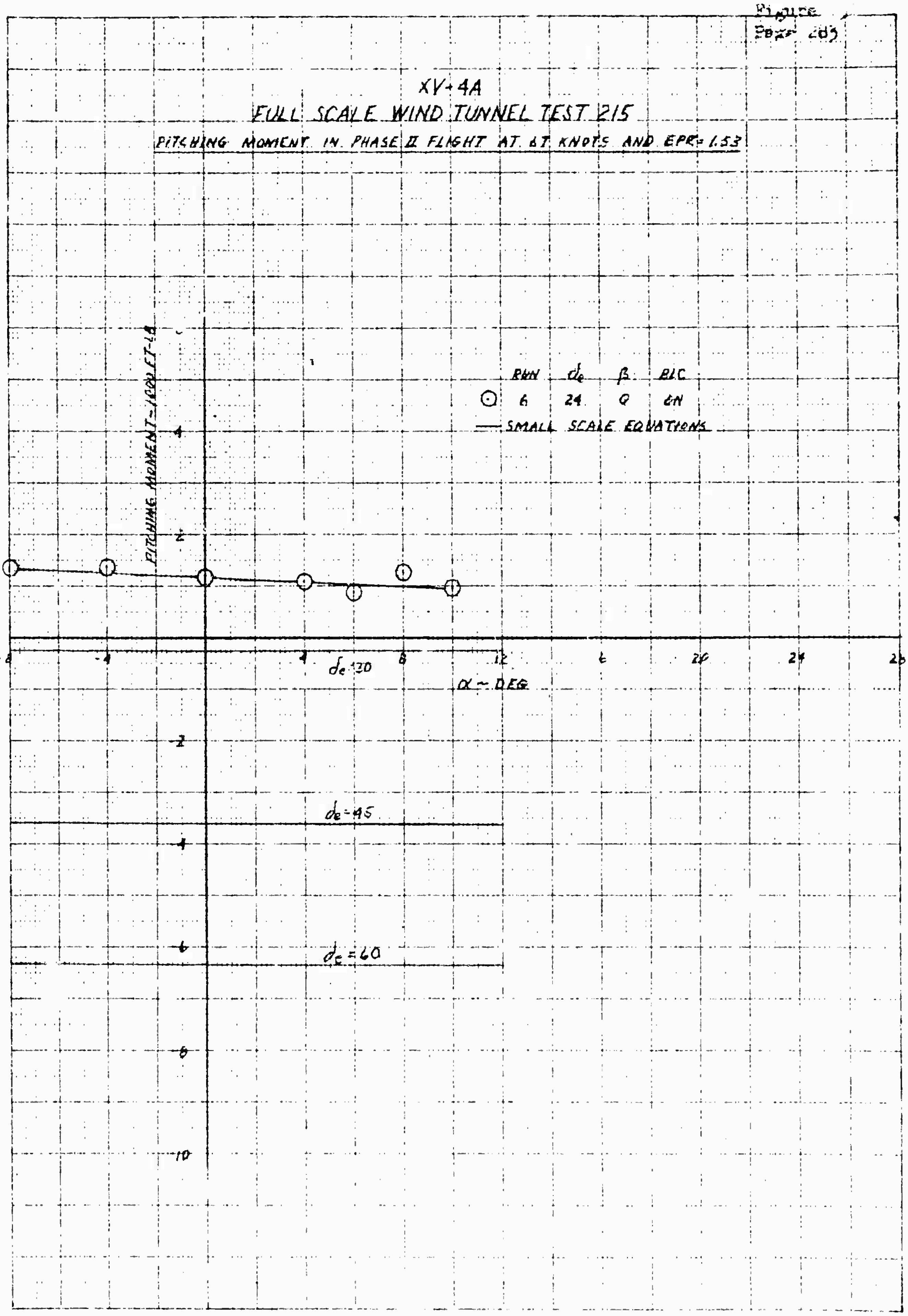
XV-4A
FULL SCALE WIND TUNNEL TEST 215
PITCHING MOMENT IN PHASE II FLIGHT AT 67 KNOTS AND EPR=1.53
RUN
β
6
24
0
SMALL SCALE EQUATIONS
PITCHING MOMENT~1000 FT-LB
α ~ DEG
δe =30
δe =45
δe =60

XV-4A
FULL SCALE WIND TUNNEL TEST 215
ELEVATOR EFFECTIVENESS IN PHASE II FLIGHT AT 67 KNOTS AND EPR=1.53

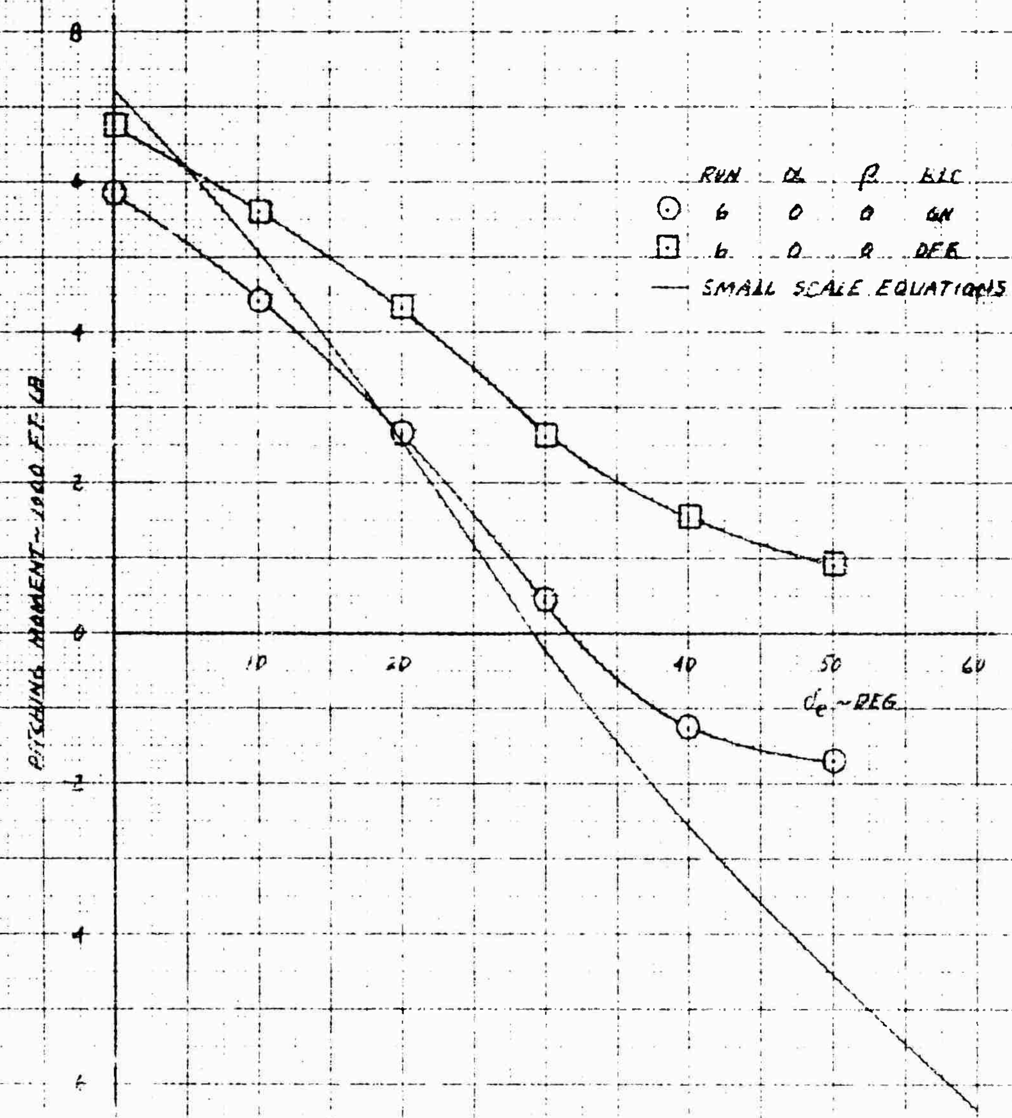

XV-4A

FULL SCALE WIND TUNNEL TEST 215

LIFT IN PHASE II FLIGHT AT 85 KNOTS AND EPR = 1.53

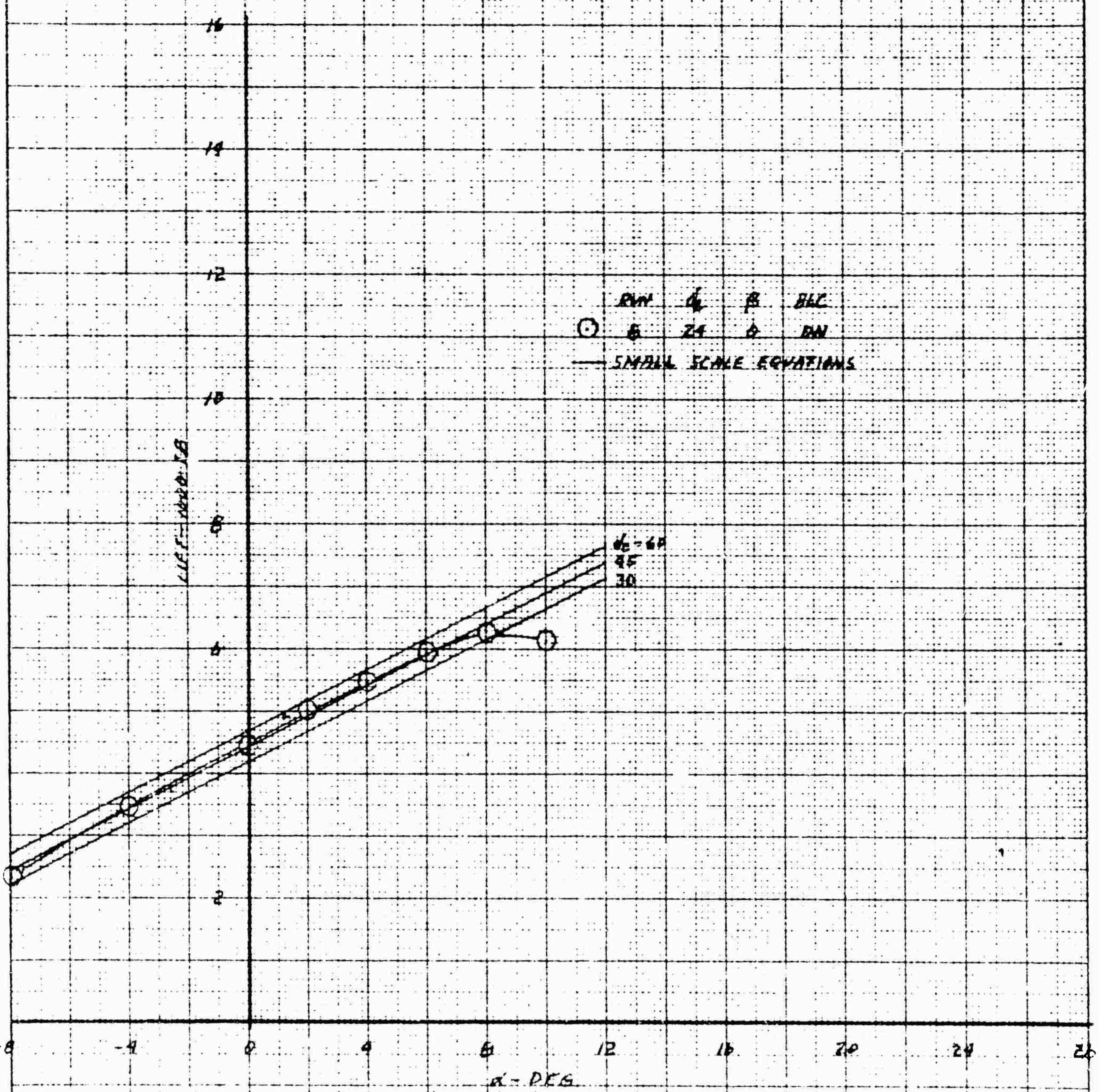

XV-4A

FULL SCALE WIND TUNNEL TEST 215

DRAG IN PHASE II FLIGHT AT 85 KNOTS AND EPR = 1.53

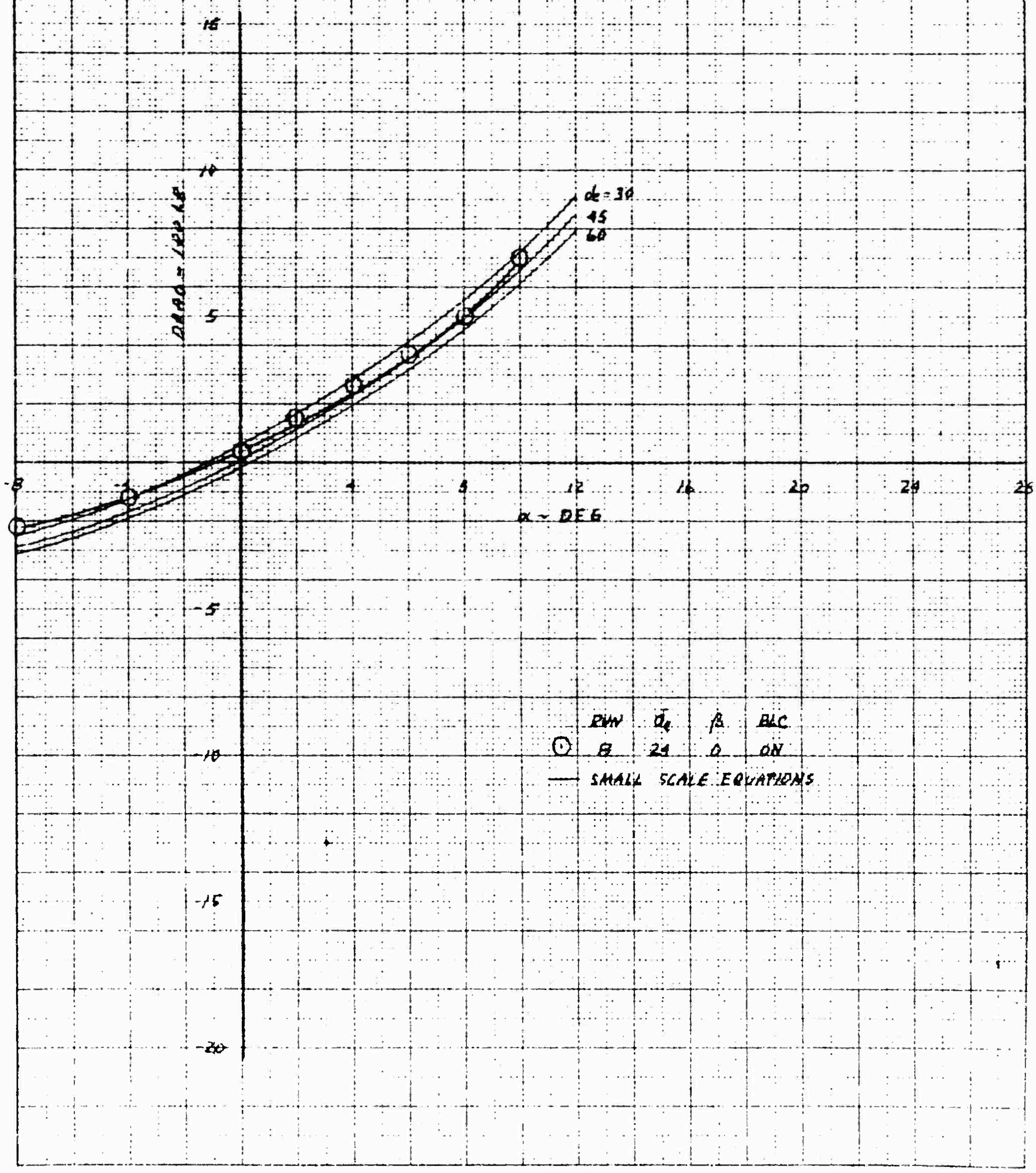

XV-4A

FULL SCALE WIND TUNNEL TEST 215

PITCHING MOMENT IN PHASE II FLIGHT AT 85 KNOTS AND EPR = 1.63

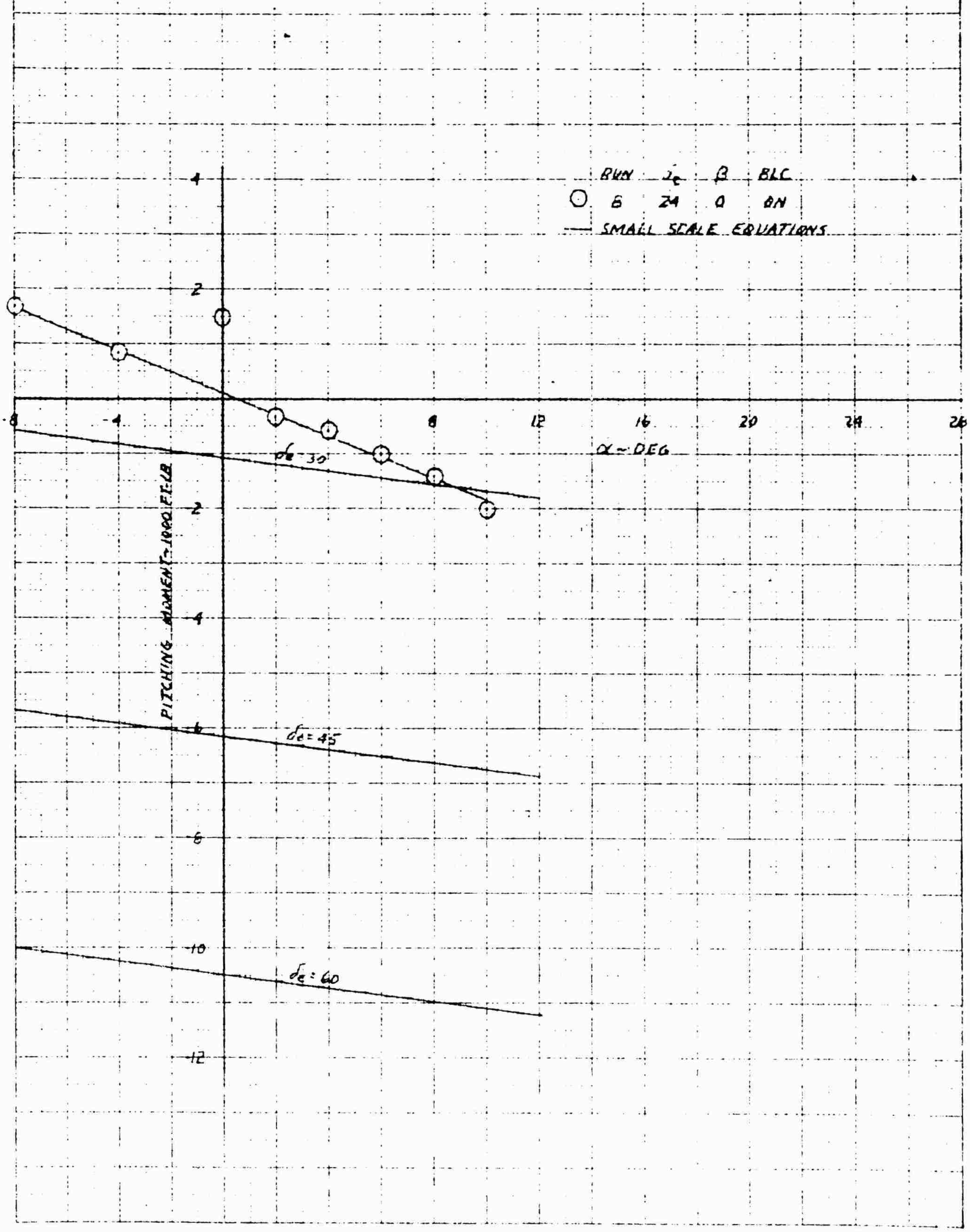

XV-4A

FULL SCALE WIND TUNNEL TEST 215

ELEVATOR EFFECTIVENESS IN PHASE II FLIGHT AT 85 KNOTS AND EPR=1.53

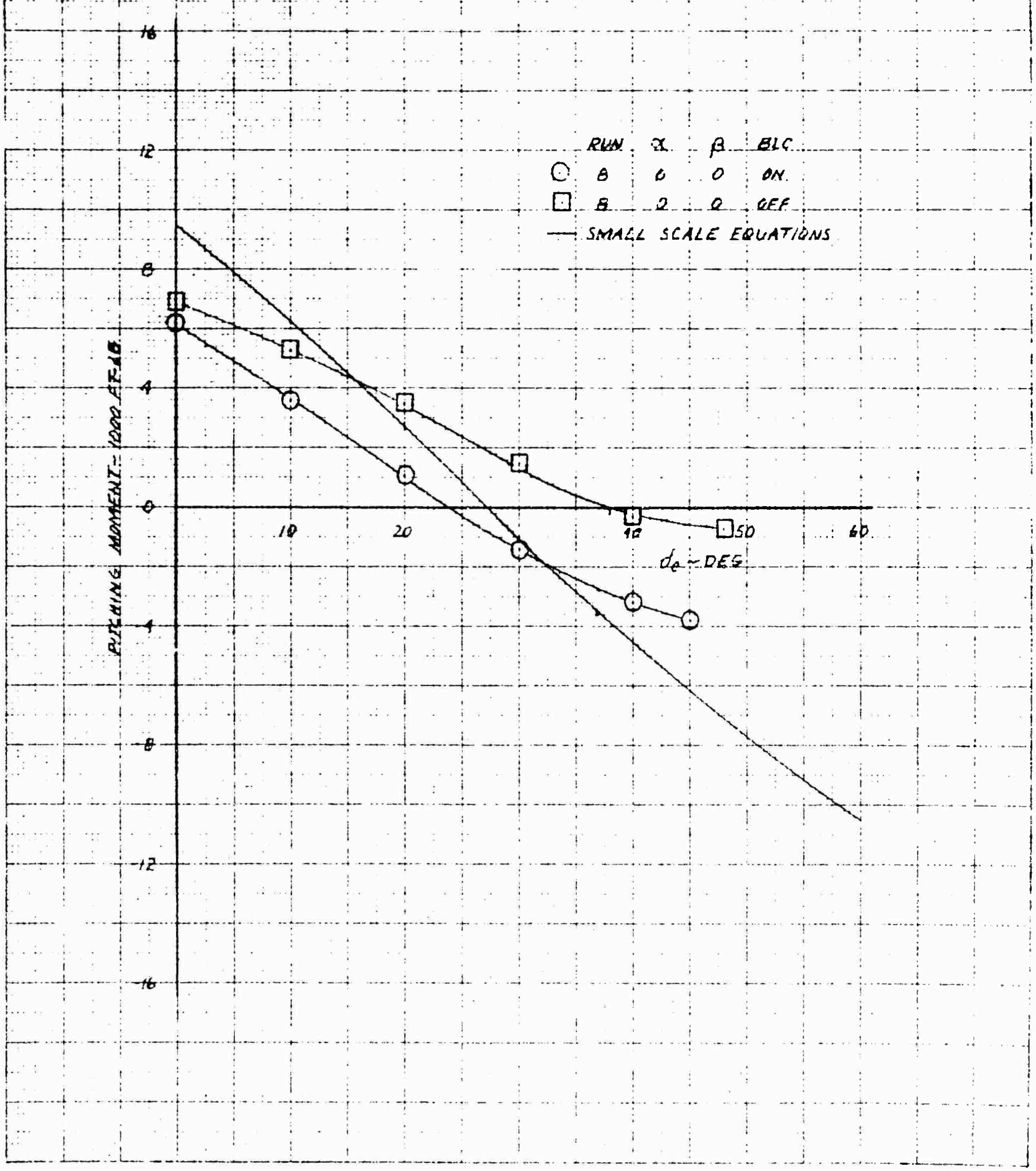

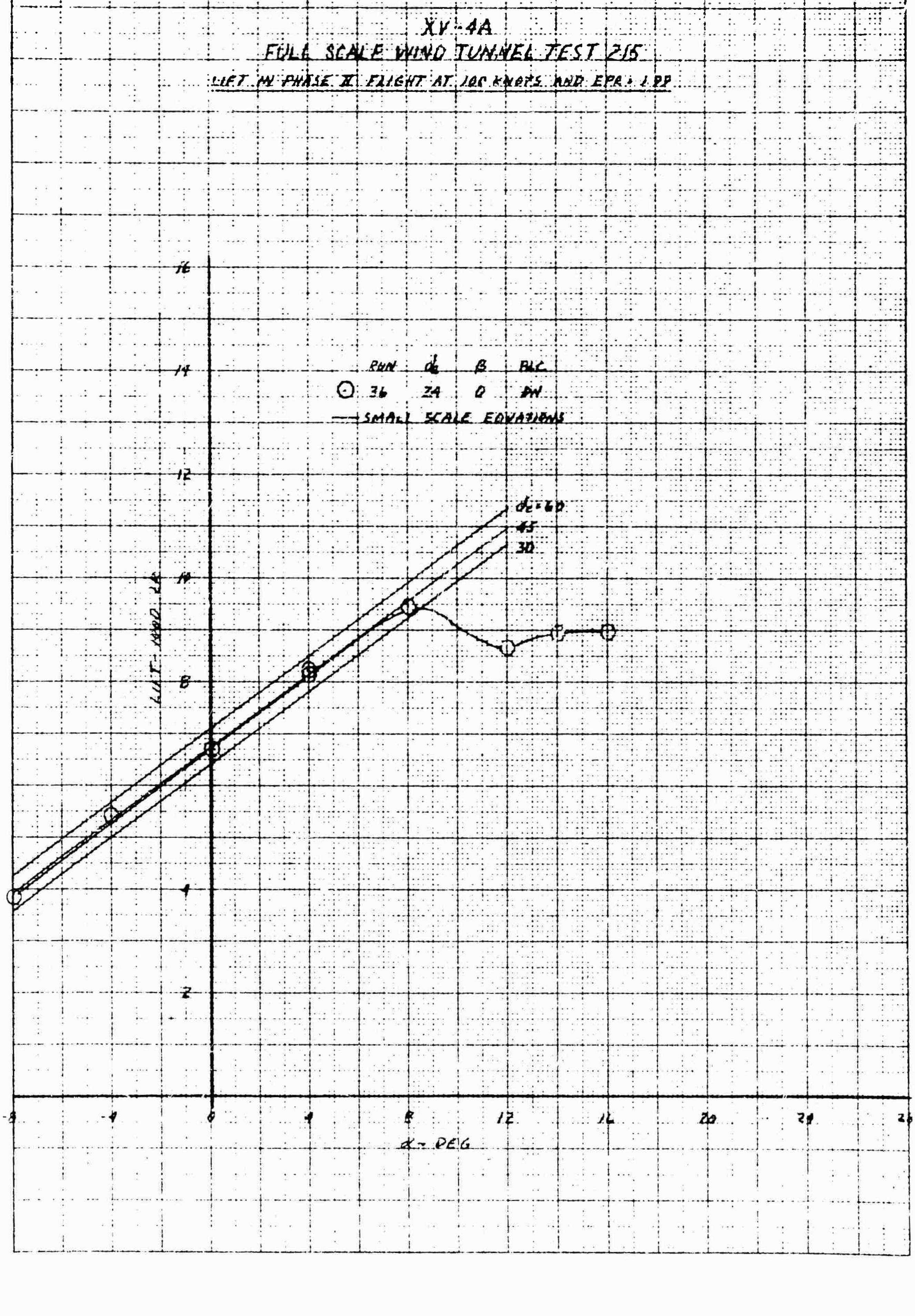
XV-4A
FULL SCALE WIND TUNNEL TEST 215
LIFT IN PHASE II FLIGHT AT 100 KNOTS AND EPR = 1.88
RUN δf β BLC
36 24 0
SMALL SCALE EQUATIONS
δf = 60
45
30
LIFT - 1000 LB
α - DEG
-8 -4 0 4 8 12 16 20 24 28
2 4 8 10 12 14 16

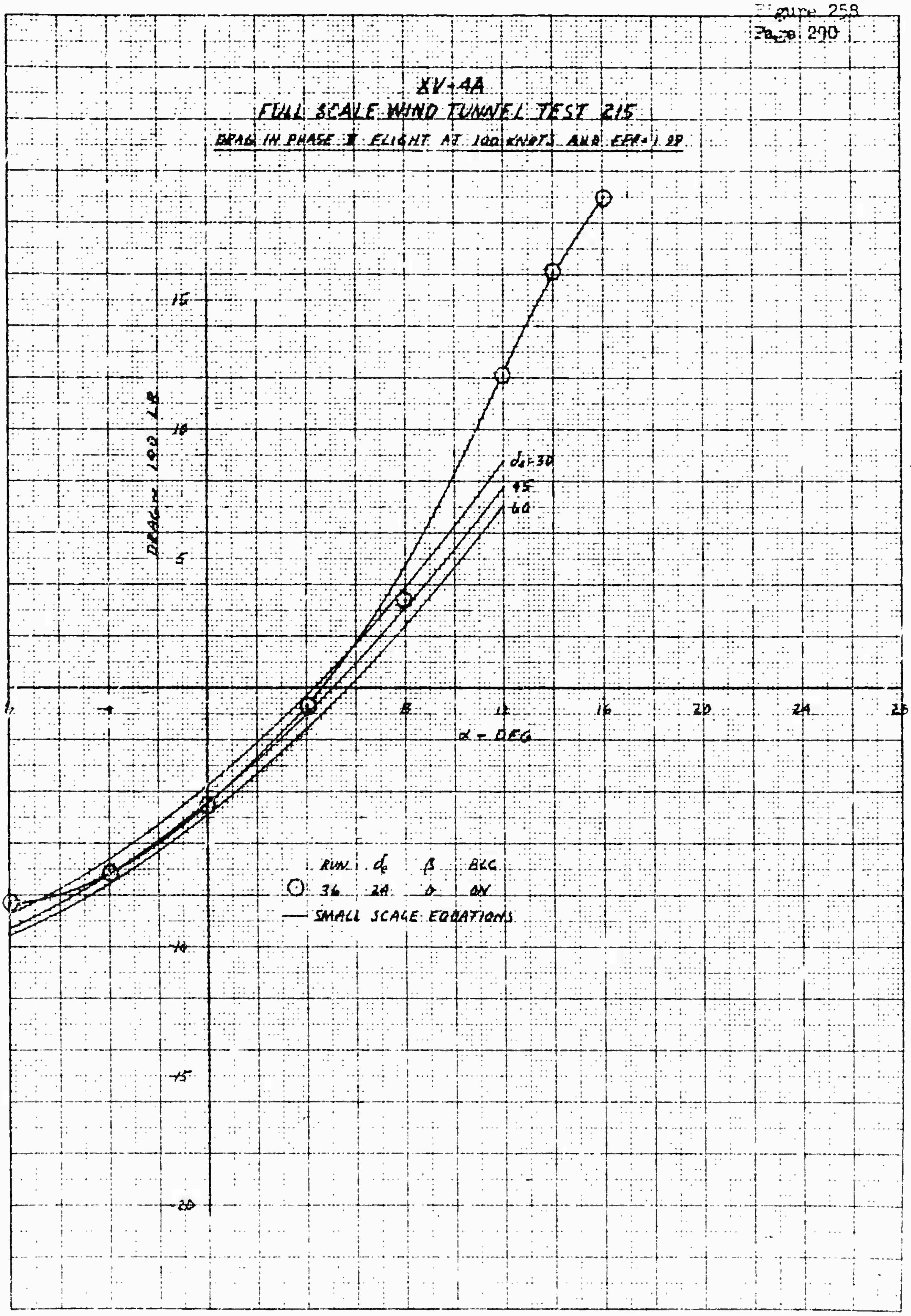
XV-4A
FULL SCALE WIND TUNNEL TEST 215
DRAG IN PHASE II FLIGHT AT 100 KNOTS AND EPR=1.09
DRAG - 100 LB
α - DEG
δf=30
45
60
RUN δf β BLC
36 20 0 ON
SMALL SCALE EQUATIONS

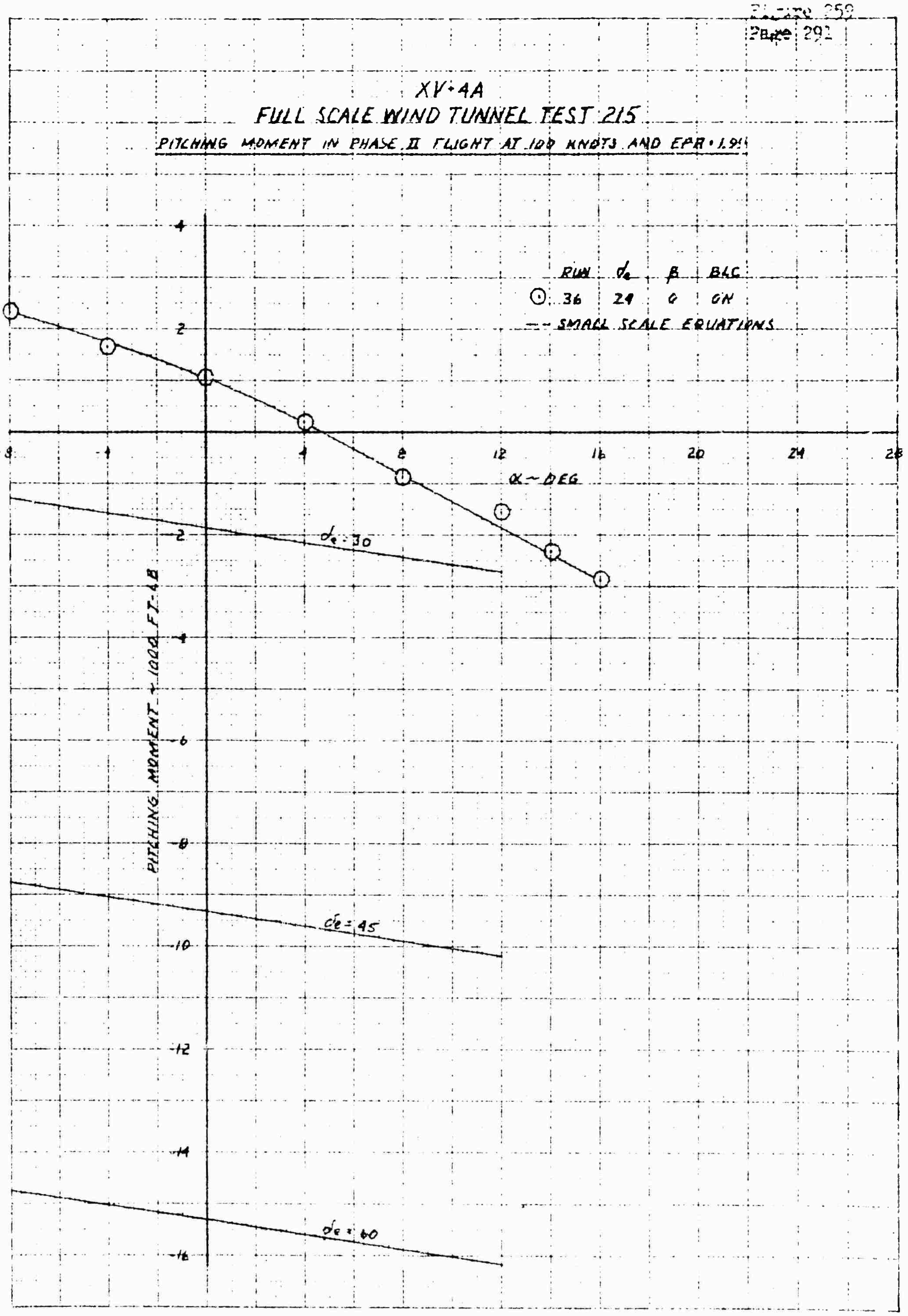

XV-4A
FULL SCALE WIND TUNNEL TEST 215
PITCHING MOMENT IN PHASE II FLIGHT AT 100 KNOTS AND EPR=1.95
RUN
36
24
6
BLC
ON
SMALL SCALE EQUATIONS
α ~ DEG
PITCHING MOMENT ÷ 1000 FT-LB
δe = 30
δe = 45
δe = 60

XV-4A
FULL SCALE WIND TUNNEL TEST 215
ELEVATOR EFFECTIVENESS IN PHASE II FLIGHT AT 100 KNOTS AND EPR 1.99

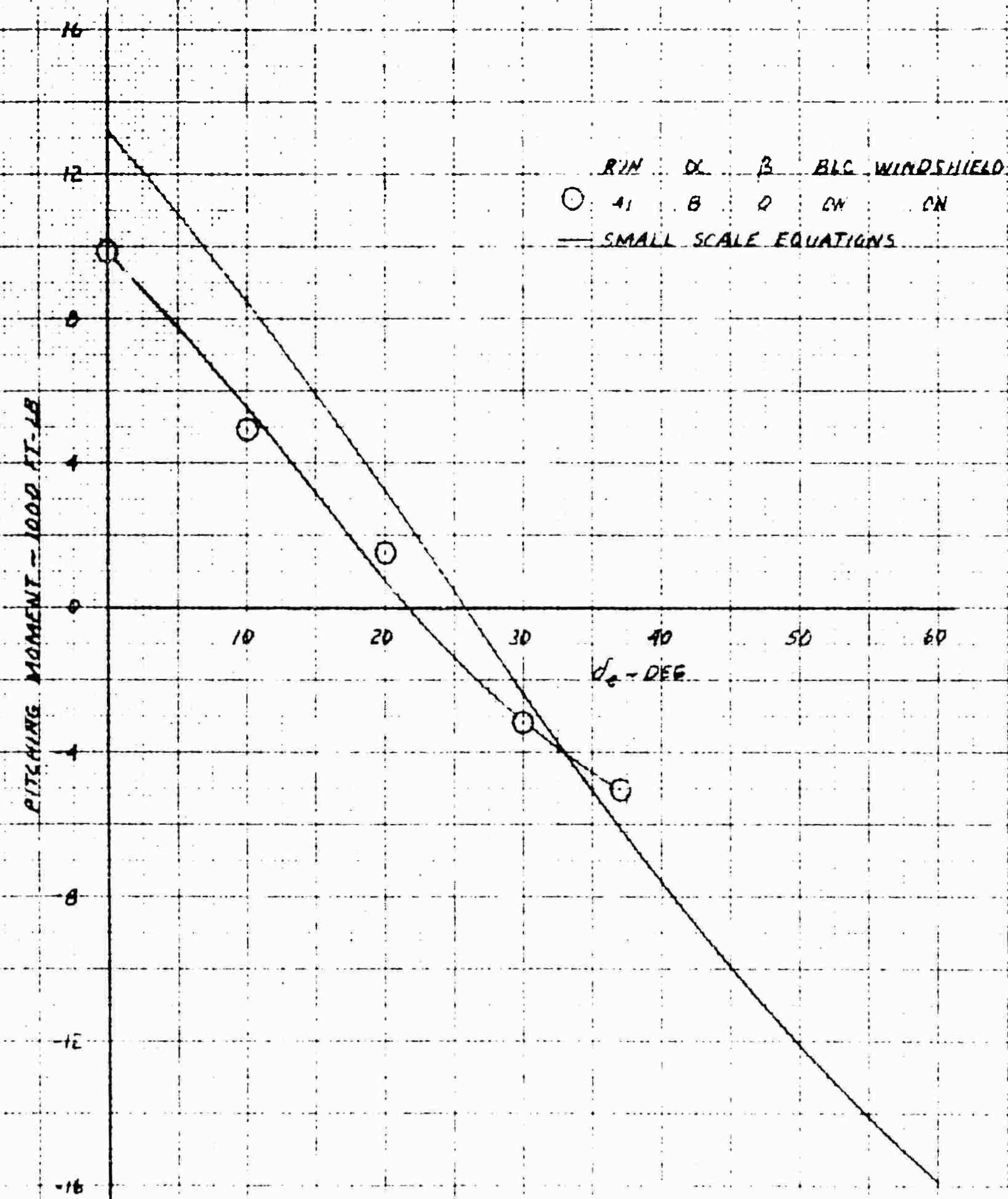

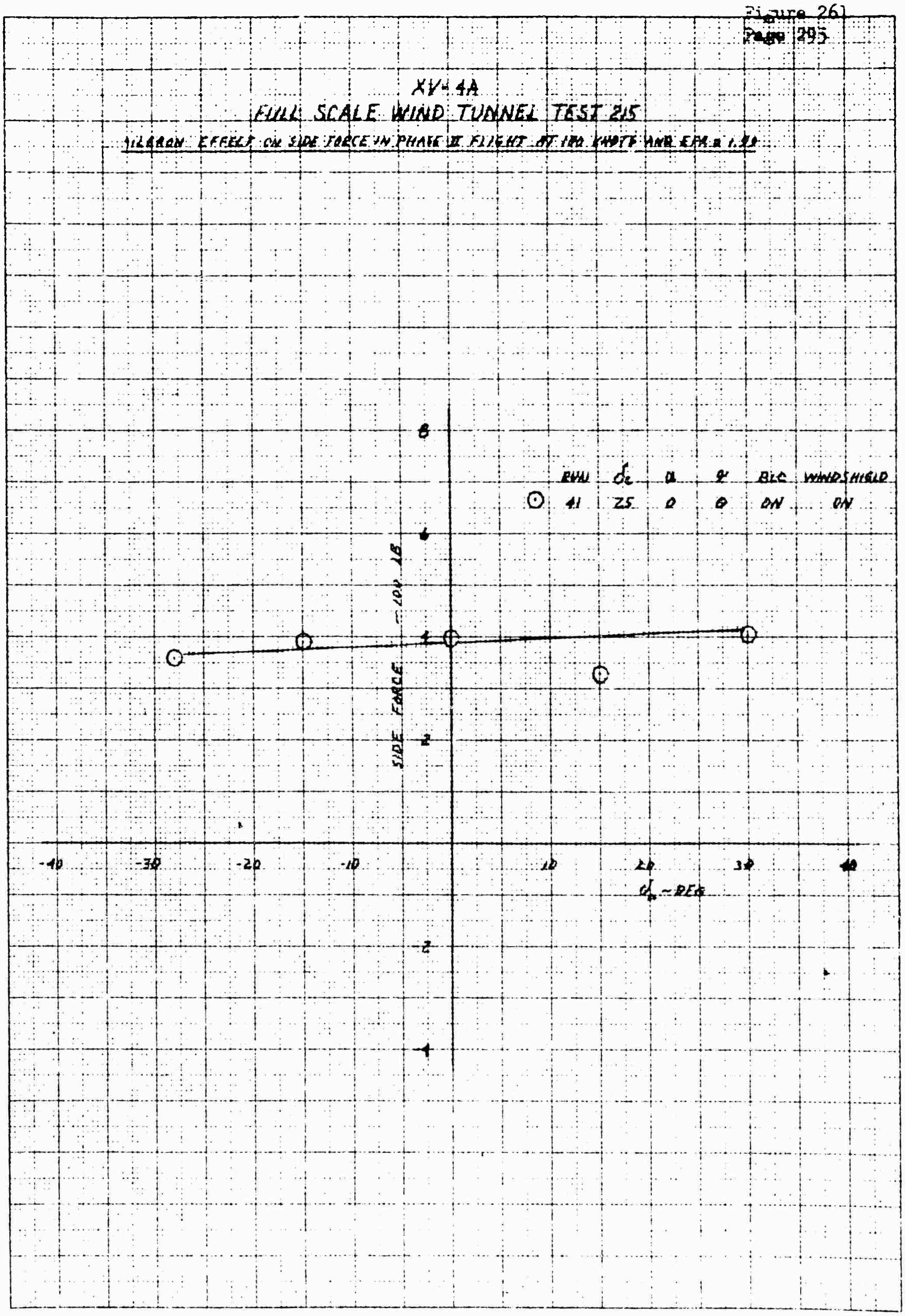
XV-4A
FULL SCALE WIND TUNNEL TEST 215
AILERON EFFECT ON SIDE FORCE IN PHASE II FLIGHT
RVU
41
25
0
0
BLC
ON
WINDSHIELD
ON
SIDE FORCE ~ 100 LB
8
6
4
2
-2
-4
-40
-30
-20
-10
10
20
30
40
~ DEG

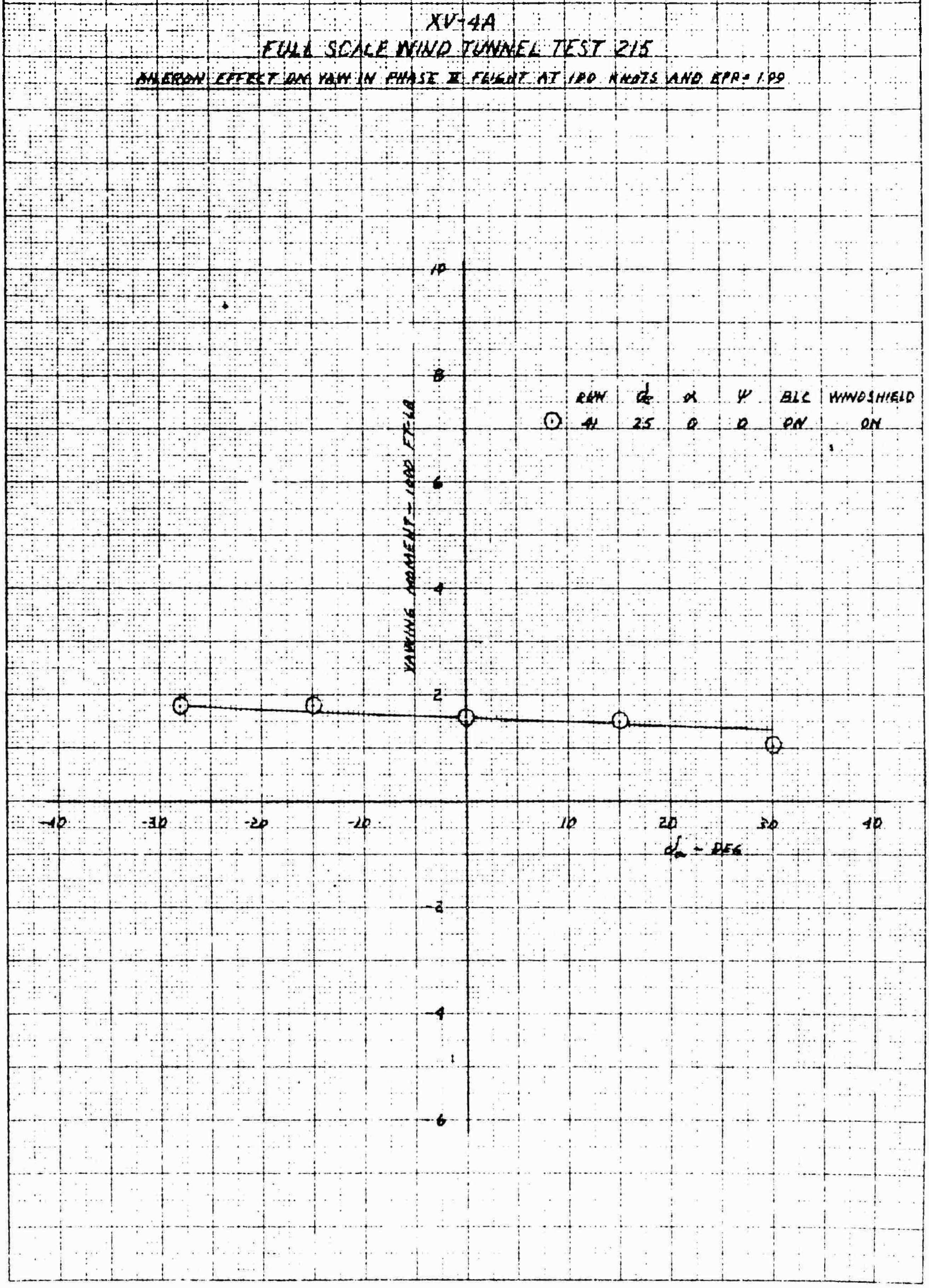
XV-4A
FULL SCALE WIND TUNNEL TEST 215
AILERON EFFECT ON YAW IN PHASE II FLIGHT AT 180 KNOTS AND EPR= 1.99
RUN
α
ψ
BLC
WINDSHIELD
41
25
0
0
ON
ON
YAWING MOMENT - 1000 FT-LB
10
8
6
4
2
-2
-4
-6
-40
-30
-20
-10
10
20
30
40
DEG

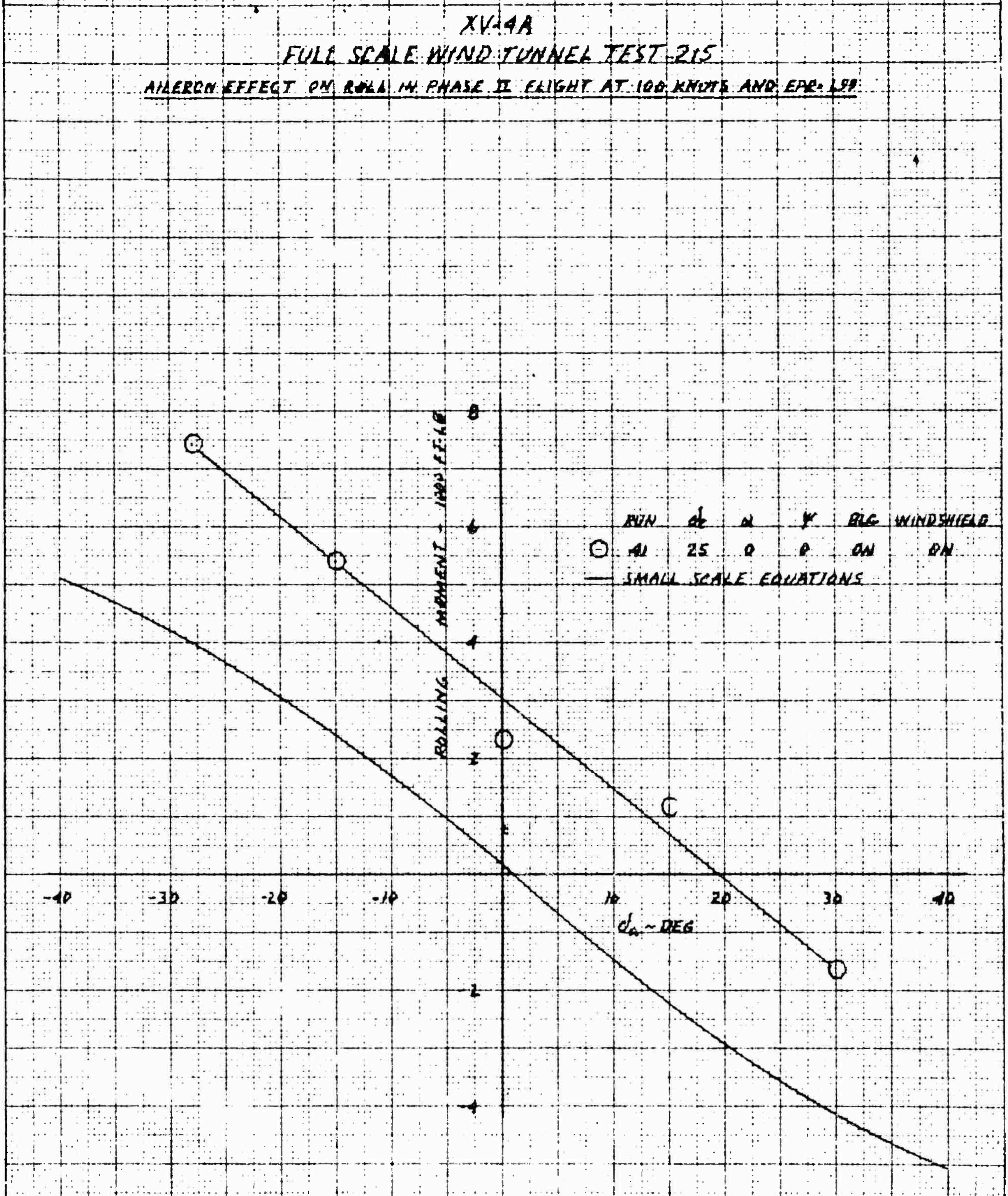
XV-4A
FULL SCALE WIND TUNNEL TEST 215
AILERON EFFECT ON ROLL IN PHASE II FLIGHT AT 100 KNOTS AND EPR=1.99
ROLLING MOMENT - 1000 FT.LB
8
6
4
2
-2
-4
-40
-30
-20
-10
10
20
30
40
δ_a ~ DEG
RUN
δ_f
α
ψ
BLG
WINDSHIELD
41
25
0
0
ON
ON
SMALL SCALE EQUATIONS

XV-4A

FULL SCALE WIND TUNNEL TEST 215

RUDDER EFFECT ON SIDE FORCE IN PHASE II FLIGHT AT 140 KNOTS AND EPR = 1.99

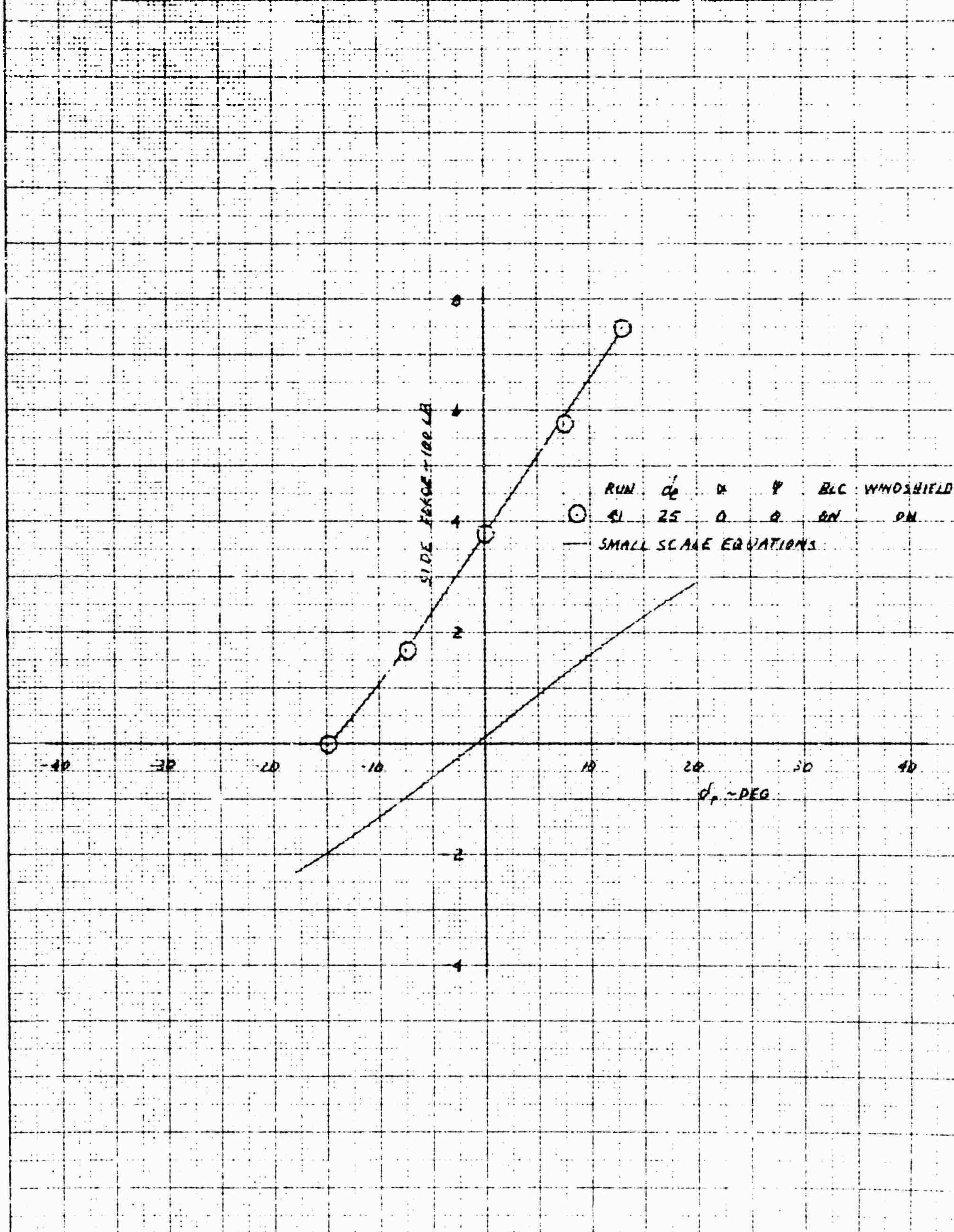

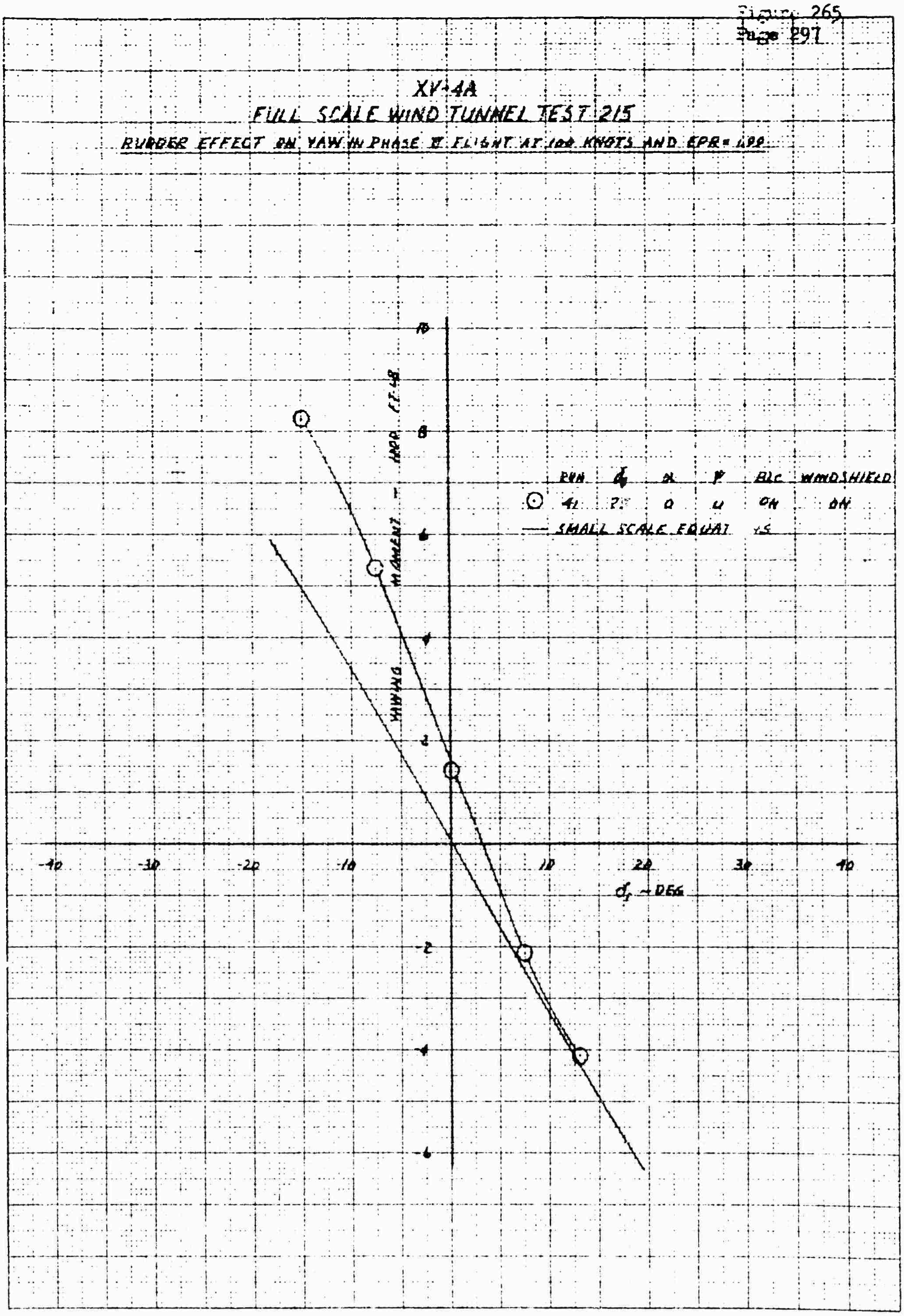
XV-4A
FULL SCALE WIND TUNNEL TEST 215
RUDDER EFFECT ON YAW IN PHASE II FLIGHT AT 100 KNOTS AND EPR = 1.99
RUN
α
BLC
WINDSHIELD
41
0
ON
ON
SMALL SCALE EQUAT
YAWING MOMENT ~ 1000 FT-LB
10
8
6
4
2
-2
-4
-6
-40
-30
-20
-10
10
20
30
40
δ_r ~ DEG

XV-4A
FULL SCALE WIND TUNNEL TEST 215
RUDDER EFFECT ON ROLL IN PHASE II FLIGHT AT 100 KNOTS AND EPR=1.99

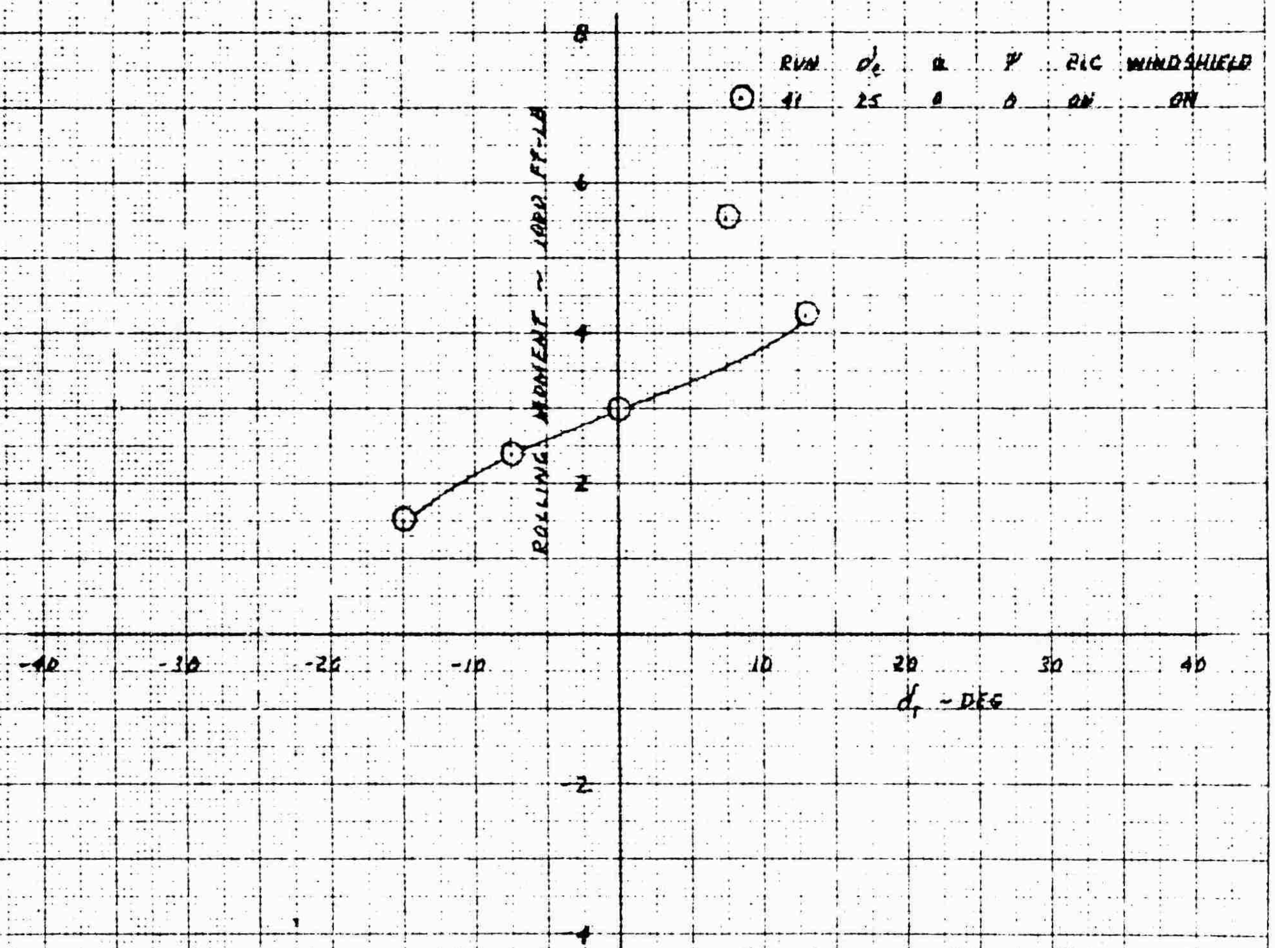

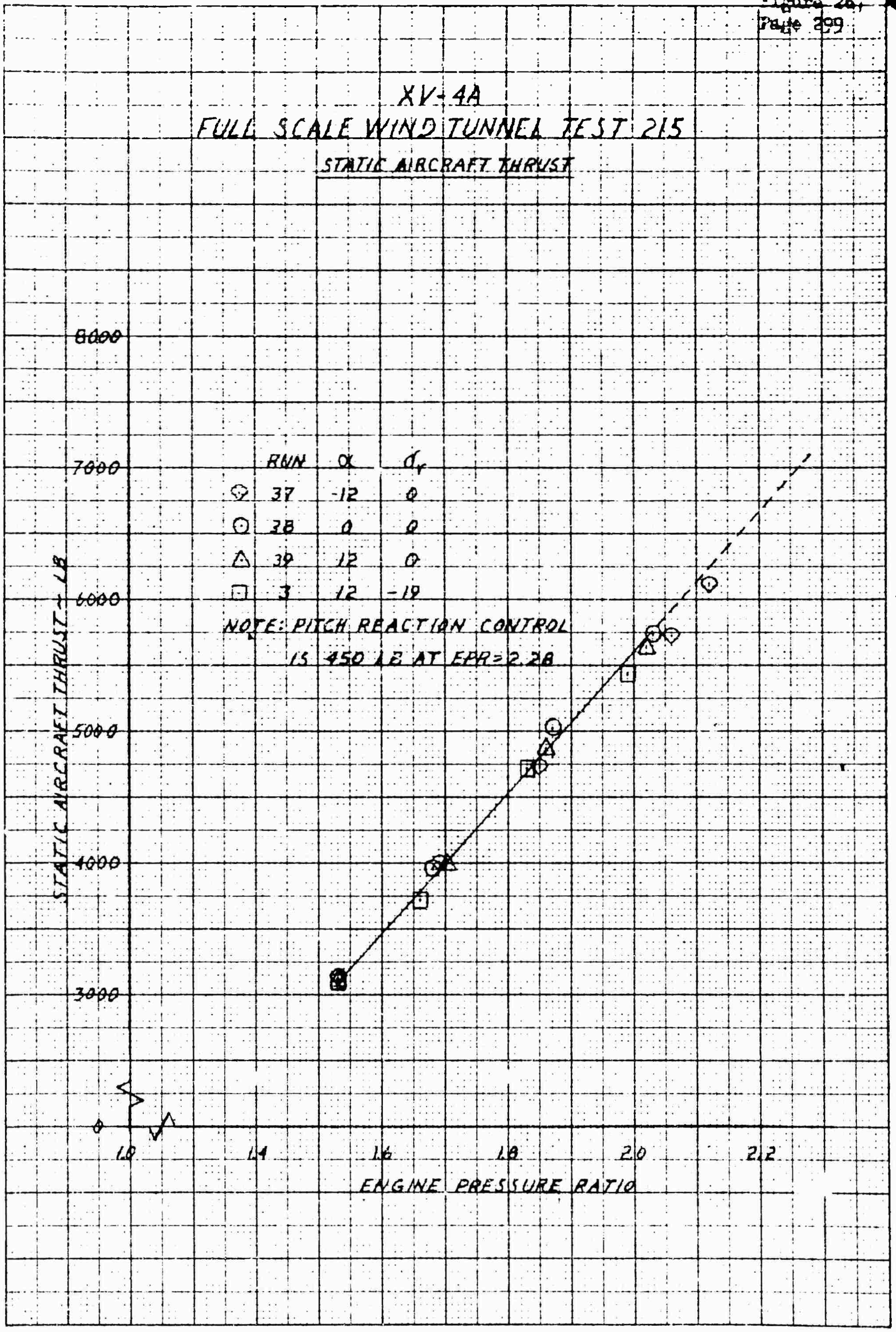
XV-4A
FULL SCALE WIND TUNNEL TEST 215
STATIC AIRCRAFT THRUST
RUN α δr
37 -12 0
38 0 0
39 12 0
3 12 -19
NOTE: PITCH REACTION CONTROL
IS 450 LB AT EPR=2.28
STATIC AIRCRAFT THRUST - LB
8000
7000
6000
5000
4000
3000
0
1.0
1.4
1.6
1.8
2.0
2.2
ENGINE PRESSURE RATIO

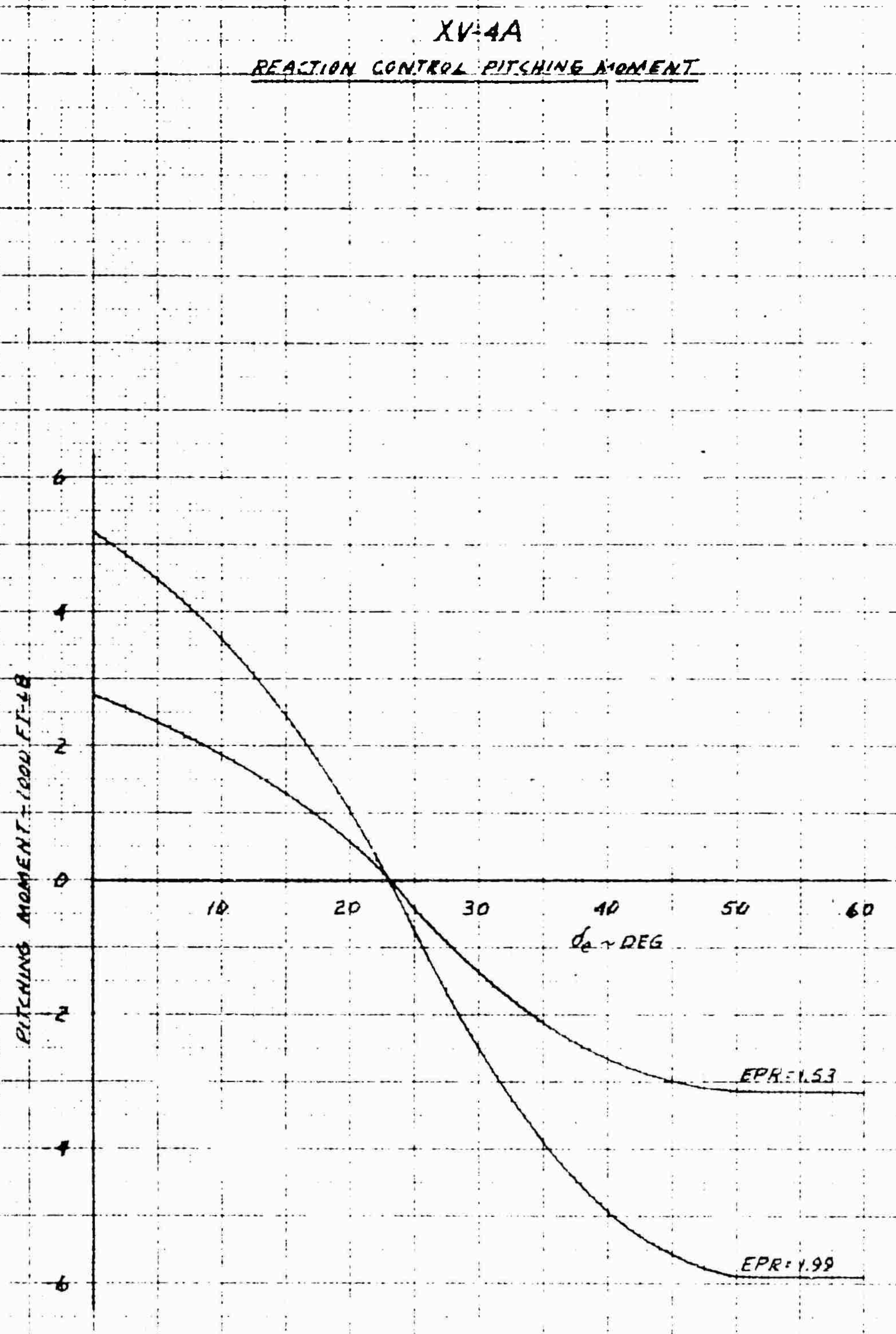
XV-4A
REACTION CONTROL PITCHING MOMENT
PITCHING MOMENT ~ 1000 FT-LB
6
4
2
0
-2
-4
-6
10
20
30
40
50
60
δ_e ~ DEG
EPR=1.53
EPR=1.99

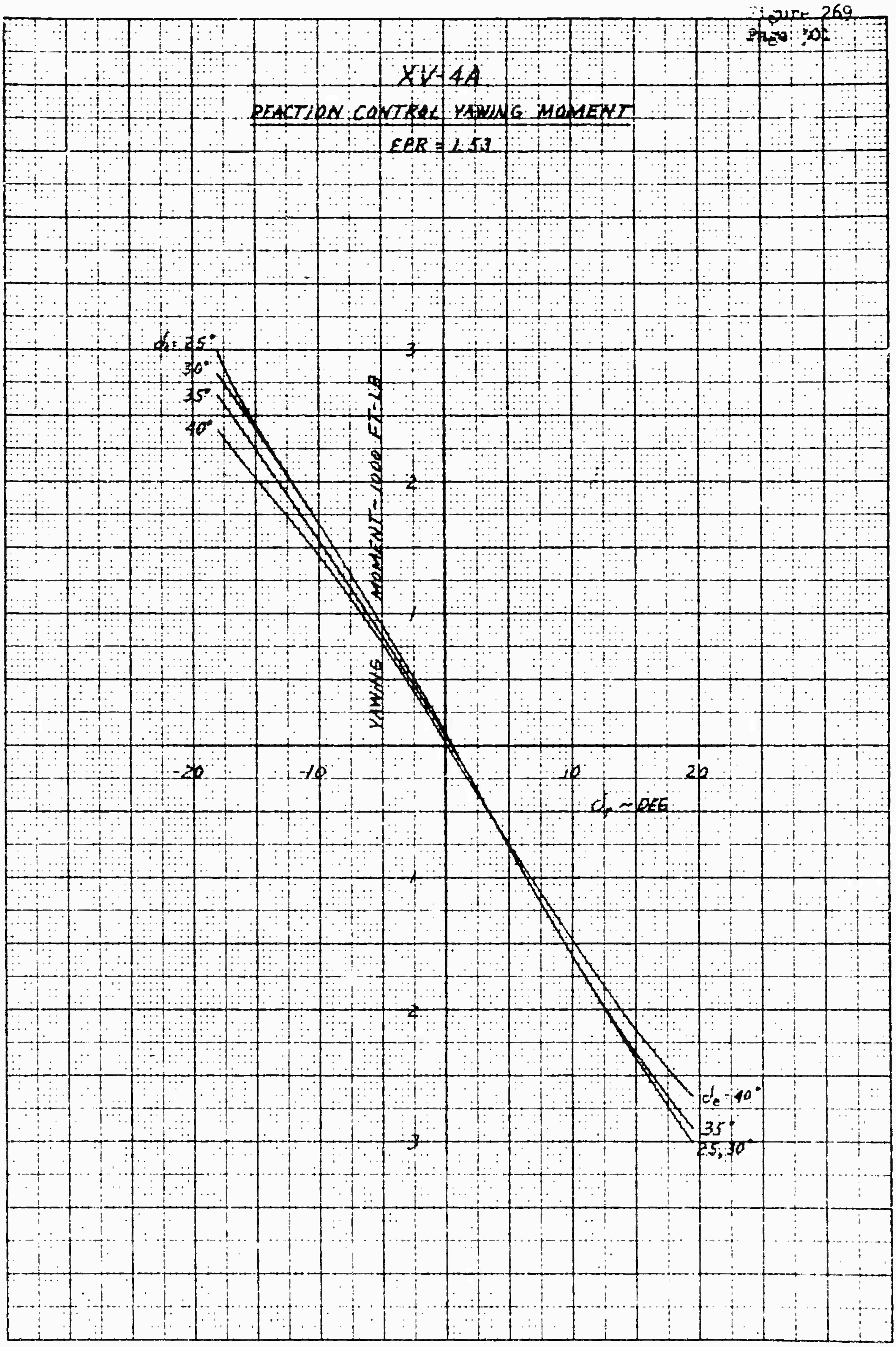
XV-4A
REACTION CONTROL YAWING MOMENT
EPR = 1.53
YAWING MOMENT – 1000 FT-LB
α_e ~ DEG
α_e = 25°
30°
35°
40°
α_e = 40°
35°
25, 30°
-20
-10
10
20
3
2
1
1
2
3

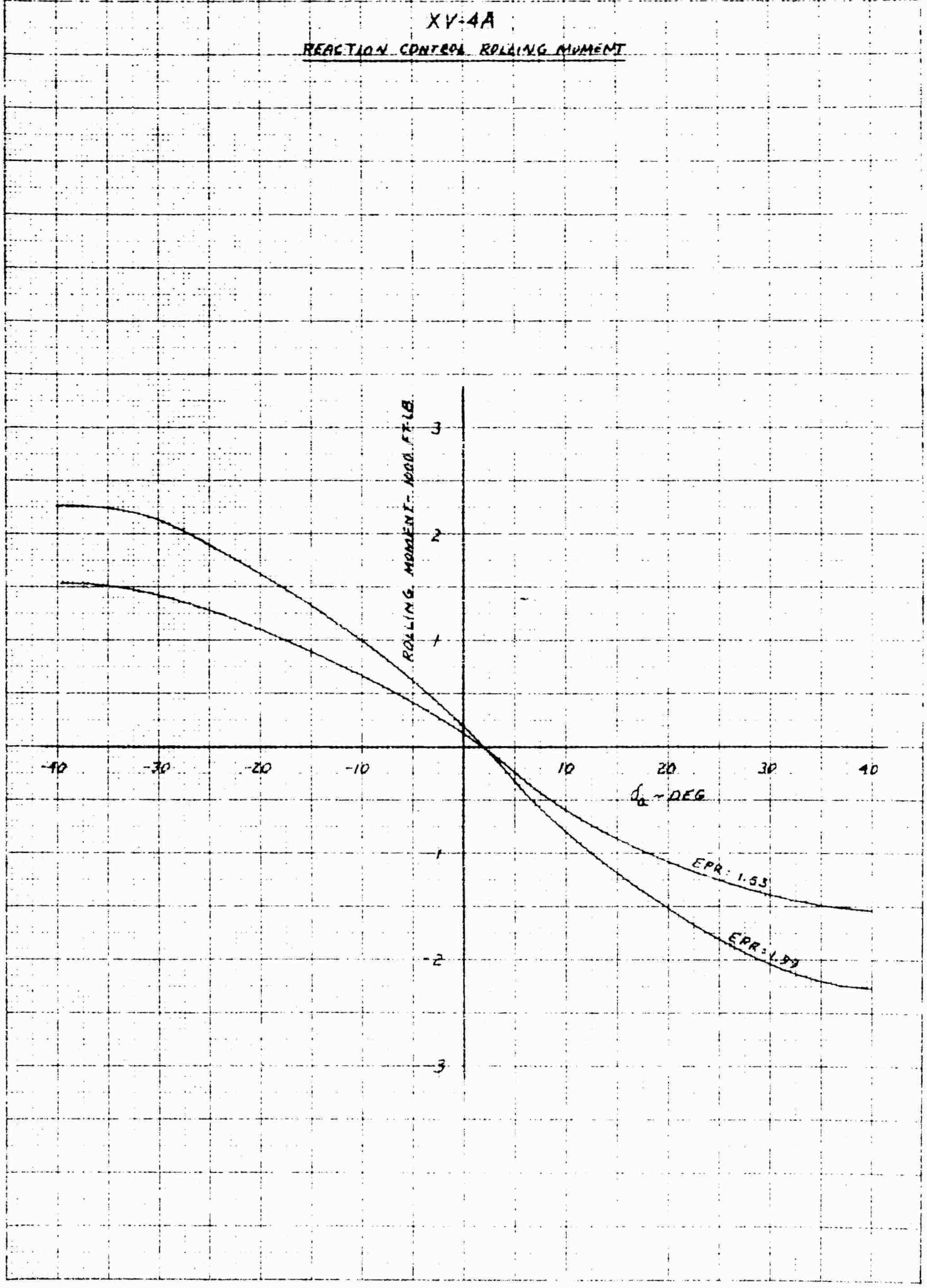
XV-4A
REACTION CONTROL ROLLING MOMENT
ROLLING MOMENT - 1000 FT-LB
3
2
1
-1
-2
-3
-40
-30
-20
-10
10
20
30
40
δ_a ~ DEG
EPR: 1.53
EPR: 1.99

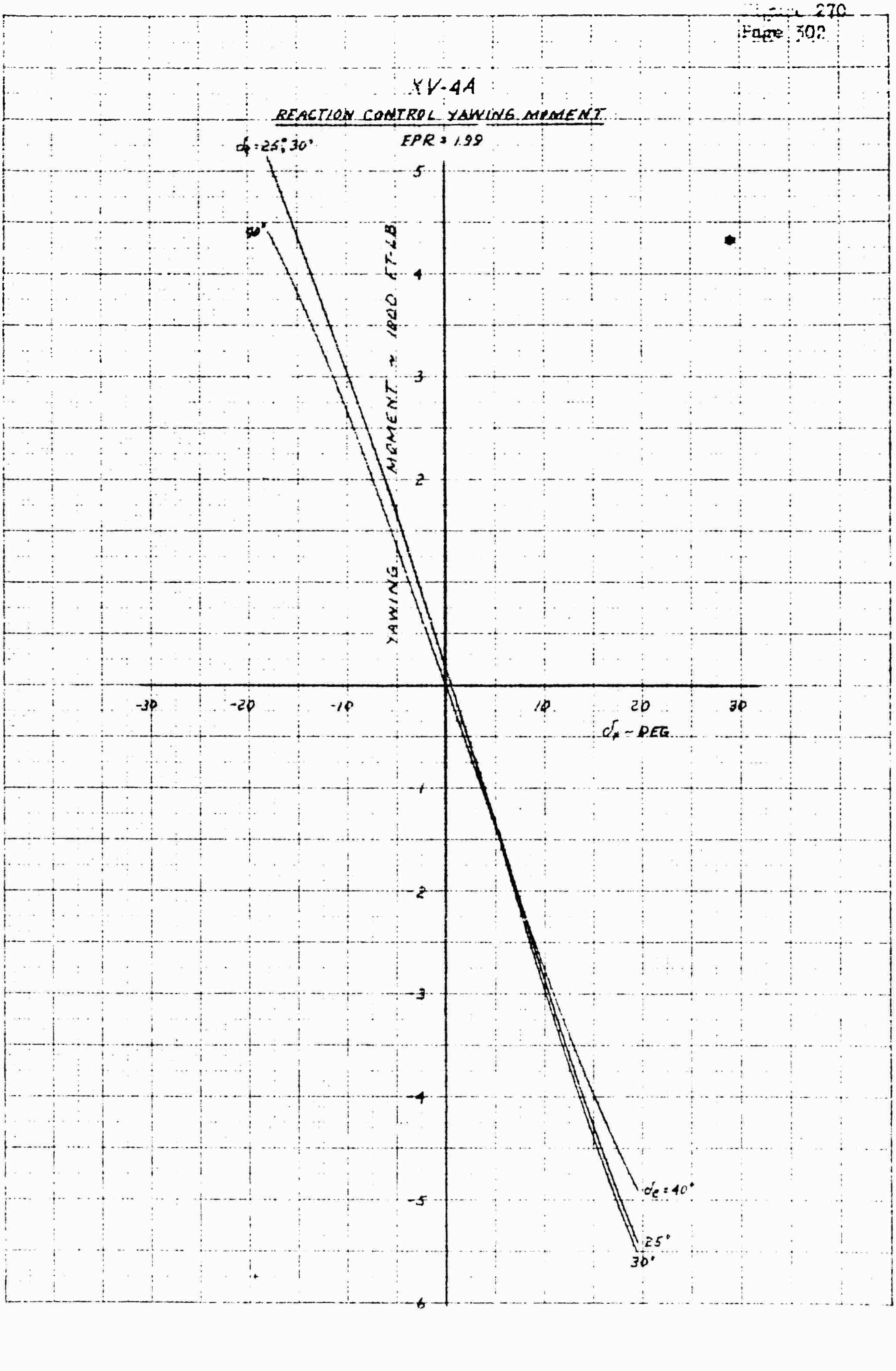
XV-4A
REACTION CONTROL YAWING MOMENT
EPR = 1.99
δ_e = 25°, 30°
40°
YAWING MOMENT ~ 1000 FT-LB
5
4
3
2
-1
-2
-3
-4
-5
-6
-30
-20
-10
10
20
30
δ_r ~ DEG
δ_e = 40°
25°
30°